

Elastic Stability of Structures

With a recall of Vlassov torsion of thin-walled shell-beams of open cross-sections

Lagrange-Dirichlet Theorem: Assuming the continuity of the total potential energy, the equilibrium of a system containing only conservative and dissipative forces is stable if the total potential energy of the system has a strict minimum (i.e., is positive-definite).

Energy approach – the MAP

$\Pi'' > 0$,	stable.
$\Pi'' = 0$,	neutral.
$\Pi'' < 0$,	unstable.

Figure 3.24: Map of total potential energy $\Delta\Pi$ of an elastic structure. Equilibrium paths corresponds to locations where $\delta(\Delta\Pi) = 0$ while keeping P constant. Stable equilibrium is achieved there where $\delta^2(\Delta\Pi) > 0$. Note the analogy with the topographical map of piece of Chamonix (Alpes).

All real structural systems are imperfect

- ✓ in form,
- ✓ in material properties,
- ✓ in the sense of residual stresses
- ✓ in the way the loads are applied

A tiny perturbation

Symmetry → breaking

Straight primary equilibrium
Is this position stable?

OTANIEMI

Djebar BAROUDI

March 11, 2021

Contents

Dear Reader	1
1 Elastic Stability of Structures	5
1.1 Introduction	5
1.1.1 The big picture - Stabiilius pähkinäkuoressa	8
1.1.2 Lagrange-Dirichlet stability theorem	9
1.2 Structural design and stability	16
1.3 Basic concepts	26
1.4 Study of Elastic stability - the method	29
1.4.1 Methods of stability analysis	30
1.4.2 What is stability as a phenomenon?	31
1.5 Equilibrium paths	46
1.5.1 Example of full non-linear and the linearised homogeneous problem	48
1.6 Types of bifurcational instabilities	50
1.6.1 Equilibrium paths for simple rigid bar systems with springs	51
1.6.2 Stable-symmetric bifurcation model	54
1.7 Effects of imperfections	62
1.7.1 Symmetric Stable bifurcation	62
1.7.2 Unstable-symmetric bifurcation model	62
1.7.3 Asymmetric bifurcation model	67
1.7.4 Example of stability of discontinuous system with many dofs	79
1.7.5 Combined loading and stability regions	83
1.8 Energy criteria for determination loss of stability of elastic structures	85
1.9 Energy criterion for bifurcational instability	86
1.10 Homogeneous linearised equations of stability	92
1.10.1 The energy criterion	94

1.11	Application examples of stability study using energy principles	109
1.11.1	Energy criteria for column buckling	110
1.11.2	Energy criteria in 'the full form'	111
1.11.3	Buckling of a beam-column	112
1.11.4	Effects of imperfections	116
1.11.5	Timoshenko column	123
1.12	Example of an application of virtual work principle - Southwell-plots	127
1.12.1	On upper- and lower bounds for the critical load	132
1.12.2	Examples of buckling load estimates	154
1.12.3	A continuous model of a pin-ended column under pulsating axial load	176
1.12.4	PAASIN TANNE 11 MARS 2021	184
1.12.5	Loss of stability of a rotating axis	184
1.12.6	Mechanical discrete models	189
1.12.7	Load combination - interaction buckling diagrams	211
1.12.8	Linear buckling analysis of simply supported column	242
1.12.9	Asymptotic post-buckling analysis of simply supported column	243
1.12.10	Lagrangian curvature	244
1.12.11	Buckling of columns on elastic foundation	252
1.12.12	Discrete energy method - FEM	265
1.12.13	Finite difference method - FDM	278
1.12.14	FE-linear buckling analysis of columns on elastic foundation	287
1.12.15	Post-buckling analysis of columns on elastic foundation	289
1.12.16	Inelastic buckling of columns	302
1.12.17	Lateral-torsional buckling of beams	303
1.12.18	The energy criterion	305
1.13	Rayleigh-Ritz energy method	317
1.13.1	Complete model when accounting the effects of shear force change during lateral-torsional buckling	324
1.14	Computational stability analysis	329
1.15	Torsional buckling	342
1.15.1	Total potential energy	343
1.16	Stability of plates	360
1.16.1	Some classical cases	368
1.16.2	Post-buckling response of plates	378
1.16.3	Computational example	381

1.16.4	Buckling of rectangular plates under uniform bi-axial loading	386
1.16.5	Buckling of rectangular plates under bi-axial loading	387
1.16.6	Buckling analysis of square and circular plates on elastic foundations	387
1.16.7	Post-buckling analysis of square and circular plates on elastic foundations	388
1.17	Buckling of arches and rings	389
1.18	Stability of cylindrical shells	390
1.18.1	Shells are imperfection-sensitive structures	392
1.18.2	About large-deflection stability equations	396
1.18.3	Energy criteria for stability loss of thin-walled cylindrical shell	401
1.18.4	Cylindrical shells under uniform axial compression . .	405
1.18.5	Finite Element based Linear buckling analysis	418
1.18.6	Finite Element based post-buckling analysis	420
1.19	Stability of cylindrical panels	420
1.20	Advanced computational simulations	420
2	Geometrically non-linear analysis of Frames	425
2.1	First words	425
2.2	Introduction	426
2.3	Combined axial loading and bending	427
2.4	Full non-linear analysis of non-sway frame	427
2.4.1	Buckling of continuous beam-column	428
2.4.2	Buckling of non-sway frame	430
2.5	Upper- and lower bound estimates for the buckling loads . .	431
2.6	Full non-linear analysis of side-sway frame	433
2.6.1	Buckling analysis of side-sway frame	434
3	Torsion of open thin-walled beams	439
3.1	Introduction	439
3.2	The geometry of motion: the value of observation	440
3.2.1	My teaching goal in starting teaching warping	443
3.3	Deplanation – demystifying the warping	444
3.4	Geometry of the motion of points on the cross-section	446
3.5	The sect – $\omega(s)$	447
3.5.1	Normal Stress resultant from Vlasov twist	452
3.5.2	Shear stresses	453
3.5.3	Torsion, Bending and Stretching	453

4 On Euler's Elastica**459**

Dear reader

These notes represents a collection of L^AT_EX-scripted pages are an illustrated version of my personal notes for the purpose of preparation of the course **CIV-E4100 - Stability of Structures** in the department of Civil Engineering and more specifically, static elastic stability of slender structures. These notes are in their raw state and provide as they are for those who want to read them. This is not an obligatory course reading material, and they do no replace good textbooks. However I warmly suggest the students to have, at least, a look to enrich their readings.

I decided to record to share my paper notes after seeing so much teachers starting their course of stability by formulating, first, complex mathematical equations (or/and principles) without showing any physical model to illustrate the phenomenon to be studied and then, claiming that 'the underlying mechanics' is a unavoidable consequence of these equations! Even sometimes, of their own equations! At a general level of fundamental physics, they may be a bit right¹ but at the pedagogical level, they are completely '*à côté de la plaque*'; wrong. This is why, I decided to show in the class, small physical models to illustrate the mechanical behaviour we want to study. Together with students we manipulate them and load them gradually by our hand, observe and feel the sudden transition of equilibrium states in our hands. We can even feel the apparent loss of rigidity at loss of stability of the small reduced structure in our hands. This *critical transition phase* from resistance to no-resistance to additional tiny deformation is what is mathematically mystified as the *loss of positive definiteness of the tangent stiffness matrix*. This is just the *mystical name* for the physical condition for neutral equilibrium to exist. I will never stop *calling a cat,*

¹Validated theories of physics as expressed by mathematics; they capture some *invariant* (like symmetries) properties of the 'reality'. Thus such mathematical theories give us access to remaining invisible part of this 'reality' because of the invariant properties; so we see the missing parts thanks to the general properties of symmetry captured in the mathematics. For instance, the gravitational waves were 'seen' by the mathematics of Einstein's gravitational theory, more than 100 years before they were actually observed.

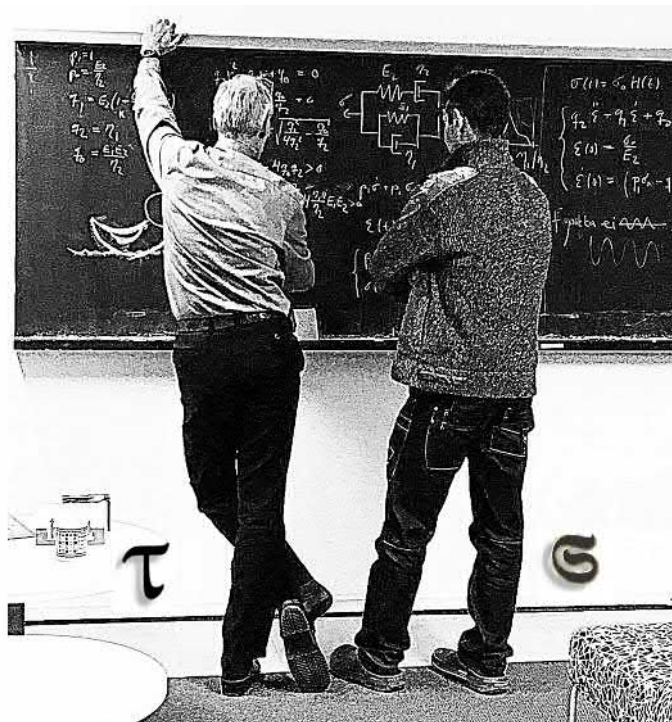
a cat, as French people say. We are ourselves small, but fine mechanical sensing devices. After that physical class experiment, we pose the *question* (physical problem setting). Then I present the physics of the related key phenomenon, as naturally being observed, and then, and only then, we start to formulate mathematical equations (Mathematical problem setting) based on fundamental (general) principles of mechanics already known to the students. Using this general principles, we arrive, mathematically, little by little, to the buckling equations which provides the needed handles to the reader. They will give the critical buckling load and the post-buckling behaviour of the studied structure. After that, we make interpretations of the solutions. This is for my pedagogical method.

Because of the bit chaotic history of these notes, the chronological flow of the presented thoughts may be not enough continuous (not linear) from time-to-time. My thoughts during writing often bifurcate forward and backward, right and left, up and down because *I do not intend to write a book*. Sometimes, when inspiration visits me, I write a bit about dynamical stability, even though this is not the topic of our course. There is plenty of good textbooks on stability, and also, unfortunately, plenty of bad textbooks too. I wanted to make the course more attractive to our engineer-students and not hide behind 'complex-looking' mathematics neither to show how brilliant the writer can be. I wanted also to write these notes as a story (more narrative than written) and best stories are those which are told not necessarily those which are written.

Consequently, this work cannot be complete. By recording my personal study notes, my intention was not to write a textbook on Structural Mechanics. As was said, there is plenty of good textbooks in the air written by legends of Structural Mechanics. My writing here is also intended to illustrate with examples, grasp the relevant physics, and then and only then, write the equations. The aim is to make the field of Structural Mechanics, in general, more attractive to young people and encourage them to read classical and also some 'newer' textbooks, if any.

Related to the language: as my mother-tong is surely not Oxford English, do not expect to read Shakespeare in my sentences. I am writing mostly my non-linear thoughts in my proper English, thus with mistakes in grammar, orthograph and style (as now). I hope this will not add difficulties in reading. These notes are under review by one of my retired and very critical professors, a legend. I will soon account for his comments and the reader will obtain an upgraded version.

Related to non-linearly flowing chapters and thoughts: as I write by



"*Virtaa sittenkin*". The Last Mohicans τ and σ ; Reijo and Djebar (2020, Otaniemi).

inspiration, and inspiration is not very often visiting my office, the reader can find some repetitions or 'hole's in the written text. While some repetitions can be pedagogically helping in learning, others can become annoying for some readers. If you find such, then either learn or skip it. However, I will appreciate if you notice me with that. Also, you can find here and there some small funny things that I hope will not disturb you from the main serious reading. One student once called them *positively distracting*. Sometimes, the writing is a bit boring, so I can make some comments that I usually make during *in-vivo* lectures or exercises sessions with living students long time ago before the BC-IXX century.

The reader is encouraged to give me any feedback leading to enhancing the quality of these lecture notes. Please, your comments and suggestions are needed. Do not keep them for yourself. (many students already provided me feedback and good questions leading to quality enhancing. I have even written new sections to answer them because the some questions shows that I did not wrote enough explicitly or there is something important missing.)

Djebar Baroudi
Otaniemi, 4/02/2021

Chapter 1

Elastic Stability of Structures

1.1 Introduction

The concept of stability is fundamental in all branches of science. In this 'lecture-notes'-looking text, we specifically deal with its applications to static stability of mechanical structures encountered in civil engineering. Such structures can be, for instance, primary or secondary substructures or elements of buildings and constructions including foundations and the supporting soils and ground. The simplest structure can be a column which may buckle under a certain load and loses its apparent rigidity: this is the well-known problem formulated and solved for the first time in the 'mankind' history by **Euler**, the Great.

Dynamic stability is quite a wide subject and it is not the topic of this course despite that *static stability* is simply a special case of dynamic stability.

This concept of *stability* is, as already said above, of *primary importance* since it allows to determine *if an equilibrium position is stable or not* under tiny perturbations. Consequently, quantifying stability provides a powerful tool for structural engineers for robust structural design and reliable control of mechanical structures. Figure (1.1) shows an example of a stability loss in a simple ramp due to overload. The upper chord of the truss buckled and consequently, the structure failed suddenly. No body was injured.¹

Let's explain in few words what does *stability* mean here:

- **Static stability:** (SS) Consider a structure (a system) being *initially*

¹In such case, already a first year master student can exactly determine the maximum allowable load (\approx number of persons) for the structure to not fail in buckling (and also, not fail at all).

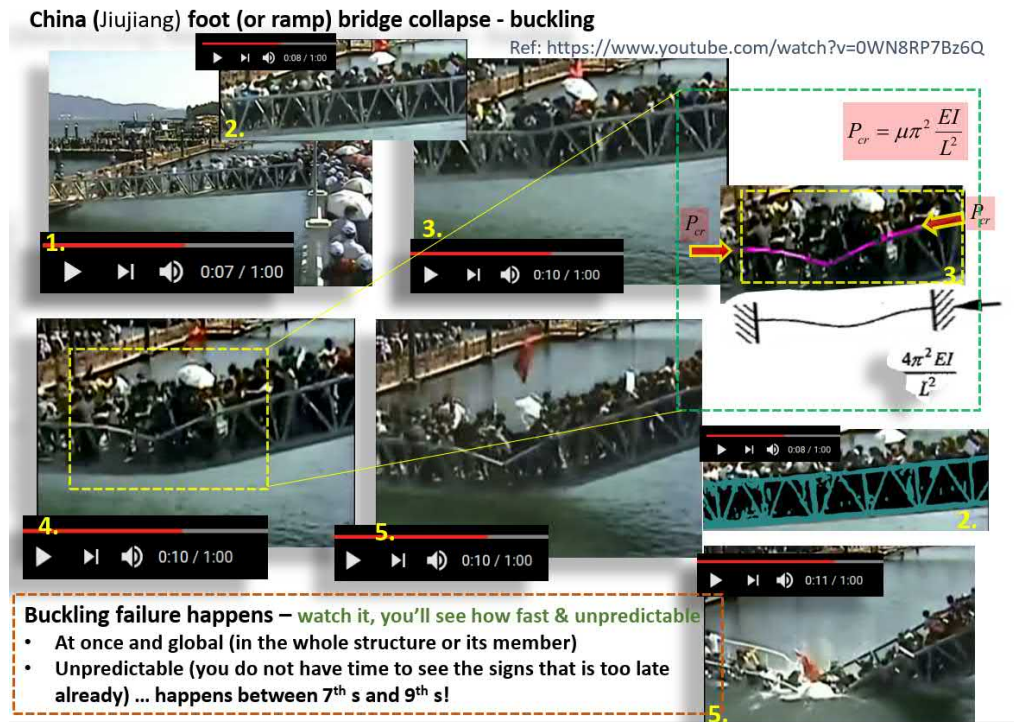


Figure 1.1: Stability loss in a foot ramp due to the simple buckling of the upper cord of the truss.



in equilibrium. We introduce an *arbitrary infinitesimal perturbation* to the system and follow what happens. If for any choice of such arbitrary perturbation, the structure sustains or comes back to its initial equilibrium configuration or very close to it, after disappearance of the perturbation, we say that, the initial equilibrium configuration is *statically stable (SS)* or shortly just *stable*. Otherwise, the equilibrium is *unstable*. Mechanically speaking, the stability loss of structure is seen, on the equilibrium path, as a loss of apparent rigidity or as a its dramatic reduction.

Stability loss or transition from one state to another is dynamic by nature To study *Dynamic stability* one needs tools from *dynamical systems theory* especially, concepts as **Lyapunov** stability. This will not be the topic of this course. We will focus on the study of static stability of structures which will be in itself a challenging course. There will be provided a short section introducing in details this concept after few pages. (For dynamic stability, go and read about **Lyapunov** stability of dynamical systems)

- **Dynamic stability:** *DS* considers the time history of the motion after a tiny perturbation. If the change in amplitude keep not enhanced in time,

after such perturbation, we say that the system is *dynamically stability*.

It is well known that the static stability is a necessary, but not sufficient condition to ensure dynamic stability.

* * *

This introductory course picks a side a bit directed toward structural engineer students. The following specific topics will be addressed: *flexural buckling* (nurjahdus), *lateral-torsional buckling* (kiepahdus), *torsional buckling* (vääntönurjahdus), *buckling of thin plates* and *buckling of cylindrical shells* (levyjen ja kuorten lommahdus). In addition, only slender elastic structures will be considered. This means that, plasticity, visco-elasticity, viscoplasticity and material damage is left outside of this course²

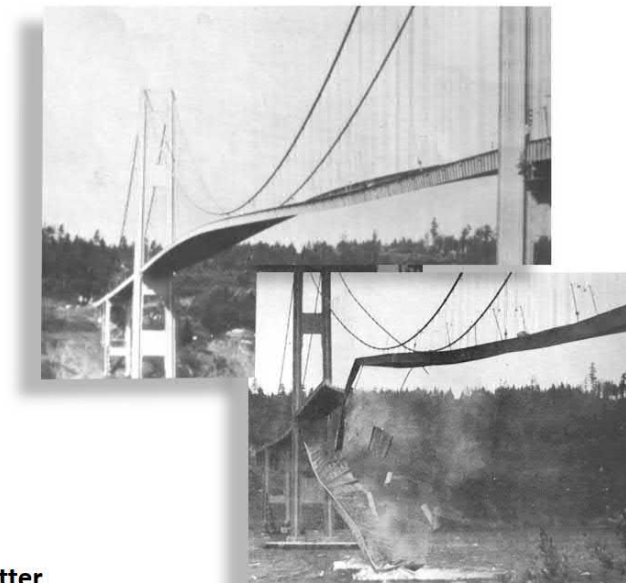
The approach adopted in these lecture notes concentrates both on applying systematically general principles on and the mechanics (=physics) of *loss of stability* phenomena, deriving the *buckling equations* and on providing examples, both analytical and computational FE-based, respectively. I think that such approach is an efficient *method* which enhances deep learning and the self-confidence of the future engineer in that when he uses *Computational tools* he knows exactly what equations and what physics he is solving in his daily work without forgetting that the *last word* is humbly reserved to experimental validation and investigation. This is how should be a *robust engineer* and not a *Robot engine-jööri*.

Central concepts like *Linear buckling analysis*, *post-buckling analysis* and *sensitivity with respect to imperfections* will become familiar as it is introduced through examples.

Let's be clear with the terminology of static and dynamic stability: the stability loss is nothing else than the motion during transition of the structure from one equilibrium state to another one and therefore *stability loss is dynamical* by nature as demonstrated by the extreme and very classical case of the collapse of the Tacoma Narrows Bridge due to dynamical loss of stability (Fig. 1.2). Despite, that, under certain conditions one can recast the problem of stability loss in the statics framework (see footnote bellow). This is specially true for conservative systems. To our chance, the set of conservative systems is huge and covers many key problems of structural analysis. On the other side, the set of non-conservative systems is also huge and of importance even for civil engineers. An example of a set of such systems are dissipative systems (path dependency) (all type of friction, dissipation,

²For those interested in these advanced topics, you can start with the classical textbook by Bazant and Cedolin. *Stability of structures - Elastic, Inelastic, Fracture, and damage theories*. (2003) Dover publications, Inc.

Oscillation and subsequent collapse of the Tacoma Narrows Bridge

**Flutter**

Coupling structure-fluid motion

Bending and torsional modes ... have same frequency

Figure 1.2: Tacoma bridge - failure due to dynamical instability (flutter).

plasticity, visco-plasticity, ...). Dynamical effects, like for instance *flutter* phenomena in bridges (Fig. 1.2), stayed cable wind-induced vibrations, etc. can be such systems (following forces, ...). Naturally, all such problems and many other problems of *stability* must be set as *dynamical problems* to be correctly solved. At the end, loss of stability is a dynamic process.

1.1.1 The big picture - Stabiilius pähkinäkuoressa

For conservative system, the stability analysis reduces to check the *positive definiteness* of the tangential stiffness matrix of the structure thanks to the *Lagrange-Dirichlet stability theorem* (will be given bellow). The total potential energy of the the linearised system is quadratic and the critical load can be determined from the stiffness matrix of the linearised system at points of critical equilibrium. This linearisation leads to the so called *Homogeneous linearised equations of stability* in the form of linearised eigenvalue problem (lineaarinen omiaisarvottehtävä, see section 1.10).

The higher terms than quadratic of the total potential energy change, expressed as a function of some generalised displacements, determine the post-buckling behaviour. The basic types of post-buckling behaviour are

classified as follow (Section 1.6):

- *stable symmetric* - always imperfection insensitive
- *unstable symmetric* - imperfection sensitive
- *unstable asymmetric* - imperfection sensitive (more than in the symmetric unstable case)

Koiter's (1945) power law describes all the initial post-buckling behaviour. According to this famous power law, for all elastic structures with a (tiny) initial imperfection causes a reduction in the maximum load is proportional either to $2/3$ or $1/2$ power of the amplitude of the initial imperfection. This reduction in the maximum load (usually, expressed by a *knock-down factor*) is specially severe in cylindrical shells under axial loading or bending and spherical domes, due to the presence of unavoidable initial imperfection; it goes down to about $1/8$ to $1/3$ of the theoretical critical load of an (imaginary) perfect structure (see sections 1.6, 1.18.1 and 1.18.4). For other structures like elastic frames, the reduction is usually moderate.

Related to elastic frames, Roorda (1971) showed experimentally evidence of asymmetric bifurcation where depending on the 'sign' of the initial eccentricity, the post-buckling behaviour suddenly changes between stable and unstable. As plates have a symmetric post-buckling behaviour in their first mode, they are insensitive to initial inherent imperfections. Adding elastic supports can, for some critical ratio of relative rigidity of the structure and the supports, render the post-buckling behaviour unstable and thus imperfection sensitive like, beams or plates on elastic foundations, for instance (even in the first buckling mode).

1.1.2 Lagrange-Dirichlet stability theorem

On a more general level, we will address stability of *conservative systems*. A global energy approach will be systematically adopted through the use of the *Stability theorem* of **Lagrange-Dirichlet**³.

³*Cf.*, classical textbook by Bazant and Cedolin. *Stability of structures - Elastic, Inelastic, Fracture, and damage theories*. (2003) Dover publications, Inc., for the proof of this theorem. Just consider Lagrange's equations $\partial L/\partial q_i - d/dt(\partial L/\partial \dot{q}_i) = 0$, for conservative systems, and set the velocities \dot{u} and accelerations \ddot{u} to zero in them because of equilibrium, and you obtain as a consequence, the stationarity (the minimum condition) of potential energy at equilibrium $\delta(\Delta\Pi) = 0$, automatically. The Lagrangian is defined $L = T - V$, where T being the kinetic energy and V the potential energy of the system ($V = \Pi$, the total potential energy, for conservative systems). ($u = q$).

Lagrange-Dirichlet Theorem: Assuming the continuity of the total potential energy, the equilibrium of a system containing only conservative and dissipative forces is stable if the total potential energy of the system has a strict minimum or in other words is positive-definite.



Lagrange



Dirichlet

Trust us, we are not politicians.

The above theorem is a *global energy criterion* for stability. We will use systematically to derive all the equations of (loss) of stability we need for any arbitrary elastic structure. The limit state of stability (stability loss, Figure 1.3) will be identified by the transition condition between *stable* and *unstable* states and which corresponds to the *neutral* equilibrium condition⁴ for which the total potential energy becomes *indefinite* (i.e., generically, we have $\Pi''(u; P) = 0$ or more generally, $\delta(\Delta\Pi) = 0$, where $\Delta(\Pi)$ being the increment in total potential energy).

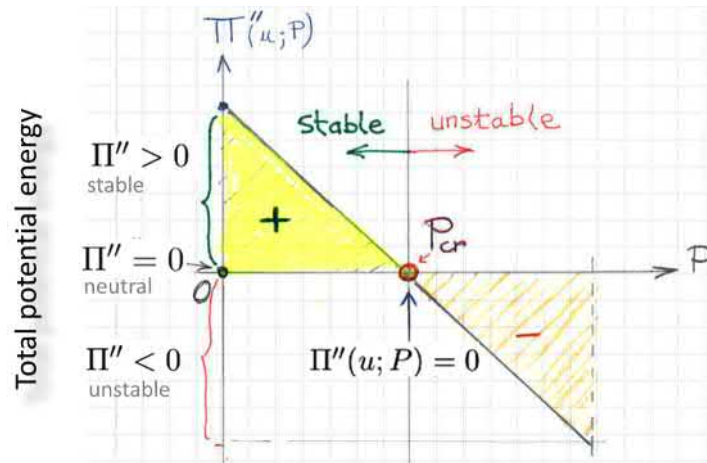


Figure 1.3: Generic illustration of the energy criterion defining stable and unstable ranges for some elastic structure. The loading P being the control parameter. The kinematics of the system is defined by u . The transition of the system between stable and unstable state occurs at the critical load P_{cr} for which a neutral equilibrium is attained when $\Pi'' = 0$; i.e., equivalently when $\delta(\Delta\Pi) = 0$, where $\Delta\Pi$ being the change in total potential energy between initial equilibrium state and the (buckled) adjacent equilibrium state.

The *stability* condition - *positive-definiteness* - for the total potential energy $\Pi(u)$ means generically that its second derivative $\Pi'' > 0$ with respect to the

⁴Also called, *criticality* condition.

kinematic variables u of the system has to be positive at these *equilibrium points* (local extrema points). Consequently, *instability* of an equilibrium corresponds to the condition $\Pi'' < 0$, respectively. So, to resume,

$$\begin{cases} \Pi'' > 0, & \text{stable,} \\ \Pi'' = 0, & \text{neutral,} \\ \Pi'' < 0, & \text{unstable.} \end{cases} \quad (1.1)$$

The derivatives are the so called generalised derivatives and will be defined later in terms of variations⁵ for continuous and discrete systems.

About the energy criteria in the form $\delta(\Delta\Pi) = 0$

I hope to clarify the notations, for total potential energy change $\Delta\Pi$ that I will use thorough these lectures-like notes. We think that first, the system is, under loading, in an initial equilibrium state (or configuration) corresponding to the total potential energy Π_0 . Often this initial state is called *initial pre-buckled state*. Now the stability of such equilibrium state is investigated by perturbing it a bit in some manner and keeping the loading unchanged. The system in the perturbed state obtains an increment $\Delta\Pi$ of the total potential energy. Therefore, *the total potential energy* of the system in the new perturbed, *post-buckled state*, is simply

$$\Pi = \Pi_0 + \Delta\Pi. \quad (1.2)$$

Now the question to pose is: *is the perturbed state an equilibrium state* or not? If the answer is yes, then the system can find another equilibrium configuration *close* to the initial one. This close equilibrium is called *adjacent equilibrium state* and since it is an equilibrium state, by definition, then we have $\delta\Pi = 0$. Therefore, the stability loss, which corresponds to the transition between these two states can be formulated, physically, as *the condition of existence for such adjacent of far equilibrium* configuration where the system can via a tiny perturbation can move without increase

⁵Even these variation of total potential energy can be recast as simple one-variable derivative with respect to a scalar parameter ϵ , their meaning is different from derivatives of functions. The total potential energy is a functional; a function of a function. The meaning given by Lagrange is the correct one. Not because the pixels of the image of a flower can be coded (described mathematically) by integers (0..255), one can claim that the flower is just a collection of structured integers. The same thought holds between the meaning of variation of a functional and the derivative of a function. Not because such variation can be described by a one-variable simple derivative that it becomes this simple derivative. Do not worry about this comment, it is more meant as an answer for a colleague.

of loading. This condition holds also to identify the existence of even *far equilibrium configurations* such the one reached after a *snap-through* like stability loss. In this cases, the condition identify what are called, on the load-displacement diagrams, *limit points*. This condition is mathematically written as is simply

$$\delta\Pi = \underbrace{\delta\Pi_0}_{=0, \text{ initial equilibrium}} + \delta(\Delta\Pi) = 0, \quad \forall \text{ perturbation } \delta v \quad (1.3)$$

$$\implies \delta(\Delta\Pi) = 0 \quad \text{at buckling}, \quad \forall \delta v \quad (1.4)$$

Consequently, the condition

$$\boxed{\text{At buckling } \delta(\Delta\Pi) = 0, \quad \forall \delta v} \quad (1.5)$$

as expressed by Equation (1.872), is the critical buckling condition. It is also called, equivalently, *condition for neutral equilibrium* to exist. At the end, it expresses the stationarity of the change of total potential energy as said by the Lagrange-Dirichlet theorem.

I prefer to work directly with the increment of the total potential energy to avoid extra 'ramifications' with extra terms related to the initial state while deriving the buckling equations, in general. So, in these notes we use the notation $\delta(\Delta\Pi) = 0$, where $\Delta\Pi$ being the change in total potential energy between initial equilibrium state and the (buckled) adjacent equilibrium state. This stability loss is often referred as *bifurcational*. We will come back to this concept while dealing with equilibrium paths and equilibrium points. It worth to tell that the above condition for neutral equilibrium holds and remain valid even to identify non-adjacent equilibrium state; *far equilibrium configurations* like those encountered in snap-through like stability loss. In this cases, the condition identify what are called, on the load-displacement diagrams, *limit points*.

* * *

About Hessians, quadratic form and stability

For discontinuous systems with N configuration degrees of freedom⁶ $\mathbf{q} = [q_1, q_2, \dots, q_N]^T$, the second derivative $\Pi'' \sim \mathbf{H}$ is simpler, and is simply the Hessian \mathbf{H} of Π at \mathbf{q}^0 , the initial equilibrium configuration. For instance for a quadratic form, the Hessian \mathbf{H} of Π defined as the coefficient matrix

$$\mathbf{H}_{i,j} = \frac{\partial^2 \Pi}{\partial q_i \partial q_j}. \quad (1.6)$$

⁶Lagrange coordinates.

In general, the leading terms (in amplitude) of the Taylor expansion of the total potential energy

$$\Pi(\underbrace{\mathbf{q}^0 + \delta\mathbf{q}}_{\mathbf{q}}) = \Pi(\mathbf{q}^0) + \sum_{i=1}^N \frac{\partial \Pi}{\partial q_i} \Big|_{\mathbf{q}^0} \cdot \delta q_i + \frac{1}{2!} \sum_{i,j=1}^N \underbrace{\frac{\partial^2 \Pi}{\partial q_i \partial q_j} \Big|_{\mathbf{q}^0}}_{\equiv \mathbf{H}(\mathbf{q}^0)} \cdot \delta q_i \delta q_j + \dots \quad (1.7)$$

$$\approx \Pi(\mathbf{q}^0) + \underbrace{\left[\frac{\nabla \Pi(\mathbf{q}^0)}{\equiv \delta \Pi} \right]^T}_{=0, \text{ equilibrium}} \delta \mathbf{q} + \underbrace{\frac{1}{2!} \delta \mathbf{q}^T [\mathbf{H}(\mathbf{q}^0)] \delta \mathbf{q}}_{\equiv \delta^2 \Pi} + \mathcal{O}(\|\delta \mathbf{q}\|^3), \quad (1.8)$$

where $\delta \mathbf{q}$ (or equivalently $\Delta \mathbf{q}$) being an infinitesimal increment, is a quadratic form in \mathbf{q} . In such cases, the stability of equilibrium can be accessed through the sign of the Hessian (the determinant of the Hessian matrix) or equivalently the sign of the second variation $\delta^2 \Pi(\mathbf{q}^0)$ of the total potential energy increment (Trefftz). Loss of stability occurs when the determinant vanishes (the Hessian matrix becomes singular). Stability is therefore determined by the sign of this Hessian which is also called *stability matrix*. If positive then stability is ensured, if negative then no. The sign of the Hessian (the determinant) is given also by the product of its eigenvalues. Note, for the moment, that the expression for the leading term in the change in total potential energy is

$$\Delta \Pi = \delta^2 \Pi + \mathcal{O}(\|\delta \mathbf{q}\|^3) \sim \frac{1}{2!} \delta \mathbf{q}^T [\mathbf{H}(\mathbf{q}^0)] \delta \mathbf{q} \quad (1.9)$$

at equilibrium ($\delta \Pi = 0$). Just keep in mind how it looks like, no worry for the moment. Let go back to our introductory generic story on the *loss of stability criterion*.

* * *

So, the sign of the second derivative of the total potential energy permits to study the stability of structures. For instance, the sign of the second derivative $\Pi''(u)$ can be in particular⁷ accessed in terms of the sign of the second variation $\delta^2 \Pi(u)$. Note that, here Π is the increment¹ $\Delta \Pi$ of the total potential energy. This last condition of neutral equilibrium ($\delta^2 \Pi(u) = 0$) is known as the **Trefftz** condition for stability of an equilibrium:

$$\begin{cases} \delta^2 \Pi(u) > 0, & \text{stable,} \\ \delta^2 \Pi(u) = 0, & \text{neutral, (Trefftz criterion of stability loss)} \\ \delta^2 \Pi(u) < 0, & \text{unstable.} \end{cases} \quad (1.10)$$

⁷as a special case of the Lagrange-Dirichlet theorem where the total potential energy increment being expanded up-to its quadratic terms.



Loss of stability of a column. Original temporary reinforcement method.

¹ Very often the symbol Δ for increment or change is dropped to lighten the writing and to confuse readers.

However, the sign of the increment $\Delta\Pi$ of total potential energy between to equilibrium states is a more general form of the stability condition. What to do when $\delta^2\Pi(u) \equiv 0$? The Trefftz condition remains silent. Therefore, we will prefer to use directly *Lagrange-Dirichlet theorem* and investigate the sign of the increment

$$\Delta\Pi = \delta\Pi + \delta^2\Pi + \delta^3\Pi + \delta^4\Pi + \dots \quad (1.11)$$

to resolve the stability question. So, for instance, here, the sign $\delta^3\Pi$, when non-null, will resolve the stability question. Otherwise, one takes higher and higher terms to find out.

Before leaving this introductory paragraph, let recall that the *Lagrange-Dirichlet stability theorem* mathematises the fundamental concept of *minimum total potential energy principle* known from physics. This *general principle* says:

A conservative system deforms or moves to an equilibrium configuration which makes its total potential energy stationary, and additionally, the equilibrium is stable if the extremum corresponds to a local minimum.

In this transition toward new configuration, the total potential energy decreases and the loss being evacuated from the system in form of kinetic energy and heat. The development of this principle took hundreds and hundreds of years from the humanity to crystallise it into *the theorem*.

Grasp the big picture

Thorough the text of this lecture notes, you will meet a general concepts called *energy stability criteria* in the **Brian**, *Timoshenko* or *Euler* forms, etc. All these *appellations* are nothing else than direct applications of the *Lagrange-Dirichlet theorem*. People likes giving thousands names for the thing they love.

Can a structural engineer seriously use a *mathematical theorem* to design a mechanical structure? Are you joking? Aren't the *Eurocodes* more powerful for that? These are natural questions coming to mind. Yes, you can make more serious and robust structural design when you rely also on a *theorem* and experiments, and consequently, the robustness of the engineer itself grows. Experiments are used both for validation of models and to uncover the behaviour of the structure or its elements, joints, etc.

Assume we are interested to find just the buckling load of a specific structure. So, our interest is to answer the question under which lowest load

the structure equilibrium loses its stability (bifurcation, or limit-point)? In these cases, the above stability criteria, or more specifically, the *Lagrange-Dirichlet*⁸ theorem will be the correct tool. For that, it is enough to expand the total potential energy increment up to quadratic terms in the kinematics. Applying the criticality condition for neutral equilibrium, one obtains a set of homogeneous linear equations (they are often in form of partial-differential equation) forming an *eigenvalue* problem. This process is called *linearisation*. The solution of such linearised problem provides the *buckling load* and the corresponding *buckling mode* and higher modes. In addition, the stability condition, sign of Π'' , can be used to determine the nature of stability of the primary (initial) equilibrium branch which now the buckling load (bifurcation point) divides into two parts.

No other information of what happens after the buckling point can be extracted. *How large are the buckling displacements? What is the post-buckled configuration? Is it stable or not?*

The above questions remain without answer because the linearised equations have lost all these information. The amplitude of the buckling shape remains indeterminate. This procedure is known as *linear buckling analysis*. In order to obtain further information on the properties of the system at the buckling point (bifurcation or limit-point) and to characterise the post-buckling behaviour, one needs to account for higher terms than quadratic ones in the expansion of the total potential energy increment. This type of analysis is termed my *post-buckling analysis*.

We will come to all this and that in details and with examples in the dedicated parts of this notes. For the moment, try to get the *big picture* and not its pixels.

Here the content of this course in four points through questions that will be addressed:

1. can we predict the buckling (critical) load?
2. what happens at the bifurcation (or limit) point?
(*i.e.*, after the buckling)
3. can we determine the post-critical branches?
What would be their shape? Nature of stability?

⁸This theorem holds only for conservative systems. However, the set of conservative systems of practical engineering interest is almost infinite. For non-conservative systems, we will adopt the dynamical approach and write directly the motion equations of dynamics and check for stability of the equilibrium in the time-evolution meaning (dynamic stability). This last approach is versatile and contains, naturally, also the conservative systems.

4. what imperfection-sensitive is the structure under study?

1.2 Structural design and stability

Structures are more and more designed to be lighter and thinner with using high-strength materials. This tendency can be seen as a consequence of aiming to reduce structural weight leading to economic saving at all levels, in fabrication, construction and service life. In analysing such 'slender' structures, *linear analysis* become inadequate even in the material elastic range. For instance, an axially loaded cylindrical thin shell behaves in a non-linear manner and can suddenly lose its load-bearing capacity even if its constituting material being still deforming within the elastic range. Such behaviour is characteristically *non-linear*, even more, *geometrically non-linear*. Such 'slender' structures are sensitive to imperfections. Therefore, for such 'slender' and 'thin' structures, this non-linear behaviour should be analysed to achieve a reliable and robust design. It is the *stability* and the *post-buckling analysis* (or equivalently, the general non-linear analysis) which permits to analysis such non-linear behaviour.

The idea of *Loss of Stability* as a *concept* and a phenomenon (Fig. 1.4) is introduced and clarified in subsequent section of this chapter. Later, examples from structures of civil engineering will analysed. Let's exercise some *reverse Polish logic* and introduce first some intuitive understanding of such stability phenomenon. Here we focus mainly on the stability of elastic solid structures of use in civil Engineering.

Mechanics⁹ is the science investigating the motion of systems under the various loading or imposed displacements. In statics we focus on the *equilibrium states*. One main goal of theory of *stability* is to study under what conditions a motion or an equilibrium state is *stable* or *unstable*. Figure (1.15) demonstrate in images the key concept of stability of equilibrium. *Primarily important is equilibrium, vital is it's stability.*

However, restricting ourselves to determine only the *stability limit* through study of neutral equilibrium state (loss of stability condition), provides us with an incomplete map¹⁰, (Figure 1.5) and (Fig. 1.6),

⁹As an example of celebrities from this discipline, let's cite few 'people' names like **Galileo**, **Newton** and **Einstein**.

¹⁰In the form of the solution of an eigenvalue problem rising from linearisation, close to the critical point, of the full non-linear equations of equilibrium. The smallest eigenvalue corresponds to the buckling load λ_{cr} and the corresponding Eigen-vector \mathbf{v}_{cr} gives the buckling mode up-to a multiplicative coefficient. So, in the figurative talk, I had,

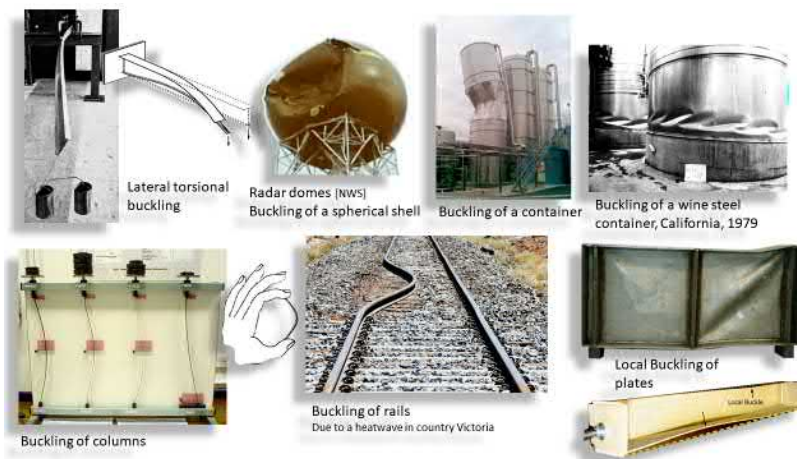


Figure 1.4: Examples of various types of loss of stability in simple structures. From left to right: lateral-torsional buckling, buckling of spherical and cylindrical shells, buckling of slender columns, buckling of a rail-road rail bonded to a support and plate buckling represented by shear buckling of the flanges and compressive buckling of web.

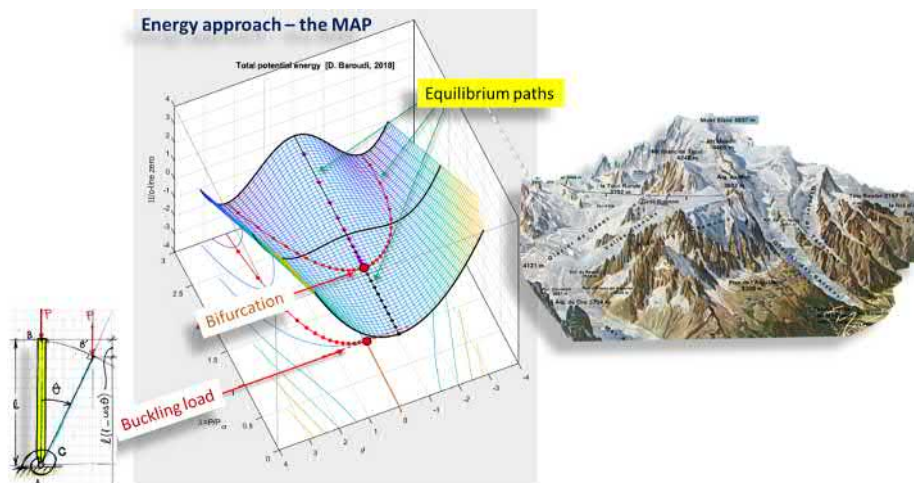


Figure 1.5: *Map* of total potential energy $\Delta\Pi$ of an elastic structure. Equilibrium paths corresponds to locations where $\delta(\Delta\Pi) = 0$ while keeping P constant. Stable equilibrium is achieved there where $\delta^2(\Delta\Pi) > 0$. Note the analogy with the topographical map of piece of Chamonix (Alpes).

the point P on the map corresponds to the pair $P(\lambda_{cr}, \mathbf{v}_{cr})$, so an entire surrounding *topography* remains invisible.

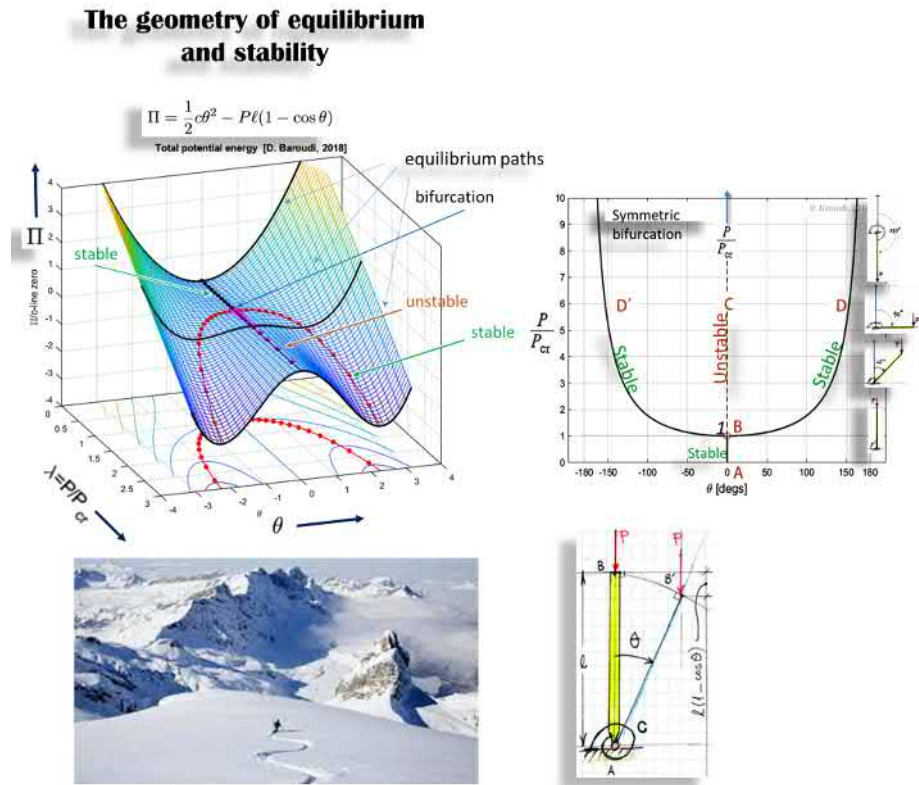


Figure 1.6: 'Topographical Map' of the total potential energy $\Delta\Pi$. Geometry of equilibria and stability.

having only *one single and only one* point on it: the *bifurcation*¹¹ or *limit point*¹². The missing entire 'topography' on the map will be provided by the *post-buckling*¹³ analysis and which will provides the designer or the analyst the relevant post-buckling behaviour of the structure. Knowing the nature of such post-critical behaviour (stable, unstable) enhances the *ro-*

¹¹At a bifurcation point, appearance of new one or more neighbouring equilibrium state for the same load, occurs. So, solution *branching* takes place.

¹²At a limit point, no branching occurs, on the equilibrium-paths, beyond this critical point, the *initial equilibrium* becomes unstable.

¹³Let's demystify the 'label' *post-buckling analysis*. Generally speaking, such analysis is simply a *non-linear analysis* which can have both geometrical and/or material nonlinearities, with the specific purpose to investigate the pre- and post-buckling behaviour of the structure while introducing arbitrary small perturbations to the initial state. So, what structural engineers call *post-buckling analysis* is a specialised sub-class of the more general *non-linear analysis* class. Post-buckling analysis is a special kind of sensitivity analysis with respect to perturbations in material properties, geometry and loads as deviations from the perfect design.

*bustness*¹⁴ and *safety* of the structural design by addressing sensitivity of the design with respect to *inherent imperfections*¹⁵ and also allow the designer to *quantify the buckling deformations* resulting from limit or buckling load within a certain range of possible loading increase¹⁶. Such excessive 'buckling deformations' or more exactly non-linear effects in displacements and rotations¹⁷ can consequently destroy joints of the buckling sub-structure to subsequent structures and results in serious collapse, even when the post-buckling behaviour being stable (Figure 1.8).

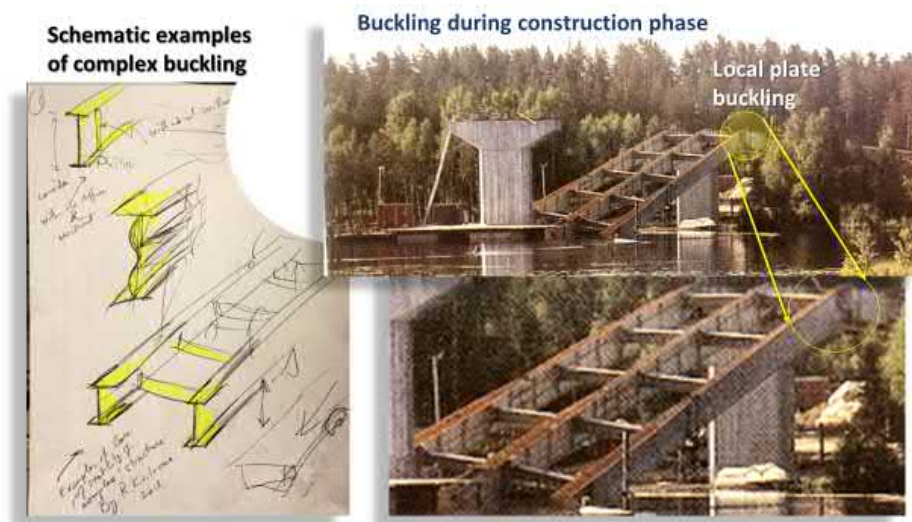


Figure 1.7: Loss of stability more complex structures (refs: left - drawings by Dr. R. **Kiviluoma**, right - flyer of *Rakenteiden mekaniikan seura*).

Let's put the above ideas in pictures: finding the bifurcation or limit point and consequently, the critical load, corresponds to discover the tiny (10%) visible tip of an iceberg. Linear buckling analysis give you access to

¹⁴Robust design "makes the structure's or product's performance insensitive to (inherent) variations in material, geometry, manufacture and operating environment", (Phadke, 1989 or later). I can add that *robust design* is a *stable design*, and *robustness* is conceptually the same as *stability* of the structure under 'all' inherent perturbations (noise) that indeed we can only quantify probabilistically. These inherent perturbations can be qualified by *noise*. For those interested in reading, you can consult the book: M. S. **Phadke**. *Quality Engineering Using Robust Design*. Prentice Hall PTR, 1995.

¹⁵*It may be safely said that all real structural systems are imperfect in form, imperfect in material properties, imperfect in the sense of residual stresses and imperfect in the way the loads are applied.* **Roorda** (1980)

¹⁶When the post-buckling behaviour is stable

¹⁷Better known to engineers as *second order effects*. In such popular language remains ambiguous what is of second-order and compared to what.

such tip and only to it. What remains unseen, through the linear buckling analysis, is the huge underwater (90%) hidden part of the iceberg which can be only reached by post-buckling analysis.

In short a correct design against stability aspects will be such 1) collapse of the structural components or the structure resulting from *buckling* will not occur at design loads, neither 2) will the *buckling deformations* will be so large to damage or render components, their parts or nearby components non-functional. Both design aspects are addressed through 1) *buckling* and 2) *post-buckling analysis*, for the first design criteria and second one, respectively.

One of the challenges is to quantify and account for the *inherent imperfections* in the real structure a which deviates from the idealised *planned, manufactured and designed* one , in order to achieve *robustness* of the final engineering product. Good engineering final result should always provide the product itself together with a *quantified safety margin* of it operation.

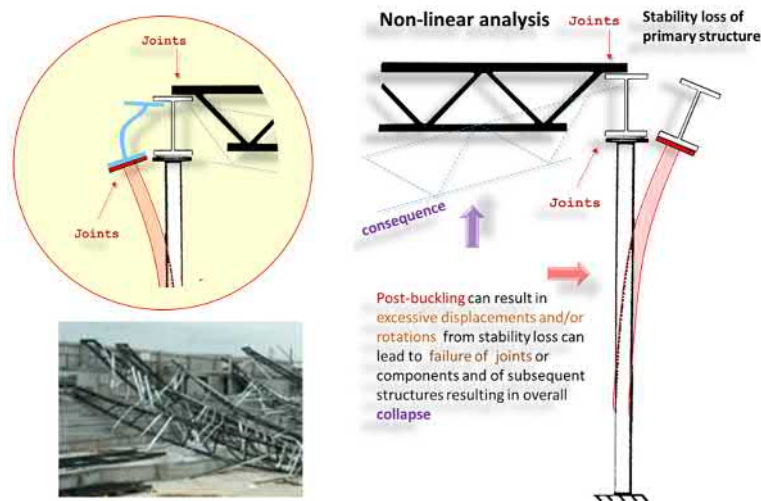


Figure 1.8: Illustration of possible consequence of too large rotations or displacements after stability loss.

On the other hand, when performing structural design, often *static stability analysis* sufficient for many design purposes (when the knowledge of critical load is sufficient). In such analysis, the study of stability of equilibrium state is enough since the designer wants to avoid the very first occurrence of loss of stability. This being said, knowing the post-buckling behaviour a the structure under design may be vital when accessing robustness (read: *safety*). This is because the type of stability the structure

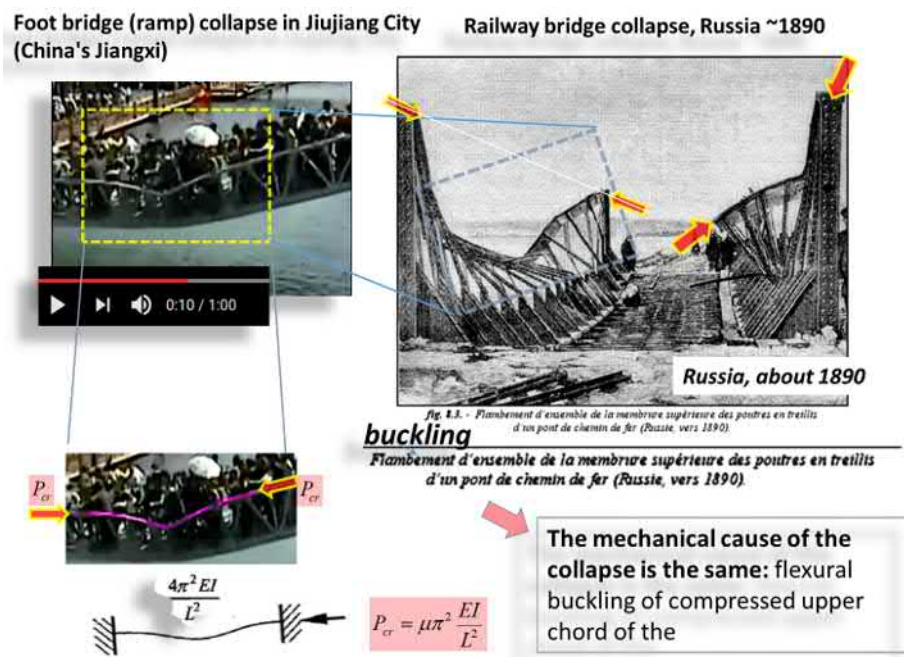


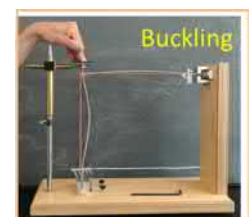
Figure 1.9: Accidents: Loss of stability.

have after buckling, *stable* or *unstable*, determines how safely it is sensitive to inherent imperfections and other perturbations. When the post-buckling behaviour is stable, the structure is not sensitive to small imperfections (safe behaviour). On the contrary, it becomes sensitive to imperfection (unsafe behaviour) when post-buckling is unstable.

However, in many other situations (aeroplane, rockets, rotor dynamics, structures under some special dynamic loading, etc.), one should consider the *dynamic nature of stability* (dynamic stability) to resolve stability issues. In Figure (1.10) a simple case of dynamic buckling of a column is reproduced for illustration purposes only. In short, this course, quantifies the behaviour depicted in the three consecutive images: *initial stress-free state*, *pre-buckling state* and *buckled state* by answering the question: "What is the general (or invariant) condition for the transition¹⁸ between pre-buckling state to buckled state for any arbitrary elastic structure?" Naturally, some other aspects will be also studied.

In structural analysis we study the stability of various type of structures

¹⁸Such transition is called a bifurcation and is possible only for perfect structures. For instance, when a column eccentrically loaded, it start directly to have a flexural mode, in addition to the compressive one. So, the bifurcation will not exist as such. In other cases of practical importance, the loss of stability occurs through a limit points. (we will come back to these basic concepts in details.)



Frame Buckling.

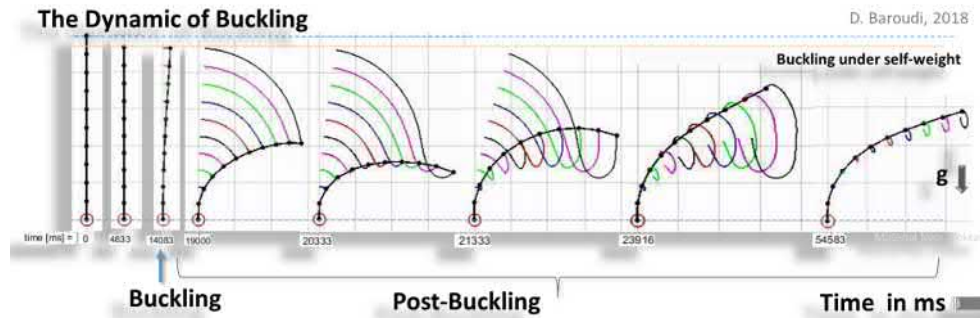


Figure 1.10: Example of dynamic behaviour of a column buckling under its self-weight. Numerical simulation using discrete Hencky-type chain model.

as, for instance, rods, beams, plates and shell. For instance, stability issues are critical in design of steel structures since, by definition, steel structural elements are usually slender and thin. The number of standards (Figure 1.11) related to stability issues in design of steel and wooden structures remind us of their importance.

For instance, the standard EN 1993-1-6 is completely dedicated to structural design and analysis issues of shells and shell-structures. This is because, these type of structures are known to be highly imperfection-sensitive and thus their stability issues and non-linear behaviour with and without imperfections is crucial and should be accounted for in design and analysis. When, in addition to geometrically non-linear behaviour, the *material non-linearity* is involved in the above analysis, the increase in complexity of the problem make the computational and experimental approaches the only feasible and practical way to have useful quantitative answer on actual loading capacity or limiting displacement response.

Material non-linearity cannot be avoided because when structure or its parts starts to have large displacements and rotations. In these cases, the material behaviour becomes non-linear and such phenomena as local damage, delamination, plasticity, with small or large deformations, viscoplasticity, partial contact regions, local friction, . . .) become determinant in the overall behaviour. In such cases, the physics becomes dissipative. There is also other additional complexity rising from complex geometry, presence of stiffeners, holes, supports, junctions, etc. which are, in practice, impossible to tackle analytically to obtain reliable quantities. However, qualitatively, analytical approach provides the concepts and handles in terms of the non-dimensional products (variables) of the problem. In many practical cases, isotropy is the exception and engineers love to uses materials or composite-materials with sub-structures. Examples can be cases including

anisotropic plates or laminates, laminated skew plates, fibre-reinforced composite laminates and so on. So, *Niet Scape*¹⁹ for the need of computational tools.

The system described above is not no any more a conservative and thus *static equilibrium* framework becomes invalid. Therefore, *path-dependence* dependency and inertia forces have to included. In one word: it is now time *do a non-linear dynamic analysis*.

This being said, the knowledge of theoretical fundamentals and underlying theories become even more crucial for doing reliable and responsible structural design. This first master course is dealing with *elastic stability*, only. So, in the following, the structure are all assumed made of elastic material.



Post-buckling of shells

Example of non-linearities: material and geometrical, large plastic deformations, contact with friction, ...

Standards: design of steel structures

- Local buckling EN 1993-1-5
- Flexural buckling EN 1993-1-1 hot rolled columns
- Lateral torsional buckling EN 1993-1-1 beams
- Lateral

- Flexural torsional buckling
- Local-global EN 1993-1-3
- Distortional EN 1993-1-5
- Shear buckling

- Shell buckling EN 1993-1-6
 - Linear elastic Bifurcation Analysis (LBA) (= linear buckling analysis)
 - Geometrically Non-linear Analysis (GNA)
 - Geometrically Non-linear Analysis with Imperfections
 - ... LA , LBA , GNA , GNIA, ... (= post-buckling analysis for perfect structure and structure with imperfections)

Standards: design of wood structures

- Stability issues & imperfections EN 1995-1-1

Standards: design of concrete structures

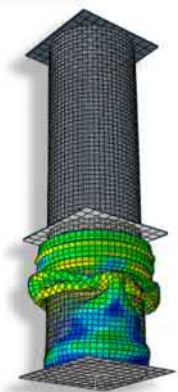
- Sect. 5.8 Second order effects with axial load..... EN 1992-1-1

Figure 1.11: Some standards related to stability issues in structural design.

Note that, in the assumed 'planar' arch (Figure 1.12), the out-of-plane motion should be prevented or the 3D stability behaviour should be anal-

¹⁹Old web browser. Here, I am playing with words, as I recall the saying of one of my Russian ex-colleague: "*NiET Scape*" he was saying for the browser name *Netscape*. In Russian language *NET* means nay or simple no. here I used in the meaning that we have no other option beside the experimental approach.

Mild-steel tube crash simulation (Abaqus/Explicit) [D. Baroudi, 2019]



Simulation: material and geometrical non-linearities and time-dependency.

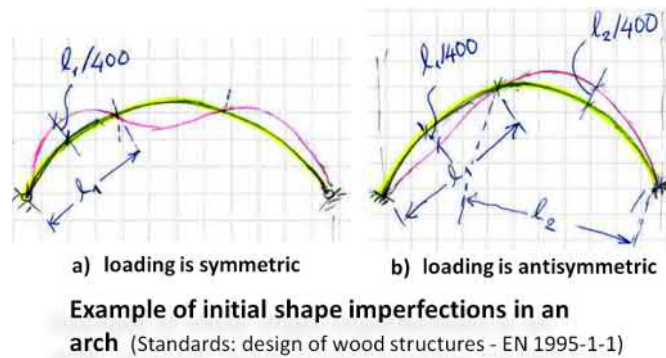


Figure 1.12: Example of initial shape imperfections (muotovirheet) in wooden arches to be accounted in the structural analysis. The geometric imperfection can be introduced into the non-linear analysis as linear combination of first buckling modes of the structure with amplitudes quantifying the discrepancy between planned and realised geometry. a) represents a symmetric imperfection mode and b) anti-symmetrical one.

used too. However, it may be easier to prevent the out-of-plane motion by additional supports.

Of course, depending on the complexity of the structure under consideration and on the material behaviour, computational approach may be the only feasible approach. However, understanding the underlying theory is necessary. Even when doing computational stability analysis one should understand what are the key content of such analysis: determination of the critical load and the sensitivity analysis with respect to imperfections (geometry, load eccentricities, ...). In other words, *How much the loading capacity or critical load will be decreased by the effect of such imperfections when compared to the mechanical response of the ideally perfect structure.*

Figure (1.12) shows an example of proposed initial shape imperfections (Standard EN-1995-1-1) for wooden arches to be accounted for in the structural analysis and in the *geometrically non-linear analysis*. Figure (1.13) reproduces a slide from my lectures-notes illustrating the basic difference between linear buckling and non-linear (buckling) analysis (GNA).

There is also other geometrical imperfections²⁰ to be quantified and accounted for and which come from the geometrical tolerances in the initial non-mounted structural members and connections, and additional tolerances resulting from mounting the structure.

On the subject of geometrical non-linear analysis, more will be told in

²⁰Muotovirheet (sf).

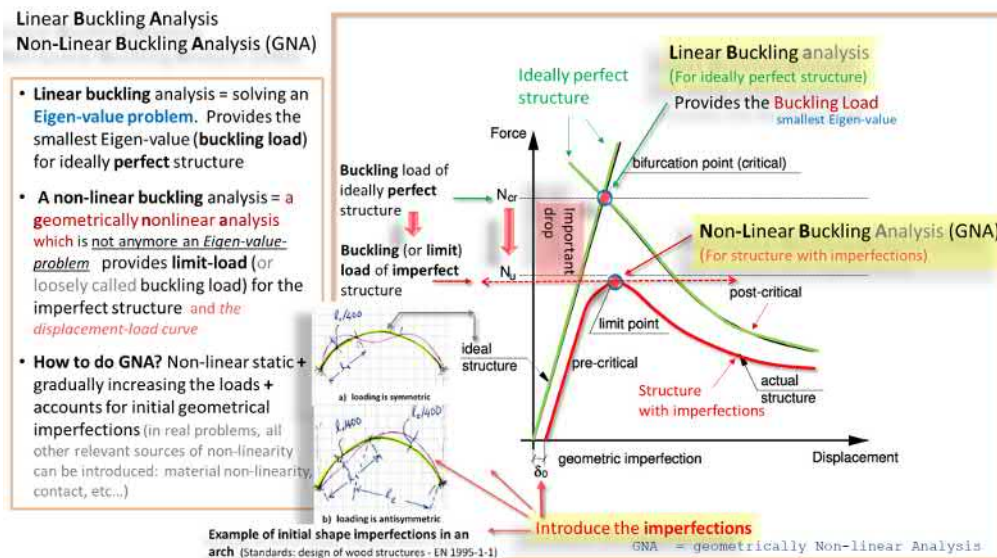


Figure 1.13: Illustration of the basic difference between Linear and non-linear buckling analysis (GNA).

coming sections. Now back to basics, first.

In such structures, the stability loss has the next terminology which corresponds also to engineering names for the macroscopic structural instability 'phenomena' (Fig. 1.14).

- Flexural buckling (nurjahdus)
- Lateral-torsional buckling (kiepahdus)
- Torsional buckling (vääntönurjahdus)
- plate and shell buckling (lommahdus)

In the following, we introduce the concepts of *static stability of conservative systems* through simplified illustrative example of a rigid ball in gravitational field with constraint to move on the ground (yellow in the Figure) without interpenetration. Note that, the following concepts are general and independent on the complexity of the structure under consideration. There exist three different types of equilibrium: *stable*, *unstable* and *indifferent (neutral)* (Figure in margin).

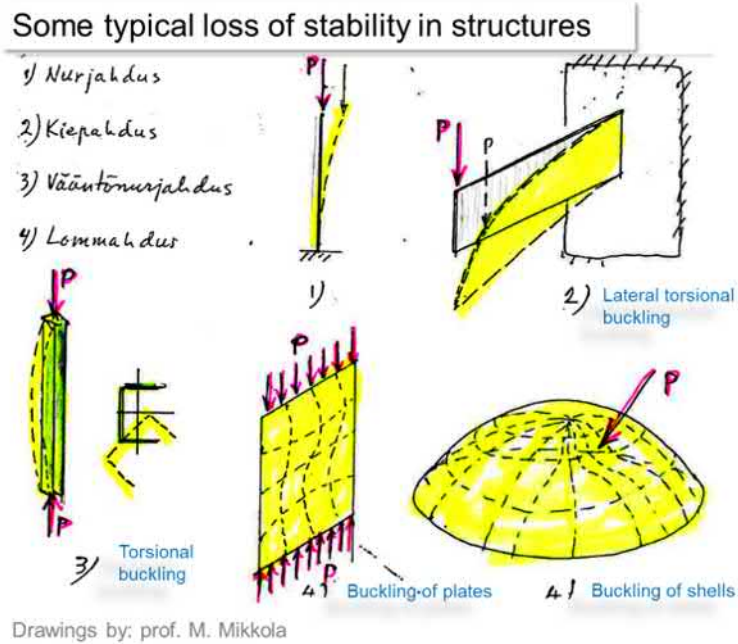


Figure 1.14: Typical instabilities in structures. (Figure adapted from BW-drawings in lecture notes by Emer. prof. Martti Mikkola.)

1.3 Basic concepts

The main idea is to make the study of stability in terms of general variational calculus applicable to the more general case of continuous cases where the displacements $\mathbf{u}(x_1, x_2, x_3)$ are continuous functions instead of a finite number of scalar kinematic variables. For the scalar case one can directly use the derivatives instead of variation and obtain the sign of Π'' deciding for the stability. Let's illustrate these three forms²¹ of equilibrium by considering *intuitively*²² the *initial equilibrium* of the ball in the following three cases: The shape of the surface on which the ball is moving is given by the graph $y = y(x)$, where the initial position of equilibrium is $x_0 = 0$. The equilibrium points for which one investigates the nature of stability are called *critical points*.

- perturbing a bit the initial equilibrium by displacing slightly the ball

²¹Nature of equilibrium - Tasapainon laatu (Finnish)

²²We have such a perfect and correct intuition which is educated by daily experiencing mechanics since we are ourselves macro-mechanical living devices mechanically interacting with our surrounding. Further, however, the type or nature of equilibrium will be investigated using the language of mathematics since we are engineers and such language is quantitative.



Three various types of equilibrium configurations.

on the *convex* surface (valley). Intuitively, we know that it will return to its original position after removing the disturbance. Such equilibrium is called *stable*.

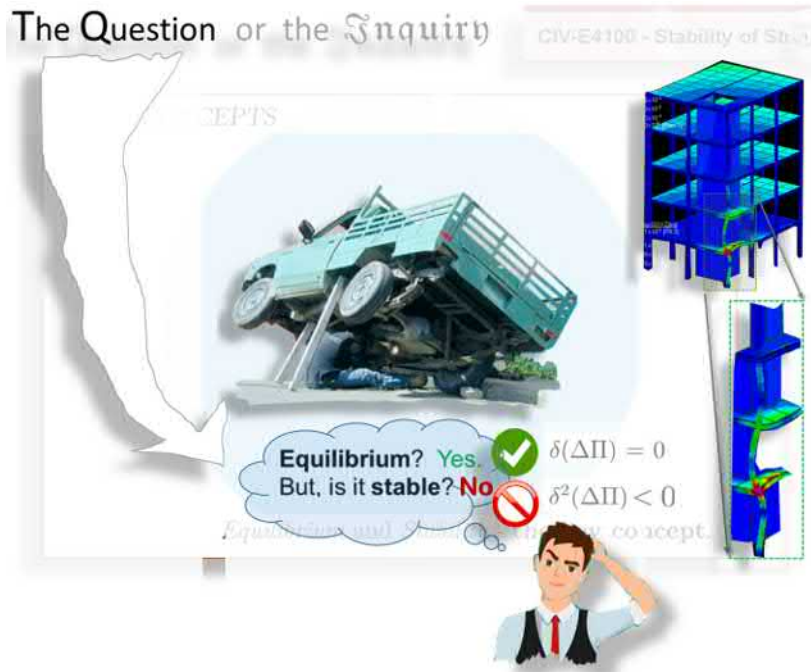


Figure 1.15: *Equilibrium and Stability - the difference.*

- now, on the contrary, the ball is locally at equilibrium on the top of the *concave* surface (hill). If now one perturbs slightly this configuration then the ball will continue to move farther away from the original position without returning to its initial configuration. Such initial equilibrium (or behaviour) is said to be *unstable*.
- assume that, locally, the ball is in equilibrium on a horizontal plane. If one displaces it slightly, the ball now remains at the position to which the small disturbance has moved it. Such equilibrium is called *neutral* or *indifferent*.

Let's now illustrate the basic stability types 1 – 3 mathematically, keeping the simplified example of the rigid ball. As the ball is perfectly rigid, the total potential energy of the system consists now only potential energy of gravitation $\Pi = \Pi_0 + mgy(x)$, where $\Pi_0 = \Pi(x_0 = 0)$ is a constant at the initial position of equilibrium x_0 . Locally, the shape of the surface is

described by the graph of $y(x) = ax^2$ which is the first term in the Taylor series for the surface around the initial point of equilibrium. The scalar $a > 0$ for convex, $a < 0$ for concave and $a = 0$ for the neutral equilibrium cases, respectively. Therefore,

$$\Pi(x) = \Pi_0 + mga x^2. \quad (1.12)$$

Now think that the initial equilibrium configuration $x_0 = 0$ is perturbed slightly by an infinitesimal amount δx . Thus, the perturbed total potential energy is

$$\Pi(x_0 + \delta x) = \Pi(x_0) + \frac{d\Pi(x)}{dx}\Big|_{x_0} \delta x + \frac{1}{2} \frac{d^2\Pi(x)}{dx^2}\Big|_{x_0} (\delta x)^2 + \frac{1}{3!} \frac{d^3\Pi(x)}{dx^3}\Big|_{x_0} (\delta x)^3 + \dots \quad (1.13)$$

$$\equiv \Pi(x_0) + \delta\Pi|_{x_0} + \frac{1}{2} \delta^2\Pi|_{x_0} + \frac{1}{3!} \delta^3\Pi|_{x_0} + \dots \quad (1.14)$$

Since x_0 is an equilibrium then $\delta\Pi|_{x_0} = 0$. Rewriting the above in a condensed form as

$$\Delta\Pi = \Pi(x_0 + \delta x) - \Pi(x_0) = \frac{1}{2} \delta^2\Pi|_{x_0} + \frac{1}{3!} \delta^3\Pi|_{x_0} + \dots \quad (1.15)$$

which provides us the sign of the increment of the total potential energy $\Delta\Pi$ between the perturbed and the initial equilibrium states. The study of stability of the initial equilibrium is conducted by studying the sign of the increment $\Delta\Pi$. First, keep only up-to the second order²³ term:

$$\Delta\Pi = \frac{1}{2} \underbrace{\frac{d^2\Pi(x)}{dx^2}\Big|_{x_0}}_{\text{Hessian of } \Pi} (\delta x)^2 = mga(\delta x)^2 + O(\delta x)^3. \quad (1.16)$$

Consequently, the initial equilibrium x_0 is stable when $a > 0$ (locally convex surface), unstable for $a < 0$ (locally concave surface) and indifferent when $a = 0$.

Bellow follows a résumé: At the critical points (equilibrium points), studying the sign of the increment of total potential energy $\Delta\Pi$, makes it possible to make statements on the nature of the actual equilibrium:

1. **stable:** (stabiili) $\Delta\Pi > 0$

²³If the second order term vanishes then higher order non-vanishing terms, for instance, $\frac{1}{3!} \frac{d^3\Pi(x)}{dx^3}\Big|_{x_0} (\delta x)^3$, will be used when $\frac{1}{2!} \frac{d^2\Pi(x)}{dx^2}\Big|_{x_0} (\delta x)^2 = 0$ to decide the sign of the increment $\Delta\Pi$ of total potential energy.

2. **indifferent** : (indiferentti) $\Delta\Pi = 0$. Often, the total potential energy increment $\Delta\Pi$ is expanded to second order only (squares of small displacements). In this case, $\Delta\Pi = 0$ and therefore, higher order terms should be included in the Taylor expansion to decide of the sign of $\Delta\Pi$ to disclose the character of indifferent equilibrium.
3. **unstable**: (labiili, epästabiili) $\Delta\Pi < 0$

Follow some terms:

- initial state: (perustila)
- perturbed state: (häritty tila)
- perturbation: (häiriö)
- increment: (poikkeama)

Note that, for this trivial discrete case with very limited number of discrete kinematic parameters (only one x), one can have the sign by direct use of Lagrange-Dirichlet stability theorem as

$$\Pi'' = 2mga. \quad (1.17)$$

So, the stability of the configuration is dictated directly by the sign of a .

1.4 Study of Elastic stability - the method

This chapter covers static elastic *stability* of some common elastic structures as beams, frames, trusses, plates, cylindrical shells of revolution and open thin-walled beams. before bifurcating to stability directly deriving equations of stability loss for such structures, 'let's stop a while' and turn and return a bit the word *stability*²⁴ to discover its *meanings* in the engineering context. So, patience.

²⁴There is a complete branch of mathematics, *Stability theory*, which is devoted to study the stability of solutions of differential equations and of trajectories of dynamical systems under tiny perturbations of initial conditions.

1.4.1 Methods of stability analysis

In short, there are three (analytical) methods for studying the stability of an equilibrium: 1) the *bifurcation approach*, 2) the *energy approach* and 3) the *dynamic approach*. The dynamic approach is versatile and holds for both conservative and dissipative systems. The energy method in the form of the Lagrange-Direchlet theorem (stable equilibrium corresponds to a local minimum of the total potential energy) is limited to conservative systems only. In these lecture notes, we systematically use the energy approach.

There exist three (analytical) methods for studying the stability of an equilibrium:

1. **Bifurcation approach** - write the equilibrium equations in a deformed configuration and determine the onset of buckling
2. **Energy approach** - the change of total potential energy of the system between two neighbouring equilibrium states is used to derive the equations of equilibrium and to study its stability
3. **Dynamic approach** - the equations of motion of the system are established. i) Natural frequencies decreasing to zero, correspond to the onset of instability or ii) investigate how an initial perturbation develops with time
4. **Computational method** (numerical simulations) For design purposes, detailed stability behaviour of structures can be analysed numerically by performing a geometrical and material non-linear (GNMA) analysis on the real structure with the inherent real and possible imperfections using capability of the Finite Element technology. Such analysis provides full load-displacement curves which are used to identify bifurcations or/and limit points for determining the limit loads
5. **Experimental approach** is necessary since models are only approximations and very often, they are a very incomplete approximations. For some structures, experiments are of primary importance

So, to say it another time, in a (may be!) shorter way: The first method consist of writing the equilibrium equations in a deformed configuration and determine the onset of buckling. In the second one, the change of total potential energy of the system between two neighbouring equilibrium states is used to derive the equations of equilibrium and to study its stability. In the third method, the equations of motion of the system are established. Natural frequencies decreasing to zero, correspond to the onset of instability.

Let's come back to what is stability.

1.4.2 What is stability as a phenomenon?

Stability or more clearly *stability of equilibrium* describes the nature of the *equilibrium* of structures. Is such equilibrium stable, indifferent or unstable. The transition from *stable* to *unstable* equilibrium (or reversely) occurs always through an *indifferent* equilibrium. Stability loss can occur through *bifurcation points* or at a *limit point*. The *point* (\mathbf{u}, P) refers to a *critical point* on the load-displacement curves (called also *load paths*).

Usually, stability is a concept related to systems having *more than one equilibrium state*. This means that there exist adjacent equilibrium configurations. In such cases some equilibrium paths (load-displacement curves) *intersect* in the configuration space (the graph of $\mathbf{u} = g(P)$). These intersections are called *bifurcation points*. We speak then of *bifurcational stability loss*. On the (total potential) energy-space representation (the graph of $\Delta\Pi = f(P, \mathbf{u})$) such special points (critical points) correspond to *local extrema*. Stable equilibriums corresponds to local *minima*: this is exactly what the Lagrange-Dirichlet theorem says in short.

There is also systems with no bifurcational stability loss. Such systems have only one equilibrium path in the configuration space. The loss of stability can occur at a special point (on the load-displacement) curve called *limit point*. At this point the apparent rigidity of the structure vanishes. The classical example of such unstable behaviour (*snap-through*) is a shallow arch under compression. However

Simplest examples for bifurcational stability loss are the *bistable* systems, with two equilibrium states where the system can rest in either one two states (Figures 1.16 and 1.17). We will study, later, an idealised example of such mechanical system known as *Mises truss*.

These equilibrium states correspond to local minima in potential energy of the system. A tiny external perturbation, in term of input energy, can make the system switch to another equilibrium state if enough energy input is given to jump the barrier separating the local minima. Between two local minima a local maximum should exist. The state at this critical point is *unstable*. This local maxima is termed as potential *barrier*. An other example of such *bi-stable* mechanical simplest system is the mechanical light switch device. It has two equilibrium states, and it switches between them upon input of a tiny external energy input when your finger initiates pushing slightly the lever making it switches trough *snap-through* to one of the on-off positions and remains there.



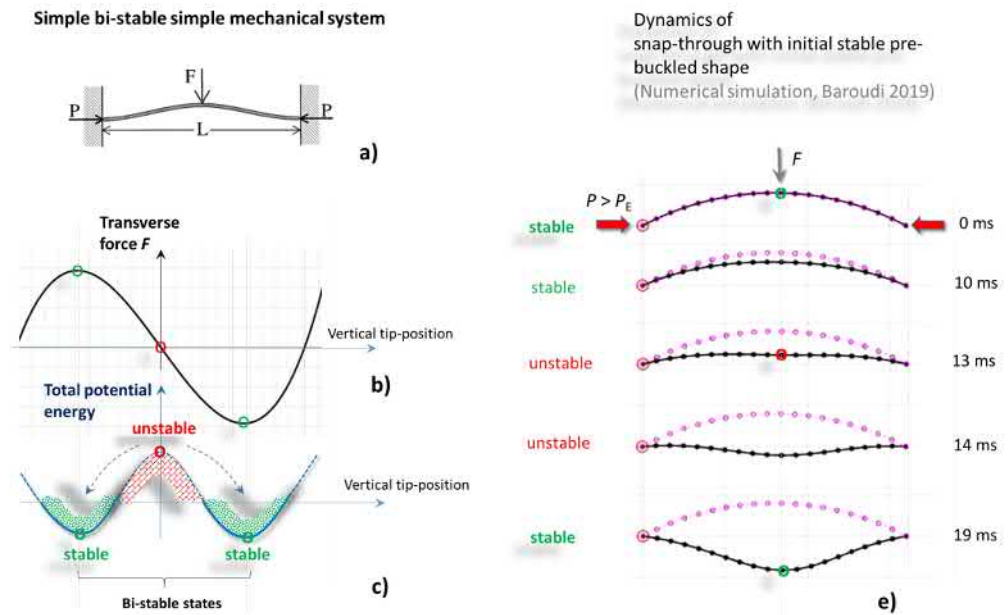


Figure 1.16: a) Simple example of bi-stable mechanical device. c) a slightly pre-buckled beam to its first mode (a shallow slightly pre-stressed arch) is a bi-stable system. c) and e) Transition between the two-equilibrium stable configurations occurs through higher modes (full dynamic simulation of snap-through. The model used is dissipative).

Snap-through of shallow arch

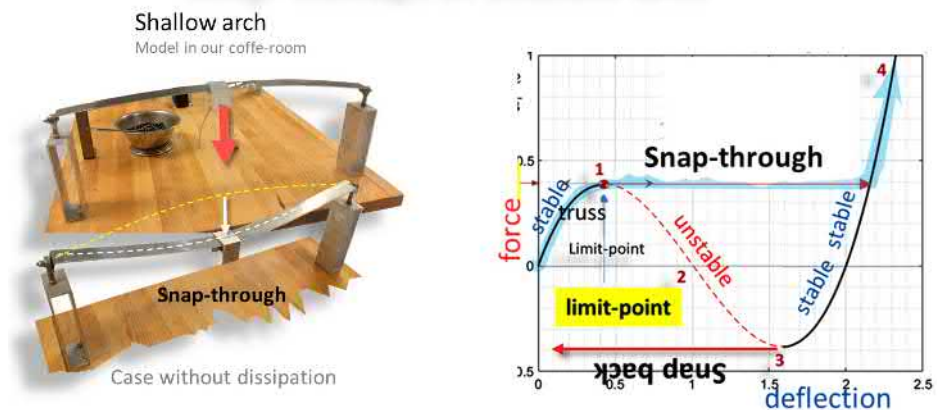
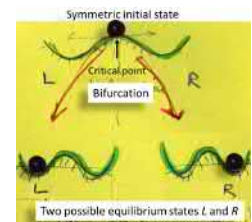


Figure 1.17: Stability of a shallow arch. The arch is an example of bi-stable systems: the transition between the two-equilibrium stable configurations occurs dynamically.

Another example of such systems with multiple equilibrium states, that the reader may recall from his high school education, is related to conditions of existence of phases of water (ice, liquid and gaseous). Of special interest, is the critical point named the *triple point* on the *phase stability diagram* (Figure 1.18). At such point all the three phases can co-exist! Such diagram shows on a graph having the pressure P as x -axis and the temperature T as y -axis, which are the *control parameters* of the system, the boundaries separating stable regions for the *stable existence* a given water phase: liquid, solid or vapour. At such *critical point* which corresponds to a *bifurcation point*, all the three possible states of water phases co-exist at such point. A *tiny* external energy input, a perturbation, makes the water ice, vapour or liquid. For instance, a supercooled water: a pure water can be cooled below zero degrees Celsius without freezing even up to -40 °C²⁵. Any impurity in the water acts as a perturbation. That is why it was purified to make it close to *ideal* pure. Now, if you hit the 'bottle' with your small finger, all the water freezes at once and becomes ice. The system bifurcated to another equilibrium state. These example above were just to immerse the reader into the meaning of the word *stability*. In this course, we will concentrate on stability of conservative systems. The stability of elastic structures such as beams, frames, trusses, plates, shells will be addressed during this course. Now stability, as a concept, is not just a word but much more than that; the nature of the response of a structure (a system) to a tiny external perturbation being encoded into this word.

We can say that emergence of our actual universe including us, is a consequence of *loss of stability* of the primary universe. Such loss of stability is called by physicists *symmetry breaking*. According to the *principle*²⁶ of *supersymmetry* it is believed that just after the big bang, *all of the forces of nature were identical and all elementary particles were the same*. But within an 'instant', this *symmetry was broken* . . . and the universe emerged.

In physics, loss of stability (bifurcational type) belongs to the class of *symmetry breaking* phenomena where action of infinitely small perturbations (fluctuations) on the system being close to a *critical point* leads to sudden branching through *bifurcation* to some other possible neighbouring state. At the bifurcation point multiple possible states emerges (branching routes). Such behaviour will be treated in details when investigating the stability of *equilibrium paths*, especially in cases of *bifurcational loss of*



²⁵such supercooled water naturally exists in the clouds as droplets. Any perturbation can initiate ice crystals formation

²⁶This principle is not yet validated (25.2.2019). [The supersymmetry is a general principle and not a theory.]

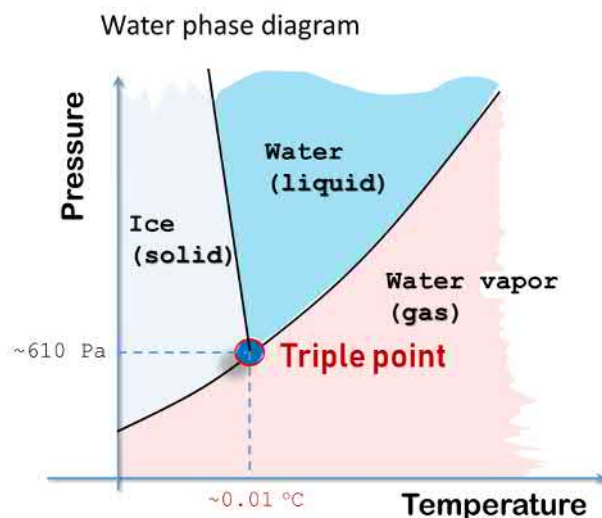


Figure 1.18: Phase diagram of water. Can be called also *phase stability diagram*.

stability of elastic structures. Such concept as equilibrium paths will of be defined properly subsequently.

From the point of view of mechanics, the phenomenon of loss of stability is dynamic by nature. The *snap-through* of a shallow arch, resonance in parametric excitation of stay-cables of a bridge or cable of guyed tower and in flutter are such examples. Generally, inertia forces should be accounted in such analysis using classical method of *dynamics stability* (**Lyapunov**²⁷ stability, for instance, **Lyapunov** (1893).

Dynamical systems are generally described by differential²⁸ or difference equations. There exist various types of stability for their solutions. The stability near to point of equilibrium²⁹ (*critical points*) is may be one of the

²⁷It can be shown that for conservative systems, the energy criterion for stability can be derived through the more general Lyapunov dynamic stability criteria. (tarkista, että viitteet)

²⁸Like non-linear dynamic system $\dot{x}(t) = f(x(t))$, $x(0) = x_0$, for instance. The equilibrium of such systems is given by points x_e such that $f(x_e) = 0$. Now the stability of such equilibrium points is of interest. For that, Lyapunov stability is often used.

²⁹They are critical points such that $\dot{x}(t) = f(x(t)) = 0$. Note that at such points the rate ('velocity') is zero. So, one have no motion. This, if we think of our mechanical system, means that in the vicinity of such point we have static equilibrium. Assuming that the external forces $\mathbf{f} = \lambda \mathbf{f}_0$ and applying mechanical energy conservation principle when $\ddot{\mathbf{u}} = 0$, $\dot{\mathbf{u}} = 0$, and linearising the obtained equations in the vicinity of the equilibrium point one obtains a linear eigenvalue problem for determining the critical (buckling) load and the corresponding eigenmodes (buckling modes). However, this is an *ad-hoc* way to say that one can may be approach stability problems, for conservative mechanical

most important. Theory of Lyapunov addresses such stability very simply in terms of initial state perturbation (Figure 1.19):

Lyapunov stability: *If at an equilibrium point x_e , two solutions (time series) having initial conditions close to each other remains close to each another for ever then the equilibrium point x_e is Lyapunov stable.*

Non-linear dynamic systems are generally described by an n -dimensional *non-linear* evolution equation

$$\begin{cases} \dot{x}(t) = f(x, t; \lambda), & t > 0 \\ x(0) = x_0, \end{cases} \quad (1.18)$$

Where λ being a control parameter. The system posses equilibrium points x_e (states) defined by $f(x_e) = 0$. Now rises the nature of stability of such equilibriums points x_e . In terms of mathematics, equilibrium point x_e is *Lyapunov stable*, (Figure 1.19), if

$$\forall \epsilon > 0, \exists \delta \text{ such that } \|x(0) - x_e\| \leq \delta \implies \|x(t) - x_e\| \leq \epsilon, \forall t \geq 0.$$

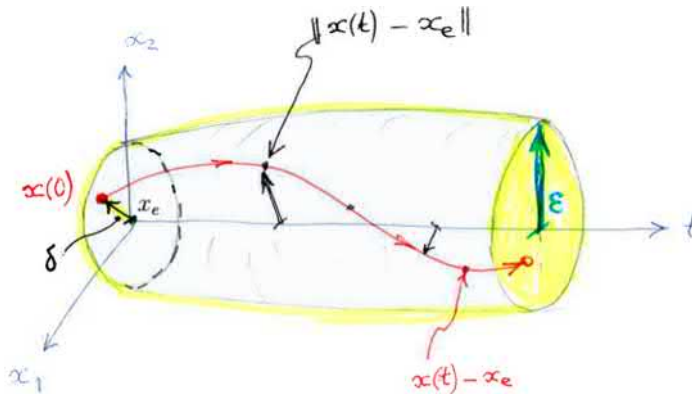


Figure 1.19: Lyapunov stability.

The discrete equation of motion of a mechanical system, can be recast in terms of a canonical non-linear dynamical problem (Equation 1.18) by

systems, by studying the stability at static equilibrium. A full prove is out the scope of this lecture.

introducing the velocity $\mathbf{v} = \dot{\mathbf{u}}$ as a change of variable in addition to displacements \mathbf{u} . The discrete equation of motion being

$$\begin{cases} \mathbf{M}\ddot{\mathbf{u}} + \mathbf{C}\dot{\mathbf{u}} + \mathbf{K}\mathbf{u} = \mathbf{f}, & \text{linear case} \\ \mathbf{M}\ddot{\mathbf{u}} = \mathbf{f}(\mathbf{u}(t), t), & \text{non-linear case.} \end{cases} \quad (1.19)$$

Consider the more general case with non-linearity³⁰; second equation in (1.19). After change of variable and accounting for that $\dot{\mathbf{v}} = \ddot{\mathbf{u}}$ one re-write the equilibrium equation in the non-linear ode form

$$\begin{bmatrix} \mathbf{M} & \mathbf{0} \\ \mathbf{0} & \mathbf{I} \end{bmatrix} \begin{bmatrix} \dot{\mathbf{v}} \\ \dot{\mathbf{u}} \end{bmatrix} = \begin{bmatrix} \mathbf{f} \\ \mathbf{v} \end{bmatrix} \implies \underbrace{\begin{bmatrix} \dot{\mathbf{v}} \\ \dot{\mathbf{u}} \end{bmatrix}}_{\dot{\mathbf{x}}} = \underbrace{\begin{bmatrix} \mathbf{M}^{-1} & \mathbf{0} \\ \mathbf{0} & \mathbf{I} \end{bmatrix} \begin{bmatrix} \mathbf{f} \\ \mathbf{v} \end{bmatrix}}_{f(x,t;\lambda)} \quad (1.20)$$

So, we see that general discrete equations of motion are reducible to the non-linear evolution equations of dynamical systems (Equation 1.18). So, Lyapunov stability criterion can naturally be applied in structural dynamics (Figure 1.20).

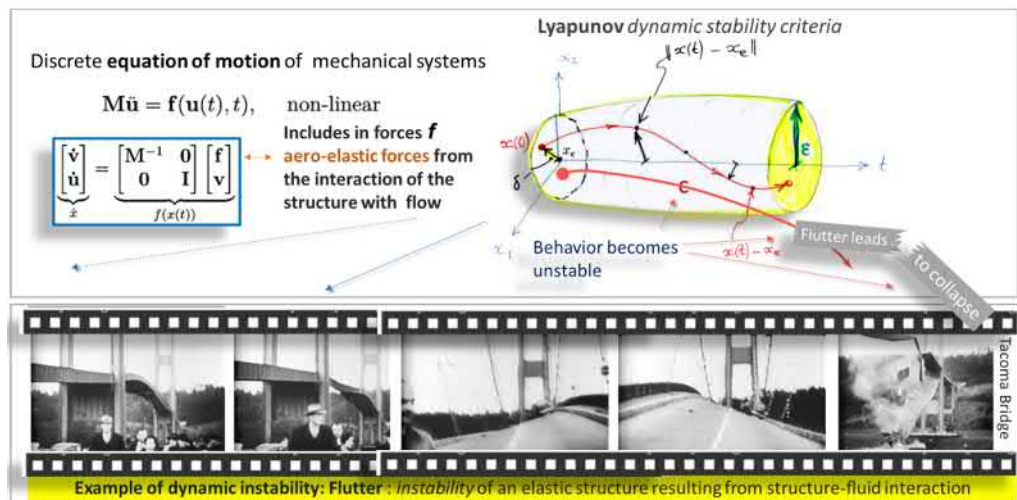


Figure 1.20: Tacoma Bridge collapse, a classical example of dynamical instability (flutter). Flutter: a coupling between bending and torsional modes through aero-elasticity exists.

Let's now return to the main subject of this writing which is focused on the *static stability* of elastic structures. Elastic structure posses *strain energy*

³⁰This is valid also for the linear case (linear coefficients), where now $\mathbf{f} := \mathbf{f} - \mathbf{C}\dot{\mathbf{u}} - \mathbf{K}\mathbf{u}$

functional. If in addition, the work of external forces do not depend on the taken path then they are conservative. Under these two conditions case our system (structure and loads) is *conservative*.

For *conservative systems* a strong *stability theorem* by **Lagrange** (1788) and **Dirichlet** (Lagrange-Dirichlet stability theorem) exists. This theorem will be our *main tool* for deriving loss of stability equations for the whole variety of structures like columns, frames, arches, plates, shells and so on. The generic name *energy criteria* of stability is nothing else than the many applications of this *theorem* saying that *system is stable if its potential energy is positive definite*³¹.

This theorem allows to approach the stability problem as a static one by investigating the 'shape' and curvature of the total potential energy surface. So thanks to this theorem, stability analysis reduces practically to a study of the positive definiteness of the tangent stiffness matrix of the structure. Consequently, the stiffness matrix of the linearised system determine the critical loads. The linearised homogeneous system is obtained from the total potential energy which is quadratic in displacements. To study the post-critical behaviour, higher terms than quadratic ones should be incorporated into the total potential energy.

For our luck, in many civil engineering structures, static approach - ignoring the effects of inertia forces - leads to the same results as when using dynamics, in terms of loss of stability (determining the critical load). This is true when the system under consideration is *conservative* (elastic structure, ideal constraints and the external loads are conservative). Therefore, in the following, we limit our selves to such conservative systems and terms this approach by *static elastic stability*.

In one word, performing *stability analysis* is to answer the **fundamental question** "*does the structure sustains its current equilibrium configuration or not, after any arbitrary infinitesimal perturbation?*" So, Stability analysis investigate next things³²:

- **Equilibrium configurations** existence of multiples equilibriums or of limit points
- **Stability of these equilibriums** with respect to small perturbations

³¹More generally, this means that the second derivative of the total potential energy increment should be $\Pi'' > 0$. The derivatives are to be defined in terms of variational calculus with respect to the kinematics. The criterion $\delta^2\Pi > 0$ is a special case for up-to quadratic terms expansion of the total potential energy functional.

³²The purpose of stability analysis is 1) to determine the critical points and 2) to study their sensitivity to small perturbations (Corridor conversation with R. Kouhia, 2018).



Equilibrium? Yes $\Leftarrow \delta\Pi|u|=0$
But, is it stable? No $\Leftarrow \delta^2\Pi|u| < 0$

Testing stability:
Push slightly. Does the bike recover its initial equilibrium configuration?

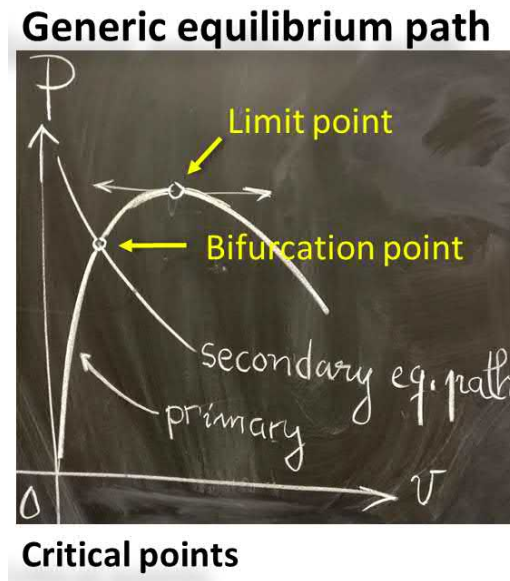


Figure 1.21: Generic equilibrium paths and types of critical equilibrium points as *bifurcation* or *limit points*. (Haarautumis- tai rajapiste, (sf))

- **Sensitivity with respect to imperfections** as for instance, shape, geometry, Loads (eccentricity) and material imperfections

In other words, one try to answer questions like:

- can we predict the critical load? the smallest value is called the *buckling load*. Such analysis is known as *linear buckling analysis*
- what happens at the bifurcation (or limit) point or at its neighbourhood?
- can we describe or determine the post-critical branches? Nature of stability?
- what about imperfection-sensitivity?

To answer the above questions one needs to do continue the linear buckling analysis with *post-buckling analysis* or a full non-linear analysis.

How to test an equilibrium state for stability?

I included the question in the title to answer in a written mode for the n -th time, the question of a good master student during the class. From

his question, one see that the concept of equilibrium, stability of an equilibrium and *testing for stability* need time to be *deconfused* correctly. The student wondered why an cantilever beam of I-cross section which is only loaded in the transversal plane of symmetry loses its stability, after the load has reached a threshold value, and buckles with a combined lateral deflection and a torsion? There is also a detailed explanation given following in sections (1.4.2 and bellow)

The student was apparently puzzled and he reformulated his question again while I was waiting for him to recall the answer by himself: "*How the I-profile knows to twist and the deflect laterally while it was only deflecting first only in the vertical plane of loading without knowing anything about torsion?*"

"*Why the I-profile have a combined twist and lateral flexural modes in the post-buckled state despite that in the initial state pre-buckled flexural mode in plane of the Loading?*" The answer is to recall what is stability? How the linearised equation of loss of stability are derived? How to study it as a phenomenon?

A short recalling answer: The *stability of an equilibrium*, or shortly the stability can be studied or *tested* experimentally, theoretically and numerically in the same way: we consider a physical system being in an *initial equilibrium* and then we *introduce a small perturbation* to the system and check does the system returns to its initial equilibrium state after removal of the perturbation or does it find another (than initial one) equilibrium state?

The perturbation can be introduced to the pre-buckled system in the form of a tiny perturbation of the initial configuration or a tiny force perturbing the initial configuration. So, in the example of I-beam cantilever, the information about post-buckled torsional and lateral-flexural modes, $\delta\phi(x)$ and $\delta w(x)$, respectively, is already *injected* by as perturbations or *post-buckling modes* into the buckling equations or the change in the total potential energy of the system between pre- and post-buckled state (Figure 1.22).

About the stability equations and Adjacent-equilibrium criterion

What are the physical basis and how are derived the stability equations? Physically speaking, we use the *criteria of adjacent-equilibrium*. What does it mean? We consider an initial equilibrium state in which the structure is already. Then, the structure is *slightly perturbed* from this *initial configuration* and moves a *neighbouring state*. The criteria of adjacent-equilibrium requires that the *neighbouring state is also an equilibrium state* (Figure

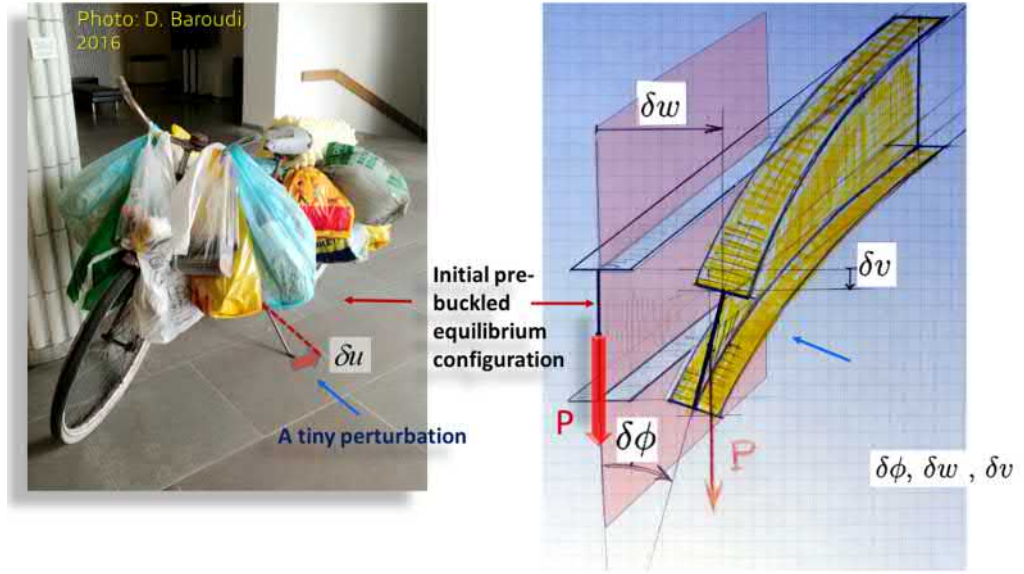


Figure 1.22: Look and see by your-self: testing for the nature of an equilibrium by introducing tiny perturbations $\delta\phi$, δw and δv .

1.23). It is based on this criterion, that the stability equations are derived. The criterion of adjacent-equilibrium is also known as *stability criterion*.

Usually, there is two approaches to use this criterion: a) *a variational* (Lagrange) and b) *a vectorial* (Newton) form. In the vectorial form, the local equations of equilibrium are imposed for the perturbed configuration for an elementary differential element of the structure. In the variational form, the equilibrium at the perturbed (deformed) configuration of the structure is imposed globally through stationarity³³ of its total potential energy. In both approaches, the geometrical non-linearities of the deformations should be accounted for, explicitly.

The variational form of the criterion for the *existence* of and equilibrium adjacent state (Figure 1.23) can be written formally or generically in the next way:

$$\text{Equilibrium initial state} \implies \delta S^0 = 0 \quad (1.21)$$

$$\text{(Requirement) Equilibrium perturbed state} \implies \delta S^* = 0 \quad (1.22)$$

$$\exists \text{ Adjacent-equilibrium state} \implies \delta(\Delta S) = \delta(S^* - S^0) = \delta S^* - \delta S^0 = 0 \quad (1.23)$$

where S - total potential energy (or action) and $\Delta S = S^* - S^0$, being the

³³Provides the weak form of perturbed equilibrium equations.

change between the two neighbouring states. The initial state (with S^0) being an equilibrium state. The perturbed state (with S^*) is thought to be achieved through a virtual perturbation δq_i of the Lagrangian coordinates q_i of the system while keeping the loading unchanged. So, in short, ΔS can stand for the increment of total potential energy $\Delta \Pi$ of the system which corresponds to the virtual variations δq_i of the initial equilibrium configuration q_i .

So, generically, the criterion of existence adjacent-equilibrium state implies that

$$\boxed{\delta S^0 = 0 \wedge \delta S^* = 0 \implies \delta(\Delta S) = 0.} \quad (1.24)$$

The criterion (1.24) is quite general. It is known by energy criterion of loss of stability.

About the energy criterion of stability

Here follows an introductory word³⁴ to have the smell, the colour and the Formula for the criteria in studying stability of an equilibrium. In further-coming section, they will be treated in the level of details they deserve.

For now, just keep in that the critical condition $\delta(\Delta \Pi) = 0$, (Cf. Figure 1.25), is a general and that the well-known classical **Trefftz** condition, $\delta(\delta^2 \Pi) = 0$, for loss of stability, can be derived as its corollary for special case when $\delta^2 \Pi \neq 0$ (as it will be shown later).

Notation and basic concepts: $\Delta \Pi$ has a physical meaning; it is the increment of the total potential energy of the system between a perturbed $u^* = \vec{u} + \delta \vec{u}$ and the unperturbed state \vec{u} (primary equilibrium) (Figure 1.25). Here, the (virtual) infinitesimal perturbation $\delta \vec{u}$ is thought to occur while keeping the loading unchanged.

In general, the perturbation $\delta \vec{u}$ of the initial state \vec{u} can be arbitrary (Figure 1.24). However, in practical cases when one is interested only by the critical load, the increment $\Delta \Pi$ is linearised in the neighbourhood of the critical point to obtain the so-called *linearised homogeneous equations of elastic-stability* (They represent an eigenvalue problem).

As a consequence of linearisation, we lose the information on the nature of such critical point and have no information concerning the post-critical behaviour (Figure 1.21). One cannot determine the buckling or deformations, for instance. Note that the reference configuration has not to be at

³⁴I, probably, will merge this paragraph with the one coming later addressing energy criteria of stability.



Adjacent-equilibrium criterion

Requiring perturbed state to be an equilibrium state $\Rightarrow \delta(\Delta S) = 0$

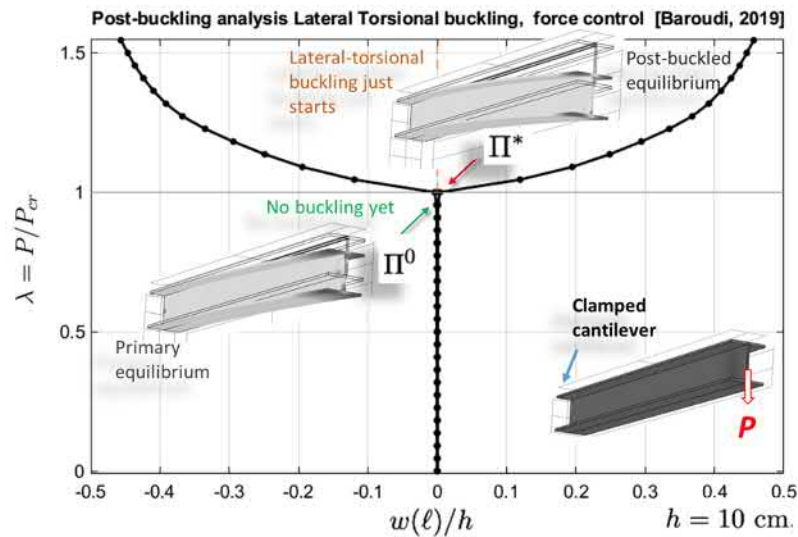
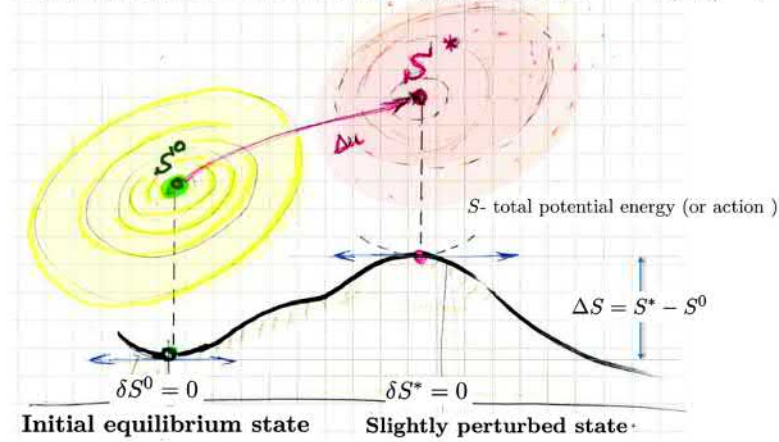


Figure 1.23: Generic illustration of the adjacent-equilibrium criterion in its variational version (up). (Δu is an infinitesimal perturbation corresponds to w on the lowest plot). Finite element post-buckling analysis (Lower figure). Note the initiation of combined lateral and torsional motion of the cross-section. Note that at buckling (zoom the infinitesimal neighbourhood of the bifurcation or limit-point) the load P does not increase. So, the value of P (external loads) remains unchanged between S^0 and S^* (Cf. horizontal tangent at buckling, see margin figure)

a critical equilibrium point. Any other equilibrium configuration can be chosen as a reference state to be perturbed.

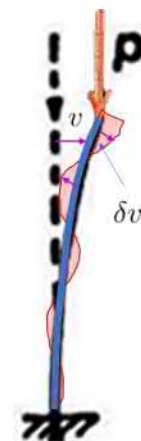
About perturbing the initial equilibrium state: what are Π^0 and Π^* in $\Delta\Pi$?

These few lines came out to clarify one question I got during a yesterday (4.3.2019) lecture. The question ... *does the value of P changes between S^0 and S^* when I form $\Delta\Pi$?* (See Figure 1.24).

1. **Real loading sequence:** One way to think how form the increment of total potential energy is through a *real loading sequence* where the load increases quasi-statically and monotonically from zero to the buckling load $P_E^+ = P_E + \epsilon$ where the real *imperfect structure* buckles, and where ϵ being infinitesimally small > 0 . The primary non-buckled configuration (primary equilibrium) corresponds to $P_E^- = P_E - \epsilon$. Now one can form the increment of the total potential energy between these two *real* states Π^0 and Π^* and takes the limit when $\epsilon \rightarrow 0$. Taking the limit is to say that we are at the bifurcation or limit-point where now the critical load being P_E . (Figures 1.23 and 1.24)

2. **The thought experiment:** the other more *classical way* (variational) We consider first, the initial pre-buckled equilibrium state (configuration) (generically, $u \neq 0$ - axial displacement and $v = 0$ - bending deflections) under membrane loading only (generically, axial load P). The total potential energy in this state is denoted Π_0 .

Then, keeping the loading unchanged, we introduce a tiny 'lateral' perturbation v^* such that, generically, $v = 0 + v^*$ and u does not change. This state is called *post-buckled* state. The total potential energy for in this state is now Π^* . Now, the *increment* or change of total potential energy is defined as $\Delta\Pi = \Pi^* - \Pi_0$. It is this increment that we consider in these reading material. Now come the time to check if this new perturbed configuration is an equilibrium state or not. If it is an neighbouring (with respect to the initial equilibrium state) equilibrium state, then, the structure can remain in this this new equilibrium state. If it so, then this motion from the primary equilibrium to the adjacent equilibrium state, is what is called *loss of stability*. Now rises the question how to check if the perturbed configuration $v \neq 0$ is an equilibrium? The answer: we introduce an arbitrary virtual displacement δv to this infinitesimally perturbed state v and require that the virtual work *thought experiment*³⁵ of all forces vanish (see margin figure and Fig. 1.24).



Is the post-buckled state v an equilibrium? The perturbed post-buckled configuration is $v + \delta v$. Is now $\delta W = 0, \forall \delta v$?

³⁵ Cf. to the virtual displacement concept in the classical theorem of virtual work. The *virtual work principle* is *fundamental* in analytical mechanics and Lagrange developed his

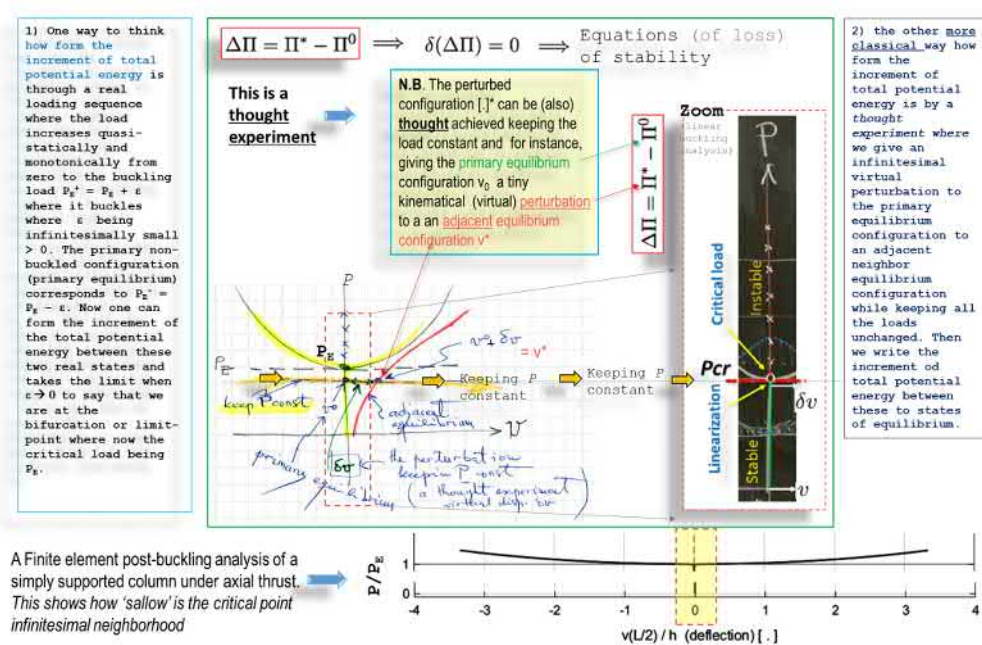


Figure 1.24: How to form $\Delta\Pi$? This is one strong way to visualise the procedure of perturbation: The initial primary equilibrium state v^0 is perturbed into an adjacent state $v^* = v^0 + \delta v$, in a *thought-experiment* by a tiny virtual displacement δv while keeping the load P constant. Then the energy criteria for loss of stability $\delta(\Delta\Pi) = 0$ requires the perturbed state to be an *equilibrium state* too. The load level P can be also chosen arbitrarily, even above the buckling load P_E .

About post-buckling analysis

In post-buckling analysis one need to solve or trace the load-deflection history while the structure is loaded incrementally in a monotonic way. Performing such task is far from trivial. Quasi-static or static analysis can be often sufficient. However, for some structures (as thin imperfect shells, shallow arch, ...) there can be some snap-back which makes the displacement control 'not correctly working' (multiple solutions for one given displacement) or snap-through making force control 'not correctly working'

Lagrangian mechanics through the use of such principle while accounting for the virtual work of acceleration forces (= -inertia forces) by D'Alembert's principle . Lagrangian and Hamiltonian methods together with the *least action principle* can be derived from this principle. In one word, all these three principles lead naturally to Newton's law of motion. By curiosity, the Hamiltonian principle directly follows from the virtual work principle, $\delta W = 0, \forall \delta \mathbf{u}$, by asking $-\int_{t_1}^{t_2} \delta W \cdot dt = 0$ where the virtual displacements have kinematically admissible.

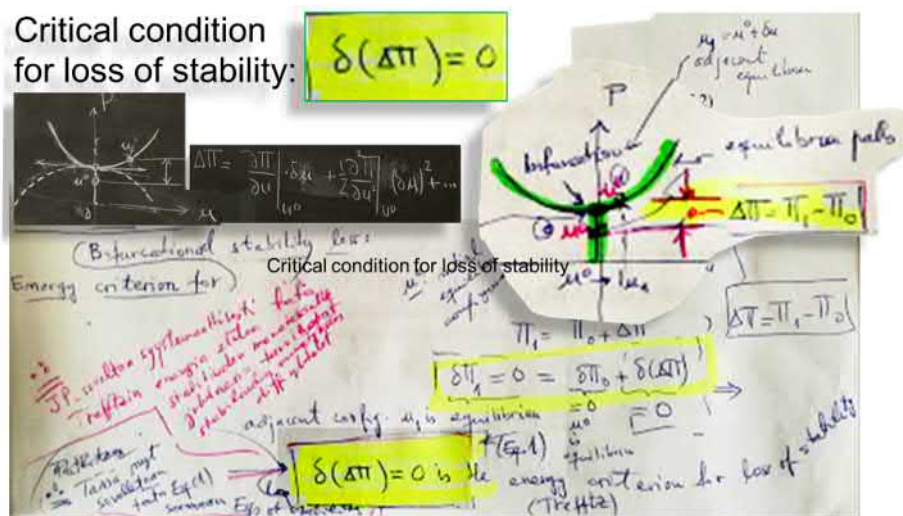


Figure 1.25: Stability of an equilibrium by energy criteria. A physical interpretation of the general critical condition $\delta(\Delta\Pi) = 0$. $\Delta\Pi$ is the increment of the total potential energy between a perturbed (post-buckled state) and the unperturbed state (primary equilibrium or pre-buckling state). Note that at buckling (zoom the infinitesimal neighbourhood of the bifurcation or limit-point) the load P does not increase (horizontal tangent at buckling).

(multiple solutions in displacements under one same load) . If we are interested in the complete load-path history, it may be wise (expensive one) to perform a dynamic analysis while introducing artificially over damping to the structure when needed.

Physically speaking, the structure suddenly loses its effective rigidity at the critical points since on the equilibrium path (curve representing imposed force *versus* displacement) when such points has horizontal tangents or they correspond to points with a dramatic change in the apparent rigidity. This is the reason why a small lateral force in a support, in the direction of buckling, is enough to prevent efficiently against buckling.

About computational analysis of stability

Addressing stability issues (*buckling load* and *post-buckling analysis*) of real structures which can be made by assembling many structural elements in a complex way, can be done only by numerical simulations (*Cf.* margin figure). However, fundamentals of stability should be learnt well in order to obtain results which are reliable since, the engineer should also provide

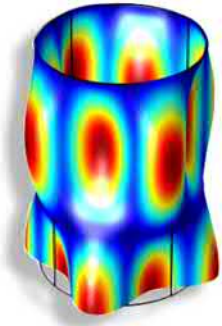


Figure 1.26: Buckling of axially compressed thin shell. Computed as a full 3D geometrically non-linear problem for illustration purposes. (3D model just to avoid the question *what shell-theory to use?*)

(experimental) validation of his results or at least a quantified estimation of the validity range of the obtained results. providing validity ranges is one of the hardest and most laborious task since experimental work is usually needed to obtain practical answers of use for cases with high consequences for safety. Even, participating to planning such experimental work an engineer needs good knowledge of fundamentals.

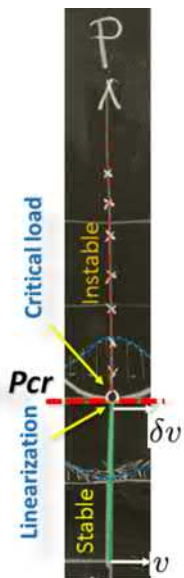
Traditional courses deal, usually, with stability of basic *single* structural members as beams, column-beams, frames, lateral torsional buckling of beams, buckling of plates and cylindrical shells, etc. In addition, such courses focus more on the determination (linear buckling analysis) of the smallest critical load (\equiv buckling load). The post-buckling analysis some of its aspects are not dealt with, independently how critical they may be in structural design³⁶

Numerical approach should be given (allocated) equally attention than the traditional basic theoretical content for such course since the *computational technology* as, for instance, **FEA**, is our days available and of everyday use. The students, during this course, should focus more on the concepts to understand the phenomena of stability in order to make more reliable numerical simulations. Therefore, making models and asking the correct questions to be addressed and solved computationally, is the second core of the learning-outcomes.

1.5 Equilibrium paths

The basics of stability concepts can be accessed by studying illustrative examples of simple elastic systems having one, two or more degrees of freedom. This means that, these concepts and approach is valid as such for more complex structures as frames, trusses, plates, shells and so on (structural elements and structures). The concepts to study are equilibrium paths, bifurcation and limit points, critical load, linearised homogeneous equations of stability, energy criteria for stability loss.

Equilibrium path(s) is a curve or curves describing the relation between the displacements at some specific locations of loaded structure and the load.



In general, apart from this one or few degrees of freedom rigid bars-

³⁶As a side note, there is a good reading material about post-buckling analysis and its technical aspects, by *full professor* Reijo **KOUHIA** at <http://www.tut.fi/rakmek/personnel/kouhia/teach/> named *Computational techniques for the non-linear analysis of structures, 2009.*"

springs systems, more complex structures are not tractable analytically. In general, equilibrium paths are derived computationally² through a full-nonlinear analysis (post-buckling analysis) for a given structures (see Fig. 1.171). Solving analytically equilibrium path (load-curves) for even a simple slender elastic rod (Elastica) is impossible. The only way to solve it is by doing geometrically non-linear Finite Element Analysis³⁷. However, the general concepts and the general methodology to study stability loss are not dependent on the degree of complexity of the examples used to illustrate them. The main peculiarities of the behaviour of the structure can be studied by considering the equilibrium paths at some characteristic points (equilibrium points).

² Actually, *load-displacement* curves are often done experimentally, at least for a parts of the structure, to obtain real limit-load together with the full mechanical response.

It will shown further that the bifurcation points of the initial equilibrium state can be determined without solving the post-critical³⁸ state. For this purpose, the non-linear equation will be *linearised* in the neighbourhood of a critical point (Figure in the margin). The set of equations is called *homogeneous linearised equations of elastic-stability* and is in the form of an eigenvalue problem. Solution of such eigenvalue problem provide us the critical load (as the smallest eigenvalue) and the corresponding new equilibrium configuration up-to a scaling factor (eigenvectors or buckling modes). It should, however, be stressed that such linearised equations of stability cannot provide any information on the type of the critical point nor give the post-critical state (finite displacements). For these purpose, one should perform (geometrically) full non-linear analysis.

Note that, linearised analysis is not applicable when the structure has significant non-linearity already before the critical load.

As previously concluded, basics of stability concepts demonstrated by studying simple elastic systems with few degrees of freedom. However, for educative purposes and to immerse the student in reality, I produce next figure (Fig. 1.27) to illustrate equilibrium paths (load-displacement curves ($w_0, p/p_{cr}$)) of more complex structure, namely, spherical shell caps. Stability of shells will be treated later. Here, the pressure is p [Pa] and the deflection at mid-span w_0 [m]. If there is one thing to retain about thin shells then it will be that their behaviour is very *sensitive to imperfections; especially shape imperfections*. This aspect will be quantified once we get there.

³⁷This is also one scope of this course.

³⁸which can be obtained by solving the non-linear equations for arbitrary displacements.

Picture and text legend are from the reference below:
http://shellbuckling.com/presentations/buckledShells/pages/page_38.html , (2018)

Load deflection curves for externally pressurized spherical caps
 This slide demonstrates the transition in behavior from that of a flat plate under uniform pressure to that of a deep spherical cap or a complete spherical shell under uniform external pressure.

The **flat plate (a)** exhibits **increasing stiffness** as the pressure is increased and membrane tension develops as the flat plate bends downward under the pressure.

A **very slightly curved plate (b)** **initially softens, then stiffens** as the external pressure is increased, but there is **no local maximum load-carrying capacity**.

The **somewhat more curved plate (c)** exhibits the type of **nonlinear buckling** called **"snap-through"**: The plate softens until it has zero stiffness, then "snaps" into an inverted position, after which it stiffens with further increase in pressure.

A **plate with more curvature yet (d)** exhibits **non-axisymmetric bifurcation buckling** (black points) **before axisymmetric "snap-through"**. The bifurcation buckling load from linear theory is somewhat higher than that from nonlinear theory in this example.

Deeper (or thinner) plates yet (e, f) exhibit the same type of behavior as (d), with the characteristic equilibrium paths having an increasing degree of the **"doubling back"** feature typical of shells the behaviors of which are extremely sensitive to initial imperfections.

Shell depth $H/h \sim$ radius/thickness

Lambda is a "shallowness" parameter $\lambda = 2[3(1 - \nu^2)]^{1/4} (H/h)^{1/2}$

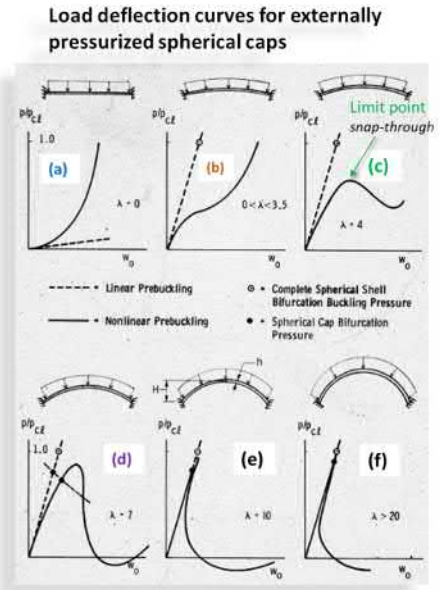


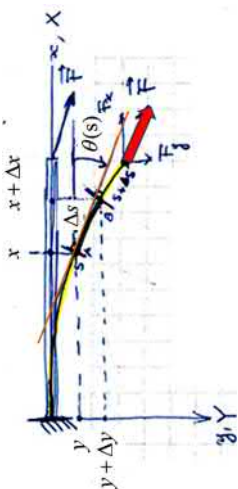
Figure 1.27: Load deflection curves for externally pressurized spherical caps. (Picture and text legend are from the reference below: http://shellbuckling.com/presentations/buckledShells/pages/page_38.html (2018).

1.5.1 Example of full non-linear and the linearised homogeneous problem

Here follows an illustrative example clarifying the main difference between *linearised equations of elastic-stability loss* (eigenvalue problem) and the *full non-linear equations* describing the *post-buckling* behaviour.

Consider the *Euler's Elastica* (Cf. Chapter 4) which consists of a slender elastic rod loaded with a conservative non-following end load P , ($F = (0, -P)$). Just imagine the pole used by Serguey **Bubka**, the legendary pole vaulter. Assume a conservative compressive loading P of such pole at one of its ends. The second end being rigidly clamped. The pole he is using is an perfect example of such Elastica. The problem is to determine the configuration (or the shape) of the pole as the loading changes. Such problem is naturally a non-linear one and is given by the the classical Euler's Elastica problem (Fig. 1.28).

For elastic behaviour the bending moment-curvature relation $M = EI\kappa = -EI\theta'$ holds. Derivations are with respect to the arch-length s . From equilibrium consideration written in the flexural deformed configuration (post-



buckled state), the non-linear post-buckling equation is obtained

$$EI\theta'' + P \sin(\theta) = 0. \tag{1.25}$$

After accounting for the boundary conditions $M(\ell) = 0$ and $\theta(0) = 0$, the above equation can completely be solved³⁹. The solutions (Left part in Fig. 1.28) describe fully the post-buckling configuration as a function of the load P . Therefore, as a conclusion, we can see that the *entire post-buckling behaviour is captured* explicitly by this non-linear problem (Eq. 1.25 and Fig. 1.28). Thus, one can now address naturally the stability nature of such post-buckled configuration and solve the configuration for any given value of the load P (Figure in margin for such configurations for various loadings.).

Now let's see what will be the linearised version of these non-linear equilibrium equations (1.25).

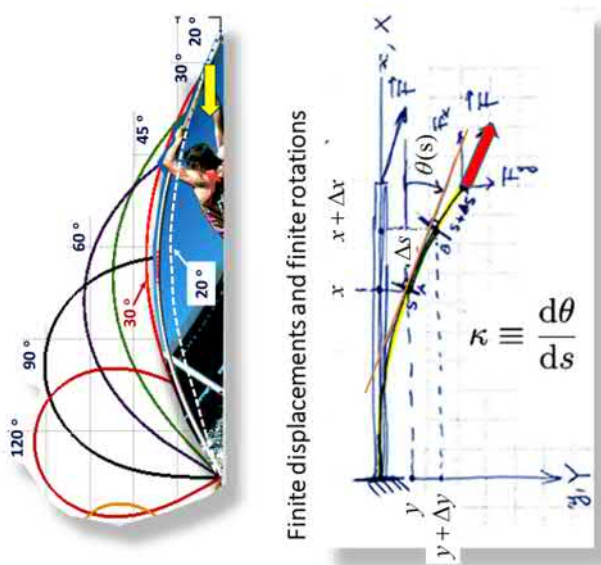
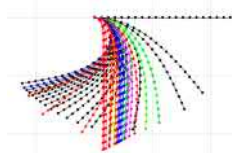


Figure 1.28: Euler's Elastica as a geometrically non-linear problem. The finite curvature being $\kappa \equiv \theta'$. The deflection being v . In the actual example, we have $F = (0, -P)$ a compressive conservative load.

In order to derive the classical Euler's buckling equation as an eigenvalue problem³ which constitutes a linearised system of equilibrium equations for (1.25) in the vicinity of the critical buckling load $P = P_{cr}$ which remains constant during buckling. In addition, the Euler-Bernoulli kinematic, $\theta = v'$,



³ Derived by **Leonhard Euler** in 1757 while investigating buckling of columns.

³⁹Please refer to classical textbooks.

is naturally assumed. The equilibrium non-linear equation (4.6) linearises in the following manner

$$EI\theta''(s) + P \sin(\theta(s)) = 0, \quad (1.26)$$

$$EI\theta''(s) + P\theta(s) = 0, \quad (1.27)$$

$$EIv'''(x) + Pv'(x) = 0, \quad (1.28)$$

when we consider small displacements⁴⁰ $x(s) \approx X(s)$, $y(s) \approx Y(s)$ and rotations for which $\sin(\theta) \approx \theta = v'$. Thus now $s \approx x \approx X$. Derivation once again the last equation above with respect to x , on obtains the classical familiar Euler's buckling equation

$$\boxed{EIv^{(4)}(x) + Pv''(x) = 0}, \quad (1.29)$$

which is the *linearised homogeneous equation of elastic-stability* and, mathematically, represents an *eigenvalue problem*. Therefore, only the critical buckling load can be solved and no information for the post-buckling behaviour can be extracted from the solution of such equation (1.29) using appropriate boundary conditions. In addition, the corresponding Eigenvectors (buckling modes) provides some information about the the corresponding new neighbouring and infinitely close equilibrium configuration up-to a scaling factor. On the contrary with the full non-linear equilibrium equation of the post-buckling of the Elastica, now, no information about the nature of the new equilibrium can be extracted.

* * *

1.6 Types of bifurcational instabilities

The nature of post-buckling behaviour determines to a large extend its safety and the robustness of the structural design. The basic type of *post-critical behaviour* of a structure can be classified into next classes (Figure 1.29):

- *stable symmetric*. Structures having this type of behaviour are always *imperfection insensitive* and have consequently a reserve of resistance
- *unstable symmetric*. This gives imperfection sensitive structures

⁴⁰Capital letters refer to the initial coordinates while the small letter, to the actual configuration, respectively (Material / spatial coordinates).

- *asymmetric or unsymmetrical*. This gives much more severe imperfection sensitive structures than above

To the above post-critical behaviour, one should add the *snap-through* behaviour. Such dynamic behaviour is pathological not desired behaviour and can be seen as asymmetric branching on the equilibrium path.

So, to summarise, bifurcational stability 'loss' can be classified into one of the types of instability shown in Figure (1.29) with examples of structure having such post-critical behaviour.

These types of *bifurcations* are not just nice drawings on paper but such behaviour has been *observed, experimentally*, in real structure as shown, for instance, by Figure (1.30).

Koiter (1945) have shown that for all elastic systems, the initial post-critical behaviour follow the famous asymptotic power law⁴¹: the reduction of the collapse or maximum load $\lambda_{\max}/\lambda_{cr} \equiv P_{\max}/P_{cr}$, for the perfect structure, is reduced proportionally to the 2/3 or 1/2 power of the imperfection magnitude⁴². Usually exponent 1/2 and thus, a higher reduction, is related to asymmetric unstable post-buckling behaviour which more 'sensitive' to perturbation than the symmetric unstable one, for which the exponent is 2/3⁴³. In some frames, the reduction can be moderate. However, for cylindrical shells, it was found that the reduction is significant: the maximum collapse load can be reduced by a factor 1/8 to 1/3 as compared to the buckling load of the perfect structure. In shells such imperfections are inherent and inevitable. (more of this in the Section dealing with shells).

1.6.1 Equilibrium paths for simple rigid bar systems with springs

As told previously, the basics of stability concepts can be accessed by studying examples of simple elastic systems having one, two or more degrees of freedom. With rigid bars, all the strain energy concentrate in the springs. With such systems, we also demonstrate, in addition to the equilibrium paths (load-displacement curves), critical points and so on, the

⁴¹Known as Koiter law or Koiter's 2/3-power and 1/2-power laws.

⁴²Do post-critical study and plot the maximum post-critical load versus the chosen imperfection parameter α . The imperfection parameter can be, for instance, eccentricity, relative initial shape imperfection, etc. It is practical to draw P_{\max}/P_{cr} or $\lambda_{\max}/\lambda_{cr}$ versus the logarithm of the relative imperfection α , for instance a geometric imperfection relative to thickness, in the case of shells. This way, the slope of the straight line will give you the exponent of the power-law.

⁴³Cross-check this; RK?

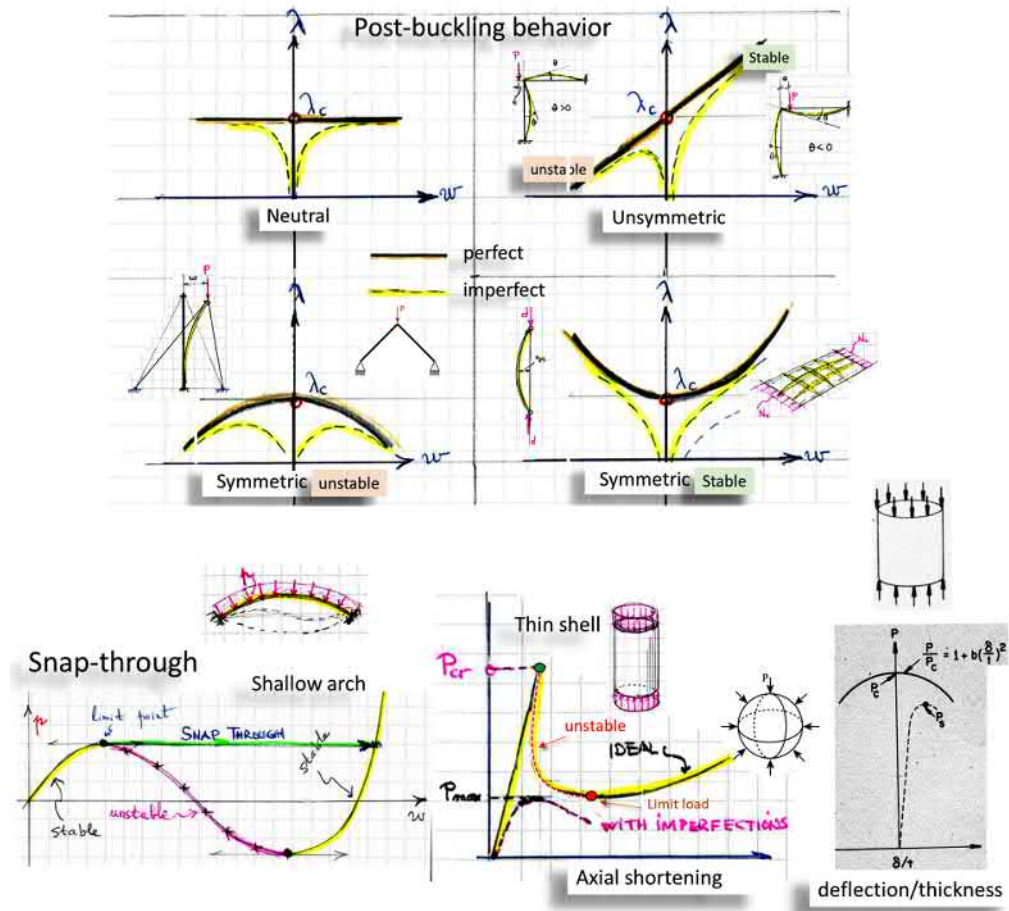
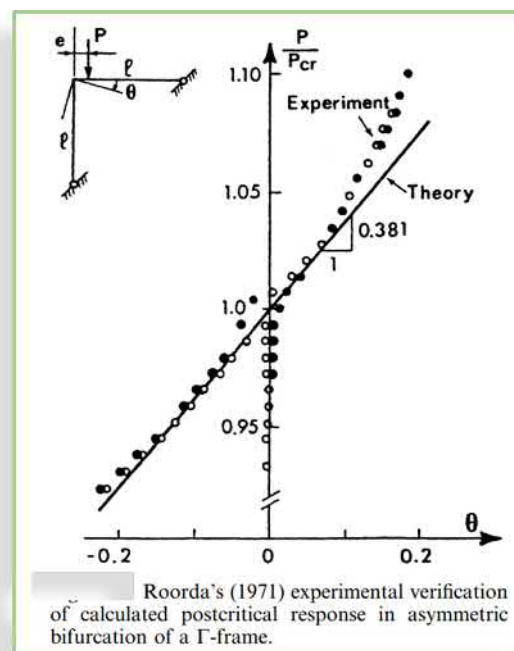


Figure 1.29: Type of loss of stability in buckling (bifurcations) for ideally perfect geometry and with imperfections. Illustrates also the effects of initial imperfections. The load parameter is λ , λ_c , the critical (buckling) load and w being displacement at a control point.

principle difference between full-non-linear equations describing the post-critical state and their linearised homogeneous versions in the vicinity of critical points. For comprehensive readings, the reader is encouraged to refer to textbooks⁴⁴. (see the footnote for proposed examples of readings, in addition to classical Timoshenko's classical textbook on *Theory of Elastic Stability*, 2nd Ed. or later).

⁴⁴1. N. A. Alfutov, *Stability of Elastic Structures*. Springer 2000 (translated from Russian). 2. H.G. Allen. *Background to Buckling*. McGraw-Hill Inc., US (May 1, 1980). 3. J. Robert, *Buckling of bars, plates and shells*. Bull Ridge Publishing. 2006. 4. S.P. Timoshenko & J.M. Gere. *Theory of Elastic Stability*.



Roorda, 1971, *An experience in equilibrium and stability*, Techn. Note No. 3, Solid Mech. Div., University of Waterloo, Canada.

Figure 1.30: Experimental evidence of asymmetric bifurcation in structures. Roorda's (1971) frame experiments (dots and circles). for positive eccentricity $e > 0$ stable behaviour, and unstable for $e < 0$. ($e > 0$ in the Figure)

In the following, we present the general types of equilibrium loss behaviour in terms of 'geometrical' considerations on special points (critical) on equilibrium paths (load-displacement curve) and in terms of critical points on the hyper-surface representation of the total potential energy.

To make it tractable, by hand, the models will have only few degrees of freedom. On the energetic surface, equilibrium points correspond, geometrically, to points on the surface having horizontal tangent-planes ($\delta(\Pi) = 0$). Stability at such points, stability of the local equilibrium, is thus recast as *geometrically* examining the sign of the curvatures at that point. If the curvature is positive in all horizontal directions (convex) then the equilibrium is locally stable, otherwise, if one of the curvatures is negative (concave), the the equilibrium is unstable. The sign of the generalised curvature will be studied in terms of signs of $\delta^2(\Pi)$ (Fig. 1.35).

1.6.2 Stable-symmetric bifurcation model

We are interested to exactly determine all its equilibrium configurations: *pre-buckling* and *post-buckling* configurations. For that, we do an *full non-linear analysis* in analytic form. This task is possible for such simplified rigid bar-springs system. The full-non linear description is necessary since we want also to capture the *post-buckled configuration(s)*. We will see after this example, *linearised version* of this analysis (*linearised buckling problem*) which, of course, will provide us with the buckling load (bifurcation point) but the post-buckled configuration will remain undetermined because of the linearisation.

In the following, the initial reference state is stress-less. The total potential energy of the system in its initial configuration is Π_0 and is constant. Since we will deal with changes $\Delta\Pi = \Pi - \Pi_0$ and changes of its changes with respect to the reference configuration, we decided, in this section, to drop-off the sign Δ from writing to make it a bit lighter.

```

10 %
11 % Global parameters: material properties
12 %
13 % Length of the bar
14 %
15 % Area of the cross-section
16 %
17 % Modulus of elasticity
18 %
19 % Initial angle
20 %
21 % Load
22 %
23 %
24 %
25 %
26 %
27 %
28 %
29 %
30 %
31 %
32 %
33 %
34 %
35 %
36 %
37 %
38 %
39 %
40 %
41 %
42 %
43 %
44 %
45 %
46 %
47 %
48 %
49 %
50 %
51 %
52 %
53 %
54 %
55 %
56 %
57 %
58 %
59 %
60 %
61 %
62 %
63 %
64 %
65 %
66 %
67 %
68 %
69 %
70 %
71 %
72 %
73 %
74 %
75 %
76 %
77 %
78 %
79 %
80 %
81 %
82 %
83 %
84 %
85 %
86 %
87 %
88 %
89 %
90 %
91 %
92 %
93 %
94 %
95 %
96 %
97 %
98 %
99 %
100 %

```

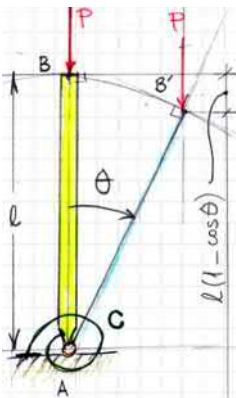
Matlab-code used to produce the energy surface.

Axially loaded perfect structure

Let's consider the axially loaded ideal structure in Figure (1.34) which is initially perfectly straight (no-imperfections, yet).

It is sufficient to consider only it's half as in the margin figure or Figure (1.35). The total potential energy change Π between the straight initial equilibrium configuration (yellow) and the perturbed one (blue) is

$$\Pi = \frac{1}{2}c\theta^2 - P\ell(1 - \cos\theta). \tag{1.30}$$



Straight equilibrium configuration (yellow), perturbed (blue).

For illustrative purposes, the surface representing total potential energy is reproduced in Figure (1.31). Now, everything becomes geometrically more clear: equilibrium corresponds, on the topography, to local extrema: points having a horizontal tangent plane ($\rightarrow \delta\Pi = 0$, not varying P). Stable equilibrium configurations corresponds to local minima (convexity $\rightarrow \delta^2\Pi > 0$), and so on. Just walk, or let a small ball rolling on this surface and feel where you're naturally will go. The equilibrium paths correspond to configurations for which

$$\delta\Pi = 0 \implies \frac{d\Pi}{d\theta} \equiv \Pi' = c\theta - P\ell \sin\theta = 0. \tag{1.31}$$

Consequently, equilibrium configuration is achieved for

$$\theta = 0 \quad \text{or} \quad P = \frac{c}{\ell} \cdot \frac{\theta}{\sin\theta}, \theta \neq 0. \tag{1.32}$$

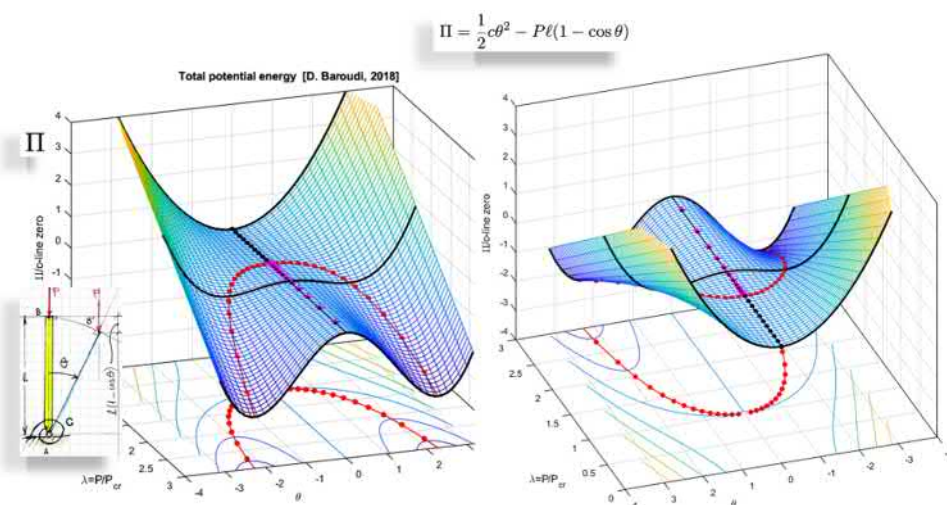


Figure 1.31: Total potential energy represented by a 3D-surface having a topography. The local extrema (big dots-lines) corresponds to equilibrium configurations. (Try to recognise the load-displacement curves (equilibrium path) on the level-curves on the horizontal plane).

The trivial equilibrium $\theta = 0$, corresponds to the initial straight configuration (no buckling), branches AB and BC . The *primary equilibrium path*, prior to buckling, corresponds to branch AB . The remaining equation

$$P = \frac{c}{\ell} \cdot \frac{\theta}{\sin \theta} \quad \text{or} \quad \frac{P}{P_{cr}} = \frac{\theta}{\sin \theta}, \quad \text{with notation} \quad \frac{c}{\ell} \equiv P_{cr} \quad (1.33)$$

corresponds to the secondary equilibrium branches BD and BD' and deviates from the vertical configuration since $\theta \neq 0$.⁴⁵ Because θ can be positive (the move to right side of the vertical) or negative (moves to the left side), we see that both solutions are possible. So now at the point ($\theta = 0, P = c/\ell$) the number of equilibrium configurations changes from one (straight, $\theta = 0$) to two: $\theta > 0$ or $\theta < 0$. This point, on the equilibrium path (load-displacement curve) is called a *bifurcation point*⁴⁶. The critical value of the load at this point

$$P = \frac{c}{\ell} = P_{cr} \quad (1.34)$$

is called the *buckling load* (Fig. (1.33)).

⁴⁵If we are interested in what happens, after buckling, in the vicinity of $\theta = 0$, one should take the $\lim_{\theta \rightarrow 0^*} [P] = \lim_{\theta \rightarrow 0^*} [c/\ell \cdot \theta/\sin \theta] \rightarrow c/\ell \equiv P_{cr}$. This is a linearisation at the bifurcation point.

⁴⁶The number of solutions changes from one to two or more.

Now comes the question of *stability of the equilibrium* points and branches. For this purpose, the sign of the second variation

$$\delta^2\Pi \implies \frac{d^2\Pi}{d\theta^2} \equiv \Pi'' = c - P\ell \cos\theta. \quad (1.35)$$

has to be investigated on the primary path $\theta = 0$ and on the secondary path where $P = (c/\ell) \cdot (\theta/\sin\theta)$, respectively.

$$\Pi''(\theta) = c - P\ell \cos\theta > 0$$

Stability of Equilibrium on the
secondary path: $\text{sign } \Pi''|_{P=c/\ell \cdot \theta/\sin\theta}?$

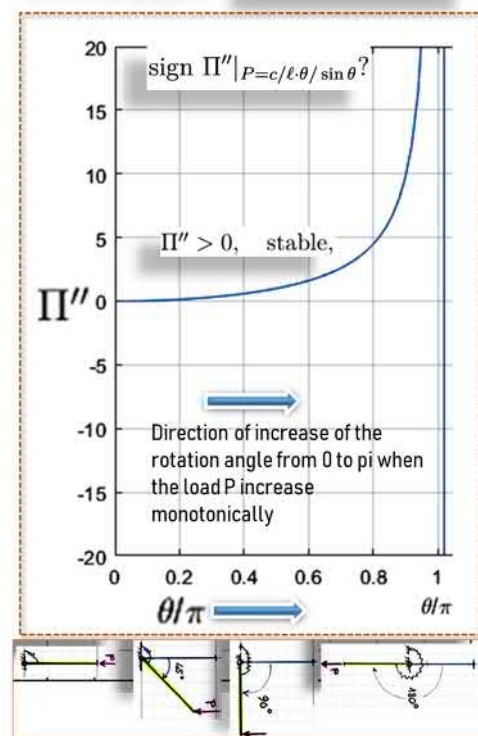


Figure 1.32: Stability of an equilibrium: Sign of the second derivative of the total potential energy.

Let's study the sign of the second derivative

$$\text{sign } \Pi''|_{\theta=0} \quad \text{sign } \Pi''|_{P=c/\ell \cdot \theta/\sin\theta} \quad (1.36)$$

and rewrite it in the form after dividing by the positive spring coefficient $c > 0$. let's check, for instance, for stable branches the sign of

$$\Pi'' = c - \ell \cos\theta = c(1 - \theta \cos\theta / \sin\theta) > 0, \text{ where } c > 0 \quad (1.37)$$

on the post-buckled path (secondary path) is shown graphically in Figure (1.32). Therefore, that the second derivative $\Pi'' > 0$ for all the secondary path. The double-prime meaning twice derivative with respect to θ . The whole equilibrium paths is reproduced in Figure (1.33).

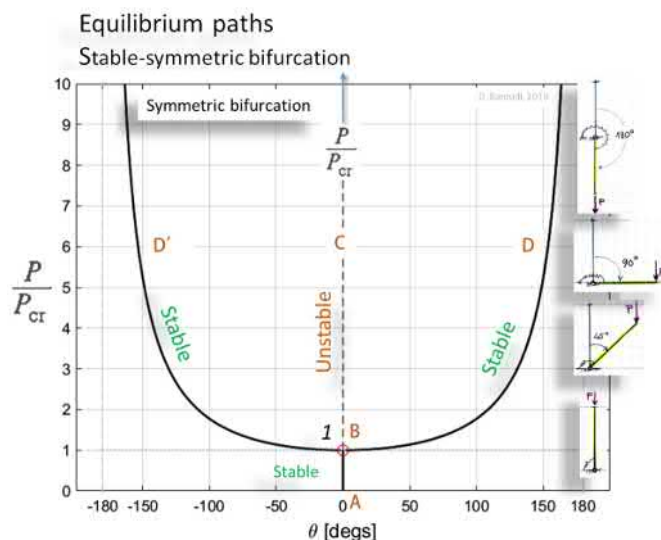


Figure 1.33: Symmetric bifurcation. Note the stiffening effects close to $|\theta| \rightarrow \pi$

Stability of equilibrium

Let's study the sign of the second derivative $\Pi''(\theta) = c - P\ell \cos \theta$ (Eq. 1.35)

- **trivial case:** $\theta = 0$ (branches AB and BC)
 - so the sign of the second derivative $\Pi''|_{\theta=0}$ on the primary path $\theta = 0$ should be considered:
 - 1.1) $\Pi''(\theta = 0) = c - P\ell = 0 \implies P_{cr} = c/\ell$ (we have a *bifurcation point* at B since the second derivative Π'' changes sign) (P_{cr} is called the **buckling load**).
 - 1.2) $AB, \theta = 0: \Pi''(0) = c - P\ell > 0 \implies P < P_{cr}$ (AB stable)
 - 1.3) $BC, \theta = 0: \Pi''(0) = c - P\ell < 0 \implies P > P_{cr}$ (BC unstable)
- **post-bucked case:** $\theta \neq 0$ (branches BD and BD')
 - so, the second derivative should be evaluated on the secondary branch $P = \frac{c}{\ell} \cdot \theta / \sin \theta$:

Eq. (1.35) $\rightarrow \Pi''(\theta) = c - Pl \cos \theta > 0? \implies$ the sign of $\Pi'' = c - l \cos \theta = c(1 - \theta \cos \theta / \sin \theta) > 0$, where $c > 0$, so we have always $\Pi'' > 0$ for $\theta \in [0, \pi]$ (see Fig. 1.33)

So $\rightarrow BD$ and BD' stable).

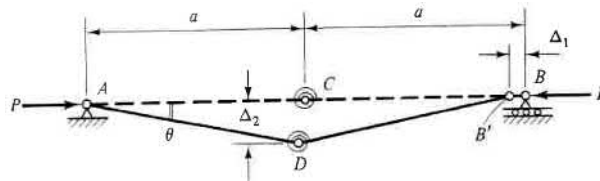


Figure 1.34: Ideal rod-spring structure exhibiting stable-symmetric bifurcation. (a re-dessiner).

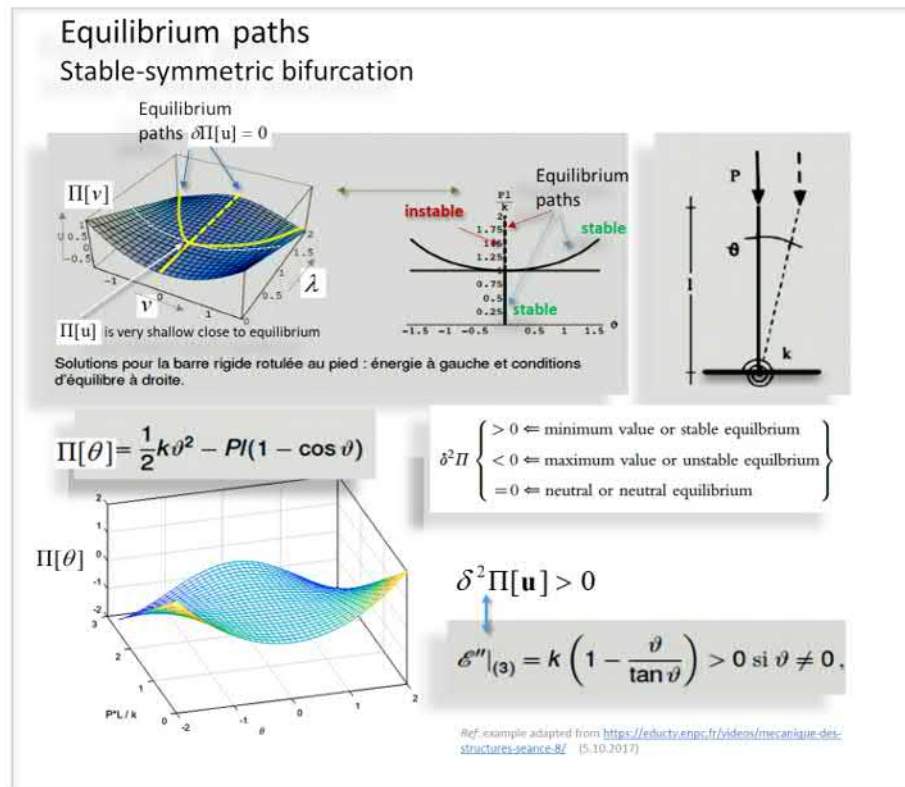


Figure 1.35: Equilibrium paths. Stable-symmetric example.

Linearised model

Let's now linearise the total potential energy (Eq. 1.30) around the neutral equilibrium position $\theta = \theta_0 = 0$ and see what is the *fundamental* the differences we obtain as regarded to the full non-linear analysis performed just above in which all the equilibrium branches were completely *determined*.

Expanding in Taylor's series the work of external forces with respect to θ and retaining up-to the quadratic terms gives

$$\Pi(\theta; P) = \frac{1}{2}c\theta^2 - P\ell(1 - \cos \theta) \approx \frac{1}{2}c\theta^2 - P\ell \cdot \frac{\theta^2}{2}. \quad (1.38)$$

Now the equilibrium condition $\delta(\Delta\Pi) = 0$ leads to

$$\boxed{\Pi' = c\theta - P\ell\theta = (c - P\ell) \cdot \theta = 0} \quad (1.39)$$

which represent the *homogeneous linearised equation of (loss) of stability* in the vicinity of $\theta_0 = 0$. We see clearly that the linearised problem (1.39) became an *eigenvalue problem*. Compare them to their non-linear expression (Eq. 1.31). This means that, one can only solve for the eigenvalue (the smallest one correspond to the buckling load P_{cr}) and the corresponding eigenmodes (the buckling modes). The amplitude of the buckling modes remains, naturally, undetermined as a consequence of the linearisation. Recall that for the full non-linear model, both pre-buckled⁴⁷ and post-buckling⁴⁸ behaviour was exactly solved (Eq. 1.32).

Let solve the stability loss problem: $(c - P\ell) \cdot \theta = 0$, (Eq. 1.39)

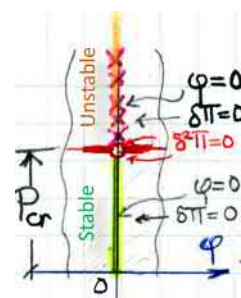
- **no buckling:** $\theta = 0$, is a solution (trivial initial straight $A - B - C$)
- **buckling:** $\theta \neq 0 \implies c - P\ell = 0 \implies P_{cr} = c/\ell$ (buckling load)

So, we see that one can determine the buckling load from the criticality condition on the linearised problem as $\det(c - P\ell) = 0$. However, as you see, we cannot determine the amplitude of θ , we just know that it is non zero (Figure in margin). However, we can check for the nature of stability of the critical point B and of the initial straight equilibrium of branches AB and BC . for this, we study the signs of the second variation $\delta^2\Pi$ of the linearised version

$$\Pi'' = c - P\ell. \quad (1.40)$$

⁴⁷the primary initial equilibrium configuration

⁴⁸the behaviour after the bifurcation point



Linearised criterion.

Consequently, $\Pi''(0) = c - P\ell > 0 \implies P < P_{cr}$ (*AB stable*). On the opposite, branch *BC* is unstable, since there $c - P\ell < 0$ for $P > P_{cr}$. One question still unresolved! What is the nature of stability at the bifurcation point *B* for $\theta = 0$? Can we decide by the criteria of the sign of second variation? Let's see:

$$\Pi''(\theta = 0; P = P_{cr}) = c - P_{cr}\ell = c - \frac{c}{\ell} \cdot \ell = 0. \quad (1.41)$$

One may wrongly or too fast, conclude that the equilibrium is *indifferent*. However, this is not true and this result is an artefact of the linearisation. We should take higher order⁴⁹ (than quadratic) terms in the expansion of $W_{ext.}(\theta; P) = -P\ell(1 - \cos \theta)$ with respect to θ , in order to decide (the sign) of the stability at the bifurcation point. For instance, the expansion $\cos \theta \approx 1 - \theta^2/2 + \theta^4/4!$ can solve the sign problem. This, physically, means that we use a *asymptotic expansion of non-linear equations* and capture the moderate rotations and displacements around $\theta = 0$.⁵⁰ *What should be re-*

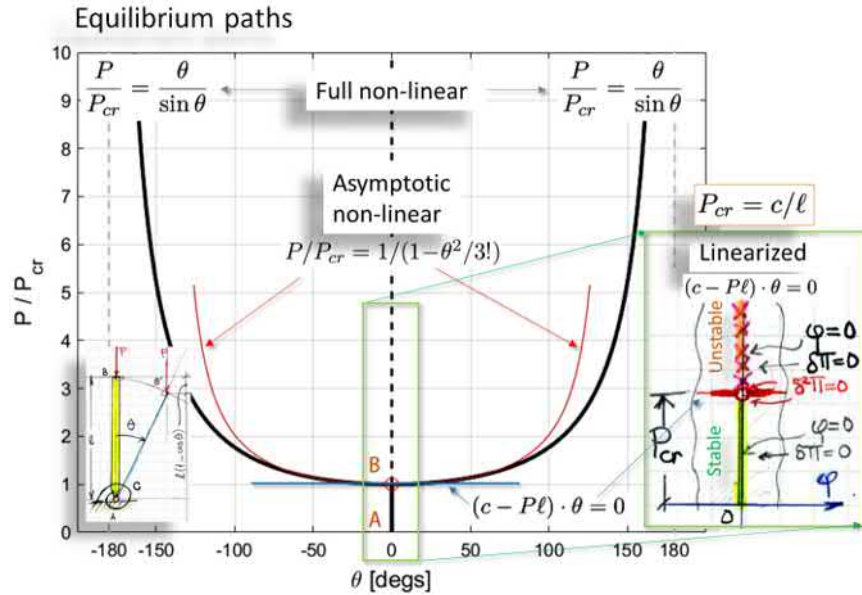


Figure 1.36: Equilibrium paths. Full non-linear model (black), asymptotic non-linear model (orange) and the linearised model (right side).

tained? The homogeneous linearised equations⁵¹ cannot give information on

⁴⁹ $\dots + \delta^2\Pi + \delta^3\Pi + \delta^4\Pi + \dots$

⁵⁰ The total potential energy will be $\Pi = 1/2c\theta^2 - P\ell\theta^2/2 + P\ell\theta^4/4!$ and $\Pi' = (c - P\ell)\theta + P\ell\theta^3/3!$. I let the reader continue solving the problem. I have no time for this now.

⁵¹ obtained through linearisation of the energy criterion

the type of bifurcation point (stable? unstable? indifferent?) nor they can provide the amplitude of the finite displacements (*Cf.* the right-side small figure in Fig. (1.36).) (known only up-to a multiplicative coefficient). However, they provides us with the buckling load and the associated buckling modes, exactly. For normal structural design, this knowledge is sufficient, since, subsequent failure is very probable to occur as a consequence of buckling. Failure may occur in buckling element, or at the joints or elsewhere as a consequence of excessive displacements and rotations. So, on need to quantify these post-buckling displacements and rotations to do the correct structural design.

Post-buckling analysis - asymptotic non-linear approach

Taking up-to fourth-order terms in $\cos \theta$ leads to the total potential energy and it's first derivative ($= \delta(\Delta\Pi)$)

$$\Pi = 1/2c\theta^2 - P\ell\theta^2/2 + P\ell\theta^4/4! \quad (1.42)$$

$$d\Pi/d\theta = (c - P\ell)\theta + P\ell\theta^3/3! = 0. \quad (1.43)$$

The above non-linear equation (the second one), as for the full non-linear system (1.32), has two solutions:

$$\theta = 0, \forall P \quad \text{or} \quad P = \frac{P_{cr}}{1 - \theta^2/3!}, \quad P_{cr} = c/\ell, \theta \neq 0. \quad (1.44)$$

Now, Equation (1.44) provides the post-buckling configuration for moderate rotations. One sees that $P = c/\ell \equiv P_{cr}$ is indeed a bifurcation point, since a non-trivial equilibrium exist in vicinity of trivial primary equilibrium ($\theta = 0$, vertical bar) for a tiny deviation from $\theta \rightarrow 0^{*52}$, as given by $P/P_{cr} = 1/(1 - \theta^2/3!)$.

The overall comparison of the various models used is summarised in Figure (1.36). One sees that the *asymptotic non-linear model* permits to follow rotations up-to 75 degrees (visually estimated). This is what is about in *post-buckling analysis* and this is a post-buckling analysis. So what we did? Firstly, we did analytically post-buckling analysis. secondly, this general approach, *asymptotic analysis*, permits to study analytically (or numerically) the post-buckling behaviour of more complex structures. In this lectures note, some illustrative examples will be provided. [to do: 22.1.2019]

^{520*} is the closest real to zero without being itself zero.

1.7 Effects of imperfections

1.7.1 Symmetric Stable bifurcation

Axially loaded structure with imperfections: Consider the axially loaded structure in Figure (1.37) having initial imperfection in its horizontality or a tiny transverse load $F_v \ll P$.

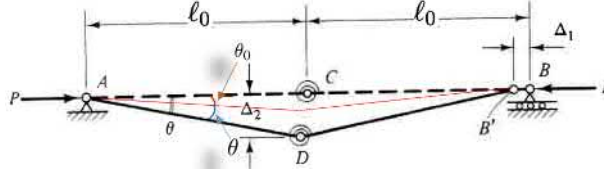


Figure 1.37: Axially loaded structure with initial imperfection θ_0 . the rotational spring stiffness is c . (*symmetrical stable*).

$$\Pi = \frac{1}{2} c [2(\theta - \theta_0)]^2 - 2P\ell_0(\cos \theta - \cos \theta_0). \quad (1.45)$$

Stationarity condition

$$\delta\Pi = 0 \implies \frac{d\Pi}{d\theta} = 0 \implies \frac{P}{P_{cr}} = \frac{\theta - \theta_0}{\sin \theta}, \quad P_{cr} = \frac{2c}{a}. \quad (1.46)$$

The effect of lack of straightness (initial imperfection angle $\theta_0 = [0, 0.1, 1, 2, 5]$ degrees.)

Should remind, students from time to time that for real structure, rotation over elasticity range lead to damage or plastic yielding. This makes the Load-displacement curve in Figure (1.38) having a limit-point (the dashed grey line in the figure) for the maximum load-bearing capacity before failure.

1.7.2 Unstable-symmetric bifurcation model

Axially loaded perfect structure: Initially perfectly horizontal configuration. No imperfections are present. The translational degrees of freedom u, v can be expressed in terms of the rotation θ as $v \equiv \Delta_2 = \ell_0 \sin \theta$ and $u \equiv \Delta_1 = 2\ell_0(1 - \cos \theta)$ (Fig. 1.39) and obtains

$$\Pi = \frac{1}{2} k v^2 - P\ell_0(1 - \cos \theta) \quad (1.47)$$

$$= \frac{1}{2} k \ell_0^2 \sin^2 \theta - 2P\ell_0(1 - \cos \theta). \quad (1.48)$$

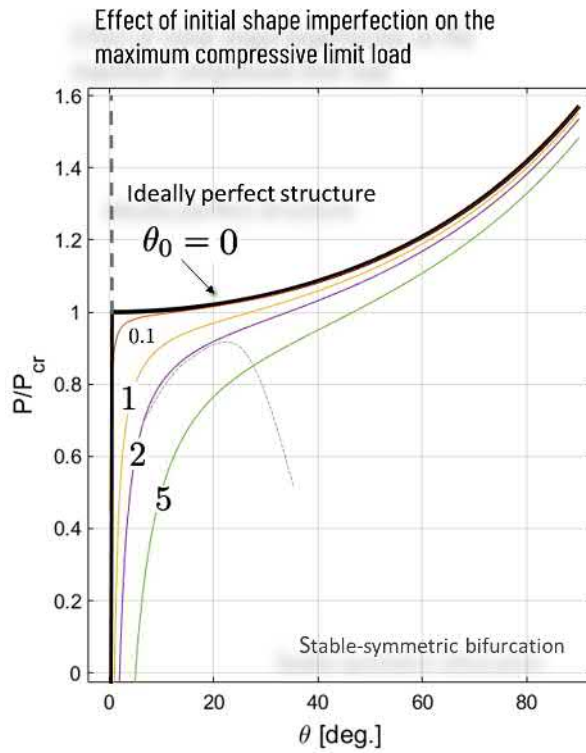


Figure 1.38: Load-displacement curve. Effects of geometrical imperfections as deviation angle θ_0 [degrees] from straightness for structure in Figure (1.37) (*symmetrical stable*). For real structure, rotation over elasticity range (elasto-plasticity, for instance) leads to damage or yielding making load-displacement curve having a limit-point (dashed grey line in the figure).

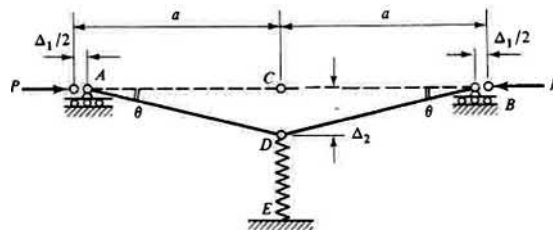


Figure 1.39: Equilibrium paths. Unstable-symmetric example. (re-dessiner à la main)

The equilibrium paths correspond to

$$\delta\Pi = 0 \implies \frac{d\Pi}{d\theta} = kl_0^2 \sin\theta \cos\theta - 2Pl_0 \cdot \sin\theta = 0 \quad (1.49)$$

Equation (1.49) defines the equilibrium paths (load-displacement curves).

Equilibrium is satisfied for $\theta = 0[\pi]$ (= zero *modulo* π), or for

$$P = \frac{k\ell_0}{2} \cos \theta = P_{cr} \cos \theta, \quad \text{where } P_{cr} \equiv \frac{k\ell_0}{2}. \quad (1.50)$$

Let's check for the stability of the obtained critical point $P_{cr} = k\ell_0/2$. This is achieved by inserting the value of the critical load in Equation (1.49) and then taking again the derivative $d(d\Pi/d\theta) = d^2\Pi/d\theta^2$ and check for the sign. If the second derivative vanishes, then one should take higher derivatives till non-zero⁵³ value is achieved, for this case, for the sign of $\delta(\Delta\Pi)$.

The stability of branches on the equilibrium curve is determined by studying the signs of $\delta^2\Pi$ which are given by the second derivative $d^2\Pi/d\theta^2$. One see (1.40 that bifurcation⁵⁴ of the equilibrium occurs for $\theta = 0$ at the critical load $P_{cr} = k\ell_0/2$. The vertical branch, for $\theta = 0$ until $P < P_{cr}$ is stable and for higher $P > P_{cr}$ becomes unstable. The symmetric branches $0 < |\theta| < \pi$ are unstable. so after the bifurcation, all the possible three paths (AB' , AB and AD) are unstable. Therefore, the structure from the critical point P_{cr} , even when the load is kept constant, will directly collapse to configuration $\theta = \pi$ where it becomes stable. However, it is too late) for the structure. This sudden (unstable) transition to this end point can be seen as a snap-through.

Axially loaded structure with imperfections: Consider the axially loaded bar-spring system of Figure (1.39) which had no imperfections. Lets add to it now an initial imperfection or a deviation from a perfect straight geometry, let's say an initial angle θ_0 as shown in Figure (1.41). We have now introduced a tiny imperfection in its horizontality: Such imperfection can also be introducing a small transverse load $F_v \ll P$.

The total potential energy is now

$$\Pi = \frac{1}{2}k\ell_0^2(\sin \theta - \sin \theta_0)^2 - 2P\ell_0(\cos \theta_0 - \cos \theta). \quad (1.51)$$

The equilibrium condition $d\Pi/d\theta = 0$ leads, after some algebraic manipulations, to the equation

$$\frac{P}{P_{cr}} = \left(1 - \frac{\sin \theta_0}{\sin \theta}\right) \cos \theta, \quad P_{cr} = k\ell_0/2. \quad (1.52)$$

⁵³Indifferent equilibrium is not possible as shown by the derived graphs (equilibrium paths).

⁵⁴Means existence of more than one equilibrium configurations.

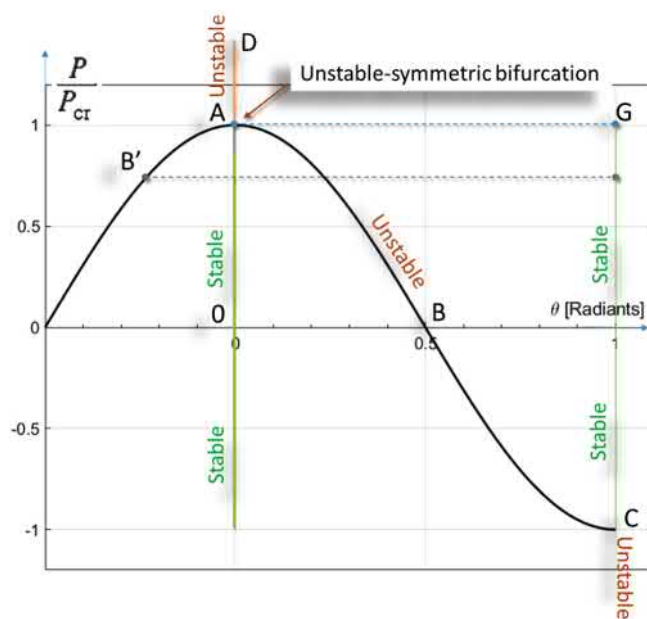


Figure 1.40: Equilibrium path. Unstable-symmetric.

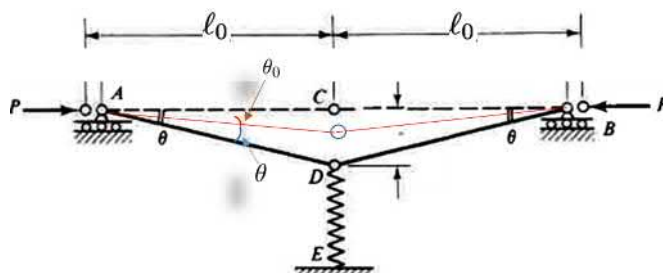


Figure 1.41: Axially loaded structure with initial imperfection (*symmetrical unstable*). The spring stiffness is k .

which is graphically reproduced in next Figure (1.42) for various values of the imperfection parameter θ_0 . The *locus of maxima* are at the points $(\theta, P/P_{cr})$ such that

$$\sin \theta = (\sin \theta_0)^{1/3}, \quad P/P_{cr} = \left[1 - (\sin \theta_0)^{2/3} \right]^{3/2}. \quad (1.53)$$

These points are found by finding the maximum of function defined by Equation (1.52).

In addition, to bifurcation analysis with imperfection, the maximum loading capacity P/P_{cr} (maximum axial load that can be carried) as a function of the relative magnitude of the imperfection θ_0/θ_{ref} will be produced analytically and graphically (Figures 1.42 & 1.43). The reduction of the

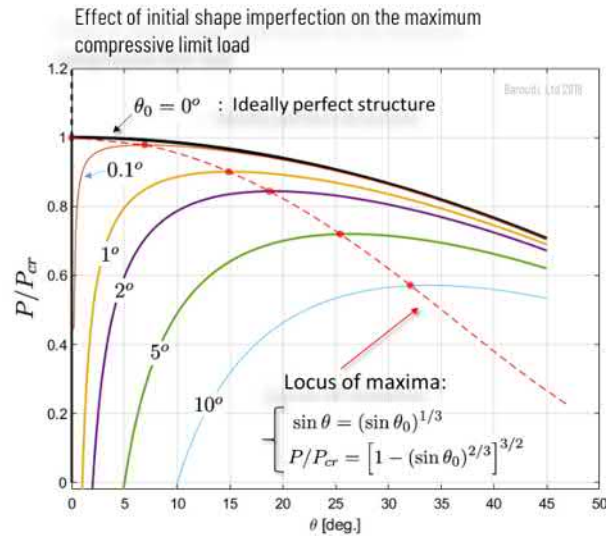


Figure 1.42: Load-displacement curve (unstable symmetric-bifurcation). Effects of various values of initial imperfections for the structure in Figure (1.41). Initial behaviour for the ideally perfect structure (Black line). The remaining continuous lines correspond to the response of the imperfect structure. The reduced axial capacity is the locus of maxima (red-dotted line).

maximum axial load increases with the increase of the relative size of the imperfection. This reduction follows the well-known **Koiter** 2/3-power law for the imperfection effects on the collapse load. The curve of the reduced axial capacity correspond to the locus of maxima shown by the red-dotted line in Figure (1.42). The reduction of the maximum axial force with respect to the amplitude of initial imperfection is shown in Figure (1.43). So, initial shape imperfections reduces the maximum axial load; the reduction is already by half for $\theta_0 \approx 12.5$. This is why, in structural design and analysis, such effects should always be included. The critical load of the ideally perfect structure $P_{cr} = k\ell_0/2$ was obtained in the previous example.

Good to keep in mind: The behaviour depicted in Figures (1.42) and (1.43) is also analogous for thin shells in compression. Thin-shells are imperfection-sensitive structures. Both structures, the column with an initial imperfection (angle θ_0 of departure from the axis of compression) and a thin cylindrical shell, for instance, having initial shape-imperfection w_0/t (a relative departure from ideal cylindrical geometry) behave the same way after the bifurcation points (buckling). Just after this point, there is a relatively 'long' unstable branch (snap-through). Consequently, the absence

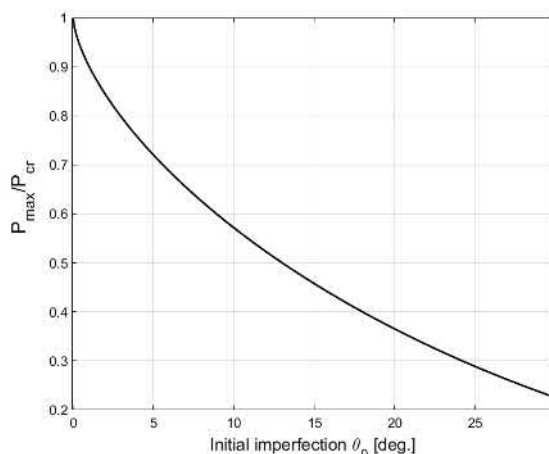


Figure 1.43: Maximum axial force reduction with respect to the amplitude of initial imperfection. P_{cr} is the collapse or buckling load of the perfect structure.

of a stable branch after the bifurcation points render such structure sensitive to imperfections. (More about this topic in the section dealing with shells.). On the contrary, for instance, flat plates, are not imperfection-sensitive since their post-buckling behaviour is symmetric-stable type. This means that there is a stable branch immediately after bifurcation.

1.7.3 Asymmetric bifurcation model

Two examples to illustrate the concept of *limit-load* will be given. The key point is that there is no *bifurcation point* where the primary equilibrium *branches* to neighbouring equilibria. Now, the critical-point is a *limit point* with no-branching. Beyond this point, the nature of equilibrium changes from stable to unstable (or reciprocally).

The first example is a simplified model of the **Mises** truss and the second example is the Mises truss, itself. (may I will change the order, later).

Snap-through model

We consider here a model of structure having a snap-through behaviour (Figure 1.44). This physical model is similar to the classical simple two-bars elastic truss (von Mises truss⁵⁵) in which the stretching of the elastic bar is accounted, here, by the spring k . Note that, especially when reading

⁵⁵In von Mises truss the support do not move. The axial stiffness of the elastic bars is $EA/(\ell/\cos \alpha)$, where ℓ being the length of the bar.

the diagram in Figure (1.45), the angular deformation is $\alpha - \theta$ and initial value for $\theta(P = 0) = \alpha$.

The total potential energy increment is

$$\Pi = \frac{1}{2}k(2L)^2(\cos \theta - \cos \alpha)^2 - PL(\sin \alpha - \sin \theta). \quad (1.54)$$

The equilibrium $d\Pi/d\theta = 0$ gives

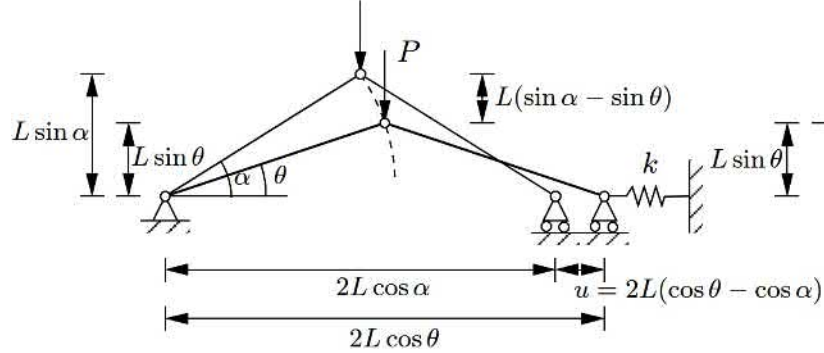


Figure 1.44: Truss for demonstrating similar snap-through behaviour of shallow arches and shells. (Ref. Emer. prof. M. Tuomala. *Rakenteiden Stabiilisuusteoria*.)

$$\frac{P}{4kL} = \sin \theta - \tan \theta \cos \alpha = \sin \theta(1 - \cos \alpha / \cos \theta) \quad (1.55)$$

Equilibrium and stability of the truss illustrated in Figure (1.44) will be investigated. Such simplified model represent well the stability behaviour of shallow arches and shells. The characteristic loss of stability phenomenon is known as *snap-trough*.

Snap-through is by nature a dynamic phenomena where the external forces are not any more equilibrated by the internal forces generated by deformation of the structure. The unbalanced difference in forces generates accelerated motion according to Newton's law of motion (At points B and B' in Figure 1.45). The structure or its part will have a dynamic motion till the internal forces are again equilibrated by the internal forces generated by an excess of deformation. After that, it behaves quasi-statically when the load is applied very slowly. At this stage the structure works more like a membrane. It is this dynamic behaviour which is called snap-through.

The equilibrium path for (Equation 1.55) is schematically drawn in Figure (1.45). The stability of the equilibrium is determined by the sign of the

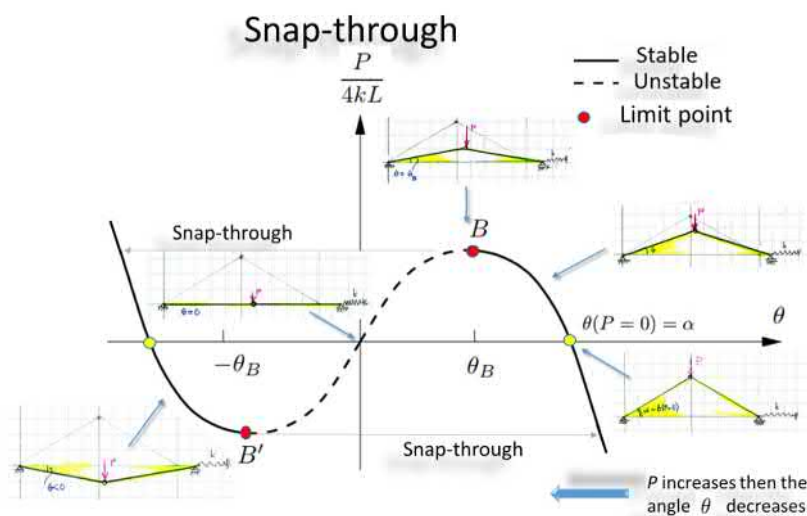


Figure 1.45: Snap through illustration. Note that the starting value for θ is not 0 but $\alpha > 0$, so $\theta(P = 0) = \alpha$ and when $\theta = 0$ the truss achieve a horizontal configuration. This graph becomes easier to read if you make the variable change $\alpha - \theta$ which correspond to the angular deformation *N.B.* To be able to follow (capture) the unstable branch (dotted-line) when performing computational (static) linear buckling analysis, one should use displacement-control. In general, adequate numerical schemes to capture the complete equilibrium path (modified **Riks** method) are implemented in good FE-software. In addition, since the phenomenon of snap-through is transient, only full dynamic analysis will reveal what happens really between to consecutive stable configurations.

second variation

$$d^2\Pi/d\theta^2 = 4kL^2(\cos \alpha / \cos \theta - \cos^2 \theta). \quad (1.56)$$

The zeros of the second derivative are

$$\theta = \pm \arccos[(\cos \alpha)^{1/3}] \equiv \pm\theta_B \quad (1.57)$$

Therefore

$$\Pi'' > 0, \quad \text{when } \theta < 0 \text{ and } \theta > \theta_B, \quad (1.58)$$

$$\Pi'' < 0, \quad \text{when } -\theta_B < \theta < \theta_B. \quad (1.59)$$

To fix the ideas, we have for instance, for an initial angle $\alpha = 30^\circ$, $\theta_B = \pm 17.6^\circ$ a bit more than half of α and consequently, $P = \pm 0.028 \cdot 4kL$.

This example is incomplete [TO DO]

Snap-through model of Mises truss

The following example illustrate the concept of *limit-load*. The idealised structure, known by Mises Truss, consists of two straight elastic bars of equal length connected to each other by a hinge and to the fixed supports. The supports allow free rotations only (Figure 1.46). The truss considered here is shallow⁵⁶ h/ℓ in order to obtain the snap-through and demonstrate the limit-load concept. The load P is kept increasing quasi-statically and we want to solve the force-displacement curve (equilibrium paths). So, let $k = EA/\ell$ the elasticity coefficient of stretching. Here, we assume⁵⁷ the bars designed such that flexural buckling will not occur. Through equilibrium⁵⁸ considerations one can directly determine the internal axial member force (equal in the bars)

$$N = \frac{P}{2 \sin \theta} = \frac{P\bar{\ell}}{2(h-v)}, \quad (1.60)$$

where

$$\bar{\ell} = \sqrt{\ell^2 + v^2 - 2vh}. \quad (1.61)$$

wher the axial shortening (stretching) is

$$\Delta(v) = \ell - \bar{\ell} = \ell - \sqrt{\ell^2 + v^2 - 2vh}. \quad (1.62)$$

Finally, the load-displacement 'curve' is given by (in the long version)

$$P \frac{\sqrt{\ell^2 + v^2 - 2vh}}{2k(h-v)} = \ell - \sqrt{\ell^2 + v^2 - 2vh} \quad (1.63)$$

One should make the above relation non-dimensional by dividing (scaling) P by kh^3/ℓ^2 . However, for *shallow trusses*⁵⁹ we have $h \ll \ell$, so we can simplify⁶⁰, and obtains the needed equilibrium relation

$$\frac{P\ell^2}{kh^3} = 2\delta - 3\delta^2 + \delta^3, \quad (1.64)$$

⁵⁶For non-shallow truss, one should consider both displacement components u and v for the tip. Dependently on the relative height h/ℓ the stability loss can occurs through bifurcation or snap-through, for high and shallow truss, relatively.

⁵⁷This 2D truss is only a simplified **example** used to illustrate the **general concept** of *limit-load*. So, be careful to not mix general concepts and the examples used to illustrate them. The concept is very general, the example is particular mean helping passing the concept.

⁵⁸TO DO: Treat this example by energy method, otherwise, it becomes practically 'intractable' to treat the stability of equilibrium branches.

⁵⁹Snap-through becomes important for shallow structures; arches, trusses.

⁶⁰ $\sqrt{1 \pm \epsilon} \approx 1 \pm \epsilon/2$.

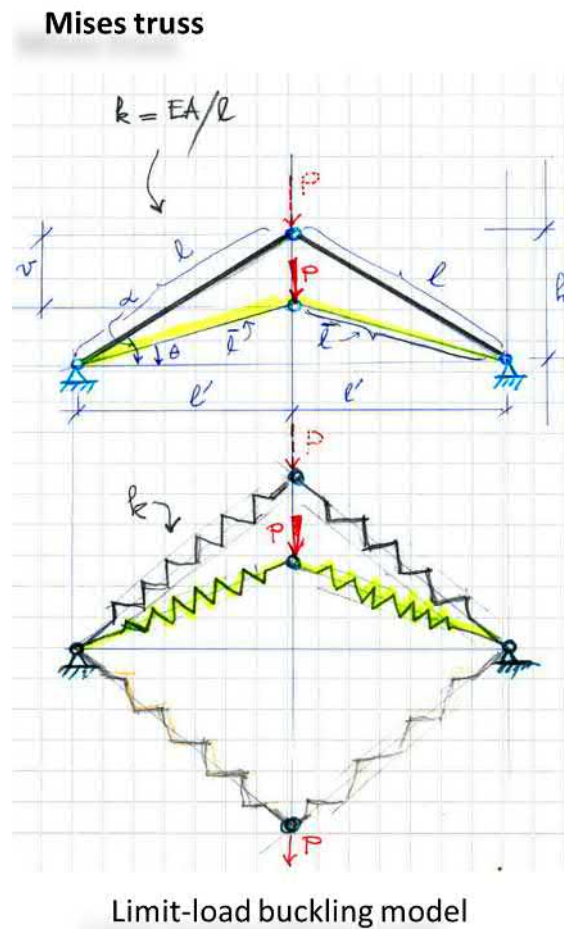


Figure 1.46: Snap through illustration

where $\delta = v/h$. We see already, based on our high-school studies, that this third order polynomial behaviour is rich in limit- and inflection-points. Let's express all this graphically (Figure 1.47). During increase of load P from 0 the maximum point 1, the structures resists (stable path). beyond the point 1 (till 3) the behaviour becomes, suddenly, unstable. The critical point 1 corresponds to a limit-point and the critical load is called limit-load.

Study the stability of the paths shown on the figure using energy criterion.

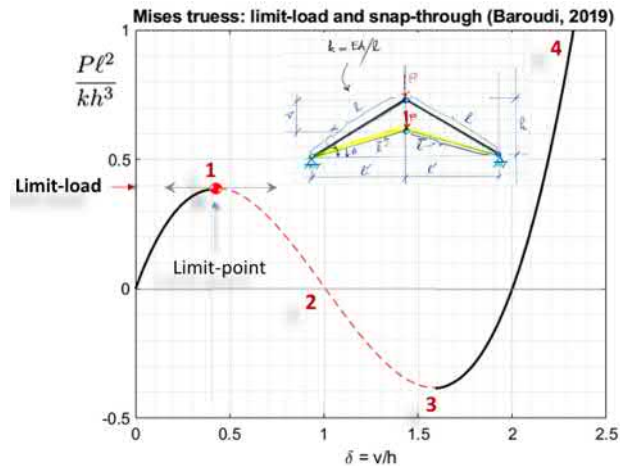


Figure 1.47: Illustration of limit-load. Load-displacement curve, stable continuous line(black) and unstable, dashed-line (red). (Curve valid for shallow truss.)

Asymmetric bifurcation of a two degrees of freedom rigid bars-springs system

In this example we will study the stability of an ideally perfect system in two steps: 1) *linear buckling analysis*, to determine the buckling⁶¹ load (eigenvalue problem) and 2) asymptotic *post-buckling analysis*, to investigate the post-buckling behaviour and to see if the bifurcated branches are stable or not. In the post-buckling analysis the problem is not any more an eigenvalue problem but becomes a geometrically non-linear (GN) problem of static where the loads are increased step-by-step and the displacement-curves being solved (in the force-control⁶² version). In such analysis, we are interested only in the first bifurcation neighbourhood corresponding to the lowest buckling load (or smaller eigenvalue). The stability of this neighbourhood (branch) is crucial for the real load-bearing capacity. If one has instability then the Euler load will be reduced. How much?

Usually, the Euler buckling load over-estimates the actual buckling (limit) load for the system with imperfections (Figure 1.48). To find out how much the reduction is, one should perform a non-linear buckling analysis (GNA) accounting for the imperfections. Sensitivity with respect to such geomet-

⁶¹Such buckling load for the perfect system is called *Euler buckling load*.

⁶²We can also have a displacement-control version where displacements are imposed at some locations and the reactions at these points being recorded to obtain the force-displacement curves. It is on these curves (in both force- or displacement control versions) that the limit-points are identified.

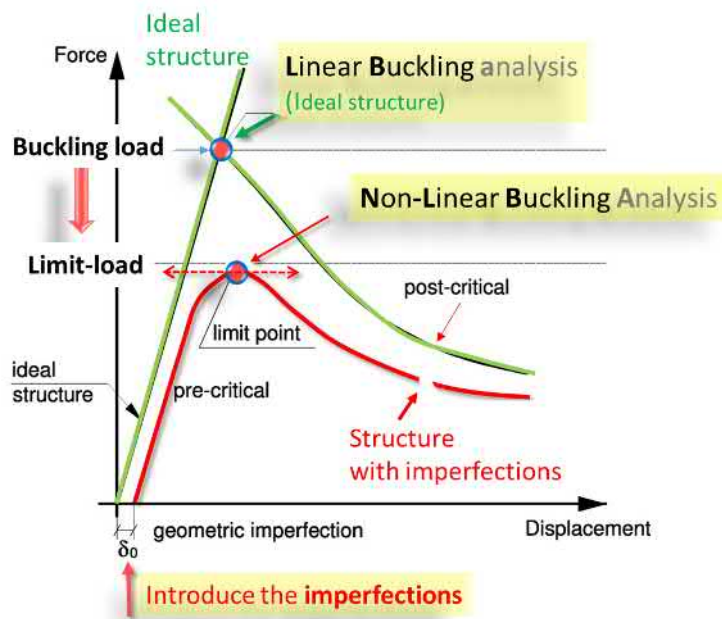
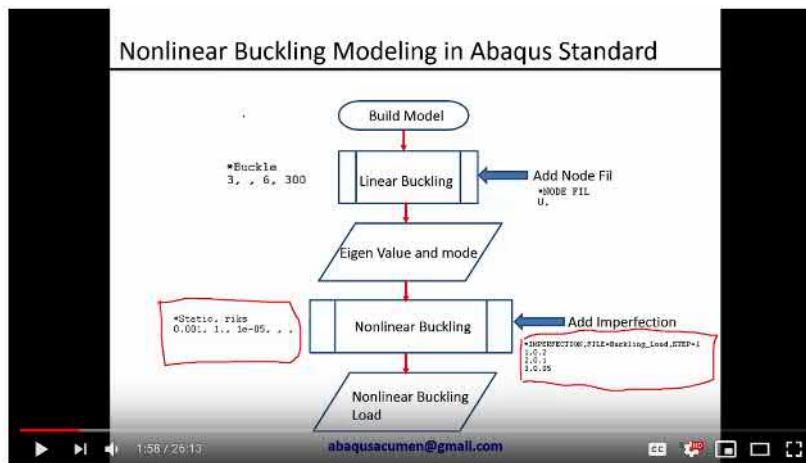


Figure 1.48: Generic illustration of Euler buckling load and limit-load.

ical imperfections can be analysed numerically as shown for Abaqus (Fig. 1.49), for instance.



Abaqus Standard: Nonlinear Buckling Example (Cylinder buckling)

Figure 1.49: Generic flow chart for doing non-linear buckling analysis in Abaqus. (a non-linear analysis)

The effect of such imperfection was studied previously (*Cf.* Figure 1.42), so the reader should refer to that. Despite what was said above, in the

current example, we consider only the perfect structure.

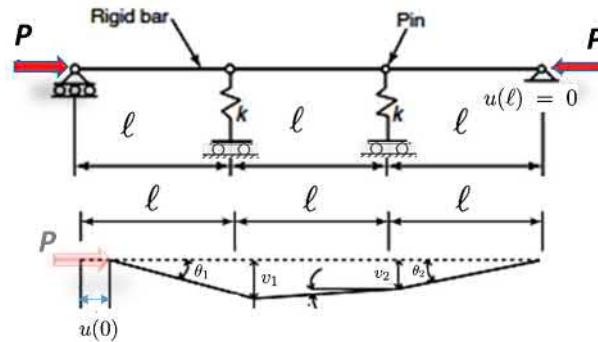


Figure 1.50: A simple system having two degrees of freedom.

Consider the system depicted in Figure (1.50). The bars being infinity rigid connected by hinges to elastic supports. The springs are linear elastic. The continuous equivalent structure can be, for instance, a column with elastic supports. A pertinent design question can be what should be the ratio of stiffness of the elastic supports k as regard to bending rigidity EI , in order to ensure stability? Since, if the post-buckling behaviour is unstable, then the Euler buckling load (for the perfect structure) will be reduced to the lower limit-load when accounting for initial imperfections. Imperfection can be geometrical as for instance, small deviations from straightness or initial eccentricities . . . So, in structural design, one should continue to step to and perform (GNA) non-linear buckling analysis including the imperfections in order to determine the actual limit-load.

Geometrically non-linear equations of equilibrium: Let's measure the deflected configuration by v_1 and v_2 , the two independent transversal deflections.

The total potential energy increment (TPEI) between the initial equilibrium (perfectly straight configuration; $v_1 = v_2 = 0$) and the perturbed configurations being

$$\Delta\Pi(v_1, v_2) = \frac{1}{2}kv_1^2 + \frac{1}{2}kv_2^2 - Pu(0). \quad (1.65)$$

Geometrical consideration (Pythagoras' theorem⁶³) on *triangles rectangles* provides the *exact* total axial displacement $u(0)$ - cumulated nodal displace-

⁶³Yet another theorem very usual even for a structural engineer!

ment - as

$$u(0) = \ell \left[1 - \sqrt{1 - \left(\frac{v_1}{\ell}\right)^2} \right] + \quad (1.66)$$

$$+ \ell \left[1 - \sqrt{1 - \left(\frac{v_2 - v_1}{\ell}\right)^2} \right] + \quad (1.67)$$

$$+ \ell \left[1 - \sqrt{1 - \left(\frac{v_2}{\ell}\right)^2} \right]. \quad (1.68)$$

Consequently, the total potential energy increment will be

$$\Delta\Pi(\epsilon_1, \epsilon_2) = \frac{1}{2}k\ell^2(\epsilon_1^2 + \epsilon_2^2) - P\ell \cdot \left(\left[1 - \sqrt{1 - \epsilon_1^2} \right] + \left[1 - \sqrt{1 - (\epsilon_2 - \epsilon_1)^2} \right] + \left[1 - \sqrt{1 - \epsilon_2^2} \right] \right), \quad (1.69)$$

where the relative shortenings are defined as $\epsilon_1 = v_1/\ell$ and $\epsilon_2 = v_2/\ell$. Note that, the obtained expression is exact and no assumption was done on the relative magnitudes of ϵ_1 or ϵ_2 as compared to ℓ .

1) Linear buckling analysis: We want to determine the Euler buckling load. In such analysis we have, by definition, both relative shortening of the column $\epsilon_1 \ll 1$ and $\epsilon_2 \ll 1$, so as the reader may recall, one expands the total potential energy increment into *Taylor expansion up-to quadratic terms* in v_1/ℓ and v_2/ℓ (or ϵ_1 and ϵ_2). So,

$$\Delta\Pi(v_1, v_2) = \frac{1}{2}k(v_1^2 + v_2^2) - P\ell \left[\frac{1}{2} \left(\frac{v_1}{\ell}\right)^2 + \frac{1}{2} \left(\frac{v_2 - v_1}{\ell}\right)^2 + \frac{1}{2} \left(\frac{v_2}{\ell}\right)^2 \right]. \quad (1.70)$$

Requiring the neutral equilibrium condition $\delta(\Delta\Pi) = 0$ (for loss of stability) one obtains the eigenvalue-problem

$$\begin{bmatrix} \lambda - 2P & P \\ P & \lambda - 2P \end{bmatrix} \begin{bmatrix} v_1 \\ v_2 \end{bmatrix} = \begin{bmatrix} 0 \\ 0 \end{bmatrix} \quad (1.71)$$

where $\lambda \equiv k\ell$. The eigenvalues being $P_{1,E} = k\ell/3$ and $P_{2,E} = k\ell$ and the corresponding buckling modes $[v_1, v_2] = [1, -1]$, so $(v_1 = -v_2)$ and $[v_1, v_2] = [1, 1]$, so $(v_1 = v_2)$, respectively (Figure 1.51). One can note that the corresponding buckling mode is the asymmetric one.

Let's go further and investigate is this mode, for small increment of deflection, stable or unstable? As you remember by now, one cannot use the criteria of the sign of the second variation of the total potential energy increment, since the linearisation will return us the soundless identity $0 = 0$

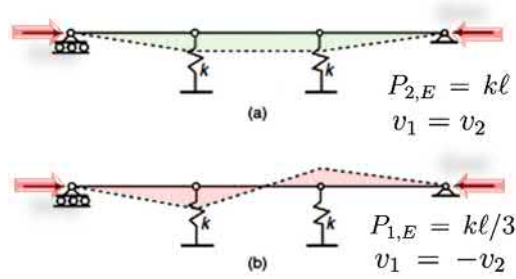


Figure 1.51: Buckling modes.

for the bifurcated (buckled) equilibrium branch. So, we cannot decide, based on linear buckling analysis, what is the stability nature for the buckled branch at buckling load $P_{1,E} = k\ell/3$, for instance. To capture the *sign*, one should add higher terms in the Taylor expansion of the energy functional.

Recall the Hessian story: Let illustrate the formalism we presented in the introduction part for the criterion of loss of stability in the form

$$\Pi''(v_1, v_2) = 0 \sim \det\{\mathbf{H}\} = 0, \quad (1.72)$$

when now the problem has more than one degrees of freedom $\mathbf{q} = [v_1, v_2]^T$. The question: *how do I take the second derivative now that we have more than one degree of freedom?* Here comes to help *variational calculus* or, even more simply, classical *linear algebra* with the Hessian of a matrix. Let's chose this simplest tool, for the moment, since every master students has completed such prerequisite course but few only studied variational calculus. Rewriting the change of total potential energy, in a matrix form, one obtains

$$\Delta\Pi(v_1, v_2) = \frac{1}{2} [v_1 \quad v_2] \underbrace{\left(\underbrace{\begin{bmatrix} k & 0 \\ 0 & k \end{bmatrix}}_{\mathbf{K}} - \frac{P}{\ell} \underbrace{\begin{bmatrix} 2 & -1 \\ -1 & 2 \end{bmatrix}}_{\mathbf{S}(P)} \right)}_{\mathbf{H}(0,0)} \begin{bmatrix} v_1 \\ v_2 \end{bmatrix} \quad (1.73)$$

So, one obtains the *quadratic form*

$$\Delta\Pi(\mathbf{q}) = \frac{1}{2} \mathbf{q}^T \mathbf{H} \mathbf{q}, \quad (1.74)$$

where \mathbf{q} being a tiny deviation from trivial equilibrium configuration $\mathbf{q}^0 = \mathbf{0}$ and

$$\mathbf{H} = \begin{bmatrix} \lambda - 2P & P \\ P & \lambda - 2P \end{bmatrix}. \quad (1.75)$$

We can also write directly the loss of stability condition in its *variational form* $\delta(\Delta\Pi) = 0$ and obtain

$$\delta(\Delta\Pi) = \frac{1}{2}\delta\mathbf{q}^T\mathbf{H}\mathbf{q} + \frac{1}{2}\mathbf{q}^T\mathbf{H}\delta\mathbf{q} = \delta\mathbf{q}^T\mathbf{H}\mathbf{q} = 0, \forall\delta\mathbf{q} \implies \quad (1.76)$$

$$\implies \mathbf{H}\mathbf{q} = \mathbf{0}, \text{ which is linear eigenvalue problem.} \quad (1.77)$$

Note that the coefficient matrix of the associated eigenvalue problem (Equation 1.71) is the same⁶⁴ than our Hessian matrix So loss of stability occurs when

$$\Pi'' = 0 \sim \det\{\mathbf{H}\} = 0 \quad (1.78)$$

and one sees that this *criterion of stability* is the same as for the associated eigenvalue problem (Equation 1.71) to require existence of non-trivial solution (buckled shape) by asking the determinant of the coefficient matrix, in the eigenvalue problem, to vanish.

2) Post-buckling analysis: *What is the nature of the bifurcated branch just in the near neighbourhood of the bifurcation point $P_{1,E} = k\ell/3$?* For that, we do an asymptotic analysis and take up-to the fourth-order in the Taylor expansion of $\Delta\Pi$. In addition, since we are in the neighbourhood of the buckling load, the ratio $v_1 = -v_2$ as given by the corresponding buckling mode, remains unchanged if we limit ourselves to very small additional deflections v_1 and v_2 from the neutral configuration. (so ratios $v_1/\ell \ll 1$ and $v_2/\ell \ll 1$). Consequently,

$$\Delta\Pi(v_1, v_2) = \frac{1}{2}k(v_1^2 + v_2^2) - P\ell \left[\frac{1}{2} \left(\frac{v_1}{\ell} \right)^2 + \frac{1}{8} \left(\frac{v_1}{\ell} \right)^4 + \right. \quad (1.79)$$

$$\left. + \frac{1}{2} \left(\frac{v_2 - v_1}{\ell} \right)^2 + \frac{1}{8} \left(\frac{v_2 - v_1}{\ell} \right)^4 + \right. \quad (1.80)$$

$$\left. + \frac{1}{2} \left(\frac{v_2}{\ell} \right)^2 + \frac{1}{8} \left(\frac{v_2}{\ell} \right)^4 \right]. \quad (1.81)$$

Inserting the relation $v \equiv v_1 = -v_2$, one finally obtains

$$\Delta\Pi(v) = k\ell^2 \left(\frac{v}{\ell} \right)^2 - 3P\ell \left(\frac{v}{\ell} \right)^2 - \frac{9}{4}P\ell \left(\frac{v}{\ell} \right)^4. \quad (1.82)$$

The stationarity condition gives us the the equilibrium equation of the bi-

⁶⁴Candide: *tout va pour le mieux dans le meilleur des mondes.*

furcated branch as by

$$\delta[\Delta\Pi(v)] = 0 \implies [\Delta\Pi]' = 0 \quad (1.83)$$

$$\implies k\ell \left(\frac{v}{\ell}\right) - 3P \left(\frac{v}{\ell}\right) - \frac{9}{2}P \left(\frac{v}{\ell}\right)^3 = 0 \quad (1.84)$$

$$\implies k\ell \left(\frac{v}{\ell}\right) \left[1 - \frac{3P}{k\ell} - \frac{3}{2} \frac{3P}{k\ell} \left(\frac{v}{\ell}\right)^2\right] = 0 \quad (1.85)$$

$$\implies k\ell \left(\frac{v}{\ell}\right) \left[1 - \frac{P}{P_{1,E}} - \frac{3}{2} \frac{P}{P_{1,E}} \left(\frac{v}{\ell}\right)^2\right] = 0 \quad (1.86)$$

$$\implies k\ell \left(\frac{v}{\ell}\right) \left[1 - \frac{P}{P_{1,E}} \left(1 + \frac{3}{2} \left(\frac{v}{\ell}\right)^2\right)\right] = 0 \quad (1.87)$$

So, the equilibrium solutions are the primary and secondary paths, respectively,

$$\begin{cases} v/\ell = 0, \forall P & \text{or} \\ P/P_{1,E} = 1/\left[1 + \frac{3}{2} \left(\frac{v}{\ell}\right)^2\right], v/\ell \neq 0 & \text{where } P_{1,E} = k\ell/3. \end{cases} \quad (1.88)$$

and

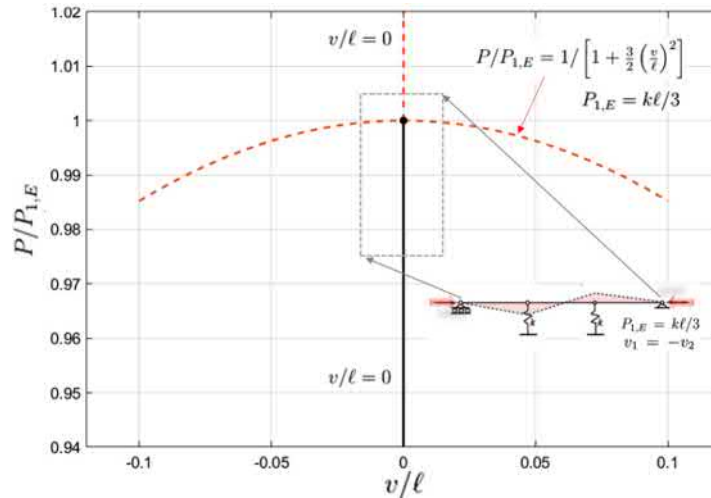


Figure 1.52: Equilibrium path (asymptotic post-buckling analysis)

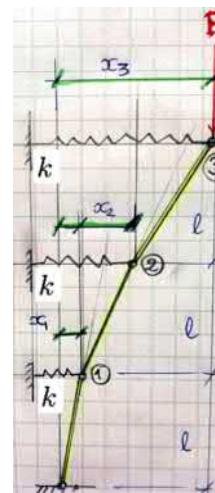
The nature of stability of this branch is provided by the sign of the second derivative (Lagrange-Dirichlet stability theorem) which gives

$$(\Delta\Pi)'' = k - \frac{3P}{\ell} - \frac{29}{2} \left(\frac{v}{\ell}\right)^2 \quad (1.89)$$

and inserting, in the above, the expression of P (second Equation in 1.88) on this branch on obtains that this bifurcated branch is *unstable*. The result of this post-buckling study is shown on the graph (Figure 1.52).

1.7.4 Example of stability of discontinuous system with many dofs

We now study the stability of a discrete system of five degrees of freedom (dof). The idea is general and extends to any number N of dofs. Let's assume that we have a 'column' with end load P (Fig. Cf. margin). In such multi-degrees of freedom structures, the buckling load corresponds to the smallest eigenvalue and the corresponding eigenmode gives the buckling mode. let's have an example. Note that the discrete structure converges to the corresponding continuous one for $N \rightarrow \infty$. It is worth to note that, if we would want to account also for bending strain energy ($\sum_i 1/2c_i\phi_i^2$, ϕ_i — relative rotations between bars $i, i - 1$), then we add simply rotational springs between the rigid bars. The spring coefficient will be $c_i = EI_i/\ell_i$. Also, stretching strain energy can be added through axial spring coefficients $k_i = EA_i/\ell_i$. This way, the discrete structure (a Hencky-type discrete chain) converges to axially loaded elastic beam-column.



In the current example, the transversal springs k may correspond to there straining effects of a **Winckler**-type elastic foundation. Therefore, the physics of our rigid bar chain is the next: straight rigid bar-chain bounded to a Winckler elastic foundation (modelled by the transversal springs k) connected by hinges is axially loaded.

The change⁶⁵ of discrete total potential energy of the deformed perfect elastic system under axial load will be

$$\Delta\Pi(x_1, x_2, \dots, x_N) = \frac{1}{2} \sum_{i=1}^N k_i x_i^2 + V(P; x_1, x_2, \dots, x_N), \quad (1.90)$$

where after assuming moderate rotations of bars ($\cos \theta_i \approx 1 - \theta_i^2/2$) one obtains

$$V(P) = -P \cdot \frac{1}{2} \sum_{i=1}^N \frac{(x_i - x_{i-1})^2}{\ell_i}, \quad x_0 = 0, \quad i = 1, 2, \dots, N \quad (1.91)$$

Asking for stationarity at the critical equilibrium point

$$\delta(\Delta\Pi) = 0, \quad \forall x_i, i = 1, 2, \dots, \implies \frac{\partial(\Delta\Pi)}{\partial x_i} = 0, \quad (1.92)$$

⁶⁵= change between straight configuration and slightly buckled one.

gives next equilibrium equations

$$\frac{\partial(\Delta\Pi)}{\partial x_1} = k_1 x_1 + \frac{P}{\ell}(2x_1 - x_2), \quad (1.93)$$

$$\frac{\partial(\Delta\Pi)}{\partial x_2} = k_2 x_2 + \frac{P}{\ell}(-x_1 + 2x_2 - x_3), \quad (1.94)$$

$$\frac{\partial(\Delta\Pi)}{\partial x_i} = k_i x_i + \frac{P}{\ell}(-x_{i-1} + 2x_i - x_{i+1}), \quad i = 2, 3, \dots, N-1, \quad (1.95)$$

$$\frac{\partial(\Delta\Pi)}{\partial x_N} = k_N x_N + \frac{P}{\ell}(-x_{N-1} + x_N), \quad (1.96)$$

rewritten into a canonical in a matrix form one obtains the linear homogeneous system and recognise the eigenvalue problem setting:

$$\left[\mathbf{K} - \frac{P}{\ell} \mathbf{S} \right] \mathbf{x} = \mathbf{0}. \quad (1.97)$$

The stiffness matrix $\mathbf{K} = \text{diag}(k_i)$, $i = 1 : N$. For constant spring coefficient, one gets $\mathbf{K} = k\mathbf{I}$, where the identity-matrix notation is evident. Both matrices are real and symmetric. So, the eigenvalues are real too. The *geometrical stiffness matrix* is

$$\mathbf{S} = \frac{P}{\ell} \begin{bmatrix} 2 & -1 & 0 & \dots & 0 & 0 \\ -1 & 2 & -1 & \dots & 0 & 0 \\ \vdots & \vdots & \vdots & \ddots & \vdots & \vdots \\ 0 & 0 & \dots & -1 & 2 & -1 \\ 0 & 0 & \dots & 0 & -1 & 1 \end{bmatrix} \quad (1.98)$$

So the full eigenvalue problem to solve now is:

$$\left(\begin{bmatrix} k_1 & 0 & 0 & \dots & 0 & 0 \\ 0 & k_2 & 0 & \dots & 0 & 0 \\ \vdots & \vdots & \vdots & \ddots & \vdots & \vdots \\ 0 & 0 & \dots & 0 & k_{N-1} & 0 \\ 0 & 0 & \dots & 0 & 0 & k_N \end{bmatrix} - \frac{P}{\ell} \begin{bmatrix} 2 & -1 & 0 & \dots & 0 & 0 \\ -1 & 2 & -1 & \dots & 0 & 0 \\ \vdots & \vdots & \vdots & \ddots & \vdots & \vdots \\ 0 & 0 & \dots & -1 & 2 & -1 \\ 0 & 0 & \dots & 0 & -1 & 1 \end{bmatrix} \right) \begin{bmatrix} x_1 \\ x_2 \\ \vdots \\ x_{N-1} \\ x_N \end{bmatrix} = \begin{bmatrix} 0 \\ 0 \\ \vdots \\ 0 \\ 0 \end{bmatrix} \quad (1.99)$$

Numerical example

Let solve it for a constant k for $N = 6$, for instance, in Matlab using the eigenvalue problem solver function $[V,D] = \text{eig}(A)$ or $[V,D] = \text{eig}(A,$

B).⁶⁶ The solution is reproduced in Figure (1.53) and the numerical code written in Matlab to solve it is shown in Figure (1.54).

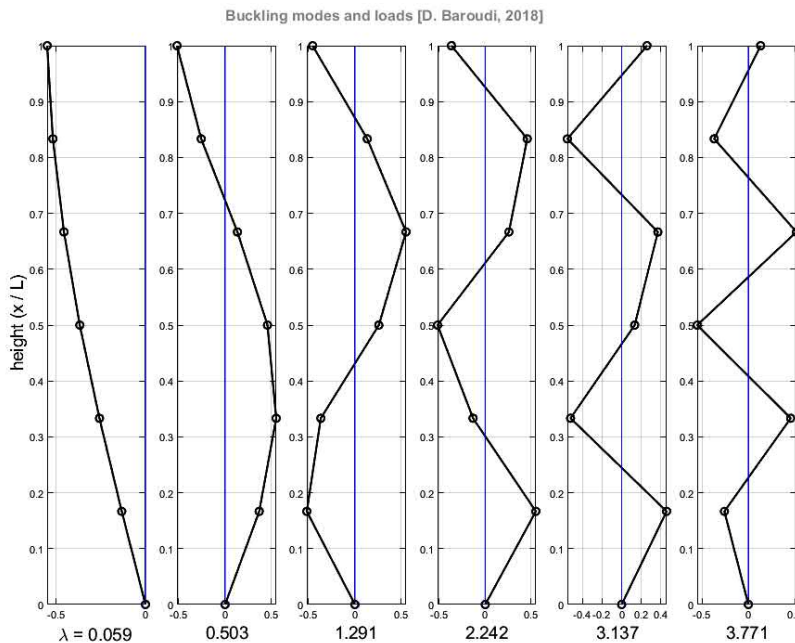


Figure 1.53: Numerically simulation. Buckling modes and the corresponding scaled eigenvalue $\lambda = P/k\ell$. Now, $N\ell = 1$ m and $N = 6$. The buckling load is now $P = 0.059/k\ell$

We can note for shortness the eigenvalues (buckling loads) $\lambda = \frac{P}{k\ell}$ corresponding \mathbf{x} are the Eigen-vector (eigenmodes). Since the stiffness matrix is invertible, one can recast the problem into the canonical form⁶⁷:

$$[\mathbf{I} - \underbrace{\lambda \mathbf{K}^{-1} \mathbf{S}}_{\equiv A}] \mathbf{x} = \mathbf{0}, \quad (1.100)$$

The criticality condition, is of course, still

$$\det [\mathbf{K} - \lambda \mathbf{S}] = 0 \implies P_N(\lambda) = a_0 + a_1 \lambda + a_2 \lambda^2 + \dots + \dots + a_N \lambda^N = 0 \quad (1.101)$$

However, instead of trying to solve for the roots (zeros) of the polynomial in λ (Eq. 1.101), we solve, directly by standard methods (QR-decomposition

⁶⁶These Matlab functions produces a diagonal matrix D of eigenvalues and a full matrix V whose columns are the corresponding eigenvectors (see Matlab functions reference manual).

⁶⁷This not obligatory to do, you can solve directly the problem in its original form (1.100)

family algorithm) the corresponding eigenvalue problem (1.100), which is, indeed, much easier and much stable to solve than to find the corresponding roots of the polynomial of order N in λ given by (eq. 1.101). Recall that the Eigen-vectors (buckling modes in Figure (1.53) are *known up-to a multiplicative factor in amplitude*. However, the rotations (relative displacements x_i/x_j are well determined) are given by the modes in their amplitude correctly. The indeterminacy in absolute values of the displacement results from the linearisation of the equilibrium equations at the critical point (neutral equilibrium).

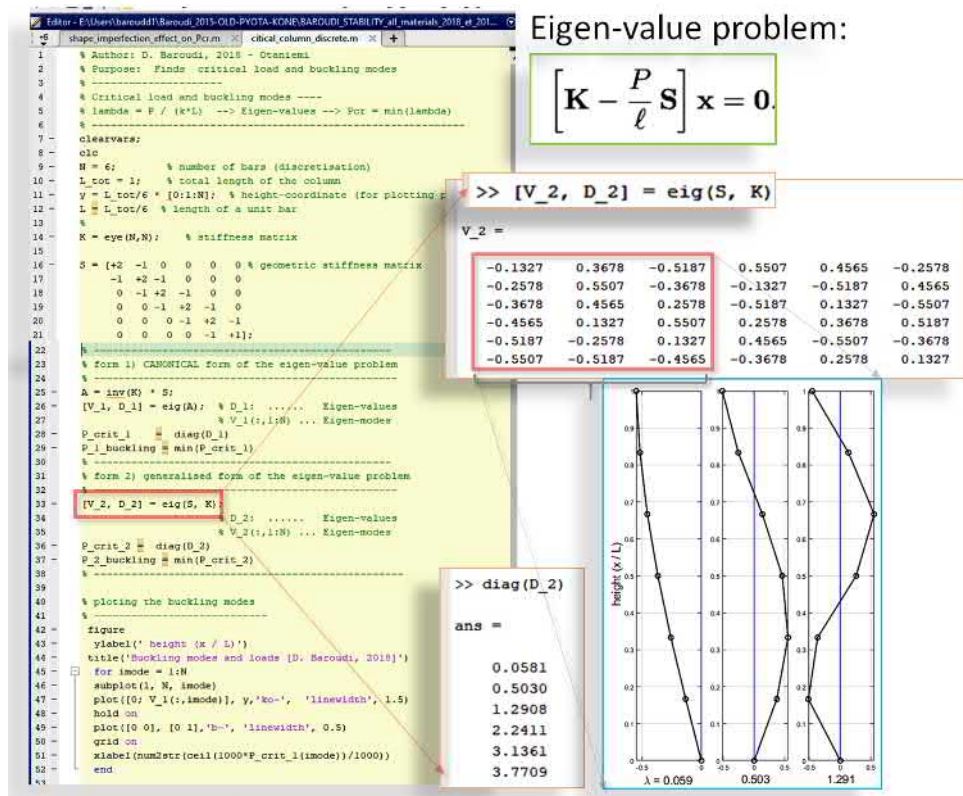


Figure 1.54: The Matlab-code used to do the numerical simulation above.

The key idea in the *linearisation* is to construct a quadratic form in terms of kinematics for the total potential energy. So, consequently, after taking the first variation of the total potential energy increment, one obtains a set of linear equations (eigenvalue problem) with respect of the kinematics. So, with this approach one can address only the value of the buckling load and the corresponding modes. for instance, one should keep in the work of external force $P \cdot v_N = P \sum_i^N \ell_0 (1 - \cos \theta_i) \approx P \sum_i^N \ell_0 (\theta_i^2/2 + \theta_i^4/4! + \dots)$,

ℓ_0 being the length of a bar segment at least up-to cubic terms. Naturally, $\cos \theta_i$ should be expressed in terms of the Lagrange coordinates x_i (There may be a homework on that: *determine the buckling load and investigate the nature of the post-buckling behaviour corresponding to the buckling mode.*) .

Higher terms than quadratic, for the kinematics, will be needed to account for in the total potential energy of the system when we need to *investigate the nature of stability of the post-buckling behaviour* (after branching at the bifurcation points). One need to form the second variation which will not, *a priori*, be any more trivially zero (not indifferent).

For the discrete system, the second variation will give a quadratic form $\delta^2(\Delta\Pi) = \mathbf{u}^T[\mathbf{K}(\mathbf{u})]\mathbf{u} > 0 \rightarrow$ means positive-definite and that the path is stable. The matrix is the *stability matrix*. It is *positive-definite* only if all its eigenvalues are positive.

1.7.5 Combined loading and stability regions

Very often, all the applied loads to an elastic structure, and especially, gravitational loads \mathbf{P} can be expressed as varying linearly with respect to only one parameter $\mathbf{P} = \lambda\mathbf{P}_0$, where P_0 being a reference load. However, in general, the applied loads can be regrouped into subgroups of reference loads which vary *independently* from each other.

Let consider two examples⁶⁸ illustrating the concept of *region of stability*. How knows, may be some future engineer will be happier learning this, too. So one can have more than one *independent systems* of loading acting simultaneously on our structure. How to *handle by hand*?

One degree of freedom spring-Rigid bar system

[TO DO]

two degree of freedom spring-Rigid bar system

[TO DO]

Thermal buckling

[TO DO] Initially uniform temperature T_0 . Uniform rise ΔT . No other

⁶⁸Ref. Section 1.7 Stability of Elastic Structures Under Combined Loading: Boundary of Stability Region. N.A. Alfutov, *Stability of Elastic Structures*. Springer-Verlag Berlin Heidelberg 2000.

mechanical loads. What will be the buckling temperature⁶⁹? α thermal expansion coefficient.

After thermal elongation the length ℓ of a bar become

$$\ell_T = (1 + \alpha\Delta T)\ell \quad (1.102)$$

due to thermal elongation. Therefore the axial displacement u_T for a rotation θ at support will be

$$u_T = 2\ell_T(1 - \cos\theta) \quad (1.103)$$

$$= 2\ell(1 + \alpha\Delta T)(1 - \cos\theta) \quad (1.104)$$

$$= 2\ell [1 - (1 + \alpha\Delta T)\cos\theta + \alpha\Delta T] \quad (1.105)$$

Typically, α is a small value of order 10^{-5} $1/^\circ\text{C}$ for most of solids, so the square $(\alpha\Delta T)^2$ of the relative thermal elongation (strain) may be ignored when compared to unity.

Total potential energy change:

$$\Delta\Pi(\theta; \Delta T) = \frac{1}{2}c(2\theta)^2 + \frac{1}{2}k\Delta_{\text{th}}^2 \quad (1.106)$$

$$= 2c\theta^2 + \frac{1}{2}k \cdot \left(\underbrace{2\ell [1 - (1 + \alpha\Delta T)\cos\theta + \alpha\Delta T]}_{\Delta_{\text{th}}} \right)^2 \quad (1.107)$$

The axial component of the overall thermal elongation is (check below Taylor expansion)

$$\Delta_{\text{th}} = 2\ell [1 - (1 + \alpha\Delta T)\cos\theta + \alpha\Delta T] \approx 2\ell \left[\frac{\theta^2}{2} + \frac{\theta^4}{24} - \alpha\Delta T \left(-2 + \frac{\theta^2}{2} + \frac{\theta^4}{24} \right) \right] \quad (1.108)$$

[DBA DO correctly] Taylor expansion for the axial displacement without ignoring the square of the thermal strain.

Stationarity at the critical equilibrium point

$$\delta(\Delta\Pi) = 0 \implies \frac{\partial(\Delta\Pi)}{\partial\Delta T} = 0, \quad (1.109)$$

provides the equilibrium paths (primary and secondary).

⁶⁹This example is inspired from the textbook by Croll J. G. A. and Walker A. C. *Elements of structural stability*. Macmillan 1972

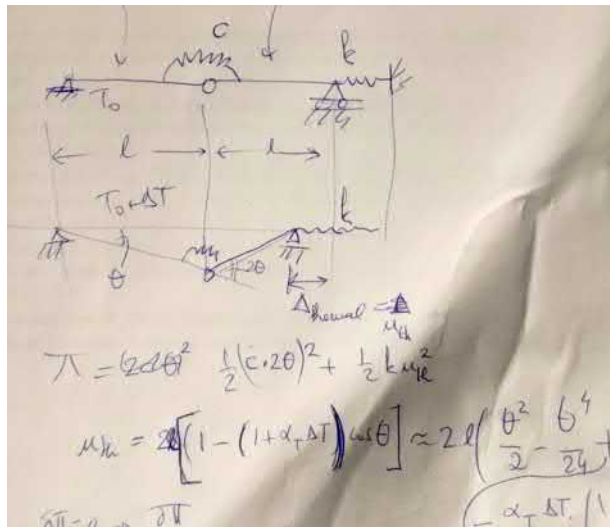


Figure 1.55: Thermal buckling of a bar-system.

1.8 Energy criteria for determination loss of stability of elastic structures

The general⁷⁰ **Trefftz** (1930, 1933) criterion says that the loss or change in stability of an elastic structure occurs when the variation of the second variation⁷¹ of the total potential energy Π of the structure vanishes, *i.e.*,

$$\delta(\delta^2\Pi) = 0. \quad (1.110)$$

Later, while discussing about bifurcational loss of stability, it will be shown that Trefftz stability condition (Eq. 1.110) is essentially an energetic criterion saying that during loss of stability and for the critical load, the equilibrium holds also in the perturbed state $u^* = u^0 + \delta u$, *i.e.*, then $\delta(\Delta\Pi) = 0$. It will be discussed later that, indeed all these energy criteria for loss of stability: ($\Delta\Pi = 0$; $P_{min} = P_{cr}$), the more general criterion $\delta(\Delta\Pi) = 0$ and the Trefftz criterion $\delta(\delta^2\Pi) = 0$ - which look at first glad different, are indeed equivalent⁷² I was few hours ago discussing with one *student* and he was puzzled with the seemingly arbitrary use of the stability loss⁷³ criterion

⁷⁰N.B. Trefftz is not a general, neither is his stability condition, general!

⁷¹So what to do when $\delta^2\Pi = 0$ and $\delta\Pi = 0$? Answer: one need to take higher order of non vanishing variations; $\delta^3\Pi$, $\delta^4\Pi$, ... of $\Delta\Pi$ to decide on stability of an equilibrium (sign). So, the Trefftz condition is not general.

⁷²With the emphasis that the criteria $\delta(\Delta\Pi) = 0$ being more general than Trefftz criteria which is a consequence of $\delta(\Delta\Pi) = 0$.

⁷³Stability loss through bifurcation or limit-point

$\Delta\Pi = 0$ and $\delta(\Delta\Pi) = 0$. Are they the same? So, Figure (1.56) shows now why, these two conditions are equivalent; just call the function f by $\Delta\Pi$.

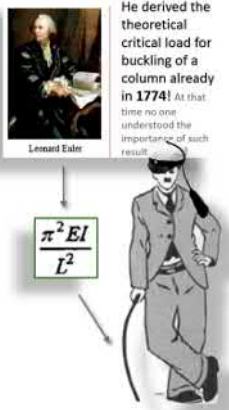
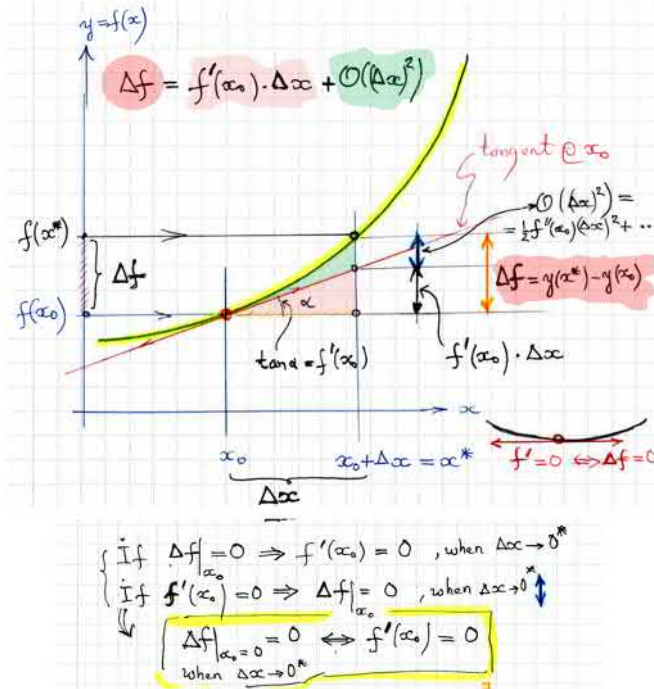


Figure 1.56: Why saying that $f'(x_0) = 0$ is equivalent to say that $\Delta f|_{x_0} = 0$.

Sometimes, to emphasize this in Equation (1.110) the variation operator is denoted $\bar{\delta}$ to emphasize that it is the perturbed state $u^* = u^0 + \delta u$ which is varied since it is its equilibrium which is investigated.

Energy method are effective for analysing the stability of complex structure.

1.9 Energy criterion for bifurcational instability

This section deals primarily with fundamentals of bifurcational instability where the *critical points* is at a *bifurcation*. However, the theorems and energy criteria presented here hold also when the *critical points* are limit points⁷⁴. Therefore in cases when the initial equilibrium path is non-linear

⁷⁴N. A. **Alfutov**, *Stability of Elastic Structures*. Springer 2000 (translated from Russian)

and not linear as it is in the bifurcational case, the energy criterion detects the limit points and points of inflection since the energy criterion is a condition for neighbouring equilibrium modes.

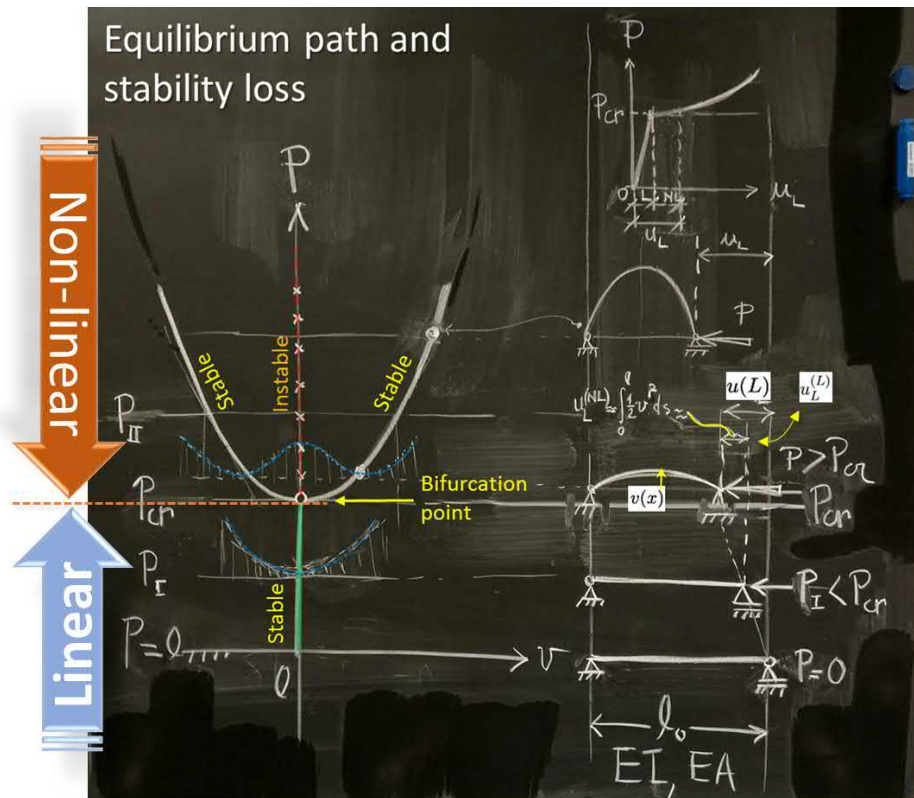


Figure 1.57: Stability of an equilibrium for a compressed elastic column. The blue dot-lines corresponds to the graph of total potential energy $\Pi(\cdot, v; P)$ for the given load P at that section. Assuming linearity of the initial state, the total axial displacement given by $u(L) = u^{(L)} + u^{(NL)} = \int_0^L [u' + \frac{1}{2}v'^2] dx$.

Let's consider that the structure under consideration, the loading are conservative and the constraints being ideal. So we have a conservative system for which the *total potential energy* is well defined and such that

$$\Pi = U + W. \tag{1.111}$$

where U being the change in strain energy and W being the potential of external loads ($= -W_{ext}$ work of external loads with a minus sign). In addition, assume that all rigid-body motion are prevented by the kinematic constraints (boundary conditions). This means that the system is not a mechanism and that is *cinematically stable*). We consider proportional loading, *i.e.*, which depends only on a single parameter P .

According to the *Lagrange theorem*⁷⁵, the total potential energy (Eq. 1.111) is *stationary* at equilibrium ($\delta\Pi = 0$) and that this equilibrium is stable if and only if (**iff**) the increment total potential energy

$$\Delta\Pi > 0, \quad \forall\delta u \quad (1.112)$$

for any small perturbations from initial state. In other words, the stationary point is a local minimum.

Consider that the structure is first in *initial equilibrium state* and described by the *theory of linear elasticity*. It is clear that for $P = 0$ the equilibrium is stable ($\Delta\Pi > 0$). Therefore, by increasing P till some finite critical value $P > P_{cr}$ this initial equilibrium ceases to be stable ($\Delta\Pi \leq 0$). The smallest load P_{cr} for which loss of stability occurs at the first time is called the *critical load*. Therefore this transition condition is the *criticality condition* for loss of stability since in case of stable state one have $\Delta\Pi > 0$ and for unstable case $\Delta\Pi \leq 0$. Therefore a transition from stable to unstable state or *vice-versa* occurs when

$$\boxed{\Delta\Pi = 0; \quad P_{cr} = P_{min}.} \quad (1.113)$$

Example of use of stability criteria in the form $\Delta\Pi = 0$

In the following, we illustrate how the energy criterion for stability of an equilibrium written in the form $\Delta\Pi = 0; \quad P_{cr} = P_{min}$ can be used. Assume that for compression $P > 0$. Consider an illustration example for the use of the energy criterion of loss of stability in the form of equation (1.113). The problem: bifurcational flexural buckling of a cantilever column under a load P it's free end. *Determine the critical load P_{cr}* . The increment (the change) of total potential energy of an elastic column between the initial equilibrium state (perfectly straight beam, pre-buckling state) with only axial deformations and the buckled flexural state (small flexural deflection) will be

$$\Delta\Pi = \frac{1}{2} \int_0^\ell EI v''^2 dx - P \int_0^\ell \frac{1}{2} v'^2 dx \quad (1.114)$$

and using explicitly the criticality condition $\Delta\Pi = 0; P_{cr} = P_{min}$ at the equilibrium point v (Eq. 1.113) leads to the critical force

$$\boxed{\Delta\Pi[v] = \frac{1}{2} \int_0^\ell EI v''^2 dx - P \int_0^\ell \frac{1}{2} v'^2 dx = 0 \implies P_{cr} = P_{min} = \frac{\int_0^\ell EI v''^2 dx}{\int_0^\ell v'^2 dx}.} \quad (1.115)$$

⁷⁵minimum total potential energy

which the well-known minimisation principle of the *Rayleigh quotient*⁷⁶

$$P_{min} = P_{cr} = \min_v R(v) = \frac{\int_0^\ell EI v''^2 dx}{\int_0^\ell v'^2 dx} \quad (1.116)$$

It is well known that Rayleigh quotient $\lambda_1 = \min_v R(v) = R(v_1)$ at the first eigenvector v_1 has a stationary point which is indeed a minimum. The above result (Eqs. 1.115 and 1.116) can be used to obtain good numerical estimations for the smallest critical load P_{cr} by choosing some even simple but adequate approximations for the modes. In addition, the Rayleigh quotient is flat near a minimum and consequently, substantial errors in eigenmode (or approximation of buckling mode) leads to only small errors in eigenvalue λ_1 or, here the buckling load P_{cr} .

Example of use of stability criteria in the form $\delta(\Delta\Pi) = 0$

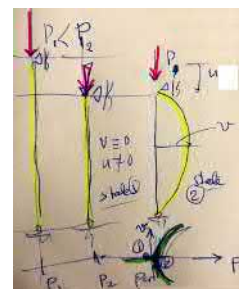
Assumes that one have compression $P > 0$ and that the initial reference state is the perfectly straight configuration with only axial deformation. We are studying the stability of a bifurcated infinitely small neighbouring flexural mode v . Such infinitely small flexion is assumed to happening with keeping all external forces constant. Therefore, the membrane state is to be taken from the reference state. Let now derive the stability equations for the same problem as above using the other form of the energy criterion (the Lagrange variational equation) as $\delta(\Delta\Pi) = 0, \forall \delta u$, where the increment of total potential energy $\Delta\Pi$ is being according to equation (1.114) given by

$$\begin{aligned} \delta(\Delta\Pi[v]) = 0, \forall \delta u &\implies \delta \left(\frac{1}{2} \int_0^\ell EI v''^2 dx - P \int_0^\ell \frac{1}{2} v'^2 dx \right) = 0, \forall \delta u \quad (1.117) \\ &= \int_0^\ell EI v'' \delta v'' dx - P \int_0^\ell v' \delta v' dx = 0 \quad (1.118) \end{aligned}$$

Integrating twice by parts and accounting for the boundary conditions in the boundary-terms leads to the well-known *Euler-Lagrange* equations of stability of a column

$$(EI v''')'' + P v'' = 0 \quad \& \quad 4 \text{ BCs.} \quad (1.119)$$

The above homogeneous differential equation describes the stability problem and its solution provides us the critical buckling load together with the associated buckling-modes once the relevant four boundary conditions are specified.



⁷⁶This quotient or ratio is named after Walther **Ritz** and Lord **Rayleigh**. Mathematically, this quotient is defined by $R(M, x) = x^* M x / (x^* x)$ where M is a complex Hermitian matrix and x non-zero vector. For real matrices and vectors, Hermitian means symmetric and $x^* = x^T$. It can be shown that, for a given matrix M , the Rayleigh quotient reaches its minimum value λ_1 for the corresponding Eigen-vector v_1 . Similarly, the ratio has a maximum too.

Example of use of stability criteria in the form $\delta(\delta^2\Pi) = 0$

Now arrives the turn to use Trefftz stability criterion $\delta(\delta^2\Pi) = 0$. Again solving the same buckling problem for the elastic columns. Recall that the stress state in the initial state is assumed not changing at the moment of buckling. In particular the axial internal force $N(x) \approx N^0$. In order to not make the repetitive reading not boring and more challenging, I will write directly the stationarity of total potential energy in the form of the virtual work principle. So, then

$$\delta\Pi = -\int_0^\ell [M\delta\kappa + N\delta\epsilon]dx + P\delta u_0 \quad (1.120)$$

$$\delta\Pi = \int_0^\ell M\delta v''dx - N\int_0^\ell \delta[u' + \frac{1}{2}v'^2]dx + P\delta u_0 \quad (1.121)$$

$$\delta\Pi = \int_0^\ell M\delta v''dx - N\int_0^\ell v'\delta v'dx - N\int_0^\ell \delta u'dx + P\delta u_0 \quad (1.122)$$

$$\delta^2\Pi = \delta(\delta\Pi) = \int_0^\ell \delta M\delta v''dx - N\int_0^\ell \delta v'\delta v'dx = 0 \quad (1.123)$$

The initial (membrane) state was an equilibrium state, therefore $-N\int_0^\ell \delta u'dx + N\delta u_0 = 0$. This is accounted for in the integrations above by cancelling this term. So, now from above the Trefftz stability criteria reads:

$$\delta^2\Pi = -\int_0^\ell EI\delta v''\delta v''dx + P\int_0^\ell \delta v'\delta v'dx = 0 \implies P_{min} = P_{cr} = \frac{\int_0^\ell EI\delta v''\delta v''dx}{\int_0^\ell \delta v'\delta v'dx} \quad (1.124)$$

In the above we accounted for $N \approx N^0 = -P < 0$ and for linear elasticity and constitutive model $M = -EIv''$. The last result is nothing more than the Rayleigh-Ritz quotient obtained earlier using the first energy criteria $\Delta\Pi = 0$. In the above, since the virtual displacements δv are arbitrary, one then can technically choose $\delta v = \alpha v$, $\alpha \rightarrow 0^+$ to obtain Equation (1.115).

Overall: All the three energy criteria for stability, $\Delta\Pi = 0$, $\delta(\Delta\Pi) = 0$ and $\delta(\delta^2\Pi) = 0$ evaluated at the critical point are indeed equivalent.

The **Lagrange** theorem (minimum total potential energy) will be systematically used to investigate or derive the Euler-Lagrange loss of stability field equations.

Physically speaking, the critical condition

$$\boxed{\delta(\Delta\Pi) = 0}, \quad (1.125)$$

means that the *adjacent configuration* next to initial one, is an **equilibrium state**. In other words, this equilibrium condition states that in the vicinity

of the initial-equilibrium state, there is an other *new neighbouring equilibrium state*. Therefore this is a *condition for bifurcation (Treffitz)* and it's defines the bifurcation point of the initial state⁷⁷. Condition (Eq. 1.125) is the *energy criterion for loss of stability*. It will be systematically used throughout this study.

Let $\Pi(u_0) \equiv \Pi_0$ be the total potential energy of the initial equilibrium state one hopes to study the stability. Let this initial state u^0 be perturbed a small amount δu to a new position u^* such that $u^* = u^0 + \delta u$ such that $\Pi(u^*) = \Pi_1 = \Pi^*$ (Fig. 1.25). Now one can write the increment of total potential energy between the two configurations (states) as (Fig. 1.25) and (Fig. 1.58).

$$\Delta\Pi = \Pi^* - \Pi^0 = \Pi_1 - \Pi^0, \tag{1.126}$$

therefore asking for the adjacent state u^* to be an equilibrium state leads to

$$\boxed{\delta(\Pi^*) = 0 = \delta\Pi^0 - \delta(\Delta\Pi) = 0 \implies \delta(\Delta\Pi) = 0,} \tag{1.127}$$

since the initial state u^0 is an equilibrium state for which holds naturally $\delta\Pi^0 = 0$.

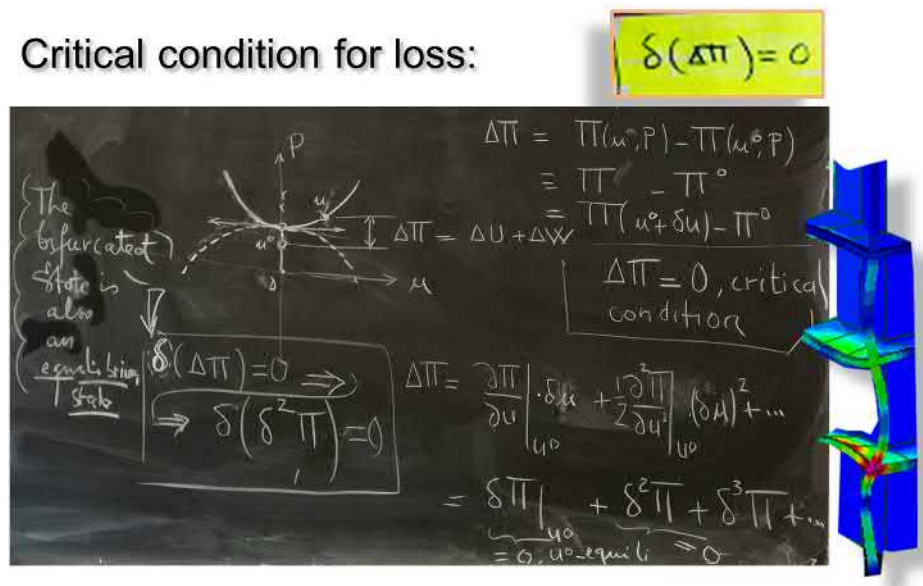


Figure 1.58: Stability of an equilibrium. The energy criterion for loss of stability.

⁷⁷This section is inspired by ideas from textbook by N. A. **Alfutov**, *Stability of Elastic Structures*. Springer 2000 (Translated from Russian)

To show that the above more general criticality condition (1.127) leads to Trefftz condition⁷⁸

$$\delta(\delta^2\Pi) = 0, \quad (1.128)$$

the total potential energy increment from the initial state to the neighbour new state is developed into Taylor series (to the second order and higher) in the vicinity of the initial equilibrium configuration u^0 and gives

$$\Delta\Pi = \Pi(u^0 + \delta u) - \Pi(u^0) = \underbrace{\delta\Pi|_{u^0}}_{=0} + \frac{1}{2}\delta^2\Pi|_{u^0} + \frac{1}{3!}\delta^3\Pi|_{u^0} + \dots \quad (1.129)$$

$$\delta(\Delta\Pi) = 0 \implies \delta\left(\frac{1}{2}\delta^2\Pi|_{u^0} + \frac{1}{3!}\delta^3\Pi|_{u^0} + \dots\right) = 0 \quad (1.130)$$

where the first variation $\delta\Pi^0 = \delta\Pi|_{u^0} = 0$ (u^0 -equilibrium initial state) and therefore, keeping only the quadratic terms, one obtains the energy criterion (Eq. 1.128)

$$\delta(\Delta\Pi) = 0 \implies \delta(\delta^2\Pi) = 0, \quad (1.131)$$

which is known as the **Trefftz** condition for stability loss. So, we see that the energy criterion for stability is physically the same as the Trefftz criterion (Fig. 1.58) when keeping till second-order terms is sufficient to decide on the nature of stability⁷⁹.

It is not useless to recall that equation (1.131) is indeed the criticality condition for loss of stability since in case of stable new state one have $\Delta\Pi > 0$ and for unstable case $\Delta\Pi < 0$. Therefore a transition from stable to unstable state or *vice-versa* occurs when

$$\boxed{\Delta\Pi|_{u^0} = 0; \quad P_{cr} = P_{min}, \quad u^0 - \text{equilibrium point.}} \quad (1.132)$$

⁴ Give an infinitesimal perturbation δu : **stable** $\delta^2\Pi > 0$, **neutrally stable**: $\delta^2\Pi = 0$ and **unstable**: $\delta^2\Pi < 0$. $\Pi[u]$ is the total potential energy.

The nature of the stability of an equilibrium⁴, more particularly in our context of a *static equilibrium* can be assessed through second and higher order variations of the total potential energy of the system. Otherwise, for more general dynamics, the engineer should use the versatile **Luyaponov stability** criteria.

1.10 Homogeneous linearised equations of stability

Assume the system is in known initial equilibrium. We are interested to determine the bifurcation point of this initial state. The sufficient condi-

⁷⁸Which follows from more general energy criterion for loss of stability (Equation 1.125

⁷⁹So, one has not $\delta^2\Pi|_{u^0} = 0$ at the critical equilibrium point u_0 .

tion for the bifurcation point is the existence of a close adjacent equilibrium state to the initial one, not far from it. Therefore, it is not necessary to consider a large deviation from the initial state of equilibrium; a sufficiently infinitesimal departure from it is sufficient. Therefore considering the *linearised equations of elastic-stability* around the critical point is to determine the bifurcation point. These equations are those of a *linearised eigenvalue problem*. The smallest eigenvalue corresponds to the critical buckling load and the corresponding *eigenmodes* gives us the *configuration of the system in the new equilibrium configuration* up to a multiplicative scalar in the vicinity of the bifurcation point.

The homogeneous equations of the *elastic-stability* can be derived based on the following three basic methods⁸⁰:

1. applying, systematically, the **energy criteria**⁸¹ for bifurcation stability loss; $\delta(\Delta\Pi) = 0$ at the critical (equilibrium) point. Note that the increment of the total potential energy $\Delta\Pi$ should be, at least, expanded to the accuracy up-to second⁸² order (the squares⁸³).
2. directly writing the **equilibrium equations in the deformed configuration** which stability we are investigating and adjacent to the initial equilibrium state.
3. of course, one can derive first the full (geometrically) **non-linear equations** in the vicinity of the critical point and then **linearise** them near the initial equilibrium point.

As seen previously, the linear strain-displacement relation is not sufficient for stability analysis. It come out that non-linear effect up to second order should be accounted for.

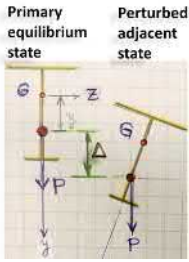
⁸⁰Ref: Alfutov . *Stability of elastic structures*

⁸¹This is the approach which will be use systematically in our current course of stability: *CIV-E4100 - Stability of Structures L*.

⁸²At least up-to the 2nd order. When needed, higher order terms should be included. For instance, in cases when the second variation vanishes or its higher orders. Since the sign of $\Delta\Pi$ will be given by the non-zero term of the Taylor expansion.

⁸³This idea is used systematically by professor Juha **Paavola** in his lecture notes when using energy method to derive stability equations in the additional written material he distributes for the course - *CIV-E410 Stability of Structures (2018)*. The written material by J. Paavola (*Structural Stability*) is valuable with plenty of examples: it is systematic and general methodology (which represents a generalisation and an extension of Bryan and Timoshenko forms type of the energy criterion) to derive the basic equations of stability for any type of elastic structural basic elements, like for instance, beam-columns, torsional buckling, lateral-torsional buckling, buckling of plates and cylindrical shells. Have a look to the material.

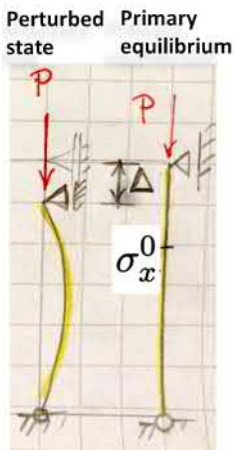
1.10.1 The energy criterion



Additional work
 $\Delta W_{\text{ext}} = P \cdot \Delta$
 (Lateral torsional buckling)

In the following three general and most common forms of energy criterion will be presented in short. The so called **Bryan**⁸⁴ form of the energy criterion for stability will be here a bit more detailed. There exist also another form for the energy criterion known as **Timoshenko** form. For more details on the two forms, please refer to the textbook by **Alfutov**⁸⁵.

There is a more general form for the energy criterion of loss of elastic stability, presented by J. Paavola in his lecture notes⁸⁶ on (*Structural Stability*). The methodology represents an extension and a generalisation of Bryan and Timoshenko forms of the energy criterion of stability. Let's refer to it as the *mixed form* which is known as the **Euler**⁸⁷. Refer, for details, to classical textbooks by **Novozhilov** and **Washizu**. Novhozhilov, in his classical textbook chapter [Chap. V: The problem of elastic stability], writes: *in investigating multiple equilibrium positions of elastic bodies, it is absolutely essential to take the effect of rotations (rotation components of the finite strains) into account.* (I added the words in brackets for later use when splitting the finite strains into linear and non-linear parts). In short, such *mixed* form accounts both for the work of initial stresses on additional deformations and for the work of external load on additional displacements caused by the transition to the perturbed configuration from the primary equilibrium state.



Additional work
 $\Delta W_{\text{ext}} = P \cdot \Delta$
 (Flexural buckling)

Bryan energy criterion for stability loss, study the accumulation or increment of total strain energy when the initial equilibrium configuration is given a small finite perturbation close to the initial state. Especially, the increment of work of external loads during this infinitesimal perturbation is accounted for through the strain energy accumulation due to the work of initial internal stress on additional perturbed strains. The strain energy accumulation due to the work of initial internal stress on additional perturbed strains is accounted for. Consequently, such approach allows also to determine the displacements before critical state in addition to the critical

⁸⁴Luis A. Godoy, The general theory of elastic stability at the end of the 19th century. *international Journal of Structural Stability and Dynamics*. Vol. 11. No. 3 (2011) 401-410

⁸⁵N. A. Alfutov, *Stability of Elastic Structures*. Springer 2000 (translated from Russian)

⁸⁶Juha Paavola, *Structural Stability* part of the course CIV-E4100 - Stability of Structures L (2018)

⁸⁷See classical textbooks of Novozhilov, *Foundation of Non-linear Theory of Elasticity* [Chap. V: The problem of elastic stability]. Graylock Press, 1953 (translation from Russian)

state (critical load and corresponding buckling mode).

However, if during the infinitesimal transition from the primary equilibrium state to the perturbed state, the external load will do additional work $\Delta W_{\text{ext}} \neq 0$, for $\Delta \neq 0$ which is not included in the work of initial stresses, than the Bryan form does not see such work (Margin Figure for lateral buckling) and then Timoshenko form is more suitable. When one includes $W_{\text{ext}} = P \cdot \Delta \neq 0$ into Bryan form of the criterion, one obtains naturally the mixed form (or the Euler form). For such cases, Timoshenko form of the criterion will be also adequate. Another example can be the flexural buckling (Margin Figure for flexural buckling) where the Bryan form is still adequate since the work of the initial stresses σ_x^0 is now equal to the work of external forces ΔW_{ext} .

As in the previous case, **Timoshenko** energy criterion studies the system deviation from initial equilibrium configuration to a infinitesimally close perturbed configuration without accounting for the deformation history away from the initial state. Such approach allows determination of the critical load, too. Now, the work of the initial stresses on the perturbed deformations is not accounted for explicitly but the work of external forces on the additional perturbed displacements is explicitly included.

There exists also a bit 'modern' or 'new' third energy criterion⁸⁸ called *criterion of critical levels of energy*.

* * *

Some basic examples of use of these criteria will be provided at the end of this section. *I will prefer to use the mixed form⁸⁹ of the energy criterion for elastic stability loss because of its generality. Both the additional work of initial stresses and of external forces is explicitly included during transition from initial equilibrium to perturbed state.*

In the following the Bryan criterion will be detailed. At the end of this section, the **Timoshenko** criterion will also be presented. For derivation details, refer to above referenced textbook by N.A. Alfutov.

⁸⁸L. Stupishin, *Comparative analysis of buckling criteria for engineering structures. Single-degree-of-freedom systems. 7th international Conference on Key Engineering Materials (ICKEM, 2017). IOP: Conf. Series: Materials Science and Engineering 201 (2017) 012020.*

⁸⁹the method presented by Prof. Paavola in his course on Stability of Structures

Bryan criterion

The energy criteria $\delta(\Delta\Pi) = 0; P = P_{cr,min}$ will be systematically used to illustrate to derive the Eigen-problem corresponding to the linearised homogeneous equations of stability loss. For notations, see (Fig. 1.158) where the idea to recall is: consider primary equilibrium state (pre-buckled configuration \mathbf{u}^0) and give perturb infinitely slightly this configuration by $\delta\mathbf{u}$ such that

$$\mathbf{u}^* = \mathbf{u}^0 + \delta\mathbf{u} \equiv \mathbf{u}^0 + \alpha\mathbf{u}_1, \quad (1.133)$$

where α being an infinitely small scalar. The displacement vector being noted as $\mathbf{u} = (u, v, w)^T$. Determining the Lagrange finite total strains⁹⁰

$$\epsilon_{ij}^* = \frac{1}{2}(u_{i,j} + u_{j,i} + u_{k,i}u_{k,j}) \quad - \text{ using Einstein summation rule} \quad (1.134)$$

$$\mathbf{E} = \frac{1}{2} \left((\nabla_X \mathbf{u})^T + \nabla_X \mathbf{u} + (\nabla_X \mathbf{u})^T \cdot \nabla_X \mathbf{u} \right), \quad (1.135)$$

from the perturbed displacements and gathering them into powers of α up to α^2 inclusive, and neglecting terms containing the derivatives⁹¹ of the initial displacement \mathbf{u}^0 , on obtains

$$\epsilon^* = \epsilon^0 + (\alpha\epsilon_1 + \alpha^2\epsilon_2) \equiv \epsilon^0 + \delta\epsilon. \quad (1.136)$$

In the above formulas, coordinates X are the material coordinates. In the strain expansion (1.136), the linear parts of the strains are the initial strain $\epsilon^0 = \mathbf{L}\mathbf{u}_0$ and the linear part of the perturbed strain (linear part of $\delta\epsilon_1$)

$$\boxed{\epsilon_1 = \mathbf{L}\mathbf{u}_1}, \quad (1.137)$$

where \mathbf{L} the linear part of the differential operator for strains defined in Eq. (1.135). One need to determine the word increment of initial stresses on the additional perturbation strains. Actually, it is found that only the non-linear part (second-order part) of such perturbed strain increment will be work conjugate with the initial stress σ^0 for computing the increment of

⁹⁰This is the Lagrangian finite strain tensor which is also known as Green-Lagrangian strain tensor. The reader should refer to some textbooks or basic course in *Continuum Mechanics*. In the definition above, the *material displacement gradient tensor* $\nabla_X \mathbf{u}$, the partial derivatives of the displacement vector are with respect to the material (Lagrangian) coordinates.

⁹¹It is assumed that the initial stress, external dead loads remains constant during the transition from the pre-buckled initial equilibrium to infinitesimally adjacent perturbed configuration. Also the derivatives of displacements from the primary equilibrium vanishes.

total potential energy $\Delta\Pi$. For that purpose, one defines the second order components (multiplying α^2 in Eq. 1.136)) of the strain vector⁹² rising from the perturbation of displacement $(u_1)_i = \mathbf{u}_1$ as

$$\epsilon_2 = [\epsilon_{11}^{**}, \epsilon_{22}^{**}, \epsilon_{33}^{**}, \gamma_{23}^{**}, \gamma_{31}^{**}, \gamma_{12}^{**}]^T \quad (1.138)$$

where the quadratic part the finite strains (1.135) as

$$\boxed{\epsilon_2 = \epsilon_{ij}^{**} = \frac{1}{2}(u_1)_{k,i}(u_1)_{k,j}}, \quad (1.139)$$

where the shear angle $\gamma_{ij} = \epsilon_{ij} + \epsilon_{ji}$.

The increment or change (accumulation) of total potential energy

$$\Delta\Pi = \Pi[\mathbf{u}^0 + \underbrace{\delta\mathbf{u}}_{=\alpha\mathbf{u}_1}] - \Pi[\mathbf{u}^0] = \underbrace{\delta\Pi|_{\mathbf{u}_0}}_{=0} + \delta^2\Pi|_{\mathbf{u}_0} + \dots \approx \underbrace{\alpha\Pi_1}_{=0} + \alpha^2\Pi_2. \quad (1.140)$$

Since the initial (primary- or pre-buckled configuration) is an equilibrium state one have, in the above equation, $\delta\Pi|_{\mathbf{u}_0} \equiv \alpha\Pi_1 = 0$. Finally, the criterion for bifurcational loss stability can be stated as, for instance,

$$\delta(\Delta\Pi) = \delta(\delta^2\Pi|_{\mathbf{u}_0}) + \dots \approx \alpha^2\delta\Pi_2 = 0, \quad (1.141)$$

where the multiplier constant α can be omitted.

Integrating the strain energy density $u = \frac{1}{2}\epsilon^T\mathbf{E}\epsilon$ over the volume of the structure, and accounting for elasticity (Hooke's law), $\sigma^0 = \mathbf{E}\epsilon^0$, $\sigma_1 = \mathbf{E}\epsilon_1$ and $\sigma_2 = \mathbf{E}\epsilon_2$, collecting the terms multiplying α^2 , and omitting the multiplier α^2 , one finally, obtains

$$\Pi_2 = \frac{1}{2} \int_V \epsilon_1^T \mathbf{E} \epsilon_1 + \epsilon_0^T \underbrace{\mathbf{E} \epsilon_2}_{\sigma_2 = \mathbf{E} \epsilon_2} + \epsilon_2^T \sigma^0 dV. \quad (1.142)$$

Now let's have a breath and recall the reciprocity theorems of **Betti-Maxwell** saying that $\epsilon_0^T \mathbf{E} \epsilon_2 = \epsilon_0^T \sigma_2 = \epsilon_2^T \sigma^0$. Accounting for that in the above expression, we finally obtain the Bryan form of the the increment of the strain energy $\Delta\Pi$, between the perturbed and primary state, can be written as

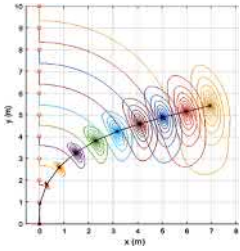
$$\boxed{\Delta\Pi = \frac{1}{2} \int_V \epsilon_1^T \mathbf{E} \epsilon_1 dV + \int_V \epsilon_2^T \sigma^0 dV.} \quad (1.143)$$

Note that initial stress σ^0 enters explicitly the Bryan energy criterion (1.143). Therefore this allows to find the critical points (bifurcation points)

⁹²Voigt's notation

independently on the origin of the cause causing the initial stresses. Such causes can be mechanical load, thermal gradients of temperature changes, initial strains, initial displacement, swelling, ... etc. So, cases with other than mechanical loading cannot be addressed naturally by the corresponding Timoshenko criterion of stability.

Note that, there is cases when some part of incremental work of external forces done on the change of the (quadratic part of) the non-linear strain increment ϵ_2 in the perturbed state cannot be accounted by the work of initial stresses. Consequently, the change in the potential of external force $\Delta V = -\Delta W_{ext}(P, \epsilon_2)$ should added to the total potential energy functional



Dynamics of buckling of slender column. Initial configuration (small circles) & node trajectories. Note that these trajectories are convergent to a stable configuration. (smooth curves) (Baroudi, 2018). /simulation/

$$\Delta \Pi = \frac{1}{2} \int_V \epsilon_1^T \mathbf{E} \epsilon_1 dV + \underbrace{\int_V \epsilon_2^T \sigma^0 dV}_{U(\sigma^0, \epsilon_2)} - \underbrace{\Delta W_{ext}(P, \epsilon_2)}_{\text{such that } \not\in U(\sigma^0, \epsilon_2)} \quad (1.144)$$

an example of such case is the lateral torsional buckling of a narrow rectangular cantilever beam with the end-load is located at a height $a \neq 0$ over (or above) the gravity center of the section. (you will have a concrete example in the section on lateral torsional buckling).

Important: in Equations (1.143 and 1.144) the deformations (linear part ϵ_1 and quadratic part ϵ_2) and the displacements are to be estimated in the slightly buckled configuration while the initial stresses σ^0 and external forces P are to be estimated in the pre-buckled configuration. It is assumed that during buckling, these initial stresses forces remain approximately constant.

About the sign of change in the potential of external forces

Example from lateral torsional buckling:

Recall that the potential of external forces being defined as the change

$$\Delta V = -\Delta W_{ext}, \quad (1.145)$$

in our conservative force system, where ΔW_{ext} being the increment in the work of external forces.

Be careful with the sign: Be specially careful with the sign when writing the change in the work ΔW_{ext} of external force \vec{F} on a displacement \vec{d} of its application point. For instance, the change in the potential of the force is $\Delta V = -\Delta W_{ext} = -\vec{F} \cdot \vec{d}$. So the work ΔW_{ext} is positive when the force and the displacement are in the same direction. On the contrary, it becomes negative when the force acts in the opposite direction of the displacement.

For instance, one very common possibility for mistake for many of us, is when considering lateral torsional buckling where the external force (gravity load) is downward directed and transversal to the neutral axis of the beam. At buckling the cross-section rotates an amount ϕ around its center of rotation (or of shear) and the point of application of the load *rises upward* by a distance d . In the case the work change is negative, since the load and the displacements are in opposite directions, so $\Delta W(F) = \vec{F} \cdot \vec{d} = -Fd < 0$ where $F > 0$, $d > 0$ and $d = a(1 - \cos \phi) \approx 1/2\phi^2$, where in this particular explaining example $a > 0$ being the location of the force bellow the shear center (SC) or the gravity center (G).

Let's illustrate with a small example we will need when studying lateral-torsional buckling. Recall the change in total potential energy being

$$\Delta\Pi = \Delta U + \Delta V, \tag{1.146}$$

where the change in the potential of the forces $\Delta V = -\Delta W_{ext}$. For the loading cased $\vec{F} = F\vec{j}$ and distributed transversal load $\vec{q}_y = q_y(x)\vec{j}$ (Figure 1.59). In both loading cases we have $d > 0$, $F > 0$ and $q_y > 0$. The force and the displacement \vec{d} of the load application point occurs in opposite direction, therefore the work is negative and given by

$$\Delta W_{ext} = \begin{cases} \vec{F} \cdot \vec{d} = [F]\vec{j} \cdot [-d]\vec{j} = -Fd < 0, & \text{point load} \\ \int_0^\ell \vec{q}_y \cdot \vec{d} dx = \int_0^\ell [q_y]\vec{j} \cdot [-d]\vec{j} dx = - \int_0^\ell q_y(x)d(x) dx, & \text{distributed} \end{cases} \tag{1.147}$$

In this particular example of lateral torsional buckling (Figure 1.59), the moderate rotation expansion is used $\cos \phi \approx 1/2\phi^2$ then $d = 1/2a \cos \phi \approx \phi^2$ and then

$$\Delta W_{ext} = \int_0^\ell \vec{q}_y(x) \cdot \vec{d}(x) dx = - \int_0^\ell q_y \cdot a(1 - \cos \phi) dx \approx - \int_0^\ell q_y \cdot a[\frac{1}{2}\phi^2] dx \tag{1.148}$$

$$= - \frac{1}{2} \int_0^\ell a(x)q_y(x)\phi^2(x) dx \tag{1.149}$$

Summa summarum, the change in potential of external forces is now

$$\Delta V = -\Delta W_{ext} = - \int_0^\ell \vec{q}_y(x) \cdot \vec{d}(x) dx = \int_0^\ell q_y \cdot a(1 - \cos \phi) dx \approx \int_0^\ell q_y \cdot a[\frac{1}{2}\phi^2] dx \tag{1.150}$$

for a transversal distributed load and equivalently for any point load.

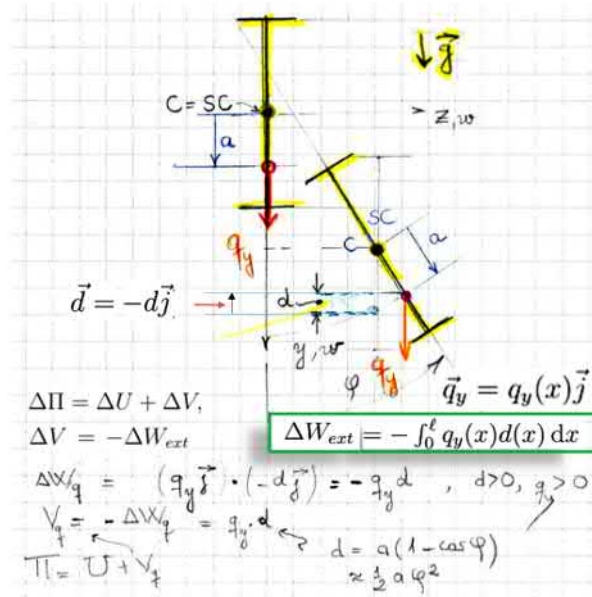


Figure 1.59: Illustration of the work of external load in lateral torsional buckling. Note the sign: the force and the displacement are in opposite directions, so the work change is negative here.

Example from Euler buckling:

Example of column buckling: Illustrative example for the criterion (Eq. 1.143): flexural buckling for simply supported column in a plan. Let the pre-buckled (primary equilibrium) state be $\mathbf{u}_0 = (u_0, v_0 \equiv 0)$. The perturbed configuration (post-buckled) is now $\mathbf{u}^* = \mathbf{u}_0 + (u, v) \equiv \mathbf{u}_0 + \alpha \mathbf{u}_1$, and using previous notation for the increment $u_1 = u, v_1 = v$ but with dropping the index 1. The total potential energy increment in the Bryan form is

$$\Delta \Pi = \frac{1}{2} \int_0^\ell EI(v'')^2 dx + \underbrace{\int_0^\ell \sigma_x^0 A \left[\frac{1}{2} (v')^2 \right] dx}_{\epsilon_2}, \quad (1.151)$$

where $v_1 \equiv v(x)$, $u_1 \equiv u(y, x) = -yv'(x)$. Consequently, the linear part of deformations $\epsilon_1 = -yv_1''(x) \equiv -yv''(x)$ and the quadratic part is $\epsilon_2 = \frac{1}{2}(v_1')^2 \equiv \frac{1}{2}(v')^2$. The pre-stress from the primary state is $\sigma_x^0 A = N^0(x)$. (in this example we've used the notation $v = v_1$ in the functional). The varied (perturbed) configuration was $v^* = v^0 + \delta v \equiv v^0 + \alpha v_1$, ($v^0 = 0$), and $u^* = u^0$ (no change in length of the centreline during buckling).

Note that the Timoshenko form of the increment of total potential en-

ergy will be

$$\Delta\Pi = \frac{1}{2} \int_0^\ell EI(v'')^2 dx - P \underbrace{\int_0^\ell \left[\frac{1}{2}(v')^2\right] dx}_\Delta, \quad (1.152)$$

where $P = -N^0$ being constant, for the simply supported column under end compression ($P > 0$). The formal difference with Bryan form is that the incremental work of external force on the perturbed configuration

$$\Delta V = -\Delta W_{\text{ext}} = -P \int_0^\ell \left[\frac{1}{2}(v')^2\right] dx \quad (1.153)$$

is included and it is equivalent internal work for initial stress σ_x^0 on the non-linear part of the incremental deformation. Now from the above Bryan form of the criterion (eq:Bryan-energy-criterion-form-flexion), we obtain $\sigma_x^0 A = N^0 = -P < 0$ which is the same than in the Timoshenko form (1.152).



Tip displacement increment after buckling.

Timoshenko energy criterion

Recalling previously discussed, this form of the energy criterion the initial stress of the primary equilibrium state does not enter explicitly. The increment of total potential energy is accounted for through the increment of the work of external forces on the perturbed finite displacements during transition from primary state to the slightly perturbed state. The increment of displacement should be expanded up-to second order, at least. Therefore, the total displacement in the adjacent new equilibrium is described by the quadratic expansion (up-to second variation)

$$\mathbf{u} = \mathbf{u}_0 + \alpha\mathbf{u}_1 + \alpha^2\mathbf{u}_2, \quad (1.154)$$

where α being infinitely small scalar. Keeping terms up-to α^2 in the deformations, one obtains

$$\epsilon = \epsilon_0 + \alpha\epsilon_1 + \alpha^2\epsilon_2, \quad (1.155)$$

and so on⁹³.

Such approach can be more nature for situations where such work is easy to formulate. An illustrative simple example can be the stability of the previous straight column (1.152).

⁹³See the Alfutov's textbook for details.

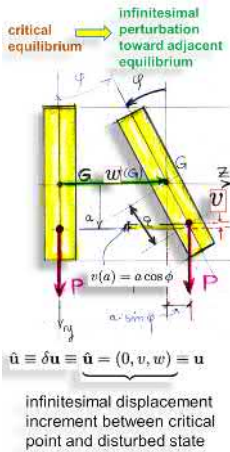
Mixed or Euler criterion

This form of the energy criterion is more versatile⁹⁴. As previously told, the methodology represents a generalisation of Bryan and Timoshenko forms of the energy criterion of stability. The approach or method used to derive the mixed form is known as the **Euler** method⁹⁵. May be one just call the mixed form the *Euler* form. Let's do so, in the following.

This Euler form *accounts explicitly for both* the additional work of the initial stresses on additional deformations and of work of external loads on the additional displacements caused by the transition to the perturbed configuration from the primary equilibrium state.

Note that the reference configuration has not to be at a critical equilibrium point. Any other equilibrium configuration can be chosen as a reference state to be perturbed.

In the following, I often, for shortness when only the stability equations are of interest, work directly, as in Bryan and Timoshenko form of the energy criterion, with the increment of total potential energy and thus directly with the increment of displacements. Therefore, I chose naturally the initial equilibrium state (configuration \mathbf{u}^0) which is slightly perturbed to a new configuration \mathbf{u}^* being infinitely close to or at the critical point for which the stability one want to study. Therefore, the dead load and displacements of primary equilibrium are kept constant during the perturbation (not varied) (*Cf.* Figure 1.61). This way, we obtain directly the equations of stability by taking the first variation of the increment of total potential energy $\delta(\Delta\Pi) \equiv \delta(\delta^2\Pi)$ with respect to the displacement increment $\delta\mathbf{u} \equiv \hat{\mathbf{u}}$ due to perturbation at critical point \mathbf{u}^0 . The primary equilibrium equations are not for interest now. Later, when dealing with the stability illustration examples, this notational difference will not be written, since it became not necessary, once we know that $\delta\mathbf{u} \equiv \hat{\mathbf{u}}$ stand for such tiny changes away from the critical equilibrium point. Therefore, from now till not otherwise stated, I will use simply the notation



$$\hat{\mathbf{u}} \equiv \delta\mathbf{u} \equiv \underbrace{\mathbf{u} = [u, v, w]^T}_{\text{this stands for changes away from critical point}} \rightarrow \text{strain changes} \rightarrow \epsilon \tag{1.156}$$

for such increment in displacement change between a critical equilibrium point and it's tiny perturbation. For instance, for the case of lateral tor-

⁹⁴Presented by J. Paavola in his lecture notes *Structural Stability* in the course CIV-E4100 - Stability of Structures L (2018)

⁹⁵Washizu. *Variational methods in elasticity and plasticity*.

sional buckling, $\hat{\mathbf{u}} \equiv \mathbf{u} = (u, v, w)$ which becomes for a narrow cross section bended in the plane (x, y) of major bending rigidity; $\hat{\mathbf{u}} = (0, v, w) \equiv \mathbf{u}$ (Cf. example later). The corresponding induced strain changes will be denoted simply by ϵ .

Therefore the dead load

(P^0) is kept constant during variation or transition from 1 \rightarrow 2: $u^* = u^0 + \delta u \equiv u^0 + \hat{u}$, $\Delta\Pi = \Delta U + \Delta V$. The tiny perturbation from u_0 to u^* will induce changes (increments) in stresses $\sigma_0 \rightarrow \sigma_0 + \sigma^*$ and in strains $\epsilon_0 \rightarrow \epsilon_0 + \epsilon^*$. It is assumed that initial stress and dead loads do not change during the tiny incremental motion.

$$\Pi^* = \Pi[u^0 + \delta u, P^0] = \underbrace{\Pi[u^0, P^0]}_{=0} + \frac{\delta\Pi|_{u^0}}{2} + \frac{1}{2}\delta^2\Pi|_{u^0} + \frac{1}{3!}\delta^3\Pi|_{u^0} + \dots \quad (1.157)$$

The idea is now to develop the increment of total potential energy up to second or higher when the second, third and so on, variation vanishes.

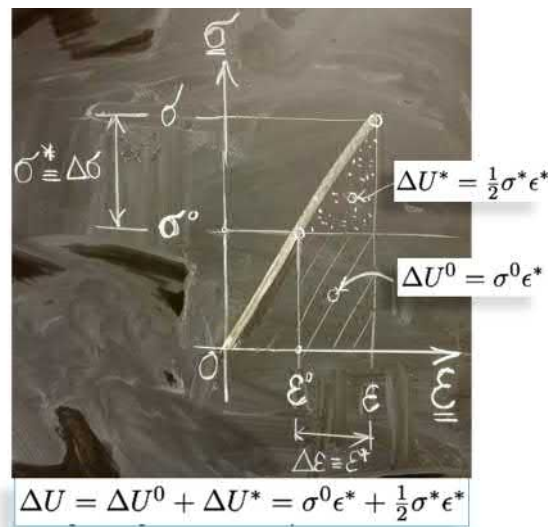


Figure 1.60: The strain energy change between reference equilibrium state \mathbf{u}^0 and a perturbed neighbouring (equilibrium) state \mathbf{u} . The change in strains being $\epsilon^* = \Delta\epsilon = \epsilon - \epsilon^0$ and in stresses $\sigma^* = \Delta\sigma = \sigma - \sigma^0$

Then the energy criterion for the stability loss is unchanged and is (physically, an equilibrium condition for the perturbed state $u^* = u^0 + \delta u \equiv$

$u^0 + \hat{u}$):

$$\delta(\Delta\Pi^*) = 0, \forall \delta u \quad \text{kin. admissible} \quad (1.158)$$

$$\delta(\Pi[u^0 + \delta u, P^0]) = \delta[\Pi[u^0, P^0] + \underbrace{\delta\Pi|_{u^0}}_{=0} + \frac{1}{2}\delta^2\Pi|_{u^0} + \frac{1}{3!}\delta^3\Pi|_{u^0} + \dots] = 0, \forall \delta u \quad (1.159)$$

$$\delta(\Pi[u^0 + \delta u, P^0]) = \underbrace{\delta[\Pi[u^0, P^0]]}_{=0} + \delta[\frac{1}{2}\delta^2\Pi|_{u^0}] + \delta[\frac{1}{3!}\delta^3\Pi|_{u^0}] + \delta[\dots] = 0, \forall \delta u \quad (1.160)$$

$$\underbrace{\delta(\Pi[u^0 + \delta u, P^0]) - \Pi[u^0, P^0]}_{\delta(\Delta\Pi)=0} = \underbrace{\delta[\frac{1}{2}\delta^2\Pi|_{u^0}] + [\frac{1}{3!}\delta^3\Pi|_{u^0}] + \delta[\dots]}_{=0} = 0, \forall \delta u. \quad (1.161)$$

When we keep terms only up-to the second order we obtain the energy criterion for stability loss in the familiar Trefftz form too as:

$$\boxed{\delta(\Delta\Pi) = \delta[\delta^2\Pi|_{u^0}] = 0, \forall \delta u, \quad \text{kin. admissible,}} \quad (1.162)$$

Physically, criterion (Eq.1.162) is saying that the perturbed configuration is an equilibrium state, too.

The homogeneous linearised equations of stability: In the following, the star-symbol * will be dropped from the perturbed strains ϵ^* will be written ϵ

- Derivatives of the primary equilibrium configuration when the structure switch from a critical point \mathbf{u}^0 to the infinitely close perturbed configuration, remains negligible⁹⁶, thus first derivatives $\mathbf{u}_{,i}^0 = 0$, $x_i = x, y, z$ when considering changes in the displacements.
- If we consider total displacement \mathbf{u}^* and include the initial state when, making variations, then \mathbf{u}^0 's derivatives should be included. It should be noted that the the primary state displacements and the additional displacements in the perturbed state are differently (separately varied). In this case, for initial state \mathbf{u}^0 we obtain the equations of equilibrium of the primary state too, in addition to the homogeneous linearised equations of equilibrium of loss of stability for the increments of the displacements $\hat{\mathbf{u}}$.

⁹⁶that can be shown true; Homework.

1.10. HOMOGENEOUS LINEARISED EQUATIONS OF STABILITY 05

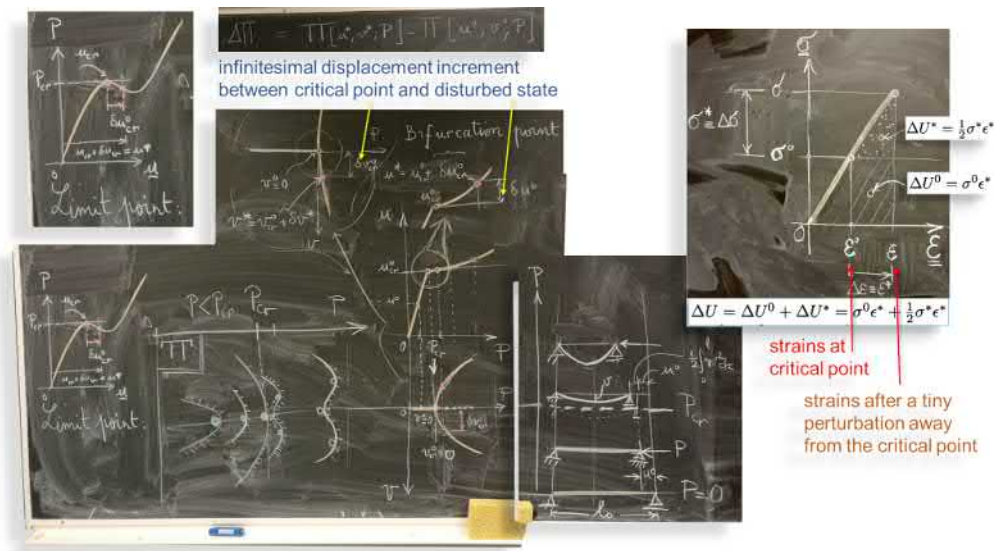


Figure 1.61: Schematic for the nature of the increment of displacements. Here, I take it as the infinitesimal additional displacement $\delta \mathbf{u} \equiv \hat{\mathbf{u}}$ happening between the transition from the critical equilibrium point \mathbf{u}_{cr}^0 to a perturbed adjacent equilibrium configuration $\mathbf{u}^* = \mathbf{u}_{cr}^0 + \delta \mathbf{u}$. During this change of configuration, it is assumed that dead loads \mathbf{f} remain constants (and thus P also is unchanged). The total potential energy increment $\Delta \Pi$ is computed between these two configurations. The linearised homogeneous equations of stability *via* energy criteria $\delta(\Delta \Pi) = 0, \forall \delta \mathbf{u}$ or $\forall \hat{\mathbf{u}}$.

Applying the mixed or Euler form: Let write again the energy criteria in its incremental form. Note that now the *total displacement* \mathbf{u}^* will be used instead of its increment between reference (primary equilibrium) and perturbed value. Later, the symbol star (*) will be dropped and denote, for instance total displacements simply by $\mathbf{u} = \mathbf{u}^0 + \delta \mathbf{u}$ and the corresponding total strains by ϵ .

It should be recalled that the reference configuration has not to be at a critical equilibrium point. Any other equilibrium configuration can be chosen as a reference state to be perturbed. Here, I take it as the infinitesimal additional displacement $\delta \mathbf{u} \equiv \hat{\mathbf{u}}$ happening between the transition from the critical equilibrium point \mathbf{u}_{cr}^0 to a perturbed adjacent equilibrium configuration $\mathbf{u}^* = \mathbf{u}_{cr}^0 + \delta \mathbf{u}$.

During this infinitesimal change of configuration, it is assumed that dead loads \mathbf{f} remain constants (and thus P also is unchanged). The total potential

energy increment $\Delta\Pi$ is computed between these two configurations as

$$\Delta\Pi = \Pi[\mathbf{u}_{cr}^0 + \delta\mathbf{u}, P^0] - \Pi[\mathbf{u}_{cr}^0, P^0]. \quad (1.163)$$

Finally, the linearised homogeneous equations of stability are derived by imposing equilibrium to the new adjacent equilibrium state through the energy criteria $\delta(\Delta\Pi) = 0, \forall\delta\mathbf{u}$ or $\forall\delta\hat{\mathbf{u}}$ (Fig. 1.62).

Now the corresponding change total strain energy of the system will be obtained by integrating the strain energy density $\Delta u = \Delta u^0 + \Delta u^*$ over the volume of the structure $\Delta u = \sigma^0 : \epsilon^* + \frac{1}{2}\sigma^* : \epsilon^*$, where $\epsilon^* = \epsilon - \epsilon^0$.

The total potential energy change (Figs. 1.60 and 1.61)

$$\Delta\Pi = \Delta U + \Delta V, \quad \Delta V = -\Delta W_{\text{ext}}, \quad (1.164)$$

where

$$\Delta U = \int_V \sigma^0 : \epsilon^* dV + \frac{1}{2} \int_V \sigma^* : \epsilon^* dV, \quad \text{where } \epsilon^* = \epsilon - \epsilon^0. \quad (1.165)$$

The strain energy change between reference equilibrium state \mathbf{u}^0 and a perturbed neighbouring (equilibrium) state \mathbf{u}^* (Fig. 1.60). The change in strains being $\Delta\epsilon = \epsilon - \epsilon^0$ and in stresses $\Delta\sigma = \sigma - \sigma^0$

In the work of external loads ΔW_{ext} , the additional displacement should be expanded, at least, up-to second order⁹⁷. Finally, the mixed energy criterion form for stability loss reads:

$$\delta(\Delta\Pi) = \delta[\delta^2\Pi|_{\mathbf{u}^0}] = 0, \forall\delta\mathbf{u}, \quad \text{kin. admissible}, \quad (1.166)$$

where now \mathbf{u}^0 being a critical equilibrium point. The contribution of $\Delta U^* = \frac{1}{2} \int_V \sigma^* : \epsilon^* dV$ has to be estimated using the linear parts of the strain changes ϵ^* . On the contrary, now the contribution $\Delta U^0 = \int_V \sigma^0 : \epsilon^* dV$ has to be done with non-linear part of the change in strains. According to J. Paavola's lecture notes, it comes out that is better to express the non-linear part of the strain energy change using the partition of the finite strain⁹⁸ (increment)

$$\epsilon_{ij} = \frac{1}{2}(u_{i,j} + u_{j,i} + u_{k,i}u_{k,j}) \quad (1.167)$$

⁹⁷Example of such expansion up-to 2nd order: lateral buckling case, see further: The incremental external work $\Delta W_{\text{ext}} = Pa(1 - \cos\phi(\ell)) \approx \frac{1}{2}Pa\phi^2(\ell)$, where a being the elevation of the point of action of the point end-load P above the neutral axis of the cross-section.

⁹⁸Recall that now u_i stands for the increments Δu_i or the perturbation of the displacement.

1.10. HOMOGENEOUS LINEARISED EQUATIONS OF STABILITY 07

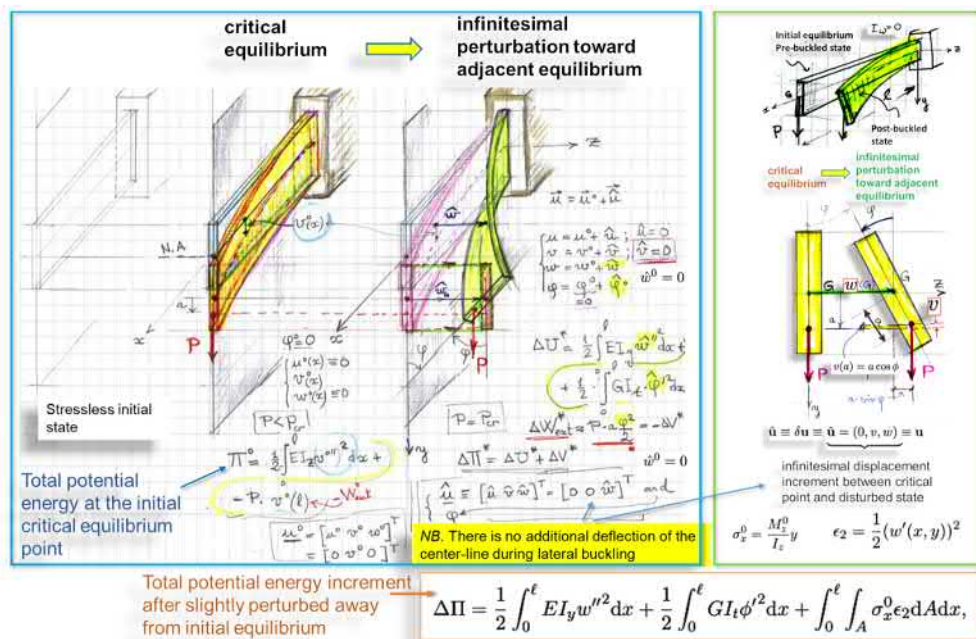


Figure 1.62: Illustration for total and of increment of displacements in the example of torsional lateral buckling of narrow beam.

(Eq. 1.135) into its linear part $\mathbf{e} = \frac{1}{2}(u_{i,j} + u_{j,i})$ and its remaining quadratic part expressed as a rotation component ω . This choice seems natural because rotation terms are many order of magnitude larger than the remaining terms in stability analysis (For details, please refer to Novhozhilov's classical textbook [Chap. V: *The problem of elastic stability*] and prof. J. Paavola lectures notes).

In the following, for defining strain-increment to account for in the stability analysis, I refer the reader to J. Paavola lecture notes (Probably, a must reading after completing the current course). I use the same notations. Let's use for convenience Voigt notation for strains and recall that shear angles $\gamma_{i,j} = \epsilon_{ij} + \epsilon_{ji}$. The rotation component of the strains are

defined as

$$\omega_x = \frac{1}{2} \left(\frac{\partial w}{\partial y} - \frac{\partial v}{\partial z} \right), \quad (1.168)$$

$$\omega_y = \frac{1}{2} \left(\frac{\partial u}{\partial z} - \frac{\partial w}{\partial x} \right), \quad (1.169)$$

$$\omega_z = \frac{1}{2} \left(\frac{\partial v}{\partial x} - \frac{\partial u}{\partial y} \right), \quad (1.170)$$

and the linear part

$$e_x = \frac{\partial u}{\partial x}, \quad e_y = \frac{\partial v}{\partial y}, \quad e_z = \frac{\partial w}{\partial z}, \quad (1.171)$$

$$e_{xy} = \frac{\partial v}{\partial x} + \frac{\partial u}{\partial y}, \quad (1.172)$$

$$e_{yz} = \frac{\partial w}{\partial y} + \frac{\partial v}{\partial z}, \quad (1.173)$$

$$e_{zx} = \frac{\partial u}{\partial z} + \frac{\partial w}{\partial x}. \quad (1.174)$$

After order of magnitude analysis for the strain increment, and keeping only up-to second order terms (the non-linear (quadratic) part can expressed in terms of rotations) one finally obtains

$$\epsilon_x = e_x + \frac{1}{2} (\omega_z^2 + \omega_y^2) \quad (1.175)$$

$$\epsilon_y = e_y + \frac{1}{2} (\omega_x^2 + \omega_z^2) \quad (1.176)$$

$$\epsilon_z = e_z + \frac{1}{2} (\omega_y^2 + \omega_x^2) \quad (1.177)$$

$$\gamma_{xy} = 2e_{xy} - \omega_x \omega_y \quad (1.178)$$

$$\gamma_{yz} = 2e_{yz} - \omega_y \omega_z, \quad (1.179)$$

$$\gamma_{zx} = 2e_{zx} - \omega_z \omega_x. \quad (1.180)$$

Deriving the equation of stability and order of magnitude in different terms:

- In stability analysis while deriving the linear stability loss equations (the linear eigenvalue problem) the amplitude of the linear part e_i of the strains, during the infinitesimal perturbation of the initial equilibrium to the (bifurcated) adjacent one, remains small^a as compared to changes in the rotation components of ω_i .
- Consequently, the quadratic terms in terms in strains e_i^2 and $\omega_i e_j$ are of second order increments as compared to changes in the rotation components, and for that reason will be dropped (ignored). In the above strain increments expressions, only terms shown in the above strains are retained for stability analysis.
- In addition to that, (*Cf.* Alfutov), terms containing the derivatives of initial primary displacements can be neglected (this, *their contribution to the increment of total potential energy $\Delta\Pi$ can be neglected*) too.

^aAs a consequence of the choice of the initial primary equilibrium and the close neighbouring adjacent (bifurcated) equilibrium. These two states are infinitesimally close.

1.11 Application examples of stability study using energy principles

The example treated here is to meant to introduce the methodology (Bryan's type) for establishing the stability equations of various simple cases of elementary structures. Naturally, the stability study for a complex structure can be done reliably only computationally together with experimental validation of the model or its parts. This does not mean that analytical approach should be forgotten. On the contrary, it should be strengthened as it is the only way to apprehend concepts correctly.

We consider the buckling of a simple slender column under constant compressive axial load. The external load can be thought being applied at one end of the column. In the following application example below, we want to derive the bucking equations (eigenvalue problem) and other secondary equilibrium equations related to the initial pre-buckled state, if needed. For this purpose, we use two various, only apparently different, forms of the total potential energy, namely $\Delta\Pi$ (Eq. 1.181) and Π^* (Eq. 1.183). Thorough these lectures note, the form $\Delta\Pi$ (Eq. 1.181), called also the Bryan form,

will be used. It is the one shown in subsection (1.11.1). The pre-buckled state close to buckling is $[u, v = 0]$ where $P \rightarrow P_E$ from below. The tiny post-buckled state is $[u + \Delta u, v \neq 0]$ for $P \rightarrow P_E$ from above. The axial displacement change $\Delta u = \Delta u_N + \Delta u_M$, where the first term is due to axial deformations ϵ_x^0 of the neutral axis and which are zero ($\Delta \epsilon_x^0 = 0$), since the load P remains constant⁹⁹, and the second part $\Delta u_M = \int_0^\ell \frac{1}{2} v'^2 dx$, due to column shortening due to curvature change while bending.

Because the buckling neighbourhood is very tiny, we can say that the axial force remains constant = P . Consequently,

$$\Delta \Pi = \Pi^*[u, v] - \Pi^0[v = 0, u] \equiv \frac{1}{2} \int_0^\ell EI(v'')^2 dx - P \int_0^\ell \frac{1}{2} v'^2 dx \quad (1.181)$$

and

$$\Pi^*[v, u] = \frac{1}{2} \int_0^\ell EI(v'')^2 dx - P \int_0^\ell \frac{1}{2} v'^2 dx + \quad (1.182)$$

$$+ \frac{1}{2} \int_0^\ell EA(u')^2 dx - P \cdot u(\ell) \quad (1.183)$$

where Π^* and Π^0 being the total potential energies in the post-buckled (initial configuration with no bending) and pre-buckled (tiny perturbed bent configuration) states, respectively.

1.11.1 Energy criteria for column buckling

The total potential energy increment in Bryan form (Eq. 1.181) was

$$\Delta \Pi = \frac{1}{2} \int_0^\ell EI(v'')^2 dx + \int_0^\ell N^0(x) \underbrace{\left[\frac{1}{2} v'^2 \right]}_{\epsilon_2} dx, \quad (1.184)$$

where the pre-stress from the primary state is $\sigma_x^0 A = N^0(x)$, deformations $\epsilon_1 = -y v''(x)$ and the quadratic part of the strain increment is $\epsilon_2 = \frac{1}{2} (v')^2$.

For the case of constant end-thrust $-P = N^0(x) < 0$ ¹⁰⁰. The energy functional can be rewritten in the form

$$\Delta \Pi = \frac{1}{2} \int_0^\ell EI(v'')^2 dx - \frac{1}{2} P \int_0^\ell (v')^2 dx. \quad (1.185)$$

⁹⁹This is true in case of symmetric bifurcation or limit point. This remains, quite a good local approximation in case of a non-symmetric bifurcation.

¹⁰⁰kts. johdot ... olen sen johtanut paperille ... työyödällä! Hitsi, missä ne on?

Taking the variation $\delta(\Delta\Pi) = 0$ one obtains

$$\int_0^\ell EIv''\delta v'' - P \int_0^\ell v'\delta v' dx = 0, \forall \delta v \quad (1.186)$$

which gives after twice integration by parts becomes

$$\int_0^\ell \underbrace{[EIv^{(4)} + Pv'']}_{=0} \delta v dx + \underbrace{[EIv'']}_{-M} \delta v \Big|_0^\ell - \underbrace{[(EIv''') + Pv']}_{-Q} \delta v \Big|_0^\ell = 0, \forall \delta v \quad (1.187)$$

The linearised buckling equation follows now straight-forwardly¹⁰¹ as

$$\boxed{EIv^{(4)} + Pv'' = 0} \quad (1.188)$$

which, mathematically speaking, is a linear eigenvalue problem. The boundary terms of the integral provides a consistent set of boundary conditions.

1.11.2 Energy criteria in 'the full form'

This subsection is reproduced here as a very short answer to a student question that was asked today. The student was wondering, and he is completely right, a question about why the initial pre-buckled equilibrium state u (initial trivial equilibrium state) has disappeared from the expression of the *change* (or the increment of) total potential energy that was used in the previous subsection (1.11.1)?

Here the answer: Let's now consider the stationarity condition of the 'full change' of total potential energy given by Eq. (1.183).

Now, Taking the variation of the 'full' total potential energy, one obtains

$$\delta\Pi^* = \int_0^\ell EIv'' \cdot \delta v'' dx - P \int_0^\ell v' \cdot \delta v' dx + \quad (1.189)$$

$$+ \int_0^\ell EAu' \cdot \delta u' dx - P\delta u(\ell) = 0, \quad \forall \delta u, \forall \delta v \quad (1.190)$$

Again, integration by part¹⁰² gives now two equilibrium equations with respective boundary terms;

$$\int_0^\ell \underbrace{[EIv^{(4)} + Pv'']}_{=0, \text{ buckled equilibrium}} \delta v dx + \underbrace{[EIv'']}_{-M} \delta v \Big|_0^\ell - \underbrace{[(EIv''') + Pv']}_{-Q} \delta v \Big|_0^\ell + \quad (1.191)$$

$$- \int_0^\ell \underbrace{[EAu'']}_{=0, \text{ initial equilibrium}} \cdot \delta u dx - \underbrace{[EAu']}_{=N} \delta u \Big|_0^\ell = 0, \quad \forall \delta u, \forall \delta v \quad (1.192)$$

¹⁰¹See references Alfutov, *Stability of Elastic Structures*. Springer 2000, for more reading on this example.

¹⁰²A question: What is the idea behind integrating by part? I let the reader think about it.

Tus on obtains two equilibrium equations (with their respective boundary terms)

1. the linearised buckling equation

$$EIv^{(4)} + Pv'' = 0, \quad \forall x \in (0, \ell), \quad (1.193)$$

which is expressing *equilibrium in the tiny buckled configuration* and

2. *the equilibrium in the initial pre-buckled state* with no bending ($v \equiv 0$, $u \neq 0$)

$$EAu'' = 0, \quad \forall x \in (0, \ell), \quad (1.194)$$

$$[EAu' - P]_0^\ell \cdot \delta u(\ell) = 0 \quad (1.195)$$

together with the associated boundary term when only the end-load P is acting.

1.11.3 Buckling of a beam-column

Illustrative and practical example for the criterion (Eq. 1.143) will be flexural buckling for simply supported compressed beam-column in a plan. The variety of engineering applications of flexural buckling theory is just tremendous. For instance, its importance in civil engineering for structural design of compressed bar-members is vital. The label '*Euler Buckling Theory*'¹⁰³ of the classical theory is, for civil engineers, as famous as is *Coca-Cola*. The only difference is that *Euler* does not receive any royalties for his formula even that the first is much more healthier than the second.

Pieter van Musschenbroek
(1692 – 1761)



A Dutch scientist
Physics, mathematics,
philosophy, medicine, astronomy

Musschenbroek

¹⁰³**Pieter van Musschenbroek** (1692 – 1761: A Dutch scientist Physics, mathematics, philosophy, medicine, astronomy) did, about 30 years before *Euler*, pioneering experimental studies on the buckling of compressed struts. He Performed experiments on column buckling (1729) and he observed that the maximum compressive load a column can sustain prior to failure is proportional to $1/\ell^2$ Compare with Euler's buckling load formula $P_{cr} = \pi^2 EI/\ell^2$ obtained theoretically and about 30 years later in 1774. At that time nobody has understood the importance of such result. Even Coulomb was saying that these results,including experimental ones are wrong because many experiments show that the compressive strength of columns was proportional to the cross-section area and not to the square of its length. These last experiments were done with short iron and wooden columns where the failure mode was the crashing or material failure and not buckling. At that time the concept of slenderness was not understood yet. At the end, they were all right but each one on the opposite side of the slenderness axis. This critical slenderness point divides the failure mode into material failure and elastic buckling, for axially compressed members.

Homogeneous equation of stability (Eq. 1.188) ; the classical *Euler buckling equation* are then

$$(EIv'')'' + Pv'' = 0 \quad (1.196)$$

$$\& \text{ four boundary conditions.} \quad (1.197)$$

The above equations describes the pure flexural buckling condition for a straight column with a centric thrust end-load $P > 0$.



Euler the Great. A Soviet union stamp in his honour.

Solutions for some classical cases

In this section, we derive, by solving the above eigenvalue problem with adequate boundary conditions, the well-known buckling formulas

$$P_{cr} = \mu\pi^2 \frac{EI}{\ell^2} \equiv P_E \quad (1.198)$$

where the inertia moment being naturally the minor $I = I_{min}$. For the not-less well-known Euler's basic buckling cases illustrated in Figure (1.63). The parameter μ accounts for variety of the boundary conditions.

For design purpose, the buckling condition is rewritten in terms of Euler critical stress for the buckling load

$$\sigma_{cr} \equiv \sigma_E = \frac{P_E}{A} = \mu\pi^2 \frac{EI}{A\ell^2} = \mu\pi^2 E \left(\frac{r_{min}}{\ell} \right)^2 = \mu\pi^2 E / \lambda_{min}^2, \quad (1.199)$$

where the minor radius of inertia (gyration) being r_{min} and λ_{min} being the relative slenderness of the column. One recognise the Euler hyperbola with graph $(\sigma_E/\sigma_Y, \lambda)$ in Equation (1.199) for the elastic regime. The yield stress of the material being denoted σ_Y .

The effect of such boundary conditions on buckling load is shown in Figure (1.64). This illustration experiment (ref?) can be also interpreted as a rudimentary but strong¹⁰⁴ validation by the Euler's basic buckling formulas for slender columns.

[**TO DO**] derive explicitly as the solution of the Eigen- value problem the basic Euler's formulas at least for two cases.

¹⁰⁴*Strong* because it does not invalidate the formulas. Think that, instead of four times the basic buckling load $4 \times \pi^2 EI / \ell^2$ of the fixed-fixed boundary condition, the experiment could produce $2 \times$ or $9 \times$ this value! However, the experiment shows a value close to $4 \times$. The probability to have it by chance equal to the theoretical is almost null.

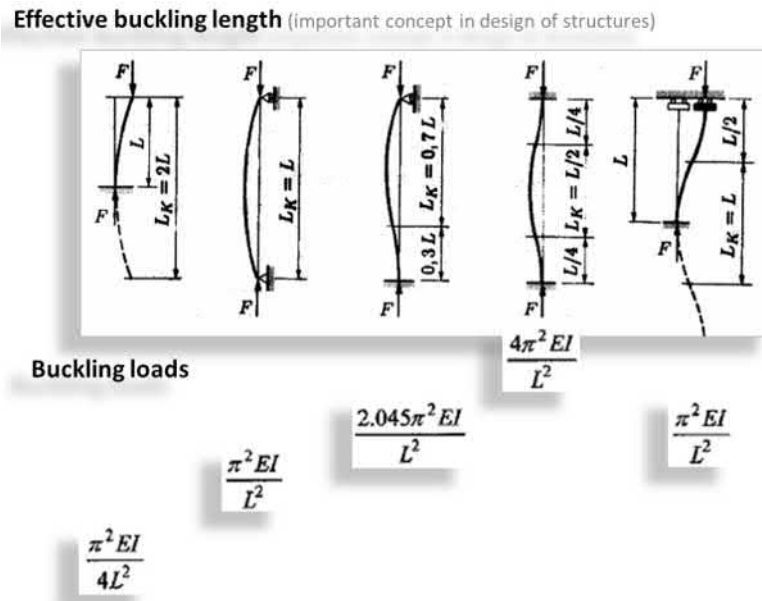


Figure 1.63: Classical Euler’s basic buckling cases.

Effects of boundary conditions – experimental evidence for Euler’s buckling formulas

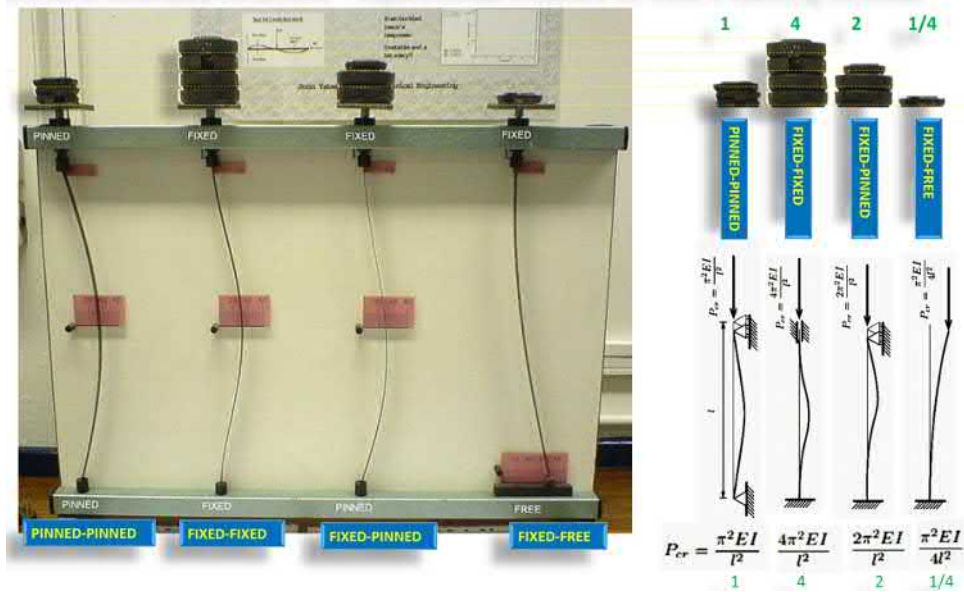


Figure 1.64: Rudimentary experimental evidence for Euler’s basic buckling formulas and the effect of boundary conditions on the buckling load.

Critical strain

One can respectively naturally be interested in the value for the critical strain $\epsilon_{cr}^0 \equiv \epsilon_E$ at buckling. How much the column relatively shorten when

it starts to buckle? What is the strain corresponding to the Euler stress σ_E ?

$$\epsilon_{cr}^0 \equiv \epsilon_E = \frac{\sigma_E}{E} = \mu\pi^2 \left(\frac{r_{min}}{\ell} \right)^2 = \mu\pi^2 / \lambda_{min}^2 \quad (1.200)$$

Consequently, the critical relative shortening of the column at buckling *does not depend on the elasticity modulus E* and thus is independent of the material. Only the relative slenderness and the boundary conditions affect ϵ_E .

Let's take a small breathing pause and I will tell you an amusing small true story. Once during a class of structural mechanics and, to mark a small pause, I asked the students the next question: "What have π , the mother of geometry, to do with Euler's buckling load, a crude force?" I continued further confusing students by concluding that π can be determined *experimentally!* Just perform a buckling experiment using a simply supported column and *measure* the buckling load 'very precisely' and then use the formula

$$\pi = \sqrt{\frac{P_{cr} \cdot \ell^2}{EI}} \quad (1.201)$$

to determine the Queen of numbers; π . After the lecture or maybe, at the start

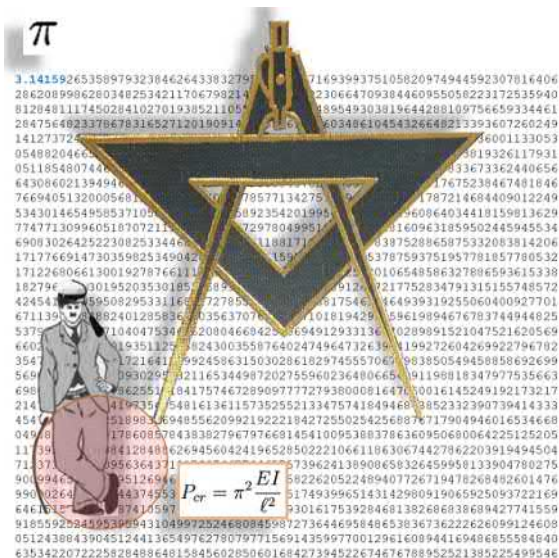


Figure 1.65: What π , the geometry itself, have to do in the Euler's buckling formulas giving the collapse forces for columns?

of the following one, one from student came to me and wondered: "the reason for the presence of π in the Euler's famous buckling formula, is because when it

start to buckle in a flexural mode, the centreline of the simply supported column initially takes the shape of a circle. I liked very much his curiosity and his answer too. So, I took the freedom to illustrate this small history in Figure (1.65).

Let's come back to a an isotropic beam-column of constant cross-section being axially loaded at its ends by P . In the following, the load can tensional ($P < 0$) or compressive. ($P > 0$). In addition, there are no transverse loading. The general solution $v(x)$ for the buckling of such column-beam s, without

$$v(x) = A \sin(kx) + B \cos(kx) + Cx + D + v_0(x), \quad P > 0 \text{ compression} \quad (1.202)$$

$$v(x) = A \sinh(kx) + B \cosh(kx) + Cx + D + v_0(x), \quad P < 0 \text{ tension} \quad (1.203)$$

where $k^2 = P/EI$.

This is the methodology for solving the critical loads for such simple column-beam: account for four boundary conditions in the general solution above and you will obtain a homogeneous linear system of four equations (four unknowns A , B , C and D). Requiring the criticality condition (= non-triviality of the integration constants \implies the determinant of system vanishes), one obtains an equation, usually, non-linear in $k\ell$, to solved. The smallest zero of this equation provides the buckling load.

We will illustrate this with few examples ... [TO DO: 28.1.2019 - you know already basics from Beams and frames course ...]

Application example from structural design

Assume one have deigned a sway column against buckling. So, the buckling load according to Euler will be $P_{E,1} = \pi^2 EI / (4\ell^2)$ and the corresponding mode $v_1(x)$ is the first mode. The question: assume the designer add a lateral elastic restrain which consists of a stiffener bar (sivujäykiste) having an effective elastic spring coefficient k [N/m] (Figure 1.66). What would be the minimum value of k (depends on EI and ℓ) in order to have the column buckling with the second mode $v_2(x)$? What would be the buckling $P_{E,2}$ load now? (this example is adapted from RK)

1.11.4 Effects of imperfections

Example 1: The secant formula

(This example is taken from your homework exercises of year 2020, so I do not give yet the solution). A column of length ℓ is eccentrically loaded with a force P . The simply supported elastic beam-column with length ℓ . The cross section is doubly symmetric with constant bending rigidity EI . The cross-section has height $h = 2c$ and area A . The aim of this exercise is to determine the load-displacement curve " $P/P_E - v(\ell/2)/\ell$ " (or equivalently $v(\ell/2)/\ell = f(P/P_E; e)$)

Example of a design problem

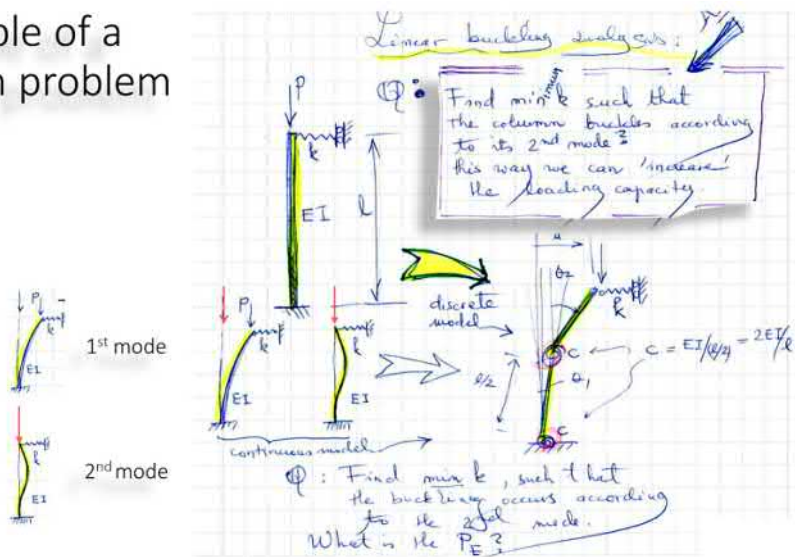


Figure 1.66: A design problem as an application of basic buckling formula.

Eccentrically loaded column FBD

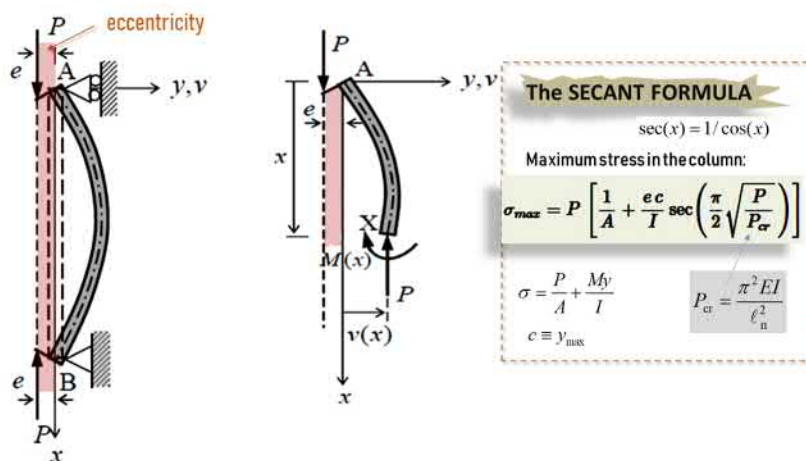


Figure 1.67: Eccentrically loaded column and the secant formula.

derive the secant-formula (see Fig. 1.67)

$$\sigma_{\max} = P \left[\frac{1}{A} + \frac{e \cdot c}{I} \sec \left(\frac{\pi}{2} \sqrt{\frac{P}{P_E}} \right) \right], \quad \text{where } \sec(x) = 1/\cos(x) \quad (1.204)$$

and $P_E = \pi^2 EI/\ell^2$ being the Euler buckling load (for perfect column with $e = 0$).

This class of problems are called *geometrically non-linear problems* (GNP). The

related differential equation of equilibrium is not homogeneous and therefore, the deflection $v(x; P, e)$ is uniquely determined.

The Question

1. Determine analytically the deflection $v(x; P, e)$
2. Determine the maximum deflection $v(\ell/2) = v(x = \ell/2, P/P_E; e)$ and draw the load-displacement curves for three different values of the parameter e , for instance $e = 0.01, 0.005$ and 0.002 . For x - axis use P/P_E and for y - axis, $v(\ell/2)/\ell$. Observations: what happens close to $P/P_E \rightarrow 1$? Conclusion?
3. Determine the maximum bending moment $M_{\max} = M(\ell/2, P; e)$ and plot this scaled maximum value $M_{\max}/(P \cdot e)$ in function of P/P_E for $e = 0.01, 0.005$ and 0.002 . Conclusions?
4. Show that the maximum stress σ_{\max} is given by formula (Eq. 1.204)
5. **EXTRA** : Answer question 2) using any FE-software¹⁰⁵ and use the geometrical non-linear (GNA) or post-buckling analysis options. Draw the obtained load-displacement curves in the same plot as the analytical ones. Compare your results (the load-displacement curves) to the analytical results you have obtained previously. Conclusions? Is there any difference when $P/P_E \rightarrow 1$? Why?

Example 2: Ayreton-Perry design formula

The well-known *Ayreton-Perry* design formula¹⁰⁶ which is in current use in Eurocodes (Eurocode 3) will be derived¹⁰⁷. The formula accounts for effects of initial imperfections on the maximum critical load (buckling resistance) that such imperfect column can carry without collapsing consequently to loss of stability. Such reduction is condensed in a buckling *reduction factor* or imperfection factor $0 \leq \chi \leq 1$ embedded into the *Eurocode buckling curves*. Imperfections cannot be avoided since they are inherent to real structures¹⁰⁸. Examples of imperfections can be geometrical in members and due to imperfections during fabrication, construction phases, tolerances due to manufacturing as lack of straightness, material imperfections and so on. Other of types of imperfections are related to loads and

¹⁰⁵Determine first, with the software, the Euler buckling load, for cross-checking your input.

¹⁰⁶European buckling curves

¹⁰⁷Dr. Alexis F. is warmly thanked for providing material used here for the Ayreton-Perry formula

¹⁰⁸The ideal world *realises* itself through imperfections. The other name of reality can be imperfect ideality.

their locations which naturally which deviates from centric idealised positions. The effects of such imperfection are crucial, especially for slender columns made of steel.

Analytical background of the Ayreton-Perry Eurocode design formula and buckling curves

The cross-section is assumed prismatic doubly symmetric and the column is simply supported. Her we consider only pure planar flexural buckling. Assume that the geometrical imperfection of the slender column is condensed in the half-sinusoidal form given in the margin figure. Then the total deflection $v(x)$ when solved from (Equation 1.197) with relevant boundary conditions $v = v'' = 0$ at $x = 0$ and $x = \ell$, will be

$$w(x) = \frac{e_0}{1 - (\lambda/\pi)^2} \sin(\pi x/\ell), \quad \lambda^2 = \frac{P\ell^2}{EI}, \quad (1.205)$$

where the initial shape imperfection was taken as

$$w_0(x) = e_0 \sin(\pi x/\ell) \quad (1.206)$$

As a design strength criteria we want that the stress in the cross section is not larger than the yield stress σ_y of the material (metal);

$$\sigma_x^{max} = \frac{N_{max}}{A} + \frac{M_{max}}{W} \leq \sigma_y \quad (1.207)$$

$$= \frac{P}{A} + \frac{M_{max}}{I} \frac{h}{2} \leq \sigma_y. \quad (1.208)$$

Now one will substitute into the above design equation (or inequality), the maximum value of the bending moment at $x = \ell/2$ obtained from (Equation 1.205) The bending moment is

$$M_{max} = M(\ell/2) = -EI(v''(\ell/2) - v_0''(\ell/2)), \quad (1.209)$$

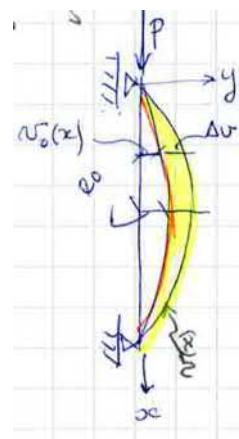
$$= P_{cr}e_0 \frac{(\lambda/\pi)^2}{1 - (\lambda/\pi)^2}, \quad (1.210)$$

$$= P_{cr}e_0 \frac{P/P_{cr}}{1 - P/P_{cr}}, \quad (1.211)$$

where the relations $(\lambda/\pi)^2 = (\lambda/\lambda_{cr})^2 = P/P_{cr}$ have been used. So, in the above equation λ is written again in terms of P/P_{cr} as in the last definition in (1.205) and the reference (Euler) buckling load $P_{cr} \equiv P_E = EI\pi^2/\ell^2 \equiv N_E$. Now inserting the above maximum bending moment in the second equation of (1.208) one obtains, at the limit,

$$\sigma_y A = P + P_{cr}e_0 \frac{h/2}{I/A} \cdot \frac{P/P_{cr}}{1 - P/P_{cr}} \implies \quad (1.212)$$

$$\frac{P_y}{P_{cr}} = \frac{P}{P_{cr}} + \frac{e_0 h/2}{i^2} \cdot \frac{P/P_{cr}}{1 - P/P_{cr}}, \quad (1.213)$$



Initial shape imperfection $w_0(x) = e_0 \sin(\pi x/\ell)$.

Now let's rewrite the above equation in a form close to the *Ayrton-Perry* formula. Before that, let's shorten the equations and use for that notation

$$a\bar{\lambda} = [e_0 h/2]/i^2 \quad (1.214)$$

$$a = \pi \sqrt{E/\sigma_y} \frac{e_0 h/2}{i} \quad (1.215)$$

$$\chi \equiv P/P_y, \quad (1.216)$$

where χ being defined as a effective load-bearing reduction factor.

Now the above equation will give

$$\bar{\lambda}^2 = a\bar{\lambda} \cdot \frac{\chi\bar{\lambda}^2}{1 - \chi\bar{\lambda}^2} + \chi\bar{\lambda}^2 \implies \quad (1.217)$$

$$\frac{1}{\chi} = a\bar{\lambda} \cdot \frac{1/\chi}{1/\chi - \bar{\lambda}^2} + 1 \quad (1.218)$$

$$\implies \frac{1}{2} \frac{1}{\chi^2} - \underbrace{\frac{1}{2} [1 + a\bar{\lambda} + \bar{\lambda}^2]}_{\equiv \phi} \frac{1}{\chi} + \frac{1}{2} \bar{\lambda}^2 = 0, \quad (1.219)$$

Finally solving the reduction factor χ from Equation (1.219) for the reduction (positive root of the second order polynomial) coefficient χ one obtains, finally, the *Ayrton-Perry* formula (Figure 1.68)

$$\chi = \frac{1}{\phi + \sqrt{\phi^2 - \bar{\lambda}^2}}, \quad \text{where } \phi = \frac{1}{2} [1 + a\bar{\lambda} + \bar{\lambda}^2] \quad (1.220)$$

and $\bar{\lambda}$ is the column relative slenderness¹⁰⁹ which can be also, for design purposes, determined as $\bar{\lambda} = \sqrt{A\sigma_y/N_E}$. How this formula (1.220) is used in design of a steel column? Consider a steel section in compression with applied load P . Initial geometrical imperfections are now accounted for through this buckling resistance reduction factor χ (Equation 1.220). For design purpose, the resistance of the column N_R to axial load should be such that the inequality

$$N_s = P \leq N_R = \chi \cdot \frac{\sigma_y A}{\gamma} \quad (1.221)$$

holds. The material safety factor being γ . The graph $(\bar{\lambda}, \chi)$, Figure a) 1.69) of Ayrton-Perry formula (Equation 1.220) forms a lower-bound curve for the reduction of the ideal buckling capacity which accounts for the effects of initial geometrical imperfections in curvature. The formula provides also the theoretical basis for buckling curves of (*Cf.* Eurocode 3 buckling curves, Figure b) 1.69)).

¹⁰⁹For ideally perfect (metallic) column one can write $\chi = \sigma_E A / \sigma_y A = 1/\bar{\lambda}^2$. This is the Euler cubic hyperbola.

Ayreton-Perry design formula (Eurocode 3)

6.3.1.2 Nurjahduskäyrät Buckling curves

(1) Aksiaalisesti puristetuille sauvoille muunnettua hoikkuutta $\bar{\lambda}$ vastaava pienennystekijä χ lasketaan seuraavasta kaavasta käyttäen kyseeseen tulevaa nurjahduskäyrää:

$$\chi = \frac{1}{\Phi + \sqrt{\Phi^2 - \bar{\lambda}^2}} \quad \text{mutta } \chi \leq 1,0$$

missä $\Phi = 0,5 \left[1 + \alpha(\bar{\lambda} - 0,2) + \bar{\lambda}^2 \right]$

$\bar{\lambda} = \sqrt{\frac{A f_y}{N_{cr}}}$ poikkileikkausluokille 1, 2 ja 3;

$\bar{\lambda} = \sqrt{\frac{A_{eff} f_y}{N_{cr}}}$ poikkileikkausluokalle 4;

α on epätarkkuustekijä;

N_{cr} on kimmoiteorian mukainen bruttopoikkileikkauksen mukaan laskettu kriittinen voima kyseeseen tulevassa nurjahdusmuodossa.

6.3.1.1 Nurjahduskestävyys

(1) Puristetut sauvat mitoitetaan seuraavasti:

$$\frac{N_{Ed}}{N_{b,Rd}} \leq 1,0$$

External axial load
Action

Resistance $N_{b,Rd} = \frac{\chi A f_y}{\gamma_{M1}}$

Nurjahduskäyrä	a_0	a	b	c	d
Epätarkkuustekijä α	0,13	0,21	0,34	0,49	0,76

Figure 1.68: Ayreton-Perry design formula as implemented in Eurocode 3. The coefficient α ($= 0.13 \dots 0.76$), in Eurocode 3, is empiric shift and accounts for various experimentally observed contributions to the overall 'imperfection' of the column. The term $\bar{\lambda} - 0.2$ in the formula accounts for plastic (limit load) failure for very short (metallic) columns ($\lambda \leq 0.2$) for which the Euler elastic buckling curve does not hold.

In the Eurocode buckling curves the effect of additional imperfections like residual stresses, eccentricities, geometric imperfections of the cross section, material variability, yielding of very short columns (for metals), and so on, are accounted for through compiling a huge amount of experimental results from various collapse tests. Naturally, all these effects remain inaccessible through mathematical modelling only.

Example: Ayreton-Perry formula. Let $e_0/\ell = 1/200$, profile I-400 \times 200 \times 12 \times 6, $I = 207.3 \times 10^6 \text{ mm}^4$, $A = 70.56 \times 10^2 \text{ mm}^2$, $i = 0.1714 \text{ m}$, $h = 0.2 \text{ m}$, $\sigma_y = 355 \text{ MPa}$, $E = 210 \text{ GPa}$, so one obtains $\bar{\lambda}^2 = \frac{\sigma_y}{E} \frac{\ell}{i\pi} \frac{h}{2} = 0.1 \text{ m}$. The parameter $a = [0.446, 0.297, 0.223]$, respectively, $e_0/\ell = [1/400, 1/300, 1/400]$ with $\ell = 2\text{m}$, for instance.

Load-deflection curves for a perfect column

Bellow is reproduced schematically the equilibrium paths for a perfect column. (1.70)

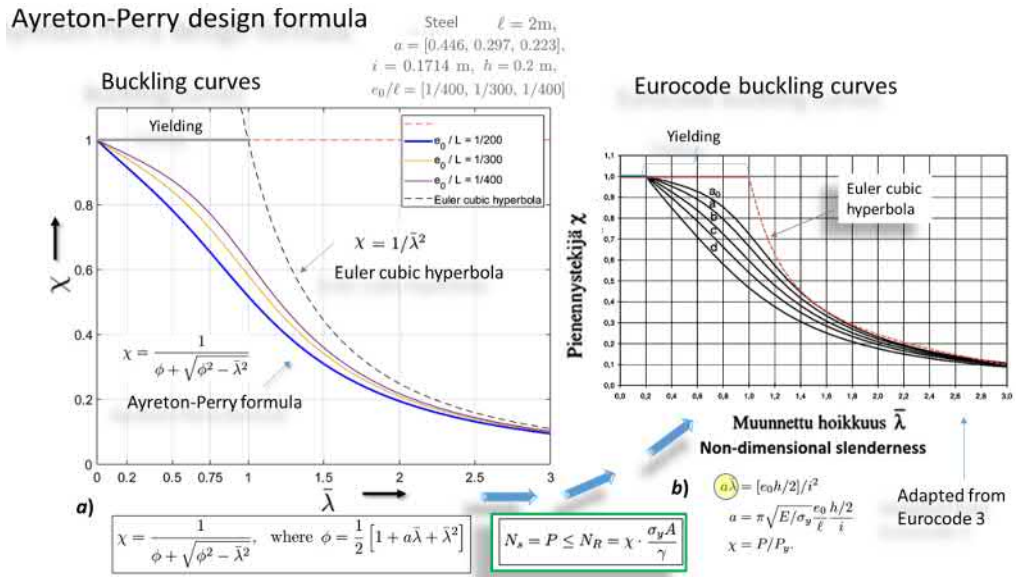


Figure 1.69: a) Theoretical buckling curve as given by Ayreton-Perry design formula for various eccentricities e_0 . b) Eurocode bucking curves.

Geometrical non-linear (GNA) effects: a study with a simple frame

seuraava teksti on raakeli, pitää työstää. The following exercise was inspired from discussions with prof. Wei Wei Lin while telling me that, in China (or in Japan?), the students have an analogous work as a laboratory work with both theoretical and experimental parts.

A lateral-sway planar elastic frame (Fig. 1.71). A simply supported elastic beam supported by two vertical cantilever columns. Both the beam and the columns are dimensioned to work elastically during the whole loading range from $P = 0 \dots P_{cr} \dots 1.5 \times P_{cr}$. The load is in the midspan of the beam. $P_{cr}/2$ is the Euler buckling load for one column.

In order to make the GNA or post-buckling analysis one adds, as a perturbation, a horizontal tiny force H at the top of one column. (let' say $H = P/1000$ or less to generate an initial eccentricity).

What we follow (record)? The deflection $v_{beam}(E)$ at the mid-span of the beam and the lateral deflection u_{col} at the top of the column.

What we do with that result? We draw load-displacement curves (equilibrium paths). On the x -axis, we put the load which increases monotonically from $P = 0 \dots P_{cr} \dots 1.5 \times P_{cr}$ and on y -axis we put two curves: $v_{beam}(E)$ and u_{col} . Then everything is clear: one sees that the deflection of the beam increases linearly with the increase of load while on the contrary, the horizontal deflection increases also linearly till P_{cr} after what it increases much faster (non-linearity)

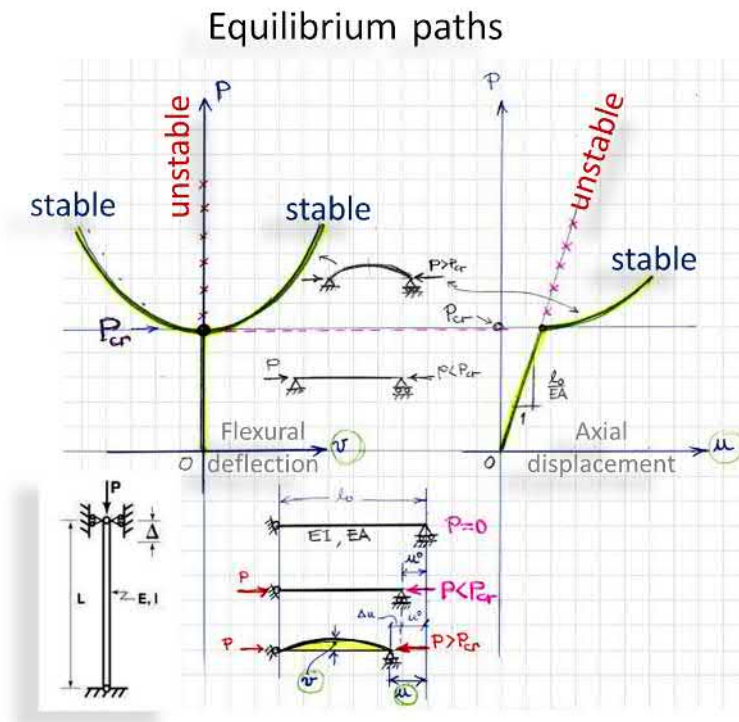


Figure 1.70: Illustration for equilibrium paths and bifurcation points for perfect structure (no imperfections).

than $v_{\text{beam}}(E)$ (order of magnitude faster).

1.11.5 Timoshenko column

Consider an axial and centric load of a straight column. If you recall your previous course of *Mechanics of beams and frames* then this the following should be already known to the reader: Timoshenko beam in bending when the classical Euler-Bernoulli kinematics does not hold any more. The basics of such theory were proposed by **Engesser** (1891) and **Timoshenko** (1921) to account for the shear effects. The idea was to separate the cross-section rotation θ from the slope v' of the deflection of the centre-line. separate

$$\gamma = -\theta + v'. \quad (1.222)$$

There is cases when the effect of shear deformation should be considered. Consider such case now. Let the mean shear angle γ of the cross-section be defined through the mean shear stress $\bar{\tau} = Q_y(x)/A$ such that

$$Q_y(x) = k_s GA \gamma = \frac{GA}{\xi} \gamma \quad (1.223)$$

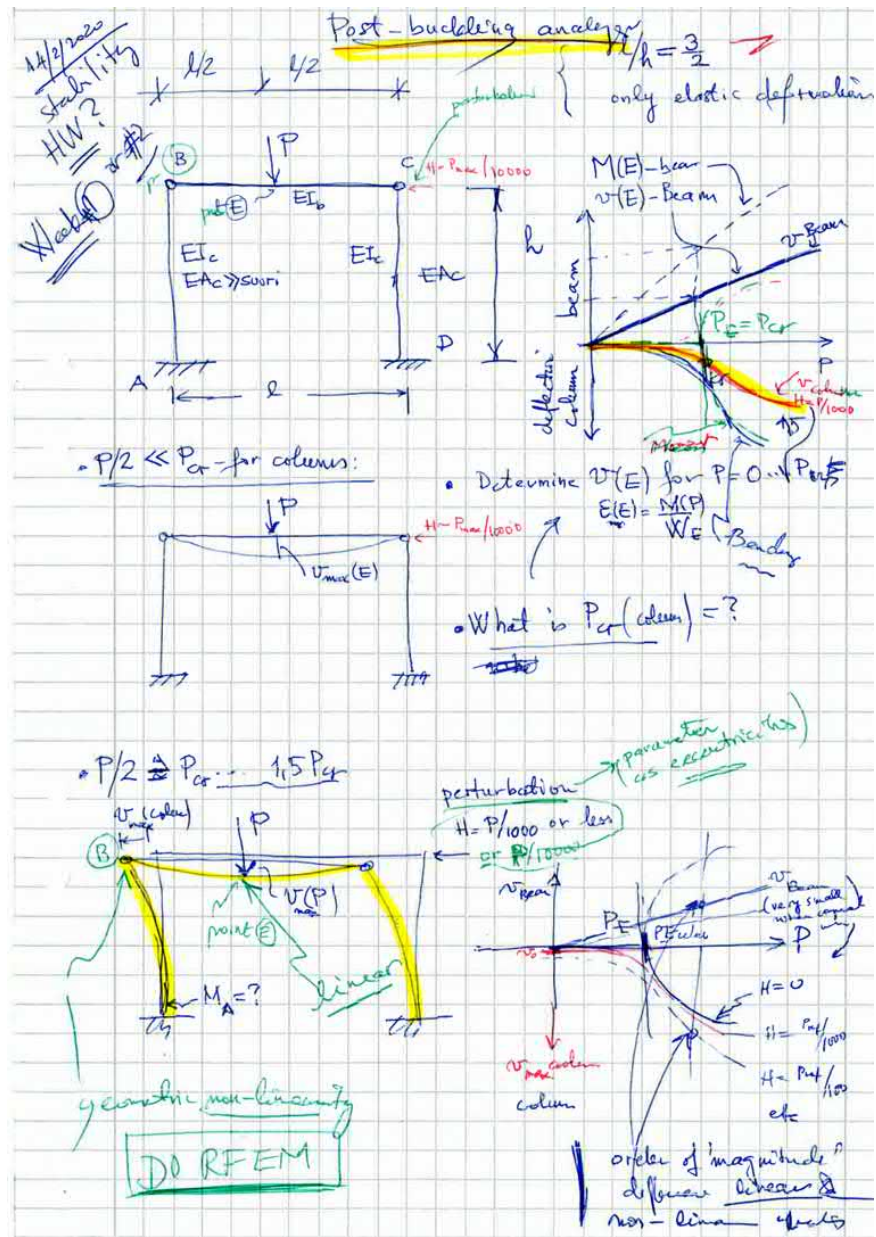


Figure 1.71: GNA for a lateral sway-frame

where for shortness one writes

$$\gamma \equiv \gamma_{xy} = \frac{T_{xy}}{G} = \xi \frac{Q_y}{GA} \equiv \alpha Q_y \tag{1.224}$$

where the shear parameter

$$\alpha = \frac{\xi}{GA} = \frac{1}{k_s GA}, \tag{1.225}$$

and ξ being the *shear correction coefficient*¹¹⁰. Recall that the shear strain is defined by

$$\gamma(x) \equiv \gamma_{xy} = u_y + v_x = -\theta(x) + v'(x), \quad (1.226)$$

where now θ being the rotation of the cross-section.

The kinematics in short: This is a recall of the Timoshenko beam theory. The kinematics is described by two independent functions $\theta(x)$ and $\gamma(x)$ such that

$$\begin{cases} u(x) = \theta(x)y, \\ \gamma(x) = v'(x) - \theta(x) \end{cases} \quad (1.227)$$

from which follows the normal linear strain

$$\epsilon = u' = -(v' - \gamma)y = \kappa y. \quad (1.228)$$

So, in linear elasticity, the bending moment and the shear force will have the expressions

$$M = EI\theta' = EI\kappa = EI(\gamma' - v'') \quad (1.229)$$

$$Q = GA\gamma/\xi = \gamma/\alpha \quad (1.230)$$

In the following the stability equation will be derived.

One way is to start from the energetic criterion

$$\Delta\Pi = \frac{1}{2} \int_{\ell} EI\kappa^2 dx + \frac{1}{2} \int_{\ell} k_s GA\gamma^2 dx - \frac{1}{2} P \int_{\ell} (v')^2 dx \quad (1.231)$$

I let this exercise for the reader.

Let's derive the stability equation from equilibrium considerations (it is straightforward for this case since it forms an update of the classical result for Euler-buckling obtained through differential approach): The idea is 1) first to write the moment equilibrium equation in the deformed configuration then 2) account for the shear correction angle for the curvature κ through the remaining equilibrium equation for shear forces. The procedure is standard. So, equilibrium for the shear force in the deformed configuration gives

$$\begin{cases} Q - Pv' & = 0 \\ M'' - Pv'' & = 0, \end{cases} \quad (1.232)$$

From the first equation one obtains

$$\gamma = \alpha Pv', \quad (1.233)$$

and finally, the needed expression for the curvature

$$\kappa = -v''(1 - \alpha P) \quad (1.234)$$

¹¹⁰ $\xi = 1.2$ for a rectangular cross-section and $\xi = 2 \dots 2.4$ for an I-profile.

to be inserted in the second equation of equilibrium to, finally, obtain, the equation of loss of stability (linearised buckling equation)

$$\boxed{(1 - \alpha P)[EIv'''' + Pv'' = 0]}. \quad (1.235)$$

Rewriting the above in a standard form gives (for constant EI):

$$v^{(4)} + k^2v'' = 0 \quad (1.236)$$

where

$$k^2 = \frac{P}{EI} \frac{1}{1 - \alpha P}. \quad (1.237)$$

The Timoshenko buckling load P^T should be solved from above (Equation 1.236) using adequate boundary conditions. There is clear relation with the Euler buckling load P^E obtained by neglecting the effect of shear deformations.

Example - buckling of a cantilever column

Assume a massive rectangular or circular cross-section which is loaded at its centroid by a thrust P . Find the critical load using the Timoshenko model and show that the critical load can be written as

$$P^T = P^E \frac{1}{1 + \alpha P^E}, \quad \alpha = \frac{\xi}{GA}. \quad (1.238)$$

Analysis of the results

Solving for some basic boundary condition cases and comparing the buckling loads P^T obtained by the Timoshenko model to Euler standard solutions P^E one finds the relation

$$P^T = P^E \frac{1}{1 + \frac{P^E}{k_s GA}} = P^E \frac{1}{1 + \alpha P^E}, \quad (1.239)$$

which holds for all columns with all end-conditions excepts for fixed-pinned. Ziegler (1982) expanded the formula for columns with fixed-pinned ends in a slightly similar form

$$P^T = P^E \frac{1}{1 + 1.1 \frac{P^E}{k_s GA}} = P^E \frac{1}{1 + 1.1 \alpha P^E}. \quad (1.240)$$

As a conclusion, the *shear deformation reduces clearly the value of the Euler buckling load* be a factor

$$1 + \frac{P^E}{k_s GA} \dots 1 + 1.1 \frac{P^E}{k_s GA}. \quad (1.241)$$

Usually the decrease of the buckling load due to transverse shear effects is negligible for bars with solid cross-section. On the contrary, for some open-cross sections, the reduction may be of 50 % even.

The coefficient α^{PE} in the reduction coefficient depends more (quadratically) on geometry than on material parameters, since

$$\alpha^{PE} = \frac{\xi}{GA} \cdot \mu \frac{\pi^2 EI}{\ell^2} \tag{1.242}$$

$$= \xi \mu \pi^2 \frac{E}{G} \left[\frac{I/A}{\ell} \right]^2, \tag{1.243}$$

where μ accounts for boundary conditions effects.

[TO DO: nomograms or graphs for usual cross-sections and materials]

1.12 Example of an application of virtual work principle - Southwell-plots

Here we present the energy principle of virtual work together with an application¹¹¹ of value for interpreting buckling test results, or more exactly how can we extract the buckling load and initial imperfection measure from the load displacement curve. The structure considered is a column with an axial compressive load. The shape of the beam-column is imperfect. The virtual work principle is written in the form principle

$$\delta(\Delta W_{int.}) + \delta(\Delta W_{ext.}) = \delta(\Delta W_{acc.}), \quad \forall \delta v \tag{1.244}$$

which tells everything. Here we do not consider dynamics, so the last virtual work increment contribution due to acceleration $\delta(\Delta W_{acc.}) = 0$. The symbol Δ means *increment* or *change* between an initial equilibrium state to the actual (another) equilibrium state. The principle (1.244) is a more general principle than the neutral equilibrium condition $\delta(\Delta \Pi) = 0$, δv which holds for conservative systems. The virtual work principle holds for any system; conservative or not, linear or not. It is universal, in the small world of mechanics.

Southwell-plots are used in interpretation of buckling experiments. It is impossible to determine buckling load by direct visual observations. This is done, usually, using Southwell-plots.¹¹² These plots are not magical, they relies on the fact that there is always some initial imperfections (often geometrical, let's

¹¹¹The reader can find many other applications of this principle in these lecture notes.

¹¹²R. V. Southwell, On the Analysis of Experimental Observations in Problems of Elastic Stability, *Proceedings of the Royal Society of London*. Series A, Containing Papers of a Mathematical and Physical Character, **Volume 135**, Issue 828, 1 April 1932, pp. 601-616.

say v_0 at $x = \ell/2$) in our member (or structure) under testing even with zero load eccentricity. The initial shape imperfection, or in other words the departure of the beam-column from the straight initial shape can be approximated by

$$v_0(x) = v_0 \cdot \sin(\pi x/\ell) \quad (1.245)$$

where v_0 is the estimated maximum imperfection amplitude that can be determined using *Southwell-plots* afterward from the same experiment as will be the critical buckling load P_E . This point will become clear at the end of the subsection.

In the experiment, the loading is done gradually without subjecting the structure (or the member) to failure. The deformations should remain in the elastic range. It is enough to bring the structure close to the critical load and record the load displacement curve at some points of the structure allows to identify the critical buckling load P_E thanks to the geometrical non-linear relation between the applied compressive load P and, let's say the transverse deflection v . The additional deflection due to loading P is $v_P(x)$, so the total deflection will be

$$v(x) = v_0(x) + v_P(x). \quad (1.246)$$

Let's present, first the result needed for the Southwell-plot and then derive it in details. So, using energy principles, that you should by now already start to know, we obtain easily the relation, for a simply supported pin-ended beam column with initial eccentricity v_0 at $x = \ell/2$, as

$$\frac{P}{P_E} = 1 - \frac{v_0}{v_1}, \quad \text{where for example can be } v_1 = v(\ell/2). \quad (1.247)$$

The graph of the equation (1.247) is shown in Figure (1.72). We are looking to linear relation between v_1/P and v_1 to which we fit the experimental data. Equation (1.247) gives us finally the needed relation as

$$P = P_E \cdot v_1(v_1 - v_0) \implies \frac{v_1}{P} = \frac{1}{P_E} \cdot (v_1 - v_0) \quad (1.248)$$

Now we plot the graph of the measured load-displacement curve using adequate variable v/P and $v_1 = v(\ell/2)$ and fit a linear equation to this data. The slope of the fit will provide the parameter $1/P_E$. Additionally, the initial imperfection v_0 can be now deduced¹¹³ from the fit *via* extrapolation (Fig. 1.73). Figure (1.74) shows real data obtained in a real experiment while loading cantilever in lateral-torsional buckling test.

Now, almost everything has been said. Almost.

¹¹³Sometimes, it is technically difficult to do a precise direct measurement of such initial imperfection v_0 . However, this can be done. It is even wise to do it and to cross-check the measured value with the one extracted from the Southwell-plot.

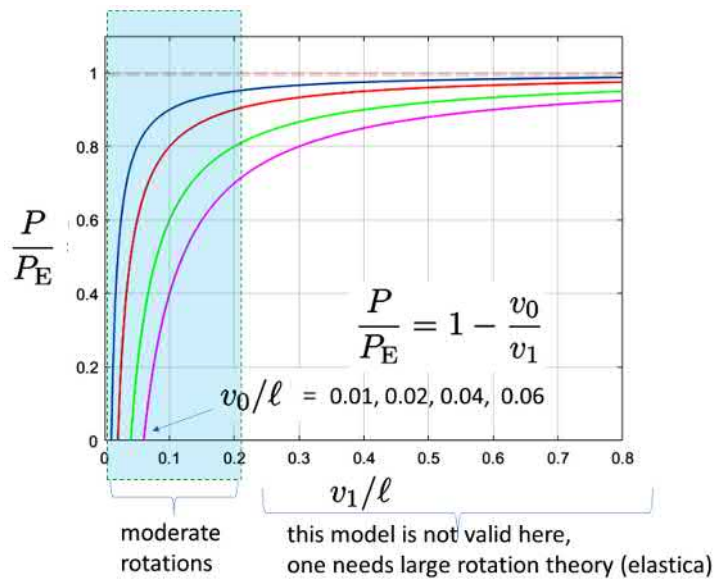


Figure 1.72: Relation between load and lateral displacement for a simply supported column having initial curvature and axially loaded. The light blue region is very approximately the domain of validity of the used hypothesis of moderate rotations.

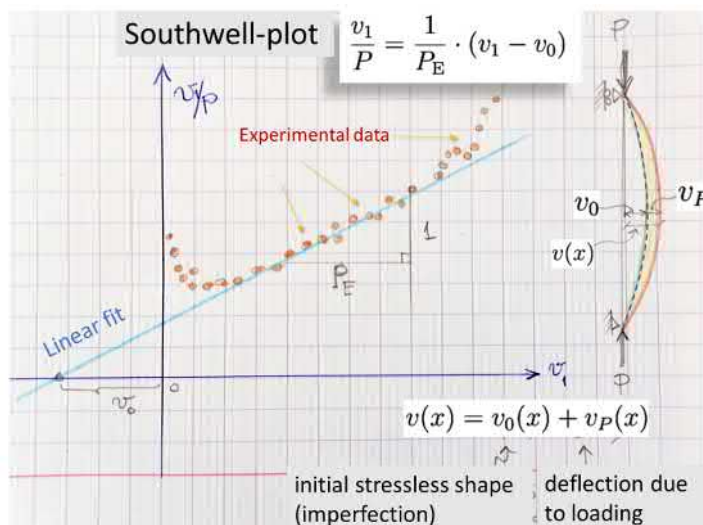


Figure 1.73: Illustration of the idea of Southwell-plots to determine, experimentally, the critical (buckling) load and estimate from the slope of the fit $1/P_E$ for the initial imperfection v_0 . Here, $v_1 = v(\ell/2)$ and $v_0 = v_0(\ell/2)$.

Let's derive the above equation (1.247) for the simply supported beam-column of

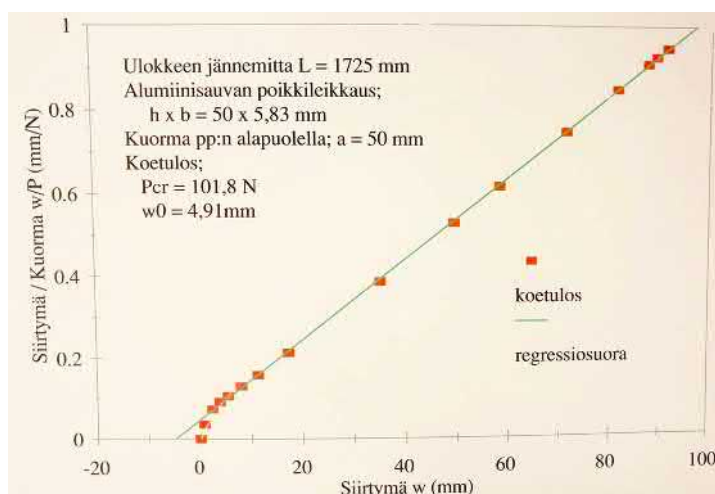


Figure 1.74: Example of use of the Southwell-plots to determine, experimentally, the critical lateral torsional buckling load and to estimate for the initial imperfection. (Ref: Prof. Reijo Kouhia and Tech. Lic. Paavo Hassinen from old TKK).

Figure (1.73). One can do it by solving the differential equation of buckling with the right term due to initial imperfection. We will do it more simply by working in the energy-space where integrals are kings. This way, we avoid, this time, solving differential equations even the related ODE is very simple¹¹⁴. Assume that today, it is the integral day and let's a bit train energy principles. For that, we take for an approximation for the deflection induced by the compressive load P . However, it will not be arbitrary choice but the exact analytical first buckling mode

$$v_P(x) = v_1 \sin(\pi x / \ell) \quad (1.249)$$

This way, using energy principle is equivalent to solving enough accurately the ODE since the (the first mode) mode is the analytical exact solution for the homogeneous ODE. However, this remains an approximation, but a very accurate one for our case. The full exact solution can be naturally obtained by expanding the displacement as a trigonometric series summing all the buckling modes. However, the effect of the other modes than the first one close to buckling load become insignificant. Now,

$$v'_P(x) = -(\pi/\ell) \cdot v_1 \cos(\pi x / \ell) \quad (1.250)$$

$$v''_P(x) = -(\pi/\ell)^2 \cdot v_1 \sin(\pi x / \ell) \quad (1.251)$$

¹¹⁴Note that it has a non-zero right term due to initial eccentricity. Therefore, the equation is not an eigenvalue problem and the amplitude of deflection can be determined exactly as a function of load P and initial imperfection v_0 .

The energy criterion is, as you surely know, is the virtual work principle

$$\delta(\Delta W_{int.}) + \delta(\Delta W_{ext.}) = 0, \forall \delta v \tag{1.252}$$

asking for equilibrium. Inserting the above expressions into the work equation, we obtain

$$\delta(\Delta W_{int.}) = - \int_0^\ell EI \kappa \cdot \delta \kappa dx \tag{1.253}$$

$$= - \int_0^\ell EI [v''(x) - v_0''(x)] \cdot \delta v''(x) dx \tag{1.254}$$

$$= -EI \left[\frac{\pi}{\ell} \right]^4 \int_0^\ell (v_1 - v_0) \sin^2(\pi x/\ell) dx \cdot \delta v_1 \tag{1.255}$$

$$= -EI \left[\frac{\pi}{\ell} \right]^4 \frac{\ell}{2} (v_1 - v_0) \cdot \delta v_1 \tag{1.256}$$

where the varied function being only $v(x)$. Equivalently,

$$\delta(\Delta W_{ext.}) = P \int_0^\ell v' \cdot \delta v' dx \tag{1.257}$$

$$= P v_1 \left[\frac{\pi}{\ell} \right]^2 \int_0^\ell \cos^2(\pi x/\ell) dx \cdot \delta v_1 \tag{1.258}$$

$$= P v_1 \left[\frac{\pi}{\ell} \right]^2 \frac{\ell}{2} \cdot \delta v_1 \tag{1.259}$$

Therefore, at equilibrium, we must have $\delta(\Delta W) = 0$, thus

$$\underbrace{\left(-EI \underbrace{\left[\frac{\pi}{\ell} \right]^2}_{\equiv P_E} (v_1 - v_0) + P v_1 \right)}_{=0} \left[\frac{\pi}{\ell} \right]^2 \frac{\ell}{2} \cdot \delta v_1 = 0, \quad \forall \delta v_1 \tag{1.260}$$

which give, as a present, the needed form for the Southwell-plots as

$$\boxed{\frac{v_1}{P} = \frac{1}{P_E} \cdot (v_1 - v_0)} \tag{1.261}$$

To recognise the equation of a straight line, replace $v_1/P \rightarrow y$, $1/P_E \rightarrow a$ and $v_1 - v_0 \rightarrow x - x_0$ and you obtain the canonical form of our childhood $y = ax + b$, where a being the slope. That's all for Southwell as well Northwell.

$$v_1/\ell \quad v_0/\ell$$

1.12.1 On upper- and lower bounds for the critical load

The following subsection is my *sandbox* for experimenting some ideas and *ajatuk-sia*. Despite this comment, *the content of this subsection gives various valuable methods with examples for the engineer to estimate buckling loads and modes based on first principles, and not less important, to derive useful parametric formulas to get access to the map.*

To recall that in this course we deal only with slender elastic structure and their failure mode is assumed elastic buckling only. However, real structures, even slender, include all type of imperfections and rarely fail only in elastic manner. The failure by buckling is only one mode of several possible failure modes of the structure. Under loading, very probably, in the neighbourhood of buckling, the real failure will be inelastic including all kind of plasticity, visco-plasticity, damage, and excessive deformations at joints, etc. So, the elastic critical buckling load can serve, for slender structures, as an absolute lower limit for safety when adequately limited by a safety factor, lets say P_{cr}/γ_s , $\gamma > 1$ (may be 1.5, 2 or even 3¹¹⁵). At the end, when using computational technology, one should perform a full non-linear analysis of his structure to estimate the lower bound of the bearing capacity. In such analysis, you include all relevant non-linearities (material and geometrical) in addition to initial imperfections. This talk is not against elastic stability analysis or its study. On the contrary. So, let's go back to our subject.

We will use two general principles for neutral equilibrium identification (buckling criteria): 1) stationarity¹¹⁶ principle of 1) *total complementary potential energy* and of 2) *total potential energy*. It is well known that second principle, used with displacement method, estimates the buckling load from above (upper bound). One can expect, at first glad, that first principle when used with the force method will provide estimates from below (lower bound) for the buckling load. However, *this last claim is not proven*¹¹⁷ *and remains a hypothesis*, at this stage of writing, despite that many examples, that will be shown later, give estimates from below for the buckling load.

What map? Let's comment a bit about the value of formulas. These maps, *i.e.*, formulas, tell on which what physical parameters depends the buckling load and how much. One may use this information to be guided in his Finite Element simulations and to reduce significantly the amount of work since the obtained the

¹¹⁵Recall that, geometric non-linearity effects become non-negligible for $P/P_E > 1/3$; refer to the section treating effect of transverse load or geometric imperfections on the deflection under axial loading.

¹¹⁶Note that, the stationarity principle is a condition for an extrema, corresponds physically to virtual work principle which expresses the neutral equilibrium condition.

¹¹⁷I have not seen publications in this direction.

formula (kaava) can be expressed in dimensionless form with less parameters and permits to identify the *dimensionless groups*. Therefore, the parametric map will have less dimensions (less variables than in the non-dimensionless form). After that, the engineer can make his numerical simulations by varying the reduced set of dimensionless products in their relevant intervals.

It is quit evident that estimating the *lower bound* of the critical load is of importance in structural design. Knowing this lower bound for buckling, for instance, we are sure that the accordingly design structure or structural member will not buckle for *a lower load*. So, we are on the *safe-side* in our design, and the designer can sleep deeply his night.

Having methods to estimate such lower- and also upper bounds is then of great importance, and is not a trivial story. For the *upper-bound*, thanks to the Rayleigh quotient P_R minimal properties for the true solution $v(x)$ we can estimate such upper bound by using minimum property of total potential energy at the investigated new equilibrium $v(x)$ obtained by a tiny perturbation of the initial trivial equilibrium configuration $v^{(0)}(x)$.

Lower bound: Estimating lower bounds is not so trivial task. There is an (academic) classical method for that given in the context of very simple structures (see Timoshenko¹¹⁸) which is called, the method of successive approximations¹¹⁹. However, this method, which based on analytical (or graphical - Mohr analogy) integration, is practically limited to very simple beam-column cases or equivalently, to statically determined cases for which bending moment can be solved easily from equilibrium equation. I have to recognize that I have not yet seen any general method for estimating lower bounds of the critical load! If there are any, they should be based on complementary energy principles.

For those interested in this topic, please refer to the *Timoshenko quotient* P_T and its relations with various bounds in the textbook by Bazant (Chap. 5.4 - *Timoshenko quotient and relation between various bounds*)

I suspect strongly that, this proposition have to be proven or disproved¹²⁰, that using cleverly the stationarity of the complementary total energy at the new equilibrium state (the buckled mode), one will obtain estimates for the lower-bound for the buckling load. The argument is that, at equilibrium, the complementary energy is an upper-bound (maximum) with respect to any statically admissible stress field (probably, we are now in the presence of a saddle equilibrium point;

¹¹⁸Chap. 2.15 in Timoshenko and Gere: *Theory of Elastic Stability*. 2nd Ed. 1985. Mc-Graw-Hill.

¹¹⁹This method, principally, solves by Picard's iterations, the PDE of the buckling, and minimise a ratio of successive solutions to give an estimate for the lower bound, is presented, in short, farther, in these notes. Excuse me for the spaghetti-structure of this sentence, I will simplify it later.

¹²⁰I am working on it with the help of my colleague Jarkko N. In addition, I am almost sure that this question has been treated in some old lost paper to be found.

satulapiste, in Finnish. Let's find out, later). I will present few examples using this approach. However, an example is not a proof, and, fortunately, a counter-example is a proof of the contrary.

Upper bound: Consider for instance, a pin-ended beam-column loaded at its end by a centric load P . Close to buckling, the column remains in the trivial equilibrium configuration $u^{(0)}(x) \neq 0$, $v^0(x) \equiv 0$. Let's introduce a tiny perturbation $v(x)$. Then, it is generally known that the true solution $v(x) \neq 0$ when it is a new equilibrium configuration (means the column buckles into an adjacent equilibrium), minimise the Rayleigh ratio

$$P_{cr} \equiv P_R = \min_{\forall v(x)} \frac{\frac{1}{2} \int_{\ell} EI [v''(x)]^2 dx}{\int_{\ell} \frac{1}{2} [v'(x)]^2 dx} \leq \frac{\frac{1}{2} \int_{\ell} EI [\hat{v}''(x)]^2 dx}{\int_{\ell} \frac{1}{2} [\hat{v}'(x)]^2 dx} = \hat{P}_R \equiv \hat{P}_{cr} \quad (1.262)$$

where $\hat{v}(x)$ being any kinematically admissible approximation of the true buckling mode $v(x)$. These are based on the *Timoshenko quotient*; P_T . According to Bazant¹²¹, the *Timoshenko quotient*¹²²

$$P_{cr} \equiv P_T = \frac{\int_{\ell} \frac{1}{2} [v'(x)]^2 dx}{\frac{1}{2} \int_{\ell} [v(x)]^2 / EI dx} \quad (1.263)$$

provides a *sharper* upper-bound¹²³ $\tilde{P}_{cr} \equiv \tilde{P}_T$ for the critical load than the Rayleigh quotient P_R (Eq. 1.265). Both quotients (Eqs. 1.265 and (Eq. 1.263)) are derived from energy principles. At the adjacent equilibrium (the tiny buckled configuration $v(x)$), the total potential energy change is minimal and thus (stationarity)

$$\delta(\Delta\Pi[v(x); P]) = \int_{\ell} EI v'' \delta v'' dx - P \int_{\ell} v' \delta v' dx = 0, \forall \delta v(x) \in V_{kin.ad}. \quad (1.264)$$

The Rayleigh quotient P_R can be directly obtained from the neutral equilibrium condition (1.264) by choosing $\delta v = v$ and solving for the buckling load P

$$P_R(v) = \frac{\int_{\ell} EI [v''(x)]^2 dx}{\int_{\ell} [v'(x)]^2 dx} \leq \frac{\int_{\ell} EI [\hat{v}''(x)]^2 dx}{\int_{\ell} [\hat{v}'(x)]^2 dx}. \quad (1.265)$$

¹²¹see Bazant's textbook: , Chap. 5.4 - *Timoshenko quotient and relation between various bounds*

¹²²This quotient can be defined for statically determined structures. For, a general structure, I propose to use the principle of stationarity of complementary total potential energy $\Delta\Pi_c$ at the adjacent equilibrium point, to obtain an estimate for the lower bound of the buckling load. This last proposition is, for the moment, a working hypothesis to be investigated (is true or false?).

¹²³Albert B. Ku. Upper- and lower bounds of buckling load. *International Journal of Solids and Structures*. Vol. 13, issue 8, 1977, pp. 709-715

It is known that this ratio is minimised¹²⁴ by the true solution v and any other kinematically admissible trial(buckling mode) \hat{v} approaches this minimum from above.

¹²⁴Gives the smallest eigenvalue of the related linearised eigenvalue problem given by the stationarity condition (1.264) which is equivalent to zero gradient $\nabla_v(\Delta\Pi) = 0$ of the quadratic form of the increment of total potential energy.

A FEM mini-story: we can directly rewrite the above result (Eq. 1.264) in a classical weak form by choosing the virtual displacement δv as a test function, so $\hat{v} \equiv \delta v$ and we obtain the weak form below directly from Eq. (1.264) ready for numerical implementations (computer and hand). For this purpose, for instance, in the Galerkin approach, we chose local (element-wise) approximations $\mathbf{v}(\mathbf{x}) = \mathbf{N}(\mathbf{x})\mathbf{a}$ and take the basis functions N_i as test functions \hat{v}_i .]

$$\delta(\Delta\Pi[v(x); P]) = \int_{\ell} EI v'' \hat{v}'' dx - P \int_{\ell} v' \hat{v}' dx = 0, \forall \hat{v} \in V_{kin.ad.} \quad (1.266)$$

In the weak form (1.266), take a local approximation for the displacement field $v(x) \approx \sum_i \phi_i(x) a_i$, $i = 1 : n$ and choose for test functions $\hat{v}(x) = \phi_j$, $j = 1 : n$. Consequently, one obtains

$$\sum_{e=1}^{N^e} \left[\sum_i \left(\underbrace{\int_{\ell^e} \phi_i'' EI \phi_j'' dx}_{K_{ij}^{(e)}} - P^e \underbrace{\int_{\ell^e} \phi_i' \phi_j' dx}_{K_{ij}^{(e)}(P)} \right) \cdot a_i \right] = 0, j = 1 : n \quad (1.267)$$

where $P^e \approx N^e$, the normal force in the element number e . The problem above (1.267) is the (linearised) eigenvalue problem of buckling. The outer sum is an assembly to obtain global equations of neutral equilibrium

$$[\mathbf{K} - \mathbf{K}(P^1, P^{(2)}, \dots, P^k, \dots, P^{N^e})] \cdot \mathbf{a} = \mathbf{0} \quad (1.268)$$

written for general non-proportional loading. In the case of proportional loading, the axial elementary forces, in an element k , can be expressed as $P^{(k)} = p_k P_0$, where the ratio p_k being known.

Consequently, we obtain the standard eigenvalue problem

$$[\mathbf{K} - P_0 \cdot \mathbf{K}(p_1, p_{(2)}, \dots, p_k, \dots, p_{N^e})] \cdot \mathbf{a} = \mathbf{0} \quad (1.269)$$

For our example, there is only one load P , so the critical load P_{cr} can be estimated as the smallest eigenvalue from the eigenvalue problem

$$[\mathbf{K} - P \cdot \mathbf{K}_G] \cdot \mathbf{a} = \mathbf{0}. \quad (1.270)$$

Note that, all matrices are symmetric and the coefficient EI is positive. The minimum properties of the Rayleigh quotient says that the smallest eigenvalue P_{cr} makes the corresponding quadratic form minimal when v is the true solution. For all other choices (kinematically admissible), the derived critical values, from above, are estimates from above (upper bounds) of the critical load.

End of the other FEM mini-story.

Choosing an estimate $\hat{v}(x)$ for the displacements, and solving for P in Equation (1.264), one obtains the upper-bound estimate for the buckling load as given by the Rayleigh quotient \hat{P}_R (Eq. 1.265). Now, a sharper estimate for this same buckling load is provided by the Timoshenko quotient (Eq. 1.263) which can be directly derived, as for the Rayleigh quotient, solving $P = \tilde{P}_{cr}$ from (and this for $\forall v(x) \in V_{kin.ad.}$) from this form of the neutral equilibrium condition¹²⁵ $\Delta\Pi_c = 0$,

$$\Delta\Pi_c[v(x); P] = \frac{1}{2} \int_{\ell} [\underbrace{M(x)}_{M=-Pv}]^2 / EI dx - P \int_{\ell} \frac{1}{2} [v'(x)]^2 dx = 0, \quad (1.271)$$

$$= \frac{1}{2} \int_{\ell} [Pv(x)]^2 / EI dx - P \int_{\ell} \frac{1}{2} [v'(x)]^2 dx = 0, \quad (1.272)$$

and, finally, gives equation (1.263) for P_T by solving it from (1.272) as

$$P_T = \frac{\frac{1}{2} \int_{\ell} [M(x)]^2 / EI dx}{\int_{\ell} \frac{1}{2} [v'(x)]^2 dx}. \quad (1.273)$$

Knowing an the estimate \hat{P}_{cr} for the upper-bound, may seem frustrating as the true buckling load can be higher; $P_{cr} \geq \hat{P}_{cr}$. So we are on the unsafe-side in the structural design! This is, in practice, not a problem, since we can refine the estimate \hat{P}_{cr} very close to the true value by refining our approximation $\hat{v}(x)$ by enriching the approximation *basis function set*. Especially, this is true while using the Finite Element Method and the, actually automated *h-* and even *p-* adaptivity, if needed. However, an estimate for the safety margin (= confidence interval) should be found by the designer or/and the structural analyst, if they respect themselves and their profession. This is why we should know, or at least know someone who knows, analytical methods; they may help to provide us a *kättä pitempää* in the form of formulas. However, for this particular case of estimating the lower bound of the critical buckling load, it seems to be very probably an impossible mission. However, asking help from people with more experience than ourselves is worth the effort.

¹²⁵The quotient can be also derived in the standard form by asking stationarity of a quadratic (linearised) form of $\delta(\Pi_c)$; i.e., $\nabla(\Delta\Pi_c) = 0$

Another FEM mini-story:

The complementary version (or force method) in the weak form: So, for $\forall (v, M) \in V_{kin.ad.} \times \Sigma_{stat.ad.}$, the condition of neutral (adjacent) equilibrium gives

$$\delta(\Delta\Pi_c[v(x); P]) = \int_{\ell} \frac{M\delta M}{EI} dx - \int_{\ell} P \cdot v' \delta v' dx \quad (1.274)$$

$$= \int_{\ell} \frac{M\hat{M}}{EI} dx - \int_{\ell} P \cdot v' \hat{v}' dx = 0 \quad (1.275)$$

with \hat{M} and \hat{v} being test functions. Let's take a displacement approximation $v(x) \approx \sum_i \phi_i(x)a_i$. Note that the couple (v, M) should satisfy *jointly* the equilibrium equation

$$(EIv'')' - (N_0')' = 0 \quad (1.276)$$

where N_0 being the initial normal force (for instance, in our simple example, for compression $N_0 = -P$, where $P^0 = P > 0$). This equilibrium equation simplifies to, in this simple case to $M - Pv = 0$. Therefore, the separate approximations (v, M) should also fulfil this equilibrium condition. Therefore, the bending moment approximation should be $M = P \cdot v \approx P \sum_i \phi_i(x)a_i$. Note that, since $\delta M = P \cdot \delta v = \sum_i P \cdot \phi_i(x)\delta a_i$, then consequently, the test function should be chosen as $\hat{M} = P \cdot \phi_j(x)$, $j = 1 : n$. Inserting all these ingredients into the weak form (1.275) one obtains

$$\sum_{e=1}^{N^e} \left[\sum_i \left(\underbrace{\int_{\ell^e} \frac{\phi_i(x)\phi_j(x)}{EI} dx}_{S_{ij}^{(LIN.)}} - \underbrace{\frac{1}{Pe} \int_{\ell^e} \phi_i' \phi_j' dx}_{S_{ij}^{(NL.)}(P)} \right) \cdot a_i \right] = 0, \quad j = 1 : n \quad (1.277)$$

which for proportional loading (and for our simple loading case with only one compressive load P), and without loss of generality becomes the classical eigenvalue problem

$$\sum_{e=1}^{N^e} \left[\sum_i \left(\int_{\ell^e} \frac{\phi_i(x)\phi_j(x)}{EI} dx - \frac{1}{P} \int_{\ell^e} \phi_i' \phi_j' dx \right) \cdot a_i \right] = 0, \quad j = 1 : n \quad (1.278)$$

Equation (1.279) can be more appreciated in its matrix-form (generalised) eigenvalue problem

$$[\mathbf{S} - \frac{1}{P} \cdot \mathbf{G}] \cdot \mathbf{a} = \mathbf{0}. \quad (1.279)$$

It should be noted that the coefficient matrices \mathbf{S} (flexibility matrix such that $\mathbf{S}^{-1} = \mathbf{K}$) and \mathbf{G} are *symmetric.*) and $P > 0$. On can be rewrite the above result as

$$[\mathbf{I} - \frac{1}{P} \cdot \mathbf{S}^{-1} \mathbf{G}] \cdot \mathbf{a} = \mathbf{0} \quad (1.280)$$

So, I stop here this side-jump in the form of a question.¹²⁶

Application example - simply supported beam-column

In the following, estimation method for the lower- and upper bounds for the smallest buckling load is shown and illustrated by two simple cases: buckling of a simply supported beam-column loaded at one end by a point load and buckling of a cantilever column under its self-weight. It goes without saying that estimating such bounds allows us to obtain objective *trust* in our *computations* having such confidence bounds. In general, to be useful, as a scientist or even an engineer, should always give results with an estimate of their confidence bounds.

The method of successive approximations

There is a classical such method for estimating such bounds of the critical load called *Method of successive approximations* which can be found in Timoshenko's and Gere classical textbook *Theory of elastic stability. 2nd Ed., Chap. 215*, in both its *analytical* and *graphical* forms. The readers interested in it can refer to Timoshenko's textbook; we will not treat it in this lecture's notes. The method of successive approximations is essentially a **Picard's** iteration of the buckling equations written in their differential equation form. Let's give an example to be clear. Consider a simply supported homogeneous column ($EI = \text{const.}$) with pinned-pinned supports, and centrally load by a point-load P at the roller-end. Then the equation of equilibrium in the buckled configuration are

$$M(x) = P \cdot v(x), \text{ equilibrium} \quad (1.281)$$

$$M(x) = -EIv''(x), \text{ kinematics \& constitutive law} \quad (1.282)$$

$$v(0) = 0, v(\ell) = 0, \text{ boundary conditions} \quad (1.283)$$

which can be combined as the boundary-value problem (differential equation)

$$-EIv''(x) = P \cdot v(x), \quad (1.284)$$

together with the boundary conditions $v(0) = 0$ and $v(\ell) = 0$.

In the above method, equation (1.284), is essentially solved iteratively by the Picard's iteration: the idea is to solve iteratively $v(x)$, the buckling mode, starting from an initial guess $v^{(i)}(x)$ ($i = 0$) in the right-side of Eq. (1.284) and then refine

¹²⁶**Question** to my colleagues Jarkko N. and Reijo K.: Can we deduce from maximum property of the quadratic form (1.279) for the true solution (v, M) and symmetries of the coefficient matrices above, as when proving the minimising properties of the Rayleigh quotient, that the smallest eigenvalue $1/P_{cr}$ minimises the maximum of this quadratic form and consequently, its inverse P_{cr} will therefore, be approximations for P_{cr} from below? (so, estimates the lower bound?) I sure, that, in addition we should, into the quadratic (complementary) form, enforce weakly the constitutive law $M + EIv'' = 0$ by some penalty or Lagrange multipliers. (I will investigate this question later in examples.)

the successively the approximation $v^{(i+1)}(x)$ by twice integrating (analytically or graphically¹²⁷) the left-side of Eq. (1.284). The estimate, at each iteration i , of the buckling load P_{cr}^{i+1} is obtained by equating two successive solutions $v^{(i)}(x) = v^{(i+1)}(x; P)$. Here a pseudo-algorithm:

1. **Initialise**, $i = 0$
2. $a)$ chose an expression for the **initial** approximation¹²⁸ $v^{(i)}(x)$ with some free parameter(s) (let's called generically v_0) and $b)$ chose an arbitrary initial value for the critical load $P^{(i)}$ the right-side of Eq. (1.284) **THEN** determine $M^{(i)}(x; P) = P \cdot v(x)$
3. **twice integrate** (analytically or graphically and enforce boundary conditions) the left-side of Eq. (1.284 with the known right-hand from previous step to obtain an updated estimate for the buckling mode $v^{(i+1)}(x)$ (there is naturally still undetermined free parameter(s) of the deflection since it is a buckling mode.)

Note that, this *twice integration* above can be *elegantly* performed using Mohr-analogy where the apparent distributed load being $\bar{q}(x) \equiv -M(x; P^i)/EI$. Then determine $v(x)$ graphically twice integrating the load $\bar{q}(x)$ which is just the moment of this apparent distributed load \bar{q} .

4. **Estimate critical load** $P_{cr}^{(i+1)}$ by **equating** two successive approximations of deflections, at some arbitrary chosen points x_k (for ex. $x_k = \ell/2$), $v^{(i)}(x) = v^{(i+1)}(x; P)$, \forall free-parameter value, let's say v_0 .
5. set in step 2, $v^{(i)} = v^{(i+1)}$ and repeat steps 2 to 4 till wished convergence.
(a faster converging way is to chose the new value as $v^{(i)} := (v^{(i)} + v^{(i+1)})/2$ and then to join step 2, refer to Timoshenko textbook given previously)

Tuning numerically the value of P (in your graphical environment) in order to visually make the two successive curves of the approximations of the deflections, coincide at some points (graphical fit) will provide an estimate for the critical load P_{cr} .

6. an upper- and lower bound for the buckling load, $P_{cr,min}$ and $P_{cr,max}$, can be estimated by finding the minimum and maximum value, with respect to x of the ratio $r(x; P)$ of two successive mode iterations, namely $r(x; P) \equiv v^{(i)}(x; P)/v^{(i+1)}(x; P)$. The corresponding critical loads obtained from r_{min}

¹²⁷The Mohr-analogy use $\bar{q}(x) \equiv -M(x; P)/EI$, with initial value for P chosen arbitrarily. Then determine $v(x)$ graphically twice integrating the load $\bar{q}(x)$ which just the moment of this apparent distributed load \bar{q} . If you cannot follow this explanation then join the Athanasios M. very famous course on graphical methods in statics.

¹²⁸The initial guess for the buckling mode; for instance $v(x) \approx v_0 x(\ell - x)/\ell^2$ can be a good start. Any other satisfying the kinematical boundary conditions is welcomed.

and r_{max} are, according to Timoshenko, the estimated upper- and lower bounds¹²⁹

Here, may be, if our dear friend Athanasios M. the Greek will have time, we can add the result of a beautiful graphical example performed using *GeoGebra* or some geometrical computational tools according to the above steps.

Let's now go to our main task to try¹³⁰ to estimate the confidence bounds of the smallest critical load using more general methods based on energy principles. This is a new story. So, *Amaa ... chahou ...* ... (once upon a time ... in O-land far before the starting of the Big-Bang, when there were only pure localised energy surfing on the waves of an infinite sea far before the start of time...)

Energy principles for estimating buckling load with examples

Here I present two general energy methods based on the displacement and the force methods in the light of simple examples.

The idea to use, in determining approximates for the buckling load, the very old *principle of virtual force*¹³¹ (in the virtual work principle) to estimate displacements, at chosen locations x_i , is inspired by my readings (A Soviet (CCCP) textbooks of *structural mechanics* by V. A. **Kisiliev**, 1980, MOCKBA, Stroi-Isdat, p. 431, in Russian, to estimate the analytically the buckling loads.

¹²⁹For me there is a question: why this quotient r has this property? Is it proven somewhere, in literature? Probably, yes in, may be the field of iteratively solving differential equations. I do not know. However, the first iterate of the quotient r for the buckling of a simply supported beam is $r(x; P) = v_1/v_2 = 12EI/\ell^2 \cdot [\ell^2(\ell - x)]/[\ell^3 - 2x^2 + x^3]$ when the approximated mode being $v_1 = 4v_0x/\ell \cdot (1 - x/\ell)$. The minimum and maximum of r , with respect to x , being 0.8 and 1. Consequently, we deduce from this two ratios estimates for lower- and upper bounds of the critical load as $P_{cr,min} \approx 0.97\pi^2 EI/\ell^2$ and $P_{cr,max} \approx 1.2\pi^2 EI/\ell^2$. The analytical 'exact' Euler buckling load is $P_E = \pi^2 EI/\ell^2$. So, effectively, the bracket contains the solution. I let this exercise for the students which have too much free time.

¹³⁰I think that is a quit difficult task, in general. Probably, another way to find such estimates for the lower- and upper bound can be a mechanical approach: one approximate 'mechanically' on paper, of course, the structure by one a more 'rigid' and the other a more 'loose' (=less rigid) structures. Then determine the buckling load of both structures. If we are good engineers (or student-engineers), the answer will give us a reliable bracket for the actual buckling load. We will train this approach in the homework dealing with buckling of continuous beam-columns and frames. I believe more in the efficiency of this last approach. This approach, in addition, forces us to better analyse and understand the mechanical behaviour of our structure.

¹³¹The 1-dummy load method which essentially is equivalent to integrates graphically twice the curvature at a chosen point x_i where the 1-dummy load $\bar{F} = 1$ is set (=Mohr integral to Mohr-Maxwell integrals

lower¹³²- and upper bounds for the buckling load. The method based on *virtual work principle* may remind, by the way it looks, the method of successive approximations presented above, but the energy method is more general and is different in *essence*. The method of successive approximations is essentially based on Picard's iterations to estimate buckling load from solving iteratively the equilibrium differential equations (Eq. 1.284) in the deformed configuration and to estimate P_{cr} by equating two successive approximates of deflections (buckling modes).

Using *energy principles* with both the *force method* and the *displacement method*, we derive an estimate for the upper- and lower bound of the critical load.

Usually, to derive estimates for the buckling load, students and teachers, use the displacement method with the energy criteria given by the Lagrange-Dirichlet theorem. The reason for that, is that it is much easier to 'guess' a compatible displacement field than to 'guess' a statically admissible stress field¹³³. However, it should be kept in mind that the obtained estimate for the buckling load is a higher upper-bound which means that the *true critical load can be lower* but not higher. If one can estimate the lower bound $P_{cr}^{(force)}$, then it a bracket (and confidence bounds) for the buckling load as

$$P_{cr}^{(force)} \leq P_{cr}^{(theor.)} \leq P_{cr}^{(displ.)} \quad (1.285)$$

a really valuable information will be at hand to help to estimating the safety margin for the given structural design against buckling. (I am not saying, that this safety question cannot be addressed also numerically. Analytical approach provides *parametric maps*, and numerical methods, provide only Tera-bytes of real numbers even with many decimals in which we can be lost without *this map*.)

My hypothesis on a lower bound estimation

Using the force method or more exactly the principle that the true stress field at equilibrium *maximises* the *complementary* total potential energy for any compatible strain and displacement fields.

¹³²Remember that, this is only my hypothesis. So, the reader should remain sceptical with its generality, unless, a proof, or a reference to it, is provided. For the moment, I show some simple examples where this claim seems to hold. However, an example is not a proof while the counter-example, is a proof for the counterary. This means, it is sufficient to find one single counter example to ruin my claim. So, do not hesitate to check, I will appreciate it and publish in these notes with thanks and references to the author, naturally.

¹³³Finding a stress field which is in equilibrium and fulfils the constitutive relation, needs more effort and not always possible to do, but is worth to do or try to find, since one can obtain an estimate for the upper-bound of the critical load. This means that we can trustfully say that the buckling load cannot be higher than that upper-bound. This knowledge is of value in structural design.

Let's, take an illustration example and take a simple end-pinned column which is axially compressed ($P > 0$) without eccentricity.

Without loss of generality, let's define the complementary total potential energy increment gained in the transition from an initial trivial equilibrium state to a tiny adjacent (buckling) equilibrium state, as

$$\Delta\Pi_c[v, M; P] = \frac{1}{2} \int_{\ell} \frac{[M(x)]^2}{EI} dx + \int_{\ell} \underbrace{N(x)}_{=-P} \cdot \frac{1}{2} [v'(x)]^2 dx \quad (1.286)$$

$$= \frac{1}{2} \int_{\ell} \frac{[M(x)]^2}{EI} dx - \int_{\ell} P \cdot \frac{1}{2} [v'(x)]^2 dx \quad (1.287)$$

It is known that the above complementary energy (Eq. (1.287)) is *maximized*¹³⁴ with respect to the stress resultant $M(x)$ when the couple $(v, M) \in V_{kin.ad.} \times \Sigma_{ad.}$, fulfil jointly, the equilibrium equation (M - statically admissible and v - kinematically admissible)

$$M'' - Pv'' = 0 \quad (1.288)$$

together with appropriate boundary conditions.

Let's denote this equilibrium solution by the couple (v, M) and rewrite generically, this maximum principle in the following form

$$(v, M) = sol. \left\{ \max_M \Delta\Pi_c[v, M; P] \right\} \quad (1.289)$$

Note that the functional can be rewritten *generically* as a real-valued f function of two variables having a parameter $P > 0$, as $f(x, y; P) := \Delta\Pi_c[v, M; P]$, where

¹³⁴To avoid confusion, let's refresh our mind with about minimum and maximum of functions. Let's the function $f(x)$ have a minimum at a local point x_c . Then this same point x_c maximises the new function $-f(x)$ obtained from the old one by multiplying it by -1 . Till now, nothing too difficult. Consider now the total potential energy functional Π and it's 'conjugate' potential Π_c called the complementary total potential energy. Now, when Π is minimised, locally, at some generic point c_e , it's complement Π_c will be simply maximised at this 'same' point, expressed in terms of forces. The simple reason is the same with $f(x)$ and $-f(x)$, when the first is minimised, it's complement is simply maximised. Think just of the parabola x^2 and $-x^2$, and everything becomes clear. No need to be Einstein. With the energy potentials, the reason is the same and is really simple: Consider the strain energy U and it's *complement* $U_c \equiv \sigma : \epsilon - U$ which is called *complementary strain energy* to make the names long. Now you see that U and U_c have a difference in the sign. Or even, more *geometrical* illustration (A. M. will love it), consider the area enclosed by the 'rectangle' $\sigma : \epsilon$ which is simply $\sigma : \epsilon = U + U_c$. Now think that the area of the rectangle is fixed, then when U is minimised, U_c is maximised to keep the area of the rectangle constant at equilibrium point $x_e (\epsilon, \sigma)$. Now, in some textbooks and also in my writing, sometimes, the sign -1 is omitted in the definition of the complementary energy. Then instead of maximising it, we are simply minimize it. This can and will lead to confusion. So, be careful how the sign in the complementary energy is written.

$x \rightarrow v$ and $y \rightarrow M$. Now, the condition that the functional (1.289) have a maximum at the equilibrium point (v, M) means, as learned from high school, at this point, 1) one have extrema $f' = 0$ and 2) the second derivative should be negative $f'' < 0$ at this extrema point (written generically). Because, now, the arguments of the function f are functions $v(x)$ and $M(x)$, the conditions for extrema and maximum can similarly written as

$$\max_{(v,M)} \Delta\Pi_c[v, M; P] \implies \underbrace{\delta(\Delta\Pi_c[v, M; P]) = 0}_{\text{neutral equilibrium}}, \text{ and } \underbrace{\delta^2(\Delta\Pi_c[v, M; P]) < 0}_{\text{maximum point}} \quad (1.290)$$

respectively.

We now see what these two conditions will give us with a simple example.

1. **Extrema condition:** The extrema condition¹³⁵ means that the point $(v, M) \in V_{kin.ad.} \times \Sigma_{stat.ad.}$, is such that we have

$$\delta(\Delta\Pi_c) = \int_{\ell} \frac{M\delta M}{EI} dx - \int_{\ell} P \cdot v' \delta v' dx = 0 \quad (1.291)$$

Note that the bending moment $M(x) = M(x; P)$, depends also on P and therefore, one should account for that in the expression of the bending moment. Now $M = M(x, P)$ depends on P through the equilibrium equation. The dependence is fortunately explicit thanks to integration of the equilibrium equation (2.23) and gives $M(x; P) = Pv(x) + Ax + B$, A and B are constant of integration. Let's assume for simplicity, in this example, and without loss of generality¹³⁶, that boundary conditions makes $A = 0$ and $b = 0$. Note that the compressive load P is defined positive. Accounting for $M = Pv$ in (1.291) gives

$$\delta(\Delta\Pi_c) = \int_{\ell} \frac{(Pv)(P\delta v)}{EI} dx - \int_{\ell} P \cdot v' \delta v' dx = \quad (1.292)$$

$$= P^2 \int_{\ell} \frac{v\delta v}{EI} dx - P \int_{\ell} v' \delta v' dx = 0 \implies \quad (1.293)$$

$$= P \int_{\ell} \frac{v\delta v}{EI} dx - \int_{\ell} v' \delta v' dx = 0, \quad \forall \delta v \in V_{kin.ad.} \quad (1.294)$$

$$\implies P = \int_{\ell} v' \delta v' dx / \int_{\ell} \frac{v\delta v}{EI} dx \quad (\text{gives the critical load}) \quad (1.295)$$

Since the variation δv can be arbitrarily chosen, we chose it as $\delta v \equiv v$ in (1.295) and obtain the critical load (Timoshenko quotient) as

$$P \equiv P_{cr} = \frac{\int_{\ell} v'^2 dx}{\int_{\ell} v^2/EI dx} \quad (1.296)$$

¹³⁵Recall that stationarity corresponds physically to asking for the neutral equilibrium, so saying that the buckled state (v, M) is an equilibrium state. This equilibrium is expressed as an eigenvalue problem.

¹³⁶*without loss of generality* is a nice sentence that I have very often heard in my courses of mathematics.

As a conclusion, we say showed that extrema point $(v, M; P_{cr})$ makes the functional stationary.

For approximation purposes, we can also use the weak form

$$P \approx \hat{P}_{cr} = \frac{\int_{\ell} \hat{v}' \delta \hat{v}' dx}{\int_{\ell} \hat{v} \delta \hat{v} / EI dx} = \frac{\int_{\ell} \hat{v}'^2 dx}{\int_{\ell} \hat{v}^2 / EI dx} \quad (1.297)$$

where \hat{v} being any kinematically admissible trial for the buckling mode.

2. **maximum point:** Let's now find what *valuable knowledge* can be extracted from the conditions that the extrema extrema point $(v, M; P_{cr})$ corresponds to a *maximum*?

$$\delta^2(\Delta \Pi_c) = \delta \left(P^2 \int_{\ell} \frac{v \delta v}{EI} dx - P \int_{\ell} v' \delta v' dx \right) < 0 \quad (1.298)$$

$$= P^2 \int_{\ell} \frac{\delta v \delta v}{EI} dx - P \int_{\ell} \delta v' \delta v' dx < 0 \quad (1.299)$$

$$= P^2 \int_{\ell} \frac{(\delta v)^2}{EI} dx - P \int_{\ell} (\delta v')^2 dx < 0 \implies \quad (1.300)$$

$$= P \underbrace{\int_{\ell} \frac{(\delta v)^2}{EI} dx}_{>0} - \underbrace{\int_{\ell} (\delta v')^2 dx}_{>0} < 0, \quad (P > 0) \implies \quad (1.301)$$

$$\implies P < \int_{\ell} (\delta v')^2 dx / \int_{\ell} \frac{(\delta v)^2}{EI} dx = \quad (1.302)$$

$$= \int_{\ell} (v')^2 dx / \int_{\ell} \frac{v^2}{EI} dx \equiv P_{theor.} = P_{cr}, \text{ when } v \equiv \delta v \text{ (=true mode)} \quad (1.303)$$

From the above result, I can *loosely*¹³⁷ conclude, that

$$P(\hat{v}, \hat{M}) \equiv \hat{P}_{cr} = \underbrace{\frac{\int_{\ell} \hat{v}'^2 dx}{\int_{\ell} \hat{v}^2 / EI dx}}_{\text{approximate mode } \hat{v}} \leq \underbrace{\frac{\int_{\ell} (v')^2 dx}{\int_{\ell} v^2 / EI dx}}_{\text{true mode}} \equiv P(v, M) \equiv P_{cr} \quad (1.304)$$

meaning that, the force method (when we choose jointly the approximation \hat{M} and (may) \hat{v}) provides a *lower bound for the buckling load*, under the additional condition (constraint) that the couple \hat{v}, \hat{M} fulfils the constitutive relation $M \hat{+} EI \hat{v}'' \neq 0$ for the approximation. However, this, in general, never the case since the constitutive law will be fulfilled exactly only if \hat{v} corresponds to the true buckling mode. In all other cases, there will be a small discrepancy (not equilibrating moment $\Delta M \equiv M \hat{+} EI \hat{v}'' \neq 0$).

¹³⁷I let my colleagues R. K. and J. N. check and finalise this conclusion.

This is why I postulate that, one may obtain an estimate for the lower bound of the buckling load only if this constraint is accounted in explicit manner in the (or can) total potential energy increment as

$$\Delta\Pi_c[v, M; P] = \frac{1}{2} \int_{\ell} \frac{[M(x)]^2}{EI} dx - \int_{\ell} P \cdot \frac{1}{2} [v'(x)]^2 dx + \lambda \int_{\ell} \underbrace{[M(x) + EIv'']^2}_{M=-EIv''} dx, \quad (1.305)$$

where λ (or equivalently $1/2\lambda^2$) being here a penalty¹³⁸ parameter to be optimally estimated. Then, it becomes clear (is it?) that the *true solution* (v, M) , fulfilling equilibrium equation (2.23) and constitutive law (1.307), *maximizes* the above *positively augmented*¹³⁹ change in total complementary energy.¹⁴⁰

My hypothesis: Therefore, (to be checked), solving $P_{cr} = P$ from the stationarity condition of Eq. (1.287) will, with high probability¹⁴¹, provide an estimate for the lower bound of the critical load when one chooses a *statically admissible stress field* (*i.e.*, the bending moment $M(x)$) and a kinematically admissible displacement field $v(x)$, such that both approximations fulfil jointly the equilibrium equation of buckling (for instance, for an end-loaded pin-ended column with point load P will be

$$M'' - Pv'' = 0 \quad (1.306)$$

or equivalently $M - Pv = 0$ together with adequate boundary conditions), and additionally, imposing that strains (here curvature κ when computed separately from the displacement approximation $\kappa = -v''$ and the bending moment approximation $\kappa = M/EI$ are equal¹⁴², at least in a weak form. This means that we must enforce the constitutive relation

$$M = -EIv'' \quad (1.307)$$

in the complementary energy integral weakly.

In other words, not in other worlds, the approximates for the bending moment $\hat{M}(x)$ and the displacement $\hat{v}(x)$ should satisfy *jointly* the buckling equilibrium equation and that the curvature (strains) determined separately from these two

¹³⁸Later, there will be given a classical variant using Lagrange multipliers called *Hellinger-Reissner* (derived) stationary principle.

¹³⁹The parameter λ^2 is a penalisation parameter or Lagrange multiplier to be chosen optimally or determined.

¹⁴⁰Anyway, using the above functional will provide more accurate approximations than those given by the Rayleigh quotient because the order of the derivatives are lower in the above functional than with Rayleigh quotient.

¹⁴¹This is my hypothesis which can be true or false, I have not investigated it theoretically

¹⁴²These two expressions are always equal only when the displacement approximation $v(x)$ corresponds to a true buckling mode.

approximations ($\hat{M}(x), \hat{v}(x)$) are equal. Usually, this is not the case¹⁴³, and the cure of this is to add to the complementary energy integral (1.287) a *positive* part enforcing the constitutive law in the following manner

$$\Delta\Pi_c[v(x); P] = \frac{1}{2} \int_{\ell} \frac{[M(x)]^2}{EI} dx - \int_{\ell} P \cdot \frac{1}{2} [v'(x)]^2 dx + \frac{1}{2} \lambda^2 \int_{\ell} \underbrace{[M(x) + EIv'']^2}_{M=-EIv''} dx, \quad (1.308)$$

where λ^2 being a penalty coefficient to be optimally chosen. Note that this integral conserve its maximum property, with respect to M , since it was augmented by a positive value. The neutral equilibrium condition (criticality) can be expressed by

$$\delta(\Delta\Pi_c[v(x); P]) = \int_{\ell} \frac{M\delta M}{EI} dx - \int_{\ell} P \cdot v' \delta v' dx + \lambda^2 \int_{\ell} [M + EIv''] [\delta M + EI\delta v''] dx = 0, \quad (1.309)$$

where $\forall(v, M) \in V_{kin.ad.} \times \Sigma_{stat.ad.}$. To find approximations for the buckling load and mode, one have to insert trials (\hat{v}, \hat{M}) into (1.309) since the approximations should mimic the true solutions.

Iterative refinement for lower bound: One may obtain from Eqs. (1.308) and (1.309) an iterative¹⁴⁴ scheme, by enforcing iteratively the constitutive law, in order to refine the estimated buckling load and therefore, fulfil better and better the constitutive constraint $\Delta M \equiv M(x) + EIv'' = 0$, which makes, probably, the estimate to converge to the lower bound. For instance, for a suitable boundary conditions (end-pinned column, for example, $M = Pv$), on can derive from the stationarity (neutral equilibrium condition) the following iteration

$$\frac{1}{P_{cr}} = \frac{\int_{\ell} v^2/EI dx + \lambda^2 \int_{\ell} [M(x) + EIv'']^2 dx}{\int_{\ell} [v'(x)]^2 dx} \implies \quad (1.310)$$

$$\frac{1}{P_{cr}} = \underbrace{\frac{\int_{\ell} v^2/EI dx}{\int_{\ell} [v']^2 dx}}_{\equiv 1/P_{cr}^{(0)}} + \lambda^2 \frac{\int_{\ell} [M + EIv'']^2 dx}{\int_{\ell} [v']^2 dx} \implies \quad (1.311)$$

$$\frac{1}{P_{cr}^{(i+1)}} = \frac{1}{P_{cr}^{(i)}} + \lambda^2 \frac{\int_{\ell} [M(P_{cr}^{(i)}) + EIv'']^2 dx}{\int_{\ell} [v']^2 dx} \quad (1.312)$$

Notice that the excess (not in equilibrium) moment is now $\Delta M \equiv M + EIv'' \neq 0$, where now the bending moment approximation is determined separately, from $M = P_{cr}^{(i)}v$ and from the curvature approximation $M = -EIv''$. An illustration example will be given.

¹⁴³This condition is not, *a priori* granted since both approximates can be chosen separately.

¹⁴⁴Compare to the method of successive approximations (Timoshenko).

Example - ends-pinned column: Taking the displacement approximation $v(x) \approx 4v_0x(\ell - x)/\ell^2 \equiv a_1\phi_1(x)$ and the bending moment (in equilibrium) $M \approx Pv = P \cdot 4v_0x(\ell - x)/\ell^2 = P \cdot a_1\phi_1(x)$, where now $\phi_1(x) = x/\ell \cdot (1 - x/\ell)$, one obtains

$$\frac{1}{P_{cr}^{(0)}} = \frac{\int_{\ell} v^2/EI dx}{\int_{\ell} [v']^2 dx} = \frac{\int_{\ell} \phi_1^2/EI dx}{\int_{\ell} [\phi_1']^2 dx} \implies P_{cr}^{(0)} = 10 \frac{EI}{\ell^2} \approx 1.01\pi^2 \frac{EI}{\ell^2} \quad (1.313)$$

Note that, now this first iterate estimation of buckling load is not approaching from below. However, it is very close (1%) difference to the analytical Euler buckling load $1 \cdot \pi^2 \frac{EI}{\ell^2}$. Probably this is due to that the approximation of the buckling load and the moment is not fulfilling the constitutive law. Effectively, there is actually a non-zero excess moment. The moment computed from equilibrium gives

$$M^{(0)} = P_{cr}^{(0)}v = 1.013\pi^2 \frac{EI}{\ell^2} \cdot a_1\phi_1(x) = 10 \frac{EI}{\ell^2} \cdot a_1 \frac{x}{\ell} (1 - \frac{x}{\ell}) \quad (1.314)$$

and determined from the constitutive law, provides

$$M^{(0)} = -EIv'' = 2EIa_1/\ell^2 \quad (1.315)$$

Clearly, the constitutive law is not satisfied, since

$$\Delta M^{(0)} \equiv M^{(0)} + EIv'' = 10 \cdot a_1 \frac{EI}{\ell^2} \cdot \frac{x}{\ell} (1 - \frac{x}{\ell}) + 2a_1 \frac{EI}{\ell^2} = \quad (1.316)$$

$$= a_1 \cdot 10 \frac{EI}{\ell^2} \cdot \left[\frac{x}{\ell} (1 - \frac{x}{\ell}) + \frac{1}{5} \right] \neq 0 \quad (1.317)$$

Notice that the excess (not in equilibrium) moment is now $\Delta M \equiv M + EIv'' \neq 0$. Let's use the iteration scheme (Eq. (1.312)) to make a better approximation of the critical load $P_{cr}^{(1)}$, as

$$\frac{1}{P_{cr}^{(1)}} = \frac{1}{P_{cr}^{(0)}} + \lambda^2 \cdot \frac{\int_0^{\ell} [M(P_{cr}^{(0)}) + EIv'']^2 dx}{\int_0^{\ell} [v']^2 dx} \quad (1.318)$$

$$= \frac{1}{P_{cr}^{(0)}} + \lambda^2 \cdot \frac{\int_0^{\ell} [\Delta M^{(0)}]^2 dx}{\int_0^{\ell} [v']^2 dx} \quad (1.319)$$

Inserting the expression of the non-equilibrating moment (Eq. 1.317) in the above iterate and choosing for penalty¹⁴⁵ $\lambda^2 = 1$ and then $\lambda^2 = 0.5$, obtains the better

¹⁴⁵If I will have time, I will discuss about the optimal choice of the penalty coefficient λ . For the moment, I take just two values. However, the idea is to plot a graph $(P_{cr}^{(i)}(\lambda_i), \lambda_i)$ and find some *optimal point* on it, or equivalently, a balance between the Timoshenko-type quotient and the constitutive constraint.

estimate of buckling load which is now converging from below as

$$\frac{1}{P_{cr}^{(1)}} : \ell^2/EI = \frac{1}{10} + 1 \cdot \frac{1}{153.333} = 0.106522 \implies P_{cr}^{(1)} = 0.951\pi^2 EI/\ell^2 \quad (1.320)$$

$$\frac{1}{P_{cr}^{(1)}} : \ell^2/EI = \frac{1}{10} + 0.5 \cdot \frac{1}{153.333} = 0.10326 \implies P_{cr}^{(1)} = 0.981\pi^2 EI/\ell^2 \quad (1.321)$$

What should be notice now, is that *imposing the constraint of the constitutive law* seems to make the estimated of the buckling load *approaching* the true vale $P_E = 1 \cdot \pi^2 EI/\ell^2$ *from bellow*. Can this result be generalised?¹⁴⁶

How does topography of $\Delta\Pi_c$ looks like? In the following, we will draw 2-D equilibrium surface example for the complementary total potential energy increment $\Delta\Pi_c$ to illustrate the neutral equilibrium at a saddle-point-like¹⁴⁷ point (tasapainopiste = satulapiste).

For illustration purposes of the how does look the geometry of the complementary total potential energy hyper-surface in 3D. Consider the one degrees of freedom systems: end-pinned column-beam and a rigid cantilever bar with a rotational spring c (Fig. 1.75). The buckling mode of the Euler elastic column is approximated by a the one-degrees of freedom $v(x) \approx 4v_0x(\ell - x)/\ell^2$, the rigid bar kinematic is parametrised by a rotation angle θ and the deformation energy is concentrated in the spring. After some simple algebraic manipulations one obtains

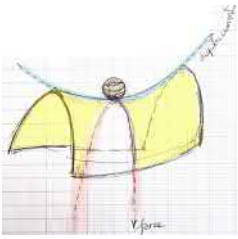
$$\Delta\Pi_c(v_0/\ell, P\ell) = \frac{1}{2} \underbrace{[4v_0/\ell]^2}_{\equiv x} \underbrace{[P\ell]}_{\equiv y} \left(\frac{P\ell}{k} - \frac{1}{3} \right), \quad k = EI/\ell \quad (1.322)$$

$$\Delta\Pi_c(\theta, P\ell) = \frac{1}{2} \theta^2 \left[\frac{P\ell}{c} \right] \left(\frac{P\ell}{c} - 1 \right). \quad (1.323)$$

Note that the expressions of energy increment $\Delta\Pi_c$ (Eqs. 1.322 and 1.323) are similar and are function of two variables only, $f(x, y)$, which can be written for

¹⁴⁶The truth should be said, that may be this discussion, will remain academic since finding an approximation, in general, for the stress field (the force method) which will be in equilibrium is not, really, feasible. To be convinced, just think to find such statically admissible stress state for the problem combined lateral-torsional buckling, which still remains not complex as compared to buckling of shells. One have almost to solve the full problem, first! Here we succeeded because, the problem was statically determined (isostatic) and thus the approximation of the bending moment was easily solved in explicit form. This is one reason why the displacement based finite element method is the most successful story as you can notice from the availability of the softwares. Can anyone find a FE-software commercially in use and which is based on the force method? There is other technical issues related to the numerical implementation of the force method; prof. Jarkko N. can tell you more.

¹⁴⁷To be checked more generally. [19/2/2021. TO DO]



Topography of a generic stability surface at a saddle-point.

instance, for the column, in a familiar form

$$f(x, y) = 1/2x^2 \cdot y \cdot (y/k - 1/3), \tag{1.324}$$

where k and c are material parameters, for illustration purposes. One can see clearly the surfaces, after choosing some values for the material parameters (Figs. 1.75 and 1.76). Note the analogy (similarity) of the energies or surfaces. They have the characteristic saddle shape-type (min-max)¹⁴⁸. This means that one have a maximum with respect to generalised force and a minimum with respect to the generalised displacements. The saddle-point like corresponds to the neutral equilibrium configuration.

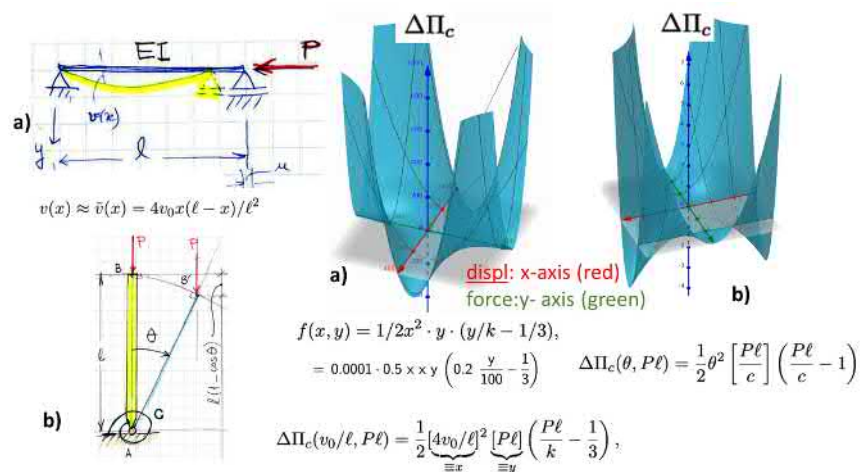


Figure 1.75: Total potential energy as a two dimensional surface. Note the saddle shape. Generalised displacements as x -axis and force as y -axis. (surface plotted with a smartphone version of GeoGebra 3D Calculator)

Let's come back to our previous discussion. So, I let the question - to *prove*¹⁴⁹ holeness-ly (aukottomasti) that using the complementary energy approach pro-

¹⁴⁸Dear colleagues, please check for this terminology.

¹⁴⁹May be, it will be easier to form the quotient $P(v, M)$, equivalently as for the Rayleigh quotient, in the form (forgetting a bit about the constraint that can be added later)

$$P(u, M) = \frac{\frac{1}{2} \int_0^\ell M^2/EI dx + \frac{1}{2} \lambda^2 \int_0^\ell [M + EIv'']^2 dx}{\int_0^\ell \frac{1}{2} (v')^2 dx}, \tag{1.325}$$

and find P from stationarity (extrema condition $\nabla P(u, M) = 0$), and then impose the maximum condition that the second derivative of P with respect to (v, M) is positive ($\nabla^2 P(u, M) > 0$ for the stationary point P to be a maximum. There is one technical difficulty when computing the gradients: one should account for that $M = M(x, P)$ depends on P through the equilibrium equation. The dependence is usually, fortunately

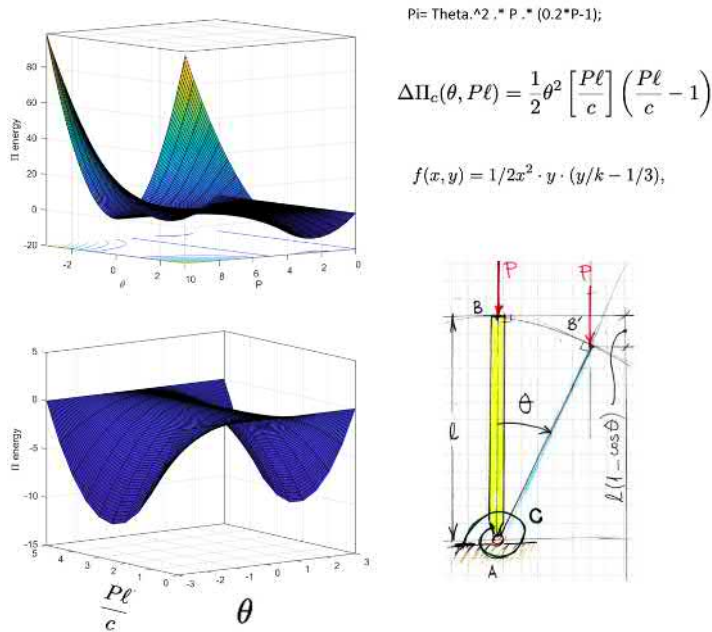


Figure 1.76: Another version of a plot for the total potential energy as a two dimensional surface. Note the saddle shape-type in a small region. (surface plotted with Matlab.)

vides (or does not) a lower bound for the critical load, open for my colleagues (R. K. & J. N.) and skip to application examples.

Hellinger-Reissner derived stationary principle

There is a classical powerful derived variational principle - called Hellinger-Reissner principle - which resembles the one I proposed in (Eq. 1.305) with the penalty constraint to enforce the constitutive law. This last variational principle constraints, in the complementary total potential energy change, the constitutive law by *Lagrange multiplier* functions $\lambda(x)$. Indeed, I recalled this from one of my old seminar work¹⁵⁰ (=textbooks) I took when I was a post-graduating student.

We will just introduce this augmented approach with the example of the beam-column buckling.

Lets tell you the story here: There was an energy functional even though

explicit thanks to integration of the equilibrium equation (2.23) which gives $M(x; P) = Pv(x) + Ax + B$, A and B are constant of integration).

¹⁵⁰M. S. El Naschie. *Stress, stability and chaos in structural engineering: and energy approach*. (Chap. 6.3: Hellinger-Reissner principle and the trial function method.)

called complementary total potential energy

$$\Delta\Pi_c[v, M; P] = \frac{1}{2} \int_{\ell} \frac{[M(x)]^2}{EI} dx - \int_{\ell} P \cdot \frac{1}{2} [v'(x)]^2 dx \quad (1.326)$$

felt itself lonely and sad. This is because the constitutive law could never be satisfied as the consequence of the free choice of trials.¹⁵¹ Then came an idea to our functional to grow and become augmented by constraining the unbalanced moment ΔM , due to arbitrary trials, to provide zero work $\lambda(x) \cdot \Delta M(x)$ when dancing with Lagrange multipliers $\lambda(x)$ along the beam. This is how the augmented functional

$$\Delta\hat{\Pi}_c[v, M, \lambda; P] = \frac{1}{2} \int_{\ell} \frac{[M(x)]^2}{EI} dx - \int_{\ell} P \cdot \frac{1}{2} [v'(x)]^2 dx + \int_{\ell} \lambda(x) \underbrace{[M(x) + EIV'']}_{\Delta M \neq 0} dx, \quad (1.327)$$

came to birth. One very important thing should be noted: the Lagrange multiplier $\lambda(x)$ is a function defined all over the structure. This is much stronger constraint than the one I had with the penalty factor. The other, not less important remark, is that $\lambda(x)$ should have the physical dimensions of *curvature*, since it works with the unbalanced moment ΔM .

The (optimal) Lagrange multiplier can be eliminated by asking stationarity (extremization) of the augmented functional with respect to λ . Therefore, for any variation δM , $\delta v'$ and $\delta v''$, we must have

$$\begin{aligned} \delta(\Delta\hat{\Pi}_c) = 0 &\implies \int_{\ell} \frac{M\delta M}{EI} dx - \int_{\ell} P v' \delta v' dx + \int_{\ell} \lambda(x) [\delta M + EI\delta v''] dx = 0 \\ &\implies \lambda(x) = -M(x)/EI(x), \quad \lambda \text{ is identified as a curvature} \end{aligned} \quad (1.328)$$

$$(1.329)$$

Now by choosing the Lagrange multiplier as given above, the *order* will be re-established and restored, and the augmented functional will feel itself *complete* and not only *complementary*. This is for the story. Inserting this optimal Lagrange multiplier into (Eq. 1.327) one obtains, finally, the Hellinger-Reissner functional

$$\boxed{\Delta\hat{\Pi}_c[v, M; P] = -\frac{1}{2} \int_{\ell} \frac{M^2}{EI} dx - \int_{\ell} P \cdot \frac{1}{2} [v']^2 dx + \int_{\ell} M v'' dx} \quad (1.330)$$

which stationarity (extremum condition) provides the neutral equilibrium condition (for buckling).

¹⁵¹It was satisfied only if the trials are the analytical true buckling modes that are *a priori* unknown.

* * * * *

In the following, I will therefore just present some application examples to illustrate the idea of using energy principles to find (good) approximates and even *formulas*¹⁵² for buckling loads in the light of simple illustrative structures. Also the new hypothesis will be tested with one or two example in its simplest form. The analysis of the method, related to the lower-bound estimate claim, will be left to do¹⁵³.

Disclaim : Notice, dear reader, that in the following examples, we obtain, in addition to, *clean* upper-bounds (\approx from known Rayleigh quotient), estimates for the buckling load from below (lähestytään alhaalta). Is this result, of the lower value for the buckling load (lower bound), general? For the moment, I do not (yet) know.

In the following examples will provided to test the hypothesis¹⁵⁴ with examples that the variation principles expressed by equations (1.291) and (1.309), may provide estimates for the lower bound of buckling loads. In addition, the examples will treated with various methods and find estimates for buckling loads in the following different ways:

1. the virtual unit-load theorem¹⁵⁵ to determine an updated approximation for the buckled deflection \hat{v} from approximations of bending moment and shear force \hat{M} and \hat{Q} , respectively. An initial buckling mode \hat{v} is postulated, too. The buckling load estimate is obtained by equating the initial and updated buckling mode estimates. This reminds the method of successive approximations. (In the MM - integral, the term $\delta\kappa = \delta M/EI \equiv \bar{M}/EI$ enforces a *bit*¹⁵⁶ the constitutive law $\hat{\kappa} = \hat{M}/EI$)

This method will be labelled as the *force method*.

N.B. In the examples treated here, this approach provided estimates from bellow for the buckling load. However, I am not claiming that this result is generally true. One reason for giving approximate for from bellow may be because this method can be interpreted as a variant of the *method of successive approximations*¹⁵⁷ which can give estimates for the lower- and upper

¹⁵²One student during one of my lectures said: "... *My God! Using energy principles, we can even derive our own F.O.R.M.U.L.A.S!* He was very excited and explaining to a classmate how **wonderful** is that. The classmate did not shared this excitement.

¹⁵³To check with professors and colleagues. Reijo K. and Jarkko N.

¹⁵⁴which is not yet proven or dis-proven.

¹⁵⁵Yksikkövoimamenetelmä, in Finnish.

¹⁵⁶I can hear Reijo from here. *This is not a scientific proposition.* True, it is not. It is for the moment just a *scientific filling* to be checked later.

¹⁵⁷Will be presented shortly farther, see also Timoshenko.

bound by finding minimum and maximum of successive approximations of deflections (buckling modes) (see Timoshenko for details).

2. approximating displacements \hat{v} and using neutral equilibrium condition of the total potential energy in its displacement form. (Rayleigh quotient-like)

This method will be labelled as the *displacement method*.

Naturally, this approach provides an upper-bound for the buckling load (see literature for Rayleigh quotient minimal property).

Consequently, all solutions given by every Finite Element (FE) software (based on the displacement method) will be upper-bound estimates for the buckling load.

3. the proposed variation principles expressed by equations (1.291) and (1.309), to, may be, provide estimate for lower-bound of the critical load.

This method will be labelled as the *mixed method*.

Examples are under work; coming soon.

1.12.2 Examples of buckling load estimates

End-pinned column

We start by using the two first methods 1) and 2) listed above. The old energy principle to be used with the 1) force method is the elegant *theorem of virtual work of the unit-dummy load*¹⁵⁸ - which is known as the brutal *unit-dummy load method* - and 2) the Lagrange-Dirichlet theorem asking for stationarity (neutral equilibrium condition) of the *change* of total potential energy $\delta(\Delta\Pi) = 0$ at buckling for any tiny virtual perturbation $\delta\mathbf{v}$.

To start and concretise the idea, let us consider the simple example of the beam-column which is simply supported and centrally loaded by a point load P at one end (Figure 1.77). We will account for both shearing and bending effects. The effective rigidities being EI and k_sGA , respectively and without more comments. (later, another example of a column-beam, buckling of a a cantilever under its own weight will be considered).

After an analysis that will be detailed bellow. When accounting for the shearing effect, next results

$$\underbrace{0.97 \cdot \frac{\pi^2 EI}{\ell^2} \left[\frac{1}{1 + \frac{48EI}{5k_sGA\ell^2}} \right]}_{\text{force method}} \leq P_{cr}^{(theor.)} \leq \underbrace{1.22 \cdot \frac{\pi^2 EI}{\ell^2} \left[1 + \frac{k_sGA\ell^2}{48EI} \right]}_{\text{displacement method}} \quad (1.331)$$

are obtained.

¹⁵⁸this is a corollary of the work of virtual force principle

Note that, the force method seems to estimate the analytical buckling load from below, in this example. We can conclude that because we know, *a priori* the analytical value - the basic Euler buckling load $P_E = \frac{\pi^2 EI}{\ell^2}$. Think how difficult, to claim that we've found an estimate for the lower-bound when we do not the true solution! So, this result of the lower bound estimate, by the force method, as presented here, cannot be extended to be general since I do not found a prove for it, yet. It suffice to find one single counter-example to disapprove the generality of such hypothesis. So, take you pencils and tell me.

Neglecting this last effect, gives the next bounds

$$\underbrace{0.97 \cdot \frac{\pi^2 EI}{\ell^2}}_{\text{force method}} \leq P_E^{(theor.)} = 1 \cdot \frac{\pi^2 EI}{\ell^2} \leq \underbrace{1.22 \cdot \frac{\pi^2 EI}{\ell^2}}_{\text{displacement method}} \quad (1.332)$$

Valuable and even very valuable is to find bounds (upper- and lower) for the critical or buckling load for purpose of structural design. Since, we then know that the true value of the critical load lays within the interval given by these bounds, and that, for instance, *buckling will not occur for loads lower than the lower-bound*.

Let now see how the above non-trivial result has been obtained. Read following chapters to find out the full story. In the following, we will go step-by-step to show the above results.

The force method

The force method gives the *lower-bound*

$$P_{cr}^{(force.)} = \frac{48}{5} \cdot \frac{\pi^2 EI}{\ell^2} \left[\frac{1}{1 + \frac{48EI}{5kGA\ell^2}} \right] \approx 0.97 \cdot \frac{\pi^2 EI}{\ell^2} \left[\frac{1}{1 + \frac{48EI}{5kGA\ell^2}} \right] \leq P_{cr}^{(true)}. \quad (1.333)$$

The idea is to approximate the real bending moment $M = M(x; v(x), P)$ and shear force $Q = Q(x; v(x), P)$ distributions in the deformed configuration, here the buckled position $v(x)$, in order to account for the geometrical non-linearity. Then to determine the buckled displacements at some specific points x_i (here $x_i = \ell/2$ and $v(\ell/2) = v_0$) by the virtue of the *virtual work principle* (the virtual force, $\delta F \equiv \bar{F}$, method). Here we use the virtual unit dummy-load theorem¹⁵⁹.

¹⁵⁹Note that not P , the value of the critical load, neither $v(x)$, the buckled deflection, are known. The only thing we know is that at buckling $v(x) \neq 0$. We will not be able to determine the buckled deflection in this analysis. For that, one need post-buckling analysis. The virtual work theorem can be used. We may do that with the virtual force method, if there is time and obtain some interesting results. May be later. Now, our interest is to determine the buckling load P_{cr} only

The *master* student should remember that *the theorems of virtual work are very general and that they remain valid not only in linear cases but also in presence of all kind of non-linearities*¹⁶⁰, *geometrical and material*. That is why I use the theorems of virtual work (here, the so called 1-dummy-load method) to determine displacements at specific locations for the buckled configuration ($v(x) \neq 0$.)

$$1 \cdot v_i = \int_{\ell} \frac{M[x; v(x); P] \cdot \bar{M}_i(x)}{EI(x)} dx + \int_{\ell} \frac{Q[x; v(x); P] \cdot \bar{Q}_i(x)}{kGA(x)} dx, \quad v_i \neq 0, \quad i = 1, 2, \dots, N \quad (1.334)$$

where, in general for the case of many degrees of freedom v_i , $i = 1, 2, \dots, N$, $\bar{M}_i(x)$ and $\bar{Q}_i(x)$ are stress resultants (bending moment and shear force) in the corresponding virtual states when the structure is loaded by a unit load at locations x_i in the direction of the deflection v_i to be determined (Fig. 1.77 b). In the following example, we have only one degrees of freedom v_0 and we chose $x_i = \ell/2$ and $v(x_i) = v(\ell/2) \equiv v_0$ ¹⁶¹, (Fig. 1.78).

Notice that we now use the force method, and we will *make approximation for the internal forces* M and Q which will depend also on deflection v and axial force $N = -P$, to account for this geometrical non-linearities in the real stress resultants M and Q . In this example, the first buckling mode is approximated by a parabolic shape to simplify hand calculations, without loss of generality. For instance, a piece-wise linear approximation may be much better when the number of discrete points is enough high, let's say 10 or more intervals x_i (Fig. 1.77 b). This will result is a homogeneous matrix equation $[\mathbf{A} - P \cdot \mathbf{B}] \mathbf{v}_0 = \mathbf{0}$, to be solved for non-trivial solutions to exist (Therefore, the condition $\det[\mathbf{A} - P \cdot \mathbf{B}] = 0$ will provide a lower bound for the critical load as the smallest eigenvalue.

In our simplified one-degrees-of-freedom example, the deflection (buckling mode) is approximated in the form (Fig. 1.77 a))

$$v(x) \approx \tilde{v}(x) = 4v_0x(\ell - x)/\ell^2 \quad (1.335)$$

This is how we introduce the geometrical non-linearity in approximations of the true stress resultants Finally,

$$M(x; v_0, P) = P \cdot v(x) = P \cdot 4v_0x(\ell - x)/\ell^2, \quad (1.336)$$

$$Q(x; v_0, P) = M' = -P \cdot 4v_0(2x - \ell)/\ell^2, \quad (1.337)$$

for $x \in [0, \ell]$. It is important to note, that the above internal force approximations are defined to fulfil the equilibrium equations, and are consistent with the approximation of the buckling mode.

¹⁶⁰Here, we are dealing with only elastic buckling and thus geometrical non-linearities. Material non-linearity will be presented when we arrive into the elasto-plastic buckling of columns. So, patience.

¹⁶¹this part of the story, you already must know from the basic course in structural mechanics.

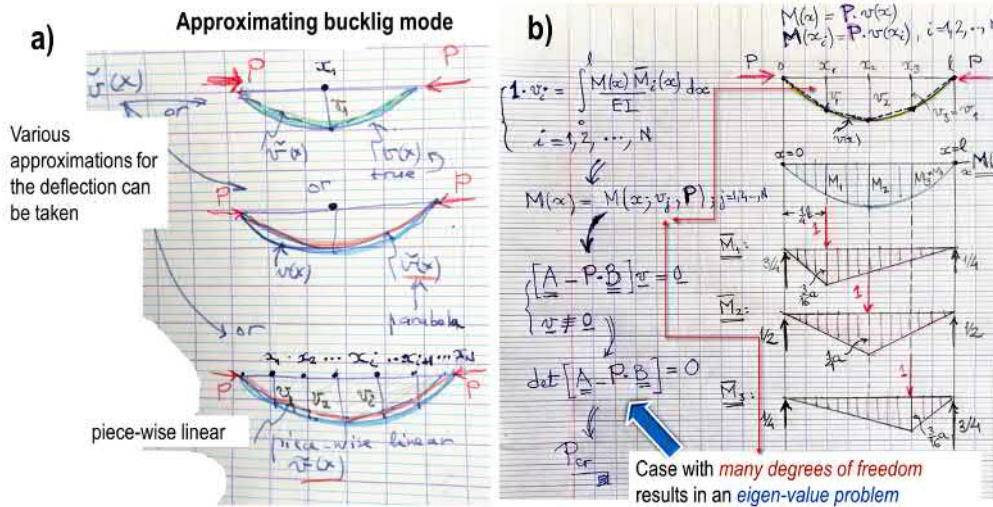


Figure 1.77: Approximating the first buckling mode: a) a parabolic and a piece-wise linear distributions using one degrees of freedom (dofs) and b) a piece-wise linear distributions using many dofs.

The bending moment \bar{M} and shear force \bar{Q} induced by the transversal unit load are

$$\bar{M}(x) = \frac{1}{2}x, \quad x \in [0, \ell/2], \text{ symmetric for } x \in [\ell/2, \ell] \quad (1.338)$$

$$\bar{Q}(x) = \frac{1}{2}, \quad x \in [0, \ell/2], \text{ antisymmetric for } x \in [\ell/2, \ell] \quad (1.339)$$

These resultants are given for $x \in [0, \ell/2]$ because the needed MM -integrals¹⁶² can be computed as

$$1 \cdot v_0 = \int_0^\ell \frac{M \cdot \bar{M}}{EI} dx + \int_0^\ell \frac{Q \cdot \bar{Q}}{kGA} dx = 2 \int_0^{\ell/2} \frac{M \cdot \bar{M}}{EI} dx + 2 \int_0^{\ell/2} \frac{Q \cdot \bar{Q}}{kGA} dx \quad (1.340)$$

thanks to symmetries of the distributions (symmetric \times symmetric and antisymmetric \times antisymmetric; Fig. 1.78).

Performing the integrations in the MM -integral (1.340)

$$1 \cdot v_0 = 2 \int_0^{\ell/2} \frac{1}{EI} \cdot \underbrace{\frac{4Pv_0x(\ell-x)}{\ell^2}}_M \cdot \underbrace{\frac{1}{2}x}_M dx + 2 \int_0^{\ell/2} \frac{1}{kGA} \cdot \underbrace{\frac{4Pv_0(\ell-2x)}{\ell^2}}_Q \cdot \underbrace{\frac{1}{2}}_Q dx \quad (1.341)$$

¹⁶²The letters MM in the notation MM -integral refers to Maxwell-Mohr integrals and not to the moments M .

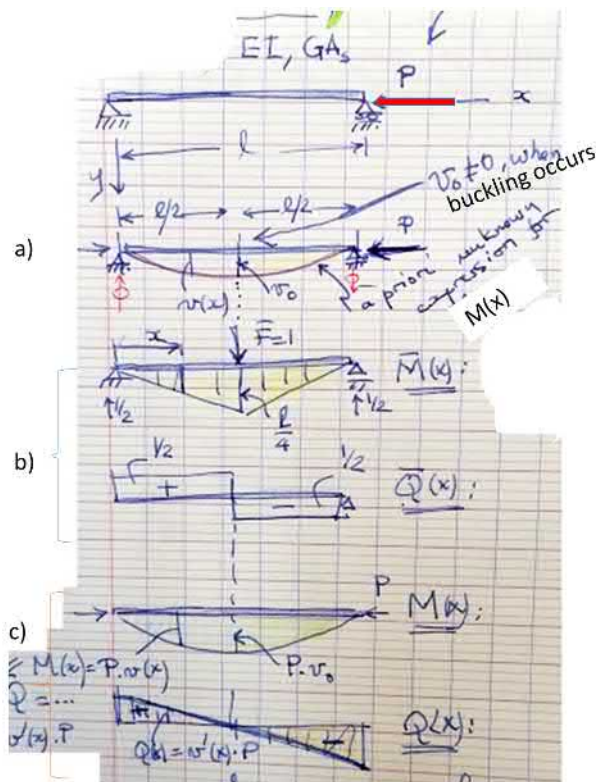


Figure 1.78: Buckling of a simply supported column. a) buckled configuration $\implies v \neq 0$ - to be approximated). b) virtual bending moment and shear force. c) real bending moment and shear force (to be approximated).

one obtains

$$1 \cdot v_0 = \frac{5}{48} \frac{Pv_0\ell^2}{EI} + \frac{Pv_0}{kGA} \implies v_0 \cdot \underbrace{\left(1 - \frac{5}{48} \frac{Pv_0\ell^2}{EI} \cdot \left[1 + \frac{48EI}{5kGA\ell^2}\right]\right)}_{\text{should be } = 0} = 0, \forall v_0 \neq 0 \quad (1.342)$$

and consequently, the needed beautiful result (Equation (1.333))

$$P_{cr}^{(force.)} \approx 0.97 \cdot \frac{\pi^2 EI}{\ell^2} \left[\frac{1}{1 + \frac{48}{5} \frac{EI}{kGA\ell^2}} \right] \leq P_{cr}^{(true.)}. \quad (1.343)$$

comes as a gift by *the force*¹⁶³, for those remaining humble with the value of virtual work principles, since the expression within the rounded brackets should vanish because $v_0 \neq 0$. Note that, the numerical approximation $48/5 \approx \pi^2$, in the above formula, can be used to compare the approximate the obtained 'buckling

¹⁶³Jumalan lahjana, in Finnish.

formula' with known analytical result. Compare the above result (Eq. 1.343) with the analytical solution (1.239) by Timoshenko *et al.*. Inserting $P^E = \pi^2 EI/\ell^2$ in Eq. (1.344) one obtains, for comparison,

$$P_T = \underbrace{\frac{\pi^2 EI}{\ell^2} \frac{1}{1 + \pi^2 \frac{EI}{kGA\ell^2}}}_{\text{analytical}} \approx 0.97 \underbrace{\frac{\pi^2 EI}{\ell^2} \frac{1}{1 + \frac{48}{5} \frac{EI}{kGA\ell^2}}}_{\text{approx. by force method}} \quad (1.344)$$

By noting, in (1.344) that $\pi^2 = 9.9 \approx 10 \approx 48/5 = 9.6$ we conclude that, the energy method (the force method) we used, provided us a quite accurate estimate of the buckling load, and, in addition, accounts quit correctly, for the shearing effects! *Long live the power of abstraction.* We notice also, that this critical load estimates approaches the analytical buckling load from bellow. We however, cannot conclude, in general, that it is an estimate for the lower bound.¹⁶⁴

Application example - buckling of a sandwich beam

For curiosity, I will rewrite the above *academic* result to show that, in fact, it is a result of *practical* importance than can be used to design sandwich beams against global buckling¹⁶⁵. Let's rewrite formula (1.344) using effective bending and shear rigidities, $EI \equiv B$ and $kGA \equiv S$, respectively. Consider a simply supported end-pinned column with a load¹⁶⁶ P at the roller support (Fig. 1.79). The (analytical) buckling load, accounting for shearing, is¹⁶⁷

$$P_T = \underbrace{\frac{\pi^2 EI}{\ell^2}}_{\equiv P_E} \frac{1}{1 + \pi^2 \frac{EI}{kGA\ell^2}} = P_E \frac{1}{1 + \frac{P_E}{S}} = \frac{\pi^2 B}{\ell^2} \frac{1}{1 + \pi^2 \underbrace{\left[\frac{B}{S\ell^2} \right]}_{\equiv \Phi}} = P_E \cdot \frac{1}{1 + \pi^2 \Phi} \quad (1.345)$$

where the *shear factor*, defined as $\Phi = B/(S\ell^2)$, have been used. The effective rigidities can be determined, for instance, using energy arguments by asking the homogeneous sandwich beam' to conserving strain energy of the original laminated structure.

¹⁶⁴This is simple to say when one knows the analytical solution. Imagine that you do not know it. Based on what, we can then conclude that the obtained approximation is an estimate for the lower bound?

¹⁶⁵In such sandwich structures, in addition to global buckling, local buckling may play a critical role in overall failure. The question of local buckling is a very important question.

¹⁶⁶One naturally, distributes uniformly the load P among a large surface of the cross section of the sandwich-beam, in order to avoid local failure. Therefore, the application surface of the force should occurs through some stiffened plate or equivalent.

¹⁶⁷This was derived previously in this notes; this is a classical result as shown by Timoshenko and others.

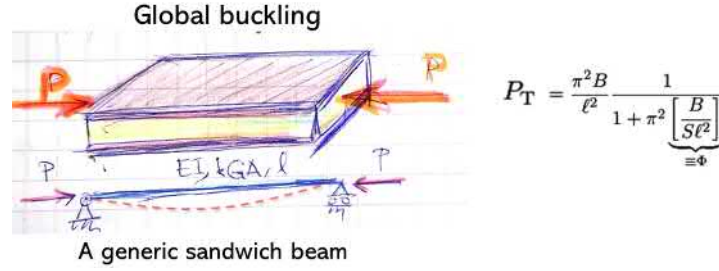


Figure 1.79: Buckling of a simple sandwich beam (model).

Important to note: now that we have an estimate for the buckling load, we can estimate the resulting bending moment M , separately from the bending moment approximation

$$\hat{M}(x) = P_{cr} \cdot v(x) = 0.97\pi^2 \frac{EI}{\ell^2} \cdot 4v_0 x(x - \ell)/\ell^2 \quad (1.346)$$

and the approximation of the displacements (constitutive law)

$$\hat{M}(x) = -EIv''(x) = -EI \cdot 2 \cdot 4v_0/\ell^2 \quad (1.347)$$

and to find that the constitutive relation, in the form of the constraint

$$M(x) + EIv''(x) = 0 \quad (1.348)$$

which gives

$$\hat{M}(x) + EIv''(x) = 0.97\pi^2 \frac{EI}{\ell^2} \cdot 4v_0 x(x - \ell)/\ell^2 + EI \cdot 2 \cdot 4v_0/\ell^2 \neq 0 \quad (1.349)$$

and thus, is not fulfilled. This will be the case (=fulfilled) only when the buckling mode approximation happens to be a true buckling mode. This is the reason why I proposed to enforce this constraint, the constitutive law, by accounting for it, as a penalty $\lambda \int_{\ell} [M(x) + EIv''(x)]^2 dx$, $\lambda > 0$ to add directly into the variational principle

The displacement method

The displacement method gives the *upper-bound*

$$P_{cr}^{(displ.)} = \frac{12}{\pi^2} \cdot \frac{\pi^2 EI}{\ell^2} \left[1 + \frac{kGA\ell^2}{48EI} \right] \approx 1.22 \cdot \frac{\pi^2 EI}{\ell^2} \left[1 + \frac{kGA\ell^2}{48EI} \right] \geq P_{cr}^{(true)} \quad (1.350)$$

Let see how it is obtained.

Recall that now

$$\Delta\Pi = \frac{1}{2} \int_{\ell} EI\kappa^2 dx + \frac{1}{2} \int_{\ell} k_s GA\gamma^2 dx - P \int_{\ell} \frac{1}{2} (v')^2 dx. \quad (1.351)$$

So the buckling criteria gives

$$\delta(\Delta\Pi) = \int_{\ell} EI\kappa \cdot \delta\kappa dx + \int_{\ell} k_s GA\gamma \cdot \delta\gamma dx - P \int_{\ell} v' \cdot \delta v' dx = 0, \forall \delta\kappa, \delta\gamma, \quad (1.352)$$

where $\kappa(x) = -v''$ and $\gamma(x)$ being the shear angle. The criteria (1.352)¹⁶⁸ is the one that will be used to derive the approximation for the lower-bound by giving trials (approximations) for $v(x)$ and $\gamma(x)$, separately.

Let's start from the start, *i.e.*, take the buckling criteria (Eq. 1.352) and use the Galerkin method and use an approximation for the displacements fields $v(x)$ and $\gamma(x)$. The variations $\delta v''$, $\delta v'$ and $\delta\gamma$ will follow by taking adequate variations of the approximated fields as good story flows from the mouth of a story-teller. Let the simplest approximation of the displacement (buckled deflection) be the same as the chosen previously (Fig. 1.80);

$$v(x) \approx \tilde{v}(x) = 4v_0x(\ell - x)/\ell^2, \quad x \in [0, \ell]. \quad (1.354)$$

For the shear angle $\gamma(x)$ we will take a simplest possible in the linear form (Fig. 1.80) (this will lead to a linear shear force $Q = kGA\gamma$ distribution which can be an enough good approximation for our purpose)

$$\gamma(x) \approx \tilde{\gamma}(x) = \frac{v_0}{\ell^2/2} \left(1 - \frac{x}{\ell/2}\right), \quad x \in [0, \ell/2] \quad (1.355)$$

and, for $x \in [\ell/2, \ell]$, $\gamma(x)$ is antisymmetric. The above kinematic approximations result in the next variations

$$v' = \frac{4}{\ell^2}(\ell - 2x)v_0 \implies \delta v' = \frac{4}{\ell^2}(\ell - 2x)\delta v_0, \quad x \in [0, \ell] \quad (1.356)$$

$$v'' = \frac{8}{\ell^2}v_0 \implies \delta v'' = \frac{8}{\ell^2}\delta v_0, \quad x \in [0, \ell] \quad (1.357)$$

$$\delta\gamma(x) = \frac{2}{\ell}(1 - 2x/\ell)\delta v_0, \quad x \in [0, \ell/2], \text{ (remaining part is antisym.)} \quad (1.358)$$

¹⁶⁸This is a weak form (equivalent to the virtual work principle). The variations $\delta v''$, $\delta v'$ and $\delta\gamma$ can be seen as the corresponding test functions \hat{v}'' , \hat{v}' and $\hat{\beta}$;

$$\int_{\ell} EIv'' \cdot \hat{v}'' dx + \int_{\ell} k_s GA\gamma \cdot \hat{\gamma} dx - P \int_{\ell} v' \cdot \hat{v}' dx = 0, \forall \hat{v}'', \hat{v}', \hat{\gamma} \quad (1.353)$$

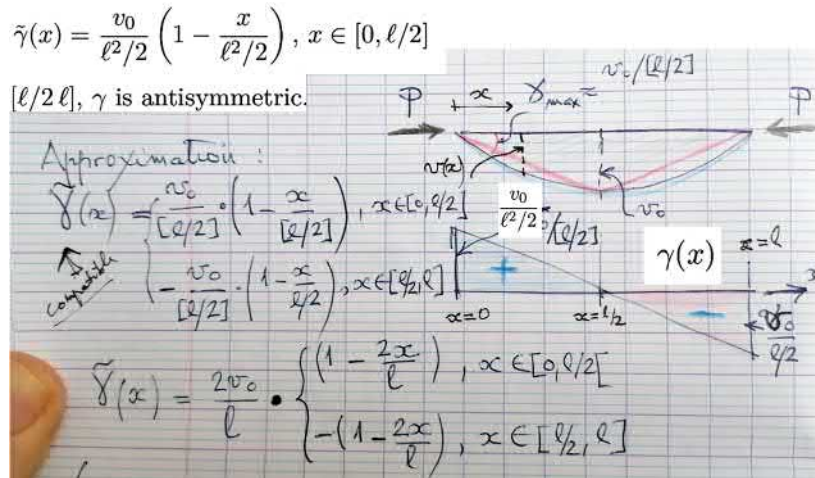


Figure 1.80: Approximating the first buckling mode: a) a parabolic and a piece-wise linear distributions using one degrees of freedom (dofs) and b) a piece-wise linear distributions using many dofs.

Inserting all the needed expressions in the criticality condition (1.352) gives

$$\delta(\Delta\Pi) = \underbrace{\int_{\ell} EI \left[\frac{8}{\ell^2} v_0 \right] \cdot \left[\frac{8}{\ell^2} \delta v_0 \right] dx}_{=4 \cdot 16 EI / \ell^3 \cdot v_0 \delta v_0} + \quad (1.359)$$

$$+ \underbrace{\int_{\ell} k_s GA \cdot \left[\frac{2}{\ell} \left(1 - \frac{2x}{\ell}\right) v_0 \right] \cdot \left[\frac{2}{\ell} \left(1 - \frac{2x}{\ell}\right) \delta v_0 \right] dx}_{=4 / (3\ell) k_s GA \cdot v_0 \delta v_0} + \quad (1.360)$$

$$- P \underbrace{\int_{\ell} \left[\frac{4}{\ell^2} (\ell - 2x) v_0 \right] \cdot \left[\frac{4}{\ell^2} (\ell - 2x) \delta v_0 \right] dx}_{=16 / (3\ell)} = 0, \quad \forall \delta v_0, v_0 \neq 0 \quad (1.361)$$

which, at its turn, provides the buckling equation

$$\left[\frac{4 k_s GA}{3 \ell} + 4 \cdot 16 \frac{EI}{\ell^3} - P \cdot \frac{16}{3\ell} \right] \cdot v_0 \delta v_0 = 0, \quad \forall \delta v_0 \neq 0, v_0 \neq 0 \implies P_{cr}^{(displ.)}, \quad (1.362)$$

which leads, with NET-¹⁶⁹ scape, to the long-awaited-for result

$$\boxed{P_{cr}^{(displ.)} \approx 1.22 \cdot \frac{\pi^2 EI}{\ell^2} \left[1 + \frac{kGA \ell^2}{48 EI} \right] \geq P_{cr}^{(true)}} \quad (1.363)$$

¹⁶⁹Russian NET. thus meaning there is o other ways! As in the old historical browser NETSCAPE. Sorry, this is an inside joke.

Cantilever column under self-weight

The force method

The displacement approximation is chosen

$$\hat{v}(x) = v_0 x^2 / \ell^2. \quad (1.364)$$

and is kinematically admissible, since $\hat{v}(0) = 0$ and $\hat{v}'(0) = 0$. Before writing

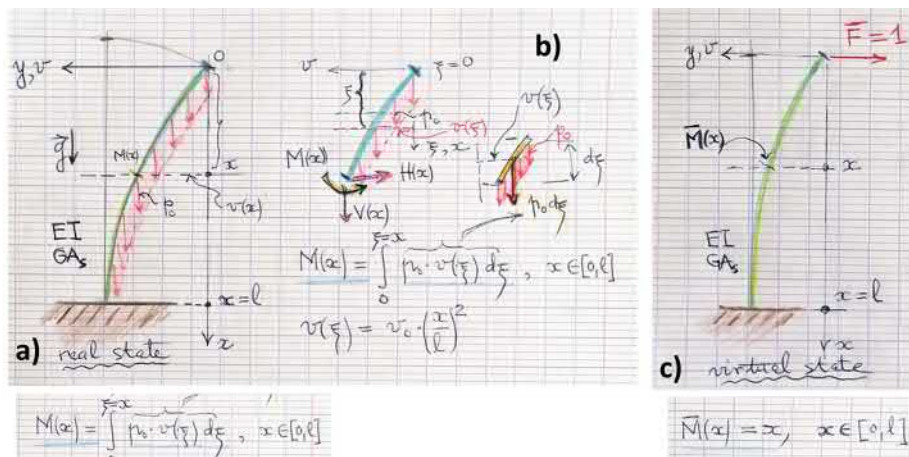


Figure 1.81: Buckling of a cantilever column-beam under its self-weight.

equilibrium equation, we need to determine the *external moment* $M_e(x)$ at a section x due to the distributed load (self-weight) p_0 as (free-body diagram in Fig. 1.81 b)

$$dM_e(\xi) = p_0 v(\xi) d\xi \implies M_e(x) = \int_{\xi=0}^{\xi=x} p_0 v(\xi) d\xi = p_0 v_0 / \ell^2 \cdot x^3 \quad (1.365)$$

Therefore, the bending moment approximation $\hat{M}(x)$ is obtained by asking the approximation of the moment to equilibrate the external moment

$$M_e(x) - \hat{M}(x) = 0 \implies \hat{M}(x) = p_0 x \hat{v}(x) = p_0 v_0 / \ell^2 \cdot x^3 \quad (1.366)$$

since it should equilibrate the external moment at every section x . In the following, the shearing effects are, for simplicity, ignored.¹⁷⁰ Estimating the displace-

¹⁷⁰They can, easily, be added through the energy term $\int_0^\ell \frac{Q \cdot \bar{Q}}{kGA} dx$ with $Q = M'$.

ment¹⁷¹ at the tip of the column gives, for all $v_0 \neq 0$,

$$1 \cdot v_0 = \int_0^\ell M \cdot \frac{\bar{M}}{EI} dx = \frac{p_0 v_0}{EI \ell^2} \int_0^\ell x^3 \cdot x dx = \frac{(p_0 \ell) \cdot \ell^2}{5EI} \quad (1.367)$$

$$\implies (p_0 \ell)_{cr} = 5 \frac{EI}{\ell^2} \approx \underbrace{0.5\pi^2 \frac{EI}{\ell^2}}_{\text{the force method}} < (p_0 \ell)_E = \underbrace{0.79\pi^2 \frac{EI}{\ell^2}}_{\text{analytical}} \quad (1.368)$$

We conclude by comparing the result with known analytical solution (see Timoshenko) that, the obtained estimation of the critical load is also coming from below in this example too.

The displacement method

First, I drop, for shortness, the hat from the approximation

$$v(x) = v_0 x^2 / \ell^2. \quad (1.369)$$

Now, one needs to determine the work increment of the external load at buckling. For that, the shortening of the column at buckling is needed. It easy to express the differential shortening¹⁷² due to bending (curvature change) as

$$du(x) = \int_0^{\xi=x} \frac{1}{2} [v'(\xi)]^2 d\xi. \quad (1.370)$$

Note that the work done by the distributed constant self-weight p_0 on the column (flexural) shortening is

$$\Delta W_e = \int_0^\ell \left[\int_0^{\xi=x} p_0 \cdot \frac{1}{2} [v'(\xi)]^2 d\xi \right] dx \quad (1.371)$$

Let's, for shortness and not bore the reader, determine the critical load estimate directly from weak form¹⁷³ one obtains from Eq. (1.375)

$$\underbrace{\int_0^\ell v'' EI \delta v'' dx}_{\delta(\Delta W_{\text{int}})} - \underbrace{\int_0^\ell \left[\int_0^{\xi=x} p_0 \cdot v'(\xi) \cdot \delta v'(\xi) d\xi \right] dx}_{\delta(\Delta W_{\text{ext}})} = 0, \forall \delta v \in V_{ad}. \quad (1.372)$$

It worth to first, notice that (neutral equilibrium condition (Eq. (1.375) corresponds to the virtual work principle $\delta W = 0, \forall \delta v$).

¹⁷¹Notice that now, we start from known bending moment distributions M and \bar{M} which are independent of coordinate system. Thus, for the MM -integration, I changed to an axis system with origin at the clamping $x = 0$ and $x = \ell$ at the tip.

¹⁷²Recall that at buckling, the change in u' is negligible as compared to the shortening resulting from bending.

¹⁷³Show this result as a homework, or just an exercise to do when you are bored.

Let's now rewrite the above neutral equilibrium condition into a familiar weak form¹⁷⁴ more easy to use computationally as Identifying $\phi := x^2/\ell^2$ and therefore

$$\int_0^\ell \phi'' EI \phi'' dx - \int_0^{x=\ell} \left[\int_0^{\xi=x} p_0 \cdot \phi'(\xi) \cdot \phi'(\xi) d\xi \right] dx = 0, \forall \delta v \in V_{ad}. \quad (1.373)$$

So,

$$\phi = x^2/\ell^2, \phi' = 2x/\ell^2, \phi'' = 2/\ell^2. \quad (1.374)$$

$$\left(\int_{\ell^e} \frac{2}{\ell^2} \cdot EI \cdot \frac{2}{\ell^2} dx - p_0 \int_0^{x=\ell} \left[\int_0^{\xi=x} [2\xi/\ell^2] \cdot [2\xi/\ell^2] d\xi \right] dx \right) \cdot v_0 = 0, v_0 \neq 0 \quad (1.375)$$

After integrations, we obtain to the result for the critical weight $(p_0\ell)$

$$(p_0\ell)_{cr} \approx 12 \frac{EI}{\ell^2} \approx 1.2\pi^2 \frac{EI}{\ell^2} > \underbrace{7.84 \frac{EI}{\ell^2} \approx 0.79\pi^2 \frac{EI}{\ell^2}}_{\text{analytical}} \quad (1.376)$$

We see that, as expected, that the estimation comes from *above* with respect to *known* analytical buckling load.

Dynamics of loss of stability of a very slender cantilever: This example is given to capture students motivation and their curiosity toward dynamics as applied to structural analysis. I reproduce a numerical simulation¹⁷⁵ where, I solved the full non-linear equations of motion of such cantilever under its self-weight. The trajectories of the motion till new equilibrium is found. In this model large displacements and rotations are solved without any approximation related to moderate rotations or whatever. In this example, the self-weight was a bit higher than the critical value. Then, a very tiny horizontal tip load served as perturbation. The resulting dynamic motion (trajectories) are reproduced in Figure (1.81). In addition, we also notice that the new equilibrium configuration is stable since the amplitudes of the motion get smaller and smaller with time. This is a sign for stability behaviour.

Cantilever column

We will consider the elastic cantilever of length ℓ with central end-load P . Estimate the buckling load. Both displacement and force method will used.

¹⁷⁴The test functions or δv are chosen as in the Galerkin method, the same as the basis functions of the approximation. Additionally, the reader should already recognise that, physically speaking, this *weak form* is nothing else than the familiar *virtual work principle*.

¹⁷⁵D. Baroudi *et. al.*, Finnish XIII - Mechanics days, 2018.

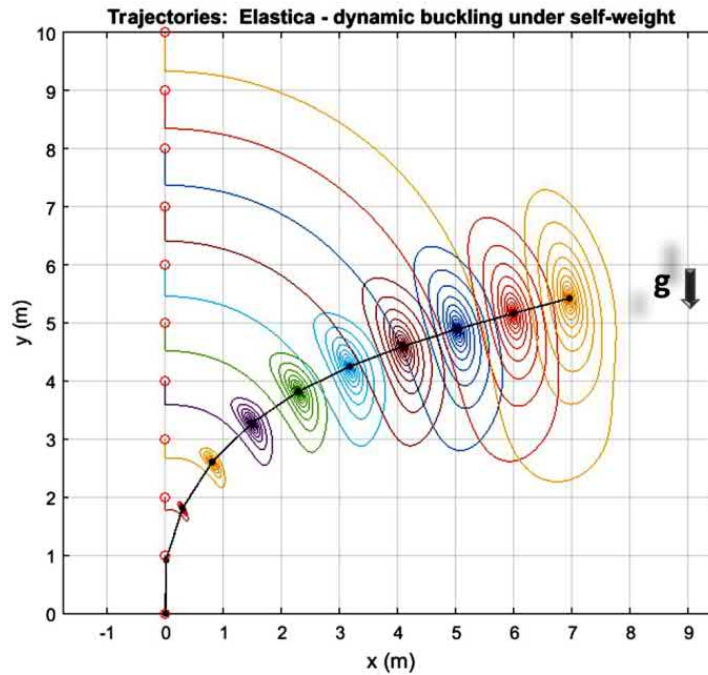


Figure 1.82: Dynamic loss of stability of the cantilever column-beam under its self-weight shown in Figure (). The trajectories of the nodes shows the time evolution of their positions.

Force method

In the force method we will consider the dummy unit-load method, sorry for this brutal naming, and the complementary energy principle.¹⁷⁶

The virtual force principle

$$1 \cdot v_0 = \int_0^\ell M \cdot \frac{\bar{M}}{EI} dx = \int_0^\ell \frac{Pv_0}{EI\ell^2} [1 - (x/\ell)^2][\ell - x] dx = \quad (1.377)$$

$$\implies P_{cr} = \frac{12 EI}{5 \ell^2} \approx \underbrace{0.24\pi^2 \frac{EI}{\ell^2}}_{\text{the force method}} < P_E = \underbrace{1/4 \cdot \pi^2 \frac{EI}{\ell^2}}_{\text{analytical}} \quad (1.378)$$

The estimated buckling load seems to approach from below.

¹⁷⁶If I remember well, we have already tackled a bit this question somewhere in these notes in details while discussing about lower bounds for the buckling load. Please, dear reader, refer to subsection (1.12.1) for that.

Displacement method

We go back to the cantilever buckling problem. We will use the energy principle in its weak form ready for computations as the eigenvalue problem

$$\sum_{i=1}^n \left[\underbrace{\int_0^\ell \phi_i'' EI \phi_j'' dx}_{K_{ij}} - P \underbrace{\int_0^\ell \phi_i'(x) \cdot \phi_j'(x) dx}_{S_{ij}} \right] \cdot a_i = 0, \forall j = 1, 2, \dots, n \quad (1.379)$$

$$[\mathbf{K} - P \cdot \mathbf{S}] \mathbf{a} = \mathbf{0}, \mathbf{a} \neq \mathbf{0} \quad (1.380)$$

The basis functions are ϕ_i and the test functions are the same ϕ_j (the Galerkin method, attend the FEM-course by prof. Jarko N. for standard notations). In this analysis, we use global approximations¹⁷⁷ for the buckling deflection

$$\hat{v}(x) = \sum_i a_i \phi_i(x), a_i \in R \quad (1.381)$$

where the basis, for this example, is

$$\phi = [1, x, x^2, x^3, x^4, \dots, x^n]. \quad (1.382)$$

From which the two first basis functions 1 and x are eliminated to fulfil kinematic boundary conditions $\hat{v}(0) = 0$ and $\hat{v}'(0) = 0$.

One can use, naturally, the trigonometric series. However, in this example, we will not do so, since otherwise, one will exactly obtain the exact solution, and we want to demonstrate the convergence properties of the approximations from above.

We will perform three successive kinematically admissible approximations using, one, two and three terms from basis functions $\{x^2\}_1$, $\{x^2, x^3\}_2$ and $\{x^2, x^3, x^4\}_3$. Therefore, the approximation (fulfilling kinematic boundary conditions) is

$$\hat{v}(x) = \sum_{i=1}^n \phi_i(x) a_i, \quad (1.383)$$

where, vuorotellen, $n = 1$, $n = 2$ and $n = 3$.

Note that the (linearised) stiffness matrices and (geometrical) stiffness matrices \mathbf{K} and \mathbf{S} are

$$K_{ij} = \int_0^\ell \phi_i'' EI \phi_j'' dx \quad (1.384)$$

and

$$S_{ij} = P \int_0^\ell \phi_i'(x) \cdot \phi_j'(x) dx \quad (1.385)$$

Inserting successively the above three approximations into the weak form (1.380), after computing the needed matrices, one obtains the three successive eigenvalue problems:

¹⁷⁷The accuracy of the truncated series can be estimated by estimating the reminding terms by the formula of Taylor series.

basis: $\{x^2\}$

$$\phi_1(x) = x^2, \phi_1'(x) = 2x, \phi_1'' = 2 \quad (1.386)$$

$$\left(4 - \frac{4P\ell^2}{3EI}\right) \cdot a_1 = 0, a_1 \neq 0 \implies P_{cr} = 3\frac{EI}{\ell^2} \approx 0.3\pi^2\frac{EI}{\ell^2} > \underbrace{\frac{1}{4}\pi^2\frac{EI}{\ell^2}}_{\text{analytical}} \quad (1.387)$$

basis: $\{x^2, x^3\}$

Now

$$\phi_1 = x^2, \phi_1' = 2x, \phi_1'' = 2 \quad (1.388)$$

$$\phi_2 = x^3, \phi_2' = 3x^2, \phi_2'' = 6x \quad (1.389)$$

and consequently

$$\left(\begin{bmatrix} 4 & 6 \\ 6 & 12 \end{bmatrix} - \frac{P\ell^2}{EI} \begin{bmatrix} 4/3 & 3/2 \\ 3/2 & 9/5 \end{bmatrix}\right) \begin{bmatrix} a_1\ell \\ a_2\ell^2 \end{bmatrix} = \begin{bmatrix} 0 \\ 0 \end{bmatrix}. \quad (1.390)$$

One obtains two eigenvalues¹⁷⁸ $P_{min} = 2.486$ and $P_{max} = 31.18$. The smallest eigenvalue corresponds to the critical load

$$\implies P_{cr} = 2.486\frac{EI}{\ell^2} \approx 0.252\pi^2\frac{EI}{\ell^2} > \underbrace{\frac{1}{4}\pi^2\frac{EI}{\ell^2}}_{\text{analytical}} \quad (1.391)$$

basis: $\{x^2, x^3, x^4\}$

Now

$$\phi_1 = x^2, \phi_1' = 2x, \phi_1'' = 2 \quad (1.392)$$

$$\phi_2 = x^3, \phi_2' = 3x^2, \phi_2'' = 6x \quad (1.393)$$

$$\phi_3 = x^4, \phi_3' = 4x^3, \phi_3'' = 12x^2 \quad (1.394)$$

and consequently

$$\left(\begin{bmatrix} 4 & 6 & 8 \\ 6 & 12 & 18 \\ 8 & 18 & 144/5 \end{bmatrix} - \frac{P\ell^2}{EI} \begin{bmatrix} 4/3 & 3/2 & 8/5 \\ 3/2 & 9/5 & 2 \\ 8/5 & 2 & 16/7 \end{bmatrix}\right) \begin{bmatrix} a_1\ell \\ a_2\ell^2 \\ a_3\ell^3 \end{bmatrix} = \begin{bmatrix} 0 \\ 0 \\ 0 \end{bmatrix}. \quad (1.395)$$

The smallest eigenvalue gives the critical load

$$\implies P_{cr} = 2.4677\frac{EI}{\ell^2} \approx 0.250045 \cdot \pi^2\frac{EI}{\ell^2} > \underbrace{\frac{1}{4}\pi^2\frac{EI}{\ell^2}}_{\text{analytical, } \approx 0.250000} \quad (1.396)$$

¹⁷⁸The generalised eigenvalue problem $[\mathbf{K} - P \cdot \mathbf{S}]\mathbf{a} = \mathbf{0}$, when needed, can be written in the standard form $[\mathbf{I} - P \cdot \mathbf{K}^{-1}\mathbf{S}]\mathbf{a} = \mathbf{0}$ which can be solved, for instance with Matlab (Fig.1.84) function `eig(A)` .

We notice that the three estimates converge¹⁷⁹ to the analytical value by approaching it from above, and thus are estimates for the upper bound of the critical load (Fig. 1.83). In addition, the estimate obtained with only three basis functions gave already a very accurate value

$$\approx 0.250045 \cdot \pi^2 \frac{EI}{\ell^2} \approx \frac{1}{4} \pi^2 \frac{EI}{\ell^2}. \tag{1.397}$$

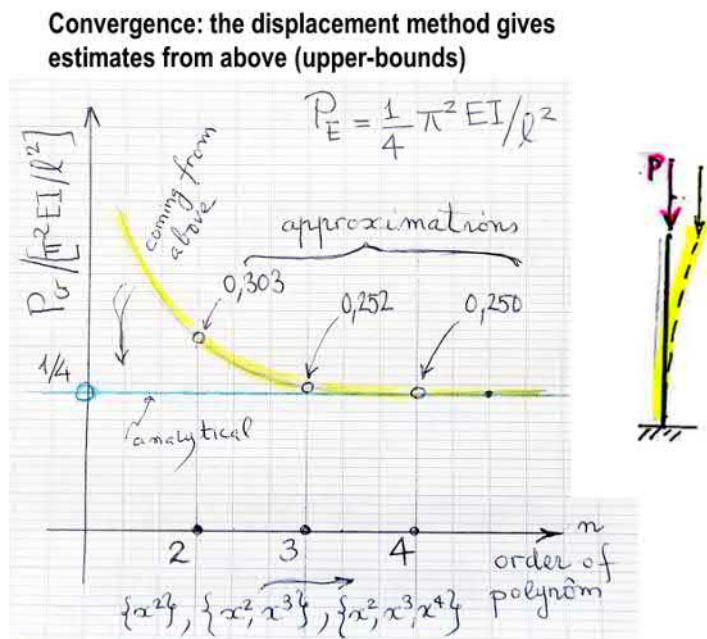


Figure 1.83: Convergence of the buckling load from above (upper bounds) as given by the displacement method. Example of axially free-end compressed cantilever column.

For curiosity, I reproduce this example solved of using the Application Addi (from GooglePlay) to solve the eigenvalue problem (Fig.1.84) that I used when I did not had access to Matlab.

¹⁷⁹This type of convergence is called *p*-convergence. Respectively, *h*-converges is related to convergence obtained by mesh refinement. In our examples we used global approximations, so the convergence is achieved by enriching the basis function set. The convergence can be also achieved by discretizing the geometric domain (triangulation) into sub-domains (elements) and by taking local approximations of lower order. Now refining the mesh, *h* becomes smaller and smaller, a convergence can e achieved, under some conditions for the choice of the basic functions. This condition, in principle is simple: one should approximate, the energy-integrals in a convergent way. For that, it suffice, to approximate the integrand by a piece-wise constant, like in the Reimann-sums for which the integrals are the limits for $h \rightarrow 0^+$.

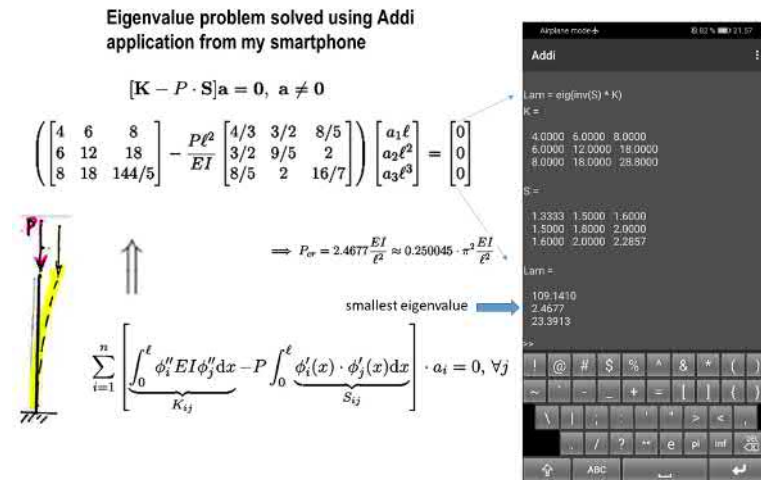


Figure 1.84: Example of eigenvalue problem solved using the Application Addi (from GooglePlay, 2020).

Coming back, to the analysis of the results, note that, we did not take trigonometric basis functions, in this example, for the reason that they will capture exactly the analytical solution. since the analytical buckling modes are trigonometric functions. We wanted to demonstrate the convergence from above of the approximations without this bias, and we therefore took polynomial basis. It is well known that *the complete set of polynomials is dense in the set of continuous functions*. This cryptic mathematical *Boorbakian-type psalms* says in clear that, *any continuous function can be approximated to any given accuracy with polynomial series*.

Force method - simply beam supported column

Let's go back to the simply-supported beam-column buckling problem and illustrate convergence of the Rayleigh-Ritz method which is another name for the energy method, the hand-version of FEM illustrated by the weak form. We will use the energy principle in its weak form ready for computations as the eigenvalue problem (Timoshenko form)

$$\sum_{i=1}^n \left[\int_0^\ell \frac{\phi_i \phi_j}{EI} dx - \frac{1}{P} \int_0^\ell \phi_i'(x) \cdot \phi_j'(x) dx \right] \cdot a_i = 0, \forall j = 1, 2, \dots, n \quad (1.398)$$

where now the kinematically admissible trial functions are (with $\xi = x/\ell$)

basis: $\{x^2, x^4\}$

¹⁸⁰ The displacement trial

$$v \approx a_1\phi_1(x) + a_2\phi_2(x). \tag{1.399}$$

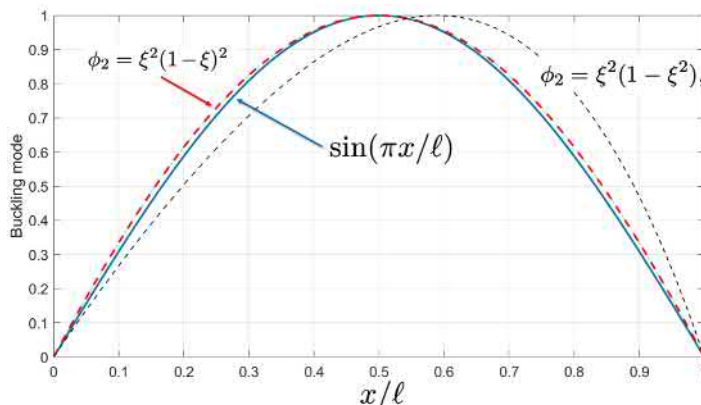


Figure 1.85: Critical buckling mode and some approximating terms.

is used (Fig. 1.85).¹⁸¹ Now

$$\phi_1 = \xi(1 - \xi), \ell\phi_1' = 1 - 2\xi, \ell^2\phi_1'' = -2 \tag{1.400}$$

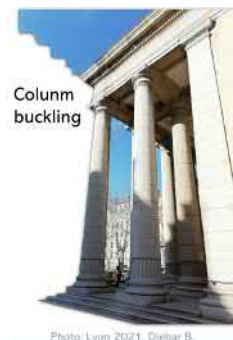
$$\phi_2 = \xi^2(1 - \xi^2), \ell\phi_2' = 2\xi - 4\xi^3, \ell^2\phi_2'' = 2 - 12\xi^2 \tag{1.401}$$

After performing the integrations we obtain the critical condition

$$\det \left\{ \begin{bmatrix} 1/30 & 11/420 \\ 11/420 & 8/315 \end{bmatrix} - \frac{EI}{P\ell^2} \begin{bmatrix} 1/3 & 4/15 \\ 4/15 & 44/105 \end{bmatrix} \right\} = 0 \tag{1.402}$$

¹⁸⁰Notice that I dropped the term x^3 which corresponds to an asymmetric mode. This is possible only because I know, for this example, that the first buckling mode is symmetric. In general, one should take a *complete* basis to ensure convergence (means that the term x^3 should be taken.) and because, we do not know necessarily, *a priori* what is the critical buckling mode. A good counter example is a simply supported column-beam with elastic supports. For some ratio of rigidities of the beam and support, the critical mode is asymmetric. This can be a good homework exercise to give.

¹⁸¹Hits! Note that it happens that in this example we know that exact mode $\sin(\pi x/\ell)$ is symmetric around $x = \ell/2$. Unfortunately, for the accuracy, the chosen basis $\phi_2 = \xi^2(1-\xi^2)$ is less 'symmetric' and that a choice like $\phi_2 = \xi^2(1-\xi)^2$ preserves this symmetry. Surely, using this last version will give more accurate results (see the example). However, the only condition for the trials, to fulfill is to be kinematically admissible as does my unfortunate choice here. Only accuracy will suffer when using a small amount of basis functions. Anyway, the idea, is that we do not know a priori into which mode (symmetric or antisymmetric) the structure will buckle and, so, we have to take a complete basis (or a good approximation for such basis: truncated complete polynomial or trigonometric series.).



Why this column did not buckled?

having the eigenvalues

$$P_{cr} = \left[\begin{array}{c} 1.0128 \\ 4.3274 \end{array} \right] \cdot \pi^2 \frac{EI}{\ell^2} \quad (1.403)$$

Finally, the estimated critical load corresponds to the smallest eigenvalue

$$P_{cr} = 1.0128 \cdot \pi^2 \frac{EI}{\ell^2} > \underbrace{1 \cdot \pi^2 \frac{EI}{\ell^2}}_{\text{analytical}}. \quad (1.404)$$

Figure (1.86) shows, as an example, how a simple determinant that can be,

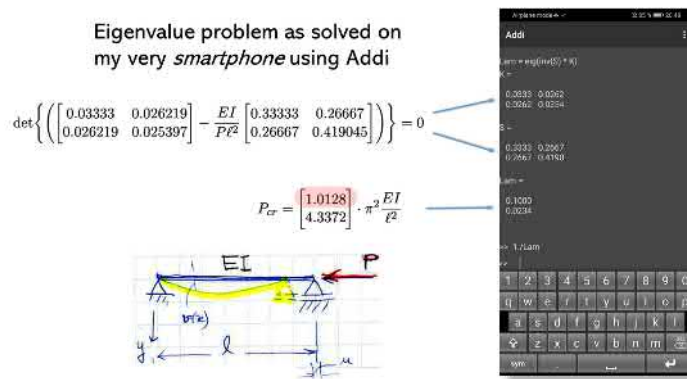


Figure 1.86: Solving the eigenvalue problem of buckling.

anyway, computed by hand, can be solved by a smartphone.¹⁸²

We can notice that the estimate is very close to the analytical solution ($\approx 1\%$) but is, unexpectedly, approaching it from above even when the force method has been used! Did we said, previously, that we should obtain an estimate for the lower bound? No. This is a good counter-example to show that the weak version of the force method without constraint for the constitutive law, in general, does not, in general, provide an estimate for the *lower bound* of the buckling load. This bias may be explained by the fact the trial solution will with high probability *not fulfil, a priori* the constitutive relation $M + EIv'' = 0$, as I have explained this point earlier.

Both basis functions are now symmetric: Again the curiosity to resolve the question was huge, so I did it. Here the story, in short. Notice that now $\phi_2(x)$ is

¹⁸²Solving the eigenvalue problem when we do not have access to computers or when we become lazy. Note that this determinant can be computed by hand in five or less minutes to obtain a quadratic equation to be solved in two minutes using Cramer rule. However, this method will not work when one finds himself lost in Sahara without any smart-phone. Anyway, then, the critical load is surely not the critical problem to solve. (*find water or a way to condense water from its soil evaporation, protect against the sun and find the way out, read the star-map.*)

symmetric (Fig. 1.85), so

$$\phi_1 = \xi(1 - \xi), \tag{1.405}$$

$$\phi_2 = \xi^2(1 - \xi)^2, \tag{1.406}$$

. The approximation for the equilibrium bending moment being simply $M = Pv$. After symbolic integrations, in Matlab, we obtain the critical condition

$$\det \left\{ \begin{bmatrix} 1/30 & 1/140 \\ 1/140 & 1/630 \end{bmatrix} - \frac{EI}{P\ell^2} \begin{bmatrix} 1/3 & 1/15 \\ 1/15 & 2/105 \end{bmatrix} \right\} = 0 \tag{1.407}$$

having the eigenvalues

$$P_{cr} = \begin{bmatrix} 1.000015 \\ 10.347957 \end{bmatrix} \cdot \pi^2 \frac{EI}{\ell^2} \tag{1.408}$$

Finally, the estimated critical is obtained with great accuracy of $\approx 1/100000\%$! However, the estimate is still, mathematically speaking, from above! Now,

$$P_{cr} = 1.000015 \cdot \pi^2 \frac{EI}{\ell^2} > \underbrace{1 \cdot \pi^2 \frac{EI}{\ell^2}}_{\text{analytical}} \tag{1.409}$$

Displacement method - simply beam supported column

Here we mean that we use the weak form (extended Rayleigh quotient) or just virtual work principle (at the critical equilibrium) written in the form

$$\sum_{i=1}^n \left[\int_0^\ell \phi_i''(x) EI \phi_j''(x) dx - P \int_0^\ell \phi_i'(x) \cdot \phi_j'(x) dx \right] \cdot a_i = 0, \forall j = 1, 2, \dots, n \tag{1.410}$$

As in the previous example, the kinematically admissible displacement basis functions are

$$\phi_1 = \xi(1 - \xi), \tag{1.411}$$

$$\phi_2 = \xi^2(1 - \xi)^2, \tag{1.412}$$

as shown in Figure (1.85) After symbolic integrations, in Matlab¹⁸³ again, we obtain the critical condition

$$\det \left\{ \begin{bmatrix} 4 & 0 \\ 0 & 4/5 \end{bmatrix} - \frac{P\ell^2}{EI} \begin{bmatrix} 1/3 & 1/15 \\ 1/15 & 2/105 \end{bmatrix} \right\} = 0 \tag{1.413}$$

having the eigenvalues

$$P_{cr} = \begin{bmatrix} 1.000056 \\ 17.23725 \end{bmatrix} \cdot \pi^2 \frac{EI}{\ell^2} \tag{1.414}$$

¹⁸³I got, finally, my internet connection *on* for doing symbolically the boring part of integration.

The critical buckling load is now

$$P_{cr} = 1.00056 \cdot \pi^2 \frac{EI}{\ell^2} \quad (1.415)$$

is a clean and *rehellinen* estimate for the upper-bound.

I now stop this story here, and just provide for those that may be interested, the Matlab-script I used.

```

\
% Buckling simply supported column -----
% Djebar B. 2021
% MATLAB symbolic
% Timoshenko and Rayleigh quotients
% -----
% ----
syms EI L P
syms x
syms phi_1 phi_2
syms K K_DIS K_G K_T K

% Basis functions
phi_1(x, L) = ( x / L ) * ( 1 - x / L );
phi_2(x, L) = ( x / L ).^2 * ( 1 - x / L ).^2;
%% phi_2(x, L) = ( x / L ).^2 * ( 1 - (x / L).^2 );

% 1st derivatives of L_i, i = 1:3
d1_phi_1(x, L) = simplify( diff(phi_1, x) );
d1_phi_2(x, L) = simplify( diff(phi_2, x) );

% 2nd derivatives of L_i, i = 1:3
d2_phi_1(x, L) = simplify( diff(d1_phi_1, x) );
d2_phi_2(x, L) = simplify( diff(d1_phi_2, x) );

% Forming stiffness matrix K_T (Timoshenko)
% -----
% a) the force method (Timoshenko quotient)
K_11 = int(phi_1 .* phi_1, [0 L]);
K_12 = int(phi_1 .* phi_2, [0 L]);
K_21 = K_12;
K_22 = int(phi_2 .* phi_2, [0 L]);

K_T(L, EI) = [K_11 K_12;
K_21 K_22] / EI;

```



```

% --
% Forming stiffness matrix K (displcement method)
% -----
% a) the force method (Timoshenko quotient)
KD_11 = int(d2_phi_1 .* d2_phi_1, [0 L]);
KD_12 = int(d2_phi_1 .* d2_phi_2, [0 L]);
KD_21 = KD_12;
KD_22 = int(d2_phi_2 .* d2_phi_2, [0 L]);

K_DIS(L, EI) = [KD_11 KD_12;
KD_21 KD_22] * EI;

%-----
% Forming geoemtrical stiffness matrix K_G
% -----
KG_11 = int(d1_phi_1 .* d1_phi_1, [0 L]);
KG_12 = int(d1_phi_1 .* d1_phi_2, [0 L]);
KG_21 = KG_12;
KG_22 = int(d1_phi_2 .* d1_phi_2, [0 L]);

K_G(L, P) = [KG_11 KG_12;
KG_21 KG_22] /P;

% b) Rayleigh quotient
% -----
K_GR(L, P) = [KG_11 KG_12;
KG_21 KG_22] * P;

% -----
%% Numerical Eigenvalues: using matlab eig() -function
% -----
L = 1;
EI =1;
P = 1;
% a) Remeber in Timoshenko quotient we have (1/P) as critical --
KT_num = double( K_T(L, EI) );
KG_num = double( K_G(L, EI) );
LAMS = double( eig( double(K_T(L,EI)), double(K_G(L,EI))) )
[P_cr_num] = 1 ./ LAMS
P_cr_E_Timo= P_cr_num / pi^2
% -----

```

```

% b) Remember in Rayleigh quotient we have P as critical --
K_num = double( K_DIS(L, EI) );
KG_num = double( K_GR(L, EI) );
LAMS_R = double( eig( double(K_DIS(L,EI)), double(K_GR(L,EI))) )
[P_cr_num] = LAMS_R
P_cr_E_R= P_cr_num / pi^2
%-----

```

1.12.3 A continuous model of a pin-ended column under pulsating axial load

Even though this course deals only with static stability, I think that it is pedagogically a good reason, to introduce a simple problem of dynamic stability. This application example will demonstrate two things: 1) How to account for inertia effects 2) The universality of the principle of virtual work (VWP). The example treated is the same example that the one shown in Timoshenko's classical textbook of stability.¹⁸⁴ Timoshenko derives the equations of motion using local differential approach. In our example, we will use a different approach: the global approach as given by virtual work principle. The good news are that the VWP provides both i) the correct equations of motion and ii) the best way to solve these equations since the VWP is itself already the variational principle (= weak form) to be discretized. Nothing can be more efficient than that.¹⁸⁵

The virtual work principle for dynamics

Maybe the reader recall the principle of virtual power that we studied in previous master course in the course called *Mechanics of beams and frames* and which is funnily labelled CIV-E1020 as if it was a food additive E1020 to make more digestible to the students. The virtual power (or work) principle in its general

¹⁸⁴In Timoshenko: Section 2.22, p. 158: *Stability of prismatic bars under varying axial force*. The textbook: Timoshenko and Gere: *Theory of Elastic Stability*. 2nd Ed. 1985. Mc-Graw-Hill.

¹⁸⁵From my experience, I can say that it is worth (maksaa vaivan) to learn to use the virtual work principle (VWP). With time, student become more and more familiar with the VWP as they use it more and more. The VWP is in the beginning hard to grasp. The student should just start using it daily and keep using it till it becomes familiar. After this learning period, you can forget about it since it is then integrated in your hardware and becomes as for your school multiplication tables: your body knows them as you breathe but you don't know how you know them.

form looks like this:

$$\underbrace{- \int_{\Omega} \sigma : \delta(\nabla \mathbf{v}) \, d\Omega}_{\delta W_{\text{int}}} + \underbrace{\int_{\Omega} \mathbf{f} \cdot \delta \mathbf{v} \, d\Omega + \int_{\partial\Omega_t} \mathbf{t} \cdot \delta \mathbf{v} \, dS}_{\delta W_{\text{ext}}} = \underbrace{\int_{\Omega} \rho \ddot{\mathbf{u}} \cdot \delta \mathbf{v} \, d\Omega}_{\delta W_{\text{acc}}} \quad , \quad \forall \delta \mathbf{v} \tag{1.416}$$

and says, that in body in motion moves and deforms such the principle is not violated, at least for velocities less than speed of light and no nuclear reactions being involved. This principle is equivalent to what says Newtonian dynamics for deformable and undeformable bodies moving with non-relativistic velocities. The Newton's motion equations for deformable bodies are called *Cauchy's equations of motion*.¹⁸⁶

We will apply this universal principle (Eq. 1.416) to the dynamics of our column under pulsating centric axial loading. We just need to integrate all constant variables, generically h , within the cross-section A over the cross-section and obtain $\int_V h \, dV = \int_{\ell} h \cdot A \, dx$ and then obtain the readily virtual power principle for the column.

However, in this notes, we will use the virtual work principle (the static version), known to student from earlier courses, and add the additional term of the work of acceleration forces (inertia forces) using the d'Alembert principle. Maybe this approach will make the student more curious about mechanics. Let's take into account the inertia forces (= -acceleration forces)

$$\mathbf{f}_{\text{inertia}} = -\mathbf{f}_{\text{acc.}} = -m\ddot{\mathbf{u}} \tag{1.417}$$

according to the d'Alembert's principle in the virtual work of the inertia forces

$$\delta W_{\text{inertia}} = -\delta W_{\text{acc.}} = -\mathbf{f}_{\text{inertia}} \cdot \delta \mathbf{u} \tag{1.418}$$

and re-write the virtual work principle in a canonical form which holds for both statics¹⁸⁷ and dynamics.

$$\delta W_{\text{int}} + \delta W_{\text{ext}} - \delta W_{\text{acc.}} = 0, \quad \forall \delta \mathbf{u} \iff \implies \text{the equations of motion} \tag{1.419}$$

where \mathbf{u} being the displacement field. The virtual work principle says that it is equivalent with the equations of motion of a (deformable or not) body.

¹⁸⁶Cauchy's equations of motion: $\nabla \cdot \sigma + \rho \mathbf{f} = \rho \ddot{\mathbf{u}}$ and Newton's equation for a body $m\mathbf{a} = \mathbf{f}$, where the acceleration $a = \ddot{\mathbf{u}}$. We notice that these two motion equations are naturally, the same. The deformation of the body, for us engineers working with deformable bodies, results in cohesion forces $\mathbf{t} = \sigma \cdot \mathbf{n}$ applied at the boundaries that should be added to the resultant of external force \mathbf{f} . As you recall the surface force term $\int_S \mathbf{t} \, dS = \int_S \sigma \cdot \mathbf{n} \, dS$ when integrated over the surface, and thanks to Gauss, the king of mathematicians, can be transformed into an equivalent volume force term $\int_V \nabla \cdot \sigma \, dV$. If you get interested, consult textbooks on *continuum mechanics*.

¹⁸⁷In statics, all accelerations are zero.

Now we will apply this principle for the column under pulsating axial load to derive the equations of motion and then to study the dynamic stability of the system.

We consider a *slender* pin-ended elastic column under a pulsating centric load (Fig. 1.87)

$$P(t) = P_0 + S \cdot \cos(\Omega t) \quad (1.420)$$

where P_0 is the constant part (positive or negative) of the axial load and S the maximum amplitude of the harmonic change (with $0 < \eta = S/P_0 < 1$). The circular frequency of the excitation being Ω . The column of the example is slender and we consider transverse vibrations only and ignore, in this application, the effect of axial deformations.¹⁸⁸ For a short column, the axial vibration (or wave propagations) are surely dominant over the flexural vibrational modes.

Natural frequency for transversal free vibrations

What we want to investigate? We are interested in finding how the first natural angular frequency ω of the loaded slender column depends on the excitation angular frequency Ω and the relative amplitude S/P_0 of the pulsating axial load $P(t)$. For the moment we ignore the effect of damping.

Let's approximate the transversal free vibration v using the first mode

$$v(x, t) = \underbrace{v_0 \sin(\pi x / \ell)}_{\text{first mode}} \cdot \underbrace{\sin(\omega t + \phi)}_{\text{harmonic evolution}} \quad (1.421)$$

where the free vibrations are assumed harmonic and the phase angle being ϕ and v_0 the mode amplitude.

¹⁸⁸Note that both deformation modes - axial and transverse, as for instance, in a tensioned cable of a stay-bridge, can be present at the same time during parametric excitation of such cable. In such excitation, one end of the cable have a forced periodic motion of relatively small amplitude and of given frequency content. The dynamic stability behaviour of such cable is critical. For example, a frequency Ω of the excitation such that $\Omega = 2\omega$, leads to instability and enhances violently the transverse vibration even when the end-motion while exiting remains relatively small. Such dynamics is very complex (=rich) because the natural frequency ω of the tensioned cable depends on the tension, and the tension is varying as a result of the end-periodic motion and the large transversal vibrations. Increase of tension increases this frequency, while decrease of tension, decreases it. Structurally, the design is very demanding because such vibrations leads to fatigue of the cable and of the cable-anchoring or supports. If someone get interested ask Dr. Risto Kiviluoma our specialist of bridges in Finland.

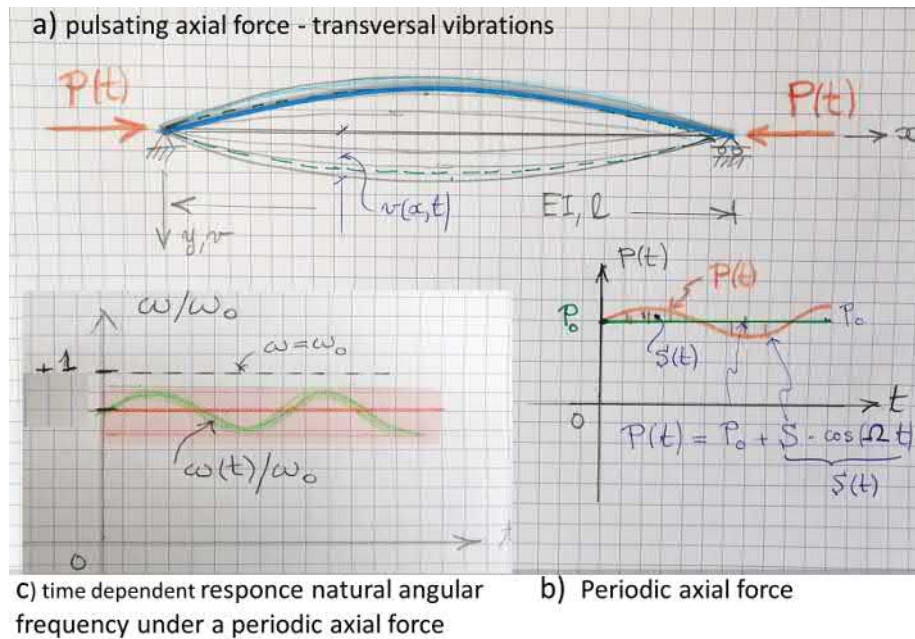


Figure 1.87: Simply supported elastic and slender column under axial pulsating load.

Before going to the total virtual work, we need next derivatives

$$v'(x, t) = \left[\frac{\pi}{l} \right] \cdot v_0 \cos(\pi x/l) \cdot \sin(\omega t + \phi), \quad (1.422)$$

$$v''(x, t) = - \left[\frac{\pi}{l} \right]^2 \cdot v_0 \sin(\pi x/l) \cdot \sin(\omega t + \phi), \quad \text{and} \quad (1.423)$$

$$\ddot{v}(x, t) = - \omega^2 \cdot v_0 \sin(\pi x/l) \cdot \sin(\omega t + \phi). \quad (1.424)$$

The variations of the generalised displacements are naturally spatial variations only. They are independent of time. Consequently, the virtual displacement δv and virtual rotation $\delta v'$ are, natürlich,

$$\delta v(x) = \delta v_0 \cdot \sin(\pi x/l), \quad (1.425)$$

$$\delta v'(x) = \left[\frac{\pi}{l} \right] \cdot \delta v_0 \cdot \cos(\pi x/l) \quad (1.426)$$

The virtual work contributions are:

$$\delta(\Delta W_{\text{int}}) = - \int_0^l v'' EI \cdot \delta v'' dx = \quad (1.427)$$

$$= - EI \left[\frac{\pi}{l} \right]^4 \int_0^l \sin^2 \left(\frac{\pi x}{l} \right) dx \cdot v_0 \cdot \delta v_0 \cdot \sin(\omega t + \phi) \quad (1.428)$$

$$= - EI \left[\frac{\pi}{l} \right]^4 \cdot \frac{l}{2} \cdot v_0 \cdot \delta v_0 \cdot \sin(\omega t + \phi) \quad (1.429)$$

$$\delta(\Delta W_{\text{ext}}) = P(t) \int_0^\ell v' \cdot \delta v' dx = \quad (1.430)$$

$$= P(t) \left[\frac{\pi}{\ell} \right]^2 \int_0^\ell \cos^2 \left(\frac{\pi x}{\ell} \right) dx \cdot v_0 \cdot \delta v_0 \cdot \sin(\omega t + \phi) \quad (1.431)$$

$$= P(t) \left[\frac{\pi}{\ell} \right]^2 \cdot \frac{\ell}{2} \cdot v_0 \cdot \delta v_0 \cdot \sin(\omega t + \phi) \quad (1.432)$$

$$\delta(\Delta W_{\text{acc}}) = \int_0^\ell \rho A \ddot{v} \cdot \delta v dx = \quad (1.433)$$

$$= -\rho A \omega^2 \int_0^\ell \sin^2 \left(\frac{\pi x}{\ell} \right) dx \cdot v_0 \cdot \delta v_0 \cdot \sin(\omega t + \phi) \quad (1.434)$$

$$= -\rho A \omega^2 \cdot \frac{\ell}{2} \cdot v_0 \cdot \delta v_0 \cdot \sin(\omega t + \phi) \quad (1.435)$$

Finally,

$$\delta W_{\text{int}} + \delta W_{\text{ext}} - \delta W_{\text{acc}} = 0, \forall \delta v \quad (1.436)$$

$$\implies EI \left[\frac{\pi}{\ell} \right]^4 - P_0 [1 + S/P_0 \cdot \cos(\Omega t)] \left[\frac{\pi}{\ell} \right]^2 - \rho A \omega^2 = 0 \quad (1.437)$$

The above equation provides the natural frequency ω of the lateral free vibrations under pulsating axial load. The first thing to notice is that this frequency $\omega = \omega(t)$ depends on time t . To take all the juice from this result, we study three cases:

1. **Buckling under static axial load:** $S = 0$, $P_0 \neq 0$ and $\omega = 0$. This is a simple static buckling situation with Euler critical load P_E given by

$$\implies P_E = EI [\pi/\ell]^2 \quad (1.438)$$

2. **Free lateral vibrations under static axial load:** $S = 0$, $P_0 \neq 0$ and $\omega \neq 0$.

$$\rho A \omega^2 = EI \left[\frac{\pi}{\ell} \right]^4 - P_0 \left[\frac{\pi}{\ell} \right]^2 \equiv \rho A \omega_0^2 \quad (1.439)$$

$$\implies \omega_0^2 = \frac{EI}{\rho A} \left[\frac{\pi}{\ell} \right]^4 \left(1 - \frac{P_0}{P_E} \right) \quad (1.440)$$

3. **Harmonically excited vibrations under pulsating axial load:** $S \neq 0$, $P_0 \neq 0$ and $\omega \neq 0$. The response angular frequency now depends

periodically on time; $\omega = \omega(t)$

$$\rho A \omega^2 = EI \left[\frac{\pi}{\ell} \right]^4 - [P_0 + S \cdot \cos(\Omega t)] \left[\frac{\pi}{\ell} \right]^2 \quad (1.441)$$

$$\rho A \omega^2 = \underbrace{\rho A \omega_0^2 - S \cos(\Omega t) \left[\frac{\pi}{\ell} \right]^2}_{\text{time varying}} \quad (1.442)$$

$$\rho A \omega^2(t) = \rho A \omega_0^2 \cdot \underbrace{\left(1 - \frac{P_0}{P_E} \left[1 + \frac{S}{P_0} \cos(\Omega t) \right] \right)}_{f(\Omega t) \text{ -time modulation}} \quad (1.443)$$

This time dependency of the response angular natural frequency (Eq. 1.443) is shown generically in Figure 1.87 c). It is this non-linear and time-dependent coupling of the natural response frequency ω with the excitation frequency Ω that give an incredible richness of dynamical ranges for the physical structure. Figure (1.88) shows such behaviour for a cable under periodically changing tension induced by parametric vertical excitation of the free-end.¹⁸⁹

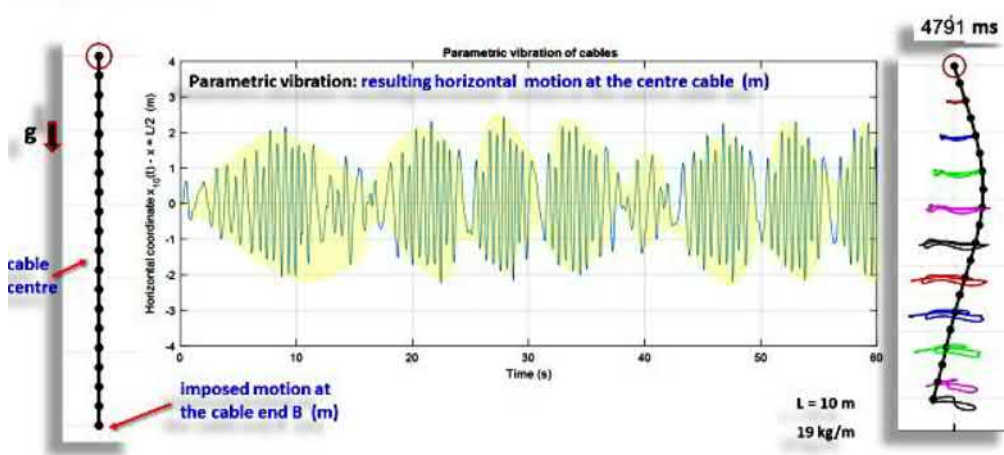


Figure 1.88: Parametric vibrations of vertical hanging cable (10 m long). The free end of the cable is given a small amplitude of vertical parametric excitation. The graph represents the transversal displacements at the middle span of the cable. The cable is not initially pre-stressed. The vertical parametric motion induces time-changing axial force $T(t)$. The natural response frequency is beating (yellow shading) with time similarly like for our column as in equation 1.443).

¹⁸⁹Ref. My own research work.

Timoshenko¹⁹⁰ studied the dynamical stability of the same example here. They derived the equations for the natural frequency ω by considering the equation of motion starting from the differential approach. They studied the dynamic stability behaviour and found that the amplitude of lateral (flexural) vibrations can grow in violent way for a set values-combinations of the non-dimensional system characteristic parameters $s = S/P_0$, $p = P_0/P_E$, ω_0/Ω . This violent lateral vibration response correspond to dynamic loss of stability. Using the reduced set of (driving or control) parameters

$$a = \frac{\omega_0^2}{\Omega^2} \cdot (1 - p), \quad b = \frac{\omega_0^2}{\Omega^2} \cdot s \quad (1.444)$$

Timoshenko determined, by probably solving numerically the corresponding equation of motion, the *regions of stability* in the phase-plane $a - b$ (Fig. 2-72 of the reference). When solving numerically the equations of motion, for a fixed numerical value of the parameters a and b , one can obtain solutions (time evolutions) which will diverge with time (the amplitude keeps growing). Then these specific 'points' correspond to unstable regions on the plot $a - b$. If on the contrary, the solution keep bounded in time, then, we found a point (a, b) which correspond to stable behaviour. By varying a and b within physically possible values, one obtains the full phase-plane with stability and instability regions determined. One result may be to keep in mind is that first dynamic instability is reached when the excitation frequency Ω is $\sqrt{\text{twice}}$ the natural frequency ω_0

$$\Omega = \sqrt{2} \cdot \omega_0 \quad \text{even for very small amplitudes } s = S/P_0 \ll 1 \quad (1.445)$$

Thus violent transversal vibrations with large amplitudes occurs under the above conditions even for small amplitudes of axial force variations (unshaded regions in Figure (1.89). The stability regions correspond to the shaded regions (Fig. 1.89). It is interesting to notice, for instance, that stability behaviour can also change for a constant $a = \text{const.}$, let's say, we fix the value $\Omega_0^2/\omega^2 \neq 2$ not corresponding to frequency resonance, but we make changes only in the relative amplitude s of the axial load along the line b . *Thus, dynamic stability can also be lost even for a discontinuous range of relative amplitudes s of the axial pulsating load.*

A word about parametric excitation of stay cables

The following example, partly from my research work¹⁹¹, is meant to wake-up curiosity of the students toward structural dynamics, in particular and to show,

¹⁹⁰Timoshenko & Gere. In: *Theory of elastic stability*, section 2.22, p. 158 *Stability of prismatic bars under varying axial force.*

¹⁹¹The equations of motion we have been using in this example were derived using the virtual work principles keeping displacements and rotation large (= keeping the $\sin \theta$ and $\cos \theta$ as they are, not expanding them into Taylor series).. Naturally, we have also dissipation (damping) which is accounted for, as in real structures.

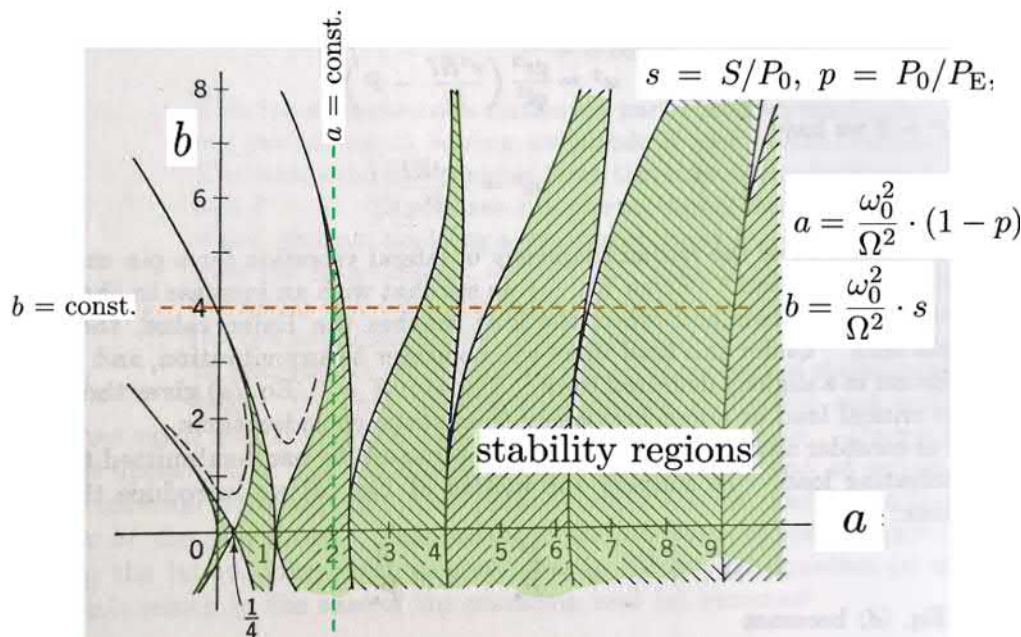


Figure 1.89: Regions of stability in the parameter space $a - b$. (Figure adapted from Timoshenko & Gere. Theory of elastic Stability.)

than once we jump from the frozen static world of quite equilibria to the rich world of dynamics, we discover a full new exciting world full of challenging key important practical questions for structural analyst and designer.

The above result (1.445) is quite similar to the case of parametric excitation of tensioned cables (stay cables of towers or stayed bridges). In the parametric excitation, one end of the pre-tensioned cable is given periodic motion (frequency Ω) of small amplitude around the equilibrium position. The initial tension of the cable being T_0 and give a natural angular frequency of transverse vibrations ω_0 . The resonance condition for this cable are the same than for the column under pulsating load ($\Omega = 2\omega_0$). The parametric excitation in the cables occurs at one or both supports or connections. One support to the pylon and the other support is to the deck. The pylon can vibrate transversally under wind effects. The deck can be also have vibrations due to wind and from the traffic motion. It is this periodic small amplitude vibrations (motion) of the support that is called parametric excitation. Such excitation may lead to catastrophic resonance (1.90) when¹⁹²

$$\Omega = \{1/2, 1, 2\} \cdot \omega_0. \tag{1.446}$$

¹⁹²V. Denoel & H. Degée Liège. *Comparison of parametric excitation and excitation of an elastic stay cable*. 7th European conference on structural dynamics, EUROLYN 2018, 7-9 July. Southampton.

Another problem is the material fatigue at the connections or in the cables. To know more on the subject, please consult Dr. R. Kiviluoma, the local specialist of bridges. The dynamic simulation shown in Figure (1.90) the connecting end

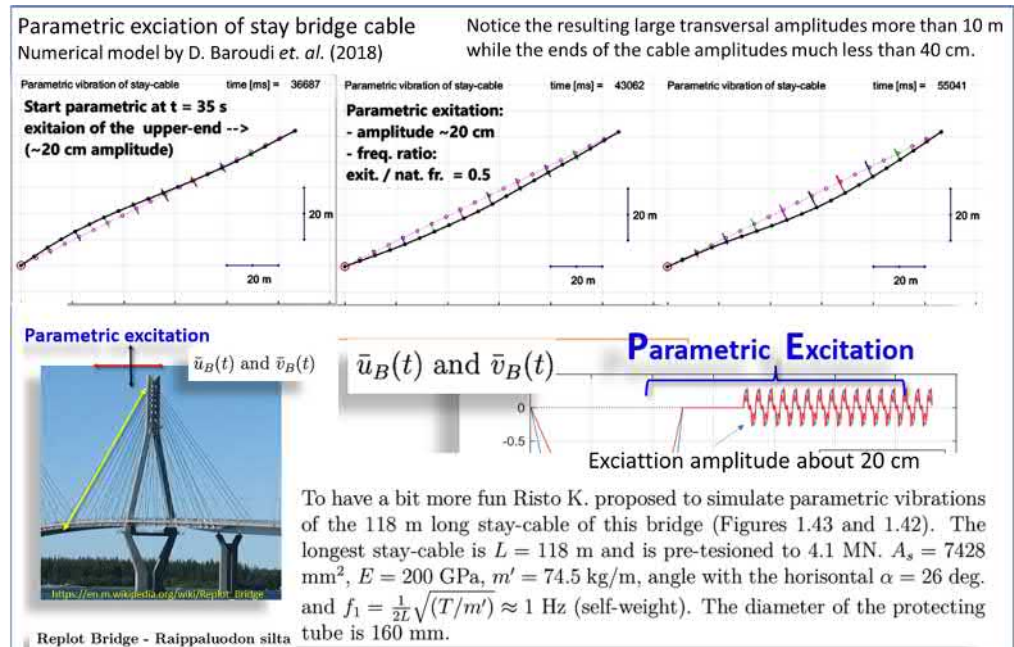


Figure 1.90: Parametric excitation of a stay cable - numerical simulation.

of the stay pre-tensioned cable was parametrically excited in both horizontal and vertical directions. The amplitude of such motion was about 20 cm and the excitation frequency such that $\Omega/\omega_0 = 1/2$.¹⁹³ Despite this relatively small amplitude (≈ 20 cm), the cable gets violent huge transversal amplitudes reaching even 10 m, due to parametric resonance.

1.12.4 PAASIN TANNE 11 MARS 2021

1.12.5 Loss of stability of a rotating axis

Consider a cantilever slender elastic beam which is rotating with constant angular velocity ω about its length-axis (Fig. 1.91). In this section we consider only the cases where the displacements v affect only the magnitude of the forces acting on the moving axis mass-element dm . The forces meant here are the centrifuge forces $df_c(x) = dm\omega^2v(x)$. The cases where the displacements affect also the

¹⁹³D. Baroudi, R. Kiviluoma, R. Kouhia, J. Paavola & L. Salokangas. Finnish XIII - Mechanics days, 2018.

direction of the loading are not considered here ¹⁹⁴.

One interesting design and operational question is to estimate what will be the lowest critical angular velocity ω to ensure that the beam will not loss its stability (buckles)? Here the transverse perturbation can be for instance, the shape imperfection (non-uniform mass distribution) around the centre of of gravity of the cross-section. Such mass eccentricity results in tiny centrifuge forces which are enough to perturb the initial straight configuration and leads motion into the neighbouring bended state (=buckling). In addition,in this example, we assume that neither torsional vibrational modes nor bending vibrational modes of the axis being excited. The cross-section of the beam is circular. The only effect of the tiny perturbation is to drive the rotating axis into a *bent mode* without flexural vibrations. This example is treated in the reference already cited¹⁹⁵ The analysis method we use now, the energy approach, is completely different from the approach used in the cited reference.

In this application consider cases where centrifuge forces are much greater than gravity forces. So, we neglect these last ones. It is straightforward to account for them when needed, just include their virtual work $\delta(\Delta W_{ext})$ into the total virtual work.

We use the virtual work principle

$$\delta(\Delta W_{int}) + \delta(\Delta W_{ext}) = \delta(\Delta W_{acc.}), \quad \forall \delta \mathbf{v}. \quad (1.447)$$

where, $\delta(\Delta W_{acc.})$ being the virtual work of acceleration forces (= minus virtual work of inertia forces). Note that the trajectories described by any material points x , during rotation of the axis, are circles. Therefore, the acceleration \vec{a} are directed toward the centres of these circles which are located on the longitudinal axis of the beam itself (Figs. 1.91 and 1.92). The acceleration is

$$\vec{a} = -\omega^2 \cdot \vec{v}(x). \quad (1.448)$$

Consequently, the acceleration force f_{acc} of a mass element dm (or end-mass m) is given by

$$d\vec{f}_{acc} = -d\vec{f}_c = -dm \cdot \omega^2 \vec{v}(x) = -\rho A \omega^2 \cdot \vec{v}(x) dx, \quad \text{distributed mass} \quad (1.449)$$

$$\vec{f}_{acc} = -\vec{f}_c = -m\omega^2 \cdot \vec{v}(\ell), \quad \text{end-mass} \quad (1.450)$$

The virtual work of the acceleration forces are then

$$\delta(\Delta W_{acc}) = \int_0^\ell \vec{f}_{acc} \cdot \delta \vec{v} dx = - \int_0^\ell \rho A \omega^2 v \delta v dx, \quad (\text{distributed mass}) \quad (1.451)$$

$$= - m\omega^2 v(\ell) \delta v(\ell), \quad (\text{end-mass}) \quad (1.452)$$

¹⁹⁴See section 3: Dependence of the loading magnitude upon the displacements. In: *Stability and oscillations of elastic systems* - Paradoxes, fallacies and new concepts. By Yakov Gilevich Panovko & Iskra Ivanovna Gubanova. (translated from Russian). Consultants Bureau, New York, 1965.

¹⁹⁵See: section 3 in: Yakov Gilevich Panovko & Iskra Ivanovna Gubanova.

Loss of stability of a rotating axis

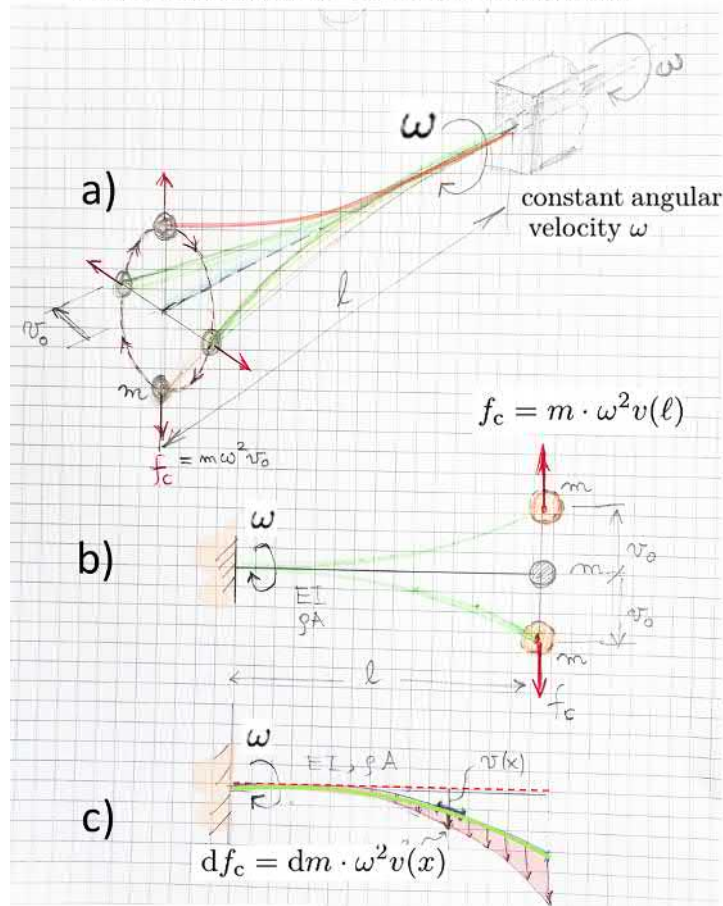


Figure 1.91: Dynamic stability loss of a rotating slender axis. The force f_c is the centrifuge force. The acceleration force is $f_{acc} = -f_c$.

The virtual work of internal force is

$$\delta(\Delta W_{int}) = - \int_0^\ell M \cdot \delta\kappa \, dx = - \int_0^\ell EI v'' \cdot \delta v'' \, dx. \tag{1.453}$$

when considering only bending. As we told previously, the virtual work of external forces $\delta(\Delta W_{ext}) \approx 0$ is assumed, again, without loss of generality (WLOG), negligible.

As we are¹⁹⁶, at least I am, interested in obtaining estimates for the critical

¹⁹⁶The student can solve this problem analytically and compare to the approximations obtained in this subsection.

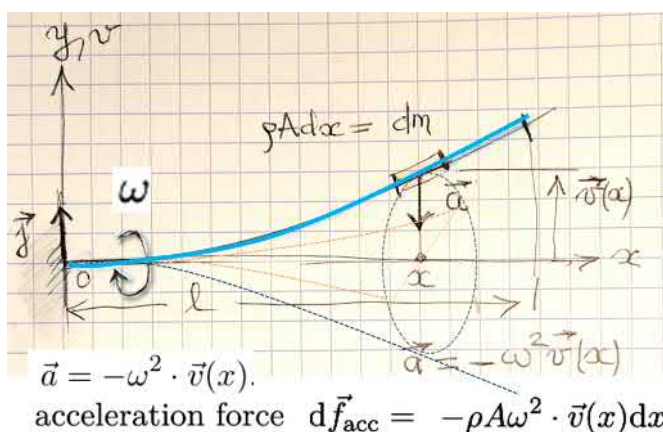


Figure 1.92: Acceleration and acceleration forces in a rotating beam. the rotation occurs around the beam axis x (see also Fig. 1.91).

rotation angular velocity ω_{cr} , we will use approximated buckling modes

$$v(x) \approx v_0 / \ell^2 \cdot x^2 \quad (1.454)$$

$$v(x) \approx v_0 \cdot [1 - \cos\left(\frac{\pi x}{2\ell}\right)] \quad (1.455)$$

which are kinematically admissible.

To say that the perturbed bent configuration (or motion) is in dynamical equilibrium is equivalent to say that the total virtual work vanishes for any perturbation of the post-buckled¹⁹⁷ configuration δv .

Let's take the mode approximation (Eq. 1.455) and do the integrations:

$$\delta(\Delta W_{\text{int}}) = - \int_0^\ell v'' EI \cdot \delta v'' dx = \quad (1.456)$$

$$= - \left(\frac{\pi}{2\ell}\right)^4 EI \int_0^\ell \cos^2\left(\frac{\pi x}{2\ell}\right) dx \cdot v_0 \cdot \delta v_0 \quad (1.457)$$

$$= - \left(\frac{\pi}{2\ell}\right)^4 EI \cdot \frac{\ell}{2} \cdot v_0 \cdot \delta v_0 \quad (1.458)$$

¹⁹⁷It is very important, for understanding, to notice that we are testing the *nature of dynamic equilibrium of the perturbed configuration* and not the equilibrium of the initial pre-buckled configuration. This last one is already in primary equilibrium. That is why it the tiny buckled configuration v which is perturbed by δv to find out if it is a possible other equilibrium configuration. If yes, then system moves from its initial (dynamic) equilibrium to the bended (buckled) neighbouring one, under tiny perturbations (Fig. 1.93). This motion is the one associated with loss of stability.

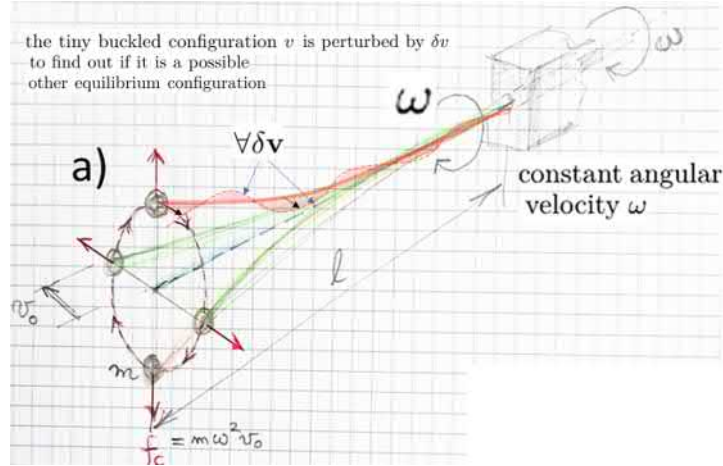


Figure 1.93: Testing for stability loss. Is the post-buckled configuration an dynamic equilibrium configuration?

$$\delta(\Delta W_{\text{acc}}) = - \int_0^\ell \rho A \omega^2 v \cdot \delta v dx = \quad (1.459)$$

$$= - \rho A \omega^2 \int_0^\ell [1 - \cos\left(\frac{\pi x}{2\ell}\right)]^2 dx \cdot v_0 \cdot \delta v_0 \quad (1.460)$$

$$\approx - 0.2267 \rho A \omega^2 \cdot \ell \cdot v_0 \cdot \delta v_0 \quad (1.461)$$

The virtual total work should vanish, for any δv , therefore

$$\delta(\Delta W_{\text{int}}) - \delta(\Delta W_{\text{acc}}) = 0 \implies \underbrace{\left[-\frac{1}{2} \left(\frac{\pi}{2\ell}\right)^4 EI + 0.2267 \rho A \omega^2\right] \ell}_{=0 \implies \omega_{\text{cr}} = \dots} \cdot \underbrace{v_0}_{\neq 0} \cdot \underbrace{\delta v_0}_{\forall \delta v_0} = 0 \quad (1.462)$$

and consequently, the critical

$$\omega_{\text{cr}} \approx \underbrace{0.371 \left(\frac{\pi}{\ell}\right)^2 \sqrt{\frac{EI}{\rho A}}}_{\text{using approximated mode}} > \underbrace{0.356 \left(\frac{\pi}{\ell}\right)^2 \sqrt{\frac{EI}{\rho A}}}_{\text{analytical, ref. Panovko \& Gubanova}} \quad (1.463)$$

The critical angular velocity given by equation (1.463) is equal to the first natural angular frequency ω_B of flexural free vibrations mode. This result is interesting. Physically speaking this makes sense. Under constant imposed angular velocity ω for the axis, the cantilever start to bend because of existence of tiny transversal perturbations (non-equilibrated mass distribution, for instance). I let this conclusion to reader to check.

Explanation: Why $\omega_{\text{cr}} = \omega_B$? Consider now the same cantilever in pure flexural free vibrations with no angular rotations of the axis. Only bending in the same

vertical plane. Let's find out, using the virtual work principle what will be the natural frequency ω_B of free flexural vibrations (for the first mode). Let's take the the same mode approximation of deflection first mode

$$v(x, t) \approx v_0[1 - \cos(\pi x/(2\ell))] \cdot \sin(\omega_B t + \phi) \quad (1.464)$$

and add the harmonic time dependency. The virtual work of internal forces will remain the 'same' as given by Equations (1.456 and (1.458). The

$$\delta(\Delta W_{\text{int}}) = - \int_0^\ell v'' EI \cdot \delta v'' dx = \quad (1.465)$$

$$= - \left(\frac{\pi}{2\ell}\right)^4 EI \int_0^\ell \cos^2\left(\frac{\pi x}{2\ell}\right) dx \cdot v_0 \cdot \delta v_0 \cdot \sin(\omega_B t + \phi) \quad (1.466)$$

$$= - \left(\frac{\pi}{2\ell}\right)^4 EI \cdot \frac{\ell}{2} \cdot v_0 \cdot \delta v_0 \cdot \sin(\omega_B t + \phi) \quad (1.467)$$

Notice that

$$\delta v(x, t) = \delta v_0[1 - \cos(\pi x/(2\ell))] \cdot \sin(\omega_B t + \phi), \quad \text{time } t \text{ is not varied} \quad (1.468)$$

The virtual work of acceleration forces is now

$$\delta(\Delta W_{\text{acc}}) = \int_0^\ell \rho A \ddot{v} \cdot \delta v dx = \quad (1.469)$$

$$= \int_0^\ell \rho A (-\omega_B^2) [1 - \cos(\pi x/(2\ell))]^2 dx \cdot v_0 \cdot \delta v_0 \cdot \sin(\omega_B t + \phi) \quad (1.470)$$

$$= - \rho A \omega_B^2 \underbrace{\int_0^\ell [1 - \cos(\pi x/(2\ell))]^2 dx}_{\approx 0.2267} \cdot v_0 \cdot \delta v_0 \cdot \sin(\omega_B t + \phi) \quad (1.471)$$

Therefore

$$\delta(\Delta W_{\text{int}}) - \delta(\Delta W_{\text{acc}}) = 0 \implies \omega_B \approx 0.371 \left(\frac{\pi}{\ell}\right)^2 \sqrt{\frac{EI}{\rho A}}, \quad (1.472)$$

which gives the approximation for the natural angular frequency ω_B for free flexural vibrations which is equal to the critical angular imposed rotation of the cantilever axis ω . For me, this make sense, even it *resonates*.

1.12.6 Mechanical discrete models

Im the following a a general physical-type discretization method (or equivalently, mechanical discretization) is presented through an example of static buckling of a column. The example is treated first as a dynamic problem to show the reader

the universality of an elegant and powerful approach based on the *principle of virtual work*¹⁹⁸:

$$\delta W_{int} + \delta W_{ext} = \delta W_{acc.}, \forall \delta \mathbf{v}. \quad (1.473)$$

where, $\delta W_{acc.}$ being the virtual work of acceleration forces. The remaining terms should be familiar from statics. The basic idea is to approximate the continuous system with an equivalent discrete system formed by linking rigid bars with concentrated masses with rotational joints having rotational stiffness. The rigidity of the bars can be released by allowing them to behave like stretching springs. In addition, to elasticity dissipative behaviour can be easily accounted for by adding non-linear dissipative rotational and axial springs. The concentrated masses at nodes account for the inertia of the structure by these lumped masses.

A discrete model of a pin-ended column

The example we will consider here is linear elastic.¹⁹⁹ In addition we assume that the distributed mass of the beam being lumped at nodes. For the moment, we ignore stretching of the bars. In this example, the axial load P is assumed constant²⁰⁰ Assume we use for discrete elements to approximate the continuous

¹⁹⁸The acceleration forces $f_{i,acc} = -f_i a_i$, where the acceleration $a = \ddot{u}$, are accounted for by the d'Alembert principle. This principle is not just moving acceleration terms to the other side of the motion equation and changing its sign.

¹⁹⁹Despite this simplification, the virtual work principle holds for any type of systems (conservative or not) and for any kind of non-linearities when present. The simplifying assumption, in this example, are done to obtain a model that is tractable by hand. Otherwise, it leads to a non-linear initial value problem where numerical integration will be needed. Being without saying, that the integration scheme should be implicit and appropriate for stiff-equations, and of low order. This type terminology will be clear when you start to work with such problems.

²⁰⁰For non-constant arbitrarily changing force $P = P(t)$ there is no problem to account for it in the virtual work of external forces $\delta W_{ext}(P) = P(t) \cdot \delta u(\ell, t)$. In addition, to obtain a physically realistic model, one should release the axial compressibility constraint and allow for axial deformation to work $\delta W_{int}(N) = \int_{\ell} N \delta \epsilon dx$. Otherwise, one cannot capture axial vibrations or waves. For the special case of pulsating axial force (compression/tension) like, for instance, $P(t) = P_0 + S \cos(\Omega t)$, where S is a small variable change around the mean value P_0 , please consult Timoshenko, section 2.22, p. 158: *Stability of prismatic bars under varying axial force* of the Timoshenko's stability textbook referenced many times already here. This last case is a nice problem of dynamic stability where the amplitude of lateral (flexural) vibrations can grow in violent way for some excitation frequencies (resonance). The student can do the same-type of experiment with a string in pulsating tension. He will find that for a certain excitation frequency, the lateral vibration of the string becomes large and violent. (note that dynamics describing both behaviours of pulsating compression and tension are the same; one is obtained from the other problem essentially by multiplying by -1 .) These problems are practically the same as the problem of *parametric excitation* in which one end of the tensioned (or compressed) structure or member is given a periodic motion about some average position. An example of such structural element can be the tensioned stay-cable fixed to the

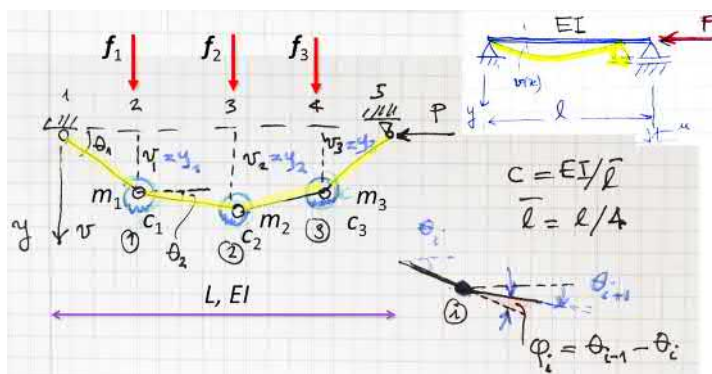


Figure 1.94: Physical discrete model. The column of length ℓ is axially compressed column with a point load P and a total mass $M = \sum m_i$ with the bending rigidity EI .

column (Fig. 1.94) using four rigid bars ($N = 4$ of equal length $\ell_i = \ell/4 \equiv \bar{\ell}$. The discrete rotational springs should have spring coefficient

$$c_i = EI/\ell_i, \quad \ell_i = \ell/4 \equiv \bar{\ell} \quad (1.474)$$

in order for the strain energy to be conserved. The lumped masses should be

$$M = \sum_i^n m_i, \quad \text{where } m_i = \rho A_i \ell_i, \quad \ell_i = \ell/4 \quad (1.475)$$

in order to conserve the mass M of the column. Let's, for simplicity in this example, assume the discrete bars to be rigid. This way of constructing a mechanical discrete model is sometimes called, Hencky-type physical discretization. It should be understood here that the model is mathematical even we sometimes specks of physical discretization. When a true physical model is dealt with, it will be reminded.

Note dear reader, that the following equations hold for any number of degrees of freedom, and are such general. For simplicity, I derive them, together with you, for few degrees of freedom (here three) and assuming, without loss of generality, moderate rotations. This last assumption can be released. Sometimes, it is more clearer to go from simplified example and generalise the result than to cover the opposite path. Sometimes, the reader can be bored by so much conceptual and general approach before reaching the goal. Sometimes, on the contrary, we prefer the general conceptual approach to catch the *map* before travelling in details.

pylon by one end when the other is fixed to the deck (of a stayed cable bridge). One of the fixation, under effect of wing or traffic is excited periodically. Under determined conditions (resonance), such vibrations can get amplified dramatically in a dangerous manner even when the amplitude of the motion of the fixation remains relatively small.

The discrete kinematics

Let's define the kinematics we need for writing the needed expressions for the virtual work. For simplicity, I mean that we will obtain a result that can be solved by hand, in order to distinguish the *tree* from the *forest*, we assume small displacements and moderate rotations.²⁰¹

We chose the independent coordinates

$$\mathbf{y} = \begin{bmatrix} y_1 \\ y_2 \\ y_3 \end{bmatrix} \quad (1.476)$$

as Lagrangian coordinates²⁰². It is worth to note that we do not assume any symmetry because one do not know, *in general* what mode is critical (comes first); symmetric? antisymmetric? So, we let sir Newton tell us through the motion equations (1.473). Note that the nodes are enumerated from $j = 1 : 4$ (the first ($j = 0$) and the last nodes ($j = 4$) are *a priori*²⁰³ dropped from the equations to account for the kinematic boundary conditions $y_0 = 0$ and $y_4 = 0$). Consequently, the slopes, within the moderate rotation hypothesis, θ_i of the bars $i = 1 : 4$ are

$$\theta = \begin{bmatrix} \theta_1 \\ \theta_2 \\ \theta_3 \\ \theta_4 \end{bmatrix} = \begin{bmatrix} (y_1 - y_0)/\ell_1 \\ (y_2 - y_1)/\ell_1 \\ (y_3 - y_2)/\ell_2 \\ (y_4 - y_3)/\ell_3 \end{bmatrix} = \begin{bmatrix} y_1/\ell_1 \\ (y_2 - y_1)/\ell_1 \\ (y_3 - y_2)/\ell_2 \\ -y_3/\ell_3 \end{bmatrix} \quad (1.477)$$

Discrete curvature: Now we will define the discrete equivalent for the curvatures at nodes as the relative difference in rotation of two consecutive bars i and $i + 1$ at node i as $\phi_i = \theta_{i-1} - \theta_i$. This will be the deformation rotation on which the internal moment M_i will work. Note that we have now three of such nodes (Fig. 1.94). So,

$$\phi = \begin{bmatrix} \phi_1 \\ \phi_2 \\ \phi_3 \end{bmatrix} = \begin{bmatrix} \theta_1 - \theta_2 \\ \theta_2 - \theta_3 \\ \theta_3 - \theta_4 \end{bmatrix} = \frac{1}{\ell} \begin{bmatrix} 2 & -1 & 0 \\ -1 & 2 & -1 \\ 0 & -1 & 2 \end{bmatrix} \begin{bmatrix} y_1 \\ y_2 \\ y_3 \end{bmatrix} \equiv \mathbf{R} \cdot \mathbf{y} \quad (1.478)$$

Note the analogy in the discrete *curvature*, in matrix \mathbf{R} , with the finite difference formula (molecule) of the second derivative $\propto [-1 \ 2 \ -1]$. Recall that the change

²⁰¹This assumption when released, leads to a geometrically non-linear equations of motion in the form of a non-linear ODE-set. It is of great simplicity to time-integrate them implicitly with some stable schemes. I will provide, later, an example when considering dynamic instability of a stay-cable in cable bridges which is a *parametrically excited*.

²⁰²In case of compressibility, one adds x_i to the set of coordinates. In three-D, just add z_i , also, and our freind Reijo K. will be pleased.

²⁰³We can also account for these boundary conditions at the end, after assembling all the equations. For hand calculation purposes, I drop the at the start to get a smaller set of equations.

ϕ in the slope θ corresponds, in the small displacement approximations, to the second derivative y'' of the slope y' , where y being the deflection.

Shortening of the column: Here we mean the axial shortening $\Delta u(0)$ due to bending.²⁰⁴ This In the moderate rotation approximation we can write

$$\Delta u(0) = \sum_{i=1}^4 \Delta u^{(i)} = \sum_{i=1}^4 \ell_i (1 - \cos \theta_i) \approx \sum_{i=1}^4 \ell_i \cdot \frac{1}{2} \theta_i^2 \implies \quad (1.480)$$

$$\delta(\Delta u(0)) \approx \sum_{i=1}^4 \ell_i \cdot \theta_i \delta \theta_i \quad (1.481)$$

Note that when we use the approximation

$$\theta_i \approx \sin \theta_i = [y_{i+1} - y_i] / \ell_i, \quad (1.482)$$

we obtain finally, the needed variation of the total shortening on which the external axial loads will work, as

$$\delta(\Delta u(0)) \approx \sum_{i=0}^3 \delta[y_{i+1} - y_i] \cdot [y_{i+1} - y_i] / \ell_i = \quad (1.483)$$

$$= \delta(\mathbf{S} \cdot \mathbf{y})^T \cdot (\mathbf{S} \cdot \mathbf{y}) / \bar{\ell}, \quad (1.484)$$

where

$$\Delta \mathbf{y} \equiv \begin{bmatrix} y_1 \\ y_2 - y_1 \\ y_3 - y_2 \\ -y_3 \end{bmatrix} \equiv \mathbf{S}_{4 \times 3} \cdot \mathbf{y}_{3 \times 1} \quad (1.485)$$

and the geometric-type matrix \mathbf{S} being defined below in the scalar product $\sum_{i=0}^3 \delta[y_{i+1} - y_i] \cdot [y_{i+1} - y_i] / \ell_i = (\delta \Delta \mathbf{y})^T \Delta \mathbf{y} / \bar{\ell}$ in

$$\Delta \mathbf{y} = \underbrace{\begin{bmatrix} 1 & 0 & 0 \\ -1 & 1 & 0 \\ 0 & -1 & 1 \\ 0 & 0 & -1 \end{bmatrix}}_{\equiv \mathbf{S}} \begin{bmatrix} y_1 \\ y_2 \\ y_3 \end{bmatrix} \equiv \mathbf{S} \cdot \mathbf{y} \quad (1.486)$$

After this long kinematic trip, we can finally start writing the virtual work contributions δW_{int} , δW_{ext} δW_{acc} , respectively, from internal, external and acceleration forces to obtain the equations of motion. From these equations of motion

²⁰⁴Note that for the continuous case, for moderate rotations, we had

$$\Delta u(0) = \int_0^\ell \frac{1}{2} [v']^2 dx \quad (1.479)$$

we will determine 1) the buckling load for the static case (zero acceleration) and 2) the natural frequency of free-vibrations. I let to the curious student, to 3) integrate numerically, in Matlab using `ode` set functions, the equation of motion to determine completely, the dynamics.

The discrete equations of motion

Before even we start, let's recall an important thing: the concept of a stable equilibrium corresponding to a local minimum of the total potential energy change, holds only for conservative systems. Question: What to do when one of us, faces one day or another, a dissipative system? Answer: *Call Isaac Newton*. The following dynamical approach, is versatile and holds also for non-conservative²⁰⁵ systems. This being said, let's start by deriving the equation of motion.

As you probably remember, the (scalar) principle of virtual work ($\delta W = 0$, $\forall \delta \vec{v}$, Eq. (1.473) and the equations of motion, $\vec{f} = m\vec{a}$, obtained by using Newtonian vectorial mechanics are equivalent and both are the two faces of the same coin. Our preference goes toward virtual work principle in deriving complex set of equation of motion. One of the reasons is that in this principle, the work couples or conjugates explicitly kinematics and kinetics what the Newtonian mechanics does not.

Let's stop here philosophy and go to equations and start to gather all the contributions to the total virtual work done on the (close) system that represent the loaded column.

Virtual internal work: The work of internal bending moment is (the summation goes over all the nodes)

$$\delta W_{int} = - \sum_i M_i \delta \phi_i = - \sum_i (c_i \phi_i) \cdot \delta \phi_i = \quad (1.487)$$

$$= - \delta (\mathbf{R} \cdot \mathbf{y})^T \cdot \mathbf{c} \cdot (\mathbf{R} \cdot \mathbf{y}) = - \delta \mathbf{y}^T \underbrace{[\mathbf{R}^T \cdot \mathbf{c} \cdot \mathbf{R}]}_{\equiv \mathbf{K}} \mathbf{y} = \quad (1.488)$$

$$= - \delta \mathbf{y}^T \cdot \mathbf{K} \cdot \mathbf{y}. \quad (1.489)$$

²⁰⁵An example of such non-conservative system can be a cantilever column with an end-load remaining constant but always tangent to the slope of the cantilever. So, the applied load \vec{P} changes direction but not intensity. The question: what is the amplitude of the load leading the column to a dynamic instability like the flutter, for instance? This is a simple engineering problem. One should have the right tools to address it. Establishing the equation of motion is such universal tool. In addition, using the principle of virtual work for that, will give you a l-o-n-g advance as regard to your friends from mechanical engineering as you are anyway familiar, already, with Newtonian mechanics.

where \mathbf{K} being the stiffness matrix. The constitutive matrix for bending is simply

$$\mathbf{c} = \begin{bmatrix} c_1 & 0 & 0 \\ 0 & c_2 & 0 \\ 0 & 0 & c_3 \end{bmatrix} \quad (1.490)$$

and becomes $\mathbf{c} = \bar{c}\mathbf{I}$ for constant $c_i = \bar{c} = 4EI/\ell$ as in our example.

Virtual external work: As external forces, we have, in this example, transversal forces \mathbf{f} composed of nodal forces f_i at nodes i and the compressive force P at the roller support. We will compute separately their virtual work and sum them at the end as $\delta W_{ext} = \delta W_{ext}^{(f)} + \delta W_{ext}^{(P)}$ to have the total contribution. Note that the transversal forces may include the self-weight $m_i g$, where $m_i = \rho A_i \ell_i$ being the lumped mass at the considered node i .

External transversal forces: The work of external forces cannot be simpler than

$$\delta W_{ext}^{(f)} = - \sum_i f_i \delta y_i = \delta \mathbf{y}^T \cdot \mathbf{f} \quad (1.491)$$

where \mathbf{f} being the external nodal force (column-) vector

$$\mathbf{f} = \begin{bmatrix} f_1 \\ f_2 \\ f_3 \end{bmatrix} + \begin{bmatrix} m_1 g \\ m_2 g \\ m_3 g \end{bmatrix}. \quad (1.492)$$

External axially force: The work of this force is also as simple as it can be - this force P will work on the virtual shortening $\delta(\Delta u(0))$ of the column, defined earlier, and results in

$$\delta W_{ext}^{(P)} = [\delta \Delta \mathbf{y}]^T \cdot P \cdot \Delta \mathbf{y} / \bar{\ell} \quad (1.493)$$

$$= \delta [\mathbf{S} \cdot \mathbf{y}]^T \cdot P \cdot (\mathbf{S} \cdot \mathbf{y}) / \bar{\ell} \quad (1.494)$$

$$= \delta \mathbf{y}^T \cdot \frac{P}{\bar{\ell}} \cdot \underbrace{[\mathbf{S}^T \cdot \mathbf{S}]}_{\equiv \mathbf{K}_G} \cdot \mathbf{y} \quad (1.495)$$

$$= \delta \mathbf{y}^T \left[\frac{P}{\bar{\ell}} \cdot \mathbf{K}_G \cdot \mathbf{y} \right] \quad (1.496)$$

where the convention signs $P > 0$ in compression and in tension $T \equiv -P < 0$ are accounted for. The above equation holds for both cases, naturally, of compression and tension.

Virtual work of acceleration forces: This work is

$$\delta W_{acc} = \left(\sum_i m_i \ddot{y}_i \right) \cdot \delta y_i \quad (1.497)$$

$$= \delta \mathbf{y}^T \cdot \mathbf{M} \cdot \ddot{\mathbf{y}} \quad (1.498)$$

where the mass matrix being naturally diagonal (lumped) is

$$\mathbf{M} = \begin{bmatrix} m_1 & 0 & 0 \\ 0 & m_2 & 0 \\ 0 & 0 & m_3 \end{bmatrix}. \quad (1.499)$$

and the lumped mass²⁰⁶

$$m_i = \frac{1}{2}\rho_i A_i \ell_i + \frac{1}{2}\rho_{i+1} A_{i+1} \ell_{i+1} \quad (1.500)$$

which becomes for our case of constant, homogeneous and uniform section is

$$m_i = \rho A \bar{\ell} \equiv \bar{m}, \quad \forall i \quad (1.501)$$

Now, finally, after a lot of real physical and intellectual work, comes the time of gathering the total virtual work and to set it equal to *zero* in any virtual displacement, therefore,

$$\delta W_{int} + \delta W_{ext} = \delta W_{acc.}, \quad \forall \delta \mathbf{v} \implies \quad (1.502)$$

$$\implies \delta \mathbf{y}^T \cdot \left[\mathbf{M} \ddot{\mathbf{y}} + \left(\mathbf{K} - \frac{P}{\ell} \mathbf{K}_G \right) \mathbf{y} - \mathbf{f} \right] = 0, \quad \forall \delta \mathbf{y}. \quad (1.503)$$

From the above *scalar equation*, one obtains, almost 'magically', the *vector form* of the equation of motion

$$\mathbf{M} \ddot{\mathbf{y}} + \left(\mathbf{K} - \frac{P}{\ell} \mathbf{K}_G \right) \mathbf{y} = \mathbf{f}, \quad (1.504)$$

which should be completed with initial value conditions, like for instance, $\mathbf{y}(0) = \mathbf{y}_0$ and $\dot{\mathbf{y}}(0) = \dot{\mathbf{y}}_0$. In our case both initial configuration and velocities are 'zero'. It is not difficult to include dissipative forces. I let this as an exercise to the reader. Just add the virtual work of such dissipative forces.²⁰⁷

Now from the motion equation (1.503) we obtain

1. the eigenvalue problem for determining the *critical buckling force* (P_{cr}) in statics by setting accelerations and transversal loads equal to zero

$$\left(\mathbf{K} - \frac{P}{\ell} \mathbf{K}_G \right) \cdot \mathbf{y} = \mathbf{0}, \quad \mathbf{y} \neq \mathbf{0} \quad (1.505)$$

²⁰⁶Note that this lumping of the mass accounts also, approximately, for the distributed mass. As the discretization becomes finer, the approximation of the distributed mass becomes better.

²⁰⁷The dissipative force can be a friction moment $M_i^{(dis)} = c_i^{(dis)} \dot{\phi}_i$ at joints. Then the dissipated virtual work will be $\delta W_{ext}^{(dis)} = \sum_i M_i^{(dis)} \delta \dot{\phi}_i$. I let you express this using matrices to obtain the friction or dissipation term $\mathbf{C} \dot{\mathbf{y}}$.

2. We can, equivalently, obtain another eigenvalue problem to determine *natural vibration frequencies* ω of the beam by setting axial force zero and external forces too. In both forms, we are usually, interested in the smallest eigenvalue. Note that, since the matrices real symmetric, all the the eigenvalues are positive and real (recall your course on matrices).

$$\mathbf{M}\ddot{\mathbf{y}} + \mathbf{K}\mathbf{y} = \mathbf{0}, \quad \implies \quad \left(-\omega^2\mathbf{M} + \mathbf{K}\right) \cdot \mathbf{y} = \mathbf{0}, \quad (1.506)$$

after making the harmonic modal assumption $\mathbf{y} = A_i \sin(\omega_i t + \phi_0)$ for free vibrations ($\ddot{\mathbf{y}} = -\omega_i^2 \mathbf{y}$). It will be seen that both problems, equations (1.505) and (1.506), are formally analogous (P_{cr} analogous to ω^2).

3. Finally, we can determine the effect of axial loading (compression/tension) on natural frequencies of the transversal vibrations of beam by solving the generalised eigenvalue problem

$$\left[-\omega^2\mathbf{M} + \underbrace{\left(\mathbf{K} - \frac{P}{\ell} \mathbf{K}_G\right)}_{\equiv \mathbf{K}(P)} \right] \cdot \mathbf{y} = \mathbf{0} \quad (1.507)$$

where compression is such that $P > 0$. For tension, we should have $T \equiv -P < 0$. This equation says, if you 'listen' to it, that axial load affects the natural vibration frequencies: 1) *compression* ($P > 0$) reduces the natural vibration frequency $\omega(P)$ since the effective stiffness $\mathbf{K}(P) = (\mathbf{K}) - P/\ell \cdot \mathbf{K}_G$ is also reduced by the compression. 2) *tension* ($P < 0$) increases the natural vibration frequency $\omega(P)$ since the effective stiffness $\mathbf{K}(P) = (\mathbf{K}) - (-P)/\ell \cdot \mathbf{K}_G$ is also increased by the tension. Recall from high-school physics that $\omega = \sqrt{k/m}$. Now we identify $k \rightarrow \mathbf{K} - P/\ell \cdot \mathbf{K}_G$ and $m \rightarrow \mathbf{M}$. From this simple high-school generic formula, we see that increasing (decreasing) effective stiffness k will increase (decrease) the frequency. *Increasing compression, decreases frequency, and inversely.*

For instance, in case of vibrating string under tension, one recovers from Eq. (1.507) the high-school formula for natural frequencies of a tensioned string by putting bending rigidity $EI \rightarrow 0$ ($c_i = 0 \rightarrow \mathbf{K} = \mathbf{0}$) and obtains

$$\left[-\omega^2\mathbf{M} + \frac{T}{\ell} \mathbf{K}_G \right] \cdot \mathbf{y} = \mathbf{0} \rightarrow \quad (1.508)$$

$$\left[-\omega^2\bar{m}\mathbf{I} + \frac{T}{\ell} \mathbf{K}_G \right] \cdot \mathbf{y} = \mathbf{0} \rightarrow \quad (1.509)$$

$$\left[-\omega^2\mathbf{I} + \frac{T}{\rho A \ell^2} \mathbf{K}_G \right] \cdot \mathbf{y} = \mathbf{0} \quad (1.510)$$

from which one can deduce easily that indeed, the natural frequency

$$\omega \propto \frac{1}{\ell} \sqrt{\frac{T}{\rho A}} \quad (1.511)$$

We know that the lowest natural frequency of such freely vibrating string is

$$\omega = 2\pi \cdot \frac{1}{2\ell} \sqrt{\frac{T}{\mu}}, \quad \text{where } \mu \equiv \rho A \quad (1.512)$$

As a conclusion, I just say that long-live both the power of abstraction and of the virtual work. We recovered the familiar FORMULA of the vibrating string almost 'magically' by the not less *magical* virtual work principle.

In a following subsection. (subsection 1.12.6), the above example will be treated analytically, to obtain a more incisive *formula* to find out how axial load change the natural frequency of transversal free vibrations in a beam. This class of physical problems is of key importance in rotating machines where the force transmitting axes are also excited dynamically by eccentric masses in addition to torque, transversal and axial loading. Finding stable operating regime is the question of life or dead. For you and me, as structural engineers, another more relevant physical situation can be the dynamic stability of columns in a high-rise building under wind excitation. Design this columns against *resonance*. Yes, I know that you know how to do it, but now the applied axial forces change the natural frequencies of the system. This needs an engineering *know-how* or *how-know* to resolve the problem in a safe way. One should consider and account for, how and how much the fundamental (natural) frequencies (those close to the wind excitation frequencies) of the columns are reduced by compression from the axial loading. In next subsection, we will derive, together with the reader, the interaction diagrams in the form $(\omega/\omega_0)^2 - P/P_{cr,0}$ for our simply supported beam. Now ω_0 is the natural free system frequency with constant axial loading ($P = 0$), and $P_{cr,0}$ is the static critical buckling (Euler) load.

Static Buckling equations

Now we have centric constant axial loading (P), no transversal loading, and no accelerations ($\omega = 0$), saying nothing more, we solve equation (1.503)

$$\left(\mathbf{K} - \frac{P}{\ell} \mathbf{K}_G \right) \mathbf{y} = \mathbf{0} \quad (1.513)$$

for our example and obtains the stiffness matrix

$$\mathbf{K} = \mathbf{R}^T \cdot \mathbf{c} \cdot \mathbf{R} = \frac{1}{\ell} \begin{bmatrix} 2 & -1 & 0 \\ -1 & 2 & -1 \\ 0 & -1 & 2 \end{bmatrix}^T \cdot \frac{EI}{\ell} \cdot \frac{1}{\ell} \begin{bmatrix} 2 & -1 & 0 \\ -1 & 2 & -1 \\ 0 & -1 & 2 \end{bmatrix} \quad (1.514)$$

$$= \frac{EI}{\ell^3} \cdot \begin{bmatrix} 5 & -4 & 1 \\ -4 & 6 & -4 \\ 1 & -4 & 5 \end{bmatrix} \quad (1.515)$$

and the geometric stiffness matrix

$$\mathbf{K}_G = \mathbf{S}^T \cdot \mathbf{S} = \begin{bmatrix} 1 & 0 & 0 \\ -1 & 1 & 0 \\ 0 & -1 & 1 \\ 0 & 0 & -1 \end{bmatrix}^T \begin{bmatrix} 1 & 0 & 0 \\ -1 & 1 & 0 \\ 0 & -1 & 1 \\ 0 & 0 & -1 \end{bmatrix} \quad (1.516)$$

$$= \begin{bmatrix} 2 & -1 & 0 \\ -1 & 2 & -1 \\ 0 & -1 & 2 \end{bmatrix} \quad (1.517)$$

Inserting all this matrix-staff in the eigenvalue problem of buckling (Eq. (1.513), one FINALLY, obtains the non-dimensional generalised eigenvalue problem

$$\left(\begin{bmatrix} 5 & -4 & 1 \\ -4 & 6 & -4 \\ 1 & -4 & 5 \end{bmatrix} - \underbrace{\frac{P\bar{\ell}^2}{EI}}_{\equiv \lambda^2} \begin{bmatrix} 2 & -1 & 0 \\ -1 & 2 & -1 \\ 0 & -1 & 2 \end{bmatrix} \right) \cdot \mathbf{y} = \mathbf{0}, \quad \mathbf{y} \neq \mathbf{0} \quad (1.518)$$

Solving the eigenvalue problem (Matlab: $[\mathbf{v}, \mathbf{D}] = \text{eig}(K, K_G)$). The smallest eigenvalue (buckling load)

$$\lambda^2 = \frac{P\bar{\ell}^2}{EI} = 0.5858 \implies P_{cr} = 9.3726 \frac{EI}{\ell^2} \approx 0.95\pi^2 \frac{EI}{\ell^2} < \underbrace{1 \cdot \pi^2 \frac{EI}{\ell^2}}_{\text{theoretical}} \quad (1.519)$$

For more details, please refer to Fig. (1.95).

Natural frequencies of the beam free vibrations

To illustrate the analogy of this natural frequencies problem, Eq. (1.506), with the one of buckling, let's solve these natural frequencies for this same pin-ended beam for which we determined the buckling load. Inserting again all the staff in

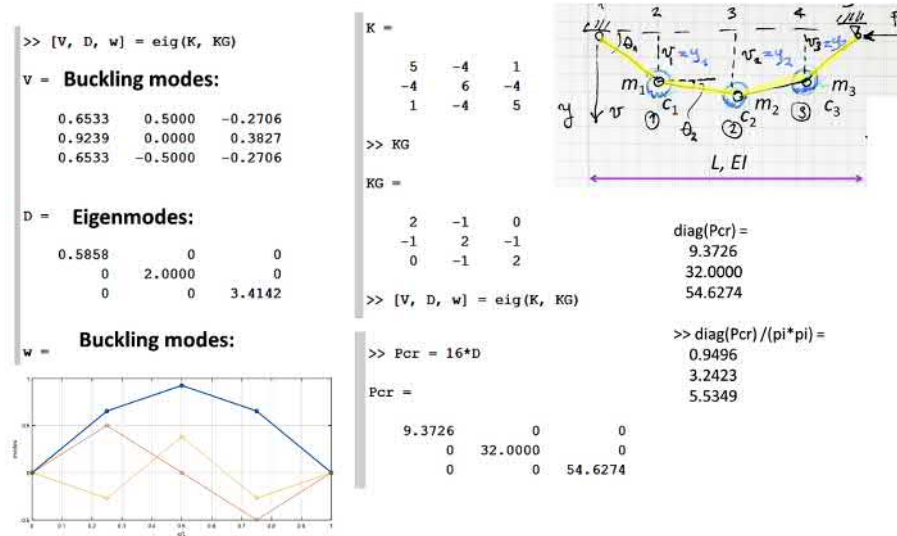


Figure 1.95: The discrete column and computational details.

this equation, one obtains for $\mathbf{y} \neq \mathbf{0}$, the homogeneous equation set

$$\left(\frac{EI}{\bar{\ell}^3} \begin{bmatrix} 5 & -4 & 1 \\ -4 & 6 & -4 \\ 1 & -4 & 5 \end{bmatrix} - \rho A \bar{\ell} \cdot \omega^2 \begin{bmatrix} 1 & 0 & 0 \\ 0 & 1 & 0 \\ 0 & 0 & 1 \end{bmatrix} \right) \cdot \mathbf{y} = \mathbf{0} \quad (1.520)$$

$$\Rightarrow \left(\begin{bmatrix} 5 & -4 & 1 \\ -4 & 6 & -4 \\ 1 & -4 & 5 \end{bmatrix} - \underbrace{\omega^2 \cdot \frac{\bar{m} \bar{\ell}^3}{EI}}_{\equiv \lambda^2} \begin{bmatrix} 1 & 0 & 0 \\ 0 & 1 & 0 \\ 0 & 0 & 1 \end{bmatrix} \right) \cdot \mathbf{y} = \mathbf{0} \quad (1.521)$$

where the eigenvalues λ^2 , once solved, for instance within Matlab `[v, lambda] = eig(K, M)`, provides the natural frequencies (here three lowest one) as

$$\omega = \lambda \sqrt{\frac{EI}{\bar{m} \bar{\ell}^3}} = \lambda \sqrt{\frac{EI}{\rho A \bar{\ell}^4}} = \lambda \sqrt{\frac{EI}{\rho A (\ell/4)^4}} = 16 \lambda \sqrt{\frac{EI}{\rho A \ell^4}} = 16 \lambda \sqrt{\frac{EI}{m \ell^3}}, \quad (1.522)$$

where the total mass of the beam being $m = \rho A \ell$. The scalar eigenvalues are

$$\lambda^2 = [0.3431 \quad 4.0000 \quad 11.6569]^T \quad (1.523)$$

which then result in next natural circular frequencies [rad./s]

$$\omega = \sqrt{\frac{EI}{\rho A \ell^4}} \cdot [9.3726 \quad 32.0000 \quad 54.6274]^T, \quad [rad/s] \quad (1.524)$$

The first obtained natural frequency (the smallest)

$$\omega_1 = \underbrace{9.37 \sqrt{EI/(\rho A \ell^4)}}_{\text{3-dofs discrete model}} \approx \underbrace{\pi^2 \sqrt{EI/(\rho A \ell^4)}}_{\approx \text{continuous analytical}} \quad (1.525)$$

The approximation quality, 6%, is good even with a such coarse model²⁰⁸. In addition to the obtained numerical estimation, the approximate results provides us a FORMULA, and says that the circular frequency depends on the block $\sqrt{EI/(\rho A \ell^4)}$. The formula enables us to design since it tells, for instance, how and how much is the frequency affected by EI/ℓ^3 and by $\bar{m} = \rho A \ell$. One can also, easily reorganise the formula to find the dimensionless products.

Now, as you may remember, if the column is excited periodically having excitation frequency ω_{ex} close enough to one value of the natural frequencies ω , the system goes into *resonance* which is one type of *dynamic instability* to be avoided by structural design.

Bellow (Fig. 1.96), I reproduce for curiosity a series of frames extracted from a video²⁰⁹, showing a failure of a structure in resonance in torsional mode under wind excitation during construction phase. The wind is not guilty. There is no torsional rigidity²¹⁰

Natural free vibrations of the string

Now setting $T = -P < 0$ and $EI = 0$, one obtains Solving the eigenvalue problem (Matlab: $[\mathbf{v}, \omega_T] = \text{eig}(\mathbf{K}_G)$). Now,

$$\left[-\omega^2 \mathbf{M} + \frac{T}{\ell} \mathbf{K}_G \right] \cdot \mathbf{y} = \mathbf{0} \implies \tag{1.526}$$

$$\left[\mathbf{K}_G - \omega^2 \cdot \underbrace{\frac{\rho A \bar{\ell}^2}{T}}_{\equiv \omega_T^2} \mathbf{I} \right] \cdot \mathbf{y} = \mathbf{0} \tag{1.527}$$

The smallest eigenvalue, given by Matlab, being

$$\omega_T^2 = 0.5858 \implies \omega = 0.765/(\ell/4) \sqrt{\frac{T}{\mu}} = \frac{3.06}{\ell} \cdot \sqrt{\frac{T}{\mu}} \approx \underbrace{\frac{\pi}{\ell} \sqrt{\frac{T}{\mu}}}_{\text{analytical}} \tag{1.528}$$

One can see that the approximation is, at least for me, enough good²¹¹ ($\pi \approx 3.06$). Naturally, refining the discrete model leads to convergence. Recall that circular

²⁰⁸Imagine! We found that $\pi^2 \approx 9.37$ before even knowing what π is, and that only by considering motion of discrete mechanical systems. So, where was hidden the *circle* from which emerges this π , the mother of the circle? Was it implicit in the *circular* frequency? I will ask our friend Athanasios M. a far friend of Euklides.

²⁰⁹Thak to our colleague Dr. Athanasios M. for sending the link.

²¹⁰Failure during construction phase should be naturally, avoided. For each phase of the construction, there should be enough temporarily supporting structures to avoid failure of any kind, like stability loss, excessive displacements/rotation and deformations and so on.

²¹¹The obtained approximation $\pi \approx 3.06$ have more much trust than the ones we often see daily in many shops claiming firmly, in their new arithmetic, that $2 + 1 = 2$ or, even

Failure under **wind excitation** during construction phase under combined **very slow torsional free vibrational mode** (less ~1 Hz) and flexural mode **resulting in excessive displacements (resonance)** and **finally joints failure**. Additional remarks: there is practically no torsional rigidity at all, to cite only one error. *(note that there was no temporary supports!)*



Reference: extracted from video Youtube 2021 (link sent by Dr. Athanasios M.)

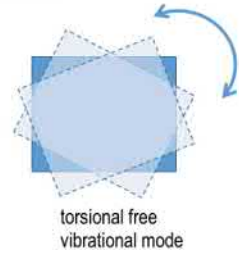


Figure 1.96: Resonance failure during constructional phase of a steel-framed structure. The failure mode seems, from the video, due to resonance in combined torsional and flexural modes. The free vibrations seem to have a very low frequency around 1 Hz. The structural failure was a consequence of excessive displacements at joints, to cite only the mechanical reason.

frequency ω , [rad./s], and frequency, [1/s], f are related by the relation $\omega = 2\pi f$. The analytical lowest natural frequency of such freely vibrating string is

$$\omega = \frac{\pi}{\ell} \sqrt{\frac{T}{\mu}}, \quad \text{where } \mu \equiv \rho A. \quad (1.529)$$

May be at this stage that a small part of the power of the virtual work principle has been demonstrated, I warmly recommend the students to start using it everywhere. Little by little, you will get more and more familiar with it. It is *le couteau suisse* of serious students of mechanics. Even sir Hamilton will recommend it because of its universality.

Vibrating column - frequency-compression interaction diagrams

In a following we consider the simply supported homogeneous beam-column (or column-beam) of length ℓ , bending rigidity EI and total mass $m = \rho A \ell$. There is a constant compressive centric axial force $P > 0$ acting at the roller support end. (The equation of motion that will be derived is versatile and hold also for a tension force $P < 0$, naturally). No transversal loading is applied.

1 + 1 = 1.

This example will be treated analytically, to obtain the 'exact' formula for the natural frequency of transversal free vibrations as function of axial compression for the simply supported beam-column.

The structural engineering motivation for such problem, or better said, exercise, can be to design such column against resonance. Now, the additional challenge being that the axial force changes the natural frequencies of the system. This question of dynamical stability can be very relevant in the columns of high-rise buildings and bracing systems under wind excitation.

The differential equation of motion is simply (just add the inertia forces to the right side of the equilibrium equation, D'Alembert principle²¹²)

$$EIv^{(4)}(x, t) - \underbrace{N^{(0)}(x, t)}_{=-P < 0} v''(x, t) + \rho A \ddot{v}(x, t) = 0 \tag{1.530}$$

$$\implies EIv^{(4)} + Pv'' + \rho A \ddot{v} = 0 \tag{1.531}$$

This equation of motion should be completed with boundary conditions and initial values $v(x, 0) = v_0(x)$ and $\dot{v}(x, 0) = \dot{v}_0(x)$. The boundary conditions are clear, and are left to the reader to recall. Recall that in this example, we consider the case of constant axial force P . For pulsating axial force²¹³, please refer to Timoshenko (Section 2.22).

Lets solve this equation by the standard method of separation of variables where

$$v(x, t) = \sum_{n=1}^{\infty} V_n(t) X_n(x) = \sum_{n=1}^{\infty} V_n(t) \sin\left(n\pi \cdot \frac{x}{\ell}\right) \tag{1.533}$$

and

$$V_n(t) = T_n \exp\{i\omega_n t\}. \tag{1.534}$$

Inserting all that stuff in the equation of motion (free vibrations) leads to the eigenvalue problem

$$\sum_{n=1}^{\infty} \underbrace{\left[\left(EI \left[\frac{n\pi}{\ell} \right]^2 - P \right) \left[\frac{n\pi}{\ell} \right]^2 - \omega_n^2 \rho A \right]}_{=0, \text{ since } V_n(t) \neq 0} V_n(t) = 0. \tag{1.535}$$

²¹²So, $\sum \vec{f}_i = m\vec{a} \implies \sum \vec{f}_i - m\vec{a} = \vec{0}$. By the way, deriving this equation of motion was last year an exercise in your homework. The student was in addition, asked to solve it, approximately, using energy principles, for $P = 0$.

²¹³In this case the equation of motion is simply

$$EIv^{(4)} + [P_0 + S \cos(\Omega t)]v'' + \rho A \ddot{v} = 0 \tag{1.532}$$

Solving the equation above will provide regions of dynamic stability for the system. P_0 is the constant part of the load and S is the maximum amplitude of the periodic part. This type of problem is not simple to solve. However, numerically, it should not be a problem for any serious student in this class.

Now, we solve for circular frequency ω_n of the mode n assuming that the applied constant axial load P known. Now came the moment to compare the discrete eigenvalue problem (Eq. 1.507) obtained using the coarse mechanical discrete model with the continuous (analytical) eigenvalue problem (1.535) obtained from the continuous problem. They are the two faces of the same axially loaded vibrating column. I am really, pleased, to see the great beauty of abstraction: starting from different sides of the thought, we arrive to the same result from two opposite sides. Experimental validations²¹⁴ tells us that this result is the correct one. Consequently, we obtain the beautiful result

$$\boxed{\omega_n^2 = \frac{n^4 \pi^4 EI}{\rho A \ell^4} \left(1 - \frac{P \ell^2}{n^2 \pi^2 EI} \right)} \quad (1.536)$$

First, equation (Eq. 1.536) is the one saying how and how much axial constant compression P reduces the natural circular frequency ω_n .

Let's rewrite the above result (Eq. 1.536) using physically more meaningful variables: let's define

$$P_{cr,n} = \underbrace{n^2 \cdot \frac{\pi^2 EI}{\ell^2}}_{\text{static Euler buckling load}} \quad \text{and} \quad \bar{\omega}_n^2 = \underbrace{n^4 \cdot \frac{\pi^4 EI}{\rho A \ell^4}}_{\text{natural frequency with zero axial force}}. \quad (1.537)$$

and the more readable, for a structural engineer²¹⁵, relation

$$\boxed{\omega_n = \bar{\omega} \sqrt{1 - \frac{P}{P_{cr,n}}}} \quad (1.538)$$

is obtained. Finally, equation (1.536) can be written in a no-dimensional form for the *long-awaited-for* interaction diagram

$$\left(\frac{\omega_n}{\bar{\omega}} \right)^2 = 1 - \frac{P}{P_{cr,n}}. \quad (1.539)$$

The graph (Fig. 1.99). of this relation cannot be simpler: a straight line going from value 1 to value 1. Note that the graph may be curved for other boundary conditions.

Now we have showed how and how much a constant applied axial compressive force reduces the natural frequencies of the system. In structural design,

²¹⁴Notice the logic: you find two different clocks showing both the same time, let's say: 12 O'clock, exactly. Can you from that deduce that it is really 12 O'clock? Surely, not. How will you proceed to find the correct local time? This is a question from high-school ... if it happens to be a sunny day.

²¹⁵He, as a civil engineer, knows for sure what is the Euler buckling load even if his major is from economy ... and much more.

we should account for this reduction of the fundamental frequencies (those close to the wind excitation frequencies) to avoid resonance of columns in high-rise buildings when, for instance, under dynamical wind load excitation. Just remember that compression reduces effective bending stiffness k , and, at its turn, this reduces the frequency according to the very well-known high-school formula $\omega = \sqrt{k/m}$ when the mass is not changing²¹⁶ (as in closed systems).

This effect of stiffness reduction by axial compression will be demonstrated in the following application example of a compressed cantilever column undergoing free-vibrations.

Why natural frequency is reduced by compression?

Consider a compressed cantilever-column of length ℓ . The axial load is constant and the cross section is constant together with the bending rigidity EI . We are interested in the transversal (bending) free-vibrations of the beam-column.

Does the frequency reduction follow the same law than as the one given by equation (1.539)? Certainly yes. We will check that directly using the high-school formula for the angular frequency

$$\omega = \sqrt{k/m} \implies \left[\frac{\omega(P)}{\omega_0} \right]^2 = \frac{k(P)}{k_0} \tag{1.540}$$

where $k(P)$ being the effective bending rigidity (stiffness) of the system under axial constant compression P and $k_0 = k(P = 0)$, being the original stiffness with no axial load. The initial angular frequency is defined as $\omega_0 = \sqrt{k_0/m}$. Naturally, we assume, in our application, that the mass is conserved. The effective mass²¹⁷ is m remains unchanged.

To determine the effective stiffness $k(P)$ and $k_0 = k(P = 0)$ we will not solve the differential equation of motion for free vibrations. We will, instead equivalently, but in a more elegant and efficient way use the virtual dummy-unit-load principle (the dummy unit-load method) to determine the tip transversal

²¹⁶Naturally, in civil engineering structural systems, the mass is conserved. They are closed systems. An example with mass changing can be a flying racket. In such system the mass decreases continuously. Such systems are called open systems.

²¹⁷In the formula $\sqrt{k/m}$, the effective mass m is the mass carrying the kinetic energy of the exited n :th mode which is best determined from the conservation of the kinetic energy $1/2mv_0^2 = 1/2 \int_{\ell} \rho h A v_n^2(x, t) dx$. Here, we consider the cantilever mass lumped to the free-end having transversal displacement v_0 . We know, and it is a small exercise of homework to show it, that the best choice, when the first mode is exited, for effective lumped mass $m = M/3$ even that $m = 1/2M$ is not bad. ($M = \rho A \ell$ is the total mass of the beam. For the effective stiffness k of the lumped (or discrete) model, the story is the same: we should conserve the strain energy; therefore the $1/2kv_0^2 = 1/2 \int_{\ell} EI[v'']^2 dx$, for instance. In one word, what ever approximation methods you use, think to conserve the original invariants of the primary system, like energy, mass, etc. That way, you'll obtain the best approximation methods. This is for the physics.

displacement v_0 under conjugate effect of axial load P and a transversal load F . This seems, in the start, complicated. It is not. On the contrary, it is a short-cut through the virtual world (conjugate problem). This way, we will determine in few lines (= Maxwell-Mohr integrals), the relation between the applied transverse tip-load F and the tip displacement v_0 . This relation is nothing more than the stiffness relation $F = k(P) \cdot v_0$. Recall that the virtual work principle is valid also even if the problem have material and geometrical non-linearities. Let's do it. (I think that the reader may not yet understood why I introduced the transversal load F ! The answer: +footnote There is a second reason. We will use this simple approach to estimate the geometrically non-linear effect of lateral sway in the presence of compressive axial static load. This will be the important case in tall buildings. We want to use directly the simple formula (1.540 to estimate frequency as function of P and not to first set-up the eigenvalue problem and the solved with appropriate boundary conditions. So, we need to determine first the effective bending rigidity $k(P)$ of the system. That is the reason.)

In the following, we derive 1) the effective rigidity relation and 2) show that, this loss of rigidity, at its turn results in a decrease of natural frequency.

1. **The effective bending rigidity decreases with increase of compression** Why effective bending rigidity decreases? Bellow follows a simple experiment we perform during the first stability lectures to demonstrate the behaviour list above as questions.

Here some experimental physics: (Refer to (Figure 1.97) to better follow this wordy example.) take a short slender ruler and compress it slightly with your two fingers. Then, push it very gently, from its mid-span with a finger of the other hand while keeping constant the tiny compression by the fingers of the other hand. While pushing slightly, try to keep your mind at the tip of the pushing finger and *feel the force*. You feel the ruler resistance to bending in your finger as a sensible reaction force. You know that rigidity is just the coefficient relating this force F , you are applying with your finger, and the resulting lateral displacement v by the relation as $F = kv$. Keep in your memory the resistance you felt. Let's call it k_0 , the reference level with almost zero level of compression. Now, increase very gently, continuously, very slowly the compression force of your two fingers till buckling, then release the force a micro-bit to come back close from below to the buckling state. Now the compression force P you are applying may be about 0.8 – 0.9 times the critical buckling load P_E . If you now test for lateral rigidity, as described earlier in the first phase, and still keeping the contact with the *force* in your pushing finger, you will feel *a much-much looser resistance* to deflection. We really feel that the lateral sensible rigidity $k(P) \rightarrow 0$ has just *vanished!* The reason is that we brought the system by our compression very close to *neutral equilibrium* condition. The small beam between our finger will deflect laterally even if you blow

air from your mouth on it. The pressure will be sufficient to bend it since bending resistance has practically vanished²¹⁸.

The effective bending stiffness $k(P)$ at a load level P is simply the tangent modulus dP/dv at point P , where v being the deflection (Figure 1.97). The transverse load F acts as a tiny perturbation and as a mean to sense the flexural rigidity under compression. This F is just the tiny force you are pushing with your finger. It serves to 'gauge' or 'sense' the bending resisting *force*. If you have had the chance to follow my physical lectures, you may recall this small experiment many students did during the class while demonstrating the physical meaning of loss of stability. The criticality condition when mathematically written generically, as

$$\|\mathbf{K} - \mathbf{K}_G(P_E)\| = 0 \tag{1.541}$$

means, physically, that the effective rigidity $k_{\text{eff}} \equiv \mathbf{K} - \mathbf{K}_G(P_E) \rightarrow 0$ of the system, just vanishes. In mathematics, many teachers, love to show how brilliant, they, are and confuse their students more, by saying that, at buckling, *the tangent stiffness matrix loses its positive definiteness*.. The truth is much simpler. It is the one you tested between your fingers to feel that the lateral rigidity (resistance) to transversal load just vanishes close to buckling (for small transverse displacements). Usually, only after understanding the physics that the mathematical formulation comes to life. However, there exist beautiful counter-examples against this logic.²¹⁹

Let's go to our business again. So, consider the cantilever shown in Figure (1.98). Let's determine his lateral displacement v_0 under both constant axial centric compression P and a transversal load F . The virtual force principle says that, we want it or not, that

$$1 \cdot v_0 = \int_0^\ell \frac{M \cdot \bar{M}_1}{EI} dx \tag{1.542}$$

²¹⁸Réciproquement, this physics explains also why one needs a very small lateral force, as provided by struts or equivalent lateral supports, to prevent buckling. One exercise can be to design the needed minimum axial rigidity for the lateral support to prevent the buckling to occur through the first mode. This way you gain in two fronts. I let you found out what are they!

²¹⁹To cite only one: the *gravitational waves*, due probably to colliding or merging of two 'huge' black holes, have been observed and measured few years ago for the first time in Mank-kind history. What is beautiful is that the existence of these now called 'physical objects' (gravitational waves) which are the vibrations of the fabric of space-time itself (our universe?) were predicted by the the EQUATIONS of the *theory of gravitation* by Einstein (general relativity) two hundreds years ago before they were observed and even their existence known. We clearly see that 'mathematics' was first, then came Einstein and then, and only then, followed gravitational waves.

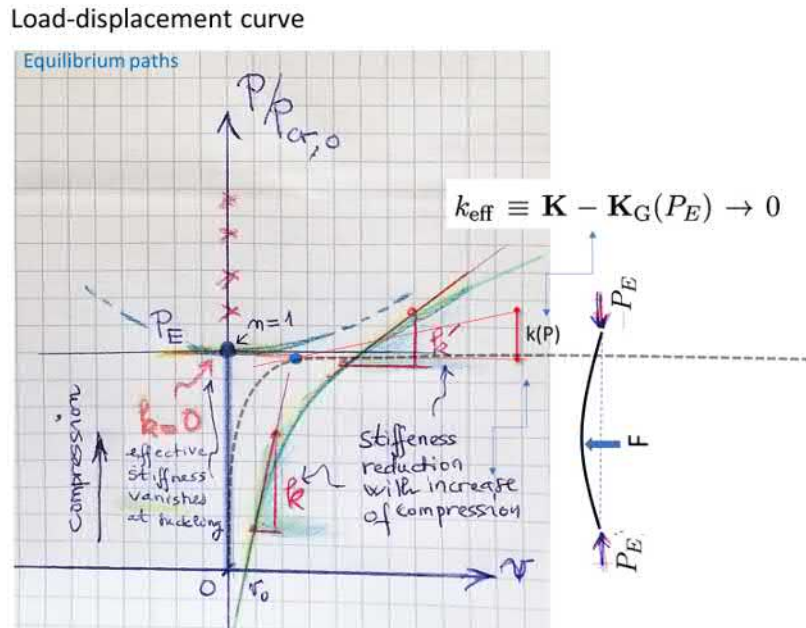


Figure 1.97: What is the effective bending rigidity? How it decreases with increase of axial compression? The load-displacement curve tells you everything.

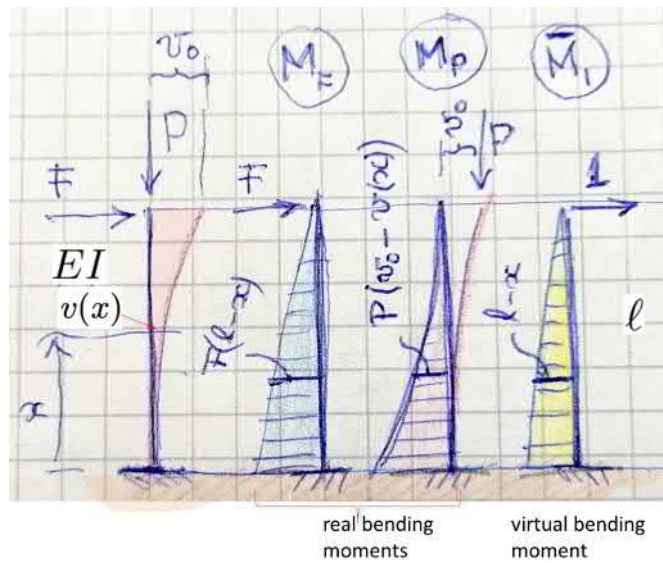


Figure 1.98: Real and virtual states used to compute the needed Mohr-Maxwell or Maxwell-Mohr or simply MM -integral $1 \cdot v_0 = \int_l M \bar{M}_1 dx$, where $M = M_F + M_P$.

where

$$M(x) = M_F(x) + M_P(x) \quad (1.543)$$

$$M_F(x) = F(\ell - x) \quad (1.544)$$

$$M_P(x) = P_0 \cdot (v_0 - v(x)) \quad (1.545)$$

$$\bar{M}_1(x) = \ell - x, \quad \text{results from unit-dummy load } \bar{F} = 1. \quad (1.546)$$

To be able to determine the second order bending moment M_P we need the transversal displacement. Since the problem is geometrically non-linear, we simply do not know it ...yet and we do not want to solve the relevant differential equation to obtain it. Let's estimate it by choosing it equal to the *exact* first buckling mode

$$v(x) = v_0[1 - \cos(\pi x/2\ell)]. \quad (1.547)$$

Inserting all this stuff *kissoineen ja koirineen* in the *MM*-integral (1.542), we obtain

$$1 \cdot v_0 = \int_0^\ell \frac{M \cdot \bar{M}_1}{EI} dx \quad (1.548)$$

$$= \frac{F\ell^3}{3EI} + \frac{P4v_0\ell^2}{\pi^2 EI} \quad (1.549)$$

$$\Rightarrow v_0 = \underbrace{\frac{F\ell^3}{3EI}}_{\text{deflection when } P=0} \cdot \underbrace{\frac{1}{1 - \frac{P}{P_E}}}_{\text{amplification factor}} \quad (1.550)$$

where the Euler buckling reference load $P_E = 1/4\pi^2 EI/\ell^2$ have been used.

We see clearly that axial compression enhances the lateral deflection by the non-linear amplification factor given in the formula. This same formula, a classical one, would be obtained by solving the differential equation of equilibrium in the tiny deflected mode. I presented, a bit, different way to derive it, using the virtual force principle to convince students to study seriously this general principle. The best study method is to start using it.

I let to the student to find out, from this formula, what will be the maximum stress if one want to design such slender column in the elastic domain. This stress is definitely larger than $P/A + M_F/W$. Find out the exact formula. This is an exercise for homework.

Such question becomes very relevant in tall buildings where P (gravity forces) can cumulate quickly down and where the lateral sway, for instance here v_0 is *non-linearly amplified by the compressive axial load P* . This type of geometric non-linearity, as simply illustrated by the above formula (1.641), $v_0 = \frac{F\ell^3}{3EI}/[1 - \frac{P}{P_E}]$ is of key importance in limiting the lateral sway in tall building. Naturally, for more complex situations, one can use FEM

or some $P - \Delta$ methods to determine the maximum deflection in order to design adequate bracing systems to limit excessive sway.

2. **Consequently, natural frequency decreases with increase of axial compression** in the following manner: The stiffness is easily obtained by inverting the above equation to have

$$F = \underbrace{\frac{3EI}{\ell^3}}_{k_0} \cdot \underbrace{\left(1 - \frac{P}{P_E}\right)}_{\text{compression reduction}} \cdot v_0 \equiv k(P)v_0 \quad (1.551)$$

$$\implies [\omega(P)/\omega_0]^2 = \frac{k(P)}{k_0} = 1 - \frac{P}{P_E} \quad (1.552)$$

where $k_0 = k(P = 0)$ being the bending rigidity with no axial loads.

Dear reader we obtained the same reduction relation as the famous equation (1.539), previously derived starting from setting the eigenvalue problem and solving it. *Tous les chemins mènent à Rome - kaikki tiet vievät Roomaan* as goes the old saying, at least on a sphere. Note that Equation (1.552) is derived only for the first mode because of the mode assumption we made for the lateral deflection being the exact analytical first mode. This formula says clearly that, indeed, constant axial compression reduces natural frequencies as shown in Figure (1.99).

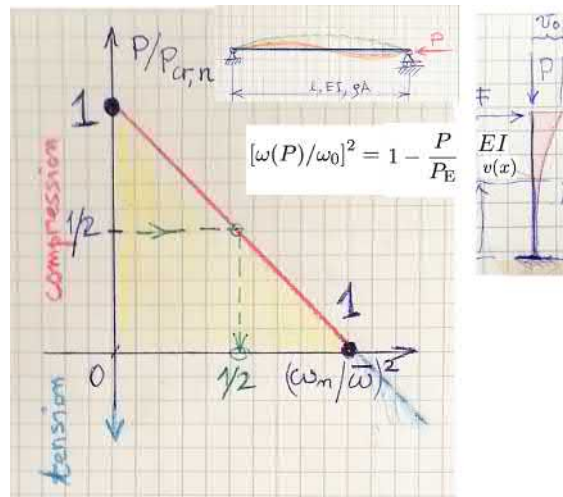


Figure 1.99: Natural frequency reduction by a compressive constant axial load for both simply supported and cantilever columns.

1.12.7 Load combination - interaction buckling diagrams

The reader can find a very well explained section, on this topic with additional examples, in the very good textbook by Alfutov ²²⁰ illustrating the concept of *region of stability*.

The design question

Assume the column shown in Figure (1.100) being loaded at each floor independently. This means that each axial load P_i resulting from the floor number i can vary independently of how varies the corresponding loads resulting from remaining floors. The question of load combination is very usual in structural design. In such combination, each load can vary independently of all others. Now the stability questions is: *how to design such column with various load combinations against buckling?* Here, we tackle the necessary question of how to, first, *analyse* such column for buckling. Be patient and read further how, it may e done correctly. Assume, for instance to make the idea

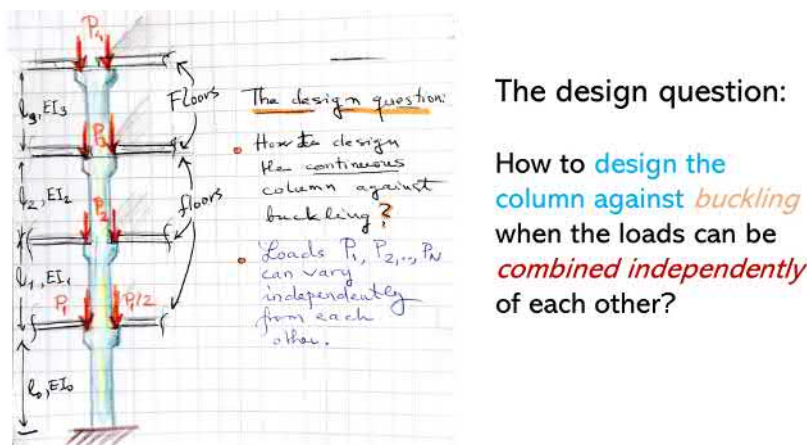


Figure 1.100: A loaded column with a set of independent axial loads P_i .

clear, a beam-column loaded by a set of compressive axial loads (Fig. 1.101) $P_i, i = 1, 2, \dots, N$ which values can be changed independently of each other. This load combination is called *non-proportional loading*. If the load values are changed simultaneously at the same time and proportionally to each other ($P_2/P_1 = \eta_2, P_3/P_1 = \eta_3 \dots P_i/P_1 = \eta_i, \dots P_N/P_1 = \eta_N$), the loading is said *proportional loading*. Only elastic buckling is now addressed.

²²⁰Ref. Section 1.7 Stability of Elastic Structures Under Combined Loading: Boundary of Stability Region. N.A. Alfutov, *Stability of Elastic Structures*. Springer-Verlag Berlin Heidelberg 2000.

In the case of proportional loading, to find the critical buckling loads, we load the column with all the loads and reset the eigenvalue problem in terms of only one reference²²¹ load P_1 , for instance, and then find $P_{1,cr}$ and consequently all the other critical values of remaining loads thanks to proportionality.

In the non-proportional loading case; independent set of load combinations are acting, therefore one *cannot expect to obtain one and only one set of critical loads*. Instead of that, a *set of load critical combinations* is obtained. This last result is best expressed as a critical load combination (interaction) diagram. The eigenvalue problem of buckling now expresses a relation between all the loads P_i and cannot anymore be expressed in terms of a unique reference buckling load. This relation when expressed geometrically, provides the interaction diagram (for instance, Fig. 1.102).

In the following an illustration example of the methodology is shown.

Buckling interaction diagram for a cantilever column

In this example, we will consider that shearing effects are negligible and only elastic buckling occurs. The elasto-plastic buckling is a bit more complex - we will give further examples, *iff* time. To go directly to the point (load interaction buckling diagram²²²; (Fig. 1.102) and not to remain trapped in mathematical 'spaghetti'-like differential equations, let's derive the buckling equation (linear eigenvalue problem) using the energy (displacement) method

The virtual work principle induced from neutral equilibrium condition (Eq. (1.266) will be, again, used to derive the needed interaction diagrams. So,

$$\underbrace{\int_{\ell} EI v'' \hat{v}'' dx}_{\equiv -\delta(\Delta W_{int})} - P \underbrace{\int_{\ell} v' \hat{v}' dx}_{\equiv -\delta(\Delta W_{ext})} = 0, \quad (1.553)$$

for $\forall \hat{v} \in V_{kin.ad}$.

The idea is to derive approximations for such interaction diagrams for the cantilever column (Fig. (1.101)). I let the analytical solution as a homework. Let's choose the simplest mode approximation

$$v \approx \hat{v} = v_0 \cdot \left(\frac{x}{\ell}\right)^2. \quad (1.554)$$

Of course, using the buckling mode of the end-loaded cantilever, namely, as an approximation $v \approx v_0[1 - \cos(\pi x/2\ell)]$ will give more accurate results (I let this,

²²¹The reference load P_{ref} can be chosen adequately. For instance, it can be the largest load $P_{ref} = \max P_i$ or when relevant, $P_{ref} = P_E$, some reference buckling load.

²²²In deed, now, one obtains an estimate of it, once I use an approximation of the displacement field.

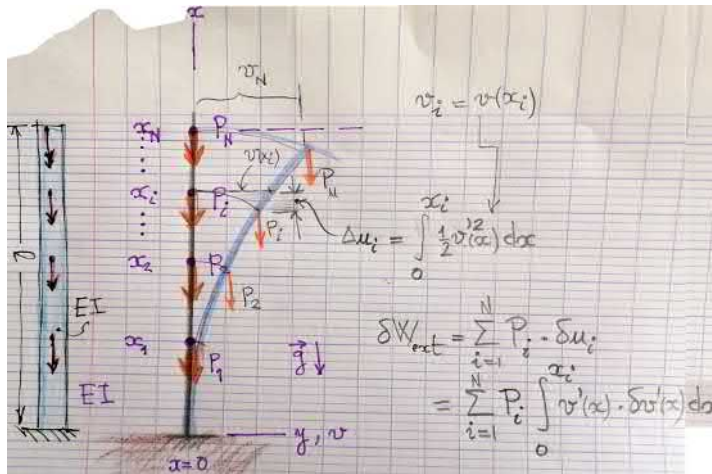


Figure 1.101: Example of axially compressed column with a set of independent loads P_i

too, as an exercise for the student to show.) Making the integrations, one obtains

$$\delta(\Delta W_{int}) : \int_0^\ell EI[2v_0/\ell^2][2\delta v_0/\ell^2]dx = \frac{4EI}{\ell^3} v_0 \delta v_0 \quad (1.555)$$

$$\delta(\Delta W_{int}^{(i)}) : P_i \cdot \int_0^{x_i} [v_0/\ell^2 \cdot 2x][\delta v_0/\ell^2 \cdot 2x]dx = \frac{4P_i}{3\ell} \left(\frac{x_i}{\ell}\right)^3 v_0 \delta v_0. \quad (1.556)$$

Finally, from the above, since always $v_0 \neq 0$ and $\delta v_0 \neq 0$, one gets the (approximative) interaction equation

$$-\sum_{i=1}^N P_i \left(\frac{x_i}{\ell}\right)^3 + \frac{3EI}{\ell^2} = 0, \quad (1.557)$$

It is not difficult to write the load combination as

$$\left[\sum_{i=1}^N P_i \left(\frac{x_i}{\ell}\right)^3 \right]_{cr} \approx 0.3\pi^2 \frac{EI}{\ell^2} \equiv \underbrace{\hat{P}_E}_{\text{system reference buckling resistance}}. \quad (1.558)$$

Let's use the ratio $\eta_i \equiv P_i/\hat{P}_E$, as a measure how close or far is the single load is from the reference buckling load \hat{P}_E of our system. Notice first that this buckling coefficient 0.3 in the buckling load (Eq. (1.558) is the approximation obtained using the somehow *barbarian parabolic* approximation for the first buckling mode. Further, we will see that this buckling coefficient will converge to a probably more realistic²²³ 1/4 using better approximation for the global first mode of buckling

²²³Not trivial to say that this buckling coefficient should remain equal 1/4 which corresponds to the case with only one single axial load for the cantilever. Now, our column is loaded with a system of axial loads and the critical buckling mode will not, *a priori* be the same as when loaded with a single load.

of the cantilever column loaded with a system of central axial loads.

Note now that reference load is the buckling (= resistance) load of the system whatever is the load combination load. We will rewrite the load-interaction result in an elegant non-dimensional way, as

$$\sum_{i=1}^N \eta_i \left(\frac{x_i}{\ell} \right)^3 = 1, \quad \eta_i \equiv P_i / \hat{P}_E. \quad (1.559)$$

Alternative form of the buckling condition: Critical condition (Eq. 1.558) can be also re-written in a form which is easier to use to determine the effective buckling load $(P)_{\text{cr}}$ of the structure under the full simultaneous loading. This form is achieved by choosing one of the loads as reference load, let's say $P_1 \equiv P$ and all remaining forces $P_2, P_3 \dots P_N$ are expressed in with the ratios η_i as $P_i = \eta_i P$. The above buckling condition becomes

$$\underbrace{\left[\sum_{i=1}^N P_i \left(\frac{x_i}{\ell} \right)^3 \right]}_{\equiv (P)_{\text{cr}}} = P_{\text{cr}} \cdot \left[\sum_{i=1}^N \eta_i \left(\frac{x_i}{\ell} \right)^3 \right] = \frac{1}{4} \frac{\pi^2 EI}{\ell^2} \equiv \hat{P}_E \quad (1.560)$$

where now P_{cr} denotes the critical value of the reference load $P \equiv P_1$ and $(P)_{\text{cr}}$, the critical *overall* buckling load of the structure, as defined by equation (1.560). Please note the difference in meanings between the different notations $(P)_{\text{cr}}$ and P_{cr} . This notation will be critical to apply correctly the *Durckerkey theorem* presented in sub-section (1.11.3).

Now, using the above form of the buckling condition, for any load combination, we can find (estimate) the critical buckling load of the system, either expressed with the reference load P_{cr} or the overall buckling load $(P)_{\text{cr}}$.

How to use this result for finding combined buckling load? Assume that we know the free-end applied load is $P_2 = \hat{P}_E/2$ and we still want to load the column at its mid-span with a axial load P_1 . The question is: *what is the magnitude of this load before buckling failure?* The answer is given by Equation (1.559) and by its application (Eq. 1.573) as

$$P_2 = \frac{1}{2} \hat{P}_E \implies \eta_2 = \frac{1}{2} \quad (1.561)$$

$$\implies \frac{1}{8} \eta_1 + \eta_2 = 1 \implies \eta_1 = 8(1 - 1/2) = 4 \quad (1.562)$$

$$\implies P_1 = 4 \cdot \hat{P}_E, \quad \hat{P}_E = 1/4 \pi^2 EI / \ell^2 \quad (1.563)$$

So, to get the column to buckle, one should load it, in addition, to the end-load P_2 , with a mid-span load of $P_1 = \pi^2 EI / \ell^2$ which is half of the critical load for P_1 when $P_2 = 0$.

A simple cross-check: Assume $\hat{P}_2 = 0$, thus zero end-load, and $\eta_2 = 0$. Above combination formula gives, for the mid-span load

$$\eta_2 = 0 \implies \eta_1 = 8 \implies P_1 = 8 \cdot (1/4\pi^2 \cdot EI/\ell^2) = 1/4\pi^2 EI/[\ell/2]^2 \quad (1.564)$$

The above results are the correct ones, we obtain directly using basic Euler' buckling formula with column length $\ell/2$. Consequently, the probability of mistaking in this exercise is very low even that the entropy is keeping growing all the time.

How to use this result for safe design? Equation (1.559) says loudly, for those who know how to read, that the system, independently of the load combination, will remain *safe = unbuckled*, as long as the inequality

$$\sum_{i=1}^N \eta_i \left(\frac{x_i}{\ell}\right)^3 < 1 \implies \text{unbuckled} = \text{safe}, \quad \eta_i \equiv P_i/\hat{P}_E. \quad (1.565)$$

holds. Geometrically speaking, this inequality separate the load-combination space (P_1, P_2, \dots, P_N) into safe region and unsafe boundary²²⁴ (when = 1). The safe region represent the interior space delimited by hyperplanes defined by $\sum_i \eta_i (x_i/\ell)^3 = 1$. There will be given a small example to illustrate this safe region in a three-dimensional case P_1, P_2, P_3 load-space.

Theorem of Durkerley

This theorem is very useful while estimating the critical buckling load under multiple loading. It can be used, also, to cross-check our estimations which are obtained by other methods.

Durkerley Theorem: *The eigenvalue (critical buckling load) $(P)_{cr}$ of a structure under simultaneous multiple independent loading $P_1, P_2, \dots, P_i, \dots, P_N$, fulfil the inequality*

$$\frac{1}{(P)_{cr}} \leq \sum_{i=1}^N \frac{1}{P_{i,cr}}, \quad (1.566)$$

where $P_{i,cr}$ are the critical buckling load of the system when only a unique load P_i is (axially) compressing the system while all remaining loads are set equal to zero.

The demonstration (todistus) of the theorem, at its basic level, is simple and relay on the minimum properties of the (smallest) eigenvalue in the Rayleigh quotients.²²⁵ *This is how:* To make the following argument easier to follow, and without loose of generality, let's think we have a continuous column. Consider

²²⁴We cannot go out the boundaries because the structure will fail (buckle) when the boundary is reached, independently where this occurs.

²²⁵Chap. 13.4 in: M. S. El Naschie. *Stress, stability and chaos in structural engineering: and energy approach.*

now that the exact buckling mode of the structure when simultaneously loaded by all the loads $P_1, P_2, \dots, P_i, \dots, P_N$ being known and denoted as v . Let's now unload the structure and re-load it only and *only* by one separate load P_i at location x_i until buckling. Note that this corresponding buckling mode v_i is now different from v when all loads act simultaneously. We can estimate now obtain an *estimate* $\hat{P}_{i,\text{cr}}$, thanks to Lord Rayleigh and Ritz, of the corresponding buckling load $P_{i,\text{cr}}$ using the global exact buckling mode v as a *trial function*, and therefore

$$\underbrace{P_{i,\text{cr}}}_{\text{exact but unknown}} \leq \frac{\int_{\ell} EI v''^2 dx}{\int_0^{x_i} v'^2 dx} = \underbrace{\hat{P}_{i,\text{cr}}}_{\text{estimate}}, \forall i \implies \frac{1}{P_{i,\text{cr}}} \geq \frac{\int_0^{x_i} v'^2 dx}{\int_{\ell} EI v''^2 dx}, \forall i \quad (1.567)$$

Let's now be the structure again be loaded by all the loads simultaneously and buckles to the exact critical mode v , already used as trial in the separate loading. Now, because v is the exact buckling mode for this loading case, we have *equality*

$$\underbrace{(P)_{\text{cr}}}_{\text{overall critical}} = \frac{\int_{\ell} EI v''^2 dx}{\sum_{i=1}^N \int_0^{x_i} v'^2 dx} \implies \frac{1}{(P)_{\text{cr}}} = \frac{\sum_{i=1}^N \int_0^{x_i} v'^2 dx}{\int_{\ell} EI v''^2 dx} \quad (1.568)$$

Now summing all the terms in (Eq. 1.567) and comparing the result with equation (1.568) we obtain, the Durkerkey theorem shown in (1.566), since

$$\frac{1}{(P)_{\text{cr}}} = \frac{\sum_{i=1}^N \int_0^{x_i} v'^2 dx}{\int_{\ell} EI v''^2 dx} \leq \sum_{i=1}^N \frac{1}{P_{i,\text{cr}}}. \quad (1.569)$$

I recall that now $P_{i,\text{cr}}$ denotes the critical value of the load $P \equiv P_i$ when it is acting alone and $(P)_{\text{cr}}$ is the critical *overall* buckling load of the structure, as defined, for instance, by equation like (1.560) or equivalently, when all the loads are simultaneously acting.

This notation will be critical to apply correctly the *Durkerkey theorem* presented in sub-section (1.11.3). We will apply it in the following examples to cross-check our results. Are the, the obtained results, *oikealla hehtaarilla vai ei?*, as M. L., a legend in soil mechanics, were often saying.²²⁶

Application example 1 - column supporting two levels

Let's the column shown in Figure (1.102) be axially loaded by two central load ($e = 0$). We take a case for two loads P_1 and P_2 , because it is easy to draw the interaction diagram in two-dimensions.

²²⁶Eng. Matti 'Legendre': *In in soil mechanics, we are happy when the obtain experimental data-points located on the same A4-paper sheet with the curves given by the models.* This was an example of a measure how close can be models with experimental data, in soil mechanics. This was not a negative measure. They are happy because obtaining reliable data in geotechnics, in general, is not as easy in a traction test for steel.

Accounting for $x_1/\ell = 1/2$ and $x_2/\ell = 1$, in the safety region (Eq. 1.559), one obtains

$$\sum_{i=1}^2 \eta_i \left(\frac{x_i}{\ell}\right)^3 = \frac{1}{8}\eta_1 + \eta_2 = 1, \quad \eta_i \equiv P_i/\hat{P}_E \quad (\hat{P}_E \approx 0.3\pi^2 EI/\ell^2). \quad (1.570)$$

Recall that this buckling coefficient ≈ 0.3 in the buckling load (Eq. (1.570)) is a crude approximation obtained using parabolic approximation for the first buckling mode. Further, it will be shown that a better approximation for this buckling coefficient will be $1/4$ which corresponds to the case with only one single axial load.

The boundary of the (safety region) is given by the straight line defined, in the plane defined by the Cartesian product $\eta_1 \times \eta_2$ by the equation $\frac{1}{8}\eta_1 + \eta_2 = 1$ as given by the interaction equation (1.570) and shown in Figure (1.102).

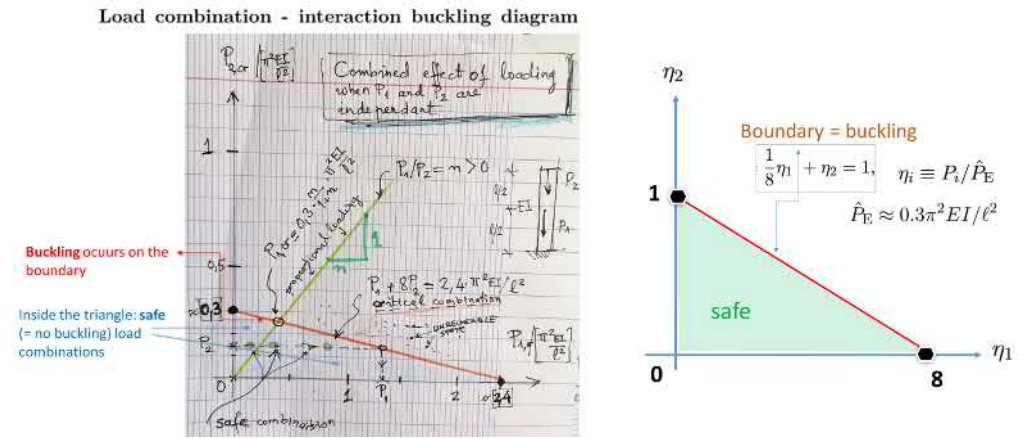


Figure 1.102: Buckling load interaction diagram for a pair of compressive loads P_1 and P_2 as given by Eq. (1.559). Note that the reference buckling load given here is obtained from the crude parabolic mode approximation. A more exact value will be $\hat{P}_E = \frac{1}{4}EI/\ell^2$, as derived at the end of this section by assuming the exact mode for buckling of a cantilever under a single free-end-load.

Application example 2 - column supporting three levels

Now the column shown in Figure (1.103) is axially loaded by three central load ($e = 0$). Analogously with the previous example, we obtain the load interaction

equation for the *buckling failure* boundary as

$$\sum_{i=1}^3 \eta_i \left(\frac{x_i}{\ell} \right)^3 = \eta_1 + \frac{8}{27}\eta_2 + \frac{1}{9}\eta_3 = 1, \quad \eta_i \equiv P_i/\hat{P}_E \leq 1 \quad (1.571)$$

$$\text{where the approximate was } \hat{P}_E \approx 0.3\pi^2 EI/\ell^2 \quad (1.572)$$

$$\text{however, a better estimamte is } P_E = 1/4\pi^2 EI/\ell^2 \text{ as will be shown} \quad (1.573)$$

since the three load-levels (floors) divide the column into three equal parts $\ell/3$. This equation is illustrated geometrically²²⁷, for the lovers of geometry²²⁸, in Figure (1.103).

Application example 3 - column supporting two levels with various type of loading

Consider the continuous column shown in Figure (1.104) supporting two floors. Here we will consider elastic buckling due to axial centric load. The elastic bending rigidity of the column is constant and equal to EI . In this exercise, we use the reference buckling load $P_E = 1/4\pi^2 EI/\ell^2$. It is, as you know, the buckling load when the column is loaded only with the end-load P_2 and $P_1 = 0$. This, in order, to keep the qualitative order of magnitude correct and in our hands.

To illustrate the efficiency of energy approach for hand analysis, we will consider two cases of loading types:

1. *Proportional loading* $P_1 = P_2 = P$; both loads are equal. Determine the critical load P_{cr} .
2. *Non-proportional loading*: assume we know that, for instance the first floor is loaded with $P_1 = 1/4 \cdot P_E$ (where $P_E = 1/4\pi^2 EI/\ell^2$) and the designer, you, are asked to find how much the second floor can be loaded $P_2 = ?$ at maximum before the continuous column buckles when supporting both load simultaneously?²²⁹

²²⁷Truth should be said, even Descartes may disagree, that geometry tells more than millions of words in one picture. Descartes is the guy who made the *geometry, analytical* and the *analysis, geometrical*.

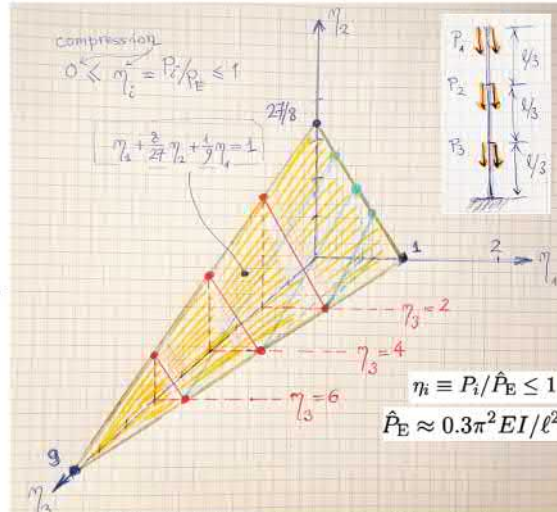
²²⁸I know at least one such person; Athanasios M. the Greek, beside R. Penrose, A. Einstein and R. Feynman. Of course, there are many others geometers, I have not mentioned and many others that I do not know. Did you notice that we say for a person who think deeply before solving difficult tasks that he is *analytical*! Why not to say, instead, that he is *geometrical*!

²²⁹Assume, in addition, that you forgot your computer at home and you are on the site and, as a trusted engineer, you should provide your answer within 15 min, otherwise the project goes to another company. You are happy because you have with you a pen and a paper sheet, and you are young but remember well your energy methods thank

How to design the column against buckling when the loads can be *combined independently* of each other?

- The safe region is inside this triangular pyramid (tetrahedron).
- On its boundary, buckling failure will occur.

$$\sum_{i=1}^3 \eta_i \left(\frac{x_i}{\ell}\right)^3 = \eta_1 + \frac{8}{27}\eta_2 + \frac{1}{9}\eta_3 = 1,$$



Note that the reference buckling load given here is obtained from the crude parabolic mode approximation. May, be a more exact value will be $\hat{P}_E = \frac{1}{4}EI/\ell^2$, as derived at the end of this section.

Figure 1.103: Buckling load interaction (approximate) diagram for a triplet loads P_1, P_2, P_3 Note that the reference buckling load given here is obtained from the crude parabolic mode approximation. Probably, $\hat{P}_E = \frac{1}{4}EI/\ell^2$ is a better approximation for the reference buckling load for such column with multiple axial loads, as shown later.

1) Proportional loading: Now $P_1 = P_2 = P$ and they are acting simultaneously. Let's approximate the buckling mode by

$$v(x) \approx a_1 \left[1 - \cos\left(\frac{\pi x}{2\ell}\right)\right] = a_1 \phi_1(x), \quad a_1 \neq 0 \quad (1.574)$$

which is the analytical exact buckling mode when only the tip load $P_2 = P$, is acting. Note well, that when both loads are acting, this buckling mode does not necessarily correspond to exact analytical one.

Recalling your energy method (Rayleigh-Ritz or much general virtual work

to actively doing homework exercises. So, you answered correctly within 10 min. The cross-check came from India: they confirmed that your estimate was correct after using a computer simulation (FEM) that took one hour to set-up. After that day, all your colleagues really respect you as a true engineer and call you *herra insinööri*, respectfully.

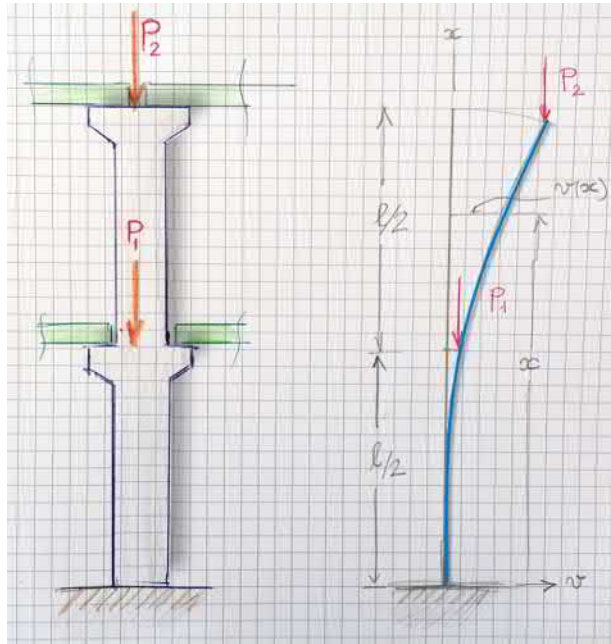


Figure 1.104: Two level continuous column. Interacting buckling loads loads P_1 and P_2 .

principle) one obtains²³⁰

$$P_{cr} = \int_0^\ell EI \phi_1'' \phi_1'' dx / \left(\int_0^{\ell/2} \phi_1' \phi_1' dx + \int_0^\ell \phi_1' \phi_1' dx \right) \quad (1.575)$$

To perform hand-integration, we need

$$\phi_1'(x) = -\frac{\pi}{2\ell} \sin\left(\frac{\pi x}{2\ell}\right) \quad \text{and} \quad \phi_1''(x) = \left(\frac{\pi}{2\ell}\right)^2 \cos\left(\frac{\pi x}{2\ell}\right) \quad (1.576)$$

and may be, to recall²³¹ that

$$\int \sin^2(ax) dx = \frac{x}{2} - \frac{1}{4a} \sin(2ax), \quad (1.577)$$

$$\int \cos^2(ax) dx = \frac{x}{2} + \frac{1}{4a} \sin(2ax). \quad (1.578)$$

²³⁰I let the details to work out for the students. You never know when you will need a paper and a pen at work and all computers are shut down. So, it is a good occasion to train.

²³¹These formulas can be derived using simply integration by parts of the squares of sin and cos functions.

The integration gives

$$\int_0^\ell EI\phi_1''\phi_1''dx = \left(\frac{\pi}{2\ell}\right)^4 \cdot EI \frac{\ell}{2} \tag{1.579}$$

$$I_{\ell/2} = \int_0^{\ell/2} \phi_1'\phi_1'dx = \left(\frac{\pi}{2\ell}\right)^2 \cdot \frac{\ell}{4} \left(1 - \frac{2}{\pi}\right) \tag{1.580}$$

$$I_\ell = \int_0^\ell \phi_1'\phi_1'dx = \left(\frac{\pi}{2\ell}\right)^2 \cdot \frac{\ell}{2} \tag{1.581}$$

Finally, one obtains, the critical estimate load as

$$(P_1)_{cr} = (P_2)_{cr} \equiv (P)_{cr} \geq 0.846 \cdot \frac{\pi^2 EI}{4\ell^2} = 0.846P_E. \tag{1.582}$$

when both equal loads act simultaneously. Notice that the column supports now both loads $P_1 = P_2 = P$ and therefore, the total loading is $2 \cdot P_{cr} = 1.69\pi^2 EI/[4\ell^2]$ with one load at $x = \ell$ and the other one, at $x = \ell/2$. At first glad, this may seem too much since already $P = 1 \cdot P_E$ will already lead to buckling when only one load is applied at the tip $x = \ell$. The obtained result (Eq. 1.582) is correct.

One fast cross-check: The column will not buckle for separate loading a) $P_1 = 0.846P_E$ and ($P_2 = 0$) and when b) $P_2 = 0.846P_E$ and ($P_1 = 0$). In case a) naturally, no buckling since the buckling load should be $0.846P_E$ is less than the needed P_E . For case b) the needed critical load is $\pi^2 EI/[4(\ell/2)^2] = 4 \cdot P_E$, so no buckling, neither.

Another more sophisticated cross-check is to use the *Durkerley theorem* shown in following sections (subsection 1.11.3). This theorem says that, the critical load P_{cr} of the structure when loaded with all the loads is such that

$$\frac{1}{P_{cr}} \leq \frac{1}{P_{1,cr}} + \frac{1}{P_{2,cr}} \tag{1.583}$$

where $P_{i,cr}$ is the critical load when P_i is applied alone. Inserting $P_{1,cr} = 4 \cdot P_E$ and $P_{2,cr} = 1 \cdot P_E$ in the bound above, we obtain

$$\frac{1}{P_{cr}} \leq \frac{1}{4P_E} + \frac{1}{P_E} = \frac{5}{4} \frac{1}{P_E} \implies \underbrace{P_{cr} \geq \frac{4}{5} P_E = 0.8P_E}_{\text{true, since we obtained } P_{cr} \approx 0.846P_E} \tag{1.584}$$

After these cross-checks, we can again sleep on both ears. However, in real situations with new complex structural system and complex loading, computational or analytical cross-check, alone, is not sufficient. The experimental check is the only one with *the last word*.

* * * * *

2) Non-proportional loading: Now first floor is already loading the column with $P_1 = 1/4P_E$. So, how much load P_2 can one put, at maximum, in the second floor before buckling?

The virtual work principle which is the expression of the neutral equilibrium condition

$$\delta(\Delta W_{\text{int}}) + \delta(\Delta W_{\text{ext}}) = 0, \quad \forall \text{ tiny virt. perturbation } \delta a_1 \quad (1.585)$$

Therefore, at buckling, we have (buckling conditions)

$$-\int_0^\ell EI\phi_1''\phi_1''dx + \underbrace{P_1}_{\text{known}} \cdot \int_0^{\ell/2} \phi_1'\phi_1'dx + \underbrace{P_2}_{\text{unknown}} \int_0^\ell \phi_1'\phi_1'dx = 0, \quad (1.586)$$

Therefore, saying elegantly, that

$$P_{2,\text{cr}} = \frac{\int_0^\ell EI\phi_1''\phi_1''dx - P_1 \cdot \int_0^{\ell/2} \phi_1'\phi_1'dx}{\int_0^\ell \phi_1'\phi_1'dx} \quad (1.587)$$

$$= \frac{\int_0^\ell EI\phi_1''\phi_1''dx}{\int_0^\ell \phi_1'\phi_1'dx} - P_1 \cdot \frac{\int_0^{\ell/2} \phi_1'\phi_1'dx}{\int_0^\ell \phi_1'\phi_1'dx} \quad (1.588)$$

$$= \frac{\pi^2 EI}{4\ell^2} - \underbrace{P_1}_{=1/2P_E} \cdot \underbrace{\frac{\int_0^{\ell/2} \phi_1'\phi_1'dx}{\int_0^\ell \phi_1'\phi_1'dx}}_{=I_{\ell/2}/I_\ell} \quad (1.589)$$

$$= 0.91P_E. \quad (1.590)$$

So, we can now load the second floor with as much as $0.91P_E$, a such relatively high value which cannot be guessed correctly. Some-one may through the value $3/4 = 0.75 \times P_E$ just by guessing to complete to $1P_E$. It is a good guess, but not, necessarily *a priori* reliable; unless one does the analysis.

I stop here and let the reader with the pleasure to cross-check the above result. Once you did it, please send me a copy, I will include it here with adequate reference. You are free to find the way to cross-check; analytical, numerical, software, FEM, experimental, etc. Please let me know.

* * * * *

Mini-FEM - buckling load of column supporting two levels

Consider the example of cantilever column axially loaded at two levels with to central loads P_1 at free-end $x = \ell$, and P_2 at the mid-span $x = \ell/2$ (Fig. 1.105). This example is the same column as the one treated in subsection (1.11.3).

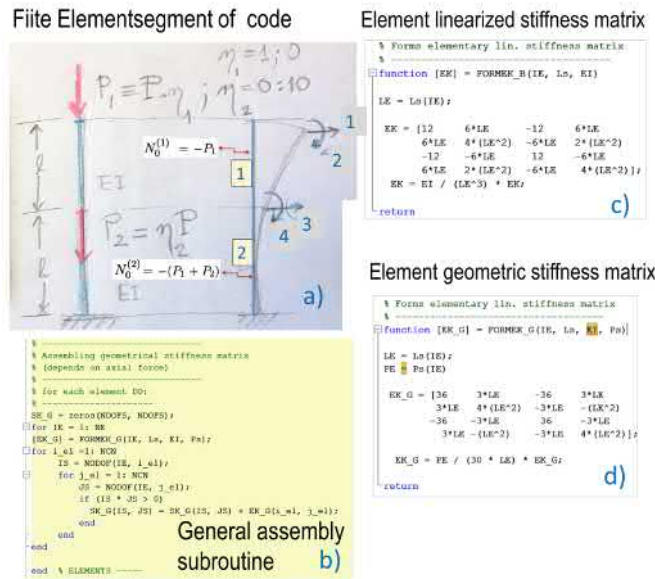


Figure 1.105: A column axially loaded with proportional loads. Notice also the assembly procedure of the global matrices.

Let's assume now *proportional loading*. Consider that the central load $P_1 \equiv P$ as the reference load and we want find out how much the global buckling load $(P)_{cr}$ is reduced by the application of the load $P_2 = \eta \cdot P$ with the parameter η varying from zero to two ($\eta = 0 : 2$). Notice that the question is a bit different from previous ones when the loading was not proportional. It is clear that with $P_2 = 0$ and $P_1 = P$, the critical buckling load should be the Euler' load $P_{cr} = 1/4\pi^2 EI/\ell^2$. Adding at the mid-span a compressive load will naturally reduce the buckling load. *How and how much?* We take a case for two loads P_1 and P_2 , because it is easy to draw the interaction diagram in two-dimensions.

In this finite element application, we will use only two elements of equal lengths. Refer to the theory and the two examples shown in subsection (1.12.12: *Discrete energy method - FEM*). The finite element formulation, with all the needed element-matrices, are derived in this (1.12.12). The global discrete (FEM) equation of neutral equilibrium are

$$(\mathbf{K}_{4 \times 4} - \lambda \mathbf{K}_{G, 4 \times 4}) \mathbf{u} = \mathbf{0}, \quad (1.591)$$

provides the critical buckling load as the smallest eigenvalue λ . For the assembly of the stiffness and geometrical matrices, refer to the examples of the cited subsection. The reader can find a general assembly procedure of the global matrices shown in Figure (1.105 b)). In this version, the global matrices are assembled from the contributions of elementary ones element by element (a loop over all the elements). There is an other very beautiful and efficient version for a hand-assembly

procedure that I will show you on black-board *in vivo* and in this application exercise *in silico*. The assembly is done globally by adding all the contributions to one global degrees of freedom (dofs) at a time, and that for all the global dofs. The assembly is nothing else than writing equilibrium of generalised forces at nodes where the internal forces are expressed using stiffness-relations.²³²

Note that the internal axial force $N_0^{(1)} = -(P_1 + P_2)$ in the lowest element while $N_0^{(2)} = -P_1$ in the upper element (of the free-end).

The relative global critical buckling load $P_{cr}/[\pi^2 EI/\ell^2]$ is shown in Figure (1.106). Notice that, even with only two elements, we obtain, almost, the Euler' analytical load $P_{cr} = 1/4 \cdot \pi^2 EI/\ell^2$ when $P_2 = 0$. This is to illustrate, the power (efficiency) of such numerical, but still analytical, approach. The full efficiency will be illustrated when analysing buckling of frames.

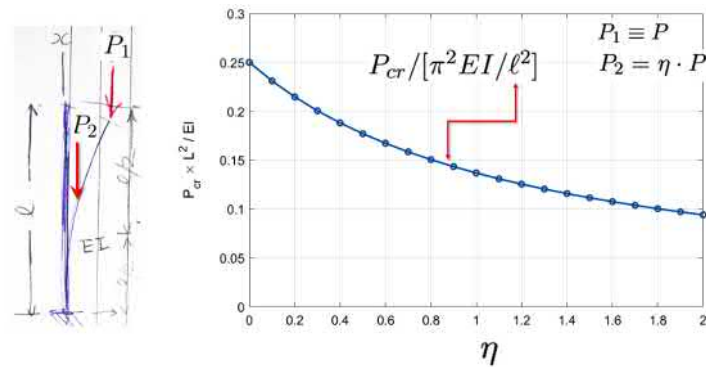


Figure 1.106: The relative global critical buckling load for a column with two proportional axial loads.

The global equilibrium equations for non-proportional loading: We will show explicitly how the eigenvalue problem, *i.e.*, the equation for neutral equilibrium condition (Eq. 1.591), looks like for a combined (non-proportional) axial loading with the two loads P_1 and $P - 2$. For that, I first reproduce here the elementary matrices that will be derived later in section (1.12.12: *Discrete energy method - FEM*). The global equilibrium equations will be assembled from the contributions of all the elements (in this example, we will have only two).

Using the analytical bending modes (as shape functions) of the Euler-Bernoulli beam when loaded only with nodal bending moment and shear forces, we obtain for a general element number e the elementary linearised stiffness matrix for

²³²Analogously for the joint method for trusses and the slope-deflection method for frames, we could write the global equilibrium equations using matrices and stiffness-internal force relations. We obtained a handy version of the finite element method to use with a paper and a pen with no need to computer other than our brain.

bending as

$$\mathbf{K}^{(e)} = \frac{EI}{\ell^3} \begin{bmatrix} 12 & 6\ell & -12 & 6\ell \\ 6\ell & 4\ell^2 & -6\ell & 2\ell^2 \\ -12 & -6\ell & 12 & -6\ell \\ 6\ell & 2\ell^2 & -6\ell & 4\ell^2 \end{bmatrix} \quad (1.592)$$

where ℓ and EI are element length and bending rigidity, respectively, and the geometric elementary matrix as

$$\mathbf{K}_G^{(e)} = -\frac{P^{(e)}}{30\ell} \begin{bmatrix} 36 & 3\ell & -36 & 3\ell \\ 3\ell & 4\ell^2 & -3\ell & -\ell^2 \\ -36 & -3\ell & 36 & -3\ell \\ 3\ell & -\ell^2 & -3\ell & 4\ell^2 \end{bmatrix} \quad (1.593)$$

where $P^{(e)} = -N_0^{(e)} > 0$ for compression, being the initial internal normal force in the element (assumed constant, element-wise). Note that ℓ and EI stand for the length of the element and its bending rigidity. Both can vary from element to element.

Let's discretize the column into two elements of equal length $\bar{\ell} \equiv \ell/2$, with now ℓ meaning the full length of the column. There is four global nodal generalised displacements which are v_1, ϕ_1, v_2, ϕ_2 in this order corresponding to global dofs denoted by 1, 2, 3 and 4, in Figure (1.105 a)).

The global neutral equilibrium equation (or equivalently, the buckling condition, Eq. (1.591)), in a non-dimensional²³³ matrix form, will be

$$\left(\begin{bmatrix} -12 & -6 & -12 & -6 \\ -6 & 4 & 6 & 2 \\ -12 & 6 & 24 & 0 \\ -6 & 2 & 0 & 8 \end{bmatrix} - \frac{\bar{\ell}^2}{30EI} \begin{bmatrix} 36P_1 & -3P_1 & -36P_1 & -3P_1 \\ -3P_1 & 4P_1 & 3P_1 & -P_1 \\ -36P_1 & 3P_1 & 36(2P_1 + P_2) & -3P_2 \\ -3P_1 & -P_1 & -3P_2 & 4(2P_1 + P_2) \end{bmatrix} \right) \begin{bmatrix} v_1 \\ \phi_1\ell \\ v_2 \\ \phi_2\ell \end{bmatrix} = \begin{bmatrix} 0 \\ 0 \\ 0 \\ 0 \end{bmatrix} \quad (1.594)$$

Let's rewrite the eigenvalue problem (Eq. 1.594) in a more tractable form, by choosing a reference load P such that $P_1 = \eta_1 P$ and $P_2 = \eta_2 P$. The buckling equation becomes

$$\left(\begin{bmatrix} -12 & -6 & -12 & -6 \\ -6 & 4 & 6 & 2 \\ -12 & 6 & 24 & 0 \\ -6 & 2 & 0 & 8 \end{bmatrix} - \underbrace{\frac{P\bar{\ell}^2}{30EI}}_{\equiv \lambda} \begin{bmatrix} 36\eta_1 & -3\eta_1 & -36\eta_1 & -3\eta_1 \\ -3\eta_1 & 4\eta_1 & 3\eta_1 & -\eta_1 \\ -36\eta_1 & 3\eta_1 & 36(2\eta_1 + \eta_2) & -3\eta_2 \\ -3\eta_1 & -\eta_1 & -3\eta_2 & 4(2\eta_1 + \eta_2) \end{bmatrix} \right) \begin{bmatrix} v_1 \\ \phi_1\ell \\ v_2 \\ \phi_2\ell \end{bmatrix} = \begin{bmatrix} 0 \\ 0 \\ 0 \\ 0 \end{bmatrix} \quad (1.595)$$

Now each load combination of $P_1 = \eta_1 P$ and $P_2 = \eta_2 P$ corresponds to a fixed choice of combination factors η_1 and η_2 in equation (1.595). For each such choice,

²³³The second and fourth global equilibrium equations were simplified by dividing them by their common factor $\bar{\ell}$.

the solution of the eigenvalue problem, for the critical buckling reference load P as $(P)_{cr} \equiv P_{cr}$ is given simply by the smallest eigenvalue $\lambda_{\min} = \min \lambda$ as

$$(P)_{cr} = \lambda_{\min} \cdot \frac{30EI}{\ell^2} \implies (P_1)_{cr} = \eta_1 P_{cr}, \text{ and } (P_2)_{cr} = \eta_2 P_{cr} \quad (1.596)$$

Some results: Figure (1.107) show critical buckling load $(P)_{cr}$, as determined from equation (1.595), for the column with two loads for two different types of loading. The explanations are on the graphs. Clearly, the buckling load is reduced from the case of having only one load; this is more than self-evident (I do not know why, I even write tautological sentence!) . Notice that, for instance, for the simple load combination $\eta_1 = 1$ and $\eta_2 = 0$ (right subfigure), we recover almost exactly the Euler basic buckling load $P_E = \pi/4 \cdot EI/\ell^2$. This is also the case, thanks God, that for $\eta_1 = 0$ and $\eta_2 = 1$, by virtue of Euler the Great , we should have, at least approximately, $P_E = \pi/4 \cdot EI/[\ell/2]^2 = \pi/4 \cdot EI/\ell^2 \cdot 4$ which gives the correct answer $1 \cdot EI/[\ell^2]$, thanks to Euler. Therefore, it seems that we did not done serious errors ...yet.

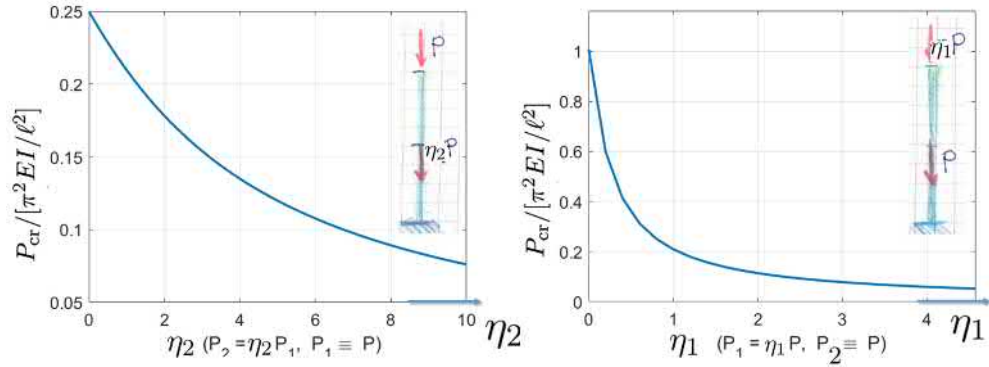


Figure 1.107: Buckling load reduction because of coupling as solved from eigenvalue problem (1.595)

A small side step: Recall that the canonical form (Eq. 1.558) used to determine the buckling interaction boundary. In this form, the reference load was chosen as the known threshold value of the global buckling load of the system P_E . However, the choice for the reference load is free. In the example above, we have chosen it as $P \equiv P_1$, for instance and therefore, $\eta_i = P_i/P$. How then does the equation of limit buckling region looks like? (only external form changes). So, now

$$P \sum_{i=1}^N \underbrace{\eta_i \left(\frac{x_i}{\ell}\right)^3}_{\equiv w_i} \approx \underbrace{1/4 \cdot \pi^2 \frac{EI}{\ell^2}}_{\equiv \hat{P}_E} \implies (P)_{cr} = \frac{\hat{P}_E}{\sum_{i=1}^N \eta_i w_i}, \quad (1.597)$$

where the weights w_i are an estimate for the buckling load interaction coefficients.

The above form (right-side of Eq. 1.597 is interesting; it tells that, the maximum resistance $(P)_{cr}$ of the structure is achieved when the numerator $\sum_{i=1}^N \eta_i w_i$ reaches its minimum with respect, either load combination factors η_i or load locations w_i or both. An interesting design problem, for instance, can be to minimise the total mass of the continuous column (or its price) - the objective function $S(\beta_k; w_i, \eta_i)$ (with β_k being the design parameters - under the the constraint inequality that the load combination is such that the design point β_k leads to loading set which remains inside the safe region of buckling region defined by the inequality you already know,

$$\min_{\beta_k} S(\beta_k; w_i, \eta_i) \quad \text{under the constraint} \quad P \sum_{i=1}^N \eta_i w_i \leq \hat{P}_E \quad (1.598)$$

where the parameters η_i can vary independently of each other. A set of the design parameters β_k can be, for instance, bending rigidity distribution EI_j , the lengths ℓ_i , the cross-section A_j , material properties, etc.

The above setting is clearly a problem of *linear programming*. This being said, let's stop this story here.²³⁴

Now, if the reader have the patience and the curiosity, I will tell him the rest of the story of how the above equation (Eq. 1.594) was assembled, step-by-step.

Global matrices assembly: Here, I present the hand-version (as opposed to the form meant for computers that was presented in Figure (1.106 b). In the computer version, we loop over all elements and add to the global matrices the respective contributions). In the hand version, the assembly (of equilibrium equations) is done by looping over each global degrees of freedom and adding the elementary contributions²³⁵ to the global matrices. Here how, I do it systematically:

Notations: $K_{ij}^{(e)}$ means the term in raw i and column j in the e :th element stiffness matrix $\mathbf{K}^{(e)}$. The global matrices are denoted without any upper-script by \mathbf{K} and \mathbf{K}_G while the upper-script $^{(e)}$ is added for local ones, where $e = 1, 2, \dots$ to the total number of elements NE . Their terms I :th and J :th terms are denoted by K_{IJ} and $K_{G,IJ}$. The capital letters I and J point to global dofs while small letters, to local (elementary) dofs. For instance, for the global degrees of freedom

²³⁴For those interested, I suggest warmly to take either the course of *structural optimization* in structural mechanics or to get a textbook on this wonderful subject. Whatever will be the optimized solution one should always ask this solution to be *robust* with respect to changes in the input parameters, like changing a bit the loading combinations, perturbing by tiny small local loads in other directions, introducing imperfections, etc. Compare this robustness with the concept of stability of an equilibrium. Thus checking for robustness of a design is equivalent to check for the stability of the solution.

²³⁵This is exactly what you do when we write node-wise equations of equilibrium after expressing the internal forces using stiffness force relations.

$I = 3$ and $J = 4$ their contributions come from elements number $e = 1$ and $e = 2$ with the corresponding elementary dofs: $i = 2$ and $j = 1$ for element $e = 1$, and $i = 3$ and $j = 4$, from element $e = 2$. So, *par exemple*

$$K_{34} = K_{12}^{(1)} + K_{34}^{(2)}. \quad (1.599)$$

The global degrees of freedom are shown in Figure (1.105 a).

The global matrix terms: In the following, all the terms of the (linearised) stiffness and geometric matrices should be multiplied by the common factor $EI/\bar{\ell}^3$ and $1/30\bar{\ell}$, respectively. The global linearised stiffness matrix elements (=terms) are

$$K_{11} = K_{33}^{(1)} = 12, \quad K_{12} = K_{34}^{(1)} = -6\bar{\ell}, \quad (1.600)$$

$$K_{13} = K_{31}^{(1)} = -12, \quad K_{14} = K_{32}^{(1)} = -6\bar{\ell} \quad (1.601)$$

$$K_{22} = K_{44}^{(1)} = 4\bar{\ell}^2, \quad K_{23} = K_{41}^{(1)} = 6\bar{\ell}, \quad K_{24} = K_{42}^{(1)} = 2\bar{\ell}^2 \quad (1.602)$$

$$K_{33} = K_{11}^{(1)} + K_{33}^{(2)} = 12 + 12 = 24\bar{\ell}, \quad (1.603)$$

$$K_{34} = K_{12}^{(1)} + K_{34}^{(2)} = 6\bar{\ell} - 6\bar{\ell} = 0, \quad (1.604)$$

$$K_{44} = K_{22}^{(1)} + K_{44}^{(2)} = 4\bar{\ell}^2 + 4\bar{\ell}^2 = 8\bar{\ell}^2. \quad (1.605)$$

Similarly, the global geometric stiffness matrix elements (=terms) are

$$K_{G,11} = K_{G,33}^{(1)} = -36P_1, \quad K_{G,12} = K_{G,34}^{(1)} = 3P_1\bar{\ell}, \quad (1.606)$$

$$K_{G,13} = K_{G,31}^{(1)} = 36P_1, \quad K_{G,14} = K_{G,32}^{(1)} = 3P_1\bar{\ell} \quad (1.607)$$

$$K_{G,22} = K_{G,44}^{(1)} = -4P_1\bar{\ell}^2, \quad (1.608)$$

$$K_{G,23} = K_{G,41}^{(1)} = -3P_1\bar{\ell}, \quad K_{G,24} = K_{G,42}^{(1)} = P_1\bar{\ell}^2 \quad (1.609)$$

$$K_{G,33} = K_{G,11}^{(1)} + K_{G,33}^{(2)} = 36(2P_1 + P_2)\bar{\ell}, \quad (1.610)$$

$$K_{G,34} = K_{G,12}^{(1)} + K_{G,34}^{(2)} = -3P_2, \quad (1.611)$$

$$K_{G,44} = K_{G,22}^{(1)} + K_{G,44}^{(2)} = 4(2P_1 + P_2)\bar{\ell}. \quad (1.612)$$

These terms are then gathered in the matrices above (Eq. 1.594) to form the eigenvalue problem.

For small problems (small number of dofs), this is the best way to do assembly by hand. When the number of dofs is high, let's say more than ten, I suggest to let the computer assemble the global matrices for you using the element-wise assembly shown previously. However, the effort of training doing it by hand even in our century, is worth for continuous beam-columns and, especially, in frames and lateral-sway frames. The systematic establishment (or writing down) of the global matrices entering the eigenvalue problem is a very effective *weapon* in the hand of an engineer. All what you need, is the local matrices.

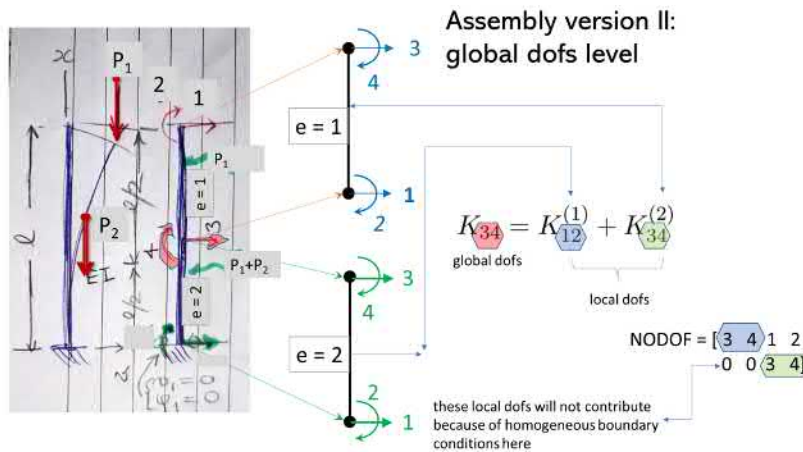


Figure 1.108: Assembly of global matrices.

* * * * *

* * * * *

About 'exact' interaction diagrams: Recall the above interaction equation (1.558) is approximate since derived using an approximation for the critical buckling mode. Probably, one approach is to use computational²³⁶ technology (FEM), to construct, for the case under study, the interaction diagram. Notice that, then, all the load combinations should be computed to determine the critical cases. Thus, you tabulate your loading cases, and for each one, do, at least, a linear buckling analysis with the software. Then, you gather all your results in a diagram that you will analyse with your brain, to find the *design* load combinations (= the most critical). This problem may also be, for simple cases, solved exactly²³⁷ but in a lengthy and boring manner that I probably let as a difficult exercise or a homework to solve, starting from the buckling differential equation

$$(EIv'''' - (N^0(x)v')') = 0 \tag{1.613}$$

²³⁶Please, let me know if some of the readers have already done such analysis in practice. I will integrate the idea into this notes for the benefit of the students.

²³⁷I confess; I have not done it. May be, it is more difficult than it seems to solve the problem exactly! Is this the reason that, such interaction buckling diagrams are found in usual textbooks? I have seen something about such interaction diagrams only in an old soviet-time formulary of strength of material but in only a tabulated form for columns with multiple non-proportional axial compression loading. The tables express, for special cases of practical importance, the ratios η_i as function of $x_i\ell$ or equivalent relative load locations along the column. I may reproduce one of such tables, if I remember.

with adequate boundary conditions. One *technical* 'difficulty' is that the known initial stress (= the normal force $N^0(x)$) is discontinuous at application points x_i along the column. However, at the end, finding roots for all load combinations may be not tractable, in practice. Another, may be more direct way than starting from the differential equation, is to use the *slope-deflection* method (with Berry's stability functions) and solve the problem as we did systematically for continuous beam-columns and frames in the basic course of *structural mechanics* famously called mechanics of beams and frames. Just write equilibrium and continuity and the problem is *almost* solved. Then account for boundary condition, and you obtain the eigenvalue problem providing us with the solutions. Remains, the may be intractable task, to find the roots of the transcendental equation expressing the criticality condition (determinant of homogeneous equilibrium equation system = 0). This last problem may be really difficult²³⁸ because the loads are not proportional. This have been said, let's stop.

* * * * *

Despite what has been said above, it will be interesting to re-do the examples above using the exact buckling mode of a cantilever, or just solving analytically the differential equation of buckling with this type of loading, and to see if the coefficient $0.3\pi^2$ will approach $1/4\pi^2$. I suspect (or hope) for beauty requirements that this coefficient should be equal to $1/4$. Please, let me know, when you will do it. For the moment, I stop here.

After 15 min, I could not resist the temptation to investigate this question. This is for the irresistible curiosity. So let the buckling mode be approximated by the exact buckling mode of the one a cantilever loaded with only one end-load P ;

$$v(x) \approx \hat{v}(x) = v_0[1 - \cos\left(\frac{\pi x}{2\ell}\right)] = v_0 \cdot \phi(x) \quad (1.614)$$

After simple integrations, one gets

$$\int_0^\ell EI \phi'' \phi'' dx = EI \frac{\pi^4}{32\ell^3} \quad (1.615)$$

$$\sum_i P_i \cdot \int_0^{x_i} \phi' \phi' dx = \sum_i P_i \cdot \frac{\pi^2}{8\ell} \left(\frac{x_i}{\ell} - \frac{1}{\pi} \sin\left(\frac{\pi x_i}{\ell}\right) \right) \quad (1.616)$$

$$\implies \sum_i P_i \cdot \left[\frac{x_i}{\ell} - \frac{1}{\pi} \sin\left(\frac{\pi x_i}{\ell}\right) \right] = \frac{1}{4} \cdot \pi^2 \frac{EI}{\ell^2} \quad (1.617)$$

$$\implies P \cdot \underbrace{\sum_i \eta_i \cdot \left[\frac{x_i}{\ell} - \frac{1}{\pi} \sin\left(\frac{\pi x_i}{\ell}\right) \right]}_{\equiv \alpha} = \underbrace{\frac{1}{4} \cdot \pi^2 \frac{EI}{\ell^2}}_{\equiv \hat{P}_E}, \quad (1.618)$$

²³⁸I have not tried it, I confess.

where P being a reference load. We see now that the critical buckling reference load $(P)_{cr}$ will be calculated concisely as

$$\alpha \cdot (P)_{cr} = \frac{1}{4} \cdot \pi^2 \frac{EI}{\ell^2}. \tag{1.619}$$

Finally the buckling coefficient ≈ 0.3 we obtained, using a lazy parabolic mode approximation, in Eq. (1.559) seems to be a not a so bad approximation of the very famous and legendary $1/4$ we know from Euler buckling cases for the cantilever. Refer to figure (1.109) to find out within what limits the interaction coefficient in Equation (1.618) varies. It varies between 0 and a bit less than 1. So, everything is well in Euler's kingdom.

Buckling failure space: It is, probably, more practical to rewrite the above interaction equation in a non-dimensional form by choosing the buckling load $\eta_i = P_i/\hat{P}_E$ as reference load, then the buckling failure boundary will be

$$\sum_i \eta_i \cdot \underbrace{\left[\frac{x_i}{\ell} - \frac{1}{\pi} \sin\left(\frac{\pi x_i}{\ell}\right) \right]}_{\equiv w_i} = \sum_i \eta_i w_i = 1, \tag{1.620}$$

where w_i being an estimate for the buckling load interaction coefficients. The safe domain will such the load combination point $(\eta_1, \eta_2, \dots, \eta_N)$ remains inside the region defined by such boundary given by the above equation in the hyperspace with coordinate axes $\eta_1, \eta_2, \dots, \eta_N$.

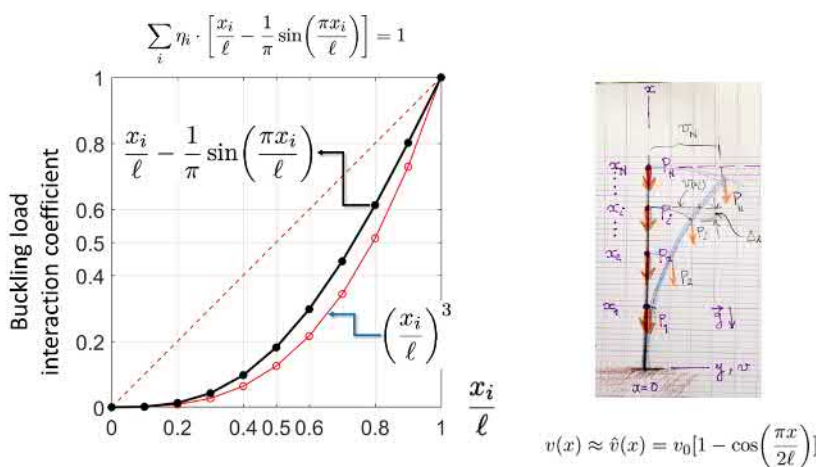


Figure 1.109: Buckling load interaction coefficient in Eq. (1.618). The interaction coefficients (or weights) were estimated using a parabolic mode approximation $v \approx v_0 \cdot (x/\ell)^2$ (the red line) and a cosine $v \approx v_0[1 - \cos(\pi x/2\ell)]$ (the black line).

However, now that we derived the load interaction buckling (approximative) diagram (Fig. 1.102), we may go back, if the reader wishes so, and apply analytical

methods and write the problem in terms of differential equations to solve. This way, he obtains, the analytical interaction equation and also to find out what will be the analytical 'exact' buckling coefficients. I will not do it here. We let it as a homework. You can find an example of such analytical approach with an application in the very classical textbook *Theory of Elastic Stability* by our grandfather of profession **Timoshenko & Gere** in *section 2.11: buckling of a bar with intermediate compressive forces, p. 98*. In the same section, Timoshenko, gives also an energy-based approximative method for solving such problems. The approach, is quite similar, in essence, as the one proposed in these notes.

Application example: Consider the cantilever column above with $P_1 = P_2 = P$ with P_1 at the free-end $x = \ell$ and P_2 at the mid-span $x_1 = \ell/2$. Assume constant bending rigidity. *Find the critical load.*

Now accounting for $\eta_1 = \eta_2 = 1$, we can write

$$P \cdot \sum_{i=1}^2 \eta_i \cdot \left[\frac{x_i}{\ell} - \frac{1}{\pi} \sin\left(\frac{\pi x_i}{\ell}\right) \right] = \frac{1}{4} \cdot \pi^2 \frac{EI}{\ell^2} \quad (1.621)$$

$$\implies P \cdot \left(\left[1 - \frac{1}{\pi} \sin(\pi) \right] + \left[\frac{1}{2} - \frac{1}{\pi} \sin\left(\frac{\pi}{2}\right) \right] \right) = \frac{1}{4} \cdot \pi^2 \frac{EI}{\ell^2} \quad (1.622)$$

$$\implies P \cdot \underbrace{(1 + 0.182)}_{=1.182} = \frac{1}{4} \cdot \pi^2 \frac{EI}{\ell^2} \quad (1.623)$$

which provides, finally, the critical buckling load for one reference axial force P as

$$(P)_{\text{cr}} = 0.846 \cdot \pi^2 \frac{EI}{4\ell^2} \approx 0.2 \cdot \pi^2 \frac{EI}{\ell^2}. \quad (1.624)$$

This result (Eq. 1.624) can be cross-checked to very probably correct by comparing it to the one given by the curves of the buckling load reduction factor in Figure (1.107) by setting $\eta_1 = 1$ or $\eta_2 = 1$. From these curves, one can see that the obtained approximate coefficient is close to 0.2 (on the graph) which was obtained using FEM (even though 'FEM' has not, necessarily, the last word.²³⁹

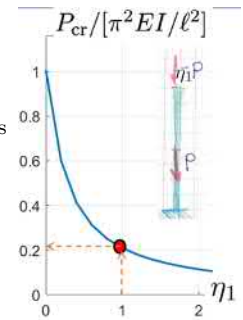
One fast and reliable cross-check is obtained when both loads are applied at

²³⁹Even when I used the reference which was obtained by FEM, we do not forget the universal GIGO-principle that *garbage in, garbage out..* One should be careful with software because one can solve exactly wrong equations or solve exactly the correct equations but using wrong data. Or even sometimes, solve correctly a correct model but *interprets erroneously the results* because of a non-solid understanding of structural mechanics. So, this is why a firm understanding of the underlying theories of the models we are working with is necessary. Additionally, any analysis or structural design done by any qualified engineer also needs naturally to be the cross-checked independently by its peers because the error is human. This is the way it is done in the profession.

the mid-span. For sure, the critical load for this case

$$2P_{cr} = \frac{1}{4} \cdot \pi^2 \frac{EI}{(\ell/2)^2} = \pi^2 \frac{EI}{\ell^2} \implies \underbrace{P_{cr} = 0.5\pi^2 \frac{EI}{\ell^2}}_{\text{both loads at mid-span}} > \underbrace{0.2 \cdot \pi^2 \frac{EI}{\ell^2}}_{\text{our example with separated loads}} \quad (1.625)$$

should be higher than for our case $0.2 \cdot \pi^2 EI/\ell^2$ with the two loads separated (one at the tip and the other at the mid-span). This is the upper-side of the verification (Cf. margin figure).



Simply supported beam-column with intermediate compressive load

FEM-Cross-check.

Consider the simply supported beam-column with two centric axial loads P_1 and P_2 ; the first load is applied at the roller and the second one, at the mid-span. This example is treated analytically in Timoshenko.²⁴⁰ In the present subsection, we²⁴¹ use energy method.

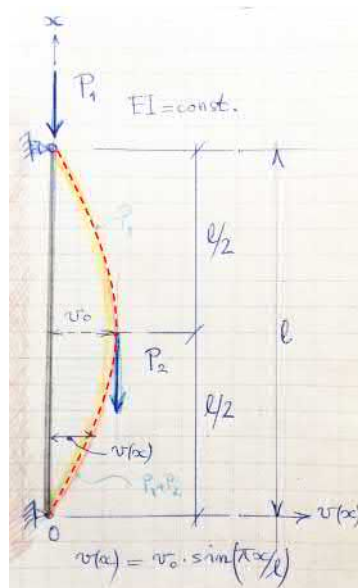


Figure 1.110: Simply supported beam-column loaded with multiple axial loads.

So let the first buckling mode be approximated by the exact analytical buck-

²⁴⁰Theory of Elastic Stability **Timoshenko** & Gere in section 2.11: buckling of a bar with intermediate compressive forces, p. 98 .

²⁴¹we = the reader + me, the writer of these notes. The subject 'we' does not mean 'we, the king', but instead, a cooperative we.

ling mode for the case with only one end-load P at the roller.

$$v(x) \approx \hat{v}(x) = v_0 \sin\left(\frac{\pi x}{\ell}\right) = v_0 \cdot \phi(x) \quad (1.626)$$

After integrations²⁴², one gets

$$\delta(\Delta U) : \delta v_0 = - \int_0^\ell EI \phi'' \phi'' dx = \frac{\pi^4}{2\ell^3} \cdot EI \quad (1.627)$$

$$\delta(\Delta W_{\text{ext}}) : \delta v_0 = \sum_{i=1}^2 P_i \cdot \int_0^{x_i} \phi' \phi' dx = P_1 \frac{\pi^2}{2\ell} + P_2 \frac{\pi^2}{4\ell} = (P_1 + \frac{1}{2}P_2) \cdot \frac{\pi^2}{2\ell} \quad (1.628)$$

$$\delta(\Delta U) + \delta(\Delta W_{\text{ext}}) = 0, \forall \delta v_0 \implies \underbrace{\left(P_1 + \frac{1}{2}P_2\right)}_{\equiv P_{cr}} = \pi^2 \cdot \frac{EI}{\ell^2} \quad (1.629)$$

where P being a reference load. We see now that the critical buckling reference load $(P)_{cr}$ will be calculated concisely as

$$\left(P_1 + \frac{1}{2}P_2\right)_{cr} = (\eta_1 + \frac{1}{2}\eta_2) \cdot (P)_{cr} = \pi^2 \frac{EI}{\ell^2}. \quad (1.630)$$

Application example: Let's in the above $P_1 = P_2 = P$ (Fig. 1.110). Consequently,

$$\left[1 + \frac{1}{2}\right] \cdot P_{cr} = \pi^2 \frac{EI}{\ell^2} \implies P_{cr} = \frac{2}{3} \cdot \pi^2 \frac{EI}{\ell^2} \approx 0.667 \cdot \pi^2 \frac{EI}{\ell^2}. \quad (1.631)$$

In other words, the above results means that, the column buckles when both loads $P_1 = P_2 \equiv P$ are applied together and when both loads are increased simultaneously (proportional loading) to reaches the critical value

$$(P)_{cr} = \frac{2}{3} \cdot \pi^2 \frac{EI}{\ell^2} \approx 0.667 \cdot \pi^2 \frac{EI}{\ell^2}. \quad (1.632)$$

This means that the column supports (kantaa), at buckling, the total load of

$$(P_1 + P_2)_{cr} = 2P_{cr} = 2 \times \frac{2}{3} \cdot \pi^2 \frac{EI}{\ell^2} = 1.333 \cdot \pi^2 \frac{EI}{\ell^2} \quad (1.633)$$

when they are located at the roller-support and the mid-span. For comparison, when the mid-span axial load is zero, the allowable load, at the roller-support, is naturally the Euler critical buckling load $P_E = 1 \cdot \pi^2 EI / \ell^2$. Recall that the above obtained estimates for the critical buckling loads (Equations 1.632 and 1.633) are energy based *approximations*.

²⁴²I confess, this time, I did these simple integrations symbolically in Matlab. Lazyness can visit anyone, from time to time ... but this will not be a habit.

Cross-checking: the above approximative solution by comparing it to the analytical solution given in Timoshenko²⁴³ in the form

$$(P_1 + P_2)_{cr} = \pi^2 \frac{EI}{L^2}, \tag{1.634}$$

where $L = \beta\ell$, being the reduced buckling length. The reduction factors β are given by Timoshenko in tabular form (Table 2-6 of same reference just cited above). These coefficients are obtained from the analytical solution. For our example $\beta = 0.87$ (Fig. 1.111), so the *total analytical* buckling load will be

$$(P_1 + P_2)_{cr} = \pi^2 \frac{EI}{L^2} = \pi^2 \frac{EI}{(0.87\ell)^2} = 1.321 \cdot \pi^2 \frac{EI}{\ell^2} \tag{1.635}$$

which corresponds to one *analytical* critical reference load $P_{cr} = 0.665\pi^2 EI/\ell^2$. As a conclusion, we can say that the approximations (Equations 1.632 and 1.633) are practically the same ($< 1\%$) than the analytical value (Eq. 1.635). In the following, we reproduce, for internal use only, Table 2-6 from Timoshenko (Fig. 1.111). In this table, next notations are used: $n = EI_2/EI_1$, $m = (P_1 + P_2)/P_1$ and $\ell_1 = \ell_2 = \ell/2$. Before closing this subsection and for pedagogical purposes,

$(P_1 + P_2)_{cr} = \pi^2 \frac{EI}{L^2}$ where $L = \beta\ell$, being the reduced buckling length. $n = EI_2/EI_1$, $m = (P_1 + P_2)/P_1$, $\ell_1 = \ell_2 = \ell/2$

TABLE 2-6. VALUES OF L/ℓ FOR COLUMN IN FIG. 2-38, WITH $\ell_1 = \ell_2$

$n \backslash m$	1.00	1.25	1.50	1.75	2.00	3.00
1.00	1.00	0.95	0.91	0.89	0.87	0.82
1.25	1.06	1.005	0.97	0.94	0.915	
1.50	1.12	1.06	1.02	0.99	0.96	
1.75	1.18	1.11	1.07	1.04	1.005	
2.00	1.24	1.16	1.12	1.08	1.05	

Theory of Elastic Stability Timoshenko & Gere in section 2.11: buckling of a bar with intermediate compressive forces, p. 98.

Figure 1.111: Analytical buckling length reduction factor $\beta = L/\ell$ for the simply supported beam-column with two axial compressive loads.

I reproduce the Matlab (symbolic) code that I used to do the *simple* integrations in the weak form (neutral equilibrium condition) above (Fig. 1.112). Here, the *weak form*, or more physically, the *virtual work principle* expresses simply the condition for the neutral equilibrium necessary to buckling.

²⁴³*Theory of Elastic Stability Timoshenko & Gere in section 2.11: buckling of a bar with intermediate compressive forces, p. 98.*

Computer algebra:

```

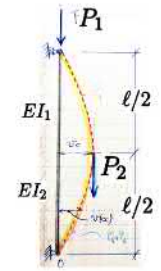
1 % Simply supported beam with ...
2 % intermediate compressive axial loads
3 % Energy method
4 % Author: Baroudi D. 2021
5 % -----
6 syms EI L P v v0 x
7 syms delta_F delta_F
8 syms EI P2
9
10 % -----
11 % multiple load simply supported
12 % -----
13 v(x, v0, L) == v0 * sin(pi * x / L)
14 d1_v(x, v0, L) == simplify(diff(v, x))
15 d2_v(x, v0, L) == simplify(diff(d1_v, x))
16
17 % -----
18 phi(x, L) == sin(pi * x / L)
19 d1_phi(x, L) == simplify(diff(phi, x))
20 d2_phi(x, L) == simplify(diff(d1_phi, x))
21 % -----
22 % variation of work increment of P1 and P2 ---
23 delta_W1(L, P1) == P1 * int(d1_phi(x, L) * d1_phi(x, L), [0 L])
24 delta_W2(L, P2) == P2 * int(d1_phi(x, L) * d1_phi(x, L), [0 L/2])
25 delta_W(L, P1, P2) == delta_W1(L, P1) + delta_W2(L, P2)
26
27 % variation of strain energy increment
28 delta_U(L, EI) == EI * int(d2_phi(x, L) * d2_phi(x, L), [0 L])
29
30

```

```

Solution by Matlab symbolic:
% solution:
% phi(x, L) = sin(pi*x/L)
% d1_phi(x, L) = (pi*cos(pi*x/L))/L
% d2_phi(x, L) = -(pi^2*sin(pi*x/L))/L^2
%
% delta_W(L, P1, P2) = (P1*pi^2)/(2*L) + (P2*pi^2)/(4*L)
% delta_U(L, EI) = (EI*pi^4)/(2*L^3)
%
% delta_U - delta_W = 0 ==> P1 + P2/2 = pi^2 * EI / L^2
%

```



$$\delta(\Delta U) : \delta v_0 = - \int_0^L EI \phi'' \phi'' dx = \frac{\pi^4}{2L^3} \cdot EI$$

$$\delta(\Delta W_{ext}) : \delta v_0 = \sum_{i=1}^2 P_i \cdot \int_0^{x_i} \phi' \phi' dx = P_1 \frac{\pi^2}{2L} + P_2 \frac{\pi^2}{4L} = (P_1 + \frac{1}{2}P_2) \cdot \frac{\pi^2}{2L}$$

Figure 1.112: Matlab symbolic code to do derive *lazily* the approximate the buckling load for the simply supported beam-column with two axial compressive loads, by energy methods.

Effect of axial force on lateral sway of columns

The idea in this subsection is to 1) demonstrate the geometric non-linearity inherent to this problem 2) to derive the *formula* giving the lateral sway v_0 as function of relative compression P/P_E in a simple case of cantilever an simply supported column (Fig. (1.113 a).

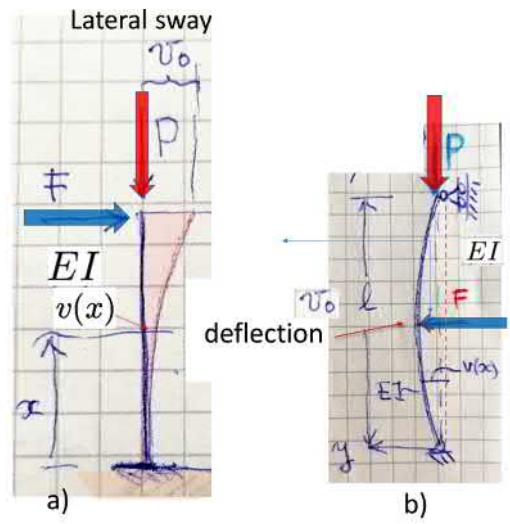


Figure 1.113: Lateral displacement is non-linearly enhanced by compression. a) Lateral sway in a cantilever column. b) mid-span lateral deflection for a pin-ended column.

The *formula* will be derived using virtual work principle (virtual unit dummy-load theorem). Naturally for real complex cases one needs, in addition, to use FEM-computational technology, experimental approach without forgetting experimental validation of the FEM-models for cases where the human life is in play. This problem is very actual in tall buildings.

The cantilever column: The column-beam of Figure (1.113 b) will be also treated in the same way to demonstrate and convince²⁴⁴ the student that virtual work principle holds also in non-linear cases.

Cantilever column: Consider again the cantilever shown in Figures (1.113 a)) and (1.98). We have determined his lateral displacement v_0 due to and a transversal load F (wind load, for instance) under constant axial centric compression P . By virtue of the virtual force principle

$$1 \cdot v_0 = \int_0^\ell \frac{M \cdot \bar{M}_1}{EI} dx \tag{1.637}$$

$$\text{where } M = M_F + M_P \tag{1.638}$$

we obtained the following result for the sway v_0

$$1 \cdot v_0 = \int_0^\ell \frac{M \cdot \bar{M}_1}{EI} dx \tag{1.639}$$

$$= \frac{F\ell^3}{3EI} + \frac{P4v_0\ell^2}{\pi^2 EI} \tag{1.640}$$

$$\Rightarrow v_0 = \underbrace{\frac{F\ell^3}{3EI}}_{\text{deflection when } P=0} \cdot \underbrace{\frac{1}{1 - \frac{P}{P_E}}}_{\text{amplification factor}} \tag{1.641}$$

where the Euler buckling reference load $P_E = 1/4\pi^2 EI/\ell^2$ have been used. In the above result, the *exact first buckling mode*

$$v(x) = v_0[1 - \cos(\pi x/2\ell)]. \tag{1.642}$$

²⁴⁴In fact you seriously speaking, you may remember that in the (primal) virtual work principle

$$- \int_V \sigma : \delta(\nabla \mathbf{u}) dV + \int_V \mathbf{f} \cdot \delta \mathbf{u} dV + \int_{\partial V} \mathbf{t} \cdot \delta \mathbf{u} dS = \int_V \rho \ddot{\mathbf{u}} \cdot \delta \mathbf{u} dV, \quad \forall \delta \mathbf{u} \tag{1.636}$$

we do not make any assumption about the material model neither on how large or small are the displacements. Such simplifying assumptions may be made later case by case. So, the principle holds for any material behaviour and for any displacement amplitude. In fact, it expresses Newton' motion law for deformable bodies in a more effective and *elegant* way. So, this is for the virtual displacement principle. The virtual force principle, is its conjugate and we have shown it in class when presenting the general force method. I may be rewrite it soon here.

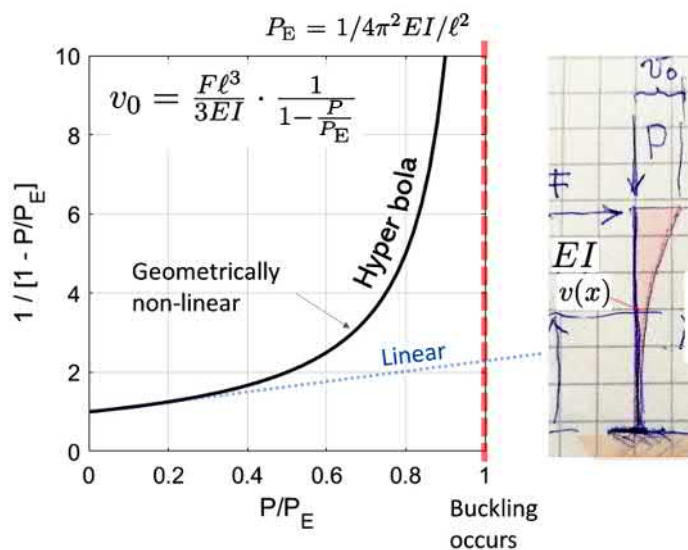


Figure 1.114: How lateral lateral sway v_0 , in a cantilever column, is non-linearly enhanced by compression.

has been used as an approximation of the deflection. To recall the reader, we had already few subsection before, solved this exercises. In this case we had

$$M_F(x) = F(\ell - x), \quad M_P(x) = P_0 \cdot (v_0 - v(x)), \quad (1.643)$$

$$\bar{M}_1(x) = \ell - x, \quad \text{results from unit-dummy load } \bar{F} = 1. \quad (1.644)$$

We see clearly, this is a classical result, that axial compression enhances the lateral sway deflection by the *non-linear amplification factor* $v_0 \propto 1/[1 - \frac{P}{P_E}]$ as given by the formula. The graph of this relation can be clearly expressed by a hyperbola (Figure 1.114).

$$v_0 = \frac{F\ell^3}{3EI} \cdot \frac{1}{1 - \frac{P}{P_E}} \quad (1.645)$$

Notice, on the graph, when the deviation from the linear behaviour theory starts, let's say this approximately begins for $P/P_E > 1/3$. It is going without saying that the bending normal (compressive) stresses are also *non-linearly* enhanced. In overall, the maximum stress will be at the clamping (at the outer-material fiber located at a distance y_{\max} from the neutral axis) and will be

$$\sigma_{\max} = \frac{P}{A} + \frac{M_{\max}}{W^{(e)}}, \quad \text{where } M_{\max} = F\ell + Pv_0. \quad (1.646)$$

where the smallest flexural elastic resistance (or section modulus, *taiivutusvastus*) of the cross-section being $W^{(e)} = I_{\max}/y_{\max}$. I let the reader rediscover the remaining notation which should be familiar from strength of material courses.

Maximum bending moment: Let's find out the expression for the amplification factor of the bending moment due to transversal load F and enhanced (amplified) by the axial compressive force P because of geometric non-linearity (buckled shape). The maximum moment at $x = \ell$, the clamped support, is

$$M_{\max} = F\ell + Pv_0 \tag{1.647}$$

$$= F\ell + P \cdot \frac{F\ell^3}{3EI} \cdot \frac{1}{1 - \frac{P}{P_E}} \tag{1.648}$$

$$= F\ell \cdot \left(1 + \frac{\ell^2}{3EI} \cdot \frac{P}{1 - \frac{P}{P_E}} \right) \tag{1.649}$$

$$= \underbrace{F\ell}_{M(P=0)} \cdot \underbrace{\left(1 + \frac{\pi^2}{12} \cdot \frac{\frac{P}{P_E}}{1 - \frac{P}{P_E}} \right)}_{\approx 0.822 \text{ amplification factor}} \tag{1.650}$$

where, again, $P_E = 1/4\pi^2 EI/\ell^2$ being the reference Euler critical buckling load. So, the maximum bending moment amplification factor is

$$M_{\max} = F\ell \cdot \left(1 + 0.822 \cdot \frac{\frac{P}{P_E}}{1 - \frac{P}{P_E}} \right) \equiv \alpha_M \cdot F\ell \tag{1.651}$$

The graphical representation is shown in Figure (1.115). One can notice that, equivalently, as for lateral sway, the maximum bending moment grows (amplified) very quickly for high compression, approximately when $P/P_E > 1/3$.

The cantilever column: Consider simply supported slender beam which is axially compressed by a centric load P (Fig. (1.113 a)). Let a transversal load F being acting at its mid-span. The question. *Determine the deflection v_0 at the mid-span. How it depends on P ?*

We can answer this question exactly by assuming the deflected shape following the first buckling mode

$$v(x) = v_0 \sin(\pi x/\ell) \tag{1.652}$$

However, to have more fun and let's see what result (or difference) we will obtain if one uses an approximation of the buckling mode as

$$v(x) = 4v_0 \frac{x}{\ell} \left(\ell - \frac{x}{\ell} \right) \tag{1.653}$$

It is quite interesting to superpose both buckling modes in one plot (Fig. ??). They are really very close, I am even a bit surprised. So, we can expect to obtain quite a good approximation for the deflection v_0 . Note that we will use the force method and thus we need only the bending moments directly determined from equilibrium. This is easy to do since our structure is statically determined.

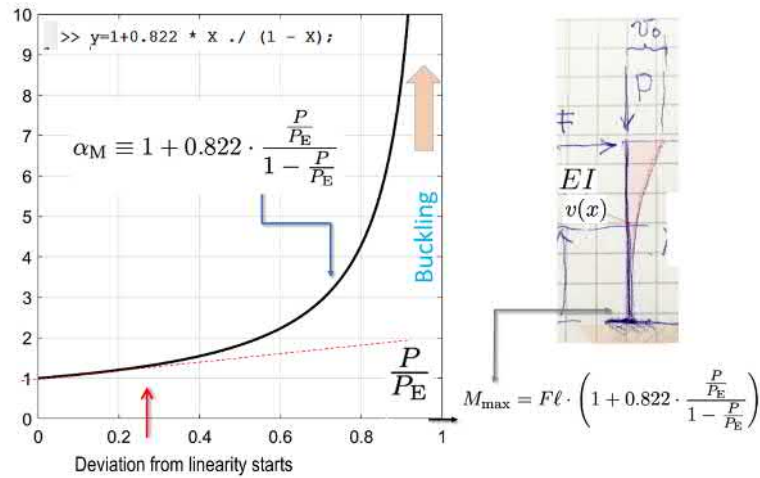


Figure 1.115: Maximum bending moment amplification factor in a cantilever column, under constant compression. The Euler reference load is $P_E = 1/4\pi^2 EI/\ell^2$.

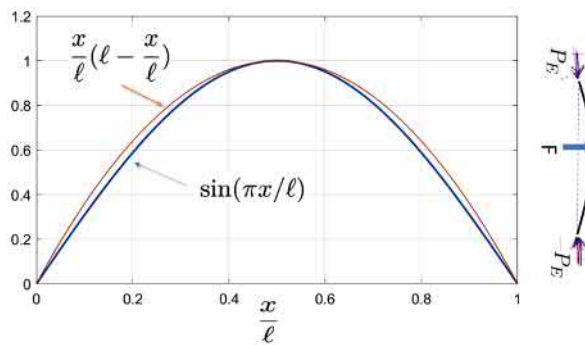


Figure 1.116: Exact and approximate first buckling mode.

The bending moment due to axial load and lateral force is symmetric about the mid-span and is simply, for the left part, given by $x \in [0, \ell/2]$

$$M = M_P + M_F = P \cdot v(x) + \frac{Fx}{2}, \quad x \in [0, \ell/2] \quad (\text{remaining part being symmetric}) \quad (1.654)$$

Let's go and do. Put a virtual force $\bar{F} = 1$ at the mid-span and, as usual,

$$1 \cdot v_0 = \int_0^\ell \frac{M \cdot \bar{M}_1}{EI} dx \tag{1.655}$$

$$= 2 \int_0^{\ell/2} \left[\frac{F}{2} x \right] \left[\frac{1}{2} x \right] \cdot \frac{1}{EI} dx + 2 \int_0^{\ell/2} \left[4Pv_0 \frac{x}{\ell} \left[1 - \frac{x}{\ell} \right] x \right] \left[\frac{1}{2} x \right] \cdot \frac{1}{EI} dx \tag{1.656}$$

$$= \frac{F\ell^3}{48EI} + \frac{5}{48} \frac{Pv_0\ell^2}{EI}. \tag{1.657}$$

The deflection v_0 can be solved after factorisation as

$$v_0 = \frac{F\ell^3}{48EI} \cdot \frac{1}{1 - \frac{5}{48} \frac{P\ell^2}{EI}} = \underbrace{\frac{F\ell^3}{48EI}}_{\text{deflection for } P=0} \cdot \underbrace{\frac{1}{1 - \frac{P}{P_E}}}_{\text{amplification factor}}, \tag{1.658}$$

where the estimated critical buckling load being

$$\hat{P}_E = \frac{48}{5} \frac{EI}{\ell^2} = 0.973 \cdot \pi^2 \frac{EI}{\ell^2} \approx \frac{\pi^2 EI}{\ell^2} \equiv P_E. \tag{1.659}$$

To find the buckling load, it is sufficient find P for which the denominator in equation (1.658) tends to zero. (amplitude v_0 is 'blowing up'.)

Let's stop a bit and analyse the results given by the formula (Eq. 1.658).

- 1) we obtained an approximation of the buckling load which approaches from below the analytical known critical load. (keep in mind that we used the force method).
- 2) The amplification factor is non-linear and follows the same form as already determined earlier for the lateral-sway of the cantilever column.

To close this subsection, let's relax a bit. This is what I recall from physics lesson on pendulums in high-school. Students were often asked to solve problem on the black-board. The fraction $48/5 = 9.6$ seems to be a good approximation (difference less than 3 %) for $\pi^2 = 9.869604401089358 \dots$. From high-school, some of us, learn that the free-falling acceleration [m/s.s] $g \approx \pi^2$ with a difference about only 0.6 %. This last approximation is often used to simplify fast hand calculations for the circular frequency ω of pendulums where appears often $\sqrt{g/\ell}$ that can be replaced approximately by $\sqrt{\pi^2/\ell} \approx \pi/\sqrt{\ell}$. The last expression being easier to estimate after expressing approximately ℓ , the length of the pendulum, with two closer squares bracketing it from below and above. To finish, let's recall that $\pi \approx 22/7$ is a very precise fractional approximation for π , even if in this era of computers in our pockets, this knowledge may seem of non-use. In older time, some people may even kill to obtain it when others were keeping it secret. Some

even established temples around such secrets to keep the power on others. This is another story.²⁴⁵

Let's leave the word of critical buckling load approximations²⁴⁶ using energy principles and enter a new section getting familiar with geometrically non-linear FE-analysis (GNA) and some other key concepts of stability as for instance, asymptotic analysis. We will also investigate how elastic supports or foundation will change fundamentally the stability behaviour. Patience.

1.12.8 Linear buckling analysis of simply supported column

Linear buckling analysis of a straight column which is simply supported. The axial compressive load P is centric. The column is initially ideally straight.

The results of the FE-analysis, critical loads and corresponding modes, are shown in Figure (1.117). In the FE-analysis, the column was treated as a two-

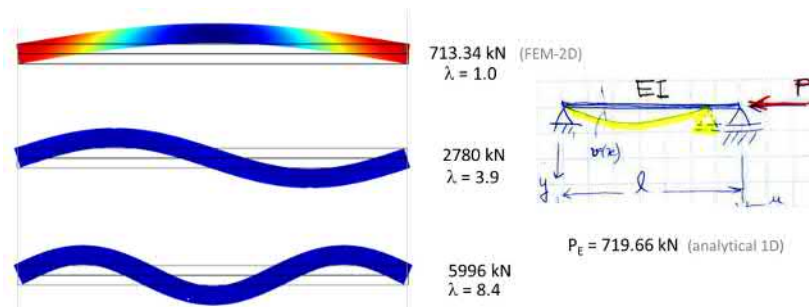


Figure 1.117: First three critical loads and respective buckling modes. Naturally, the smallest load being the buckling load. the load parameter $\lambda = P/P_{cr,2D}$. In this computation $P_{E,1D}/P_{cr,2D} = 1.01$.

dimensional elastic domain (not as a one-dimensional beam²⁴⁷) of width b . The buckling load $P_{cr,2D} = 713$ kN and the Euler $P_{E,1D} = 720$ kN. In this computation the one-dimensional model seems, with respect to the buckling load, being a

²⁴⁵You may be not know that for long time the irrationality of $\sqrt{2}$ was kept secret by one sect in ancient Greece (the Pythagorians). When one member of the sect came and said that, there is someone outside demonstrated that $\sqrt{2}$ is irrational, he was quickly killed to keep the secret from other members. The truth of this last 'legend' is not verified.

²⁴⁶I recall one related joke about approximations: Some physicists are convinced that the reality is only an approximation for their equations, while an engineer, especially a civil engineer like you and me, think humbly that, it is these equations which are approximations of the reality. However, some aspects of reality are brought to life by mathematical models as it is the case with gravitational waves.

²⁴⁷I have my reasons that the reason does not know for doing that.

bit stiffer²⁴⁸ than the two-dimensional 'beam' $P_{E,1D}/P_{cr,2D} = 1.01$, where the classical Euler buckling load being $P_{E,1D} = \pi^2 EI/\ell^2$.

The data for this example are : rectangular cross-section length $\ell = 1$ m, height $h = 50$ mm, width $b = \ell/10$, $P_E = 720$ kN (1-D), $EI = 72.917$ kN.m², $E = 70$ GPa, $\nu = 0.33$.

1.12.9 Asymptotic post-buckling analysis of simply supported column

In the following, analytical approach will be used. The aim in this section is to determine asymptotically the post-buckling behaviour of the axially compressed simply supported column. The increase of load $P = P_E + \Delta P$ being centric (Figure 1.118). This means that one should derive the force-displacement relation $f(P, v) = 0$ for moderate rotations in the neighbourhood of $P_{cr} \equiv P_E = \pi^2 EI/\ell^2$. Recall again, that by definition the asymptotic analysis can drive conclusions only

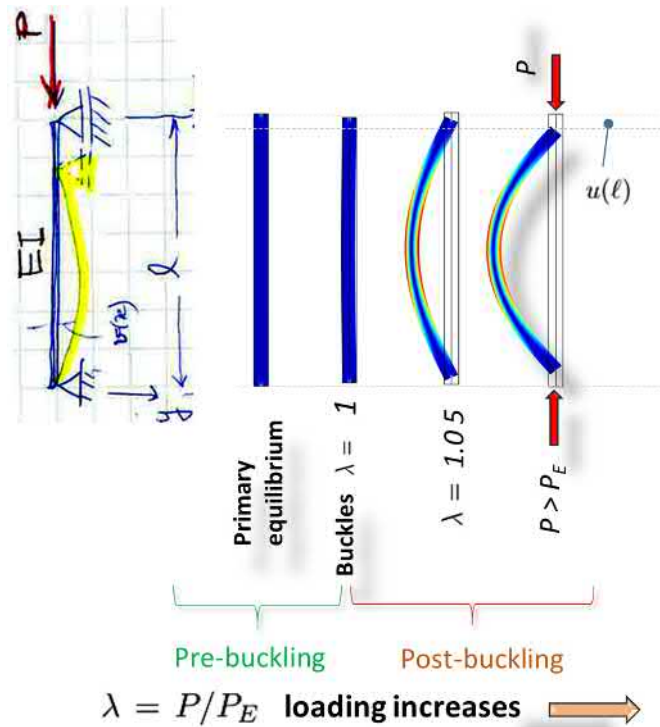


Figure 1.118: Post-buckling of simply supported column.

about the local stability around the *point* the asymptotic expansion is performed.

²⁴⁸Recall Rayleigh quotient minimising property.

So, nothing can be said about stability beyond this tiny expansion neighbourhood. for that, appropriate computational or experimental tools should be taken.

In the following we use the Lagrangian formulation. We want to use approximate energy methods to solve the problem by 'hand'²⁴⁹. Assume a (bifurcational) flexural deflection mode in the form²⁵⁰

$$v(x) = v_0 \sin(\pi x/\ell). \quad (1.660)$$

which corresponds to the *lowest buckling load and mode*, potentially, more 'dangerous' geometric imperfection²⁵¹.

1.12.10 Lagrangian curvature

Assuming that in the neighbourhood of post-buckled configuration the additional stretching from axial force being negligible as compared to the one from bending

$$du = du(N) + du(M) \approx du(M) \quad (1.661)$$

and therefore the infinitesimal length of a material element $dx = ds$ does not change (incompressible) (1.119)

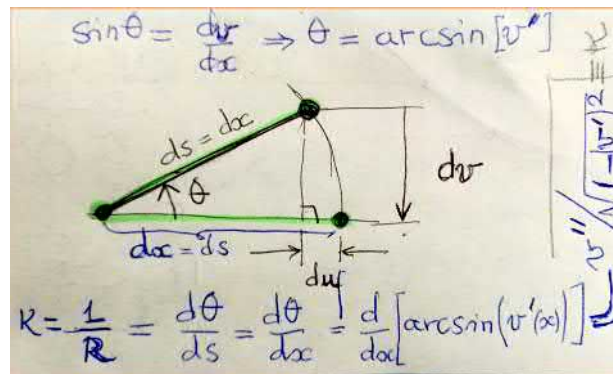


Figure 1.119: Kinematics of a Lagrangian element dx and the definition of curvature κ .

$$\kappa = -\frac{v''}{\sqrt{1 - v'^2}} \quad (1.662)$$

²⁴⁹It's late, I prefer right now to programme this in Matlab symbolic toolbox in `Post-buckling-simple-beam.m`, to avoid mistakes.

²⁵⁰In the following, we study only the case for $a_0 > 0$. The complement case $a_0 < 0$ can be deduced by changing the direction of y - axis to its opposite, and then the study is exactly the same as for $a_0 > 0$ with the same results.

²⁵¹To add a reference for this claim.

where the minus sign being a sign convention for positive curvature. From the right-angle triangle (1.119) and using Pythagoras one obtains the shortening

$$du = [1 - \sqrt{1 - v'^2}]dx \quad (1.663)$$

and therefore, the shortening $u(\ell)$ at the point of application of the load P will be

$$u(\ell) = \int_0^\ell du = \int_0^\ell [1 - \sqrt{1 - v'^2}]dx. \quad (1.664)$$

Consequently, the work increment of the load P during buckling is

$$\Delta W_e = Pu(\ell) = P \int_0^\ell du = P \int_0^\ell [1 - \sqrt{1 - v'^2}]dx. \quad (1.665)$$

So, now in the total potential energy increment (equation 1.185) one should use an asymptotic expansion for the increment of Lagrangian curvature κ and for the shortening, due to flexural buckling, of the column. For such moderate displacements and rotations, thus

$$\kappa = -\frac{v''}{\sqrt{1 - v'^2}} \approx -v''[1 + \frac{1}{2}v'^2 + \frac{3}{8}v'^4 + \dots] \quad (1.666)$$

where, now

$$\Delta \Pi = \frac{1}{2} \int_0^\ell EI \kappa^2 dx - Pu(\ell) \quad (1.667)$$

$$= \frac{1}{2} \int_0^\ell EI \left(\frac{v''}{\sqrt{1 - v'^2}} \right)^2 dx - P \int_0^\ell [1 - \sqrt{1 - (v')^2}] dx. \quad (1.668)$$

The idea further, in the asymptotic approach, is that one considers equilibrium paths locally in the vicinity some interesting point.

Such point can be the bifurcation point. You want to find the load-displacement curve (equilibrium path) around this point in an approximative way. The approximation is achieved by asymptotic developments (Taylor series) of of the terms in the total potential energy increment. That is why, here, for instance, the curvature and the shortening can be approximated with truncated Taylor series. (this is for the story).

For moderate rotations and displacements, let's keep only two terms of the Taylor expansions of the curvature (Figure 1.120) and the stretching (compression), so

$$\kappa \approx -v''[1 + \frac{1}{2}v'^2] \quad (1.669)$$

$$du/dx = 1 - \sqrt{1 - (v')^2} \approx 1 - [1 - \frac{1}{2}v'^2] = \frac{1}{2}v'^2 \quad (1.670)$$

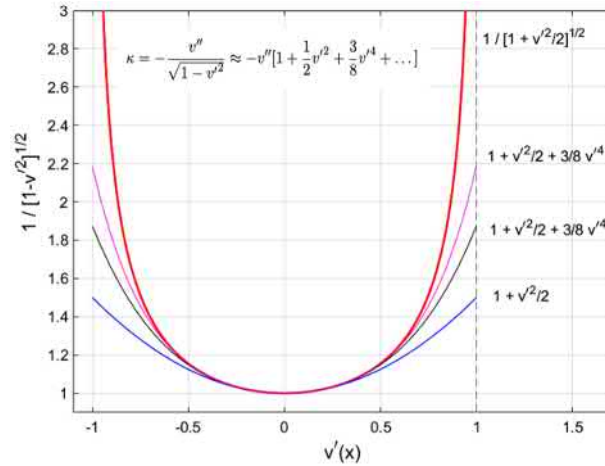


Figure 1.120: Taylor expansions of the denominator of Lagrangian curvature.

So, the approximate increment of the potential energy is now

$$\Delta\Pi \approx \frac{1}{2} \int_0^\ell EI v''^2 [1 + \frac{1}{2} v'^2]^2 dx - \frac{1}{2} P \int_0^\ell (v')^2 dx, \quad (1.671)$$

which holds for moderate rotations²⁵² and displacement and assuming, again, that the centreline for such load increment ΔP , remains practically incompressible.

Using two terms for the expansion of the curvature, and after performing the mathematical operations one obtains the change in total potential energy only as function of P , v_0 and the parameters L and EI .

I reproduce the total potential energy increment in its raw form²⁵³ as produced by the `Matlab symbolic toolbox`, after symbolic differentiation `Delta-Pi(v0, L) = -(P * v0^2 * pi^2)/(4 * L) + (EI * v0^2 * pi^4 * (32 * L^4 + 8 * pi^2 * L^2 * v0^2 + pi^4 * v0^4))/(128 * L^7)` which after being (`= LATEXed`), reads

$$\Delta\Pi = -\frac{\pi^2}{4} P \ell \left(\frac{v_0}{\ell}\right)^2 + \frac{\pi^2 EI}{\ell^2} \cdot \frac{\pi^2}{128} \left(\frac{v_0}{\ell}\right)^2 \cdot \ell \left[32 + 8\pi^2 \left(\frac{v_0}{\ell}\right)^2 + \pi^4 \left(\frac{v_0}{\ell}\right)^4\right] \quad (1.672)$$

$$= -\frac{\pi^2}{4} P \ell \delta^2 + P_E \cdot \frac{\pi^2 \ell}{128} \delta^2 [32 + 8\pi^2 \delta^2 + \pi^4 \delta^4] \equiv \Delta\Pi(\delta, \lambda; \ell), \quad (1.673)$$

where $\delta = v_0/\ell$ and $\lambda = P/P_E = (P_E + \Delta P)/P_E$ being the relative deflection, and force, respectively. From the stationarity condition

$$\delta(\Delta\Pi(v_0; P)) = 0 \implies d\Delta\Pi(v_0; P)/dv_0 = 0 \implies \quad (1.674)$$

²⁵²Limits to be defined.

²⁵³Reproduced for satisfying curiosity of the reader.

follows the equilibrium equation (force-displacement curve) , in its raw form²⁵⁴ as produced by the Matlab symbolic toolbox, after symbolic differentiation being (= L^AT_EXed) gives the *load-deflection* (equilibrium path) as

$$-32P\ell^6 + 32EI\pi^2\ell^4 + 16EI\pi^4\ell^2v_0^2 + 3EI\pi^6v_0^4 = 0 \implies \quad (1.675)$$

$$\implies P = \frac{\pi^2EI}{\ell^2} + \frac{1}{2} \frac{\pi^2EI}{\ell^2} \cdot \pi^2 \left(\frac{v_0}{\ell}\right)^2 + \frac{3}{32} \frac{\pi^2EI}{\ell^2} \cdot \pi^4 \left(\frac{v_0}{\ell}\right)^4 \quad (1.676)$$

$$P = P_E \left[1 + \frac{1}{2} \cdot \pi^2 \left(\frac{v_0}{\ell}\right)^2 + \frac{3}{32} \cdot \pi^4 \left(\frac{v_0}{\ell}\right)^4 \right]. \quad (1.677)$$

Rewriting the load-deflection 'curve' in dimensionless form, one obtains, finally,

$$\lambda \approx 1 + \frac{1}{2}\pi^2\delta^2 + \frac{3}{32}\pi^4\delta^4 = 1 + \frac{1}{2}\pi^2\delta^2 \left[1 + \frac{2 \cdot 3}{32}\pi^2\delta^2 \right], \quad (1.678)$$

where $\delta = v_0/\ell$ and $\lambda = P/P_E$ being the relative deflection, and thrust force,

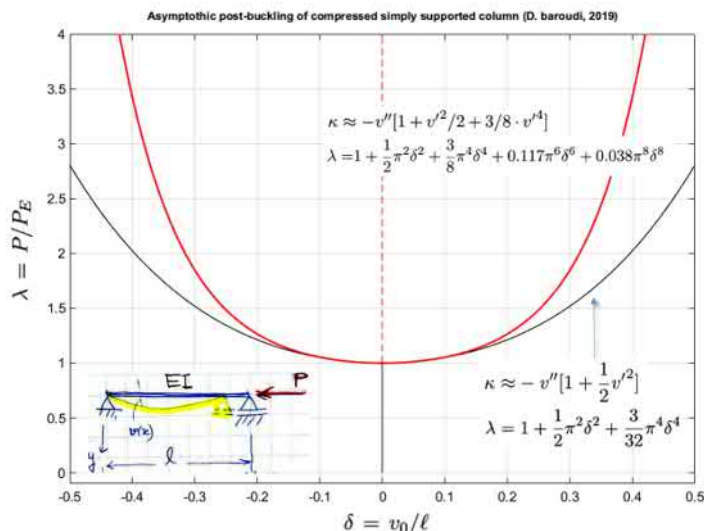


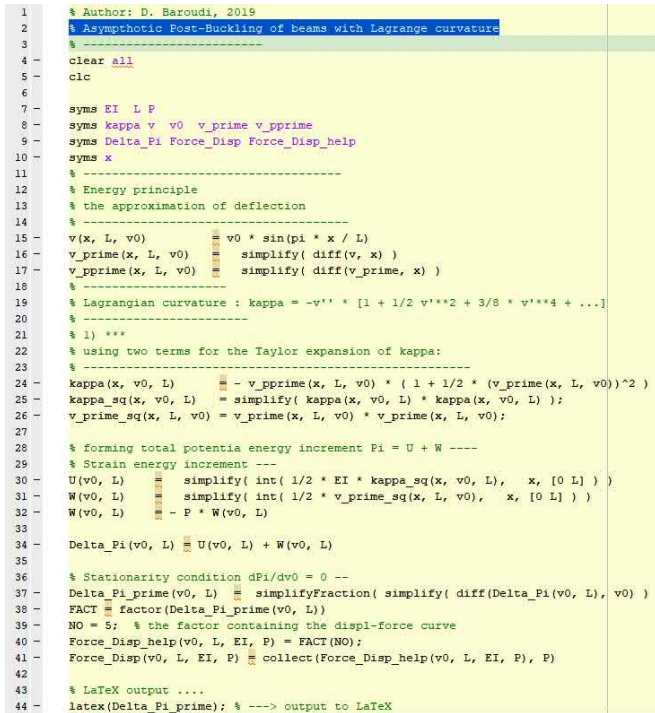
Figure 1.121: Asymptotic post-buckling when retaining only two and three terms in the Taylor expansion of the Lagrangian curvature $\kappa = -v''/\sqrt{1-v'^2}$ (holds for moderate rotations, so in close vicinity of the bifurcation point).

respectively. The above result, naturally, holds for moderate rotations, so in close vicinity of the bifurcation point.²⁵⁵ So, the final post-buckling neighbourhood being the branch λ, δ around the bifurcation point $(0, 1)$ on the bifurcated

²⁵⁴Reproduced for satisfying curiosity of the reader.

²⁵⁵I will draw a box showing that on the Figure, later.

equilibrium path. Equation (1.678), provides us, in addition, a quantitative estimation of 'buckling' deflection' and rotation (moderate post-buckling configuration). From the graph (Figure 1.121) one can see, clearly that the Asymptomatic post-buckling behaviour is symmetric stable.²⁵⁶ I reproduce the Matlab code

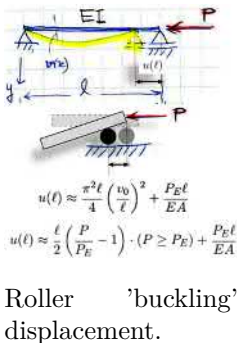


```

1 % Author: D. Baroudi, 2019
2 % Asymptotic Post-Buckling of beams with Lagrange curvature
3
4 clear all
5 cloc
6
7 syms EI L P
8 syms kappa v v0 v_prime v_pprime
9 syms Delta_Pi Force_Displ Force_Displ_help
10 syms x
11
12 % Energy principle
13 % the approximation of deflection
14
15 v(x, L, v0) == v0 * sin(pi * x / L)
16 v_prime(x, L, v0) == simplify( diff(v, x) )
17 v_pprime(x, L, v0) == simplify( diff(v_prime, x) )
18
19 % Lagrangian curvature : kappa = -v'' * [ 1 + 1/2 v''*2 + 3/8 v''*4 + ... ]
20
21 % 1) ***
22 % using two terms for the Taylor expansion of kappa:
23
24 kappa(x, v0, L) == - v_pprime(x, L, v0) * ( 1 + 1/2 * (v_prime(x, L, v0))^2 )
25 kappa_sq(x, v0, L) == simplify( kappa(x, v0, L) * kappa(x, v0, L) );
26 v_prime_sq(x, L, v0) == v_prime(x, L, v0) * v_prime(x, L, v0);
27
28 % forming total potentia energy increment Pi = U + W ----
29 % Strain energy increment ---
30 U(v0, L) == simplify( int( 1/2 * EI * kappa_sq(x, v0, L), x, [0 L] ) )
31 W(v0, L) == simplify( int( 1/2 * v_prime_sq(x, L, v0), x, [0 L] ) )
32 W(v0, L) == - P * W(v0, L)
33
34 Delta_Pi(v0, L) == U(v0, L) + W(v0, L)
35
36 % Stationarity condition dPi/dv0 = 0 --
37 Delta_Pi_prime(v0, L) == simplifyFraction( simplify( diff(Delta_Pi(v0, L), v0) ) )
38 FACT == factor(Delta_Pi_prime(v0, L))
39 NO = 5; % the factor containing the displ-force curve
40 Force_Displ_help(v0, L, EI, P) = FACT(NO);
41 Force_Displ(v0, L, EI, P) == collect(Force_Displ_help(v0, L, EI, P), P)
42
43 % LaTeX output ...
44 latex(Delta_Pi_prime); % ----> output to LaTeX

```

Figure 1.122: Matlab-code written for the asymptomatic post-buckling analysis.



I wrote to solve symbolically the full problem above. I hope, it may be useful for some students, now or later ... or never. However, seriously, programming is very efficient in structuring our understanding, as engineers. To programme, one should create the algorithm (Figure 1.122).

N.B. It is important, for design of the support length, for instance, to determine the axial displacement resulting from bending. The non-linear theory we are using, makes it possible to determine such axial displacement by integration

$$u(x) = \int_0^x (du/dx) dx = \int_0^x 1 - \sqrt{1 - (v')^2} dx \approx \int_0^x \frac{1}{2} v'^2 dx. \quad (1.679)$$

When applied to the deflection mode (1.660), we obtain

$$u(x) \approx \frac{\pi l}{8} \left(\frac{v_0}{l} \right)^2 \left[2\pi \left(\frac{x}{l} \right) + \sin \left(\frac{2\pi x}{l} \right) \right] \quad (1.680)$$

²⁵⁶The reader can check by the sign of the second variation-test for stability.

The above equations were obtained easily, or lazily, to be honest, using `Matlab` symbolic toolbox. I reproduce them, to encourage learning programming;

```

v(x, L, v0)      = v0 * sin(pi * x / L)
vprime(x, L, v0) = simplify( diff(v, x) )
vpprime(x, L, v0) = simplify( diff(vprime, x) )
u(x, L, v0)      = simplify(int( 1/2 * vprime(x, L, v0)^2, x, [0 x]));
    
```

So, let's go back to our business: how long should be the support to avoid falling of the beam? So, particularly, the maximum axial displacement, due to flexure deformation²⁵⁷, $u_L(\ell)$, at the moving support (roller)

$$u(\ell) \approx \frac{\pi^2 \ell}{4} \left(\frac{v_0}{\ell} \right)^2. \tag{1.681}$$

Adding the pre-buckling axial deformation at P_E gives the total axial displacement at the roller

$$u(\ell) \approx \frac{\pi^2 \ell}{4} \left(\frac{v_0}{\ell} \right)^2 + \frac{P_E \ell}{EA}. \tag{1.682}$$

Now, for a given load level $\lambda = P/P_E$, maximum deflection v_0/ℓ can be solved from Equation (1.678) and inserted into Equation (1.682) to obtain the displacement at the roller for a desired load P . Recall that in the introduction of these lecture notes, we wrote the non-linear analysis (or post-buckling analysis) also provides the designer tools for quantifying such 'buckling' displacements²⁵⁸. Ignoring the forth order term $(v_0/\ell)^4 \ll (v_0/\ell)^2 \ll 1$ in (1.678) for the Equation (1.682), we arrive to a useful engineering formula to quantify the horizontal dis- placement of the roller after buckling (moderate values for P/P_E over unity)

$$u(\ell) \approx \frac{\ell}{2} \left(\frac{P}{P_E} - 1 \right) \cdot (P \geq P_E) + \frac{P_E \ell}{EA}, \tag{1.683}$$

where the logical proposition $(P \geq P_E) = 1$ when `true`, otherwise, zero.

Now using three terms, $\kappa \approx -v''[1 + v'^2/2 + 3/8 \cdot v'^4]$, in the Taylor expansion of the curvature, we obtain the load-displacement curve (Figure 1.121)

$$\frac{P\ell^2}{\pi^2 EI} = 1 + \frac{1}{2}\pi^2 \left(\frac{v_0}{\ell} \right)^2 + \frac{3072}{8192}\pi^4 \left(\frac{v_0}{\ell} \right)^4 + \frac{960}{8192}\pi^6 \left(\frac{v_0}{\ell} \right)^6 + \frac{315}{8192}\pi^8 \left(\frac{v_0}{\ell} \right)^8 \tag{1.684}$$

$$\implies \lambda = 1 + \frac{1}{2}\pi^2 \delta^2 + \frac{3072}{8192}\pi^4 \delta^4 + \frac{960}{8192}\pi^6 \delta^6 + \frac{315}{8192}\pi^8 \delta^8 \tag{1.685}$$

$$\lambda = 1 + \frac{1}{2}\pi^2 \delta^2 + \frac{3}{8}\pi^4 \delta^4 + 0.117\pi^6 \delta^6 + 0.038\pi^8 \delta^8. \tag{1.686}$$

²⁵⁷The initial axial displacement $u_L(P_E) = P_E \ell / EA$ at the roller which is due to pure axial stretching prior to bending, should be added.

²⁵⁸These are the 'second order' or ' $P - \Delta$ ' effects as engineers usually call them.

I also provide the Matlab-code, I used, hoping that it can be useful for someone.

```

% -----
% Matlab code symbolic computation of the post-buckling equilibrium branch
% -----
v(x, L, v0)      = v0 * sin(pi * x / L)
vprime(x, L, v0) = simplify( diff(v, x) )
vpprime(x, L, v0) = simplify( diff(vprime, x) )
% --> three terms in kappa
kappa(x, v0, L) = - v_pprime(x, L, v0) * ( 1 + 1/2 * (v_prime(x, L, v0))^2 +
                                             + 3/8 * (v_prime(x, L, v0))^4 )
% -----
% Strain energy and work of P increments ---
U(v0, L) = simplify( int( 1/2 * EI * kappa_sq(x, v0, L), x, [0 L] ) )
W(v0, L) = simplify( int( 1/2 * v_prime_sq(x, L, v0), x, [0 L] ) )
W(v0, L) = - P * W(v0, L)
Delta_Pi(v0, L) = U(v0, L) + W(v0, L)
% -----
% Stationarity condition dPi/dv0 = 0 -->
% -----
Delta_Pi_prime(v0, L) = simplifyFraction( simplify( diff(Delta_Pi(v0, L), v0) ) )
FACT = factor(Delta_Pi_prime(v0, L))
NO = 5; % the factor containing the displ-force curve
Force_Displ_help(v0, L, EI, P) = FACT(NO);
Force_Displ(v0, L, EI, P) = collect(Force_Displ_help(v0, L, EI, P), P)
% -----
% The raw result being now: Force_Displ(v0, L, EI, P) =
- 8192*P*L^10 + 8192*EI*pi^2*L^8 + 4096*EI*pi^4*L^6*v0^2 +
+ 3072*EI*pi^6*L^4*v0^4 + 960*EI*pi^8*L^2*v0^6 + 315*EI*pi^10*v0^8
% -----

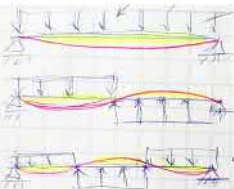
```

In the following section, a Finite Element full post-buckling analysis will be done for the same column and the results (graphs) compared.

FE-based post-buckling analysis of axially compressed column

A column of length $\ell = 1$ m made of aluminium is compressed with a centric load P . The column is simply supported. The column is initially straight. A tiny transverse load combination (Figure margin) is introduced as an initial perturbation for the purpose of the post-buckling analysis. Linearly increasing axial displacement u was imposed at both ends of column. The displacements (flexural and axial) are shown in (Figure 1.123). We see clearly that after the bifurcation, the post-buckling behaviour is of symmetric-stable type as was found in the previous asymptotic analysis (Figure 1.121). Figure (1.124) combines the results of the post-buckling analysis, both analytical asymptotic and FE-based. *N.B.*, how shallow is the shape of the post-bifurcation neighbourhood (black curve). This

Perturbed with tiny distributed load



Transverse perturbation tiny loads.

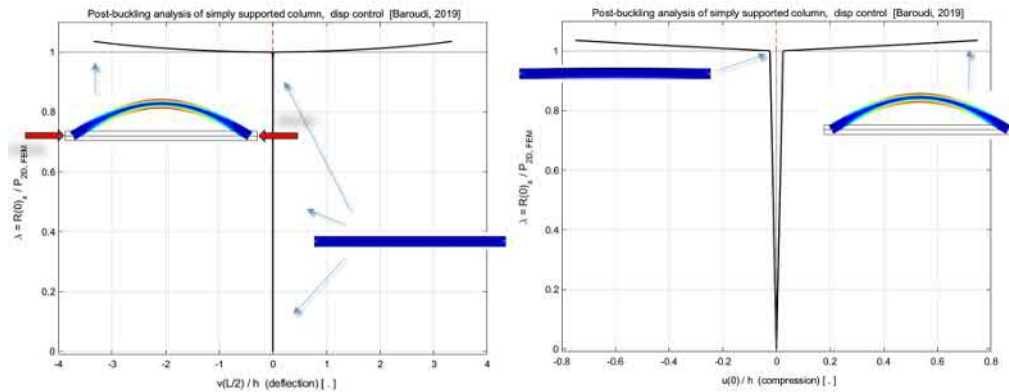


Figure 1.123: Post-buckling FE-analysis of a simply supported column (displacement control). Deflection at $\ell/2$ (left) and the column axial shortening (right). The column was initially perturbed by a combination of tiny transverse loads. *Notez bien*, how shallow is the shape of the post-bifurcation neighbourhood (black curve).

means that, the asymptotic analysis needs much more terms if one wants to see safely farther that, let's say $\delta > 0.15$.

Recall that the axial shortening of the column after buckling (in right Fig. 1.123) is mainly due the second order term $\int_0^\ell 1/2 v'^2 dx$, so summing the pre-buckling axial deformation at P_E gives the total axial displacement at the roller $u(\ell) \approx \frac{\pi^2 \ell}{4} \left(\frac{v_0}{\ell}\right)^2 + \frac{P_E \ell}{EA}$ as shown by Equation (1.682).

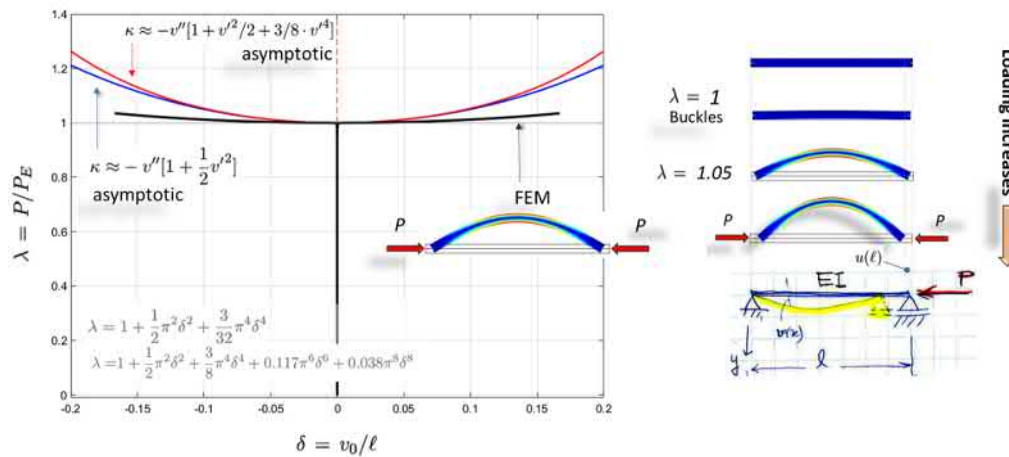
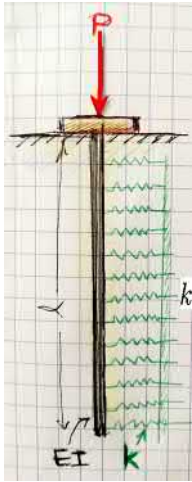


Figure 1.124: Post-buckling analysis by FEM and analytical asymptotic method. Note the very shallow shape at bifurcation point neighbourhood. *N.B.*, how shallow is the shape of the post-bifurcation neighbourhood (black curve).



Schematic of foundation pile under axial thrust which is elastically restrained by the soil (Geotechnical design; Eurocode 7).

The data for this example are: rectangular cross-section $\ell = 1$ m, $h = 50$ mm, $b = \ell/10$, $P_E = 720$ kN, $EI = 72.917$ kN.m², $E = 70$ GPa, $\nu = 0.33$.

1.12.11 Buckling of columns on elastic foundation

Let's start by giving examples of existence of such yet not visible conceptual object being labelled as *column-beam on elastic foundation*, by engineers. Indeed, new names, I mean the label of the box and the concept it contains, comes to life only through mathematically well-posed models, at least for us, engineers. The first example that the reader must know comes from civil engineering applications known as *pile foundations* (Margin figure) in which the soil-structure mechanical interaction can be captured by the one-parameter model of **Winkler**²⁵⁹. The buckling considerations of such is crucial for safety of the structural design. Pile Buckling (instability) failure can be of two types: a) global buckling or b) local buckling where the (large) deformation and consequently the damages remains local. Global buckling may occur when piles are partially exposed or are in highly soft soil or under driving loads while installing them. Local buckling may occur in end-bearing piles fully embedded in stratified soil with soft layers, especially during earthquakes as a consequence of liquefaction of soils²⁶⁰.

The second example, high practical importance of use of such simplified model for such soil-structure interaction model are railway rails (track) bonded to the soil or to carrying substructure. The rail can be continuous welded rail track or jointed track. When loaded compressively by inertia acceleration forces coming from trains or extreme increase of temperature rail track can buckle (Figure 1.125) with catastrophic consequences for the people safety in moving trains. The extreme increase of temperature leads to restraint thermal elongations which consequently can lead to excessive compressive thermal stresses resulting in thermally induced buckling. Track buckling occurs, usually, in the lateral plane. However, observations of cases with vertical buckling exists. The stability behaviour of such rails can be modelled using the well-known most simple theory named *beam on elastic foundation*.

Consider a simply supported beam or pile bounded to an elastic foundation with centric and axial compressive end-load P . what would be the critical load? Consider only flexural buckling in the weakest plan of inertia. Assume a constant

²⁵⁹**Emil Winkler** (1835-1888), German civil engineer and professor. He was the first to formulate and solve the now classical problem of elastic beam on deformable foundation. He has, among other books, published a book closely related to rails: *Lecture on Railway Engineering* (1867). His model assumes a linear relationship between the foundation reaction and the beam deflection (Winkler foundation).

²⁶⁰Ref: S. Bhattacharya, T.M. Carrington & T.R. Aldridge *Buckling considerations in pile design*. Frontiers in Offshore Geotechnics: ISFOG 2005 – Gourvenec & Cassidy (eds) 2005 Taylor & Francis Group, London, ISBN 0 415 39063 X. DOI: 10.1201/NOE0415390637.ch93

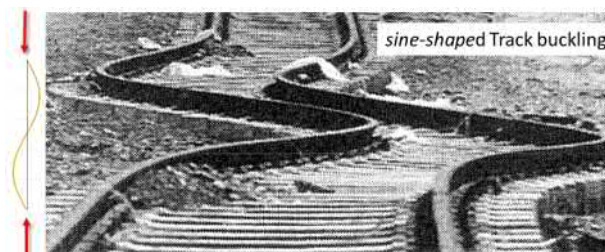


Figure 1.125: Buckled rail track. Keep in mind, for later use, the *sine-shaped* buckles. (Ref: Technical report: M.A. Van *Buckling analysis of continuous welded rail track*. Technical University Delft, Department of Civil Engineering, Mechanics and Structures Group, Stevinweg 1, 2628 CN Delft.)

cross-section with EI constant and the soil elasticity coefficient k also modelled by a constant. A axially loaded pile within a soil (foundation piles, Margin figure) or a beam-column having transversal elastic restraints (Figure 1.126) behave as a compressed beam on elastic foundation.

The buckling behaviour of such columns or piles becomes very rich and depends highly on the relative rigidities (bending rigidity EI of the beam and stiffness coefficient k , $[\text{N}/\text{m}\cdot\text{m}]$ ²⁶¹, of the elastic foundation). The soil-pile interaction is modelled by a **Winkler** model (one parameter model) as linear bilateral springs. In such model, the soil-reaction is simply proportional to deflection

$$r(x) = kv(x). \tag{1.687}$$

and the contact is bilateral (the beam and the soil remain bonded during defor-

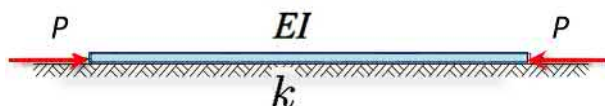


Figure 1.126: Beam bonded to an elastic foundation under axial thrust.

mations)²⁶².

²⁶¹The units of k are $[\text{N}/\text{m}]$ over the unit width $b = 1 \text{ m}$ of the beam cross-section. so $[k] = \text{N}/\text{m}\cdot\text{m}$

²⁶²There exists contact models with unilateral interaction but they are more complex to deal with analytically. In the simplest of such models the soil reaction (or interaction force) is given as $r(x) = kv(x)$ when the beam and the soil move together in the same direction, $\vec{w} \cdot \vec{n} \leq 0$, and $r(x) = 0$ otherwise. It is his discontinuous relation which makes such model analytically more challenging. So, we may come back to such interaction model in some numerical example. In this lecture note, only bilateral continuous contact model will be addressed.

Assume a straight primary (initial) equilibrium configuration. By increasing the compressive end-force P to a threshold-value P_{cr} , the column on the elastic foundation buckles in a flexural mode. The deviation from the straight line corresponds to deflection $v = v(x)$. The total potential energy increment is the same as for a beam-column in compression. There is an additional strain-energy term $1/2kv^2(x)$ accounting for the elastic deformation of the foundation. Therefore

$$\Delta\Pi = \frac{1}{2} \int_0^\ell EI[v''(x)]^2 + k[v(x)]^2 dx - P \int_0^\ell \frac{1}{2}[v'(x)]^2 dx. \tag{1.688}$$

Equation (1.688) can be used for finding approximate solutions (Rayleigh-Ritz) or for deriving the discrete eigenvalue problem by FE-element and obtain the needed stiffness- and geometric matrices \mathbf{K}_L and \mathbf{K}_G , respectively. This last subject on numerical methods will be addressed later. The linearised stiffness matrix is already known to the reader from previous course of structural mechanics; \mathbf{K}_L is the one obtained for the Euler-Bernoulli beam in bending for a beam on elastic foundation.

Applying the energy criterion $\delta(\Delta\Pi) = 0$ will give the linearised stability equations. The additional term as compared to the standard previous beam-column problem is given by the variation of the new term

$$\delta \left(\frac{1}{2} \int_0^\ell kv(x)^2 dx \right) = \int_0^\ell \underbrace{kv}_{\text{new add to ODE}} \delta v dx. \tag{1.689}$$

Taking the variation $\delta(\Delta\Pi) = 0$ one obtains

$$\int_0^\ell EIv''\delta v'' + kv\delta v dx - P \int_0^\ell v'\delta v' dx = 0, \forall \delta v \tag{1.690}$$

which becomes after twice integration by parts

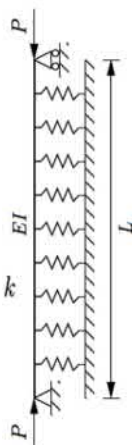
$$\int_0^\ell \underbrace{[EIv^{(4)} + kv + Pv'']}_{=0} \delta v dx + \underbrace{[EIv'']}_{-M} \delta v \Big|_0^\ell - \underbrace{[(EIv'' + Pv)']}_{-Q} \delta v \Big|_0^\ell = 0, \forall \delta v \tag{1.691}$$

The linearised buckling equation follows now straight-forwardly²⁶³ as

$$\boxed{EIv^{(4)} + Pv'' + kv = 0}. \tag{1.692}$$

The boundary terms of the integral provides the consistent boundary conditions. **Important:** Already at this stage, the reader is encouraged to keep in mind the structure of the linearised buckling equation (1.692) since it is *similar*, as will be addressed later, to axisymmetric linearised buckling equation of thin cylindrical shells under axial compression.

²⁶³See references Alfutov, *Stability of Elastic Structures*. Springer 2000, for more reading on this example.



Schematic of simply supported axially compressed column on elastic foundation.

Let's go back to our actual problem of beam buckling on elastic foundation and consider simply supported boundary conditions where

$$v(0) = v''(0) = 0, \tag{1.693}$$

$$v(\ell) = v''(\ell) = 0, \tag{1.694}$$

The solution is easy to find by following the classical case of Euler buckling. Direct substitution of trial²⁶⁴ (eigenmodes, Fig. 1.127)

$$v_n(x) = \sin \frac{n\pi x}{\ell}, \quad n = 1, 2, 3, \dots \tag{1.695}$$

into the differential equations shows that they satisfy it together with the boundary conditions. Therefore, the function set constitute the solution²⁶⁵.

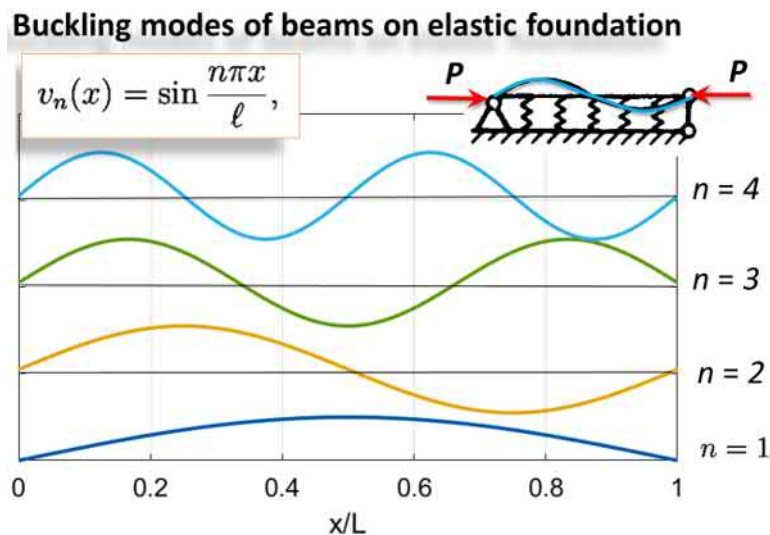


Figure 1.127: Buckling modes.

²⁶⁴The homogeneous linear differential equation with constant coefficients has a general solution of the form $v(x) = \sum_{i=1}^4 A_i e^{r_i x}$. The variables r_i are the four roots of the bi-quadratic characteristic equation. This is the correct way to solve the problem for arbitrary four boundary conditions. Inserting the boundary conditions and asking for existence of non-trivial solution (zero-determinant), one obtains the buckling load.

²⁶⁵This procedure is done to shorten the derivations. The reader should find the complete system of solutions by solving the ode with constant coefficient in a canonical and more systematic way

The critical load is now

$$P_n = \left(\frac{n\pi}{\ell}\right)^2 EI + \left(\frac{\ell}{n\pi}\right)^2 k \quad (1.696)$$

$$= n^2 \underbrace{\left[\frac{\pi^2 EI}{\ell^2}\right]}_{P_E} + \frac{1}{n^2} \frac{k\ell^2}{\pi^2} > n^2 P_E \quad (1.697)$$

$$= \left[\frac{\pi^2 EI}{\ell^2}\right] \left[n^2 + \frac{1}{n^2} \underbrace{\frac{k}{EI} \left(\frac{\ell}{\pi}\right)^4}_{\equiv \beta} \right], \quad n = 1, 2, 3, \dots \quad (1.698)$$

$$= P_E \left[n^2 + \frac{\beta}{n^2} \right]. \quad (1.699)$$

The smallest critical load $P_{cr} = P_n$ depends on the half-wave number n . Assuming the variable n continuous one obtains the smallest critical load from the extremum condition

$$\frac{dP_n}{dn} = 0 \implies n^2 = \sqrt{\beta}, \quad (1.700)$$

which leads to

$$P_{cr} = 2P_E \sqrt{\beta} = 2\sqrt{kEI}. \quad (1.701)$$

In reality, the number of half-waves n is integer variable (discrete) and the minimum for the critical buckling load given by Equation (1.701) is a limit for relatively long beams $\bar{\ell} \equiv \beta^{1/4} \geq 3$ (see following discussion). The exact buckling load is given in Figure (1.128 c)) for arbitrary relative length.

In the above equation next dimensionless parameters were defined as

$$\beta = \frac{k\ell^4}{\pi^4 EI}, \quad (1.702)$$

$$\bar{P}_n = \frac{P_n \ell^2}{\pi^2 EI} \equiv \frac{P_n}{P_E} \quad (1.703)$$

The critical load P_n can be written now in the dimensionless form as

$$\bar{P}_n \equiv \frac{P_n}{P_E} = P_n n^2 + \frac{\beta}{n^2}, \quad (1.704)$$

which represents, graphically, a set of straight lines for $n = 1, 2, 3, \dots$, etc. in function of the relative stiffness β . The graph $\bar{P}_n - \beta$ shows the lowest values for \bar{P}_n which correspond to the critical loads as function of the parameter β .

Analysis of the results

The buckling as function of a the relative length of the beam will be investigate and compared to the case of a compressed column without foundation restraining

effects. For this let define a relative length by

$$\bar{\ell} \equiv \beta^{1/4} = \frac{\ell}{\pi} \left[\frac{k}{EI} \right]^{1/4} \quad (1.705)$$

and a relative compression load by

$$\bar{P} \equiv \frac{P}{\sqrt{kEI}}. \quad (1.706)$$

These dimensionless parameters define here the physics of the buckling and they

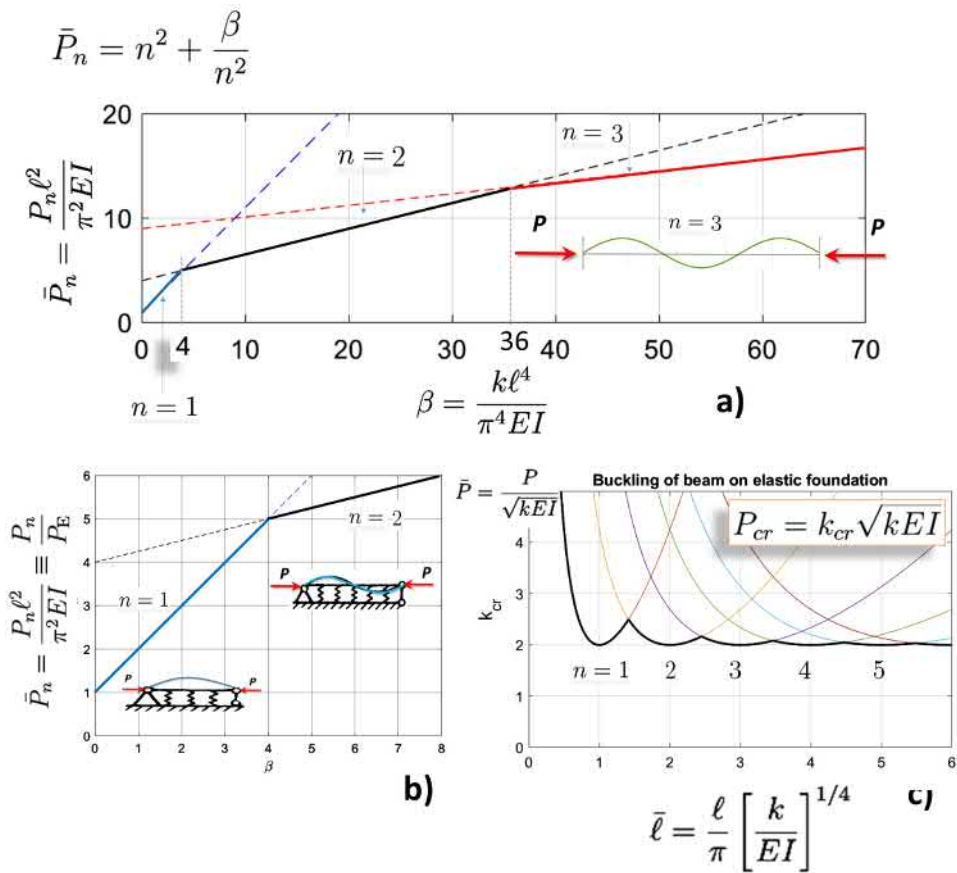


Figure 1.128: Stability behaviour of an elastic beam bonded to an elastic foundation.

are related by the buckling equation defined previously as

$$\bar{P}_n = \underbrace{\frac{n^2}{\bar{\ell}^2}}_{\equiv k_{cr}} + \frac{\bar{\ell}^2}{n^2} = \frac{P}{\sqrt{kEI}} \rightarrow P_{cr} = k_{cr} \sqrt{kEI}. \quad (1.707)$$

The graph of buckling relation (1.707) and for buckling coefficient k_{cr} is shown in (Figure 1.128 c)).

Recall that for a column in the air (no elastic restraining along the axis of the column), the critical load decreases monotonically with the increase of the column length. On the contrary, for a column bonded to an elastic foundation, the critical load does not decrease monotonically with the increase of the length. For instance, for $\bar{\ell} \geq 3$ (Figure 1.128 c)), the critical load becomes practically constant and equal to

$$P_{cr} \approx 2\sqrt{kEI}. \quad (1.708)$$

In general, the critical load will be given by

$$\boxed{P_{cr} = k_{cr}\sqrt{kEI}} \quad (1.709)$$

where the stability coefficient²⁶⁶ $k_{cr} \equiv \bar{P}$ is provided by the graph in figure (1.128 c)).

Note that the relative elasticity of the foundation β plays a critical role: for $0 \leq \kappa < 4$ the beam buckles in one half-wave. Two half-wave appear for $4 < \kappa < 36$ for a bit higher critical load (Figure 1.128 a) & b)). This mode transition phenomenon is sometimes called by *mode switching*. Increasing the relative stiffness of the foundation lead to *wrinkling*²⁶⁷ of the surface because of mode accumulation.

Figure (1.129) illustrates an example of buckling modes that a column on elastic foundation may have. It is a result of linear buckling analysis done using FEM²⁶⁸. The FE-analysis will be presented in details in a dedicated subsection. The idea of providing, already now, the figure was just to give a picture and to open more the appetite of the reader.

Other types of boundary conditions

For cases other than simply supported for both ends, one should obtain a general complete solution of the ODE (1.692) through standard solution procedure for differential equations with constant coefficients

$$v^{(4)} + p^2v'' + b^4v = 0 \quad (1.710)$$

²⁶⁶Nurjahduskerroin, lommahduskerroin (sf).

²⁶⁷This problem of *wrinkling* is closely related to the *surface instability problem* of **Biot**.

²⁶⁸Important note: It is about dimension reduction and use of correct physical parameters in only are known the beam properties : ℓ , EI , k_{beam} [N/m.m]. The beam in this example was modelled by a narrow thin plate on an elastic foundation. So what will be the corresponding foundation spring coefficient to be used in the narrow plate model? The width of the plate was b and its length ℓ equal the length of the beam. The foundation spring coefficient k_{plate} (spring constant per unit area) [N/m.m²]. So, the relation $k_{plate} = k_{beam}/b$ holds. To cross-check this result, compute the resultant of foundation reactions in both cases for a constant and uniform deflection w_0 : $R_{beam} = k_{beam}w_0\ell$ and $R_{plate} = k_{plate}w_0b\ell$. Equating $R_{beam} = R_{plate} \implies k_{plate} = k_{beam}/b$.

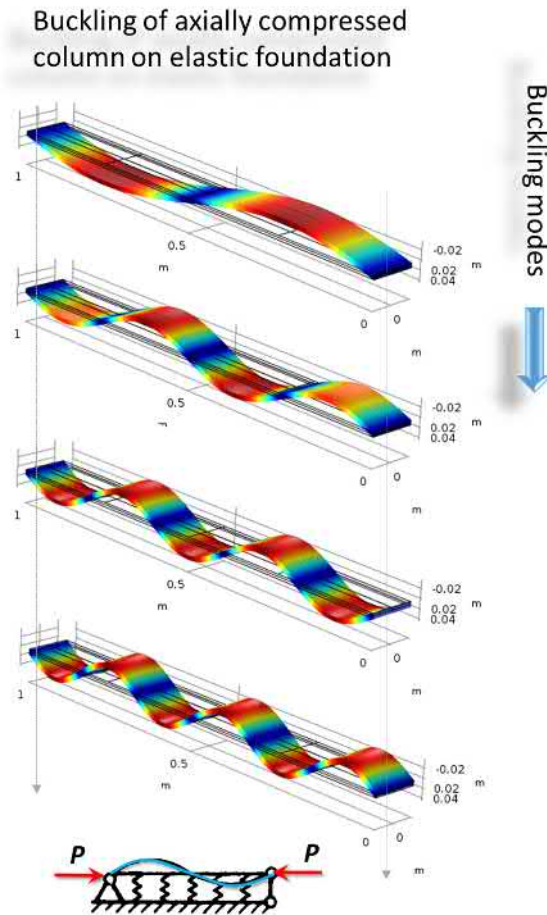


Figure 1.129: Example of buckling modes of a column bonded to an elastic foundation. The number of half-waves, n , increases with increase of the relative stiffness parameter $\beta = \frac{\ell^4}{\pi^4} \frac{k}{EI}$.

where $p^2 \equiv P/EI$ and $b^4 \equiv k/EI$. It comes out that to have a canonical and clean treatment of the general solution for all cases, one have to rewrite the above ODE using notation²⁶⁹

$$a^2 = \frac{p^2}{2} \equiv \frac{P}{2EI}, \quad b^4 \equiv \frac{k}{EI}. \quad (1.711)$$

The general solution of (Equation 1.710) is the standard basis

$$v(x) = Ae^{rx}. \quad (1.712)$$

²⁶⁹See M. Tuomala. *Rakenteiden Stabiilisuusteoria*. Lecture notes (in Finnish).

Once one solves the roots r_i , the full solution will be constructed as

$$v(x) = \sum_{i=1}^4 A_i e^{r_i x}. \quad (1.713)$$

Inserting the trial into the ODE one obtains the bi-quadratic *characteristic equation*

$$r^4 + 2a^2 r^2 + b^4 = 0, \quad (1.714)$$

with solution

$$r^2 = -a^2 \pm \sqrt{a^4 - b^4}. \quad (1.715)$$

Next the general solutions will be discussed as function of the sign of the discriminant $\Delta \equiv a^4 - b^4$.

- $\Delta > 0$, the roots are

$$r_i = \pm i \sqrt{a^2 \pm \sqrt{\Delta}}, \quad i = 1, \dots, 4 \quad (1.716)$$

where $i^2 = -1$ and $r_1 = -r_2 \equiv ik_1$, $r_3 = -r_4 \equiv ik_2$. and the general solution is

$$v(x) = c_1 \cos k_1 x + C_2 \sin k_1 x + C_3 \cos k_2 x + C_4 \sin k_2 x \quad (1.717)$$

where $(k_1, k_2) = \sqrt{a^2 \pm \sqrt{\Delta}}$.

- $\Delta = 0$, the roots are

$$r_1 = r_3 = ib, \quad r_2 = r_4 = -ib. \quad (1.718)$$

and the corresponding general solution

$$v(x) = (C_1 x + C_2) \cos bx + (C_3 x + C_4) \sin bx. \quad (1.719)$$

- $\Delta < 0$, the roots are

$$r_i = \pm i \sqrt{a^2 \mp i \sqrt{-\Delta}}, \quad i = 1, 2, 3, 4. \quad (1.720)$$

Let's define $(k_1, k_2) = \sqrt{b^2 \pm a^2} / \sqrt{2}$. Then we have

$$r_i = \pm k_1 \pm ik_2. \quad (1.721)$$

and the corresponding general solution

$$v(x) = A_1 e^{r_1 x} + A_2 e^{r_2 x} + A_3 e^{r_3 x} + A_4 e^{r_4 x} \quad (1.722)$$

or in an equivalent but more practical form for computing

$$v(x) = C_1 \cos k_1 x \cosh k_2 x + C_2 \sin k_1 x \cosh k_2 x + \quad (1.723)$$

$$+ C_3 \cos k_1 x \sinh k_2 x + C_4 \sin k_1 x \sinh k_2 x \quad (1.724)$$

Buckling of a column on elastic foundation - a summary

This section is some kind of summary for the previous subsection above. In textbooks, usually, repetitions are avoided or even banned. The following, approximately one and a half page length, subsection is a such repetition. I found a summary resuming solutions of buckling of columns on elastic foundation²⁷⁰ that I decided to share an adaptation of it with the student readers. *Repetitio est mater studiorum*²⁷¹ the Latin proverb (This proverb exists in all languages). So let's start.

Assume constant k and EI , the basic buckling equation is the well-known fourth order ordinary differential equations with constant coefficients

$$v^{(4)} + \frac{P}{EI}v'' + \frac{k}{EI}v = 0 \tag{1.725}$$

$$v^{(4)} + \lambda_P^2 v'' + \frac{\beta_k^4}{4}v = 0 \tag{1.726}$$

where $\lambda_P^2 \equiv P/EI (= p^2)$ and $\beta_k^4 \equiv 4k/EI (= 4b^4)$ ²⁷².

Recall the general solutions:

- $\lambda_P > \beta_k$,

$$v(x) = C_1 \cos px + C_2 \sin px + C_3 \cos qx + C_4 \sin qx \tag{1.727}$$

$$p = \frac{1}{2}\sqrt{\lambda_P^2 + \beta_k^2} + \frac{1}{2}\sqrt{\lambda_P^2 - \beta_k^2} \ \& \ q = \frac{1}{2}\sqrt{\lambda_P^2 + \beta_k^2} - \frac{1}{2}\sqrt{\lambda_P^2 - \beta_k^2}$$

- $\lambda_P < \beta_k$,

$$v(x) = C_1 \cosh px + C_2 \sinh px + C_3 \cosh qx + C_4 \sinh qx \tag{1.728}$$

$$p = \frac{1}{2}\sqrt{\lambda_P^2 + \beta_k^2} + \frac{1}{2}\sqrt{\beta_k^2 - \lambda_P^2} \ \& \ q = \frac{1}{2}\sqrt{\lambda_P^2 + \beta_k^2} - \frac{1}{2}\sqrt{\beta_k^2 - \lambda_P^2}$$

- $\lambda_P = \beta_k$,

$$v(x) = (C_1 + C_2x) \cos(\lambda_k/\sqrt{2}) + (C_3 + C_4x) \sin(\lambda_k/\sqrt{2}) \tag{1.729}$$

To close the problem, boundary conditions should be specified.

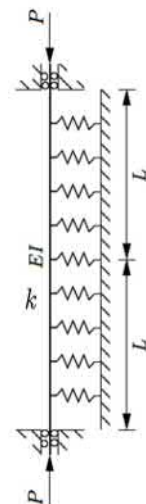
Example - buckling of a clamped beam on elastic foundation

Determine the buckling load for the pile shown in margin. Consider only the case with $\Delta = a^4 - b^4 > 0$. It can be shown that for other cases, there will be no bifurcation. Let's recall that

²⁷⁰[Chap. 4.5] in: Wai-Fah Chen, Toshio Atsuta *Theory of Beam-Columns, Volume 1: In-Plane Behavior and Design*. J. Ross publishing (2008). (First published in 1976 by Mc-Graw-Hill)

²⁷¹Repetition is the mother of learning.

²⁷²Notation p and b are those of previous subsection.



Axially compressed pile modelled as a column on Winkler elastic foundation.

$$a^2 \equiv \frac{P}{2EI}, \quad b^4 \equiv \frac{k}{EI}. \quad (1.730)$$

For this case we have previously obtained the general solution as

$$v(x) = C_1 \cos k_1 x + C_2 \sin k_1 x + C_3 \cos k_2 x + C_4 \sin k_2 x \quad (1.731)$$

where $(k_1, k_2) = \sqrt{a^2 \pm \sqrt{\Delta}}$. The boundary conditions are

$$v(-L) = v(L) = 0, \quad (1.732)$$

$$v'(-L) = v'(L) = 0. \quad (1.733)$$

Accounting for the four boundary conditions on obtains

$$\begin{bmatrix} \cos k_1 L & \sin k_1 L & \cos k_2 L & \sin k_2 L \\ \cos k_1 L & -\sin k_1 L & \cos k_2 L & -\sin k_2 L \\ -k_1 \sin k_1 L & k_1 \cos k_1 L & -k_2 \sin k_2 L & k_2 \cos k_2 L \\ k_1 \sin k_1 L & k_1 \cos k_1 L & k_2 \sin k_2 L & k_2 \cos k_2 L \end{bmatrix} \begin{bmatrix} C_1 \\ C_2 \\ C_3 \\ C_4 \end{bmatrix} = \begin{bmatrix} 0 \\ 0 \\ 0 \\ 0 \end{bmatrix}. \quad (1.734)$$

The criticality condition (zero determinant for non-trivial solution) will provide the critical load. Instead of solving the above four equations in once, we consider separately the symmetric and antisymmetric buckling cases for which the corresponding critical load will be solved. Then the smallest critical load from the two will be critical buckling load of the complete problem.

Symmetric buckling: The above four equations simplify to two for a symmetric buckling mode. So, because of symmetry $C_2 = C_4 = 0$ and the system of equations simplifies to

$$\begin{bmatrix} \cos k_1 L & \cos k_2 L \\ k_1 \sin k_1 L & k_2 \sin k_2 L \end{bmatrix} \begin{bmatrix} C_1 \\ C_3 \end{bmatrix} = \begin{bmatrix} 0 \\ 0 \end{bmatrix}. \quad (1.735)$$

Finally, non-trivial solution (zero determinant) gives

$$\boxed{f(k_1 L, k_2 L) = k_1 L \tan k_1 L - k_2 L \tan k_2 L = 0}. \quad (1.736)$$

The smallest positive zero gives P_{cr} for this case. The equation above is 'easier' to solve graphically. For this purpose, let express the arguments $k_1 L$ and $k_2 L$ in the characteristic equation (zero determinant) in more tractable form as

$$(k_1 L)^2 = \eta \sqrt{\frac{kL^4}{EI}} [1 - \eta^2], \quad (1.737)$$

$$(k_2 L)^2 = \eta \sqrt{\frac{kL^4}{EI}} [1 + \eta^2], \quad (1.738)$$

where $\eta = \eta(P_{cr}) = P_0/P$, with $P_0 = 2\sqrt{kEI}$. Inserting the above definition into Equation (1.736) on obtains the non-triviality condition rewritten in function of a non-dimensional argument η as

$$f\left(\eta; \frac{kL^4}{EI}\right) = 0 \tag{1.739}$$

where $kL^4/(EI)$ plays the role of a parameter that should be supplied. Now the smallest critical load P_{cr} correspond to the smallest positive zero η_{cr} of the function f . Naturally, it comes out that it is easier to find the roots graphically by drawing the graph of $f(\eta)$ as function of the scalar $\eta = 0 : \Delta\eta : \max(\eta)$ (for instance, one may chose $\max(\eta) = 10 \dots 100$).

Antisymmetric buckling: Now we obtain ($C_1 = C_3 = 0$)

$$\begin{bmatrix} \sin k_1L & \sin k_2L \\ k_1 \cos k_1L & k_2 \cos k_2L \end{bmatrix} \begin{bmatrix} C_2 \\ C_4 \end{bmatrix} = \begin{bmatrix} 0 \\ 0 \end{bmatrix}, \tag{1.740}$$

where the critical load P_{cr} is found as the smallest root of

$$\boxed{g(k_1L, k_2L) = k_1L \cot k_1L - k_2L \cot k_2L = 0}. \tag{1.741}$$

As was done previously for the symmetric buckling case, the smallest critical load will be found from the smallest root η_{cr} of

$$g\left(\eta; \frac{kL^4}{EI}\right) = 0. \tag{1.742}$$

Finally the smallest critical load from the two symmetric and antisymmetric cases will be the *buckling load*. This buckling load will be expressed in the form

$$\boxed{P_{cr} = \mu \cdot 2\sqrt{kEI}}, \tag{1.743}$$

where the numerical value of μ is found from the smallest root of the determinants.

Numerical application Lets fix some values for kL^4/EI in order to finalise the numerical solution of this example. Assume that the relative stiffness of the foundation and the beam bending rigidity is such that the parameter $kL^4/EI = 2\pi^4$. Graphical solution of Equations (1.736 & 1.741) gives the smallest root as $\eta_{cr} = 0.4173^{273}$ and it corresponds to the antisymmetric mode (Figure 1.130). Therefore the buckling load will be

$$P_{cr} = P_0/\eta_{cr} \approx \underbrace{2.4}_{\mu} \cdot \underbrace{2\sqrt{kEI}}_{P_0}, \tag{1.744}$$

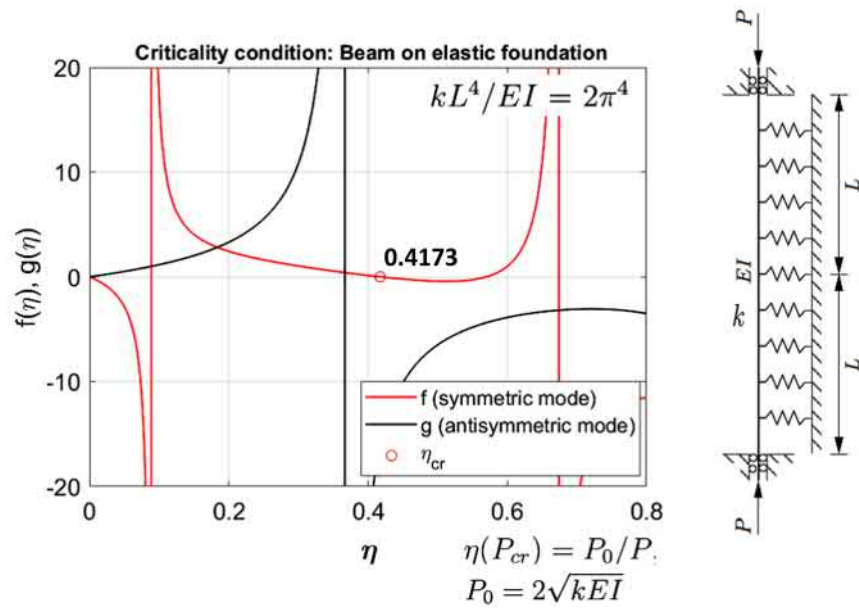


Figure 1.130: The zeros of the determinant for the buckling of a column on elastic foundation.

where $P_0 = 2\sqrt{kEI}$ corresponds to the limit case of buckling of simply supported beam on elastic foundation. Note that the buckling mode corresponding to the smallest critical load is antisymmetric since there is only one root of the determinant and which correspond to this mode. The Matlab-code used too draw the graphs is also provided in Figure (1.131).

Often, even as an engineer, it is valuable to be able to reduce a complex problem to the essential in order to obtain the key parameters deciding of some key behaviour aspects. For that, one need then to solve the reduced problem exactly analytically or approximately analytically. When analytical solutions are not possible, hand-size numerical solutions are the solution. Rayleigh-Ritz method, a powerful one, is already known to the reader. In the following two subsections, we will present two additional such numerical methods which conserve the analytical parameters of the specific problem (the handles of the problem: the *dimensionless groups* Π -numbers²⁷⁴.) and at the same time which result in a tractable and solvable numerical eigenvalue problem. The methods are: 1) *Finite element method (FEM)* and 2) *Finite difference method (FDM)*. Note that the FEM meant here is not a software but a handy calculation procedure. No need to re-write badly Abaqus²⁷⁵ or similar well-established software. Examples

²⁷³This result should be cross-checked. I have not yet done it!

²⁷⁴Good to read on the **Buckingham** Pi- theorem

²⁷⁵SIMULIA Abaqus.

```

1  % Author: D. BAROUDI, 2019
2  %
3  % Buckling of a column on elastic foundation
4  % Both ends are clamped (jäykkäkiinnitys - molemmat päät)
5  % -----
6  %
7  % eta = [2 sqrt(k * EI)] / P
8  % ==> Pcr = [2 sqrt(k * EI)] / eta
9  % -----
10 eta = 0:0.001:10;
11
12 KL4_EI = 2* pi^4;
13 k1_L_sq = eta .* (sqrt(KL4_EI)) .* (1 - sqrt(1 - eta .* eta))
14 k2_L_sq = eta .* (sqrt(KL4_EI)) .* (1 + sqrt(1 - eta .* eta))
15
16 k1_L = sqrt(k1_L_sq);
17 k2_L = sqrt(k2_L_sq);
18
19 % Determinant is zero: det = 0 ==>
20 f = k1_L .* tan(k1_L) - k2_L .* tan(k2_L);
21 g = k1_L .* cot(k1_L) - k2_L .* cot(k2_L);
22
23 % -----
24 figure
25 plot(eta, f, 'r-');
26 hold on
27 plot(eta, g, 'k-');
28 grid on
29 legend('f (symmetric mode)', 'g (antisymmetric mode)', '\eta_{cr}')
30 xlabel('\eta')
31 ylabel('f(\eta), g(\eta)')
32 title('Criticality condition: Beam on elastic foundation')
33 % -----

```

Figure 1.131: The Matlab-code to determine the zeros of the determinant for the buckling of a column on elastic foundation of Figure (1.130).

will be provided.

1.12.12 Discrete energy method - FEM

Assume a beam-column under centric thrust causing the internal axial force $N^0(x)$ to equilibrate. The compression is thought here positive. For instance, in case of end compression load $P = -N^0(x) > 0$. During buckling, we consider only change in the flexural strain energy of the beam and consequently, the additional strain energy change in the elastic foundation. Consider a column of length L discretized into elements of length $\ell^{(e)}$. The element e has two nodes with two degrees of freedom per node: transversal displacement v and rotation θ . Note that, when not necessary, and to make lighter notation, the superscript (e) will be dropped.

For Euler-Bernoulli beam of constant EI , the cubic **Hermite** polynomials solve exactly the classical homogeneous equation of equilibrium without elastic foundation ($k = 0$). Let's use these polynomials as a basis function set (shape functions) for the problem of the buckling of the beam bonded to elastic founda-

tion. Recall Hermite shape functions (Figure 1.132):

$$N_1(x) = 1 - 3(x/\ell)^2 + 2(x/\ell)^3, \quad (1.745)$$

$$N_2(x) = x(1 - x/\ell)^2, \quad (1.746)$$

$$N_3(x) = 3(x/\ell)^2 - 2(x/\ell)^3, \quad (1.747)$$

$$N_4(x) = x((x/\ell)^2 - x/\ell) \quad (1.748)$$

as shape functions (Figure 1.132) Note that one obtains the exact elementary

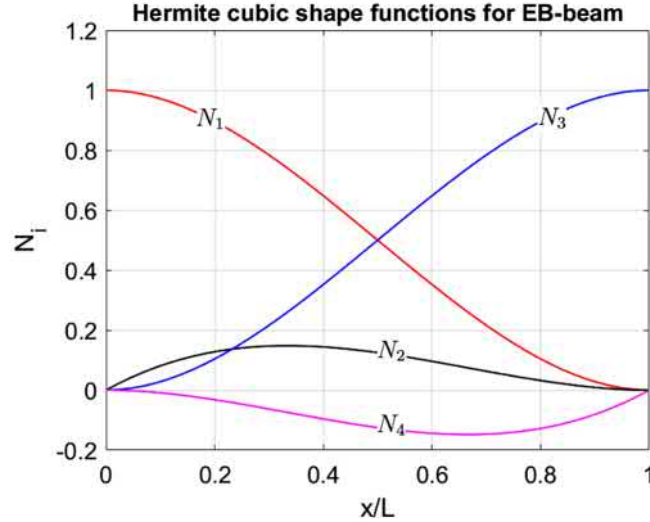


Figure 1.132: Hermite cubic splines.

linearised stiffness matrix for bending only ($k = 0$), $\mathbf{K}_L^{(B)}$ will be

$$\mathbf{K}_L^{(B)} = \frac{EI}{\ell^3} \begin{bmatrix} 12 & 6\ell & -12 & 6\ell \\ 6\ell & 4\ell^2 & -6\ell & 2\ell^2 \\ -12 & -6\ell & 12 & -6\ell \\ 6\ell & 2\ell^2 & -6\ell & 4\ell^2 \end{bmatrix} \quad (1.749)$$

and the consistent stiffness matrix from the elastic foundation

$$\mathbf{K}_L^{(F)} = \frac{k\ell}{70} \begin{bmatrix} 26 & 11\ell/3 & 9 & -13\ell/6 \\ 11\ell/3 & 2\ell^2/3 & 13\ell/6 & -\ell^2/2 \\ 9 & 13\ell/6 & 26 & -11\ell/3 \\ -13\ell/6 & -\ell^2/2 & -11\ell/3 & 2\ell^2/3 \end{bmatrix} \quad (1.750)$$

and the geometric elementary matrix is

$$\mathbf{K}_G = -\frac{P}{30\ell} \begin{bmatrix} 36 & 3\ell & -36 & 3\ell \\ 3\ell & 4\ell^2 & -3\ell & -\ell^2 \\ -36 & -3\ell & 36 & -3\ell \\ 3\ell & -\ell^2 & -3\ell & 4\ell^2 \end{bmatrix} \quad (1.751)$$

where $P = -N^0(x)$ for compression.

Some times instead of using the consistent full stiffness matrix of the foundation (Equation 1.750), it is better to use its lumped version obtained by an integration scheme leading to a diagonal stiffness matrix. Physically, this means that rotational contributions are ignored and only deflectional component are incorporated. This is indeed, the primary idea of the physics of Winkler foundation in the equation $r(x) = kv(x)$ - deflection $v(x_k)$ at neighbour points do not affect the reaction $r(x_i)$ at point x_i where $i \neq k$. So, the diagonalised stiffness matrix from the elastic foundation

$$\mathbf{K}_L^{(F)} = \frac{k\ell}{2} \begin{bmatrix} 1 & 0 & 0 & 0 \\ 0 & 0 & 0 & 0 \\ 0 & 0 & 1 & 0 \\ 0 & 0 & 0 & 0 \end{bmatrix}. \quad (1.752)$$

The above elementary matrices $\mathbf{K}_L^{(F)}$, $\mathbf{K}_L^{(F)}$ and \mathbf{K}_G are obtained by exactly integrating the elemental integrals of the stability energy criterion given by the weak form below. For pedagogical purpose, the explicit procedure of obtaining elementary matrices is done in `Matlab` symbolic toolbox and is provided here for those interested (Figure 1.133).

The starting point for deriving the elementary matrices above is the total potential energy functional (1.688) or more directly, its variation which is known as *Virtual Work Principle*. The idea is to write the variation of the total functional as a sum over the elements

$$\delta(\Delta\Pi) = \sum_{e=1}^N \left[\int_0^{\ell^{(e)}} EIv''(x)\delta v'' + kv(x)\delta v(x)dx + \int_0^{\ell^{(e)}} \underbrace{N^0(x)}_{-P^{(e)}} v'(x)\delta v'(x)dx \right] = 0 \quad (1.753)$$

$$= \sum_{e=1}^N \left[\int_0^{\ell^{(e)}} EIv''(x)\delta v'' + kv(x)\delta v(x)dx - P^{(e)} \int_0^{\ell^{(e)}} v'(x)\delta v'(x)dx \right] = 0 \quad (1.754)$$

$$= \sum_{e=1}^N (\delta \mathbf{a}^{(e)})^T \left[\underbrace{\int_0^{\ell^{(e)}} \mathbf{N}''^T(x) \cdot EI \cdot \mathbf{N}''(x)dx}_{\mathbf{K}_L^{(B)}} + \underbrace{\int_0^{\ell^{(e)}} \mathbf{N}^T(x) \cdot k \cdot \mathbf{N}(x)dx}_{\mathbf{K}_L^{(F)}} + \right. \quad (1.755)$$

$$\left. - \int_0^{\ell^{(e)}} \mathbf{N}'^T(x) \cdot P^{(e)} \cdot \mathbf{N}'(x)dx \right] \mathbf{a}^{(e)} = 0, \forall \delta \mathbf{a}^{(e)} \quad (1.756)$$

where $P^{(e)} = -N^0(x)$ (compression $P^{(e)} > 0$) and $N^0(x)$ being the membrane stress-resultant in the element number e . The element matrices are shown in the under-braced terms of the weak form. Note that the axial force $P^{(e)}$, in the geometric stiffness matrix, plays formally the role of an effective 'stiffness' when comparing with bending and foundation terms. The transversal displacement being approximated locally as

$$v^{(e)}(x) = \sum_{i=1}^M \phi_i(x) a_i^{(e)} \equiv \mathbf{N}(x) \mathbf{a}^{(e)}, \quad (1.757)$$

where the number of degrees of freedom per element, being $M = 4$ and the nodal degree of freedom vector being

$$\mathbf{a}^{(e)} = [v_1 \quad \theta_1 \quad v_2 \quad \theta_2]^T \quad (1.758)$$

The shape functions $\mathbf{N}(x) = [N_1(x) N_2(x) N_3(x) N_4(x)]$ being now the analytical solution for the classical bending problem of Euler-Bernoulli beams. In other words, **Hermite** cubic splines (polynomials) are used as shape functions to achieve the needed C^1 -continuity.

Some words of explanations for the transition from the weak form (virtual work principle) to the discretized FE-form: According to **Galerkin** approach, the arbitrary variation $\delta v(x)$ is chosen locally within each element e as

$$\delta v(x) = \mathbf{N}(x) \delta \mathbf{a}^{(e)}, \quad (1.759)$$

where $N_j(x)$ are the shape functions in Equation (1.757). In other words the shape functions and the variations (or test functions) are the same. (The reader is encouraged to refer to some Basic textbooks²⁷⁶ on Finite Element Method).

Diagonalized foundation stiffness matrix: For the diagonalised stiffness matrix version of the foundation $\hat{\mathbf{K}}_L^{(F)}$, the result (1.752) is obtained using the following thought. Let's integrate the elementary contribution of the foundation

$$\delta(\Delta\Pi)_{\text{found.}}^{(e)} = \int_0^{\ell^{(e)}} kv(x) \delta v(x) dx \quad (1.760)$$

to the total strain energy such that convergence is ensured. For that, it is enough to ensure at least a piece-wise constant integrand. Here, we use a piecewise linear approximation of the deflection $v(x) = \hat{\mathbf{N}} \mathbf{a}^{(e)}$ for the contribution of the integral in (Equation 1.760). Using for the foundation displacement approximation

$$\hat{\mathbf{N}}_F = \begin{bmatrix} 1 - x/\ell & 0 & x/\ell & 0 \end{bmatrix} \quad (1.761)$$

²⁷⁶The classical: **O. Zienkiewicz**, R. Taylor & J.Z. Zhu. *The Finite Element Method: Its Basis and Fundamentals*. 7th Edition. 2013. (1st Ed. 1967 published by Mc-Graw-Hill)

and test function $\delta v(x) = \hat{\mathbf{N}}\delta\mathbf{a}^{(e)}$ where $\mathbf{a}^{(e)}$ being the full elementary nodal degrees of freedom vector given by Equation (1.759). One can, of course, use a more harmonious approach and keep the same shape and test functions for all the terms in the weak form. The diagonalisation of the foundation stiffness matrix being achieved by performing an under-integration²⁷⁷.

Deriving elementary matrices using computer algebra: Bellow an example of how to use Symbolic toolboxes (Matlab) or any other Computer Algebra tools to derives elementary matrices (1.133). The elementary matrices are re-

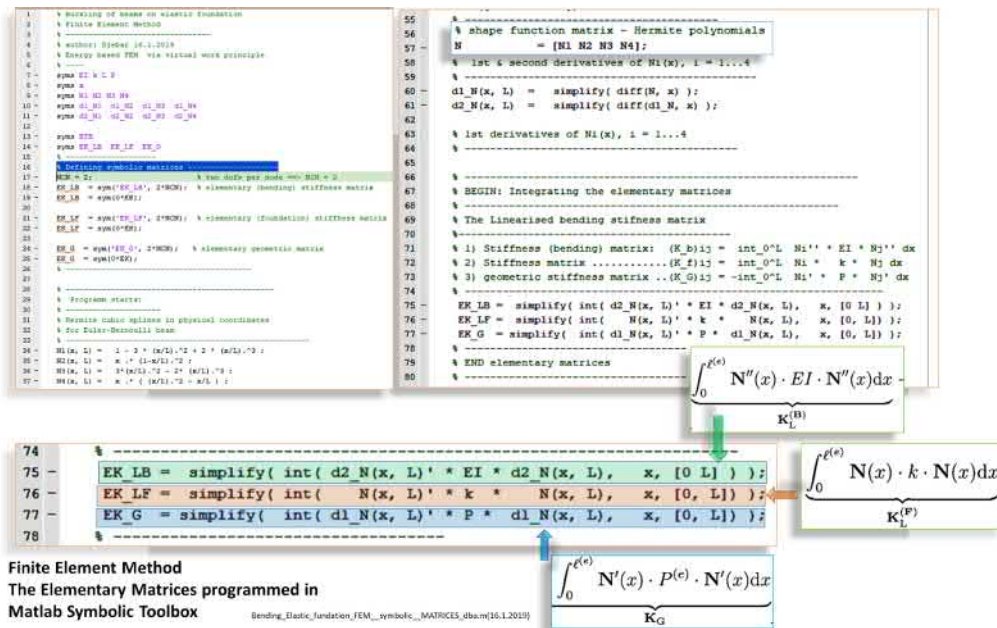


Figure 1.133: Example of Matlab-code to determine symbolically the element matrices.

written explicitly to show how they are derived in a Matlab symbolic toolbox

$$\mathbf{K}_L^{(B)} = \int_0^{\ell^{(e)}} \mathbf{N}''^T(x) \cdot EI \cdot \mathbf{N}''(x) dx, \quad (1.762)$$

$$\mathbf{K}_L^{(F)} = \int_0^{\ell^{(e)}} \mathbf{N}^T(x) \cdot k \cdot \mathbf{N}(x) dx, \quad (1.763)$$

$$\mathbf{K}_G = - \int_0^{\ell^{(e)}} \mathbf{N}'^T(x) \cdot P^{(e)} \cdot \mathbf{N}'(x) dx. \quad (1.764)$$

and an example of the script used for the determining the term $(K_B)_{12}$ (1.133) is provided: The shape functions and their derivatives:

²⁷⁷We will come back to this point later (TO DO).

```

% -----
% Hermite cubic splines in physical coordinates
% for Euler-Bernoulli beam
% -----
N1(x, L) = 1 - 3 * (x/L).^2 + 2 * (x/L).^3 ;
N2(x, L) = x .* (1-x/L).^2 ;
N3(x, L) = 3*(x/L).^2 - 2*(x/L).^3 ;
N4(x, L) = x .* ( (x/L).^2 - x/L ) ;
% -----

The elementary stiffness and geometrical matrices

% -----
% shape functions and derivative matrices - Hermite polynomials
% -----
N          = [N1 N2 N3 N4];
d1_N(x, L) = simplify( diff(N, x) );
d2_N(x, L) = simplify( diff(d1_N, x) );
% -----
% Elementary matrices - symbolic integration
% -----
EK_LB = simplify( int( d2_N(x, L)' * EI * d2_N(x, L), x, [0 L] ) );
EK_LF = simplify( int( N(x, L)' * k * N(x, L), x, [0, L] ) );
EK_G  = simplify( int( d1_N(x, L)' * P * d1_N(x, L), x, [0, L] ) );
% -----

```

which finally results in the following elementary matrices below

The elementary matrices (Figure 1.134) are the result of the symbolic integration by the script programmed in the `Matlab` symbolic toolbox. Sometimes, it is useful to use the help of such computer algebra, at least from cross-checking.

In the following two examples of application of the above '*pocket-size*' FE-approach will be shown.

Other numerical approaches as Rayleigh-Ritz or finite difference method can be also used to solve approximately various problems of stability. It should be reminded that our purpose here is not to compete with full well-established **Finite Element Software** but to gain conceptual understanding of stability behaviour of structures²⁷⁸.

²⁷⁸Deriving formulae forces us to create meta-concepts which are the 'handles' for understanding and doing correct structural analysis and design. Recall that one you solve a stability problem by a 3D-FE model, in some computer software, you will obtain only real numbers mapped to 3D nodal or integration points. No true understanding is possible through numbers only. For instance, the meta-concepts or phenomena, known to you as *lateral-torsional buckling*, *torsional buckling*, *combined flexural-torsional buckling*, *shell and plate buckling*, do not simply exist in the 3D cloud of real numbers.


```

EK_LB(EI, L) =

[ (12*EI)/L^3, (6*EI)/L^2, -(12*EI)/L^3, (6*EI)/L^2]
[ (6*EI)/L^2, (4*EI)/L, -(6*EI)/L^2, (2*EI)/L]
[ -(12*EI)/L^3, -(6*EI)/L^2, (12*EI)/L^3, -(6*EI)/L^2]
[ (6*EI)/L^2, (2*EI)/L, -(6*EI)/L^2, (4*EI)/L]

EK_LF(EI, L) =

[ (13*L*k)/35, (11*L^2*k)/210, (9*L*k)/70, -(13*L^2*k)/420]
[ (11*L^2*k)/210, (L^3*k)/105, (13*L^2*k)/420, -(L^3*k)/140]
[ (9*L*k)/70, (13*L^2*k)/420, (13*L*k)/35, -(11*L^2*k)/210]
[ -(13*L^2*k)/420, -(L^3*k)/140, -(11*L^2*k)/210, (L^3*k)/105]

EK_G(P, L) =

[ (6*P)/(5*L), P/10, -(6*P)/(5*L), P/10]
[ P/10, (2*L*P)/15, -P/10, -(L*P)/30]
[ -(6*P)/(5*L), -P/10, (6*P)/(5*L), -P/10]
[ P/10, -(L*P)/30, -P/10, (2*L*P)/15]
    
```

Bending_Elastic_fundation_FEM_symbolic_dba.m (14.1.2019)

Figure 1.134: Elementary matrices obtained by symbolic integration.

Application example - no soil interaction

Let's start with a simple case of a column loaded as shown in the Margin Figure without soil interaction ($k \equiv 0$). Taking only the active²⁷⁹ global degrees of freedom

$$\mathbf{a} = [\phi_1, \phi_2]^T \quad (1.765)$$

(or $[\theta_1, \theta_2]$) (see Margin figure), we obtain the system matrices (assembled matrices)

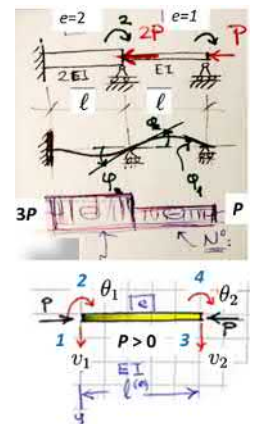
The global linearised stiffness and geometric matrices are

$$\mathbf{K}_L = \frac{2EI}{\ell} \begin{bmatrix} 2 & 1 \\ 1 & 6 \end{bmatrix}, \quad (1.766)$$

$$\mathbf{K}_G = -\frac{Pl}{30} \begin{bmatrix} 4 & -1 \\ -1 & 16 \end{bmatrix} \quad (1.767)$$

The assembly of the matrices is done in a manner very practical for hand-

²⁷⁹This means that zero the degrees of freedom are automatically dropped from the beginning to account for the corresponding boundary conditions. This procedure allows to obtain a smaller system of equations from the start. Consequently, only terms related to the active degrees of freedom are assembled into the system matrices.



procedure²⁸⁰ as

$$K_{11} = K_{44}^{(1)} = \frac{EI}{\ell^3} 4\ell^2 - \frac{P}{30\ell} 4\ell^2 \quad (1.768)$$

$$K_{12} = K_{21} = K_{42}^{(1)} = \frac{EI}{\ell^3} 2\ell^2 + \frac{P}{30\ell} \ell^2 \quad (1.769)$$

$$K_{22} = K_{22}^{(1)} + K_{44}^{(2)} = \frac{EI}{\ell^3} 4\ell^2 - \frac{P}{30\ell} 4\ell^2 + \frac{2EI}{\ell^3} 4\ell^2 - \frac{3P}{30\ell} 4\ell^2 \quad (1.770)$$

Maybe, the student should be careful and notice that the compression internal force $P^{(1)} = P$ in the first element and is $P^{(2)} = 3P$ for the second element, consequently. The loss of stability condition is given by the global eigenvalue problem

$$\left(\frac{2EI}{\ell} \begin{bmatrix} 2 & 1 \\ 1 & 6 \end{bmatrix} - \frac{P\ell}{30} \begin{bmatrix} 4 & -1 \\ -1 & 16 \end{bmatrix} \right) \begin{bmatrix} \phi_1 \\ \phi_2 \end{bmatrix} = \begin{bmatrix} 0 \\ 0 \end{bmatrix}. \quad (1.771)$$

Next notation is used: global matrices are given by their terms as K_{IJ} for the global degrees of freedom I and J . Local contributions from an element e is denoted $K_{ij}^{(e)}$, where i and j correspond to local degrees of freedom.

Criticality condition $\det(\mathbf{K}) = 0$ gives the two eigenvalues

$$P_{1,cr} = 1.62\pi^2 \frac{EI}{\ell^2} \quad (1.772)$$

$$P_{2,cr} = 3.97\pi^2 \frac{EI}{\ell^2} \quad (1.773)$$

$$(1.774)$$

where the buckling load being the smallest value $P_{cr} = 1.62\pi^2 \frac{EI}{\ell^2}$. The corresponding Eigen-vectors (or buckling modes) are

$$\phi_1 = \begin{bmatrix} 0.266 \\ -0.196 \end{bmatrix} \quad (1.775)$$

and

$$\phi_2 = \begin{bmatrix} -0.428 \\ -0.159 \end{bmatrix}. \quad (1.776)$$

Application example - cantilever

Consider a cantilever column with end-load P . Using two elements of equal length, one obtains (Fig. 1.135))

$$P_{cr}^{(\text{FEM})} = 0.250128 \cdot \pi^2 \frac{EI}{\ell^2} \approx \underbrace{\frac{1}{4} \cdot \pi^2 \frac{EI}{\ell^2}}_{\text{analytical}}. \quad (1.777)$$

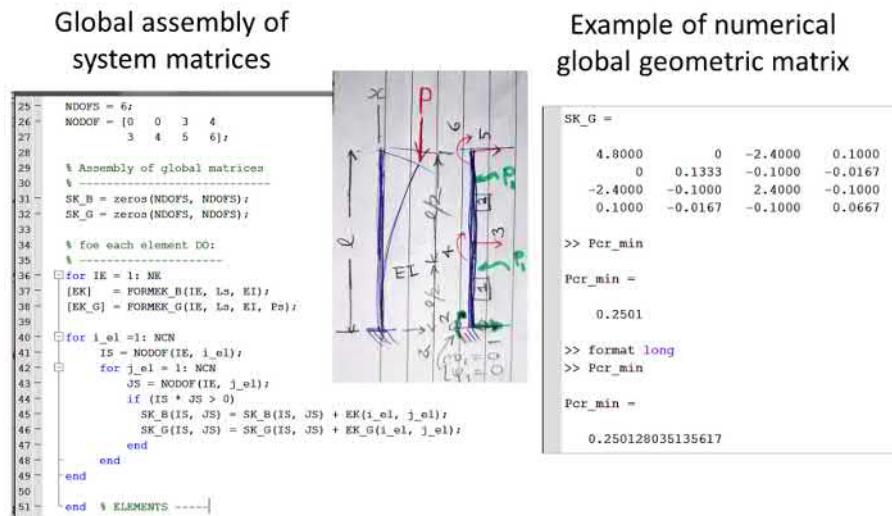


Figure 1.135: Axially loaded cantilever column as solved by the FEM presented in these notes.

The Matlab code is reproduced below for the curious.²⁸¹

```

% Djebar B. 2021 -----
% --- Cantilever column with two loads P1 and P2
% ---- x L and x = L/2 ---
% -
clear all;
% ----- DATA -----
L = 1;
Ls = [L/2 L/2];

% multiple load
P1 = 1;
P2 = 1;

Ps = [P1 P1]; % [P1 P2]
% Ps = [P1 P1+P2]; % [P1 P2]

```

²⁸⁰Writing nodal discrete force equilibrium from elementary contributions results naturally in the matrices assembly procedure used here.

²⁸¹Please, notice the simple infinite aesthetic beauty of the general assembly code-segment. I learnt it from one of my old teachers, Emeritus professor Jukka A., during my first summer job (teekkarina). We then, were programming in FORTRAN using CAPITAL LETTERS DKT- and DMT-elements for thin and thick plates.

```

EI = 1;
% -----
% -----
% Connectivity
% -----
NCN = 4;
NE   = 2;
NDOF = 4;
NDOFS = 6;
NODOF = [0  0  3  4
          3  4  5  6];

% Assembly of global matrices
% -----
SK_B = zeros(NDOFS, NDOFS);
SK_G = zeros(NDOFS, NDOFS);

% foe each element DO:
% -----
for IE = 1: NE
[EK]   = FORMEK_B(IE, Ls, EI);
[EK_G] = FORMEK_G(IE, Ls, EI, Ps);

for i_el = 1: NCN
IS = NODOF(IE, i_el);
for j_el = 1: NCN
JS = NODOF(IE, j_el);
if (IS * JS > 0)
SK_B(IS, JS) = SK_B(IS, JS) + EK(i_el, j_el);
SK_G(IS, JS) = SK_G(IS, JS) + EK_G(i_el, j_el);
end
end
end

end % ELEMENTS -----

% Boundary conditions (at clamped end)
% Eliminating equation at homogeneous BCs
% -----
SK_B(1:2,:) = [];
SK_B(:,1:2) = [];
SK_G(1:2,:) = [];
SK_G(:,1:2) = [];

```

```

% Solving the egneralised eigenvalue problem
% -----
[v, Lam] = eig(SK_B, SK_G);

Pcr = diag(Lam) ;
PcrE = Pcr / (pi*pi); % in standard form as devided by pi^2

Pcr_min = min(PcrE) % The smalles buckling load
% -----

```

Application example - frame

Application example - with soil interaction

[TO BE CONTINUED ... 12.1.2019]

A discrete mechanical model for lateral-torsional buckling

Till now, we considered only buckling resulting from direct axial loading (compression, usually) normal to the cross-section of beam-columns. Now we leave this land and enter the word of beams that can buckle even under bending loading when the rigidity of the cross section in some principal inertia direction is very high as compared with the orthogonal direction. A cantilever beam having having for instance very narrow rectangular cross-section is a good example.

When such beam is loaded in bending (transversal load or end-bending moments), the deflection, in the plane of the load, grows with the increase of loading till the deflection reaches some critical value after which, the beam *suddenly moves laterally with rotation*. The cross-section deflects laterally and rotates, without increase of transversal deflection. All this occurs in the tiny neighbourhood of what is called a bifurcation point. The corresponding maximum load prior lateral-torsional buckling is the critical buckling load, in short.

The loss of stability we mean here called *lateral torsional buckling* by engineers of our field.

Let's demonstrate the physics of such behaviour using the simplest discrete mechanical model that I know as shown in Figure (1.136). The continuous problem will be treated in coming sections. The discrete model consists on one single rigid element where the elastic deformation is concentrated in the elastic sprigs C_w , C_v and C_{θ_T} , corresponding, respectively to lateral deflection w , transversal deflection v and rotation (torque) about the axis $x - x$ of the beam θ_T . The rotation around axis $y - y$ corresponding to lateral deflection w is denoted θ_w and respectively, θ_v denotes rotation around axis $z - z$.

Consider a horizontal concentrated end-load P applied at the center of gravity G of the cross-section. without any imperfections. (Note that in the figure, the load is applied at a distance a from G . We will consider this case in the continuous model). Let's increase the point load P gradually and slowly. As described above, the cantilever have only a vertical motion given by the deflection (as a rigid body) by an amount v which moves the center of gravity G to G' .

When the load reaches a critical threshold value (the buckling load) P_{cr} , the rigid cantilever loss it's stability and the cross-section have a *simultaneous combined tiny motion of lateral deflection w associated with a rotation θ_T* (lateral-torsional motion). Notice that during this *tiny* 'buckling' combined motion *the center of gravity G' does not move vertically any more but remains in a horizontal tiny motion of amplitude w which moves to G'' with a combined rotation of the cross-section by the angle θ_T* . All his motion occurs in the tiny neighbourhood of the bifurcation point without increase of P from it's critical value. What happens, after that is called post-buckling behaviour. We will not treat it here. We will just determine the critical load using energy principles This is for the setting of the story. Notice how long is the preparation of the subject. Let's go to formulas, the butter on our bread.

Here follow the two configurations to be considered: 1) initial pre-buckled state: $v \neq 0$, $w = 0$ and $\theta_T = 0$ and 2) the lateral-torsional buckled state (post-buckled-state): $\Delta v = 0$, $w \neq 0$ and $\theta_T \neq 0$. It is between these two state that energy changes are computed.

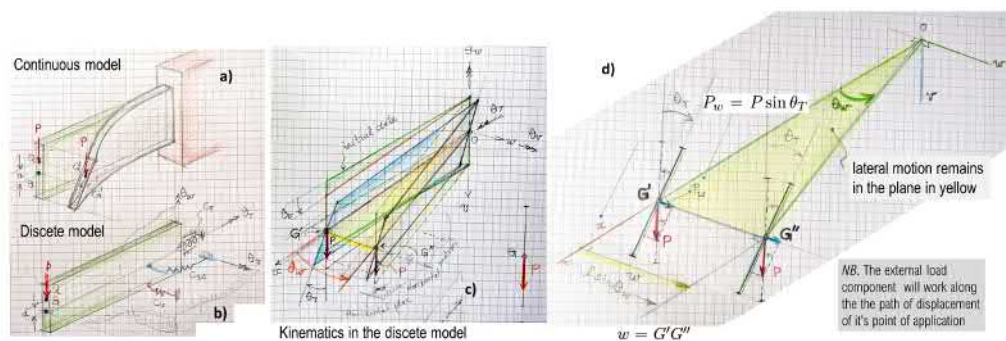


Figure 1.136: Lateral torsional buckling of a cantilever. A simple discrete model and its kinematics. Notice that during the tiny lateral motion at buckling, the center of gravity G does not move vertically any more but remain in a simultaneous horizontal tiny motion w to the point G'' and rotation of the cross-section rotates by an angle θ_T . In this example, we consider only the case where $a = 0$.

We need first to pay a bit attention to the increment of external work ΔW_e during this tiny buckling motion described above. To determine the correspond-

ing change in work of external load, one should account for the geometrical non-linearity that rotated cross-section while moving horizontally, introduces. So, it is the projection, or the component $P_w = P \sin \theta_T$ that will work during the horizontal motion $w = G'G''$. Stop a second for pedagogical reasons: one very important general thing to notice and to remember when we will come to treat the stability loss of the continuous model in lateral-torsional buckling. is that the increment of the work of the initial shear stress component τ_w^0 in the direction of the lateral tiny motion w , after rotation of the cross-section, will contribute to the change of the external work in subsection (1.13.1). Let's now come back to our problem and continue the story.

Therefore, the change in the work of external load P at buckling is

$$V = -\Delta W_e = - (P \sin \theta_T) \cdot w \tag{1.778}$$

$$= - (P \sin \theta_T)(\ell \sin \theta_w). \tag{1.779}$$

The total potential energy change between the initial pre-buckled state and post-buckled-state becomes

$$\Delta \Pi = U + V \tag{1.780}$$

$$= \underbrace{\frac{1}{2}C_w\theta_w^2 + \frac{1}{2}C_v\theta_v^2 + \frac{1}{2}C_T\theta_T^2}_U - \underbrace{(P \sin \theta_T)(\ell \sin \theta_w)}_V. \tag{1.781}$$

Note in the post-buckled configuration (=the tiny buckled configuration) we have only two degrees of freedom which becomes active, namely, w and θ_T . The neutral equilibrium equations are obtained by taking the variations with respect to $\delta\theta_w$ and $\delta\theta_T$ and keeping P unchanged in the vicinity of the bifurcation point. In short,

$$\delta(\Delta \Pi) = \underbrace{[C_w\theta_w - P \sin \theta_w \ell \cos \theta_w]}_{=0, \text{1st equilibrium equation}} \cdot \delta\theta_w + \tag{1.782}$$

$$+ \underbrace{[C_T\theta_T - P \cos \theta_T \ell \sin \theta_w]}_{=0, \text{2nd equilibrium equation}} \cdot \delta\theta_T = 0, \quad \forall \delta\theta_T, \delta\theta_w \tag{1.783}$$

The above non-linear equilibrium equations describes the post-buckling equilibrium paths. They permit to investigate the stability (or instability) of such paths by analysing the sign of the second generalised 'derivatives'²⁸². To find the critical buckling load, P_{cr} , it is enough to linearise the above equilibrium equations by taking $\sin \theta \approx \theta$ and $\cos \theta \approx 1$. Doing this on obtains

$$C_w\theta_w - P \sin \theta_w \ell \cos \theta_w = 0 \rightarrow C_w\theta_w - P\ell\theta_w = 0 \tag{1.784}$$

$$C_T\theta_T - P \cos \theta_T \ell \sin \theta_w = 0 \rightarrow C_T\theta_T - P\ell\theta_w = 0. \tag{1.785}$$

²⁸²There is plenty of examples given in these notes about how to check for the nature of stability. Please refer to them.

The homogeneous equations above (the linearised ones) correspond to the linearised eigenvalue problem

$$\begin{bmatrix} C_w & -P\ell \\ -P\ell & C_T \end{bmatrix} \begin{bmatrix} \theta_w \\ \theta_T \end{bmatrix} = \begin{bmatrix} 0 \\ 0 \end{bmatrix} \quad (1.786)$$

from which we obtain, finally, the critical load in the form of the beautiful and simple *formula*

$$P_{\text{cr}} = \frac{\sqrt{C_w C_T}}{\ell} \quad (1.787)$$

Note that C_w corresponds to bending rigidity in w -direction. So the inertia moment will be $I_w = hb^3/12$ and not $bh^3/12$ for a rectangular narrow cross-section of height h (in y -direction) and width b (in z -direction), please refer to sub-figure a (Fig. (1.136) how the springs are defined. Let's compare this result with the known analytical result

$$P_{\text{cr}} = 4.01 \frac{\sqrt{EI_y GI_t}}{\ell^2} \quad (1.788)$$

for critical load in lateral-torsional buckling of a continuous cantilever with narrow rectangular cross-section. Identifying $C_w = 3EI/\ell$ and $C_T = GI_t/\ell$ and inserting them into the estimated critical load, the one discrete element model gives

$$\hat{P}_{\text{cr}} = 1.73 \frac{\sqrt{EI_y GI_t}}{\ell^2}. \quad (1.789)$$

The results are quantitatively a bit different, as expected using a so crude approximation (one single discrete element). However, the discrete model provides us with the qualitatively correct *formula*. So, we can be happy again because energy principles seems, what I am saying, is the correct approach when we start investigating and want estimates and *formulas*.

1.12.13 Finite difference method - FDM

Warming up: What is nice with finite difference method is that: it is simple, understandable with only high-school mathematics, efficient and straight forward to the point. Really, *to the point*. Compare with the more *aristocrat* and elaborated concept of *Finite element method* where we need to understand something about *variational calculus* and weak forms. In the *proletarian* difference method, things are much simpler: the partial differential equations are enforced to hold *points-wise* in an approximate form of finite differences. The only deep philosophical concept to recall is that the derivative is indeed essentially the limit of a finite difference (*osamäärä*) which the denominator $\Delta x \rightarrow 0^*$ approaching zero without being zero! Hard to imagine! However, engineers instead of bothering themselves with limits, just limit the denominator to a tiny positive non-zero

number and everything works. To account for boundary conditions and field equation near boundaries, we can use one-sided differences to keep the discrete equations inside the physical domain. I disagree with those using symmetric difference schemes close to the boundaries and for boundary conditions with some difference nodes extending out-off the physical domain. I just do not agree that this corresponds to the right physics whatever argument of symmetry they give. A counter-example against that claim can be for instance, when we have chock-fronts or discontinuities symmetry arguments is broken The problem is that the chock-front locations (or regions) can be part of the unknowns to solve.²⁸³

Finite difference starts: Recall, first, the differential equation to be solved and we rewrite it in a more appropriate form

$$EIv^{(4)} + Pv'' + kv = 0, \quad \text{for any } x \in]0, \ell[\tag{1.790}$$

$$v^{(4)} + \lambda^2 v'' + \beta^4 v = 0, \tag{1.791}$$

where notation²⁸⁴ $\lambda^2 \equiv P/(EI) = a^2/2$ and $\beta^4 \equiv k/(EI) = b^4$ have been used. To close the problem, boundary conditions should be provided at $x(0)$ and $x(\ell)$.

The finite difference (FD-) equations for the PDE are direct and straight forward to write even by hand and even more, based only on high-school mathematics. One has just to recall the definition of a derivative of a function f' as the limit of a difference quotient $\Delta f/\Delta x$ when Δx becomes very small without being exactly null. Then the derivative $f' \approx \Delta f/\Delta x$ for some chosen small value of Δx . Higher derivatives are then approximated, by the same difference formula, as derivatives of derivatives. For instance $f'' \approx \Delta f'/\Delta x = [f'(x + \Delta x) - f'(x)]/\Delta x$, and so on.

The goal is, in general, to solve the partial differential equation system (PDE) describing loss of stability (Linearised homogeneous equations of equilibrium). The key idea is the approximate the derivatives in the (PDE) with their respective difference quotients²⁸⁵. The difference schemas can be obtained by Taylor expansions. This way, one obtains also an estimate for the truncation error.

We will use central differences. Sometime, especially for boundary nodes, it is even better to use one-side differences (left- or right-side). We will, come to this case later. Think that the interval $[x_1, x_N[$ representing the column

²⁸³Such one-sided differences can be for instance, tailored from Taylor expansions centred on the boundary point and directed toward the physical domain. Another way, is to approximate the unknown function by Lagrange polynomials and, again, the function or it's derivatives at the boundary point using only nodes directed toward the physical domain.

²⁸⁴Be attentive with notations that unfortunately may be not 'yet' consistent between chapters or even sections (notation will be homogenised in updated versions). The symbol β used now has not the exactly same meaning than β used for instance in Equation (1.699).

²⁸⁵Derivaatat approximoidaan niiden osamäärillä (sf).

centreline being discretized by N nodal points x_i . The length of the column being $\ell = x_N - x_1$. Assume for simplicity, that a constant step $\Delta x_i \equiv h = x_i - x_{i-1}$. For notational reasons, we write f_i to say $f(x_i)$, for any function f . The central differences²⁸⁶ at a point x_i are

$$v'_i \approx \frac{1}{2h} [v_{i+1} - v_{i-1}], \quad (1.792)$$

$$v''_i \approx \frac{1}{h^2} [v_{i+1} - 2v_i + v_{i-1}], \quad (1.793)$$

$$v'''_i \approx \frac{1}{2h^3} [v_{i+2} - 2v_{i+1} + 2v_{i-1} - v_{i-2}], \quad (1.794)$$

$$v^{(4)}_i \approx \frac{1}{h^4} [v_{i+2} - 4v_{i+1} + 6v_i - 4v_{i-1} + v_{i-2}]. \quad (1.795)$$

It is very practical, for hand calculations, to draw a on a transparent or semi-transparent support graphical representation of the differences above with the spacing h having the same physical dimensions as the one in the paper drawing of the finite grid $[x_1, x_2, \dots, x_i, x_{i+1}, \dots, x_N]$. By placing the central molecule of on the node i , one can safely write the differences equations (1.796) as given bellow. Such graphical representations are called *computational molecule* (Figures 1.137 and 1.138).

Replacing in (Equation 1.791) the derivatives by their difference quotients and re-arranging terms on obtains that nodal equilibrium

$$\begin{bmatrix} +1 & -4 & (6 + h^4\beta^4) & -4 & 1 \end{bmatrix} + h^2\lambda^2 \begin{bmatrix} 0 & 1 & -2 & 1 & 0 \end{bmatrix} \begin{bmatrix} v_{i-2} \\ v_{i-1} \\ v_i \\ v_{i+1} \\ v_{i+2} \end{bmatrix} = 0 \quad (1.796)$$

should hold at each point internal x_i , $i = 2, 3, \dots, N - 1$.

One may recognise the raw i of the linearised global 'FD-stiffness' matrix $\mathbf{K}_L^{(B)} + \mathbf{K}_L^{(F)}$ and \mathbf{K}_G written for node x_i

$$\mathbf{K}_L^{(B)}(:, i) + \mathbf{K}_L^{(F)}(:, i) = \begin{bmatrix} +1 & -4 & \underbrace{(6 + h^4\beta^4)}_{\text{node } i} & -4 & 1 \end{bmatrix}, \quad (1.797)$$

$$\mathbf{K}_G(:, i) = h^2\lambda^2 \begin{bmatrix} 0 & 1 & \underbrace{-2}_{\text{node } i} & 1 & 0 \end{bmatrix}, \quad (1.798)$$

$$\text{where } h^2\lambda^2 = \frac{Ph^2}{EI} \text{ and } h^4\beta^4 = \frac{kh^4}{EI}. \quad (1.799)$$

Writing Equation (1.796) at the specified points $i = 2 : N - 1$ and accounting for the discrete boundary conditions, one obtain an eigenvalue problem

$$\left([\mathbf{K}_L^{(B)} + \mathbf{K}_L^{(F)}] + \mathbf{K}_G(\lambda^2) \right) \mathbf{v} = \mathbf{0}, \quad (1.800)$$

²⁸⁶Theses formulas are of order $\mathbf{O}(h^2)$

where $\mathbf{v} = [v_1, v_2, \dots, v_i, \dots, v_N]^T$ the nodal displacement vector. The boundary conditions should be also discretized at points x_1 and x_N . The smallest eigenvalue corresponds to the buckling load. The corresponding eigenmode gives the buckling mode.

The computational molecule for the difference equation (1.796) at an arbitrary point x_i is given in Figure (1.137). *How to use this molecule?* Start by

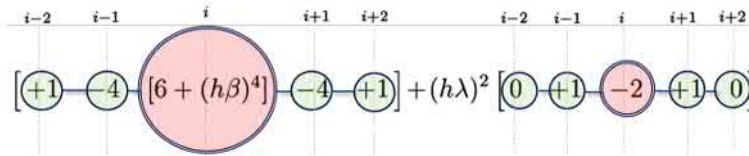


Figure 1.137: FDM representation as computational molecule for the difference equation (1.796) at x_i .

numbering²⁸⁷ the internal free nodes from $i = 1 : N$. Put its central 'atom' (marked with double line circle and semi-transparent red) on the first free node (not a boundary node) and the coefficients row will be the first row in the system equations for the corresponding node $i = 1$ marked above the molecule. repeat the operation for all internal nodes $i = 1 : N$ by sliding the central atom of the FDM-molecule to the node i , and write the row number i of the global system of equations for the current node. The number of free nodes is N . For the nodes close to the boundary nodes, the FDM-molecule goes partly out of the free-nodes. Then, account for the boundary nodes using relations for external nodal values obtained from the FDM-version of the boundary conditions (*Cf.* subsection below on boundary conditions).

Example of boundary conditions

Consider a boundary node m ($m = 1$ or $m = N$), then we have

Clamped:

$$v(x_m) = 0 \implies v_m = 0, \tag{1.801}$$

$$v'(x_m) = 0 \implies v_{m+1} - v_{m-1} = 0 \implies v_{m+1} = v_{m-1} \tag{1.802}$$

²⁸⁷For practical reasons, it is better to number the internal free nodes from $i = 1 : N$. The boundary nodes can numbered by adequately. For instance, if the boundary node corresponds to zero displacement, then numbering it by '0' is not a bad idea. I usually, number external nodes by '-' something.

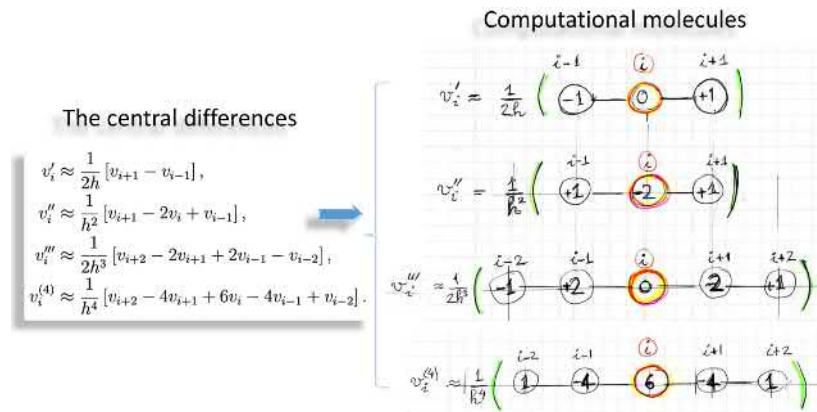


Figure 1.138: FDM representation of derivatives as computational molecules as difference quotients.

Free:

$$M(x_m) = -EIv''(x_m) = 0 \implies v_{m+1} - 2v_m + v_{m-1} = 0, \quad (1.803)$$

$$Pv'(x_m) - Q = 0 \implies \frac{P}{2h}(v_{m+1} - v_{m-1}) + EI(v_{m+2} - 2v_{m+1} + 2v_{m-1} - v_{m-2}) = 0 \quad (1.804)$$

$$(1.805)$$

Hinged:

$$v(x_m) = 0 \implies v_m = 0, \quad (1.806)$$

$$M(x_m) = -EIv''(x_m) = 0 \implies v_{m+1} - 2 \underbrace{v_m}_{=0} + v_{m-1} = 0, \quad (1.807)$$

$$(1.808)$$

Roller:

$$v'(x_m) = 0 \implies v_{m+1} - v_{m-1} = 0 \implies v_{m+1} = v_{m-1} \quad (1.809)$$

$$Q(x_m) = -EIv'''(x_m) = 0 \implies v_{m+2} - 2v_{m+1} + 2v_{m-1} - v_{m-2} = 0 \quad (1.810)$$

$$\implies v_{m+2} = v_{m-2} \quad (1.811)$$

Note that the boundary condition terms above use central differences. Later, when I will have more time, I will derive and use one-side difference schemes for boundary conditions involving derivatives. Why? Because, for me, the finite-difference expression should involve *only material points* and not any fictitious points located on fictitious prolongation of the structure. So, for me, this is my

physical argument for using left- or right sided differences for boundary terms, even if some of my colleagues do not agree with the argument. For them, probably, mathematics generates the physics, for me, not. My argument becomes self-evident when we deal with dynamics. Then, when waves are reflected at boundaries, so we face discontinuities (like velocity changes sign at the boundary after reflection, presence of chock-waves, etc.), the only correct way to take information is to take it within the body, not outside it, to estimate motion, velocities and so on. This is why, the all the finite difference 'molecules' should involve only material points.

Application example: both end clamped axially compressed column

Let's solve for the critical load P_{cr} for the case in Figure (1.139). For hand estimation purpose, we use the coarse grid depicted in the figure. Note that we do not assume symmetrical mode since v_1 and v_2 are chosen *independent* degrees of freedom. It is quite dangerous to assume symmetry in stability analysis because asymmetric modes can be the critical one. Consider two cases: 1) $k = 0$ and 2) $k \neq 0$. For case 1) with $k = 0$, we know (from Euler's basic buckling cases) that the first buckling mode is symmetric and that the theoretical critical Euler buckling load $P_{cr} = 39.4EI/\ell^2$. Let see what result we will achieve by using FDM.

With elastic foundation: The boundary conditions corresponds to

$$v(0) = 0 \implies v_0 = 0 \tag{1.812}$$

$$v'(0) = v'(\ell) = 0 \implies v_{-1} = v_1 \text{ and } v_{-2} = v_2. \tag{1.813}$$

Using the FD-molecule of the problem (1.796) and accounting for the boundary conditions, we obtain two difference equations

$$i = 1 : (v_1 + [6 + (h\beta)^4]v_1 - 4v_2) + (h\lambda)^2(-2v_1 + v_2) = 0, \tag{1.814}$$

$$\implies [7 + (h\beta)^4]v_1 - 4v_2 + (h\lambda)^2(v_2 - 2v_1) = 0, \tag{1.815}$$

$$i = 2 : (-4v_1 + [6 + (h\beta)^4]v_2 + v_2) + (h\lambda)^2(-2v_2 + v_1) = 0, \tag{1.816}$$

$$\implies [7 + (h\beta)^4]v_2 - 4v_1 + (h\lambda)^2(v_1 - 2v_2) = 0. \tag{1.817}$$

Regrouping the above system of equation in a matrix form, we see better the eigenvalue problem structure of the equations as

$$\left(\begin{bmatrix} 7 + (h\beta)^4 & -4 \\ -4 & 7 + (h\beta)^4 \end{bmatrix} + (h\lambda)^2 \begin{bmatrix} -2 & +1 \\ +1 & -2 \end{bmatrix} \right) \begin{bmatrix} v_1 \\ v_2 \end{bmatrix} = \begin{bmatrix} 0 \\ 0 \end{bmatrix}. \tag{1.818}$$

Let now solve for the two cases discussed previously.

1) Without elastic foundation: So, now one consider the classical Euler-buckling of a column without foundation. The parameters are $h^2\lambda^2 = \frac{Ph^2}{EI}$ and

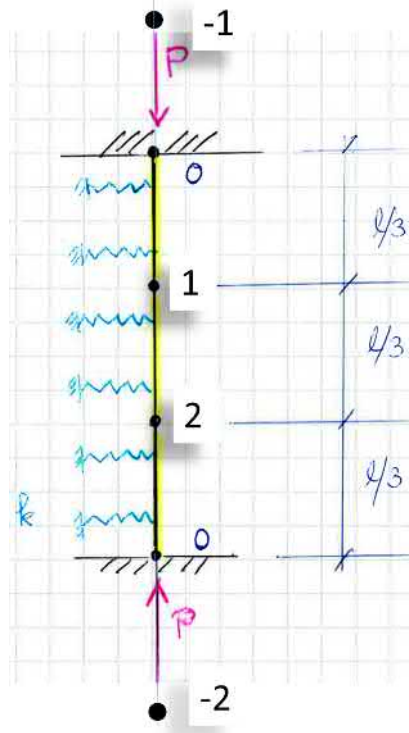


Figure 1.139: Axially loaded column on elastic foundation. The grid points labelled '-1' and '-2' are fictive nodes needed by the differences of higher derivatives.

$h^4 \beta^4 = \frac{kh^4}{EI} = 0$. Therefore,

$$\left(\underbrace{\begin{bmatrix} 7 & -4 \\ -4 & 7 \end{bmatrix}}_{\mathbf{K}_L} + \underbrace{\frac{Ph^2}{EI} \begin{bmatrix} -2 & +1 \\ +1 & -2 \end{bmatrix}}_{\mathbf{K}_G(P) \equiv \bar{P}} \right) \begin{bmatrix} v_1 \\ v_2 \end{bmatrix} = \begin{bmatrix} 0 \\ 0 \end{bmatrix}. \quad (1.819)$$

The above eigenvalue problem can be solved symbolically or numerically by hand or in general, using computer algebra tools, like for instance, Matlab function `eig` with the script `[v, P] = eig(KL, KG)`. The following solution is obtained and the smallest eigenvalue corresponds to the buckling load

$$\bar{P}_{cr,1} = \frac{P_{cr} h^2}{EI} = 3 \implies P_{cr} = 27 \frac{EI}{\ell^2} = 2.74 \frac{\pi^2 EI}{\ell^2} \quad (1.820)$$

where $h = \ell/3$. The corresponding buckling mode is *symmetric* one (Figure 1.140). The second critical load being higher $\bar{P}_{cr,2} = 3.7$. The corresponding buckling mode being *asymmetric*.

The exact solution being $P_{cr} = 4\pi^2 EI/\ell^2$. Note that the used mesh is very-coarse: only two-nodes! Despite that, we've obtained a usable numerical solution together with *design handler* EI/ℓ^2 determining completely the stability behaviour and on which one can act in order to achieve the need loading capacity. This is not much, you'll say. But assuming, one knows, *a priori* nothing about the exact solution, what we obtained is indeed very much.

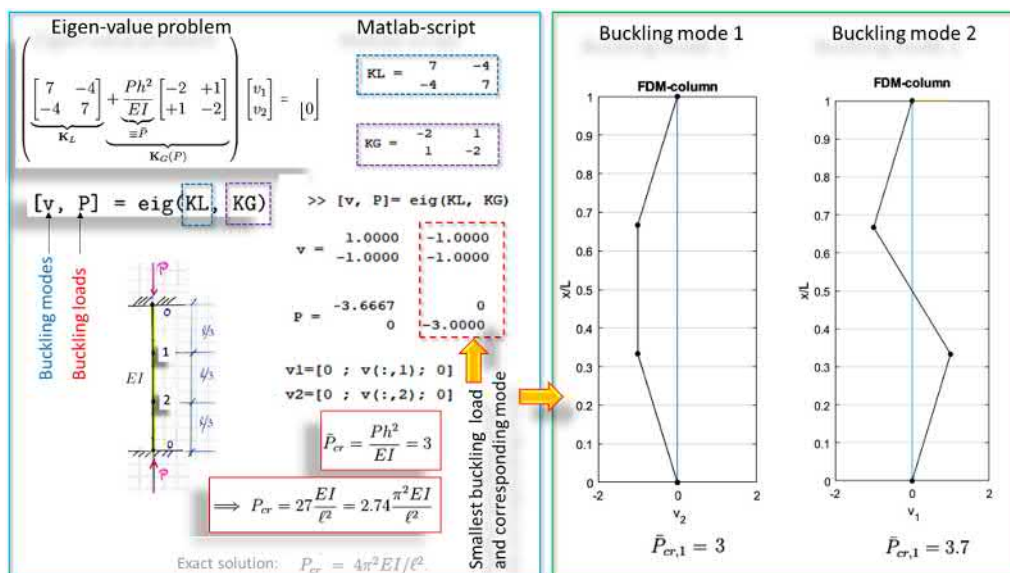
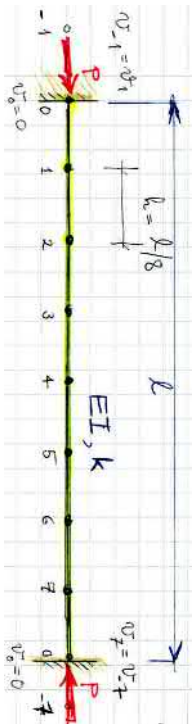


Figure 1.140: Buckling of an axially loaded column on elastic as solved by FDM-method. (a very coarse grid)

Three comments may be relevant: *a)* The approximated buckling load (Equation 1.820) seems²⁸⁸ to be a *lower bound*. This is very welcome as regard to safety aspects of such analysis: we know²⁸⁹ for that the true buckling load should be higher. The solution is depicted in Figure (1.140). *b)* We did not assumed symmetry. It comes out as the lowest motion solution. While dealing with additional effects of the foundation, the first mode may change. This is why, in stability analysis, no symmetry assumptions should be done, *a priori*. Such assumptions are even *dangerous*. *c)* Last but not least: the FD-molecule is valid also for non-constant properties $k(x_i)$ and $EI(x_i)$. If the property is discontinuous at a node x_i , then take an average value from both sides.

²⁸⁸We need some theoretical results to state this observation as a rule. Is there any such work? To be investigated.

²⁸⁹To check scientific publications on the subject. For the moment we say that it seems so. However, using Rayleigh-Ritz, we obtain buckling loads which are a lower bound for sure. For this, as we have seen before, there exists theoretical results on which one can stand.



Column buckling; FD-grid. Free-dofs $\mathbf{v} = [v_1, v_2, v_3, v_4, v_5]^T$.

Refining the FD-mesh - convergence

The idea is to see that, indeed, by refining the mesh, when can achieve convergence of the numerical result to the exact analytical.

Let's subdivide, for illustration purposes, the length of the column into eight equal parts $h = \ell/8$. It is straightforward to write the FD-equations (1.800) where the system stiffness matrix is now

$$\mathbf{K}_L = \begin{bmatrix} 7 + (h\beta)^4 & -4 & 1 & 0 & 0 & 0 & 0 & 0 \\ -4 & 6 + (h\beta)^4 & -4 & 1 & 0 & 0 & 0 & 0 \\ 1 & -4 & 6 + (h\beta)^4 & -4 & 1 & 0 & 0 & 0 \\ 0 & 1 & -4 & 6 + (h\beta)^4 & -4 & 1 & 0 & 0 \\ 0 & 0 & 1 & -4 & 6 + (h\beta)^4 & -4 & 1 & 0 \\ 0 & 0 & 0 & 1 & -4 & 6 + (h\beta)^4 & -4 & 1 \\ 0 & 0 & 0 & 0 & 1 & -4 & 6 + (h\beta)^4 & -4 \\ 0 & 0 & 0 & 0 & 0 & 1 & -4 & 7 + (h\beta)^4 \end{bmatrix} \quad (1.821)$$

and the geometrical system matrix being

$$\mathbf{K}_G(\bar{P}) = (\lambda h)^2 \begin{bmatrix} -2 & 1 & 0 & 0 & 0 & 0 & 0 \\ 1 & -2 & 1 & 0 & 0 & 0 & 0 \\ 0 & 1 & -2 & 1 & 0 & 0 & 0 \\ 0 & 0 & 1 & -2 & 1 & 0 & 0 \\ 0 & 0 & 0 & 1 & -2 & 1 & 0 \\ 0 & 0 & 0 & 0 & 1 & -2 & 1 \\ 0 & 0 & 0 & 0 & 0 & 1 & -2 \end{bmatrix}. \quad (1.822)$$

The eigenvalue problem (1.800) with $N = 7$ being the number free nodal values of displacement $v_i, i = 1 : 7$, is solved again numerically assuming no elastic foundation $k = 0 \implies \beta = 0$. The smallest eigenvalue gives the buckling load

$$\bar{P}_{cr,1} = \frac{P_{cr} h^2}{EI} = 0.5858 \implies P_{cr} = 37.5 \frac{EI}{\ell^2} = 3.8 \frac{\pi^2 EI}{\ell^2}, \quad (1.823)$$

$$\text{(Exact buckling load: } P_{cr} = 4.0\pi^2 EI/\ell^2\text{)}. \quad (1.824)$$

One can see that the FD-solution approaches well from bellow the exact value. I let the full (numerical) convergence analysis²⁹⁰ for the reader, who I hope has more time than me. The corresponding buckling mode for the smallest buckling load being *symmetric* one (Figure 1.141). The second critical load being higher $\bar{P}_{cr,2} = 1.111 \implies P_{cr,2} = 1.8P_{cr,1}$. The corresponding buckling mode being *asymmetric*.

1) With elastic foundation: So now $k \neq 0$. The discretized eigenvalue problem with a coarse and a bit finer FD-grid are written above for the general case of

²⁹⁰Recalculate with now a mesh $h_{\text{new}} = h_{\text{old}}/2$ and plot convergence curves for $P_{cr}(h)$ in a log-log scale.

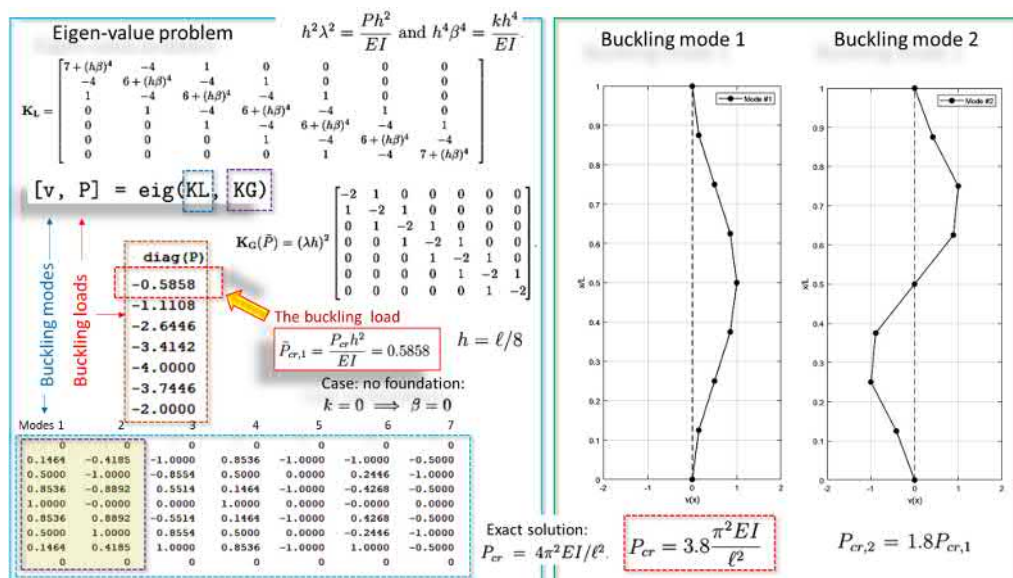


Figure 1.141: Buckling of an axially loaded column on elastic as solved by FDM-method. (a bit finer grid with seven free-nodes)

$k \neq 0$. As also previously, shown, the buckling mode activated first depends on some relative parameter in k and EI (1.128). So now, we will fix this ratio for illustrative reasons. Let's start by determining the buckling load of the case already solved analytically (Figure 1.130). Recall that, for this case, we had the following data and results: The elasticity coefficient k of the foundation was such that $kL^4/EI = 2\pi^4$. The buckling occurs in an antisymmetric mode with buckling load being

$$P_{cr} = 2.4 \cdot 2\sqrt{kEI}. \tag{1.825}$$

[To be continued ... 20.1.2019]

1.12.14 FE-linear buckling analysis of columns on elastic foundation

In the following, for illustrative pedagogical purposes, we analyse a simply supported column on elastic foundation with centric axial compressive load P . Simulation data: $\ell = 1$ m, $b = \ell/10$, $h = 50$ mm. $E = 70$ GPa ($\nu = 0.33$). We investigate, how the relative 'stiffness number' $\beta \equiv k\ell^2/(\pi^4EI)$ determine the number n of half-waves of the buckling modes corresponding to the (smallest) buckling load P_{cr} , according to Figure (1.128). Obtained FEA²⁹¹ buckling loads $P_{cr}^{(FEM)}$ will be compared to analytical values given by $P_{cr}^{(theor.)} = k_{cr}\sqrt{kEI}$,

²⁹¹Two dimensional FE-analysis. 1-D-column-elastic-fondation-2D-Example-OK.mph

where the stability coefficient $k_{cr} = (n/\bar{\ell})^2 + (\bar{\ell}/n)^2$ with $\bar{\ell} \equiv \ell/\pi(k/EI)^{1/4}$. The limit buckling load P_{cr}^{lim} for $\bar{\ell} \geq 3$ is also given in the table below. The bending stiffness of the column is now $EI = 72917 \text{ Nm}^2$. The results of the analysis and comparison with analytical behaviour are summarised in Table (1.1). There is on

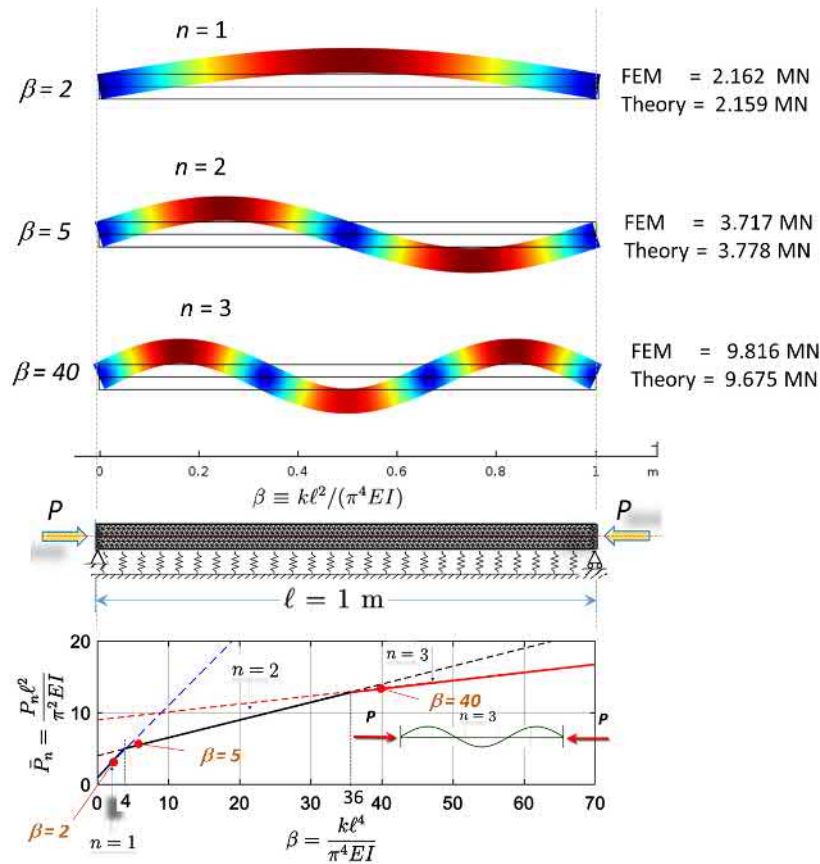


Figure 1.142: Linear FE-buckling analysis. Buckling of axially compressed column on elastic foundation. Buckling loads and corresponding buckling modes as function of the relative stiffness parameter β .

important to not miss: the buckling mode corresponding to the smallest critical load (the buckling load) has not to correspond to one half-wave (Figure 1.142). Indeed, the column can buckle for the first time in one, two or more half-waves depending on the relative stiffness β . The stiffer is, relatively, the foundation (or k) the more wrinkles (half-waves) has the load reaches from below the buckling load.

Table 1.1: FE-linear buckling analysis. The loads are given in [MN] units.

β	$\bar{\ell}$	n	$P_{cr}^{lim.}$	k_{cr}	$P_{cr}^{(theor.)}$	P_{cr}^{FEM}	$P_{cr}^{(theor.)}/P_E$	k [N/m ²]
2	1.189	1	2.04	2.121	2.159	2.162	3	14.2
5	1.495	2	3.22	2.348	3.778	3.717	5.3	35.5
40	2.515	3	9.10	2.126	9.675	9.816	13.4	284.1

1.12.15 Post-buckling analysis of columns on elastic foundation

NB. The results of this subsection, related to deriving the asymptotic post-buckling non-linear equation of equilibrium, is not finalised to give a flowing reading. I will come back as soon as I get time. For the moment, *you can at least try to read it. The derived formula for initial post-buckling is cross-checked.*

One may recall that the *linearise buckling equation* (1.692) of an column-beam on an elastic foundation is mathematically *similar* to *linearised buckling equation* (1.1183) of an axisymmetric thin-walled cylindrical shells under axial compression. Emphasis should be made that this mathematical *similarity concerns only the linearised equations of stability* and not, a priori, the post-buckling behaviour. Consequently, even if the formulas for buckling loads have to be similar on can not extrapolate on similarity post-buckling behaviours. Obviously, the post-critical kinematics are quite different since the physics involved in the post-buckled state are different, think just of the kinematics in a bifurcation point perturbed state.²⁹² A scientific published paper²⁹³ shows that *initial* post-buckling behaviour is *symmetric stable*²⁹⁴ in the neighbourhood of the bifurcation point. However, the statement of *Kounadis* on stability on the initial post-buckled configuration, cannot be general, despite that he claims the contrary in the referenced publication. It is shown, from work of colleague prof. R. Kouhia and the finite element post-buckling analysis, I did in this lecture notes, that there is a critical value for the relative rigidities β after which, the post-buckling behaviour becomes unstable²⁹⁵. . Combinations of k and EI can be found where the post-buckling

²⁹²The question: "whether the post-buckling equilibrium paths of an axially compressed beam bonded on an elastic foundation and axially compressed thin-walled cylindrical shells under symmetrical buckling, can be of similar shape?" comes to naturally to mind. However, it is much more subtle.

²⁹³A.N. Kounadis, J. Mallis & A. Sbarounis. Postbuckling analysis of columns resting on an elastic foundation. *Arch Appl Mech* (2006) **75**: 395-404 DOI 10.1007/s00419-005-0434-1.

²⁹⁴On the contrary, post-buckling behaviour thin-walled cylindrical shells under axial compression is well-known to be unstable.

²⁹⁵This work will be published soon.

behaviour becomes unstable.

In this section, post-buckling analysis of axially compressed columns on elastic foundation will be dealt with. Two approaches will be addressed: 1) using FE-post-buckling analysis and 2) an analytical asymptotic approach.

The starting point is to use an exact expression for the curvature in material²⁹⁶ coordinates (Lagrangian curvature), as given by the *Elastica*, in order to obtain the correct post-buckling equilibrium path. Then, at a second stage, the asymptotic approximation stage to access the *initial* post-buckling path. For that, we account for moderate rotations and make an asymptotic expansion of the exact (Lagrangian) curvature and inserting it in the equilibrium equations while keeping just enough terms to obtain a non-zero right hand in these equations. This allow to solve for displacements v for any P and thus the initial post-buckling equilibrium path which was not possible to do with the eigenvalue problem.

Once, we've re-written non-linear equilibrium equation of the *Elastica* for moderate rotations, we simply add the reaction from the linear springs as $r(x) = kv(x)$ to it. Let's go to the *Elastica* for moderate rotations.

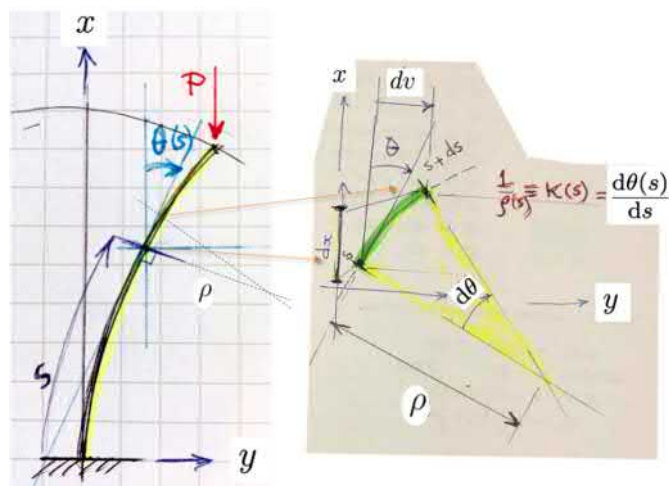


Figure 1.143: Euler's Elastica and kinematics.

Asymptotic post-buckling analysis

Before even starting, let's remind that asymptotic analysis by its nature can address only the the question of local stability.

Recall the geometrically non-linear setting of the problem of axially loaded slender rod; the Euler's Elastica (Figure (1.143) and Equation 1.838). The equation holds for arbitrary large rotations. Figure (1.144) shows an example of

²⁹⁶To have consistency between the strains and stresses to be used.

solutions obtained by numerically integration the *Elastica* equation with simply supported end conditions. The rotations $\alpha = \alpha(s)$ can be very large in magnitude till 160° degrees in the simulation.

One may wonder why use Euler's *Elastica* equation? The answer is simple: first, it is a direct, natural and reliable way to obtain the *correct* and *exact Lagrangian expression for the curvature* $\kappa \equiv \theta'$ in Lagrangian coordinates (2nd equation in 1.847) expressed as function of the deflection v . This way, the reader and I get convinced for the correctness of the Lagrangian curvature formula. Secondly, this approach is pedagogically motivated since it makes a link, for the reader, to a familiar subject treated in previous Chapter addressing *Elastica*. Naturally, *Elastica* Equation (1.838) is limited to the case of a statically determined case of the axially loaded cantilever illustrated in Figure (1.143). For, general case of boundary conditions, we will use the more general equilibrium equation

$$-EI\kappa'' + P \cdot \underbrace{v''(x)}_{\text{should be } (\sin \theta)'} + kv(x) = 0, \tag{1.826}$$

$$\left[\frac{v''(x)}{\sqrt{1 - v'^2(x)}} \right]'' + \frac{P}{EI}v''(x) + \frac{k}{EI}v(x) = 0 \tag{1.827}$$

written in the deformed geometry. The Lagrangian²⁹⁷ exact expression for the curvature $\kappa \equiv 1/\rho$ will be derived a bit further, in this section. In the above equation, the derivatives are taken with respect to $x \in [0, \ell]$ ²⁹⁸. In the above equation, the term Pv'' holds for small rotations where $(\sin \theta)' \approx v''$ ²⁹⁹. For consistency, the term $P \sin \theta$ coming from the *elastica*, should be

$$P(\sin \theta)' \approx P(\theta - \theta^3/6)', \quad \text{where} \tag{1.828}$$

$$\theta - \theta^3/6 \approx v' + \frac{1}{6}v'^3 - \frac{1}{6} \left[v'^3(1 + \frac{1}{2}v'^2) \right] \tag{1.829}$$

$$= v' - \frac{1}{12}v'^5 \approx v' \quad \text{since } v'^5 \ll v'^2 \ll 1 \tag{1.830}$$

$$\implies (\sin \theta)' \approx v''! \tag{1.831}$$

for moderate rotations. As a conclusion, the approximation Pv'' in the second equation of (1.827) seems enough here. Now let's approximate the curvature

²⁹⁷The Eulerian curvature is given by $\kappa = -\frac{d^2v}{dx^2} / \left[1 + \left(\frac{dv}{dx}\right)^2 \right]^{3/2}$ with spatial coordinates.

²⁹⁸The above equations can be written in a non-dimensional form. Take $\xi = x/\ell$, $df/dx = 1/\ell \cdot df/d\xi$, $f_{,xx} = 1/\ell^2 f_{,\xi\xi}$, etc.

²⁹⁹This is (inconsistent approximation but it holds. See further the argument

(moderate rotations) in Equation (1.827)

$$\left[\frac{v''(x)}{\sqrt{1-v'^2(x)}} \right]'' + \frac{P}{\underbrace{EI}_{\lambda_P^2}} v''(x) + \frac{k}{\underbrace{EI}_{\lambda_k^2}} v(x) = 0, \quad \text{where} \quad (1.832)$$

$$\left[\frac{v''}{\sqrt{1-v'^2}} \right] \approx v'' \left[1 + \frac{1}{2} v'^2 \right], \quad (1.833)$$

$$\left[\frac{v''}{\sqrt{1-v'^2}} \right]' \approx v''' + \frac{1}{2} v'^2 v''' + v''^2 v', \quad (1.834)$$

$$\left[\frac{v''}{\sqrt{1-v'^2}} \right]'' \approx v^{(4)} + \frac{1}{2} v'^2 v^{(4)} + 3v' v'' v''' + v''^3, \quad (1.835)$$

$$\implies v^{(4)} + \lambda_P^2 v'' + \lambda_k^2 v = - \left(\frac{1}{2} v'^2 v^{(4)} + 3v' v'' v''' + v''^3 \right) \quad (1.836)$$

So to summarise, the post-buckling behaviour not far from the bifurcation point (= initial post-buckling or for moderate rotations) is obtained by solving the equilibrium equations

$$\boxed{v^{(4)} + \lambda_P^2 v'' + \lambda_k^2 v + \left[\frac{1}{2} v'^2 v^{(4)} + 3v' v'' v''' + v''^3 \right]} = 0, \quad x \in]0, \ell[\quad (1.837)$$

for adequate boundary condition. The above equation is the asymptotic non-linear ODE of we obtained from the equilibrium equation (1.827) by approximating the curvature in order to capture the *initial* post-buckling behaviour. The same equation can be also found in the field literature³⁰⁰. In the cited article, there is an analytical study of the initial post-buckling behaviour.

For the asymptotic analysis of the post-buckling behaviour, we limit ourselves to moderate rotations, let's say, $\alpha \leq 10^\circ$ degrees in amplitude.

Lagrangian exact curvature: Recall, for refreshing memory, the equation of equilibrium of the elastica-cantilever (in Lagrangian coordinates)

$$EI\theta''(s) + P \sin(\theta(s)) = 0, \quad (1.838)$$

where the rotation $\theta(s)$ and the the Lagrangian curvature (Figure (1.143) being related as

$$\boxed{\frac{1}{\rho(s)} = \frac{d\theta(s)}{ds} \equiv \kappa(s)} \quad (1.839)$$

where are Lagrangian type variable. To, finally, obtain the exact curvature

³⁰⁰A.N. Kounadis, J. Mallis & A. Sbarounis. Postbuckling analysis of columns resting on an elastic foundation. *Arch Appl Mech* (2006) **75**: 395–404 DOI 10.1007/s00419-005-0434-1.

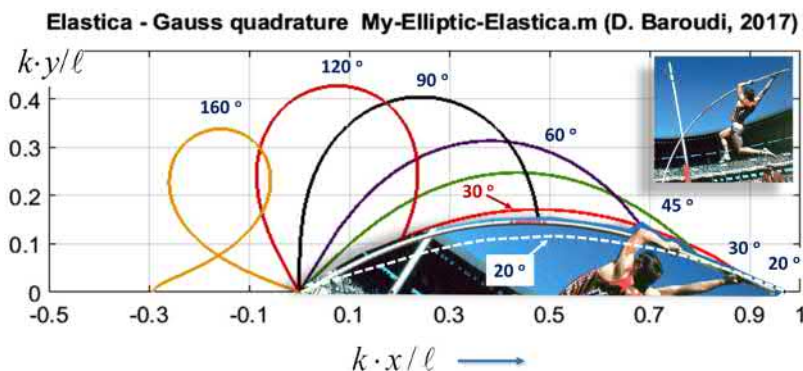


Figure 1.144: Elastica for various ends-angles (α). The solutions are obtained by numerical quadrature of the elliptic integrals. The parameters $k^2 = P/EI$ and $\ell \approx 3.8$ m were used.

formula, one has to express in the above definition $\theta(s)$ in terms of Cartesian material coordinates x and y and to take the derivative $d\theta(s)/ds$ with respect to x . Recall that the material arch-length coordinate $s = s(x, y)$. So, in the following we will do what we promised to do.

The derivatives are with respect to the arch-length s . The displacement of an arbitrary material point $P(s)$ of the deformed rod. From geometry of deformation of initially straight slender rods, we obtain the relations

$$\sin(\theta(s)) = dy(s)/ds, \quad (1.840)$$

$$\cos(\theta(s)) = dx(s)/ds, \quad (1.841)$$

We can write that the differential material element does not change length during deformation, so, $ds = dx$ ³⁰¹ since, we assume incompressibility of the centreline and initially, the bar is straight, so $ds(0) = dx(0)$. So, the geometry of the differential element $ds = dx$ provides directly the trigonometric relation which leads to the exact formula (Graal) for the material curvature:

$$\sin \theta = \frac{dv}{ds} = \frac{dv}{dx} = v' \implies \theta = \arcsin(v') \implies \theta' = (\arcsin(v'))' \equiv \kappa \quad (1.842)$$

³⁰¹Incompressibility assumption holds naturally for incompressible materials. However, in the context of stability, such assumption is an approximation which holds, even for compressible materials, during buckling and a bit in the neighbourhood of the initial post-buckled configuration for relatively moderate rotations. When rotation gets large, this assumption does not hold anymore and the stretching (or compression) of the centreline should be accounted for. *N.B.* In making assumptions, a respectable engineer should provide facts on which he is founding for the validity of his assumptions and their validity range. The word *assumption* means usually making arbitrary choice. Such logic should not be used. Only facts based assumption will be used. Otherwise, any made assumption should be verified for its validity range.

Another way, is to go through displacements. as it will be shown, for pedagogical reasons. So, the displacement of an arbitrary material point $P(s_i)$ on the centreline of rod is given as

$$u(s_i) = x(s_i) - X(s_i), \quad (1.843)$$

$$v(s_i) = y(s_i) - Y(s_i), \quad (1.844)$$

where $X(P) = x(P; t = 0)$, and $Y = y(P; t = 0)$ are the initial material coordinates. Finally,

$$\frac{dv}{ds} = \frac{d(y - Y)}{ds} = \frac{dy}{ds} = \frac{dy}{dx} = v' = \sin(\theta), \quad (ds = dx). \quad (1.845)$$

The asymptotic equation for post-buckling analysis can obtained assuming moderate rotations and expanding the term $\sin(\theta)$ in Equation (1.838) keeping two terms as $\sin \theta \approx \theta - \theta^3/6$ and accounting for the kinematics of Bernoulli-Euler

$$v' = \sin(\theta) \implies \theta = \arcsin(v') \quad (1.846)$$

$$\theta' = [\arcsin(v')] = \frac{v''}{\sqrt{1 - v'^2}} \equiv \kappa, \quad \text{Exact Lagrangian curvature.} \quad (1.847)$$

Now we can finally, re-write the exact curvature (second equation in 1.847) and the needed derivatives, in terms of Lagrangian coordinates x and its approximation for moderate rotations as the curvature being

$$\theta' \equiv \kappa(x) = - \frac{v''(x)}{\sqrt{1 - v'^2(x)}} \approx -v''(x) \left[1 + \frac{1}{2}v'^2(x) \right] \implies \quad (1.848)$$

$$\theta'' = \kappa' \approx - \left(\frac{1}{2}v'^2v''' + v''' + v'v''^2 \right) \quad (1.849)$$

$$\theta''' = \kappa'' \approx - \left(v^{(4)} + \frac{1}{2}v'^2v^{(4)} + 3v'v''v''' + v''^3 \right) \quad (1.850)$$

where the sign '-' being according to our sign-conventions.

$$\sin \theta \approx \theta - \frac{1}{6}\theta^3, \quad (1.851)$$

$$\theta = \arcsin(v') \approx v' + \frac{1}{6}v'^3, \quad (1.852)$$

$$\theta^3 \approx \left[v' + \frac{1}{6}v'^3 \right]^3 = v'^3 \left[1 + \frac{1}{6}v'^2 \right]^3 \approx v'^3 \left[1 + \frac{1}{2}v'^2 \right] \quad (1.853)$$

$$\theta - \theta^3/6 \approx v' + \frac{1}{6}v'^3 - \frac{1}{6} \left[v'^3 \left(1 + \frac{1}{2}v'^2 \right) \right] = \dots \quad (1.854)$$

$$1 = 1 \dots \quad \text{To be continued} \quad (1.855)$$

About the approximation for moderate rotations: The exact curvature holds for arbitrary large displacements and rotations and the approximation for

moderate rotations till $\approx 10^\circ$ (degrees) of angle. The displacement $v(x)$ being the displacement of an arbitrary material point x . We expand the denominator of the curvature expression into Taylor expansions³⁰² and obtain Now the derivatives are with respect to x ³⁰³. The Taylor expansion, for moderate rotations, of the denominator of the curvature gives

$$[1 - v'^2]^{1/2} \approx 1 - \frac{1}{2}v'^2. \tag{1.856}$$

Figure (1.145) shows the bounds of such expansion. The non-zero left-side term

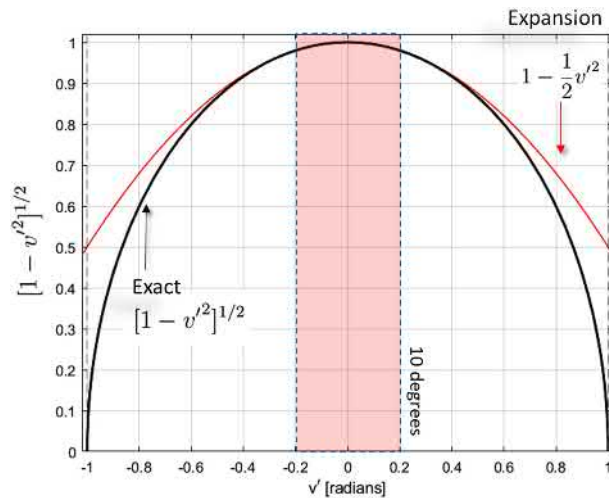


Figure 1.145: Asymptotic approximation of the denominator of the Lagrangian curvature.

being the difference when comparing to the linearised buckling equation (eigenvalue problem)

$$v^{(4)} + \lambda_p^2 v'' + \lambda_k^2 v = 0 \tag{1.857}$$

which holds at the bifurcation point-

This small difference makes the problem not an eigenvalue problem any more. Now, for given P , one can solve $v(x; P)$ from non-linear asymptotic equation and obtain the equilibrium path in the vicinity or at the bifurcation point (around the *branching point*³⁰⁴), the asymptotic non-linear ODE can be solved by accounting for the bifurcation condition (Equation 1.857).

The curvature is expanded by Taylor's series and should keep necessary terms to capture the post-buckling behaviour.

³⁰²Holds for moderate rotations: $v' \leq 10$ degrees in absolute value.)

³⁰³ $v'(x) = v_{,x}(x), v''(x) = v_{,xx}(x)$.

³⁰⁴Haarautumispiste (sf).

So, how to continue? One should solve the non-linear ODE system, numerically or analytically³⁰⁵, for given boundary conditions and obtains the post-buckling behaviour (equilibrium paths $v = f(P)$) for moderate rotations (TO DO). As previously, told, we will do first³⁰⁶ with FDM

$$v^{(4)} + \lambda_P^2 v'' + \lambda_k^2 v + \left[\frac{1}{2} v'^2 v^{(4)} + 3v'v''v''' + v''^3 \right] = 0, \quad x \in]0, \ell[\quad (1.858)$$

and corresponding boundary conditions.

Mechanical discrete model based post-buckling analysis

A Hencky-type physical discretization can be analytically and naturally computationally another way of obtaining discrete-equations from the continuous formulation.

Let's limit this example to a one-degree of freedom (Figure 1.146) such discrete system of the axially compressed column on an elastic foundation³⁰⁷. This allow to study equilibrium paths and post-buckling behaviour analytically for various combination of the system parameters. The bending rigidity of the beam being EI and the spring coefficient of the elastic foundation being k . The discretisation is as follow: two rigid bars with a rotational spring having a spring coefficient k_R , for the flexion of the beam and a translational spring k , for the soil. Naturally, the physical approximation should conserve (consistence) the strain-energy of the system. Here the parameters are chosen as $k_T = k\ell/2$ and $k_R = 1/4\pi^2 EI/\ell$. recall that the non-dimensional variable $\beta = k\ell^4/[\pi^2 EI]$. Now we can study the equilibrium paths and their stability in terms of, let's say, ϕ and P and the parameter β . This way, one obtains the full map of the behaviour of (this simplified) compressed column on elastic foundation as function of relative stiffness β of the soil and the column (Figure 1.147).

What to take with you? From the above study we can conclude that: *the buckling load increases with the increase of the stiffness of the foundation. However, at the same time, the bifurcation switches from stable to becomes of unstable-type after a critical value for $\beta > 8/3$.*

Show³⁰⁸ the following result:

$$P_{cr}(\beta) = \left(1 + \frac{\beta}{8}\right) \frac{\pi^2 EI}{\ell^2}. \quad (1.859)$$

This was the story. We will come to this example later.

[TO DO, 2.2.2019 HW]

³⁰⁵see the referenced article.

³⁰⁶May be, one can try later, if it is possible to use some analytical asymptotic method where the small parameter being v' !

³⁰⁷This illustration example is provided by prof. R. Kouhia from τ -TAU.

³⁰⁸This may be an assignment HW.

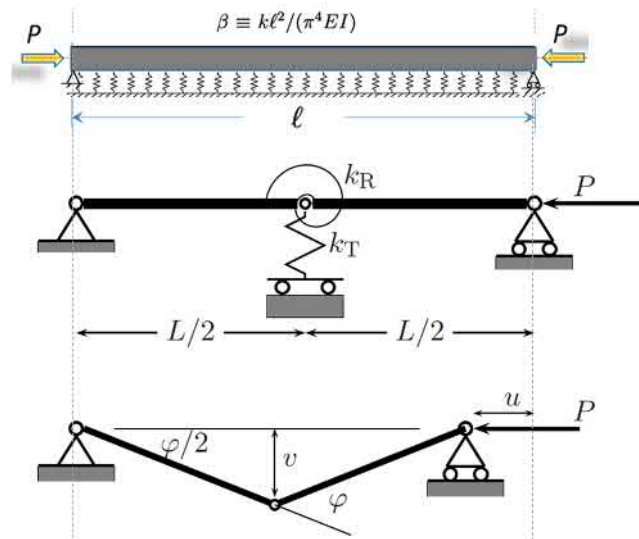


Figure 1.146: Introducing initial perturbation through a small transversal distributed load combination. (Ref. two lower drawings are from R. Kouhia).

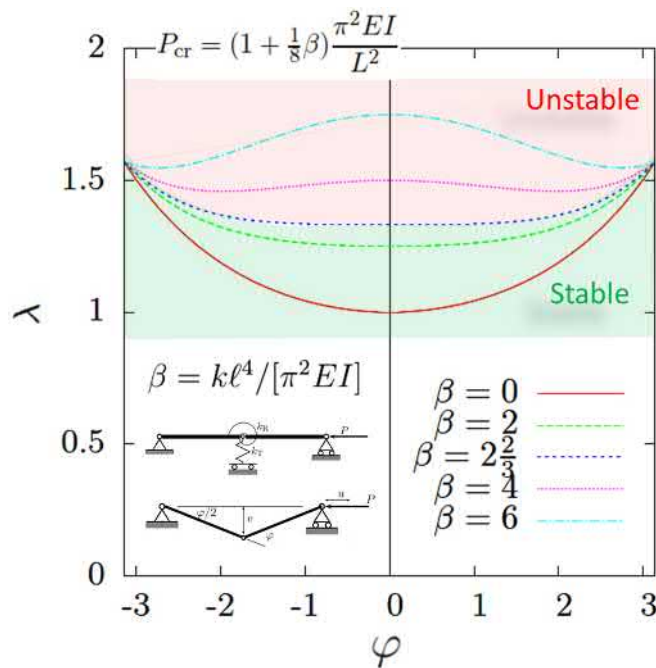


Figure 1.147: Equilibrium paths for various $\beta = k\ell^4/[\pi^2 EI]$. Note the transition from stable (green) to unstable (pink) after a critical value $\beta > 8/3$. (Ref. Figure originally, by R. Kouhia (2019) using Gnuplot).

Finite element based post-buckling analysis

The material data used are the same as those used in the previous FE-example of linear buckling analysis. For the purposes of this demonstration, next data was used: The length of the beam being ℓ and $\ell/10$ being its width. The height of its rectangular cross-section being 50 mm. So the bending rigidity $EI = 72917 \text{ N.m}^2$. The spring coefficient of the foundation was chosen to give $\beta = 5$ ($n = 2$). Thus, one obtains $k = \beta\pi^4 EI/\ell^2 = 35.5 \text{ MN/m}^2$. The elasticity modulus being $E = 70 \text{ GPa}$ and $\nu = 0.33$ ³⁰⁹

Introducing a small transversal perturbation as combination of distributed forces³¹⁰ $q_{\text{pert.}} = P_{\text{cr}}/L \cdot \epsilon$, with $\epsilon = 1/100, 1/1000, 1/10000, \dots$ (Figure 1.148) allows to do the geometrical non-linear analysis where the axial compressive load P is increased from 0 to 1.2 times the theoretical buckling load P_{cr} (Force control³¹¹) and to solve the deformations $u(x; P)$ and $v(x; P)$ (Figure 1.149).

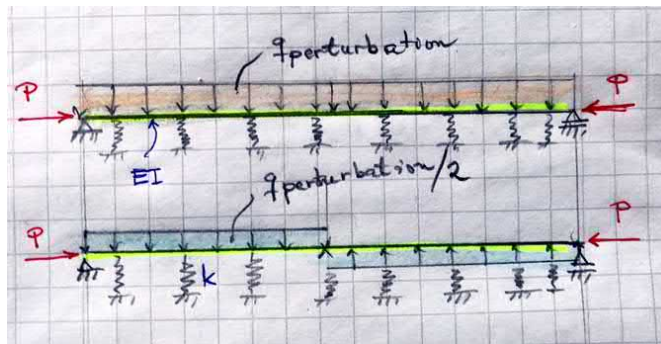


Figure 1.148: Introducing initial perturbation through a small transversal distributed load combination.

Post-buckling with force-control

The post-buckling behaviour as computed is shown in Figure (1.150) Two comments concerning the results of this partial³¹² computational : 1) the initial post-buckling behaviour is stable in the vicinity of the bifurcation. So, the behaviour corresponds to a *symmetric-stable* behaviour. 2) on the other hand, the margin of increase of the load, after buckling, while stability still ensured is, in

³⁰⁹The Poisson ratio is needed for 2D and 3D models. The current simulation is done using 2D elasticity. Of course, one can use a 1D beam-model.

³¹⁰Equivalently, one can give initial geometrical imperfections or initial small transversal displacement $\epsilon v_0(x)$.

³¹¹so, the unstable branches on the equilibrium paths will not be captured. we may, resolve this point when I will have more time.

³¹²Because only force control, here.

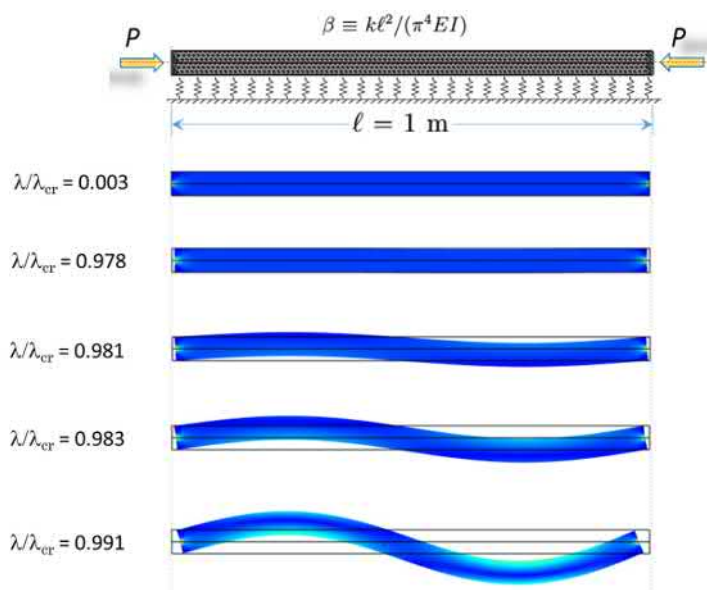


Figure 1.149: Post-buckling displacements in 1:1 scale (FE simulation). The perturbation scale $\epsilon = 1/1000$. After $\lambda/\lambda_{cr,FE} > 0.991$, the behaviour seems (in this simulation) to become unstable and could not be captured because of force control approach used (I will do a displacement control soon). ($EI = 72917 \text{ N}\cdot\text{m}^2$, $\beta = 5$ ($n = 2$)), theoretical 1-D value for $P_{cr} = 3.778 \text{ MN}$ (2D-elasticity FE based linear buckling analysis gave $P_{cr,FE} = 3.720 \text{ MN}$). .

this simulation, too tiny (about 1%) as regard to practical safe use of such structural resistance reserve. In the simulation, after this point (corresponds to 6 cm of maximum deflection), the system seems to become unstable³¹³.

Post-buckling with displacement-control

The same problem is recomputed using *displacement control*. Now, instead of imposing axial force λP_{cr} as in the force-control version, the control parameters are the imposed dens-displacements ($\Delta\lambda = 0.05$)

$$u(0) = \lambda \cdot u(0)_{cr}, \quad \text{for } \lambda \in [0 : \Delta\lambda : 3] \quad (1.860)$$

$$u(\ell) = -\lambda \cdot u(0)_{cr}, \quad (1.861)$$

of the ends of the beam-column. The critical displacement being determined by the post-buckling analysis being $u(0)_{cr} = 6.646 \text{ mm}$. The total critical length change of the column is therefore, $\Delta\ell_{cr} = \Delta u(0) + \Delta u(\ell) = 2 \times 6.646 \text{ mm}$. The

³¹³This result should be confirmed. Notice that k and EI are such that the initial buckling mode corresponds to $n = 2$, so, two half-waves mode.

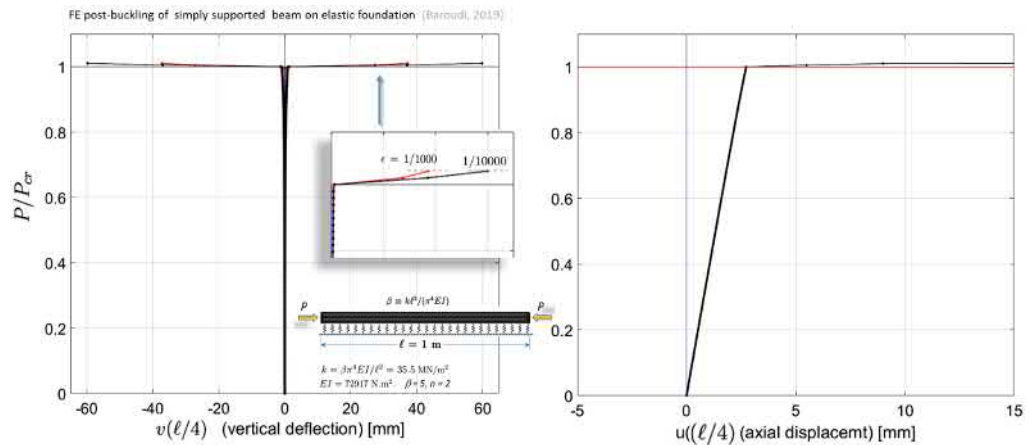


Figure 1.150: Post-buckling equilibrium paths (FE-simulation, force-control). The perturbation scale for the transverse loads was $\epsilon = 1/1000$ and $1/10000$. The loading parameter P/P_{cr} is relative to $P_{cr} = P_{cr,FE} = 3.717$ MN (obtained from D-elasticity FE-based linear buckling analysis, corresponding buckling mode half-wave number $n = 2$). From the stretching curve, one sees that critical axial displacement is about 2.75 mm at $\ell/4$. The overall critical ends-stretching of the beam $\Delta\ell_{cr} = \Delta u(0) + \Delta u(\ell) = 2 \times 6.646$ mm (figure not shown). After the last point presented on these graphs, the computed behaviour seems unstable and could not be captured because of the force control approach.

reaction³¹⁴ forces $R_x(\lambda)$, at the applied ends-displacements, are recorded during solution of this geometrically non-linear problem. The equilibrium-paths represent the graphs: $(R_x(0)/P_{cr,1D}, v(\ell/4)/h)$ and $(v(\ell/4)/h, R_x(0)/P_{cr,1D})$ (Figure 1.151). The obtained post-buckling paths (1.151) need a couple of comments:

- this non-linear analysis (post-buckling analysis) provides the numerical values (quantifies) of actual displacements after buckling. Such knowledge of the deformation scale may be crucial in design of joints, or allowable displacements and rotations, for instance.
- the second observation is that equilibrium paths are very shallow after bifurcation. So, the post-buckling behaviour starts to be stable until a relative compression or order $u(0)/h \approx 0.4$. After this point, the behaviour becomes unstable. However, this substantial shortening of the bar corresponds to an increase of the axial load which is much less than 1% (very shallow shape). So, very-very narrow safety margin to be possible to even think to use it as a reserve of strength. Practically, the post-buckling behaviour is unstable.

³¹⁴Note that this reaction corresponds to P , the applied ends axial force.

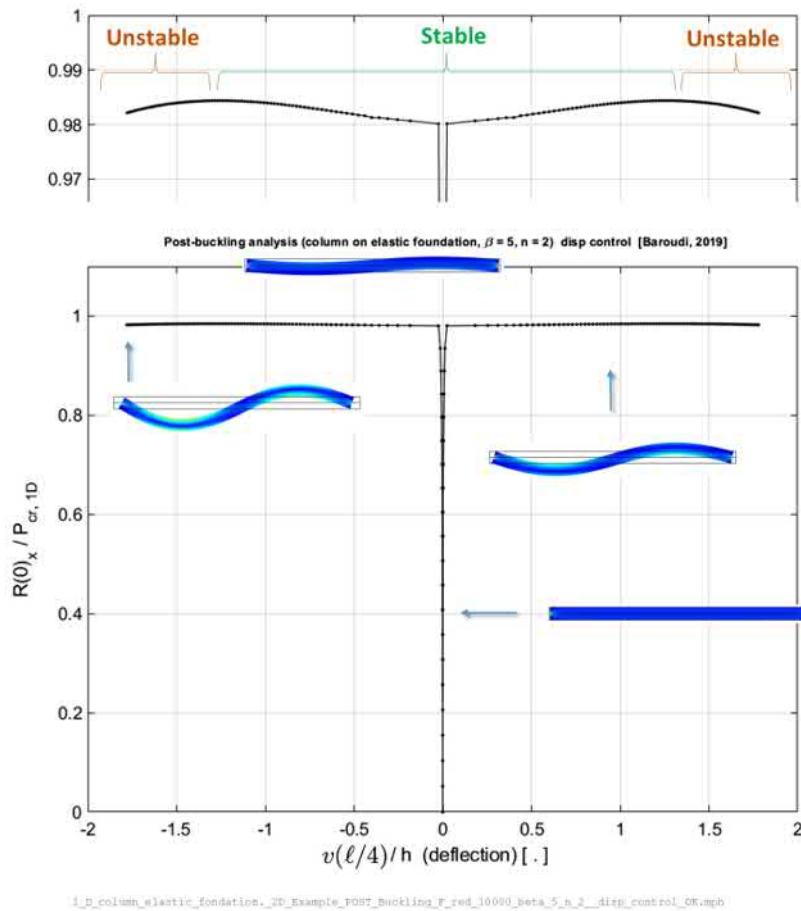


Figure 1.151: Post-buckling equilibrium paths; $v(\ell/4)$ versus P/P_{cr} , (FE-simulation, displacement-control). The parameters ℓ , k and EI are such that $\beta = 5$ and the initial post-buckling mode corresponds to two-half waves ($n = 2$). The perturbation scale for the transverse loads was $\epsilon = 1/10000$. (the post-buckled displacements are in scale 1:1 in the deformed column).

Effect of foundation stiffness on post-buckling behaviour

We study the parameter affecting the transition from stable to unstable behaviour (and vice-versa). Such parameter is clearly condensed in β (the relative stiffness). We did a displacement-controlled FE post-buckling analysis. The bifurcation diagrams (equilibrium-paths) are displayed in Figure (1.153). We see clearly, that the the bifurcation is *unstable* for this set of parameters.

The simulation is performed with next data: $E = 70$ GPa, $\nu = 0.33$, $k = 21.31$ MN/m², $EI = 72.917$ kN.m², $\ell = 1$ m, $h = 50$ mm, $b = \ell/10$ such that $\beta = 3$, $n = 1$. The theoretical critical load was, consequently $P_{cr} = 2.88$ MN.

I will come back to continue this section [TO DO 31.1.2019]. Specially, a

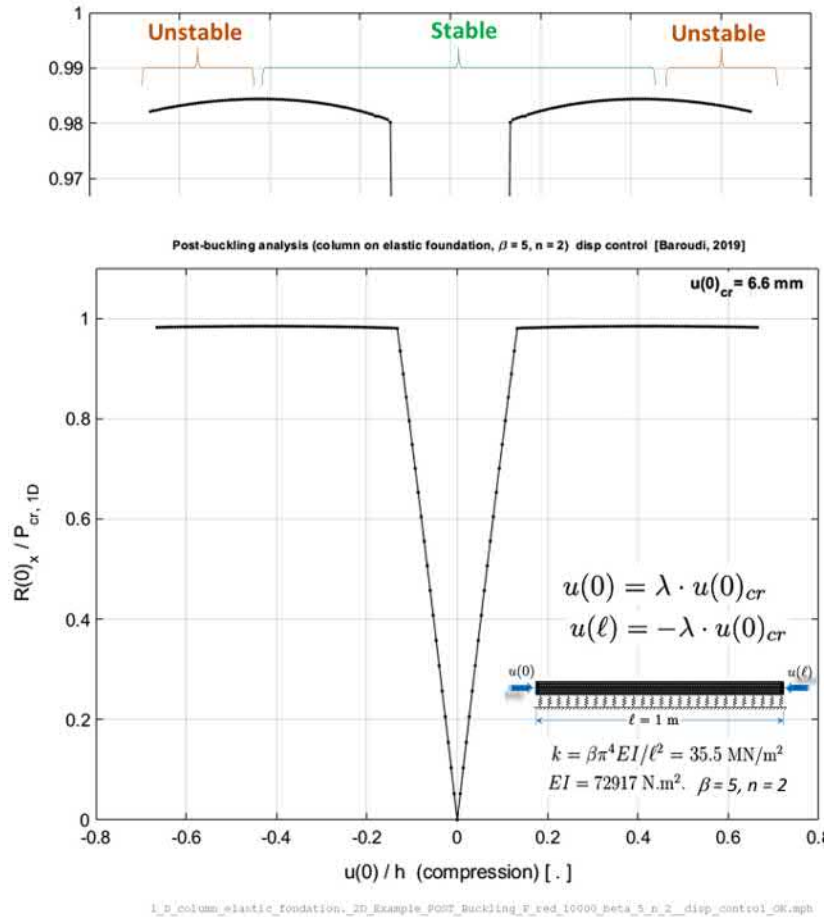


Figure 1.152: Post-buckling equilibrium paths; $u(\ell/4)$ versus P/P_{cr} , (FE-simulation, displacement-control). The parameters ℓ , k and EI are such that $\beta = 5$ and the initial post-buckling mode corresponds to two-half waves ($n = 2$). The perturbation scale for the transverse loads was $\epsilon = 1/10000$. (the post-buckled displacements are in scale 1:1 in the deformed column).

comparison with some published theoretical results ...

Recall from the previous simplified 1-dof we found a critical value for $\beta > 8/3$ after what, the post-buckling behaviour became unstable. It seems that this limit value corresponds well with the FE-examples studied here.

1.12.16 Inelastic buckling of columns

The inelastic buckling of a relatively short (not slender) column will be considered. In such columns, the elasticity limit may be exceeded during defor-

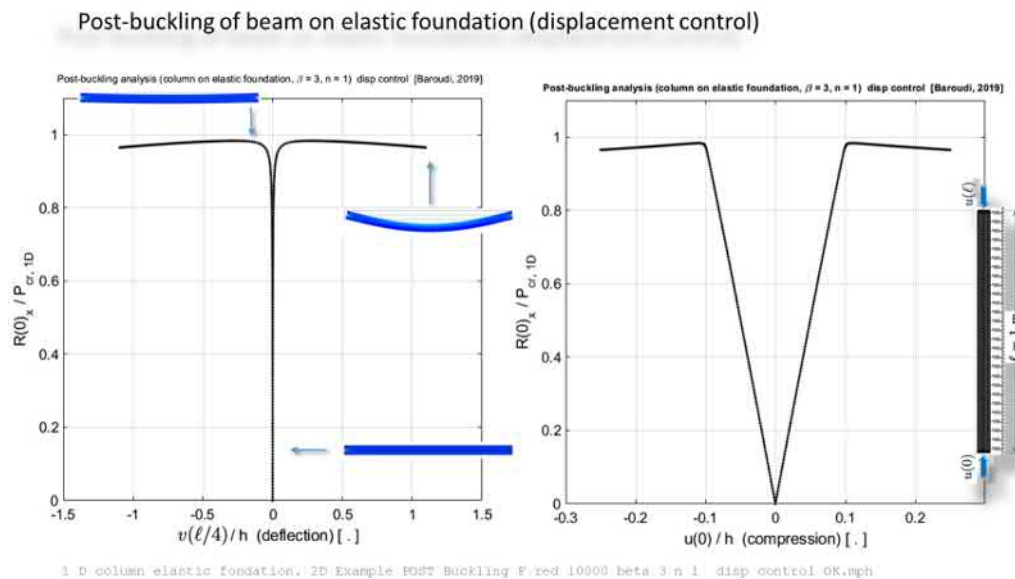


Figure 1.153: Post-buckling equilibrium paths (FE-simulation, displacement-control) of a uniformly compressed column on elastic foundation. The ends-load is centric. The parameters ℓ , k and EI are such that $\beta = 3$ and the initial post-buckling mode corresponds to one-half waves ($n = 1$). The perturbation scale for the transverse loads was $\epsilon = 1/1000$.

mation. The *Essenger's tangent modulus theory* (1889) and the *double modulus theory* (Engesser, 1895) will be exposed.

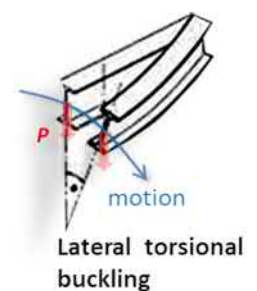
To be continued ... [DBA, 6.1.2019]

1.12.17 Lateral-torsional buckling of beams

Previously, the loading was axial, normal to the cross-section of the beam-column. After a given critical value of the compression, the column buckles in a flexural and loses its stability.

In the following we address stability of beam having a thin-walled open cross-section. Such beams can have torsional modes of stability loss due to their relatively low torsional rigidity with respect to bending rigidity in the plane of loading. Such torsional stability loss can be also observed when the out-of loading plane bending rigidity is very small as regard to the in-plan loading rigidity (Figure 1.154).

So, what new in this section? Now the loading is changed: now, it is transversal to the centreline axis of the beam. When the load is increased till a threshold value, stability loss can occur and the initially straight may lose its stability and



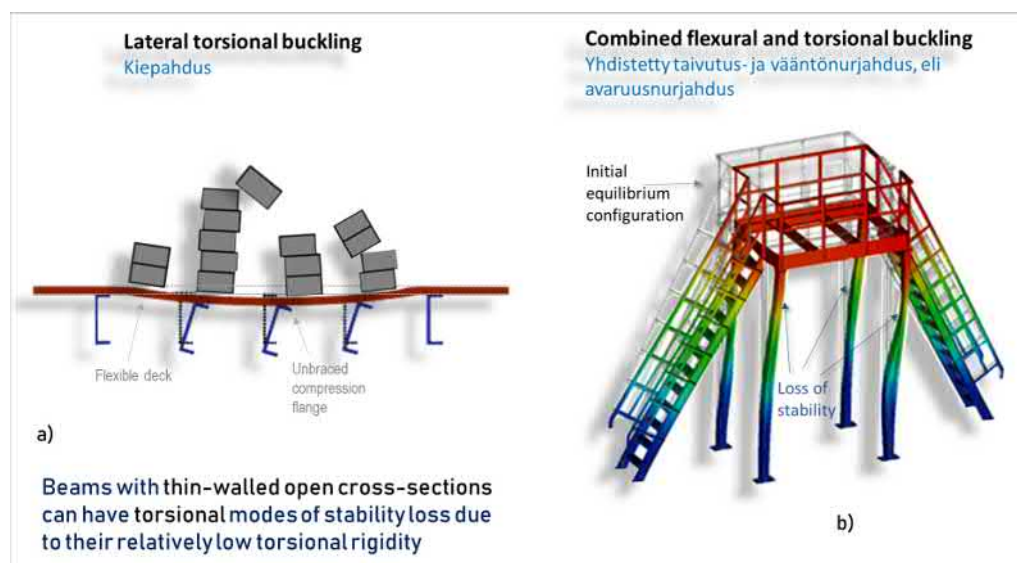


Figure 1.154: Examples of torsional stability loss modes (illustration). a) lateral torsional buckling and b) combined flexural-torsional buckling (FE-simulation).

have both flexural and torsional buckling modes when the compression flange is free to displace laterally.

The transversal load causes a bending moment resulting in compression and tension in the cross-section flanges³¹⁵. The compressed strips of the flange buckle which leads to lateral deflection and twist about the longitudinal axis (Figure 1.156)

Intuitive kinematics in lateral-torsional buckling: The kinematics of the lateral buckling can be understood more intuitively if one thinks the flanges as thin plate being physically discretized as a grid or network of slender interconnected thin bars³¹⁶ (Figure 1.155). The initial bending moment is the stress resultant of linear normal stresses $\sigma_x x^0(y)$. Each compressed longitudinal bar of the strips buckles with a lateral deflection increasing with increase of compressive $\sigma_x x^0(y)$. The tension part of the bars (lower part of the flange) tries to keep the neighbouring member straight. The bars orthogonal to the longitudinal strips are bonded to axial strips and because of continuity have an overall flexural motion along the axis of the which correspond to the twist of the cross-section.

Parameters affecting lateral-torsional buckling behaviour: The principle parameters affecting the lateral torsional buckling load are: the application point of the transverse load with respect centre of rotation (centre of shear) of the cross-

³¹⁵Consider for simplicity a narrow rectangular cross-section (simply symmetric).

³¹⁶Arina, sf.

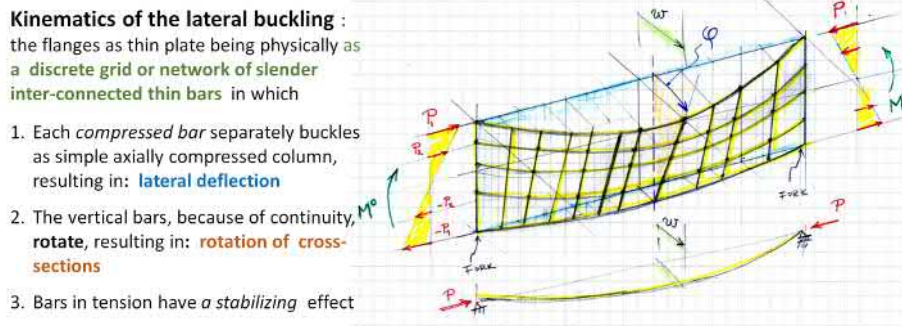


Figure 1.155: Kinematics of lateral torsional buckling as seen by a physical equivalent network of elastic buckling bars as a physical discretisation of a thin plate.

section, the distribution of the transverse initial bending moment, the boundary conditions end supports). When adding restraints against lateral motion or to twist of the cross-section, the buckling load increases. The restraining bars or rods are usually considerably smaller than the main structure since the needed lateral stabilizing force is very small as a consequence of loss of effective rigidity at buckling.

1.12.18 The energy criterion

The example treated here is to mean to introduce the methodology (Bryan's type) for establishing the stability equations for a simple but not trivial case and not of generality.

Consider a cantilever with a traverse load applied at its end. We start simply and consider that the configuration in pre-buckled state is of straight beam and that post-buckled state have free torsion (Saint Venant) and lateral bending in direction of minor axis of inertia. The cross-section of the beam is narrow rectangular. Thus, warping of the cross-section can be ignored ($I_\omega \approx 0$) since shear centre (SC) and centre of mass (G) coincide. Now, for educational purpose³¹⁷, we ignore the effect of shear stresses³¹⁸.

³¹⁷The main idea, in teaching, is to bring to the problem more complexity little-by-little. This way, the student capable of following what are the energy deformation modes integrated into such complex problem as can be *combined-lateral-torsional-flexural buckling*. If we start, teaching, in a general form, then by experience only 1-2 students from 20 are able to follow. However, if only two of twenty follow, then what are you then doing as a teacher? Just *lecture-and-go!*

³¹⁸This means that the internal work of shear stresses from the pre-buckled state with the non-linear deformations of the perturbed (or post-buckled) state $\int_V \tau_{xs}^0 \gamma_{xs}^{NL}$ can be, for now, omitted. However, later, it will be accounted for to obtain a complete model.

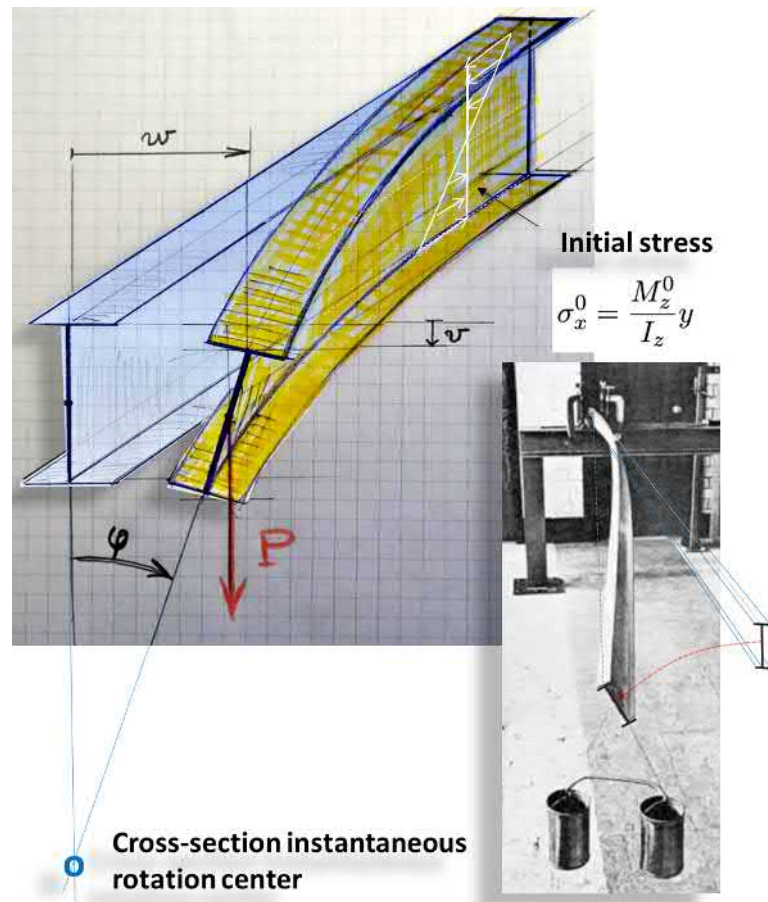


Figure 1.156: Kinematics of lateral torsional buckling: lateral deflection w , vertical displacement v and the rotation ϕ of the cross-section.

In further section, warping effects and effect of shear³¹⁹ stress (Chapter 1.13.1) both from transverse loading and torsion will be integrated into the model. The inertia moments of the cross section are such that $I_y \ll I_z$, where I_y being the *minor*³²⁰ and I_z the major moments of inertia of the cross-section. One can also account approximately for the effect of shear stresses

$$\tau_{xs}^0 = Q_y(x)S_z(y)/(I_z t(s)) \quad (1.862)$$

of the initial state from the transverse load P by assuming that the direction of this shear stress remains the same as in the primary state and does not follow the

³¹⁹The effect of shear stresses is accounted for once we derived the equations of stability without the shear effect. Refer to for-coming section.

³²⁰Note that, now $I_y = hb^3/12$ and $I_z = bh^3/12$, where b and h being, respectively the width and height of the cross-section.

Railway bridge



Figure 1.157: Old heavy railway bridge (Lyon, FR). Example of web stiffeners.

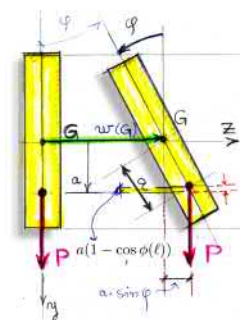
rotation of the thin wall of the cross section. Later, the change in the direction of the shear stress will be accounted for, too.

The idea, after deriving and solving for some cases the stability equations for critical load, a numerical FE-analysis will be carried to present the numerical methodology. Then, the stability problem will be augmented to be a study of effects of imperfections. This last problem is a full-non-linear problem (second order effects). As imperfections, shape imperfection and eccentricity (or a small horizontal force) will be added to the initial loading. The full equilibrium path will be computed³²¹. After this first numerical study with isotropic linear material, and to demonstrate the power of computation, we make the material of the beam orthotropic, for instance. More geometrical complexity can be added as for instance a super-structure ...

The homogeneous equations of stability

The energy criteria $\delta(\Delta\Pi) = 0; P = P_{cr,min}$ will be systematically used to illustrate to derive the Eigen-problem corresponding to the linearised homogeneous equations of stability loss. For notations, see (Fig. 1.158) where the idea to recall is: consider primary equilibrium state (pre-buckled configuration) and perturb infinitely slightly this configuration by $\delta\mathbf{u}$ such that

$$\mathbf{u}^* = \mathbf{u}^0 + \delta\mathbf{u} \equiv \mathbf{u}^0 + \alpha\mathbf{u}_1, \quad \phi^* = \phi^0 + \delta\phi \tag{1.863}$$



$w = w(G) + y \sin \phi$
 $\approx w(G) + y\phi$. The rise of the load application point being $a(1 - \cos \phi)$.

³²¹For this, it may be wise to follow the change in configurations by a performing a dynamic analysis with some simplifications: ignoring inertia forces (or putting them small) and adding damping to follow only the quasi-static solution.

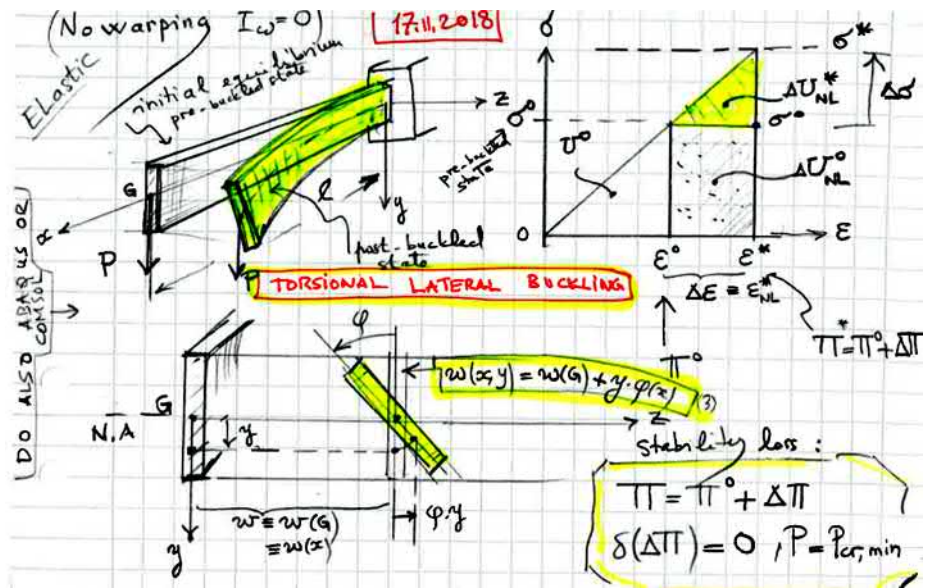


Figure 1.158: Schematic for Lateral torsional of thin beam.

where the increments of generalised displacements are (see Figure in the margin)

$$\delta \mathbf{u} \equiv (0, 0, w), \quad \delta \phi \equiv \phi, \quad (1.864)$$

$$\mathbf{u}_0 = (u_0, v_0, w_0), \quad \phi^0 = 0, \quad (1.865)$$

In the following, and in general in stability analysis, the symbol " δ " and " Δ " for increments of displacements, deformations or stresses, are dropped of (omitted) to make the notation lighter. Let's study the change $\Delta\Pi$ in the total potential energy of the system as in (eq. 1.143). Therefore when can write, again

$$\Delta\Pi = \Pi^* - \Pi^0. \quad (1.866)$$

Let recall the basic factual hypothesis:

- the basic kinematics of the displacement increments of the mid-plane $z = 0$:

$$\begin{cases} w(x, y) = w(G) + y \sin \phi \approx w(x) + y\phi(x) \\ u(x, y) = 0, \\ v(x, y) = 0 \end{cases} \quad (1.867)$$

- the additional vertical deflection v during buckling is neglected, therefore $v^* \approx v_0$.

- **N.B.** at this stage, we first, **omit**³²² the effect of shear stress in the pre-buckled state therefore we assume that the increment work of the initial shear stress τ_{xs}^0 on the shear deformations of the perturbed state. *In further section the shear stress will be accounted for to complete the model as its contribution cannot be neglected in the work increment of initial stresses.*

$$\int_V \tau_{xs}^0 \gamma_{xs,NL}^* dV \quad (\text{now, just omitted}) \quad (1.868)$$

where $\gamma_{xs,NL}^*$ being the second order part of the shear strain in the perturbed state.

(N.B)². This assumption will be released later in Chapter (1.13.1) where the complete equations of loss of stability (1.961) are derived.

- negligible or no warping $I_\omega \approx 0$ and consequently, no warping stresses.

Pre-buckled and buckled configurations (FE- stability analysis) are shown in the figure in the margin: cross section deflects much more laterally than vertically, thus, assumption $v \ll w$ during buckling for beam with narrow cross-section holds and one can neglect $v \approx 0$ during buckling. The external transversal loading goes through the centre of inertia G (sometimes denoted by C) of the cross-section. The centre of shear S coincides with G . The initial stress state σ^0 in pre-buckled state is given by the bending stresses

$$\sigma_x^0 = \frac{M_z^0}{I_z} y \quad (1.869)$$

The end-load P is acting at the centroid G of the cross section ($a = 0$) in the plane of major bending rigidity. The cross-section is rectangular and narrow such that $I_z \gg I_y$ ³²³ and no warping $I_\omega \approx 0$.

Integrating the change of strain energy over the structure one, finally, obtains the increment of total potential energy in Bryan form (Cf. 1.143) and (Fig. 1.158)

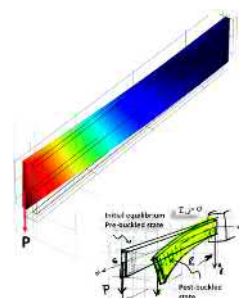
$$\Delta\Pi = \underbrace{\frac{1}{2} \int_V \epsilon_1^T \mathbf{E} \epsilon_1 dV}_{\text{linear part of strain increments}} + \underbrace{\int_V \epsilon_2^T \sigma^0 dV}_{\text{quadratic part of strain increments}} - \underbrace{\Delta W_e}_{\text{part not yet in work of initial stresses}} \quad (1.871)$$

³²²Refer to following section where the effect of shear stress (force) is accounted to obtain the full model. It came out that the work of initial shear stresses cannot be neglected.

³²³Note that now the inertia moments are defined as

$$I_y = \int_A z^2 dA, \quad I_z = \int_A y^2 dA. \quad (1.870)$$

For the rectangular narrow section, we will have $I_y = hb^3/12$, where the thickness being $b \ll h$ and h the height.



$v \ll w$ in buckling for narrow cross-section; one can neglect $v \approx 0$.

which applied within beam theory leads to

$$\Delta\Pi = \frac{1}{2} \int_0^\ell EI_y w''^2 dx + \frac{1}{2} \int_0^\ell GI_t \phi'^2 dx + \int_0^\ell \int_A \sigma_x^0 \epsilon_2 dA dx, \quad (1.872)$$

where the increments of strains $\epsilon_x = \epsilon_1 + \epsilon_2$ and where ϵ_1 being the *linear part* of the strain increments and ϵ_2 the *quadratic part* which are conjugate to σ_x^0 . Therefore,

$$\epsilon_2 = \frac{1}{2} (\omega_z^2 + \omega_y^2) \quad (1.873)$$

$$= \frac{1}{2} \underbrace{(u_{,z} - w_{,x})^2}_{=0} + \frac{1}{2} \underbrace{(v_{,x} - u_{,y})^2}_{=0} \quad (1.874)$$

$$= \frac{1}{2} (w_{,x})^2. \quad (1.875)$$

Important: As in Equations (1.144) and (1.871) the deformations (linear part ϵ_1 and quadratic part ϵ_2) and the displacements are to be estimated in the slightly buckled configuration while the initial stresses σ^0 and external forces P are to be estimated in the pre-buckled configuration. It is assumed that during buckling, these initial stresses forces remain approximately constant. Note that the linear part of the strain increments are neglected, since their spatial derivatives in $\Delta\Pi$ with respect to x_i , $i = 1, 2, 3$ are negligible.

Lets note the mass centroid by $G = G(x, y = 0, z = 0)$ which is here the same as the centre of shear (S). Inserting the perturbed displacement is $w(x, y) = w(G) + y \sin \phi \approx w(G) + y\phi$, and its derivatives together with the bending stress σ_x^0 in the energy criteria on obtains, finally:

$$\Delta\Pi = \frac{1}{2} \int_0^\ell EI_y w''^2 dx + \frac{1}{2} \int_0^\ell GI_t \phi'^2 dx + \underbrace{\int_0^\ell M_z^0 w' \phi' dx}_{\text{bending only}} + \left(\underbrace{\int_V \tau_{xs}^0 \gamma_{xs, NL}^* dV}_{\text{now omitted, accounted for later}} \right) \quad (1.876)$$

in the above expression, the cross-section moments $\int_A y dA = 0$, $\int_A y^3 dA = 0$ and $\int_A y^2 dA = I_z$ was accounted for during integration of the increment work of initial stresses. (the coordinates system $(x-, y-, z-)$ is a principle inertia coordinate system). Also the notation w for the deflection $w(G) \equiv w(x)$ of the centre of mass is used.

Now, for the actual narrow rectangular cross-section, the warping moment of inertia I_ω is such that $EI_\omega \ll GI_t$. When, on the contrary, warping rigidity would be significant then we should add the term

$$\Delta U_\omega = + \frac{1}{2} \int_0^\ell EI_\omega (\phi'')^2 dx \quad (1.877)$$

to the strain energy part in Equation (1.876). Warping will be treated in it's own section. Refer to **Vlasov's** theory on that.

For our case of no-warping, the increment of the work of the pre-stress will be

$$\int_0^\ell \int_A \sigma_x^0 \epsilon_2 dA dx = \int_0^\ell \frac{M_z^0(x)}{I_z} \int_A y \cdot \left[\frac{1}{2} w'(x)^2 + \frac{1}{2} (y\phi'(x))^2 + y\phi'(x)w'(x) \right] dA dx \quad (1.878)$$

$$= \frac{1}{2} \int_0^\ell \frac{M_z^0}{I_z} w'^2 dx \underbrace{\int_A y dA}_{S_z=0} + \frac{1}{2} \int_0^\ell \frac{M_z^0}{I_z} \phi'^2 dx \underbrace{\int_A y^3 dA}_{=0} + \quad (1.879)$$

$$+ \int_0^\ell \frac{M_z^0}{I_z} w' \phi' dx \underbrace{\int_A y^2 dA}_{=I_z} \quad (1.880)$$

$$= \int_0^\ell M_z^0 w' \phi' dx \quad (1.881)$$

and therefore, the total potential energy increment is according to equation (1.876).

It should be noted that on have two independent unknown functions for the additional displacement $w(x)$ and $\phi(x)$. The energy criterion gives the linearised equations of stability loss. This represents also the condition for existence of adjacent equilibrium to the primary initial one. Thus, taking the first variation of $\Delta\Pi$ (which is the same as taking the second variation of Π) with respect to the increments w and ϕ gives

$$\delta(\Delta\Pi[w, \phi]) = 0, \quad \forall \delta w, \delta \phi \text{ kin. admissible} \implies \quad (1.882)$$

$$\delta(\Delta\Pi[w, \phi]) = \int_0^\ell EI_y w'' \delta w'' dx + \int_0^\ell GI_t \phi' \delta \phi' dx + \quad (1.883)$$

$$+ \int_0^\ell M_z^0 w' \delta \phi' dx + \int_0^\ell M_z^0 \delta w' \phi' dx = 0, \quad (1.884)$$

$$\forall \delta w, \delta \phi \text{ kin. admissible.} \quad (1.885)$$

Since the arbitrary but cinematically admissible variations of the displacement increments are δw and $\delta \phi$ one needs to repeat integration by parts $\delta w'' \rightarrow \delta w' \rightarrow$

δw and $\delta\phi' \rightarrow \delta\phi$ to have finally,

$$\delta(\Delta\Pi[w, \phi]) = \int_0^\ell \left[EI_y (w'')'' - (M_z^0 \phi')' \right] \delta w dx + \quad (1.886)$$

$$- \int_0^\ell \left[(GI_t \phi')' + (M_z^0 w')' \right] \delta\phi dx + \quad (1.887)$$

$$- \left[(GI_t \phi' + M_z^0 w') \delta\phi \right]_0^\ell + \quad (1.888)$$

$$+ \left[-(EI_y w'')' + M_z^0 \phi' \right] \delta w \Big|_0^\ell + \quad (1.889)$$

$$+ [EI_y w'' \delta w]_0^\ell = 0, \quad (1.890)$$

$$\forall \delta w, \delta\phi \quad \text{kin. admissible.} \quad (1.891)$$

Finally, the Euler equations³²⁴ which are the equations of loss of stability or linearised homogeneous equations of stability (equilibrium equations) for the increment of displacements, for any $x \in]0, \ell[$

$$\boxed{\begin{cases} EI_y (w'')'' - (M_z^0 \phi')' = 0, \\ (GI_t \phi')' + (M_z^0 w')' = 0 \end{cases}} \quad (1.892)$$

and the corresponding homogeneous boundary conditions at $x = 0$ and $x = \ell$ for instance,

$$\text{at } x = \ell, \quad \text{at } x = 0 \quad (1.893)$$

$$GI_t \phi' + M_z^0 w' = 0, \quad w' = 0 \quad (1.894)$$

$$-(EI_y w'')' + M_z^0 \phi' = 0, \quad \text{or} \quad w = 0 \quad (1.895)$$

$$EI_y w'' = 0, \quad \phi = 0. \quad (1.896)$$

In the following two simple cases of lateral torsional buckling of thin beams will be studied to determine the buckling load by solving the eigenvalue problems of (Eqs. 1.892). The cases³²⁵ are 1) thin simply supported beam loaded with a constant moment M^0 and 2) a cantilever with end load P at a height $a = 0$ from the neutral axis of the cross-section.

End load at a height $a \neq 0$ from the neutral axis: The increment of the work of external load between the initial pre-buckled state and the perturbed state is, consequently (Figure 1.159)

³²⁴Note that in these equations the effect of shear stresses (rising from bending) is not accounted for, yet. In such a problem, the work of these initial shear stresses should be incorporated into the model to have a physically more correct model. Refer to the full equations in next chapters.

³²⁵Molemmat on jo laskettu paperilla, kirjoita puhtaaksi

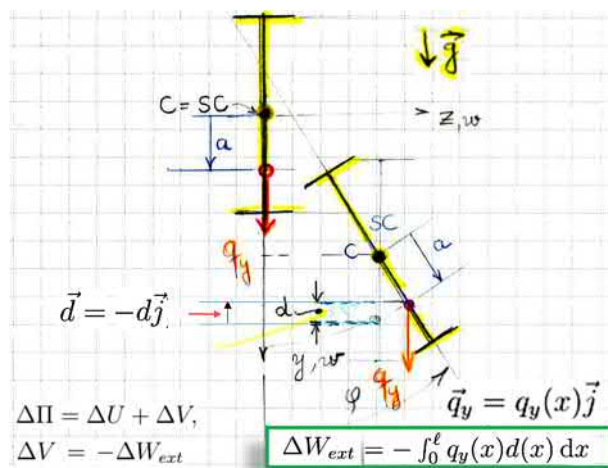


Figure 1.159: Illustration of the change in the work of external work at buckling. Note that the force q_y of equivalently, a point force P and the displacement d of the application point have opposite directions and so, consequently, the work change is negative.

$$\Delta V = -\Delta W_{ext} = -\int_0^\ell \vec{q}_y(x) \cdot \vec{d}(x) dx = \int_0^\ell q_y \cdot a(1 - \cos \phi) dx \approx \int_0^\ell q_y \cdot a \left[\frac{1}{2} \phi^2 \right] dx \quad (1.897)$$

for a distributed load $q_y(x)$ along transversal axis of the beam or

$$\Delta V = -\Delta W_{ext} = Pa(1 - \cos \phi(\ell)) \approx Pa \frac{1}{2} \phi(\ell)^2. \quad (1.898)$$

For a point load directed downward in the gravity field. Notice that in both loading cases, the transversal motion of the application point of the dead load and the direction of the load itself are of opposite signs. Therefore, the increment of the work is *negative*. The change in the potential of external load (dead load) should be naturally accounted by writing the increment of the total potential energy in the Timoshenko form. Now, for the case $a = 0$, the case under investigation, the Bryan form (1.871) was used.

Pure bending

A constant external moment $M_z^0 = M_0$ at both ends is acting. In these case the shear stresses are identically zero since the shear force vanishes. The differential equations derived previously with ignoring the shear effects are correct for pure bending. The cross-section is constant. The material isotropic linear elastic. The boundary conditions for the simply and rotation restraints (fork) at the ends supports are shown in Figure (1.160). Equations of stability (1.892) become

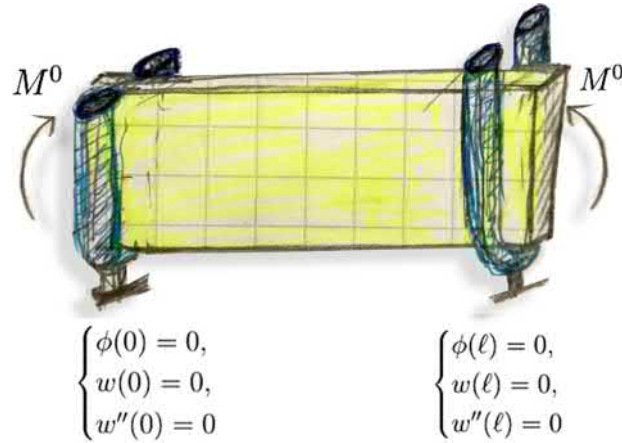


Figure 1.160: Lateral torsional buckling of a simply supported forked beam.

$$\begin{cases} EI_y w^{(4)} - M_0 \phi'' = 0, \\ GI_t \phi'' + M_0 w'' = 0. \end{cases} \quad (1.899)$$

The above system of equilibrium differential equations can be re-written as

$$\begin{cases} w^{(4)} + k_t^2 w'' = 0, & k_t^2 = M_0^2 / (GI_t EI_y) \\ \phi'' = -\frac{M_0}{GI_t} w''. \end{cases} \quad (1.900)$$

Note that the above first equation is analogous to the classical buckling equation of a simply supported column (Euler buckling) under a load P where $k_P^2 = P/EI_y \rightarrow k_t^2 = M_0^2 / (GI_t EI_y)$ (recall solution $P_{cr} = EI_y \cdot \pi^2 / \ell^2$). Therefore, one could directly write the solution by analogy³²⁶. As in the classical Euler buckling case, inserting the trial solution (eigenmode)

$$w_n(x) = A_n \sin\left(\frac{n\pi x}{\ell}\right), \quad A \neq 0, n = 1, 2, 3, \dots \quad (1.901)$$

in the first equation of the ODE-system above (1.899), one obtains

$$\left(\frac{n\pi}{\ell}\right)^2 \underbrace{\left[\left(\frac{n\pi}{\ell}\right)^2 - k_t^2\right]}_{=0} A_n \sin\left(\frac{n\pi x}{\ell}\right) = 0, \quad n = 1, 2, \dots \quad \text{eigenmodes} \quad (1.902)$$

$$\Rightarrow M_n = \left(\frac{n\pi}{\ell}\right) \sqrt{EI_y GI_t} \quad \text{eigenvalues.} \quad (1.903)$$

³²⁶ $M_{0,cr} = k_P^2 = P/EI_y \rightarrow k_t^2 = M_0^2 / (GI_t EI_y)$. Recall solution $P_{cr} = EI_y \cdot \pi^2 / \ell^2 \rightarrow M_{0,cr} = \sqrt{EI_y GI_t} \cdot \pi / \ell$.

Finally, the buckling (critical) end-moment is the smallest one for $n = 1$;

$$M_{0,cr} = \frac{\pi}{\ell} \sqrt{EI_y GI_t} \quad (1.904)$$

The critical stress from equation (1.904) is

$$\sigma_{cr} = \frac{M_{0,cr}}{W_y^{(e)}} = \frac{\pi}{W_y^{(e)} \ell} \sqrt{EI_y GI_t} \quad (1.905)$$

where $W_y^{(e)}$ is the elastic bending resistance. The above equation is widely used in many standards of structural design (*Cf.* Figure in margin) for checking lateral buckling capacity.

Please note the definitions of the inertia moments:

$$I_y = \int_A z^2 dA, \quad I_z = \int_A y^2 dA. \quad (1.906)$$

So, for the rectangular narrow section, we will have $I_y = hb^3/12$ and not $bh^3/12$, where the thickness being $b \ll h$ and h the height. Therefore, the bending rigidity entering the buckling formula, are to be defined naturally, in the lateral buckling direction (the weakest).

Let solve for the torsional mode too. Since

$$\phi'' = -\frac{M_0}{GI_t} w'' = -\frac{M_0}{GI_t} A_n \left(\frac{n\pi}{\ell}\right)^2 \sin\left(\frac{n\pi x}{\ell}\right). \quad (1.907)$$

Integrating twice, accounting for boundary conditions and inserting in the above equation the critical end-moment, one obtains the corresponding (critical) eigenmodes

$$\begin{cases} v_{cr}(x) &= A \sin\left(\frac{\pi x}{\ell}\right) \\ \phi_{cr}(x) &= -B \sqrt{\frac{EI_y}{GI_t}} \sin\left(\frac{\pi x}{\ell}\right). \end{cases} \quad (1.908)$$

For comparison, when the cross-section warping has to be accounted for, the critical end-moment have the expression³²⁷ (Timoshenko)

$$M_{0,cr} = \frac{\pi}{\ell} \sqrt{EI_y GI_t} \sqrt{1 + \frac{\pi^2}{\ell^2} \frac{EI_\omega}{GI_t}} \quad (1.909)$$

$$= \frac{\pi}{\ell} \sqrt{EI_y} \sqrt{GI_t + \frac{\pi^2}{\ell^2} EI_\omega} \quad (1.910)$$

Critical lateral buckling stress in EN 1955-1-1 (section 6.3.3) for wooden beams

$$\sigma_{m,cr} = \frac{M_{y,cr}}{W_y} = \frac{\pi \sqrt{E_{0,05} I_z G_{0,05} I_{tw}}}{\ell_{ef} W_y}$$

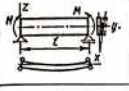
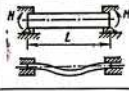

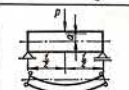
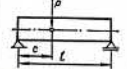
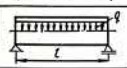
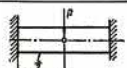
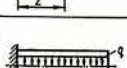
Critical stress in torsional buckling for a wooden beam in uniform bending as given in the standard (check 1955!).

³²⁷This formula will be derived when dealing with open cross-sections.

Therefore, for beams of moderate length, when warping rigidity is of the same order than torsional rigidity, one should account for warping. Or the other way around for structural designer: warping rigidity increases stability with respect to torsional lateral buckling. Of course, the product of bending and torsional rigidities is a key parameter too. This is one reason why high beams need lateral supports. The needed lateral supporting force are relatively very small since the effective rigidities (bending in the weakest direction and torsional) decreases dramatically close to buckling,

I reproduce a table (1.161) from an old formulary of strength of material (2nd Ed. 1982) giving some solutions for various cases Sorry, for the language not

Critical lateral torsional buckling loads

Таблица 8.14. Критические нагрузки		$\frac{GI_k}{T}$	0,50	0,45	0,40	0,35	0,30	0,25	0,20	0,15	0,10	0,05	
Схема балки и нагрузки		Критическая нагрузка	β	16,93	17,15	17,82	19,04	21,01	24,10	29,11	37,88	56,00	111,6
Стержень изгибается парами сил M , приложенными по концам. Концы балок могут свободно поворачиваться относительно осей z и y		$M_{кр} = \frac{\pi}{l} m$											
Нагрузка та же, но концы балки заделаны (торцовые сечения относительно вертикальных осей поворачиваться не могут)		$M_{кр} = \frac{2\pi}{l} m$											
Стержень с одним заделанным концом нагружен сосредоточенной силой в свободном конце. Точка приложения нагрузки отстоит от оси стержня на расстоянии a		$P_{кр} = \frac{4,013}{\beta} \left(m - \frac{aEI}{l} \right)$											
Стержень нагружен сосредоточенной силой посредине. Закрепления шарнирные. Точка приложения нагрузки отстоит от оси стержня на расстоянии a		$P_{кр} = \frac{16,93}{\beta} \left(m - 3,48 \frac{a}{l} EI \right)$											
Закрепления шарнирные. Нагрузка приложена на расстоянии c от ближайшей опоры на оси стержня		$P_{кр} = \frac{\beta}{\beta^2} m$											
Стержень закреплен, как и в предыдущем случае. Нагрузка, действующая на него, равномерно распределена по длине		$(q l)_{кр} = \frac{28,3}{\beta^2} m$											
Стержень, заделанный концами, нагружен посредине сосредоточенной силой. Точка приложения нагрузки находится на оси стержня		$P_{кр} = \frac{26,6}{\beta^2} m$											
Стержень, заделанный одним концом, нагружен равномерно распределенной нагрузкой		$(q l)_{кр} = \frac{12,85}{\beta^2} m$ $m = \sqrt{EJG_k}$											

Reference: Fecik C. P. (Фецук С. П.) Formulary of strength of materials. 2nd Ed. Kiev, C

Figure 1.161: Some critical loads for some cases of lateral torsional buckling.

being translated. I do not think that, it will disturb so much, since the formula and drawings are universal³²⁸.

³²⁸There was one related Russian joke: Americans were complaining that the late Russian space shuttle looks quite like the American one which was constructed and launched first by Americans. In addition, they says that Russians have stolen their technical plans by industrial spying on them. The Russians replayed: "The reason why the two shuttles look exactly like each other is simply because the law of (nature) aerodynamics are universal and the same for both shuttles and consequently, they (the laws) result in a quite close design."

1.13 Rayleigh-Ritz energy method

The energy criterion in the form $\delta(\Delta\Pi) = 0$ means that solutions of the stability problem make the change in the total potential energy (1.876) stationary. This fact can be used to find approximations for the critical buckling load. The method is called **Rayleigh-Ritz**. The idea, is to postulate cinematically admissible displacement fields, now for instance, $w(x)$ and $\phi(x)$, and to solve the buckling load from the stationarity condition

$$\delta(\Delta\Pi(a_i; P)) = 0, \quad \forall \delta a_i \implies \frac{\partial}{\partial a_j} \Delta\Pi(a_1, a_2, \dots, a_n; P) = 0, \quad (1.911)$$

where a_i are the parameters in the displacements approximation. The above stationarity condition leads to the homogeneous system of equations (Eq. 1.912) below:

$$\mathbf{K} - P\mathbf{S} = 0, \quad (1.912)$$

where, the effect of pre-stresses

$$M_z^0(x; P) = P \cdot \bar{M}_z^0(x), \quad (1.913)$$

from the reference equilibrium state are, naturally, solved in the primary equilibrium configuration in the framework of linear elasticity and small deformation theory. The bending moment distribution $\bar{M}_z^0(x)$ is the one one obtains by setting $P = 1$.

This way we obtain, in general, an eigenvalue problem in a matrix form. Therefore solving the linearised stability problem becomes a problem of finding eigenvalues and corresponding Eigen-vector of a matrix as a condition of existence of non-trivial solution;

$$\det[\mathbf{K} - P\mathbf{S}] = 0, \quad (1.914)$$

where the critical load will approximately correspond to the smallest³²⁹ eigenvalue. Stiffness-matrix terms K_{ij} and geometric-matrix terms S_{ij} emerge naturally from the stationarity condition of the change of approximated total potential energy.

Let's illustrate this procedure by an example (do with with Matlab symbolic).

High Cantilever beam

Recall the increment of total potential energy:

$$\Delta\Pi = \frac{1}{2} \int_0^\ell EI_y w''^2 dx + \frac{1}{2} \int_0^\ell GI_t \phi'^2 dx + \int_0^\ell M_z^0 w' \phi' dx. \quad (1.915)$$

³²⁹It can be shown that $P_{cr} \leq P_{cr, \text{approx}}$. This is easy to see from the *Rayleigh-quotient* minimisation properties.

Assumes the same high and narrow beam as previously. The boundary conditions are different. In this example, we will study how to use the previously derived energy criterion of stability to obtain good approximative solutions for the buckling loads. The idea is already known to you: *Rayleigh-Ritz* method. We try to find a smallest approximate \bar{P}_{cr} to the critical load as P_{cr} by postulating approximations for the change in the displacement field (for buckled shape) such that the increment of total potential energy (1.876) is stationary $\delta(\Delta\Pi) = 0$ or writing directly $\Delta\Pi = 0$ (recall the section dealing with equivalence of stability criteria).

It is known (the minimisation property of the Rayleigh-quotient for the first eigenvalue) that the exact solution is

$$P_{cr} \leq \bar{P}_{cr}. \quad (1.916)$$

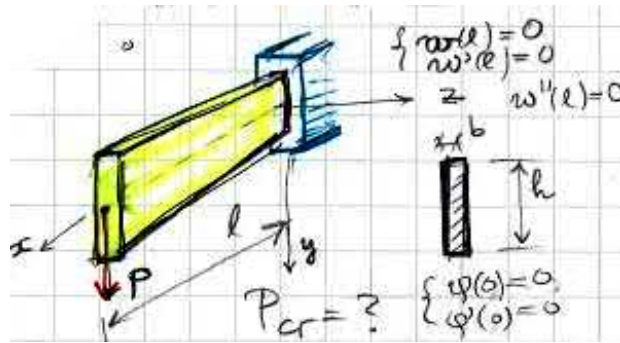


Figure 1.162: Illustration of end-loaded cantilever. The cross-section is narrow; stability loss conditions for lateral torsional buckling are present.

The Rayleigh-quotient is obtained from the equilibrium condition $\Delta\Pi = 0$. For that, we will eliminate $\phi(x)$ from the energy-functional integrating equilibrium equation

$$GI_t\phi'' + (M_0w')' = 0 \implies GI_t\phi' + (M_0w') = C \quad (1.917)$$

$$w'(\ell) = 0, \phi(\ell) = 0 \implies C = 0, \quad (1.918)$$

$$\implies \phi' = -\frac{M_z^0}{GI_t} w' \quad (1.919)$$

where the initial bending moment is

$$M_z^0(x; P) \equiv P \cdot \bar{M}_z^0(x). \quad (1.920)$$

Inserting the boxed relation into the energy-functional one obtains finely in the Rayleigh-Ritz quotient form

$$P_{cr}^2 = \frac{\int_0^\ell EI_y w''^2 dx}{\int_0^\ell (\bar{M}_z^0)^2 w'^2 / GI_t dx} \quad (1.921)$$

There is a two ways to obtain the approximate critical load:

- 1) by approximating separately $\bar{w}(x) \approx w(x)$ and $\bar{\phi}(x) \approx \phi(x)$ in the energy functional (1.915) and using the criticality condition (stationarity). This is a more general approach.
- 2) approximating only $w(x)$ in the Rayleigh-quotient³³⁰ (1.921) after eliminating the second unknown function $\phi(x)$ using the second equilibrium equation. (not a general method. In general, it may become impossible to proceed explicitly with the elimination for other types of problem.)

In both cases the displacements approximations should fulfil the kinematic boundary conditions and give non-zero contribution to the energy potential.

Approximation of buckling load using Rayleigh-quotient

Load P at the torsion centre G : The simplest polynomial cinematically admissible approximation³³¹ can be

$$\bar{w}''(x) = A(\ell - x) \implies \bar{w}'(x) = Ax(\ell - x/2) \tag{1.922}$$

for kinematic boundary conditions at $x = 0$

$$\begin{cases} w(0) = 0 \\ w'(0) = 0 \\ \phi(0) = 0 \end{cases} \tag{1.923}$$

The chosen approximation fulfils also (this condition is not necessary but it increases the accuracy of the approximate critical load) the mechanical boundary conditions at $x = \ell$

$$M_y(\ell) = -EI_y w''(\ell) = 0. \tag{1.924}$$

Let's illustrate this procedure by an example (do with with Matlab symbolic). The approximation obtained for the critical load is

$$\bar{P}_{cr} = \sqrt{(35GI_tEI_y)/(2\ell^4)} \tag{1.925}$$

$$= \frac{4.18}{\ell^2} \sqrt{GI_tEI_y}. \tag{1.926}$$

The analytical exact solution³³² is

$$P_{cr} = \frac{4.013}{\ell^2} \sqrt{GI_tEI_y}. \tag{1.927}$$

Effect of location of the load



Load at compression flange reduces the buckling load when compared to load at tension flange.

³³⁰Is also known as the *Rayleigh-Ritz ratio*.

³³¹It wise to approximate directly $w'' \propto M_y(x)$ and $\rightarrow w''(\ell) = 0$. Of course, you can start by approximating $w(x)$.

³³²Needs Bessel's function to obtain the result. **Brandtl** was the one who first derived this result.

and is enough close to the approximation for practical purposes. By extending the approximation basis functions, one converges to the analytical solution. (show this by adding one monome to the current approximation, as a home work for you).

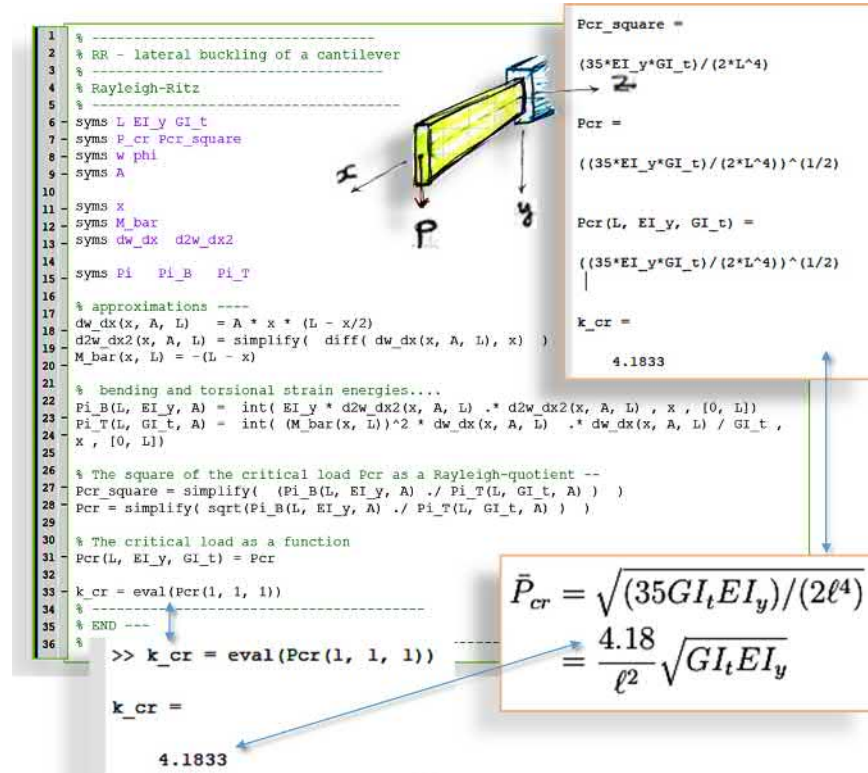


Figure 1.163: Rayleigh-Ritz method as implemented in Matlab using the symbolic toolbox to evaluate the Rayleigh-quotient \bar{P}_{cr} for the cantilever beam. Compare to analytical solution $P_{cr} = 4.013/\ell^2 \cdot \sqrt{GI_tEI_y}$ (Cf. Timoshenko).

Load P is $a > 0$ below the torsion centre G : In this case the increment of the work of external load between the initial pre-buckled state and the perturbed state is

$$\Delta V = Pa(1 - \cos \phi(\ell)) \approx +Pa \frac{1}{2} \phi(\ell)^2. \quad (1.928)$$

Therefore, when expanding the $\cos \phi$ up-to the quadratic terms and the increment of total potential energy will be now

$$\Delta \Pi = \frac{1}{2} \int_0^\ell EI_y w''^2 dx + \frac{1}{2} \int_0^\ell GI_t \phi'^2 dx + \int_0^\ell (M_z^0 \phi)' w' dx + 1/2 Pa \phi(\ell)^2 \quad (1.929)$$

Now, for educational purpose, let's approximate separately the deflection and the rotation.

- a) chose cinematically admissible $w(x)$ or directly for $w'(x) \approx Ax(\ell - x/2)$ and $\phi(x) \dots$ we can take advantage (not necessary) of the equilibrium equation $\phi' = -M_z^0/GI_t w' \approx -M_z^0/GI_t \cdot Ax(\ell - x/2)$
- or b), simplest way: take separate approximations $w'(x) \approx Ax(\ell - x/2)$ and $\phi(x) = Bx$, where A and B are independent constants. The approximations have only to fulfil the kinematic boundary conditions. Let's use these approximations.
- ask stationarity of $\Delta\Pi$ separately for ϕ and w if separate approximates. Otherwise, only δA
 $\delta(\Delta\Pi) = 0, \forall \delta A, \delta B$
- solve the problem ...

* * *

Begin: Caution- the bellow illustration example should be re-checked:

It may contain a mistake in the sign of the last term of Equation (1.930) when the load is below the center of rotation (to be checked 14.3.2019).

Solving for case b) we get the change in total potential energy as

$$\Delta\Pi(A, B) = \frac{1}{2}A^2 \frac{EI}{3\ell^3} + \frac{1}{2}B^2 GI_t \ell + \frac{1}{8}ABP\ell^4 - \frac{1}{2}B^2 P. \quad (1.930)$$

Asking for stationarity $\delta(\Pi) = 0$ leads to the homogeneous system of equations

$$\frac{\partial(\Delta\Pi)}{\partial A} = \frac{1}{3}AEI_y \ell^3 + \frac{1}{8}BP\ell^4 = 0 \quad (1.931)$$

$$\frac{\partial(\Delta\Pi)}{\partial B} = \frac{1}{8}AP\ell^4 + B(GI_t \ell - Pal^2) = 0 \quad (1.932)$$

re-arranging in matrix form

$$\begin{bmatrix} \partial(\Delta\Pi)/\partial A \\ \partial(\Delta\Pi)/\partial B \end{bmatrix} = \begin{bmatrix} \frac{1}{3}EI_y \ell^3 & \frac{1}{8}P\ell^4 \\ \frac{1}{8}P\ell^4 & (GI_t \ell - Pal^2) \end{bmatrix} \begin{bmatrix} A \\ B \end{bmatrix} = \begin{bmatrix} 0 \\ 0 \end{bmatrix}. \quad (1.933)$$

Since, in buckled configuration, $A \neq 0, B \neq 0$ (non-trivial solution) implies that the determinant of the coefficient matrix vanishes. Therefore,

$$P^2 + \frac{63}{3} \frac{Pa}{\ell} \frac{EI_y}{\ell^2} - \frac{64}{3} \frac{EI_y GI_t}{\ell^4} = 0. \quad (1.934)$$

The solution is

$$P_{cr} = K \frac{\sqrt{EI_y GI_t}}{\ell^2} \cdot [\pm \sqrt{1 + \alpha^2} - \alpha], \quad (1.935)$$

where

$$\alpha = \frac{4}{\sqrt{3}} \frac{a}{\ell} \sqrt{\frac{EI_y}{GI_t}}, \quad K = \frac{8}{\sqrt{3}}. \quad (1.936)$$

Let consider the practical case when $a \ll \ell \implies \alpha$ is small then $\pm\sqrt{1+\alpha^2} - \alpha \approx \pm 1 - \alpha/2$. The obtained approximation for the critical load P_{cr} is not very accurate (10 – 15% relative error even for $a = 0$). Thus, one should enrich the approximations to obtain more accurate results. However, ourdays, computational software are available to obtain quite accurate solutions.

The above exercise was aimed to train our understanding on how structures behave through hand-calculations and analysis. In fact, equation (1.935) reflects the physics of the problem. We see clearly what 'meta'- and macro-properties properties we can tune in design order to fulfil some design criteria. For, instance, if one use solid elements (3D) or shell-elements, then the emergent properties as EI_y and GI_t will be absent. We will just have access to ℓ and the thickness! Therefore, analytical formulas are very useful for understanding and design. Bending and torsional rigidities are new emergent meta-concepts and properties absent from a finer numerical modelling. They are also *handlers* in design for global behaviour.

This being said, bellow follows a more accurate solution for the problem

$$P_{cr} = 4.013/\ell^2 \cdot \sqrt{EI_y GI_t} \left[\pm 1 - \frac{a}{\ell} \sqrt{\frac{EI_y}{GI_t}} \right]. \quad (1.937)$$

END: Caution- the above illustration example should be re-checked

* * *

Exercise: Lateral torsional buckling with warping

Use energy principles and determine an approximative expression for the buckling load P_E of the simply supported elastic beam of length ℓ is centrally loaded by a compressive axial load P as shown in Figure (1.164). The end-rotations support is a fork-type. The buckling load should be expressed as $P_E = f(EI_y, EI_\omega, GI_t, \ell, a)$. The increment of total potential energy is now

$$\Delta\Pi = \frac{1}{2} \int_0^\ell EI_y w''^2 dx + \frac{1}{2} \int_0^\ell GI_t \phi'^2 dx + \int_0^\ell EI_\omega \phi''^2 dx + \int_0^\ell (M_z^0 \phi)' w' dx + 1/2 P a \phi(\ell)^2, \quad (1.938)$$

where the warping and the location a of the end-load are accounted for. For comparison, the analytical exact solution is given and is

$$\frac{P_E \ell}{4M_{ref}} \approx 1.35 \left[\sqrt{1 + [0.54 P_{E,y} a / M_{ref}]^2} + 0.54 P_{E,y} a / M_{ref} \right], \quad (1.939)$$

where $P_{E,y} = \pi^2 EI_y / \ell^2$ and $M_{ref} = \sqrt{P_{E,y} [GI_t + \pi^2 EI_\omega / \ell^2]}$

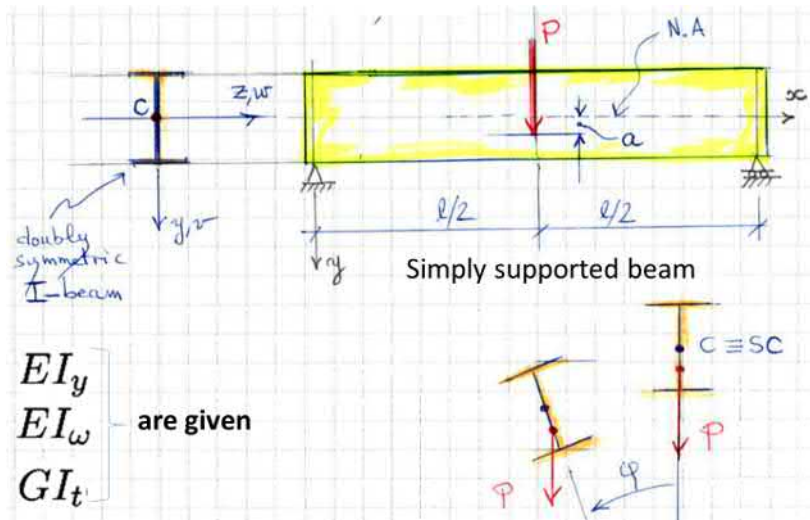
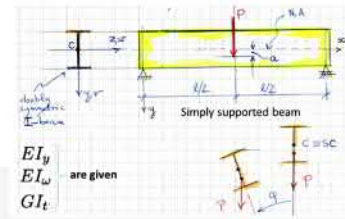


Figure 1.164: Simply supported beam. The support condition for end-rotations is a fork-type. The load P is at a distance a from from the neutral axis. The cross-section of the I-beam is doubly symmetric.

One can use trigonometrical trials: For instance, $\phi(x) \approx A \sin(\pi x/l)$ and $w(x) \approx B \sin(\pi x/l)$ is enough for illustration. The approximated solution can be extracted from Figure (1.165 and 1.166) by solving the roots of the determinant (second order polynomial in P).

Lateral-torsional buckling by Rayleigh-Ritz



$\phi[x_] := B \text{Sin}\left[\frac{\pi x}{L}\right]$
 $w[x_] := A \text{Sin}\left[\frac{\pi x}{L}\right]$
 $Mz[x_] := \frac{P}{2} x$

$$\Delta \Pi = \frac{1}{2} \int_0^l EI_y w''^2 dx + \frac{1}{2} \int_0^l GI_t \phi'^2 dx + \int_0^l EI_w \phi''^2 dx + \int_0^l (M_z^0 \phi) w' dx + \frac{1}{2} P a \phi(\ell)^2$$

Energy = $\frac{1}{2} \int_0^l (e I_y (w''[x])^2 + g I_t (\phi'[x])^2 + e I_w (\phi''[x])^2) dx + 2 \int_0^{\frac{l}{2}} (D[Mz[x] \phi[x], x]) w'[x] dx + \frac{1}{2} P a B^2$

$$\frac{1}{2} a B^2 P + \frac{1}{16} A B P (4 + \pi^2) - \frac{A^2 e I_y \pi^4 + B^2 (g I_t L^2 \pi^2 + e I_w \pi^4)}{4 L^3}$$

Collect[D[Energy, A] // FullSimplify, {A, B}]
Collect[D[Energy, B] // FullSimplify, {A, B}]

$$\frac{A e I_y \pi^4}{2 L^3} + \frac{1}{16} B P (+4 + \pi^2)$$

$$\frac{1}{16} A P (+4 + \pi^2) + B \left(a P + \frac{g I_t L^2 \pi^2 + e I_w \pi^4}{2 L^3} \right)$$

Exact analytical solution:
 $\frac{P_E \ell}{4 M_{ref}} \approx 1.35 \left[1 + [0.54 P_{E,y} \alpha / M_{ref}]^2 + 0.54 P_{E,y} \alpha / M_{ref} \right]$
 $M_{ref} = \sqrt{P_{E,y} (G I_t + \pi^2 E I_w / \ell^2)}$
 $P_{E,y} = \pi^2 E I_y / \ell^2$

Criticality means that the **determinant vanishes**. The roots of the quadratic polynomial in P gives the critical loads. The smallest one is the buckling load.

$$\begin{pmatrix} \frac{e I_y \pi^4}{2 L^3} & \frac{1}{16} P (+4 + \pi^2) \\ \frac{1}{16} P (+4 + \pi^2) & \left(a P + \frac{g I_t L^2 \pi^2 + e I_w \pi^4}{2 L^3} \right) \end{pmatrix};$$

Figure 1.165: *Mathematica* beautiful solution by our course assistant Dr. & Civ. Eng. Summer S. (However, I did not cross-checked this solution). Here you see the determinant of the eigenvalue problem obtained from the criticality condition $\delta(\Delta \Pi(A, B)) = 0$. Notation $e \equiv E$, $g \equiv G$. The remaining symbols are clear when you compare to the equations above (Eq. 1.939).

1.13.1 Complete model when accounting the effects of shear force change during lateral-torsional buckling

Recall that, in the previous section, when deriving the equations of stability for the lateral torsional buckling, the additional work of shear forces were omitted (for educational purposes)³³³ during slight perturbation. In this small chapter, we will account for their effects in order to obtain the complete the model. *It comes out that, the work of initial shear stresses at buckling cannot be ignored to*

³³³I wanted to construct a complete model by adding little-by-little complexity in order to make the student follow.

Solution kindly provided by your classmate Tuomas L. (Year 2020)

Note that, we are here looking for approximate solutions and not the exact one.

Code with Mathematica:

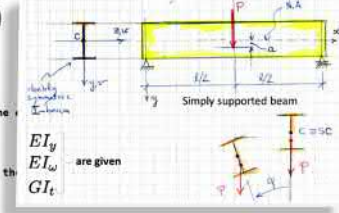
```

Collecting terms A and B
Out[10]:  $\frac{1}{16} \frac{8 H^2 y^2 \pi^4}{2 L^4} - \frac{1}{16} \frac{8 H^2 y^2 \pi^4}{2 L^4} + \frac{G J t L^2 \pi^2 + H J w \pi^4}{2 L^2} - \frac{1}{16} \frac{8 H^2 y^2 \pi^4}{2 L^4}$ 
Out[11]:  $\frac{8 H^2 y^2 \pi^4}{2 L^4} - \frac{1}{16} \frac{8 H^2 y^2 \pi^4}{2 L^4}$ 
Out[12]: Derivatives in matrix form when x=0:

$$\begin{pmatrix} a P + \frac{G J t L^2 \pi^2 + H J w \pi^4}{2 L^2} & \frac{1}{16} P (4 + \pi^2) \\ \frac{1}{16} P (4 + \pi^2) & \frac{H J y \pi^4}{2 L^3} \end{pmatrix}$$

Out[13]: The determinants of the matrix must be zero for non trivial solutions
Out[14]:  $\frac{P^2}{16} - \frac{P^2 \pi^4}{32} - \frac{8 H^2 y^2 \pi^4}{2 L^4} - \frac{P^2 \pi^4}{256} - \frac{8 H^2 J t y \pi^4}{4 L^4} - \frac{H^2 J w y \pi^4}{4 L^4}$ 
Out[15]:  $\left\{ \left\{ P = \frac{1}{L^2} \frac{8 H^2 y^2 \pi^4}{(4 + \pi^2)^2} \right\}, \left\{ 8 H^2 J t y \pi^4 - \sqrt{H^2 y \left( 32 J t L^2 (4 + \pi^2)^2 + H^2 \pi^4 (64 H^2 y^2 + 32 (4 + \pi^2)^2) \right)} \right\} \right\}$ 
Out[16]:  $\left\{ \left\{ P = \frac{1}{L^2} \frac{8 H^2 y^2 \pi^4}{(4 + \pi^2)^2} \right\}, \left\{ 8 H^2 J t y \pi^4 + \sqrt{H^2 y \left( 32 J t L^2 (4 + \pi^2)^2 + H^2 \pi^4 (64 H^2 y^2 + 32 (4 + \pi^2)^2) \right)} \right\} \right\}$ 

```



```

Text["Fork supports at the ends"]
f = A * Sin[Pi * x / L]
fd1 = D[f, x]
fd2 = D[f, {x, 2}]
Text["Simple supports at the ends"]
w = B * Sin[Pi * x / L]
wd1 = D[w, x]
wd2 = D[w, {x, 2}]
Text["Bending moment from 0 to L/2"]
Mz = P * x / 2
Text["Local torsion at L/2"]
T0 = 1 / 2 * P * a * (f /. x -> L / 2)^2
Text["Terms of total potential energy without integrals"]
Purebending = H * Jy * wd2^2
Warping = H * Jw * fd2^2
Puretorsion = G * Jt * fd1^2
Bendingenergy = D[(Mz * f), x] * wd1
Localtorsion = T0
Text["Total potential energy - Integral"]
Potint = 2 * 1 / 2 * Integrate[H * Jy * wd2^2, x] + 2 * 1 / 2 * Integrate[H * Jw * fd2^2, x] + 2 * 1 / 2 * Integrate[G * Jt * fd1^2, x] + 2 * Integrate[D[(Mz * f), x] * wd1, x] + T0

```

$$\Delta \Pi = \frac{1}{2} \int_0^L EI_y w''^2 dx + \frac{1}{2} \int_0^L GI_t \phi'^2 dx + \int_0^L EI_\omega \phi''^2 dx + \int_0^L \{M_z^0 \phi'\}' w' dx + 1/2 P a \phi(\ell)^2$$

Figure 1.166: *Mathematica* another beautiful and correct solution by your classmate & Civ. Eng. 2020; Tuomas L. who found and corrected the famous mistake or *Mathematica* 'bug' "-4 + π²" from the last year solution to the correct one "+4 + π²"; (reproduced here with permission) .

obtain the correct model.

The Euler-Bernoulli kinematic hypothesis is assumed valid. Let's recall the kinematic hypothesis:

$$w(x, y) = w(G) + y \sin \phi \approx w(x) + y \phi(x) \tag{1.940}$$

The pre-stress shear τ_{xy}^0 can be decomposed into two components: $\tau_{xy}^0 \sin \phi \approx \tau_{xy}^0 \phi$ (works with γ_{xz}^*) and component $\tau_{xy}^0 \cos \phi \approx \tau_{xy}^0$ (works with γ_{xy}^*). It comes out that the second order part of shearing angle $\gamma_{xy}^* = -\omega_y \omega_x \neq 0$ and that $\gamma_{xz}^* = 0$.

The total work per unit volume of the initial shear stress on the quadratic components of the strain increments is

$$\tau_{xy}^0 \gamma_{xy}^* + \tau_{xz}^0 \gamma_{xz}^* = \tau_{xy}^0 \gamma_{xy}^* \tag{1.941}$$

because $\gamma_{xy}^* = -\omega_x \omega_z = -w_{,x}(v_{,x} - u_{,y}) = 0$ since from the kinematic assumption follows $v_{,x} = u_{,y} = 0$. Therefore, we can ignore the work of the components $\tau_{xz}^0 \gamma_{xz}^*$, where $\tau_{xz}^0 = \tau_{xy}^0 \sin \phi \approx \tau_{xy}^0 \phi$.

In short we want to account for the work of pre-stress shear stress component $\tau_{xy}^0 \cos \phi \approx \tau_{xy}^0$ on the second order part $\gamma_{xy}^* = -\omega_y \omega_x$ of shearing angles

$$\gamma_{xy} = 2e_{xy} - \omega_y \omega_x = \gamma_{xy}^L + \gamma_{xy}^{NL} \equiv \gamma_{xy}^L + \gamma_{xy}^* \tag{1.942}$$

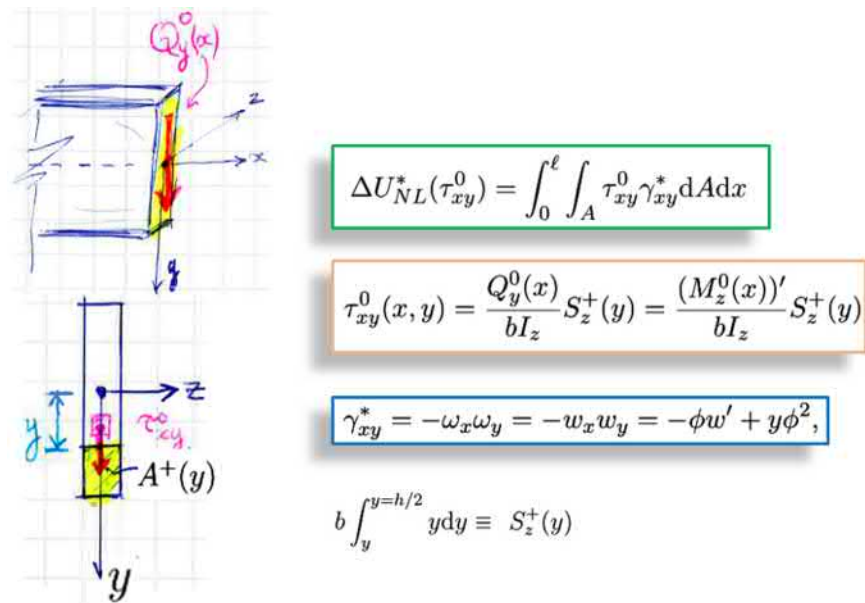


Figure 1.167: Shear stress in the pre-buckled configuration. Note that, in the work increment done by this initial stress component on the quadratic part of the shear strain γ_{xy}^* of the post-buckled configuration, this *initial shear stress* $\tau_{xy}^0(x, y)$ retains its amplitude and original direction of the pre-buckled state.

Recalling that, now we can ignore the derivatives (changes) the primary variables u^0, v^0, w^0 . We can also ignore e_{xy} while writing the increment of work done by the pre-stresses. Therefore, we write the increment of work of such pre-stress component as

$$\Delta U_{NL}^*(\tau_{xy}^0) = \int_0^\ell \int_A \tau_{xy}^0 \gamma_{xy}^* dA dx \quad (1.943)$$

The second-order (shear) rotation components are

$$\gamma_{xy}^* = -\omega_x \omega_y = -w_x w_y = -\phi w' + y \phi^2, \quad (1.944)$$

where the increment of displacements being $(0, 0, w)$ and ϕ . The lateral displacement $w(x, y)$ of arbitrary point $P(x, y)$ of the cross-section can be decomposed into lateral displacement $w(x)$ of the center of mass G of the section and into its rotation $\phi(x)$ around G ³³⁴.

³³⁴Recall that the section is a very thin narrow rectangle which have no shape distortion during deformation. This mean that the cross-section have only rigid body displacements and rotations

It will be also assumed that the forces, stresses from the primary state do not change amplitude nor direction. Therefore, we assume the *initial shear stress*

$$\tau_{xy}^0(x, y) = \frac{Q_y^0(x)}{bI_z} S_z^+(y) = \frac{(M_z^0(x))'}{bI_z} S_z^+(y) \quad (1.945)$$

retains its amplitude and original direction of the pre-buckled state. Note that, in equation (1.945) the static moment³³⁵ is defined as (Figure 1.167)

$$S_z(y) = \int_{A(y)} y dA = b \int_{y=-h/2}^y y dy = -b \underbrace{\int_y^{y=h/2} y dy}_{\equiv S_z^+(y)} \equiv -S_z^+(y), \quad (1.946)$$

in order to keep the sign '+', which is a more familiar view, for shear stress in equation (1.945). Straight forward integration gives $S_z^+(y) = -S_z(y) = \frac{b}{2}(\frac{h^2}{4} - y^2)$. The change in total potential energy when accounting for the work of shear stresses³³⁶ is

$$\Delta\Pi = \frac{1}{2} \int_0^\ell EI_y w''^2 dx + \frac{1}{2} \int_0^\ell GI_t \phi'^2 dx + \underbrace{\int_0^\ell M_z^0 w' \phi' dx}_{\text{bending: } \sigma^0 \epsilon_x^*} + \underbrace{\int_V \tau_{xy}^0 \gamma_{xy}^* dV}_{\text{shear}} \quad (1.947)$$

$$= \frac{1}{2} \int_0^\ell EI_y w''^2 dx + \frac{1}{2} \int_0^\ell GI_t \phi'^2 dx + \underbrace{\int_0^\ell M_z^0 w' \phi' dx}_{\text{bending: } \sigma^0 \epsilon_x^*} + \underbrace{\int_0^\ell Q_y^0 \phi w' dx}_{\text{shear: } \tau_{xy}^0 \gamma_{xy}^*} \quad (1.948)$$

$$= \frac{1}{2} \int_0^\ell EI_y w''^2 dx + \frac{1}{2} \int_0^\ell GI_t \phi'^2 dx + \underbrace{\int_0^\ell M_z^0 w' \phi' dx}_{\text{bending}} + \underbrace{\int_0^\ell (M_z^0)' \phi w' dx}_{\text{shear}} \quad (1.949)$$

The last two contributions in the integral above can be combined as follow

$$\int_0^\ell M_z^0 w' \phi' dx + \int_0^\ell (M_z^0)' \phi w' dx = \int_0^\ell (M_z^0 \phi)' w' dx \quad (1.950)$$

to obtain, finally, the change in the total potential energy (for narrow rectangular non-warping cross-section)

$$\boxed{\Delta\Pi = \frac{1}{2} \int_0^\ell EI_y w''^2 dx + \frac{1}{2} \int_0^\ell GI_t \phi'^2 dx + \underbrace{\int_0^\ell (M_z^0 \phi)' w' dx}_{\text{bending \& shear}}} \quad (1.951)$$

³³⁵First moment of area

³³⁶Should be accounted for in lateral torsional buckling. In addition, recall that now, we have no warping yet.

Note in the above integral that shear force equilibrium equation $(M_z^0 \phi)' = Q_y^0$ is automatically accounted for.

To account for strain energy change for warping³³⁷ $1/2 \int_0^\ell EI_\omega \phi''^2 dx$ should be added and the work of external force when not coinciding with cross-section centroid (= center of rotation for doubly symmetric sections). For such case of symmetry and distributed transversal load one will have,

$$\Delta \Pi = \frac{1}{2} \int_0^\ell EI_y w''^2 dx + \frac{1}{2} \int_0^\ell EI_\omega \phi''^2 dx + \frac{1}{2} \int_0^\ell GI_t \phi'^2 dx + \tag{1.952}$$

$$+ \int_0^\ell (M_z^0 \phi)' w' dx + \frac{1}{2} \int_0^\ell q_y(x) a_y(x) \phi^2 dx + \frac{1}{2} P a_y(x_P) \phi^2(x_P) dx, \tag{1.953}$$

where x_P being the location of the load P along the x -axis, if any point-load³³⁸

* * *

Now let's go back to the energy increment of interest (the new part as regarded to the case where we omitted the effect of shear)

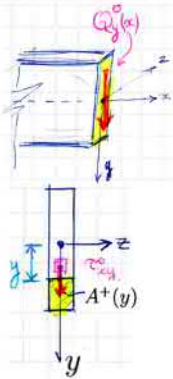
$$\Delta U_{NL}^*(\tau_{xy}^0) = \int_0^\ell \int_A \tau_{xy}^0 \gamma_{xy}^* dA dx \tag{1.954}$$

$$= \int_0^\ell \frac{Q_y^0}{bI_z} \phi w' dx \underbrace{\int_A S_z(y) dA}_{=bI_z} + \tag{1.955}$$

$$- \int_0^\ell \frac{Q_y^0}{bI_z} \phi^2 dx \underbrace{\int_A y S_z(y) dA}_{=0} \tag{1.956}$$

$$= + \int_0^\ell Q_y^0 \phi w' dx = + \int_0^\ell (M_z^0)' \phi w' dx. \tag{1.957}$$

Sign convention



$$\tau_{xy}^0(x, y) = \frac{Q_y^0(x)}{bI_z} S_z^+(y)$$

$$b \int_y^{y=h/2} y dy \equiv S_z^+(y)$$

In the above result we have the static moment $S_z(y) = -\frac{b}{2}(\frac{h^2}{4} - y^2)$ and used the fact that $\int_A y S_z(y) dA = 0$ without even computing it; just notice that the function $y(z)$ is antisymmetric (linear) and $S_y(z)$ is symmetric (parabola) with respect to $y = 0$. Therefore, the integral of their product vanishes. The integral $\int_A S_z(y) dA = -bI_z$ ³³⁹.

To find out the additional terms coming into the stability equations (1.892) one should take the first variation

$$\delta(\Delta U_{NL}^*) = + \int_0^\ell (M_z^0)' w' \delta \phi dx + \int_0^\ell (M_z^0)' \phi \delta w' dx. \tag{1.958}$$

³³⁷Will be treated in following paragraphs.

³³⁸If many P_k then take the sum.

³³⁹Also computed, graphically, as the area of the parabola - the graph of $S_z(y)$ - which is $= 2/3 \times h \cdot (bh^2/8)$.

After integration by part of the second term and factoring and adding terms with the same variations in (1.891), we obtain (retaining only the field equation) the Euler equations:

$$\underline{\delta w} : \quad EI_y (w'')'' - \left(M_z^0 \phi' \right)' - \underbrace{\left((M_z^0)' \phi \right)'}_{\text{from } \tau_{xy}^0 \cdot \gamma_{xy}^*} = 0 \quad (1.959)$$

$$\underline{\delta \phi} : \quad (GI_t \phi')' + \left(M_z^0 w' \right)' - \underbrace{\left(M_z^0 \right)' w'}_{\text{from } \tau_{xy}^0 \cdot \gamma_{xy}^*} = 0. \quad (1.960)$$

The above equation can be simplified a bit and obtain³⁴⁰, finally **the complete equations for lateral torsional buckling** with transverse planar loading:

$$\boxed{\begin{cases} EI_y (w'')'' - (M_z^0 \phi)'' & = 0 \\ (GI_t \phi')' + M_z^0 w'' & = 0. \end{cases}} \quad (1.961)$$

M_z^0 the above equations are identical with the previous ones without accounting for the initial shear force. (In pure bending, the shear force vanishes).

1.14 Computational stability analysis

Let's first clarify terms: *Computational stability* analysis is part of doing *non-linear analysis* of structures. The idea of this notes is limited to illustrating elastic stability analysis through computational examples performed with the help of some Finite Element software³⁴¹ of current use, like Abaqus, Ansys, Comsol and so on.

For detailed theoretical and related computational algorithms, the reader is encouraged to consult the very-concise lecture notes³⁴² by professor Reijo **KOUHIA** at <http://www.tut.fi/rakmek/personnel/kouhia/teach/> named *Computational techniques for the non-linear analysis of structures, 2009.*

The idea in the current notes is to also introduce computational elastic stability analysis (linear buckling and post-buckling problems) through computational starting from simple examples (single structural elements) to getting more complexity involved as in real structures (full structures).

It should be noted that when analysing the post-buckling behaviour of structures or structural elements, the response may naturally leads to large or excessive displacements and deformations resulting consequently in material failure through damage (plastic limit state for metals or damage for concrete and so

³⁴⁰Cross-checked 3.12.2018 against JP's Eq. 7.84 p : OK

³⁴¹I will, this year limit myself to use only Comsol and abaqus.

³⁴²The link is from 26.1.2019

on). Such material behaviour should be included when analysing stability or post-buckling behaviour of real structures.

In this course of *Elastic Stability* we limit our analysis to elastic behaviour of material even with large deformations. The idea in this course is to obtain the fundamentals of elastic stability. In another course³⁴³, *thermo-mechanical behaviour of solid materials* that I will give, such material damaging behaviour will be addressed; so feel free to attend.

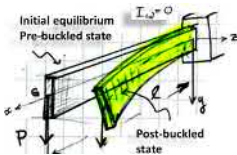
Stability analysis consists of performing next steps:

- **linear stability analysis** to determine the the critical buckling load: *buckling loads and corresponding buckling modes* (The *homogeneous linearised equations of elastic-stability* form an eigenvalue problem)
- **non-linear analysis** to study the full *post-buckling* behaviour and to investigate the *sensitivity of critical points with respect to imperfections* in shape, loading and material, and to determine also *limit load*. (= a full non-linear problem with non-zero right-hand).

The steps necessary to do the linear stability analysis are (1.168):

1. *Solve initial stress state* in the pre-buckled state for unit loading
2. *Solve the linearised homogeneous equations of stability* to obtain the critical load and buckling mode

Linear buckling analysis



In the following example we solve, computationally, the linear elastic stability problem. The physical setting is buckling of a narrow beam bended in the plan of greatest flexural rigidity. It is known that for a certain value (critical load) of the end load, such beam loses stability by lateral torsional buckling. Especially sensitive to such loss of stability are cases when flexural rigidity in plane of bending is much higher as compared to lateral bending rigidity. The beam will be stable for loading below the critical value. In design, lateral support are often used to prevent such behaviour.

Thus, the problem under consideration consists of lateral torsional buckling of a relatively high cantilever beam having a narrow I-shaped cross-section. The end transverse load P is acting at centre of mass of the cross-section along the vertical axis of symmetry. The major moment of inertia is such that $I_y \ll I_z$. The loading height below the centre of mass G of the cross-section being now $a = 0$. The length being $\ell = 347$ mm, height $h = 50$ mm and width $b = 5.83$ mm. Material properties for steel: $E = 200$ GPa and $\nu = 0.3$. Numerically (FE-analysis) obtained critical load is $P_{cr} = 7.11$ kN (Fig. 1.168).

³⁴³CIV-E4080 - Material Modelling in Civil Engineering L

The classical analytical solution³⁴⁴ within beam theory (Cf. Timoshenko 1910) gives

$$P_{cr} = \frac{4.013}{\ell^2} \sqrt{EI_y GI_t} \left[1 + \frac{a}{L} \sqrt{\frac{EI_y}{GI_t}} \right]. \quad (1.962)$$

Note that formula (1.962) was first obtained by Brandtl in 1889. The computa-

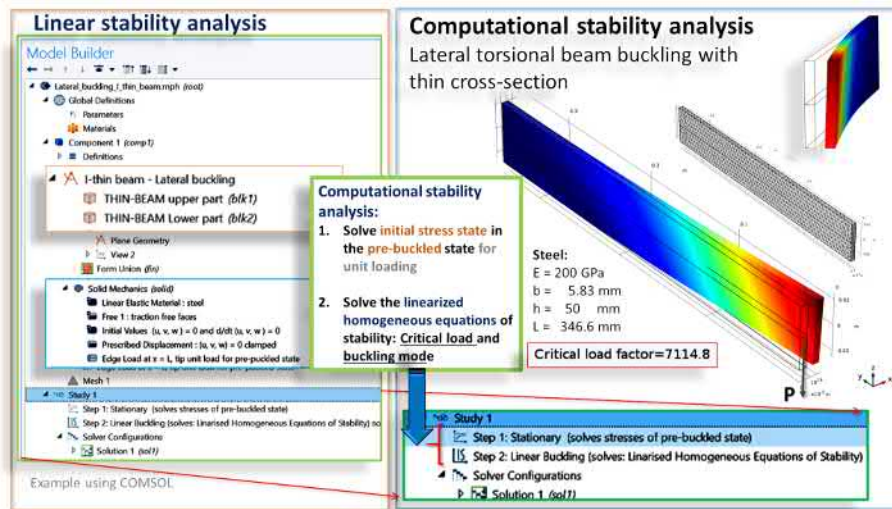


Figure 1.168: [Linear buckling analysis] Lateral torsional buckling of a thin cantilever. Computational approach for linear stability analysis. The numerical full 3-D model gives a critical load $P_{cr} = 7.11$ kN (analytical 1-D beam-theory solution $P_{cr} = 6.84$ kN (Eq. 1.962)). The FE-model used here is a full 3-D elasticity. For actual purposes shell-elements are more adequate and computationally economic than 3D-elements.

tional approach with a full 3-D numerical model (Fig. 1.168) gives a critical load $P_{cr} = 7.11$ kN. The analytical 1-D beam-theory solution $P_{cr} = 6.84$ kN, $a = 0$ (Eq. 1.962)). Recall that in the analytical model, the effect of shear stress was ignored. The above theoretical and numerical 3D-models are validated against experiments (Fig. 1.169).

The FE-model used here is a full 3-D elasticity. In general, shell-elements are more adequate and computationally economic than 3D-elements for this kind of simulation.

³⁴⁴The analytical solution involves use of Bessel functions. $P_{cr} = 4.013/\ell^2 \cdot \sqrt{EI_y GI_t/\gamma}$, where $\gamma = 1 - I_y/I_z$. Now one sees that for $I_y \ll I_z$ we have $\gamma \rightarrow 1$. On the contrary, $I_y = I_z$ gives $\gamma = 1$ a means that such beam will not loss stability by lateral torsional buckling since $P_{cr} \rightarrow \infty$.

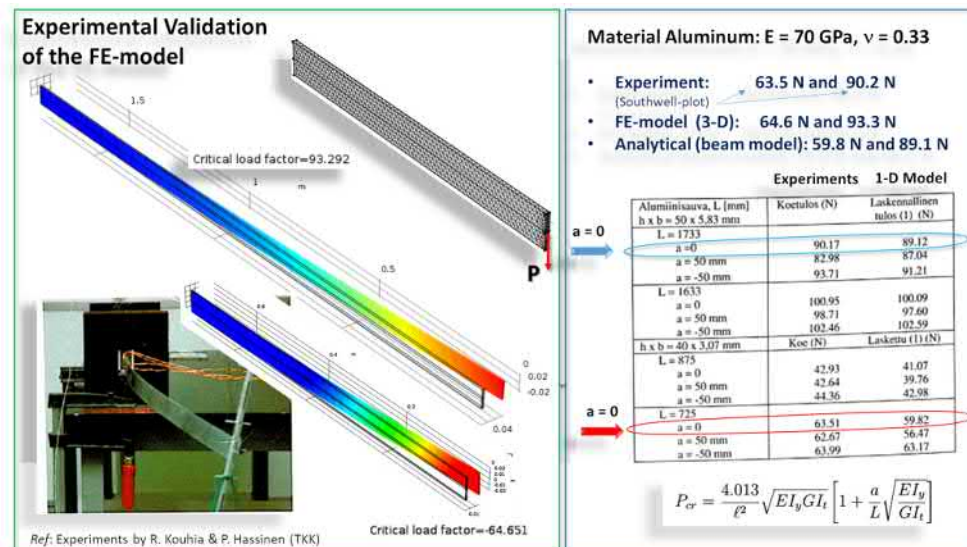


Figure 1.169: [Linear buckling analysis] Lateral torsional buckling of a thin cantilever. Experimental validation of the 3-D computational and the 1-D beam theory based theoretical stability models.

Post-buckling analysis

Non-linear Post-buckling³⁴⁵ analysis is performed (Fig. 1.170). The full geometrically non-linear simulation was done in FE-software *COMSOL Multiphysics*. A narrow cantilever loaded by a point load $P \in [0 \dots 3 \times P_{cr}]$ which was incrementally increased from 0 to its maximum. The critical load being $P_{cr} = 1.176$ kN. The material model was assumed elastic over all the deformation range.

A tiny horizontal load $H = P/1000$ was used as a perturbation. After the analysis, the load-displacements curves (v and w) were derived for the tip of the cantilever at the center of mass of the cross-section.

Data: A thin aluminium cantilever with a vertical tip load $P = 2$ kN and a horizontal perturbation force $H = P/1000$. The critical load being $P_{cr} = 1.176$ kN. Simulation data: $\ell = 0.5$ m, $b = 5.83$ mm, $h = 50$ mm. $E = 70$ GPa, $\nu = 0.33$. Location of the horizontal perturbation load was at $y = h/4$ away from the center of mass of the cross-section. The displacement in the weakest direction of inertia are denoted by w and vertical deflection in the strongest direction of inertia v , respectively.

After the analysis, the recorded tip displacements were used to draw the load-displacement curves or equilibrium paths (Fig. 1.171) which should be very close to the true one since the perturbation was nearly very small (1/1000).

³⁴⁵Lateral-buckling-I-thin-beam-Point-load-post-buckling-Analysis-parametric-OK-KURSSI-ESIM-1.mph and idem.avi

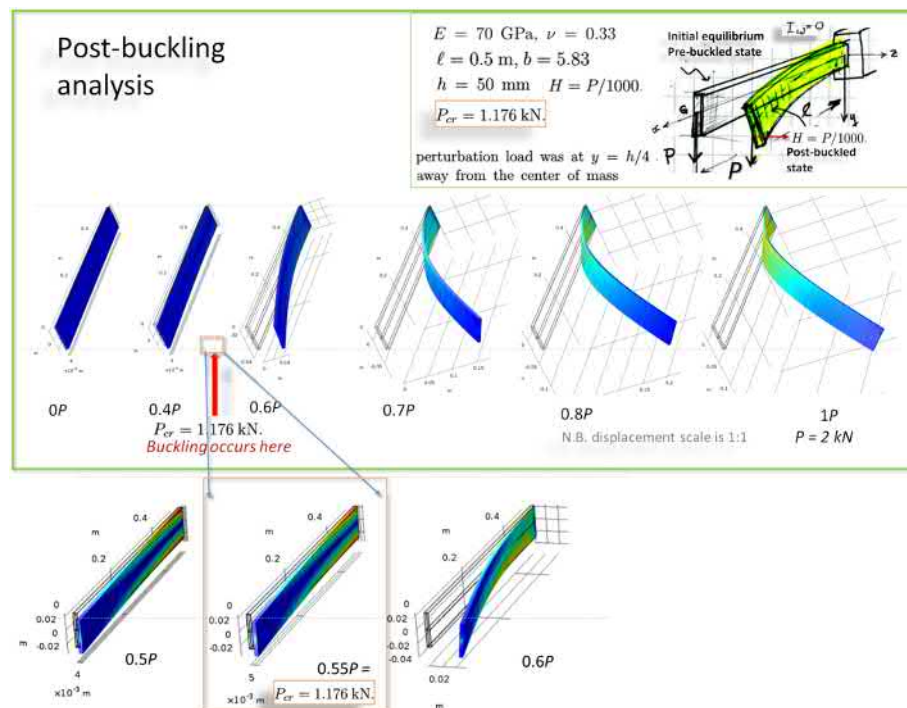


Figure 1.170: [Post-buckling analysis] A thin aluminium cantilever with a vertical tip load $P = 2$ kN and a horizontal perturbation force $H = P/1000$. The critical load being $P_{cr} = 1.176$ kN. Simulation data: $\ell = 0.5$ m, $b = 5.83$ mm, $h = 50$ mm. $E = 70$ GPa, $\nu = 0.33$. Location of the horizontal perturbation load was at $y = h/4$ away from the center of mass of the cross-section.

Lateral-torsional buckling for beams with warping

The equations of stability for a I -shaped narrow cross-section beam in transversal bending was treated previously. In the precedent example, the warping effects were ignored since $I_\omega \approx 0$ for the section and the shear centre S and the mass centre G (or C) were coinciding. Now we add a bit of complexity to the problem treated in Section (1.12.17) by considering cross-section with $I_\omega \neq 0$. Let's assume a *singly symmetric* I -beam type (Figure 1.172) about the y -axis. Additional torsional moment is generated when the transverse load does not pass through the shear center. To avoid such behaviour it is wise to use flexural members with at least on plane of symmetry. So, here, the transversal load passes through the rotation axis (shear center) laying on the plane of symmetry which is also the plane of bending. Consequently, at buckling, the additional flexural deflection with respect to the strongest axis of inertia is ignored³⁴⁶. Transverse

³⁴⁶contribution from v and its derivatives are ignored

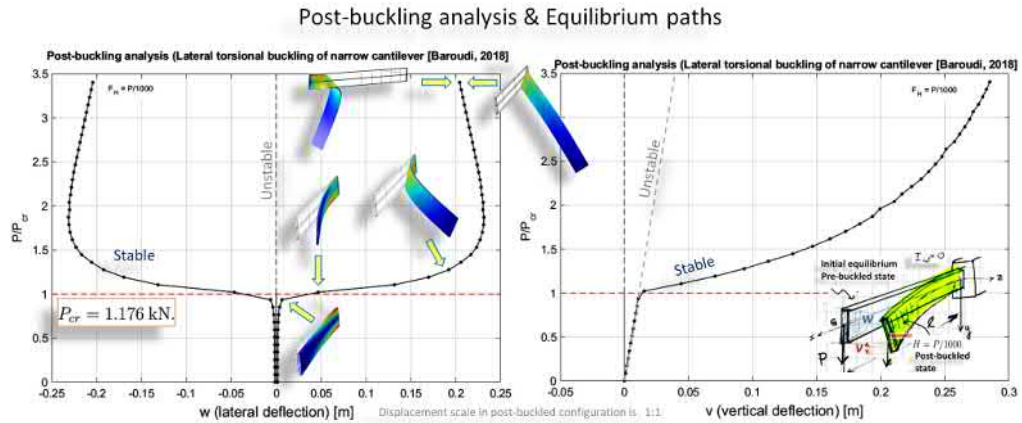


Figure 1.171: [Post-buckling analysis - equilibrium path] computed equilibrium paths for deflection in weakest direction (left) and vertical deflection in strongest direction of inertia (right). A thin aluminium cantilever with a vertical tip load P and a horizontal perturbation force $H = P/1000$.

load $q(x)$ passes through the plane passing through the web. Therefore, it also passes through the centre of shear S (called also centre of rotation). The total potential energy increase (Equation 1.876) will have two additional terms: strain energy increment due to *warping* $1/2 \int_0^\ell EI_\omega \phi''^2 dx$ and the term, we already seen earlier when the load is not applied to the centre of rotation (S), $-a_y/2 \int_\ell q_y \phi^2 dx$ of the incremental external work due to rotation of the cross-section around the shear centre.

The arm of the moment of external force q_y around the rotation centre (S) is $a_y \equiv (y_s - y_0)$, where $(y_s, z_s = 0)$ being the coordinates of S and $(y_0, z_0 = 0)$ being the coordinates of point of application of the load.

The kinematics of the cross section is defined entirely when knowing the translation motion v, w of the shear center together with the rotation ϕ of the cross-section about this shear center S (1.172). As in previous chapters, it is assumed that the orthogonal projection of cross-section on x -axis retains its shape. So, no distortion occurs (refer to previous or following discussion on this assumption). Consequently, the motion of this cross-section in the orthogonal plane to x -axis is described by a *rigid body motion* as defined in Subsection (1.12.17) and Equation (1.867).

The total potential energy increment (Equation 1.965) contains now the term coming from the additional work of initial shear stresses as $\Delta U_{\tau_0} = \int_V \tau_{xs}^0 \gamma_{xs}^* dV$. Note that the contribution of such initial shear stresses (rising from bending) in lateral torsional buckling should be included. Consequently, the initial equilibrium state is one of bending and of shear in the symmetry-plane.

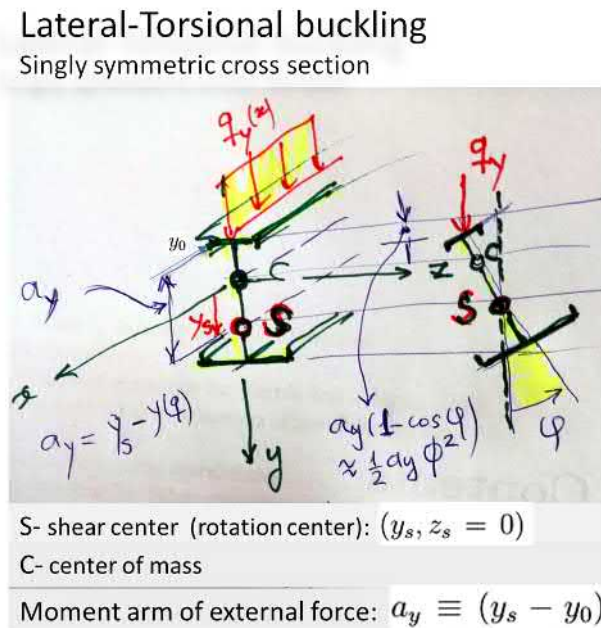


Figure 1.172: Lateral-torsional buckling of singly symmetric thin-walled open section beam under transversal load q_y .

For pedagogical reasons, we take advantage of the formulation of the increment of $\Delta\Pi$ we've already derived for the lateral-torsional buckling of the narrow rectangular cross-section. This step-by-step approach will consist of completing by adding to the previous functional the additional terms coming from considering warping which was absent from the case of the narrow cross-section and also adding other contributions not accounted for.

So, in the following, the effect warping and also additional work of initial shear stresses is accounted for in the final equations of stability³⁴⁷.

$$\Delta\Pi = \frac{1}{2} \int_0^\ell EI_y w''^2 dx + \frac{1}{2} \int_0^\ell GI_t \phi'^2 dx + \underbrace{\frac{1}{2} \int_0^\ell EI_\omega \phi''^2 dx}_{\text{new contribution to } \Delta U} \quad (1.963)$$

$$+ \underbrace{\int_0^\ell (M_z^0 \phi)' w' dx}_{\text{both bending \& shear initial stresses}} + \underbrace{\int_0^\ell M_z^0 \beta_y (\phi')^2 dx}_{\text{new contribution to } \Delta W(\tau_{xs}^0)} \quad (1.964)$$

$$+ \underbrace{\frac{a_y}{2} \int_0^\ell q_y \phi^2 dx}_{\text{new contribution to } W_{\text{ext}}} \quad (1.965)$$

where $a_y = y_q - y_s$ being the distance between the load location y_q and the shear

³⁴⁷For details in deriving (1.965), refer to the lecture-notes by Prof. J. Paavola

center y_s . Note that $a_y < 0$ when the load is above the center of rotation and $a_y > 0$ otherwise.

Now while taking the variation of $\delta(\Delta\Pi)$, $\forall\delta\phi, \delta w$ it is enough to find the variation of the new terms only and include them as *new contributions* to the linearised equilibrium equation of stability (Eq. 1.892) already obtained. Therefore

$$\delta\left(\frac{1}{2}\int_0^\ell EI_\omega\phi''^2 dx\right) = \int_0^\ell EI_\omega\phi''\delta\phi'' dx, \quad (1.966)$$

$$\delta\left(\frac{a_y}{2}\int_0^\ell q_y\phi^2 dx\right) = \frac{a_y}{2}\int_0^\ell q_y\phi\delta\phi dx, \quad (1.967)$$

$$\delta\left(\int_0^\ell M_z^0\beta_y(\phi')^2 dx\right) = \int_0^\ell M_z^0\beta_y\phi'\delta\phi' dx. \quad (1.968)$$

The contribution from additional complexity coming from warping effects and initial shear stresses to (the weak form) the Equations are (for case when the external load is applied along the center-line of the beam.)

$$\boxed{\begin{cases} (EI_y w'')'' - (M_z^0 \phi)'' = 0, \\ (EI_\omega \phi'')'' - (GI_t \phi')' - M_z^0 w'' - 2\beta_y (M_z^0 \phi')' + e_y q_y^0 \phi = 0 \end{cases}} \quad (1.969)$$

where $a_y = e_y = y_q - y_s$ the distance from the loading point to the shear center. Note that in the configuration of our example a_y (and e_y) are both negative³⁴⁸

Additional terms to the strain energy increment will be only in the torsional 2nd equation and is $-EI_\omega\phi^{(4)}$ and $-a_y q_y \phi$ to the same equations. *Homework:* derive the above equations starting from the variation of the above functional. (A bit simpler job).

No if one ignore the effect of initial shear stresses, the above equations simplify to

$$\boxed{\begin{cases} (EI_y w'')'' - (M_z^0 \phi)'' = 0, \\ (EI_\omega \phi'')'' - (GI_t \phi')' - M_z^0 w'' + a_y q_y^0 \phi = 0 \end{cases}} \quad (1.970)$$

where now the position of the transversal load above the area-center (C) is accounted for.

In the following, we will first study *analytically* two cases of practical importance for gaining understanding on how (design) parameters define the behaviour of singly-symmetric beams in lateral-torsional buckling. The effect of initial shear stress can be ignored in the following example.

Later one or two computational examples will be also provided.

³⁴⁸The correct sign for a_y or e_y can be easily cross-checked. A transversal on the compression flange will reduce sensibly the buckling load as compared with case where the load acts at the tension flange.

Example: simply supported beam with edges subjected to constant moment only

Consider such simply supported beam with singly-symmetric constant cross-section which is loaded at both ends by a constant moment $M_z^0 = \bar{M}_z^0$. The above equations (1.970) simplify to

$$EI_y w^{(4)} - \bar{M}_z^0 \phi'' = 0, \quad (1.971)$$

$$EI_\omega \phi^{(4)} - GI_t \phi'' - \bar{M}_z^0 w'' = 0. \quad (1.972)$$

These differential equations can be solved in many ways. One way is to eliminate $\phi(x)$ from the first equation and insert it in the second equation. Then, one solves the last PDE in terms of $\phi(x)$.

However, the above system of PDE with constant coefficients (1.972) is quit straight-forward to solve by taking trial solutions³⁴⁹ as

$$w(x) = A \sin(\pi x/\ell), \quad (1.973)$$

$$\phi(x) = B \sin(\pi x/\ell). \quad (1.974)$$

The linear terms $A_1 + A_2 x$ and $B_1 + B_2 x$ in the trial solution are not necessary since they cancel after twice differentiation. The above trial functions fulfil next boundary conditions

$$w(0) = w(\ell) = 0, \quad w''(0) = w''(\ell) = 0 \quad (1.975)$$

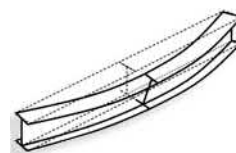
$$\phi(0) = \phi(\ell) = 0, \quad \phi''(0) = \phi''(\ell) = 0 \quad (1.976)$$

Inserting the trial solutions into the PDE (Equation 1.972) one obtains the criticality condition

$$\det \begin{bmatrix} [\pi/\ell]^2 EI_y & \bar{M}_z^0 \\ -\bar{M}_z^0 & [\pi/\ell]^2 EI_\omega + GI_t \end{bmatrix} = 0. \quad (1.977)$$

The buckling moment M_{cr} is found as the zero of the determinant as

$$M_{cr} = \frac{\pi}{\ell} \sqrt{EI_y [EI_\omega (\pi/\ell)^2 + GI_t]}. \quad (1.978)$$



Lateral buckling of I-beam subject to end moments.

Example: Simply supported beam subjected to transversal constant load

Distributed load q_y on a simply supported beam acting along the center-line. The initial bending moment (= initial stresses in the pre-buckled state) is

$$M_z^0 = \frac{q_y}{2} x(\ell - x). \quad (1.979)$$

³⁴⁹These are in fact the exact analytical Eigen-vectors. So, the solutions one obtains will be analytically exact.

Inserting this expression in the stability equations (1.970) we obtain

$$EI_y w^{(4)} - \frac{q_y}{2} [x(\ell - x)\phi]'' = 0, \quad (1.980)$$

$$EI_\omega \phi^{(4)} - GI_t \phi'' - \frac{q_y}{2} x(\ell - x)w'' = 0, \quad (1.981)$$

for the case when load is acting along the center-line of the beam. The above PDE-system forms a system of coupled equations with non-constant coefficients. A versatile method to solve the problem is to use infinite series. The solution was given by Timoshenko.

$$(q_y \ell)_{cr} = \gamma \sqrt{EI_y GI_t / \ell^2} \quad (1.982)$$

where the coefficient γ depends on

$$\gamma = f\left(\frac{GI_t \ell^2}{EI_\omega}\right) \quad (1.983)$$

The table below (by Timoshenko) provides some values for γ for a doubly symmetric I-beam cross-section for various locations (upper flange, centroid and lower flange) of the loading

VALUES OF THE FACTOR γ FOR SIMPLY SUPPORTED I BEAMS WITH UNIFORM LOAD

Load applied at	$\gamma = f\left(\frac{GI_t \ell^2}{EI_\omega}\right)$						
	0.4	4	8	16	24	32	48
Upper flange	92.9	36.3	30.4	27.5	26.6	26.1	25.9
Centroid	143	53.0	42.6	36.3	33.8	32.6	31.5
Lower flange	223	77.4	59.6	48.0	43.6	40.5	37.8
Load applied at	$\gamma = f\left(\frac{GI_t \ell^2}{EI_\omega}\right)$						
	64	80	128	200	280	360	400
Upper flange	25.9	25.8	26.0	26.4	26.5	26.6	26.7
Centroid	30.5	30.1	29.4	29.0	28.8	28.6	28.6
Lower flange	36.4	35.1	33.3	32.1	31.3	31.0	30.7

$$(q_y \ell)_{cr} = \gamma \sqrt{EI_y GI_t / \ell^2}$$

Lateral torsional buckling. Stability parameter γ . Table edited from: Timoshenko *Elastic Stability of structures*.

I-beam Cantilever

Let's consider the lateral-buckling of a singly symmetric I-beam loaded by a transversal tip-load P at the centroid. This is a classical problem treated by Timoshenko in 1910. The equations of loss of stability are given by Equations (1.970).

$$EI_y w^{(4)} - [P(\ell - x)\phi]'' = 0, \tag{1.984}$$

$$EI_\omega \phi^{(4)} - GI_t \phi'' - P(\ell - x)w'' = 0 \tag{1.985}$$

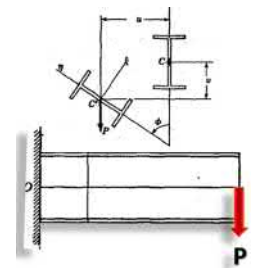
Timoshenko solved the above problem (1910) and found

$$P_{cr} = \gamma_2 \sqrt{EI_y GI_t / \ell^2} \tag{1.986}$$

where the parameter

$$\gamma_2 = 4.013 / [1 - \sqrt{EI_\omega / GI_t \ell^2}]^2 \tag{1.987}$$

$$P_{cr} = \gamma_2 \sqrt{EI_y GI_t / \ell^2} \quad \gamma_2 = 4.013 / [1 - \sqrt{EI_\omega / GI_t \ell^2}]^2$$



Lateral buckling.

VALUES OF THE FACTOR γ_2 FOR CANTILEVER BEAMS OF I SECTION

$\frac{GI_t \ell^2}{EI_\omega}$	0.1	1	2	3	4	6	8
γ_2	44.3	15.7	12.2	10.7	9.76	8.69	8.03
$\frac{GI_t \ell^2}{EI_\omega}$	10	12	14	16	24	32	40
γ_2	7.58	7.20	6.96	6.73	6.19	5.87	5.64

Figure 1.173: Lateral buckling of I-beam cantilever.

FE-computational example

Let's consider a doubly symmetric I-beam loaded at its cross-section centroid at one end by a transversal load P . The other end is clamped. The material is aluminium with $E = 70$ GPa and $\nu = 0.33$. The thickness is constant 1 cm and the web has $a = 10$ cm high and the flanges of $a = 10$ cm width (see left illustration in Figure 1.174).

Lateral-torsional buckling of I-beam

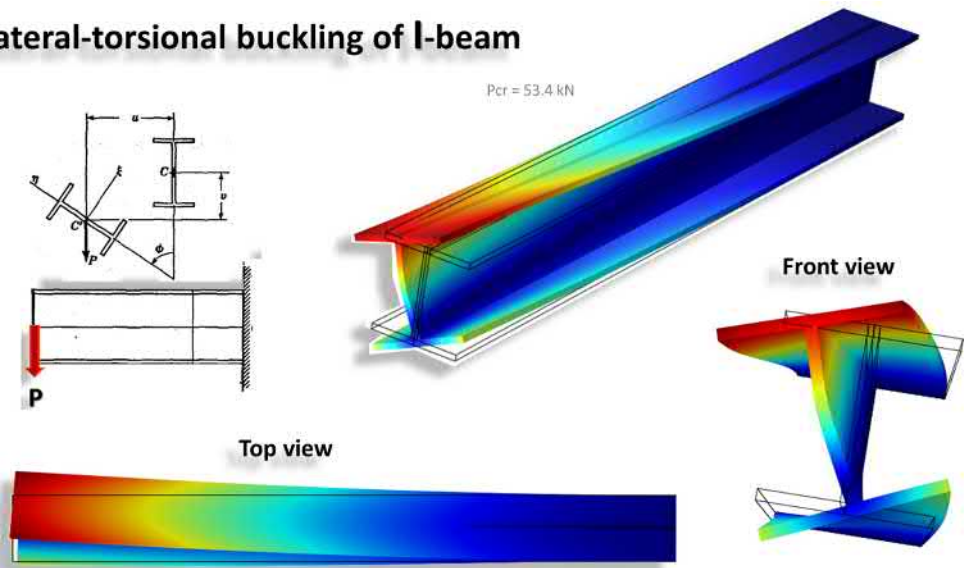


Figure 1.174: FE-Buckling analysis: Lateral torsional buckling of doubly symmetric I-beam. The transversal load is at the cross-section centroid. $P_{cr} = 53.4 \text{ kN}$. Note the small amount of distortion of the web (flexural mode of the web)

The result of the linear buckling analysis is depicted in figure (Figure 1.174). Firstly two small details are worth to keep in mind: 1) a small amount of distortion of the web is present while the beam model (1D) assumes a rigid-body kinematics for the cross-section. This is the consequence of the bending of the web as a plate. 2) the lateral displacement (see top-view) is much significant than the additional vertical displacement which is practically insignificant (of lower order of magnitude). When approaching the bifurcation point or, in other word, the buckling load, the effective rigidity (or stiffness) of the structure decreases dramatically. Consequently the motion in the direction of loss of stiffness becomes very easy because of apparent loss of stiffness: a 'butterfly' pushing in the same direction of loss of stiffness is enough to have a sensible lateral deflection. Reciprocally, *a small force or relatively weaker structural member is enough to restraint a much stronger structural member against such lateral motion or lateral buckling.*

Analytical versus FE-solution: Let's compare the result $P_{cr}^{(FE)} = 53.4 \text{ kN}$ obtained by the 3D FE-Buckling analysis to the one given by the 1D-model of

the beam-theory by Timoshenko’s formula (1.986) which, we recall here:

$$P_{cr} = \gamma_2 \sqrt{EI_y GI_t} / \ell^2, \quad \text{where} \quad (1.988)$$

$$\gamma_2 = 4.013 / [1 - \sqrt{EI_\omega / GI_t \ell^2}]^2 \quad (1.989)$$

For that we have to determine first the needed geometric properties of the cross-section as I_t , I_y and I_ω .

Energetic solution

Let’s use the energy-approach to find a approximate solution for the above problem. The increment of total potential energy is (Equation 1.965)

$$\Delta\Pi = \frac{1}{2} \int_0^\ell [EI_y w''^2 + GI_t \phi'^2 + EI_\omega \phi''^2] dx + \int_0^\ell (M_z^0 \phi)' w' dx. \quad (1.990)$$

Next we should find cinematically admissible a pair of independent trial functions $w(x)$ and $\phi(x)$. The kinematic boundary conditions to be satisfied are

$$\begin{cases} w(0) = w'(0) = 0, \\ \phi(0) = \phi'(0) = 0. \end{cases} \quad (1.991)$$

The following pair is an example of simple candidate

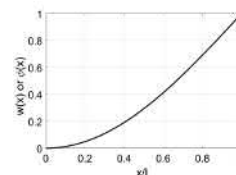
$$\begin{cases} w(x) = w_0(1 - \cos \frac{\pi x}{2\ell}) \\ \phi(x) = \phi_0(1 - \cos \frac{\pi x}{2\ell}) \end{cases} \quad (1.992)$$

fulfils the kinematic constraints above since

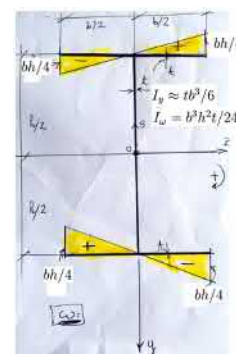
$$\begin{cases} w'(x) = w_0 \pi / 2\ell \sin \frac{\pi x}{2\ell} \\ \phi'(x) = \phi_0 \pi / 2\ell \sin \frac{\pi x}{2\ell} \end{cases} \quad (1.993)$$

The needed derivatives are $w' = w_0 \pi / 2\ell \cdot \sin \frac{\pi x}{2\ell}$. The factor 2 in the trigonometric function is there to obtain a eigenmode like shapes (see Margin). This exercise will be continued later using Matlab symbolic toolbox (this is an exercise for the reader).

Note that for a doubly symmetric open thin walled cross-section, the shear center (S) and the centroid (C) (centre of gravity) coincide. Here needed geometrical parameters for the generic I-beam cross-section with height h and width



Approximates modes $w(x)$ & $\phi(x)$.



Sectorial coordinate ω

b (see 1.175 for other types of cross-sections). The thickness being $t_f = t_w = t$:

$$A = \int_s t(s)ds = (2b + h)t, \tag{1.994}$$

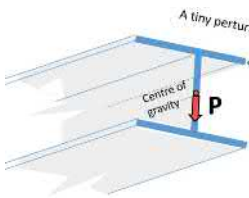
$$I_y = \int_A z^2 dA = \int_s z^2(s)t(s)ds \approx tb^3/6, \tag{1.995}$$

$$I_\omega = \int_A \omega^2(s)dA = \int_s \omega^2(s)t(s)ds = b^3h^2t/24, \tag{1.996}$$

$$I_t \approx \frac{1}{3} \sum_i \ell_i t_i^3 = \frac{1}{3}(h + 2b)t^3. \tag{1.997}$$

To be continued, compare analytical, energetic and FE-solutions [7.1.2019, DBA]
 ...

Post-buckling analysis



The aluminium I-beam of the previous linear buckling analysis example is analysed further in post-buckling behaviour (Figures 1.176 and 1.177) by Finite Element method (Comsol). As a perturbation, a tiny horizontal force H was added to generate a small perturbation torsion. Please note, in the figure, the transition from pure flexural behaviour ($\lambda \leq 1$) to torsional one after the threshold corresponding to the buckling load.

Lateral torsional buckling under a transverse load applied at centroid (G) and a perturbation H .

Recall of the method: *What does $\Delta\Pi$ means?* It is, may be, now that we have advanced so far from the start, the right time to *Stop*, friends³⁵⁰ strengthen and illustrate some key concepts of stability as for instance, *energy criterion, primary equilibrium state, perturbed equilibrium state, increment of total potential energy*, ... , we have had in the introductory part of this lecture notes booklet. Figure (1.178) tells you everything in pictures. Take time to look at it.

فَمَا تَبْكُ مِنْ ذِكْرِي حَبِيبٍ وَمَنْوِيلٍ
 بِسَيْفِ اللَّوِيِّ بَيْنَ الدَّخُولِ فَحَوْمَلٍ

A Poem by **Imru-al-Qais**: 'Oh, Stop, my Freind... and let's Remember...

1.15 Torsional buckling

In the previous section we considered *lateral-torsional buckling* where the beam was loaded *transversally*. In this section, *Torsional buckling*, we consider a beam-column with the thrust loading P is directed axially normal to the cross-section. The stability behaviour of such column-beam will be studied.

For columns with *thin-walled open cross-sections*, the torsional rigidity EI_t is dramatically smaller as compared to the same but closed section. When torsional rigidity is much small as compared to flexural rigidity in the principal directions loss of stability through torsional mode may occur. Such stability loss is termed as *torsional buckling*.

³⁵⁰Poet **Imru-al-Qais (500-544)**: *Stop, oh my friends, let us pause to weep over the remembrance of my beloved. Here was her abode on the edge of the sandy desert between Dakhool and Howmal. ...*



Torsional-buckling. Axial load is applied at centroid (G).

Shape of cross section	Location of shear centre, S	$J = \sum_{i=1}^n J_i$	I_ω	Shape of cross section	Location of shear centre, S	$J = \sum_{i=1}^n J_i$
	$y_0 = -e$ $z_0 = 0$	$J = J_1 + J_2$ $J_1 = \frac{1}{3}bt^3$ $J_2 = \frac{1}{3}bt^3$	$\frac{bt^3}{18} = \frac{A^3}{144}$		$y_0 = z_0 = 0$	$J = 2J_1 + J_2$ $J_1 = \frac{1}{3}bt_f^3$ $J_2 = \frac{1}{3}dt_w^3$
	$y_0 = -e_1$ $z_0 = -e_2$	$J = J_1 + J_2$ $J_1 = \frac{1}{3}b_1t^3$ $J_2 = \frac{1}{3}b_2t^3$	$\frac{t^3}{36}(b_1^3 + b_2^3)$		$y_0 = \frac{e_2t_2 - e_1t_1}{t_1 + t_2}$ $z_0 = 0$	$J = J_1 + J_2 + J_3$ $J_1 = \frac{1}{3}b_1t_1^3$ $J_2 = \frac{1}{3}b_2t_2^3$ $J_3 = \frac{1}{3}dt_w^3$
	$y_0 = -e$ $z_0 = 0$	$J = J_1 + J_2$ $J_1 = \frac{1}{3}dt_w^3$ $J_2 = \frac{1}{3}bt_f^3$	$\frac{t_w^3d^3}{36} + \frac{t_f^3b^3}{144}$			$I_\omega = d^2 \frac{I_1 I_2}{I_1 + I_2}$
	$y_0 = e \left(1 + \frac{e^2 A}{4t_f^2}\right)$ $z_0 = 0$	$J = 2J_1 + J_2$ $J_1 = \frac{1}{3}bt_f^3$ $J_2 = \frac{1}{3}dt_w^3$	$\frac{d^2}{4} \left[I_c + e^2 A \times \left(1 - \frac{e^2 A}{4t_f^2}\right) \right]$		$y_0 = z_0 = 0$	$J = 2J_1 + J_2$ $J_1 = \frac{1}{3}bt_f^3$ $J_2 = \frac{1}{3}dt_w^3$
						$I_\omega = \frac{d^2}{4} I_a^b$

^a I_1 and I_2 are the moments of inertia of the top and the bottom flanges, respectively, with respect to the Y -axis

^b I_a is the moment of inertia of the cross-section with respect to the centerline $a-a$ of the web

Figure 1.175: Geometric parameters of some thin-walled open cross-sections. ($S =$) shear center and the ($C =$) centroid. (Ref: Murari L. Gambhir. *Stability Analysis and Design of Structures*. Springer-Verlag Berlin Heidelberg 2004)

Despite the title of this section, we will derive the equations of stability for the general case of combined flexural (in both directions v and w and torsional buckling. The loading considered here remains only an axial thrust having no initial bending effects in the initial pre-buckled configuration. After this, the pure torsional buckling will be considered as a special case.

1.15.1 Total potential energy

In general, both flexural and torsional modes of deformation combine in a *three-dimensional buckling*. The beam can be experiencing bending in both directions ov

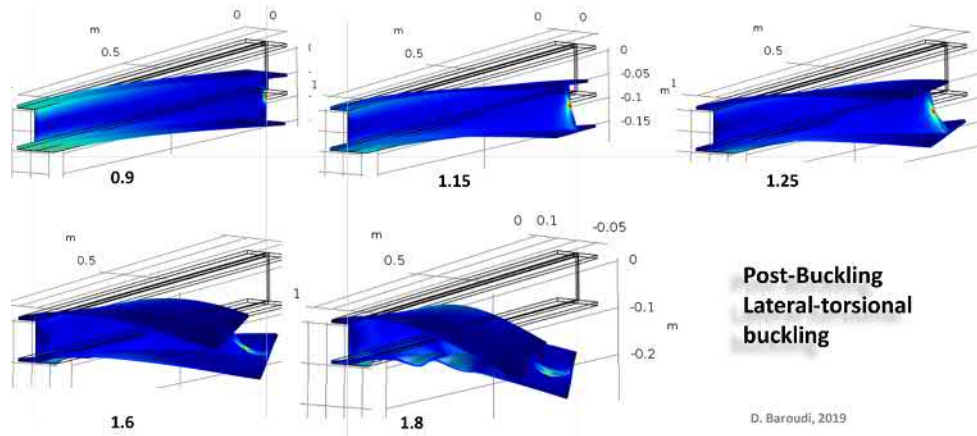


Figure 1.176: FE-post-buckling analysis of an aluminium I-beam cantilever. The transversal tip-load is at the centroid. The scalar numbers $\lambda = P/P_{cr}$ in the sub-figures correspond to the the scaled transversal load. Note that for $\lambda \geq 1.8$ local (plate-)buckling (lommahdus) of the lower flange occurs.

and w together with torsion or the cross-section around the shear center (SC). The loading considered here is still an axial thrust having no initial bending effects in the initial pre-buckled configuration.

for combined flexural and torsional buckling and when neglecting the work of shear stresses, the increment of total potential energy can be evaluated in its standard Bryan form as

$$\Delta\Pi = \frac{1}{2} \int_0^\ell EI_y w''^2 dx + \frac{1}{2} \int_0^\ell EI_z v''^2 dx + \quad (1.998)$$

$$+ \frac{1}{2} \int_0^\ell GI_t \phi'^2 dx + \frac{1}{2} \int_0^\ell EI_\omega \phi''^2 dx + \quad (1.999)$$

$$+ \int_0^\ell \int_A \sigma_x^0 \frac{1}{2} [(w'_Q)^2 + (v'_Q)^2] dA dx \quad (1.1000)$$

where the buckling incremental displacement v and w in the cross-sectional plane of an arbitrary material point $Q(y, z)$ of the cross-section is the combined motion of translation and a small rigid body rotation $\phi(x)$ of the cross-section around the shear center $(S(y_s, z_s))$

$$\begin{cases} v_Q(x) = v - (z - z_s)\phi, \\ w_Q(x) = w + (y - y_s)\phi, \end{cases} \quad (1.1001)$$

where $v = v(x)$ and $w = w(x)$ being the increments of the displacements of the centroid (C) and $\phi = \phi(x)$ the twist of the cross-section around the shear center (S). It is assumed that during buckling, the centre-line remain inextensible.

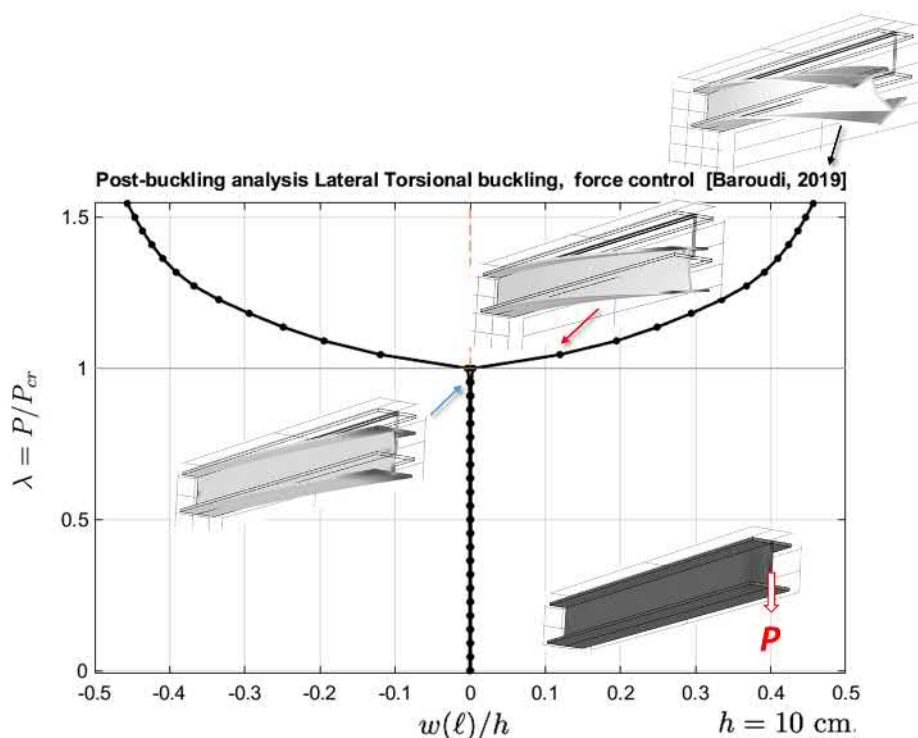


Figure 1.177: Equilibrium paths. FE-post-buckling analysis of an aluminium I-beam cantilever. The transversal tip-load is at the centroid. A tiny horizontal force H laipan yläpäässä is added as a perturbation (causes a tiny torsional moment). (TO DO: lisää vielä pystysiirtymän kuvaaja)

Accounting for the quadratic part of the strains computed from the kinematic given by (Equation 1.1001), the work of initial stress can be written, for a centric thrust P , as

$$\frac{1}{2} \int_V \sigma_x^0 [(w'_Q)^2 + (v'_Q)^2] dV = \quad (1.1002)$$

$$= \frac{P}{2} \int_0^\ell [(w')^2 + (v')^2 + r^2(\phi')^2 - 2z_s v' \phi' + 2y_s w' \phi'] dx \quad (1.1003)$$

where $r^2 = I_p/A = (I_z + I_y)/A + (y_s^2 + z_s^2)$. Expressing the initial stress in terms of initial thrust P and taking the stationary condition will lead to the Euler equations (linearised buckling equations; further in the text). The above energy functional can be also used to find good approximations for the buckling load by the Rayleigh-Ritz method.

Recall that the kinematics of an arbitrary material point $Q(x, y, z)$ laying on centreline of the wall a straight beam having open thin-walled cross-section is

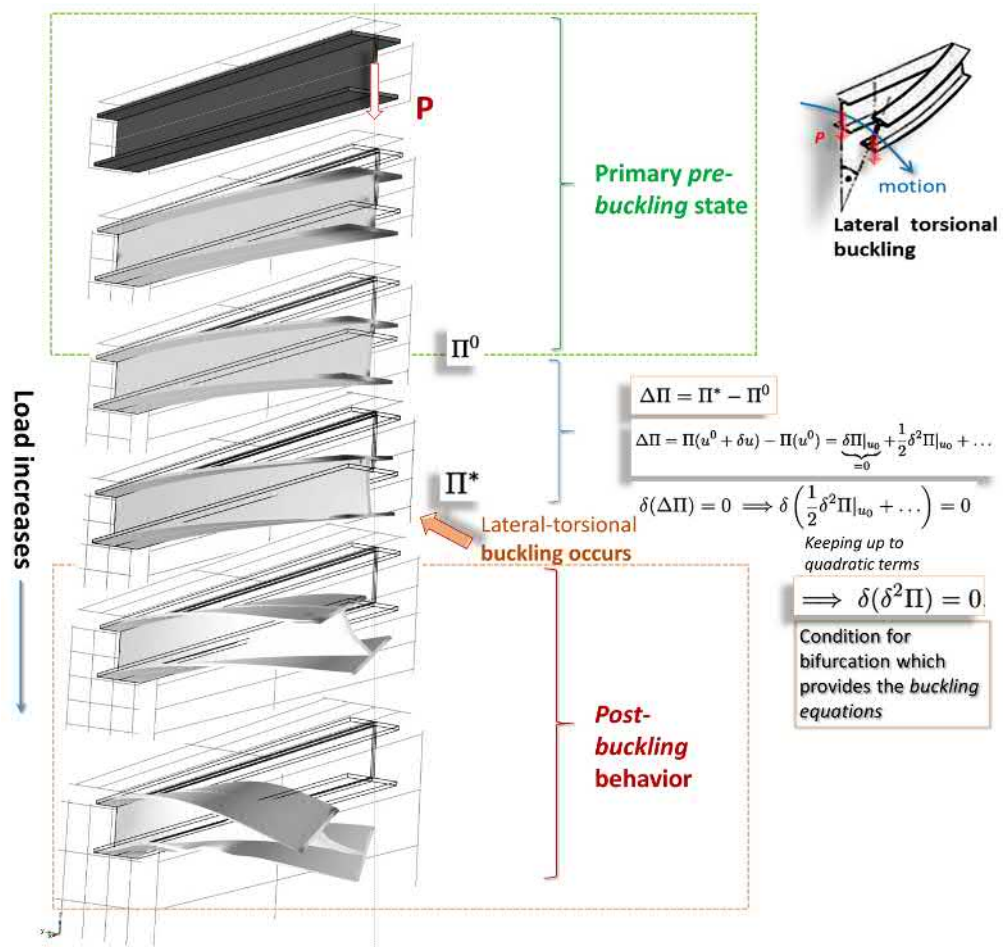


Figure 1.178: *Wysiwyg* recall and graphical illustration of key concepts of stability analysis through a FE-post-buckling analysis example.

(Figure 1.180)

$$\vec{u} = (u - yv' - zw' - \omega\phi')\vec{i} + (v - (z - z_s)\phi)\vec{j} + (w + (y - y_s)\phi)\vec{k}. \quad (1.1004)$$

This equation describes the general combined motion of such point consisting of translation and a small rigid body rotation of the cross-section around the shear center and the additional axial displacement $\Delta u_\omega(x, Q) = -\omega(s_Q)\phi'(x)$ due to warping³⁵¹. The local coordinate along the mid-plane of the thin-wall is denoted s . In a component form, we can re-write

$$\begin{cases} u_Q(x) = u - yv' - zw' - \omega\phi', \\ v_Q(x) = v - (z - z_s)\phi, \\ w_Q(x) = w + (y - y_s)\phi, \end{cases} \quad (1.1005)$$

³⁵¹Käyristyminen (sf)

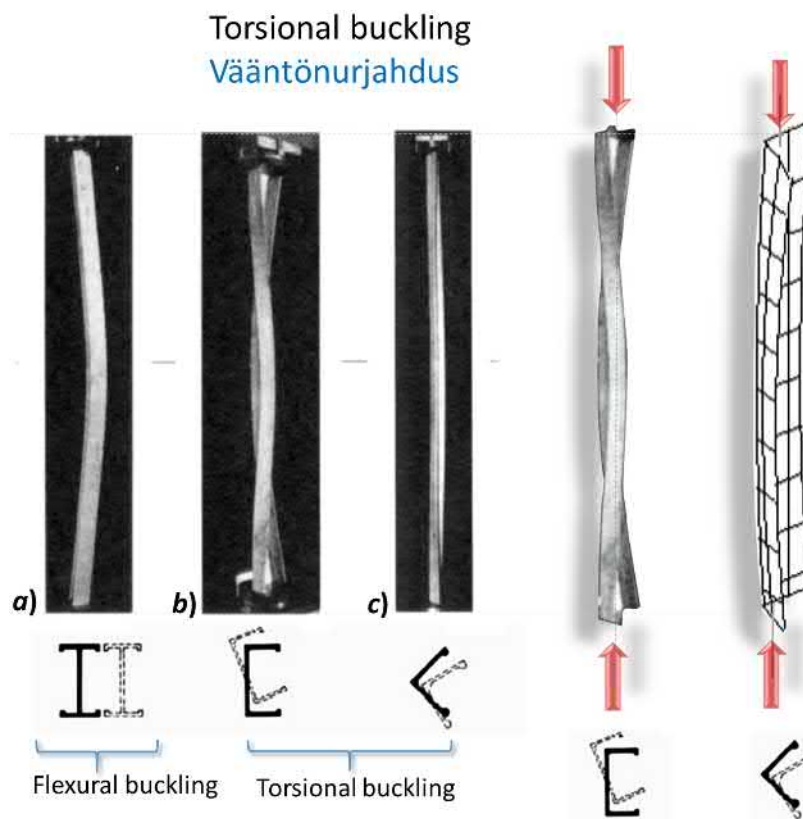


Figure 1.179: Flexural buckling a), pure torsional buckling b) and c). (Adapted from H. Hirsi's lecture notes 2019.)

where the coordinate of the rotation center (S) being (y_s, z_s) , the angle of twist $\phi(x)$ and the sectorial coordinate $\omega = \omega(x(s), y(s))$, where s being the arch-length coordinate along the mid-line of the wall of the cross-section. Recall that, the coordinate system coincides with the principle inertia axes³⁵² of the cross-section.

It should be reminded that the kinematics described by (Eq. 1.1004) corresponds to the rigid-body motion of the cross-section in orthogonal plane to x . Therefore, it implicitly assumes that the cross-section geometry remains without any distortions. In other words, the geometry of the orthogonal projection of cross-section remains unchanged during motion. *In order for this assumption to hold in reality, the thin-walled cross-section should have enough stiffeners to avoid possible shape distortions (Cf. Figure margin).* Otherwise, the Vlasov theory on which the above kinematic assumptions are based, will not hold. In this, case accounting analytically for such shape distortions makes the theory unnecessarily complex. This is however, done in many published work. Our-days, it

³⁵²Pääjäyhyyskoordinaatisto (SF)



Distortional local buckling. Vlasov theory does not account for such deformation mode.

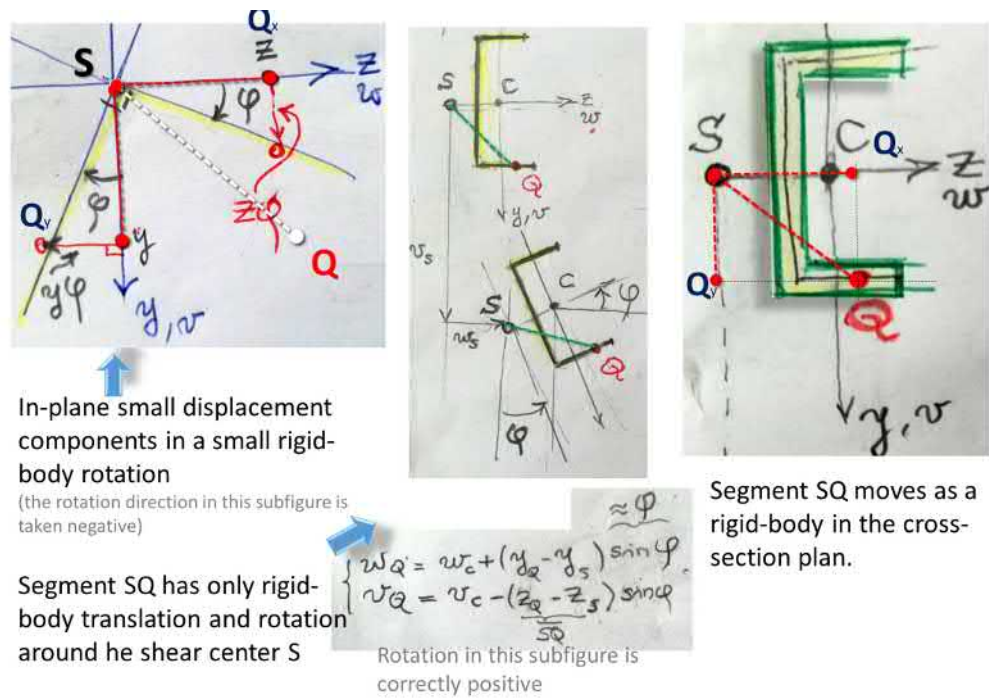


Figure 1.180: In-plane displacement components of an arbitrary point Q of the cross section of a thin-walled beam.

will be more wise, in such cases, to use also computational simulation tools and *treat the thin walls as thin shells or beam-shells*. However, for many cold-formed steel thin-walled cross-section, it is often not practical nor possible to weld any additional stiffener.

To repeat for not repeating but for pedagogical purposes, let say again with other words that, the analysis of such structural elements that one may call *thin-walled beam-shell* is not reliable within the Vlassov's theory because of the presence of local distortional modes in buckling or in geometrically non-linear analysis. This means that the geometric hypothesis of non-distorting cross-section is invalid. So, one should turn to computational and experimental tools to reliably make the structural analysis part of such structures. Our-days, the FE-technology is so developed that the engineer can very easily account also for the material non-linearities and all other sources of such non-linearities in the analysis. Analysing the results is another story. For this job one needs high level education in mechanics, structural mechanics, strength of material and so on. In one word, the computer compute and the engineer thinks.

Let's consider the eccentric compression³⁵³ of the cross-section of an open

³⁵³The following examples are inspired by lectures given by Emeritus professor **Jukka Aalto** that I was following when I was a younger student at TKK.

thin-walled beam (Figure 1.181). The eccentricities being e_y and e_z (not to be confused with the linear part of the strain tensor denoted also by e_i) Following

Torsional buckling

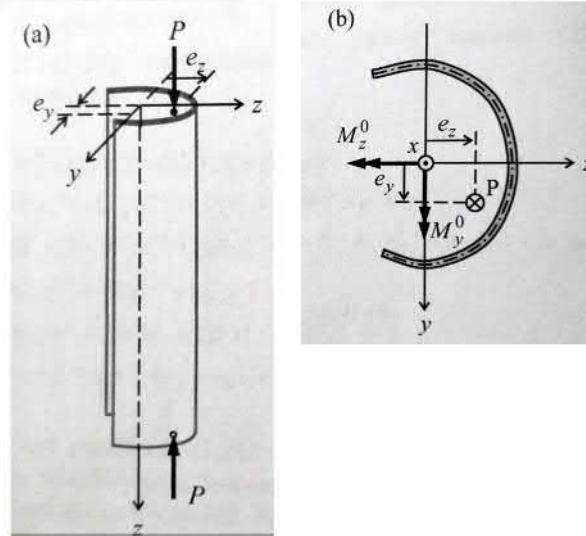


Figure 1.181: Eccentric compression of a straight beam with a thin-walled cross section. (Ref: Emeritus J. Aalto)

the same methodology as before and varying the total potential energy increment, one obtains³⁵⁴ the linearised homogeneous equilibrium equations of stability (loss) as

$$EI_z v^{(4)} + P [v'' + (z_s - e_z)\phi''] = 0, \tag{1.1006}$$

$$EI_y w^{(4)} + P [w'' - (y_s - e_y)\phi''] = 0, \tag{1.1007}$$

$$EI_\omega \phi^{(4)} - GI_t \phi'' + P [(z_s - e_z)v'' - (y_s - e_y)w'' + \gamma\phi''] = 0, \tag{1.1008}$$

where the axial internal pre-stress resultant $N_x^0 = -P$, ($P > 0$). In the above equations, the geometric factors of the cross-section are defined below:

$$r^2 = \frac{I_y + I_z}{A} + y_s^2 + z_s^2, \tag{1.1009}$$

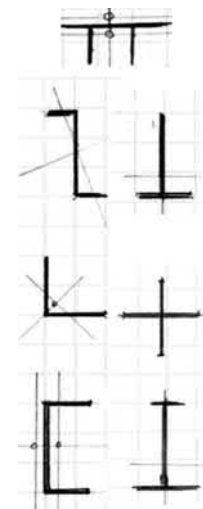
$$\beta_y = \frac{1}{2I_z} \int_A y(y^2 + z^2)dA - y_s, \tag{1.1010}$$

$$\beta_z = \frac{1}{2I_y} \int_A z(y^2 + z^2)dA - z_s, \tag{1.1011}$$

$$\gamma = (r^2 + 2\beta_y e_y + 2\beta_z e_z). \tag{1.1012}$$

In the following, we consider simplifications of the above equations rising from symmetries of the cross-section and the loading.

³⁵⁴I will, naturally present the full steps of deriving the equations, later with time.



Some types of thin-walled cross-sections that may buckle in torsional or combined flexural-torsional mode.

Singly symmetric cross-section

The equations simplify when the loading acts in the plane of symmetry: $z_s = 0$, $e_z = 0$, $\beta_z = 0$ (Figure margin)

$$EI_z v^{(4)} + P v'' = 0, \tag{1.1013}$$

$$EI_y w^{(4)} + P [w'' - (y_s - e_y)\phi''] = 0, \tag{1.1014}$$

$$EI_\omega \phi^{(4)} - GI_t \phi'' + P [-(y_s - e_y)w'' + (r^2 + 2\beta_y e_y)\phi''] = 0, \tag{1.1015}$$

Pure torsional buckling

Pure torsional under a vertical load. This case is much simpler than the previous one.

Consider a thin-walled beam where only a compressive centric load P or uniform axial stress is present. There can be cases, when the beam can buckle only in a torsional way while the longitudinal axis remains straight. For instance, this is may be case when torsional rigidity is enough weaker than flexural rigidities or the flexural buckling mode is simply mechanically restraint laterally.

To understand this phenomena, called *pure torsional buckling*, let's consider a doubly symmetric section such that the centre of mass (C) and the rotation centre or equivalently the shear center (S) coincide. Make it simple enough and assume a cruciform section with four identical flanges (Figure in margin). This case is a classical one treated by Timoshenko in his not less classical textbook on Elastic Stability.

In this case, for a critical value of the thrust force, each flange globally³⁵⁵ buckles and rotate about the axial axis which remains straight. The overall motion of the flanges is a rotating since they are bonded together.

As seen previously, the pure torsional buckling will be driven by the following equation

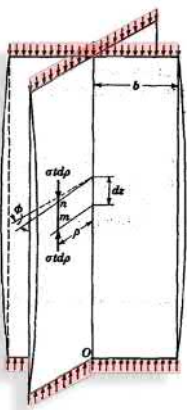
$$EI_\omega \phi^{(4)} + (Pr^2 - GI_t)\phi'' = 0, \tag{1.1016}$$

$$\phi^{(4)} + \underbrace{\frac{Pr^2 - GI_t}{EI_\omega}}_{k^2} \phi'' = 0, \tag{1.1017}$$

$$\phi^{(4)} + k^2 \phi'' = 0. \tag{1.1018}$$

The buckling load for the pure torsional mode is

³⁵⁵local buckling of flanges should be treated separately. Recall that we use the Vlasov kinematics of rigid body rotation of the orthogonal projection of the cross-sections. Thus, transversal stiffeners should be used to minimise the cross-section distortions, otherwise distorsional buckling (local buckling) should be considered (Figure in margin).



Pure torsional buckling (Ref. Timoshenko)



Pure torsional buckling of an X-beam. $\sigma_{cr} = 60.2$ MPa. (End-load is thrust force and clamped on the other end.)

$$P_{cr} = \frac{1}{r^2} \left[\frac{\pi^2 EI_\omega}{L_\phi^2} + GI_t \right], \quad (1.1019)$$

where the buckling length L_ϕ^2 should be determined according to the boundary conditions. This last result will be also derived in details. Note that the general solution for stability equation (1.1018) giving the buckling load for stability loss in pure torsion is analogous to the general solution for Euler buckling of a beam-column where $v \rightarrow \phi$. So,

$$\phi(x) = A + Bx + C \sin kx + D \cos kx, \quad \text{where } k^2 = (Pr^2 - GI_t)/EI_\omega. \quad (1.1020)$$

Centric load with doubly symmetric X-section

Pure torsional buckling: A column of $\ell = 1$ m length is loaded by a centric load P at one end. The other end is clamped. The material is aluminium with $E = 70$ GPa and $\nu = 0.33$. The thickness is 1 cm and the webs are $b = 5$ cm large, each.

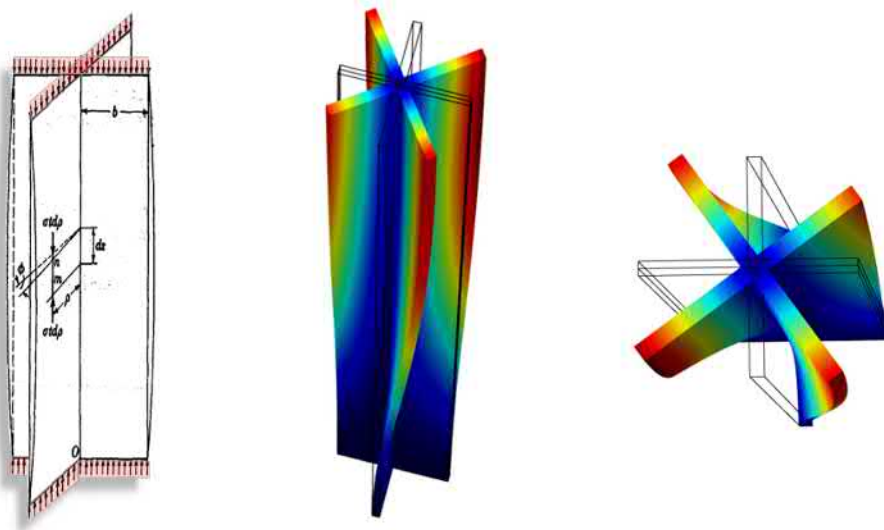


Figure 1.182: Pure torsional buckling. Computational linear buckling analysis. *right:* an illustrative example from Timoshenko book of elastic stability. *left:* Computation; pure-torsional buckling of loaded 1 m long column with doubly symmetric thin-walled X- cross-section. The thrust load P is centric and applied at the centre of mass C of the top-end. The lower end is clamped. The obtained $P_{cr} = 602$ kN.

* * *

When solving buckling load for both flexural and pure torsional modes, one find out, for instance for the X-profile that the pure torsional buckling load $P_{\phi,E}$ is independent of length of the column. Determining the missing two flexural buckling loads (Euler buckling) will provided $P_{v,E}$ and $P_{w,E}$ (recall that buckling loads are defined as the smallest critical ones). Drawing this result on a curve as a function of the length of the colm, one obtains the buckling resistance of the column (Figure 1.183).

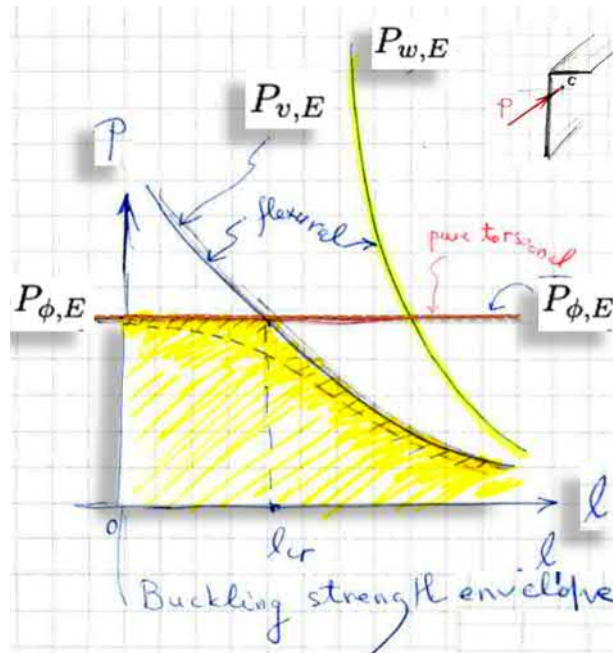


Figure 1.183: The buckling envelope (yellow) for pure torsional and flexural buckling.

* * *

Doubly symmetric cross-section & centric thrust

The equations simplify when the loading acts in the plane of symmetries and no-eccentricities $y_s = z_s = 0$, $e_y = e_z = 0$, $\beta_y = \beta_z = 0$ (Figure margin)

$$EI_z v^{(4)} + P v'' = 0, \quad (1.1021)$$

$$EI_y w^{(4)} + P w'' = 0, \quad (1.1022)$$

$$EI_\omega \phi^{(4)} - GI_t \phi'' + P r^2 \phi'' = 0. \quad (1.1023)$$

We note that now, the flexural and the torsional buckling are decoupled. The two first equations describe the Euler's flexural buckling and the last one is called *pure torsional buckling*. The smallest critical value of P is the buckling load.

The critical loads can be solved separately³⁵⁶ for pure flexural and pure torsional buckling and denote them by (decoupled modes)

$$\begin{cases} P_{cr,v} = \pi^2 EI_z / L_v^2, \\ P_{cr,w} = \pi^2 EI_y / L_w^2, \\ P_{cr,\phi} = \frac{1}{r^2} [\pi^2 EI_\omega / L_\phi^2 + GI_t] \end{cases} \quad (1.1024)$$

where, the respective buckling length are L_v^2 , L_w^2 and L_ϕ^2 depending on specific boundary conditions.

Centric loading of beams having symmetric cross-section

The cross section can be simply or doubly symmetric. Here, for generality, it is assumed singly symmetric and that the y, z -coordinate system coincides with the principal axes of inertia of the section. The stability equations for combined buckling (Equation 1.1008) for $e_y = e_z = 0$ are

$$EI_z v^{(4)} + Pv'' + Pz_s \phi'' = 0, \quad (1.1025)$$

$$EI_y w^{(4)} + Pw'' - y_s \phi'' = 0, \quad (1.1026)$$

$$EI_\omega \phi^{(4)} - GI_t \phi'' + Pz_s v'' - Py_s w'' + Pr^2 \phi'' = 0. \quad (1.1027)$$

should be solved with various boundary conditions. Recall the critical loads separately for pure flexural and torsional buckling

$$P_{cr,v} = \pi^2 EI_z / L_v^2, P_{cr,w} = \pi^2 EI_y / L_w^2, P_{cr,\phi} = \frac{1}{r^2} [\pi^2 EI_\omega / L_\phi^2 + GI_t], \quad (1.1028)$$

where, the respective buckling length are L_v^2 , L_w^2 and L_ϕ^2 depending on specific boundary conditions. We want to solve for special boundary condition setting where all the buckling lengths are equal to L_n .

Following the standard procedure for finding the critical load $P = P_{cr}$ for combined torsional-flexural buckling, one write the general solution of the fourth order differential equation with constant coefficients as

$$\begin{cases} v(x) = A_1 + B_1 x + C_1 \sin[\pi/L_n(x - x_0)], \\ w(x) = A_2 + B_2 x + C_2 \sin[\pi/L_n(x - x_0)], \\ \phi(x) = A_3 + B_3 x + C_3 \sin[\pi/L_n(x - x_0)]. \end{cases} \quad (1.1029)$$

³⁵⁶Their solutions are all three analogous as in the classical Euler buckling with general solution $v(x) = A + Bx + C \sin(kx) + D \cos(kx)$, where $k^2 = P/EI$ and accounting for the boundary conditions. One comes up with a homogeneous system of equation. Finally, the criticality condition (existence of non-trivial solution) provides the critical load P_{cr} . Note that the general solution can be also written as $v(x) = A_1 + B_1 x + C_1 \sin(kx + \phi_0)$ where we have a phase shift ϕ_0 .

Requiring that this trial solutions fulfil the differential equations above one obtains

$$\begin{bmatrix} P_{cr,v} - P & 0 & -z_s P \\ 0 & P_{cr,w} - P & y_s P \\ -z_s P & P y_s & r^2(P_{cr,\phi} - P) \end{bmatrix} \begin{bmatrix} C_1 \\ C_2 \\ C_3 \end{bmatrix} = \begin{bmatrix} 0 \\ 0 \\ 0 \end{bmatrix}. \quad (1.1030)$$

Existence of non-trivial solutions leads to require that the determinant of the coefficient matrix vanishes, *i.e.*,

$$\det \begin{bmatrix} P_{cr,v} - P & 0 & -z_s P \\ 0 & P_{cr,w} - P & y_s P \\ -z_s P & P y_s & r^2(P_{cr,\phi} - P) \end{bmatrix} = \begin{bmatrix} 0 \\ 0 \\ 0 \end{bmatrix} \quad (1.1031)$$

The above eigenvalue problem can be written in a standard general eigenvalue problem form

$$\mathbf{A} - P \mathbf{B} = \mathbf{0}, \quad (1.1032)$$

that can be easily solved by symbolically or numerically by computer algebra like for instance, `Matlab` function `eig`³⁵⁷. The matrices

$$\mathbf{A} = \begin{bmatrix} P_{cr,v} & 0 & 0 \\ 0 & P_{cr,w} & 0 \\ 0 & 0 & r^2 P_{cr,\phi} \end{bmatrix} \quad (1.1033)$$

and

$$\mathbf{B} = \begin{bmatrix} 1 & 0 & z_s \\ 0 & 1 & -y_s \\ z_s & -y_s & r^2 \end{bmatrix}. \quad (1.1034)$$

Notez bien: Thanks to the questions by your classmate *S. Katharina*, I noticed that the above matrices should be expressed with more consistence in physical units. After dividing the third homogeneous equation in (1.1030) by $r \neq 0$ and using $r \cdot C_3$ as a new third constant, we obtain an eigenvalue problem having *consistency in physical units* (the coefficient matrix is in Newtons), so now

$$\begin{bmatrix} P_{cr,v} - P & 0 & -z_s/r \cdot P \\ 0 & P_{cr,w} - P & y_s/r \cdot P \\ -z_s/r \cdot P & P \cdot y_s/r & (P_{cr,\phi} - P) \end{bmatrix} \begin{bmatrix} C_1 \\ C_2 \\ r \cdot C_3 \end{bmatrix} = \begin{bmatrix} 0 \\ 0 \\ 0 \end{bmatrix}. \quad (1.1035)$$

So, we can rewrite the above matrices of the eigenvalue problem as follow:

$$\mathbf{A} = \begin{bmatrix} P_{cr,v} & 0 & 0 \\ 0 & P_{cr,w} & 0 \\ 0 & 0 & P_{cr,\phi} \end{bmatrix} \quad (1.1036)$$

³⁵⁷ `[C, P] = eig(A, B)`

and

$$\mathbf{B} = \begin{bmatrix} 1 & 0 & z_s/r \\ 0 & 1 & -y_s/r \\ z_s/r & -y_s/r & 1 \end{bmatrix}. \quad (1.1037)$$

Use the above matrices, they are beautiful with homogeneous physical units. One can even chose a reference *buckling load*, let's say $P_{cr,ref}$ and rewrite the matrix \mathbf{A} as follow:

$$\mathbf{A} = \begin{bmatrix} P_{cr,v}/P_{cr,ref} & 0 & 0 \\ 0 & P_{cr,w}/P_{cr,ref} & 0 \\ 0 & 0 & P_{cr,\phi}/P_{cr,ref} \end{bmatrix} \quad (1.1038)$$

or in other words

$$\mathbf{A} = P_{cr,ref} \cdot \begin{bmatrix} \lambda_w & 0 & 0 \\ 0 & \lambda_w & 0 \\ 0 & 0 & \lambda_\phi \end{bmatrix} \quad (1.1039)$$

where the ratios $\lambda_v = P_{cr,v}/P_{cr,ref}$, $\lambda_w = P_{cr,w}/P_{cr,ref}$ and $\lambda_\phi = P_{cr,\phi}/P_{cr,ref}$ are dimensionless.

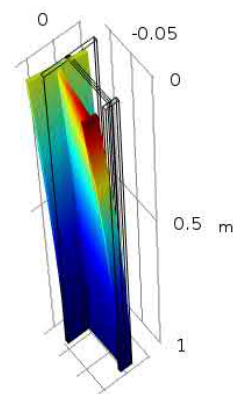
Numerical example - centric load column with singly symmetric T-section

Let's illustrate the eigenvalue problem (Eq. 1.1032) above with an application and solve for the critical load (Figure 1.184). Here are the geometry-data: length of the column is $\ell = 10a$, $G = 0.4E$, $t = a/15$. The centre of gravity (of area) of the cross-section is C . The thrust load P is centric and applied at centroid C of the cross-section.

Analytical solution

The idea is to solve the buckling load from the criticality condition given by the stability equation (1.1032). For that we need some geometrical parameters of the cross-section to determine the needed pure buckling critical loads P_v , P_w and P_ϕ to form the coefficient matrix in the criticality condition given by Equation (1.1032).

Recall that we use the principle coordinate system³⁵⁸ coincides with the principle axes of inertia of the cross-section (or principal centroidal axes) (Figure 1.184). Let's start with the geometrical parameters of the cross section as, for instance, location of the mass center (C) and of the shear center (S) or equivalently of the rotation center, etc. which are just listed below, since they belong



Combined flexural-torsional buckling of a cantilever-column loaded at its cross-section centroid (FE-Linear Buckling Analysis.)

³⁵⁸Pääjähyykskoordinaatisto (po finska).

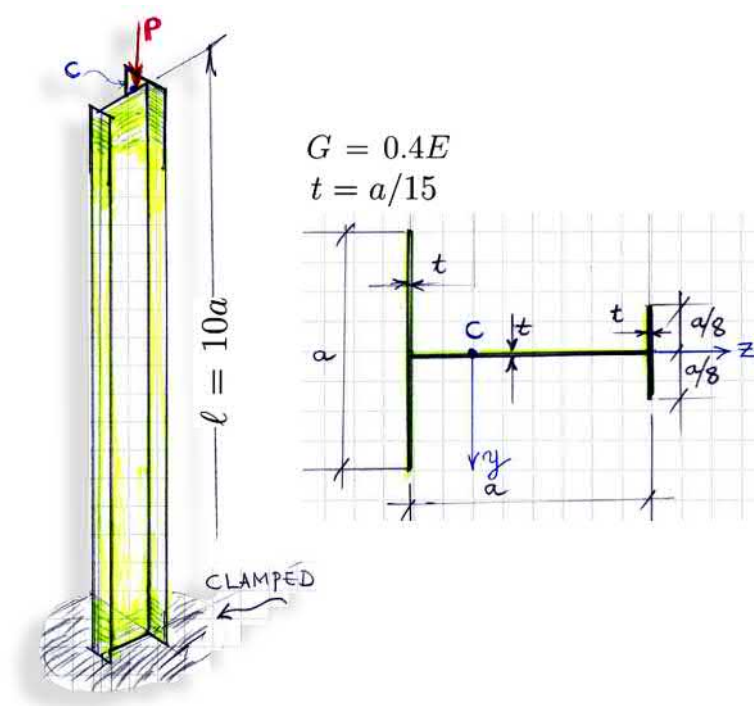


Figure 1.184: Flexural-torsional buckling of centrally loaded column with simply symmetric thin-walled cross-section. The thrust load P is centric and applied at the centre of mass C .

to basics.

$$e_c = 2/3a, \quad (1.1040)$$

$$e_s = 64/65a, \quad (1.1041)$$

$$z_s = -62/195a = -0.318a \quad (1.1042)$$

$$y_s = 0 \quad (1.1043)$$

$$I_z = 13/2304a^4 = 5.642 \times 10^{-3}a^4, \quad (1.1044)$$

$$I_y = a^4/45 = 2.222 \times 10^{-2}a^4, \quad (1.1045)$$

$$I_t = a^4/4500 = 2.222 \times 10^{-4}a^4 (= I_y/100), \quad (1.1046)$$

$$I_w = a^6/11700 = 8.570 \times 10^{-5}a^6, \quad (1.1047)$$

$$r^2 = (I_y + I_z)/A + y_s^2 + z_s^2 = 0.287a^2, \quad (1.1048)$$

$$L_n = L_v = L_\phi = L_w = 2\ell = 20a. \quad (1.1049)$$

The buckling loads in pure flexural and torsional modes are given by equation

(1.1028) as

$$\begin{cases} P_{cr,v} = \pi^2 EI_z / L_v^2 & = 1.392 \times 10^{-4} Ea^2, \\ P_{cr,w} = \pi^2 EI_y / L_w^2 & = 5.483 \times 10^{-4} Ea^2, \\ P_{cr,\phi} = [\pi^2 EI_\omega / L_\phi^2 + GI_t] / r^2 & = 3.217 \times 10^{-4} Ea^2, \end{cases} \quad (1.1050)$$

```

36 % Rigidities ----
37 EI_z = E * I_z;
38 EI_y = E * I_y;
39 EI_omega = E * I_omega;
40 GI_t = G * I_t;
41 -----
42 % Pure flexural and torsional buckling loads
43 -----
44 P_v = pi^2 * EI_z / (L_v^2)
45 P_w = pi^2 * EI_y / (L_w^2)
46 P_phi = ( pi^2 * EI_omega / (L_phi^2) + GI_t ) / r2
47 -----
48 % Eigen-value problem
49 -----
50 A = [P_v 0 0
51      0 P_w 0
52      0 0 r2*P_phi]
53 -----
54 B = [1 0 z_s
55      0 1 -y_s
56      z_s -y_s r2]
57 -----
58 % Solving the three critical forces
59 [C, P] = eig(A, B); % C- the constants
60 % the critical loads := Ps = diag(P)
61 Ps = diag(P)
62 P_cr = min(Ps) % THE BUCKLING LOAD
63 -----

```

Figure 1.185: Matlab code.

Now we come back to our problem. The critical buckling can be a combined mode. In order to find out, we go to the criticality condition in its canonical form $[C, P] = \text{eig}(A, B)$, where P being the three eigenvalues (or critical loads) and the matrices are (Figure 1.185)

$$\mathbf{A} = \begin{bmatrix} P_{cr,v} & 0 & 0 \\ 0 & P_{cr,w} & 0 \\ 0 & 0 & r^2 P_{cr,\phi} \end{bmatrix} = 10^{-3} \begin{bmatrix} 0.139 & 0 & 0 \\ 0 & 0.548 & 0 \\ 0 & 0 & 0.091 \end{bmatrix} \cdot Ea^2 \quad (1.1051)$$

and

$$\mathbf{B} = \begin{bmatrix} 1 & 0 & z_s \\ 0 & 1 & -y_s \\ z_s & -y_s & r^2 \end{bmatrix} = \begin{bmatrix} 1 & 0 & -0.318a \\ 0 & 1 & 0 \\ -0.318a & 0 & 0.287a^2 \end{bmatrix}. \quad (1.1052)$$

Programming the problem³⁵⁹ in MATLAB leads to $[C, P] = \text{eig}(A, B)$ and the

³⁵⁹the characteristic polynomial of the determinant is a third order polynomial which can be solved analytically by **Cardano's** formula to find all the three roots. Historically, it is known that **Tartaglia** contributed to the formula.

buckling load will be $P_{cr} = \min(\mathbb{P})$. The result is

$$= 10^{-4} \begin{bmatrix} 1.158 \\ 5.483 \\ 5.886 \end{bmatrix} \cdot Ea^2, \quad (1.1053)$$

where the smallest critical load

$$\boxed{P_{cr} = 1.158 \times 10^{-4} Ea^2} \quad (1.1054)$$

being the buckling load. Let's now compare, further, to the value obtained by computational analysis which is $P_{cr} = 75$ kN (Analysis done in next subsection). For $E = 70$ GPa and $a = 10$ cm, one obtains $P_{cr} = 86$ kN from the analytical solution above. We will analyse this small difference in next subsection.

Computational linear buckling analysis

Singly-symmetric cross-section: The problem presented previously is now analysed using Finite Element Method.³⁶⁰

Let's come back to the results of such numerical simulation presented in Figure (1.186). We note from the figure that the buckling occurs in a combined flexural-torsional which corresponds to the first buckling mode. Notice the bending mode of the flange (Figure 1.186) seen as a departure from the straight initial shape shown by white dot-line. This deformation mode is not accounted for in the Vlasov beam-theory used in this course. The obtained $P_{cr} = 75$ kN. The 1-D beam model gives $P_{cr} = 11.6 \cdot 10^{-3} Ea^2 = 81$ kN. The deformation modes of the

³⁶⁰**Think 1-D versus 3D:** A full three-dimensional problem was done to compare the solution with the one given by the beam-theory of previous chapters. It is also a way to access the goodness of such one-dimensional models. Such 1-D models are very valuable as they provide as, the engineers, handles to structural design and to construct our understanding using meta-concepts emerging from the dimension reduction approach. To give an example of such meta-concept (or handle) let it be the bending and torsional rigidities EI_y , EI_z , GI_t and EI_ω , and the buckling lengths of such column which just *do not exist* in the corresponding 3D-conceptual model even that they are the major handles deciding the value of the buckling load that the column can take.

In 3-D we have only a set of material points $P_i(x, y, z)$, their coordinates and displacements u_i, v_i, w_i and the corresponding strains and stresses. That's all one can have. Even the thickness is not seen explicitly in such 3D-model. What I am saying! Even the column itself is not seen in 3D-world! The column is a meta-concept too rising from dimension reduction.

So what, you'll say! However, if the simple design question will be *how to change the geometry (cross-section and length)* in order to avoid buckling, then using the 3D-simulation alone will make the trials long and many to find one good solution since your *handles* are only the coordinates now. So, finally, gaining details through 3D-models (FEM) is not necessary synonym with gaining understanding. Understanding, conceptual, can rise only by moving to a meta-level through dimension reduction.

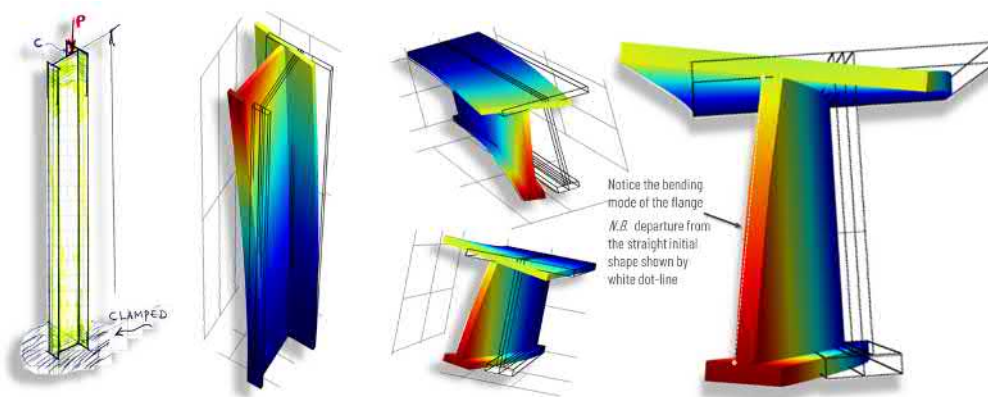


Figure 1.186: Computational linear buckling analysis (3D). Flexural-torsional buckling of axially loaded column at centroid. The cross-section is simply symmetric thin-walled T cross section. The thrust load P is centric and applied at the centre of mass C . The obtained $P_{cr} = 75$ kN.

1-D analytical model do not include the actual bending-mode shown in the figure for the flange. We say that the 1-D model is a bit *stiffer* than the full 3D-model and is one reason³⁶¹ why it provides a bit-higher buckling load value.

³⁶¹Recall the property of minimising of the smallest eigenvalue λ of the Rayleigh quotient: the true deformation mode (or displacements) makes the quotient minimum. One can think that 1-D displacement field is poorer approximation as compared to the 3-D approximation, when correctly done, of the displacement field and consequently, $\lambda_{1D} > \lambda_{3D} \geq \lambda_{\text{true}}$

1.16 Stability of plates

Literature shows that buckling of rectangular plates as a study starts with investigations by Bryan³⁶² where stability of ship plate portions under various loading conditions was investigated.

Many structures or structural elements have plate elements or substructures that under certain loading conditions can buckle. Here some examples of such common structures of civil and mechanical engineering practice

- flanges and webs of rolled or build-up beams & columns (Figure 1.187)
- hollow metallic bars (rectangular cross-sections)
- shear walls in buildings
- aircraft fuselage panels
- aircraft wings, rudder and wing panels

In the section, we consider buckling of thin plates with relative thickness $h/\ell \leq 1/10$. The mechanical models are known as the **Kirchhoff–Love** theory of plates³⁶³. Later, **von Kármán** extended it to deal with moderate rotations. Accounting for thick plates **Mindlin** and **Reissner** extended the classical theory of plates to account for shear deformation effects in thick plates³⁶⁴.

In this section, we treat buckling of plates. This topic is important in thin structures. Like for instance, metallic structural elements or structures made of thin tubes riveted or welded plates and thin plates made of other materials (concrete shells and plates from micro-fibres concrete or from composite or laminar composite layers or similarly). Such structures or structural parts can fail through damage or loss of stability (buckling).

In this section the stability aspect of plates is introduced: *a*) buckling load bifurcation type for a perfect geometry, and *b*) effects of imperfections. It will be shown that, for plates, the type of *bifurcation is symmetric-stable*. Consequently, the plane plate is *not so sensitive to imperfections* on the contrary for thin shells.

We derive the linearised homogeneous equations of (loss) of stability according to the energy criterion which yields

$$D\Delta\Delta w - N_{\alpha\beta}^0 w_{,\alpha\beta} = 0, \quad (1.1055)$$

$$D[w_{,xxxx} + 2w_{,xyxy} + w_{,yyyy}] - N_{xx}^0 w_{,xx} - 2N_{xy}^0 w_{,xy} - N_{yy}^0 w_{,yy} = 0. \quad (1.1056)$$

³⁶²H. Bryan, On stability of a Plane Plate under thrust in its own plane with applications to the buckling of sides of a ship. *Proceedings of the London Mathematical Society*, Vol. 22, nov-dec 1890-91, pp. 54-67.

³⁶³This is an extension of Euler-Bernoulli beam model.

³⁶⁴This is an extension of Timoshenko's beam model.

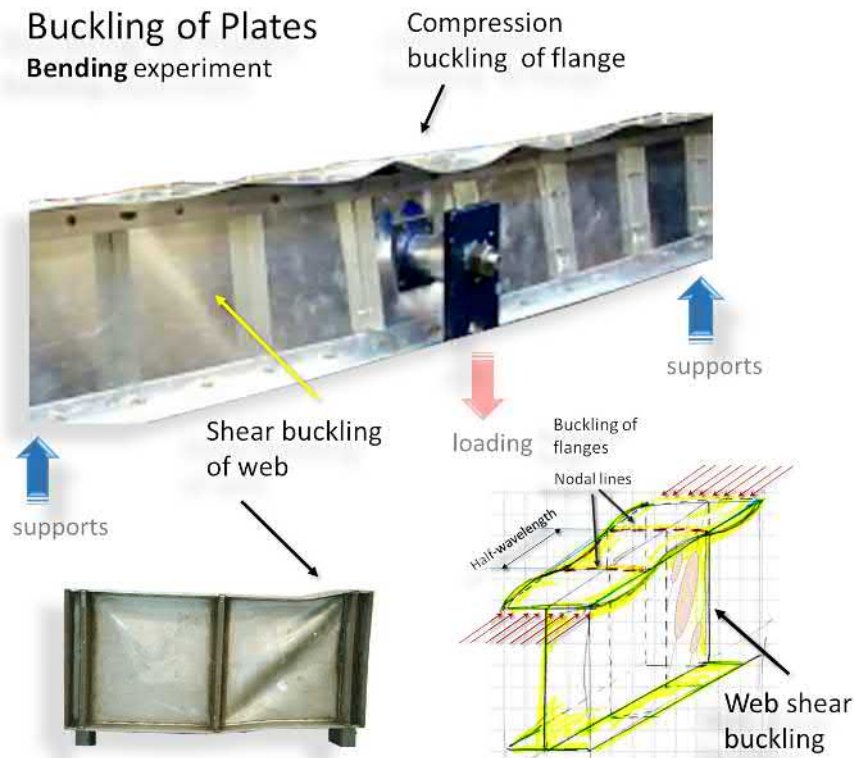
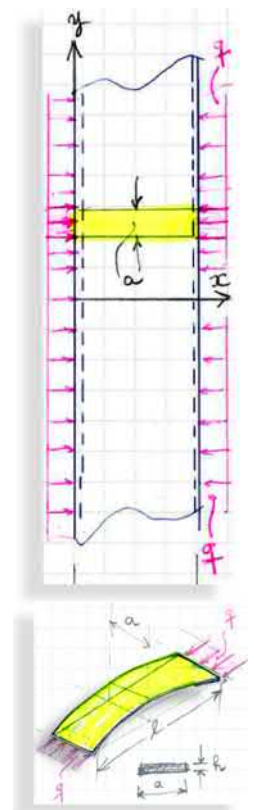


Figure 1.187: Plate buckling in structures.

As previously many time mentioned, let's recall that equation (1.1056) means that this post-buckled (bending) state, in the vicinity of the initial pre-buckled plane (membrane state) configuration, is an equilibrium state, too. The initial membrane stress-resultants $N_{\alpha\beta}^0 := [N_{xx}^0, N_{yy}^0, N_{xy}^0]$ satisfy the equilibrium equation in the pre-buckled plane state. Terms with repeated indices are summed according to Einstein summation convention. The operator Δ is the *Laplacian*³⁶⁵. In addition, it is assumed that there is no external surface membrane forces $p_x \equiv 0, p_y \equiv 0$ acting in the mid-plane of the plate. The membrane stress-resultants $N_{\alpha\beta} = \int_{-h/2}^{h/2} \sigma_{\alpha\beta} dz$, in [N/m]. Naturally, boundary conditions should be incorporated to the system.

Equations (1.1056) are already known to the reader in their version applied to the buckling of a column (Euler buckling) with axial compressive forces $P = a \cdot q$ and bending rigidity EI (Equation 1.1058). For the buckling of a unit width strip $a = 1$ [m] of an 'infinitely' long plate (Margin Figure) for which all derivatives

³⁶⁵In Finnish *Lappalaisen* operaattori.



Cylindrical-type Buckling of plate slab.

with respect to y vanishes one obtains

$$D \frac{d^4 w}{dx^4} + q \frac{d^2 w}{dx^2} = 0, \quad (1.1057)$$

$$EI \frac{d^4 w}{dx^4} + P \frac{d^2 w}{dx^2} = 0, \quad (1.1058)$$

where $EI = a \cdot D$, axial compressive forces $P = a \cdot q$ and the compressive edge forces being $N_{xx}^0 = -q$, $N_{yy}^0 = N_{xy}^0 = 0$. Note that the two equations above are analogous $EI \leftrightarrow D$ and $P \leftrightarrow a \cdot q$ and consequently, their solutions, too, are analogous.

Euler critical load for the simply supported column was $P_{cr} = \pi^2 EI / \ell^2$. Consider the elongated plate with simply supported long edges (Margin Figure). The critical load q_{cr} [N/m] will be analogously,

$$q_{cr} = \pi^2 D / \ell^2. \quad (1.1059)$$

Analysis of an Engineering formula

For that, we rewrite formula (Equation 1.1059) in terms of critical stresses and obtain

$$\sigma_{cr} = \frac{q_{cr}}{h} = \frac{\pi^2 D}{h \ell^2} = \frac{1}{h} \cdot \frac{\pi^2 E h^3}{12(1-\nu^2)\ell^2} = \quad (1.1060)$$

$$= \frac{\pi^2 E}{12(1-\nu^2)} \left[\frac{h}{\ell} \right]^2 \quad (1.1061)$$

$$= \frac{\pi^2 E}{(1-\nu^2)} \left[\frac{r}{\ell} \right]^2 \equiv \frac{\pi^2 E}{(1-\nu^2)\lambda^2}, \quad (1.1062)$$

where the gyration radius r for the plate slab of width a , being such that $r^2 = I/A = (ah^3/12) \times 1/(ah) = h^2/12$.

Equation (1.1062) emphasizes that critical compressive stresses $\sigma_{cr} \propto [h/\ell]^2$. In other words, the critical stresses decrease *quadratically* with the decrease of relative thickness of the plate. Consequently, thin plates can buckle under small compressive stress far below yielding stress. The factor $[h/\ell]^2$ represents some kind of slenderness effects of the plate as in columns. The slenderness now being $\lambda = \ell/r$.

Effects of boundary conditions

Usually, buckling stress formulas are presented as the buckling stress for some reference case multiplied by a *buckling coefficient* K accounting for different boundary conditions. A bit similar to buckling loads of columns having various boundary conditions. The Euler reference buckling load P_E (for a simply supported column) is multiplied by a coefficient μ accounting for various boundary conditions $P_{cr} = \mu P_E$.

Analogously, buckling stress formulas for plates will be, for instance, presented in form of Equation (1.1062) where the boundary conditions are accounted by a stability (or buckling)³⁶⁶ coefficient K , as

$$\sigma_{cr} = K \cdot \underbrace{\frac{\pi^2 E}{12(1-\nu^2)} \left[\frac{h}{\ell} \right]^2}_{\text{reference buckling stress}} \quad (1.1063)$$

where ℓ is some characteristic length of the plate. (*Cf.* $K \leftrightarrow \mu$). The buckling coefficient K depends on loading, boundary conditions and on the aspect ratio length to width $\alpha = a/b$ for rectangular plates. For design purpose, buckling coefficients K are tabulated or in form of nomograms for various cases in loading and boundary conditions.

How do I read Equation (1.1063)? For my plate under consideration, the buckling stress is K - times larger than the reference case for a simply supported unit strip. This reading, allows us to have a real understanding of the order of magnitudes of the actual critical stresses. The reference case can be compared to the reference case in Euler column buckling which corresponds to a simply supported column with end-load P and constant bending rigidity EI and of length ℓ and critical load

$$P_{cr} = \mu \cdot \underbrace{\frac{\pi^2 EI}{\ell^2}}_{\text{reference buckling load}} \implies \sigma_E = \frac{P_{cr}}{A} = \mu \pi^2 E \left[\frac{r}{\ell} \right]^2, \quad (1.1064)$$

where $r^2 = I/A$ and μ has analogous role as the buckling stress coefficient K .

An example basic buckling formula from SFS-EN-1993-1-5

The standard above addresses design of steel plated structural elements. Section 4 deals with buckling of rectangular plates. I reproduce here in the margin a snap-shot of a basic buckling formula from the standard just for pedagogical purposes to see the link between theory and practical design.

Deriving the equations of stability

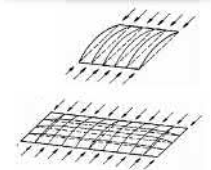
Energy criteria ... johdettu paperillasi ... $\delta(\Delta\Pi) = 0$ The kinematic of the mid-plane $w(x, y)$, $u(x, y)$, $v(x, y)$. The non-negligible increments during buckling are only $\Delta w(x, y) \equiv w$ and the change in membrane strain energy is ignored. We account only in the change in bending strain energy ΔU_B with linear deformation increments. Consider an isotropic elastic plate.

³⁶⁶Lommathduskerroin (sf).

4.5.3 Column type buckling

- (1) The elastic critical column should be taken as the buckling stress
- (2) For an unstiffened plate the

$$\sigma_{cr,c} = \frac{\pi^2 E t^2}{12(1-\nu^2) a^2}$$



Basic buckling formula for a column-like buckling mode taken from SFS-EN-1993-1-5 (section 4.5.3). Thickness is denoted t (*Cf.* Eq. (1.1062)).

Initial mid-plane kinematics, in the reference primary equilibrium state:

$$\begin{cases} u = u^0(x, y) \\ v = v^0(x, y) \\ w = w^0(x, y) \equiv 0 \end{cases} \quad (1.1065)$$

Mid-plane kinematics increments, in the post-buckled configuration:

$$\begin{cases} \Delta u = u - zw_{,x} \\ \Delta v = v - zw_{,y} \\ \Delta w = w \end{cases} \quad (1.1066)$$

Recall that at bifurcation or buckling of a beam-column, the centre-line does not change length (inextensible; $u_{,x}(x, y = 0) = 0$) for infinitesimal flexural change. Analogously, for a plate, the buckling is not accompanied with length change. Therefore, in Equation (1.1066) the derivatives of u and v will vanish (or ignored), for the mid-plane at buckling (Equation 1.1071). Therefore, only additional bending or change in curvature will contribute to the change into the strain energy at buckling.

Deformations ... (Tänne paperilla johdettua osuutta ...)

Recall that for the the case of buckling of a column in flexural mode (Euler buckling) we accounted for the change in the bending strain energy and for the additional work of initial stresses on the increment of the non-linear part of the conjugate strain

$$\Delta \Pi = \frac{1}{2} \int_0^\ell \underbrace{EI w_{,xx}^2}_{EI \kappa_x^2} dx + \int_0^\ell \underbrace{N_x^0 \left(\frac{1}{2} w_{,x}^2 \right)}_{\Delta W(\sigma_x^0, \Delta \epsilon_{x,NL})} dx \quad (1.1067)$$

This is just for info: (footnote) For the plate loaded only the boundary by surface external loading $N_{\alpha\beta}$ (edge-loads) we will do the same ... and have, analogously,

The initial membrane stress-resultants $N_{xx}^0, N_{yy}^0, N_{xy}^0$ satisfy the equilibrium equation in the pre-buckled plane state. No surface forces $p_x = p_y \equiv 0 \forall (x, y) \in \Omega$. nor transversal loads. Only boundary membranes tractions are acting on the edges of the plate.

The pre-stress resultants $N_{xx}^0, N_{yy}^0, N_{xy}^0$ will work, respectively, on the second-order³⁶⁷ components of the conjugate deformations

$$\epsilon_2 \equiv [\epsilon_{xx}^*, \epsilon_{yy}^*, \gamma_{xy}^* = 2\epsilon_{xy}^*]^T \quad (1.1068)$$

³⁶⁷Recall that second-order part $\epsilon_{ij}^* = 1/2 u_{k,i} u_{k,j}$, where $i, j = 1, 2, 3 (=x, y, z)$ and summation over index $k = 1 : 3$.

which are explicitly

$$\epsilon_{xx}^* = \frac{1}{2} \underbrace{[u_{,x}^2 + v_{,x}^2 + w_{,x}^2]}_{\approx 0 \ll w_{,x}^2} \approx \frac{1}{2} w_{,x}^2, \quad (1.1069)$$

$$\epsilon_{yy}^* = \frac{1}{2} \underbrace{[u_{,y}^2 + v_{,y}^2 + w_{,y}^2]}_{\approx 0} \approx \frac{1}{2} w_{,y}^2, \quad (1.1070)$$

$$\gamma_{xy}^* \equiv 2\epsilon_{xy}^* = \underbrace{u_{,x}u_{,y} + v_{,x}v_{,y}}_{\approx 0} + w_{,x}w_{,y} \approx w_{,x}w_{,y}. \quad (1.1071)$$

In the above, at buckling, the mid-plane becomes practically inextensible (incompressible) as during buckling of columns for the centre-line. This means that the derivatives of the mid-plane in-plane displacements are zero.

The variations³⁶⁸ of the second-order part of the strain increments are, consequently,

$$\delta\epsilon_{xx}^* = w_{,x}\delta(w_{,x}) = w_{,x}\delta w_{,x}, \quad (1.1072)$$

$$\delta\epsilon_{yy}^* = w_{,y}\delta(w_{,y}) = w_{,y}\delta w_{,y}, \quad (1.1073)$$

$$\delta\gamma_{xy}^* = w_{,y}\delta w_{,x} + w_{,x}\delta w_{,y}. \quad (1.1074)$$

Recall the Bryan form of the increment of the total potential energy in Bryan form (1.143)

$$\Delta\Pi = \underbrace{\frac{1}{2} \int_V \epsilon_1^T \mathbf{E} \epsilon_1 dV}_{\text{linear part of strain increments in } \Delta U} + \underbrace{\int_V \epsilon_2^T \sigma^0 dV}_{\text{quadratic part of strain increments in } \Delta W(\sigma^0)} \quad (1.1075)$$

where the total increment of deformation being

$$\epsilon = \underbrace{\epsilon_1}_{\text{Linear part}} + \underbrace{\epsilon_2}_{\text{quadratic part}} \quad (1.1076)$$

and \mathbf{u} being the increment of displacements.

³⁶⁸Recall that the variation and differentiation operators are interchangeable: $\delta(df/dx) = d(\delta f)/dx = \delta(f_{,x}) = (\delta f)_{,x}$.

For an isotropic³⁶⁹ plate, one obtains

$$\Delta U = \frac{1}{2} \int_V \sigma : \epsilon_1 dV = \frac{1}{2} \int_V \epsilon_1^T \mathbf{E} \epsilon_1 dV = \frac{1}{2} \int_A \vec{M} \cdot \vec{\kappa} dA \quad (1.1078)$$

$$= \frac{1}{2} D \int_A \left[w_{,xx}^2 + w_{,yy}^2 + 2\nu w_{,xx} w_{,yy} + 2(1-\nu) w_{,xy}^2 \right] dA \quad (1.1079)$$

being the change in strain energy³⁷⁰ where, the linear part of the strain increment at buckling are

$$\epsilon_1 = [\partial u / \partial x, \partial v / \partial y, \partial u / \partial y + \partial v / \partial x]^T \quad (1.1080)$$

$$= -z[w_{,xx}, w_{,yy}, w_{,xy} + w_{,yx}]^T \quad (1.1081)$$

$$= -z[\kappa_x, \kappa_y, 2\kappa_{xy}]^T, \quad (1.1082)$$

accordingly to Equation (1.1066) when assuming incompressibility of the mid-plane at buckling. The plane-strain assumption for the plate and linear elasticity gives the constitutive behaviour

$$\begin{bmatrix} \sigma_x \\ \sigma_y \\ \tau_{xy} \end{bmatrix} = \underbrace{\frac{E}{(1-2\nu)(1+\nu)}}_{\mathbf{E}} \begin{bmatrix} 1-\nu & \nu & 0 \\ \nu & 1-\nu & 0 \\ 0 & 0 & \frac{1-2\nu}{2} \end{bmatrix} \begin{bmatrix} \epsilon_x \\ \epsilon_y \\ \gamma_{xy} \end{bmatrix} \quad (1.1083)$$

The work increment of pre-stresses on the increment of second order part of strains being

$$\Delta W(\sigma_0, \Delta \epsilon_{NL}) = D \int_V \sigma^0 : \Delta \epsilon_{NL} dV = \quad (1.1084)$$

$$= \int_A \int_{-h/2}^{+h/2} \left[\sigma_{xx}^0 \epsilon_{xx}^* + \sigma_{yy}^0 \epsilon_{yy}^* + \tau_{xy}^0 \epsilon_{xy}^* + \tau_{yx}^0 \epsilon_{yx}^* \right] dz dA \quad (1.1085)$$

$$= \int_A \int_{-h/2}^{+h/2} \left[\sigma_{xx}^0 \epsilon_{xx}^* + \sigma_{yy}^0 \epsilon_{yy}^* + \tau_{xy}^0 \gamma_{xy}^* \right] dz dA \quad (1.1086)$$

$$= \int_A \left[N_{xx}^0 \frac{1}{2} w_{,x}^2 + N_{yy}^0 \frac{1}{2} w_{,y}^2 + N_{xy}^0 w_{,x} w_{,y} \right] dA \quad (1.1087)$$

³⁶⁹For an orthotropic plate, one will have,

$$\Delta U = \frac{1}{2} \int_A \left[D_x \kappa_x^2 + 2D_{xy} \kappa_x \kappa_y + D_y \kappa_y^2 + 4D_s \kappa_{xy}^2 \right] dA, \quad (1.1077)$$

where, bending and torsional rigidities being $D_x = E_x / (1 - \nu_x \nu_y) h^3 / 12$ and $D_y = E_y / (1 - \nu_x \nu_y) h^3 / 12$ are the unit flexural rigidities around x - and y - axes. Torsional unit rigidity $D_{xy} = E_x \nu_y / (1 - \nu_x \nu_y) h^3 / 12$, $D_{yx} = E_y \nu_x / (1 - \nu_x \nu_y) h^3 / 12$ and $D_s = Gh^3 / 12$. Recall this when we, if we will have time, treat an example of the effect of stiffeners on buckling of plates.

³⁷⁰This change is dominantly due to flexural buckling mode at bifurcation.

The increment of total potential energy is now

$$\Delta\Pi = \frac{1}{2}D \int_A [w_{,xx}^2 + w_{,yy}^2 + 2\nu w_{,xx}w_{,yy} + 2(1-\nu)w_{,xy}^2] dA + \quad (1.1088)$$

$$+ \frac{1}{2} \int_A [N_{xx}^0 w_{,x}^2 + N_{yy}^0 w_{,y}^2 + 2N_{xy}^0 w_{,x}w_{,y}] dA \quad (1.1089)$$

Variation of the strain energy increment term will result in the classical part known for bending of plate (ignoring the boundary terms: they will give the mechanical boundary conditions)

$$\delta(\Delta U) = \int_A [w_{,xxxx} + 2w_{,xxyy} + w_{,yyyy}] \delta w dA \quad (1.1090)$$

Variation of increment of work of pre-stresses on the increment of deformations (ignoring boundary terms) will be

$$\delta(\Delta W) = -\frac{1}{D} \int_A [N_{xx}^0 w_{,xx} + N_{yy}^0 w_{,yy} + 2N_{xy}^0 w_{,xy}] \delta w dA \quad (1.1091)$$

In the above, it is accounted that the initial stresses satisfy the equilibrium equation in the pre-buckled state and that distributed membrane external forces $p_x = 0$ and $p_y = 0$.

Summa summarum, finally we obtain

$$\delta(\Delta\Pi) = \int_A D [w_{,xxxx} + 2w_{,xxyy} + w_{,yyyy}] \delta w + \quad (1.1092)$$

$$- [N_{xx}^0 w_{,xx} + N_{yy}^0 w_{,yy} + 2N_{xy}^0 w_{,xy}] \delta w dA = 0, \quad \forall \delta w \quad (1.1093)$$

leads to the stability loss equation:

$$D \underbrace{[w_{,xxxx} + 2w_{,xxyy} + w_{,yyyy}]}_{\Delta\Delta w} - \underbrace{[N_{xx}^0 w_{,xx} + N_{yy}^0 w_{,yy} + 2N_{xy}^0 w_{,xy}]}_{N_{\alpha\beta}^0 w_{,\alpha\beta}} = 0 \quad (1.1094)$$

Finally, one obtains the field equation for loss of stability (presented in the start of this section)

$$D\Delta\Delta w - N_{\alpha\beta}^0 w_{,\alpha\beta} = 0, \quad (x, y) \in S \times [-h/2, h/2], \quad (1.1095)$$

$$D\nabla^4 w - N_{\alpha\beta}^0 w_{,\alpha\beta} = 0, \quad (x, y) \in S \times [-h/2, h/2] \quad (1.1096)$$

where membrane stress resultant $N_{\alpha\beta}^0$ are thought solved and satisfy the governing equation of equilibrium in the pre-buckled state. Relevant boundary conditions (BCs) should be added to close the buckling problem.

Post-buckling behaviour

It is known that plates have a stable-symmetric bifurcation type. This makes it less sensitive to imperfections. After bifurcation, a stable close neighbourhood exists. Consequently, plates are not imperfection sensitive structures (Figure 1.188). It will be shown, in section dealing with thin shells, that, on the contrary, thin shells are imperfection-sensitive structures as a consequence of their unstable post-buckling behaviour after the bifurcation (snap-through like). In this section, I just recall some results for ideally plate and for plate with shape imperfections as a departure from the planar ideally flat geometry.

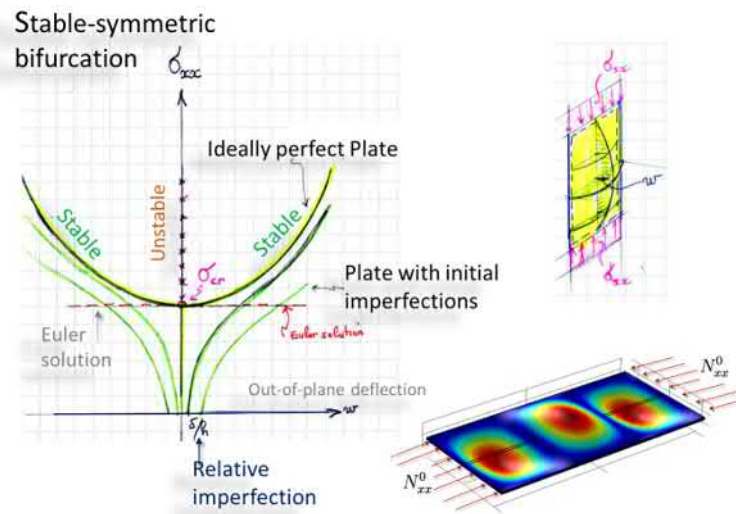


Figure 1.188: Post-buckling behaviour of thin elastic plate. Plate is not imperfection sensitive structure.

1.16.1 Some classical cases

As an illustration example, we consider a classical problem of plate buckling.

Buckling of a simply supported rectangular plate - on-side compression

Let's the two opposite edges be loaded by a compressive load $-N$ ($N > 0$) [N/m] and the two remaining edge, be load-free. The four edges are freely supported and the plate is free to move horizontally in the y -direction. Therefore, $N_{yy} = 0$ (the Poisson's expansion is free to occur in the y -direction) and thrust $N_{xx} = -N < 0$.

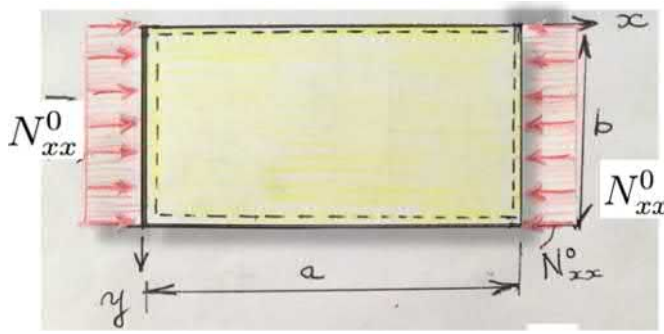


Figure 1.189: Buckling of simply supported thin plate.

The buckling of the plate is described by the eigenvalue problem below:

$$w_{,xxxx} + 2w_{,xxyy} + w_{,yyyy} = \frac{N_{xx}^0}{D} w_{,xx} \tag{1.1097}$$

where, the boundary conditions are now

$$w(0, y) = w(a, y) = 0, \quad w(x, 0) = w(x, b) = 0 \tag{1.1098}$$

$$M_x(0, y) = M_x(a, y) = 0, \quad M_y(x, 0) = M_y(x, b) = 0 \tag{1.1099}$$

It is known to you from your previous course on *thin Plates* that the classical double sine-series

$$w(x, y) = \sum_{m=1}^{\infty} \sum_{n=1}^{\infty} a_{mn} \sin \alpha_m x \sin \beta_n y \tag{1.1100}$$

where $\alpha_m = m\pi/a$ and $\beta_n = n\pi/b$, solve already the bending of such thin plate with the above boundary conditions. Let's take the above expansion as a trial solution with indeterminate non-trivial $a_{mn} \neq 0, \forall m, n$ coefficients. Inserting the trial solution into (1.1097) leads to

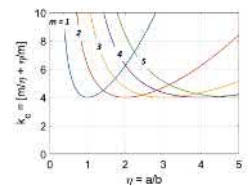
$$\sum_{m=1}^{\infty} \sum_{n=1}^{\infty} a_{mn} \underbrace{\left[\pi^4 \left(\frac{m^4}{a^4} + 2 \frac{m^2 n^2}{a^2 b^2} + \frac{n^4}{b^4} \right) + \frac{N_{xx}^0}{D} \pi^2 \frac{m^2}{a^2} \right]}_{=0, \forall m, n} \sin \alpha_m x \sin \beta_n y = 0. \tag{1.1101}$$

Consequently, the buckling occurs when

$$N_{cr} \equiv -N_{xx}^0 = D\pi^2 \frac{a^2}{m^2} \left(\frac{m^2}{a^2} + \frac{n^2}{b^2} \right)^2 \tag{1.1102}$$

$$= \frac{D\pi^2}{a^2} \underbrace{\left(m + \frac{n^2}{m} \left[\frac{a}{b} \right]^2 \right)^2}_K, \tag{1.1103}$$

$$= \frac{D\pi^2}{a^2} \left(m + \frac{1}{m} \left[\frac{a}{b} \right]^2 \right)^2, \quad (n = 1) \tag{1.1104}$$



Buckling coefficient for various aspect ratio (alin verhokäyvä).

where K being the buckling coefficient when comparing to the *reference cylindrical buckling stress* resultant of the thin plate discussed in the introductory example.

The smallest value of the thrust $N_{xx}^0(m, n; a/b, D)$ with respect to m and n corresponds to the buckling load. One should find m and n making $N_{xx} = N_{xx}(m, n)$ in Equation (1.1104) a smallest one, in amplitude. Clearly, for all values of a , b and m , the smallest value of the critical stress-resultant $N_{xx,cr}$ (the buckling) is achieved for $n = 1$.

Usually, formula (Equation 1.1104) for $a > b$ is represented, in literature, using b as characteristic length and not with the actual length a of the non-loaded edge (ℓ in Equation 1.1059) in the standard form

$$N_{cr} = \frac{D\pi^2}{a^2} \underbrace{\left(m + \frac{n^2}{m} \left[\frac{a}{b} \right]^2 \right)^2}_{K}, \quad (1.1105)$$

$$= \frac{D\pi^2}{b^2} \frac{b^2}{a^2} \underbrace{\left(m + \frac{n^2}{m} \left[\frac{a}{b} \right]^2 \right)^2}_{K_\sigma}, \quad (1.1106)$$

$$= \frac{D\pi^2}{b^2} \left(m \frac{b}{a} + \frac{n^2}{m} \frac{a}{b} \right)^2, \quad (1.1107)$$

$$= \frac{D\pi^2}{b^2} \underbrace{\left(\frac{m}{\eta} + \frac{n^2}{m} \eta \right)^2}_{K_\sigma}, \quad (1.1108)$$

$$= \frac{D\pi^2}{b^2} \underbrace{\left(\frac{m}{\eta} + \frac{\eta}{m} \right)^2}_{K_\sigma}, \quad (n = 1) \quad (1.1109)$$

where the buckling coefficient K_σ depend on the aspect ratio $\eta = a/b$ as shown in Figure (1.190).

Side note: When the we have $a < b$, usually, the characteristic length in the formula is changed to a . I hope that this notational aspects not mixing the readers. Just be careful when dealing with tables, graphs or formulas giving the stability coefficient: what is the used characteristic length? a or b ? To have an idea of the relative order of magnitudes, it is useful to compare buckling stresses (or stress resultants)

$$N_{cr} = K_\sigma \cdot \pi^2 D / b^2 = \underbrace{K_\sigma \left[\frac{a}{b} \right]^2}_K \cdot \underbrace{\pi^2 D / a^2}_{\text{ref. cylindrical buckling}} \quad (1.1110)$$

obtained for some specific case to the reference buckling stresses $N_{cr}^{\text{cylind.}} = K \cdot$

$\pi^2 D/a^2$ ($K = 1$ when simply supported, a being the loading direction) obtained for the cylindrical buckling of an infinite thin plate.

(In the following, I drop the initial-stress superscript for clear writing reasons.) Now remains to minimise with respect to m . Clearly, the ratio of the sides, $\eta = a/b$ will play a determinant role on buckling. The above expression for thrust ($-N_{xx} \equiv N > 0$) is now rewritten as (for $n = 1$)

$$N = D \frac{\pi^2}{b^2} \left(\frac{m}{\eta} + \frac{\eta}{m} \right)^2 \equiv K_\sigma D \frac{\pi^2}{b^2}. \tag{1.1111}$$

Stationary condition for a minimum $dN/d\eta = 0 \implies \eta = m$ gives, finally, the critical load as (for $m = \eta$)

$$|N_{xx,cr}| = 4 \frac{\pi^2 D}{b^2}. \tag{1.1112}$$

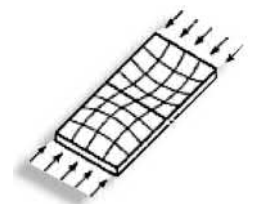
Note that the critical stress-resultant N_{xx} is four time larger than what was obtained previously for a very long plate in Equation (1.1059).

The minimum of critical load can be achieved even for $\eta = a/b$ not being an integer. In this case one can chose a closest integer for m . The absolute minimum is achieved for a set of discrete values of η (Figure 1.190). May be the cleanest way the find the minimum, for this case, is to do it graphically by inspecting the graph of the buckling coefficient $k_c = k_c(\eta; m)$ for $m = 1, 2, 3, \dots$ which is reproduced in (Figure 1.190). This graph can be already found in the classical textbook of Elastic Stability by Timoshenko.

$$k_c = \left(\frac{m}{\eta} + \frac{\eta}{m} \right)^2 \equiv K_\sigma \tag{1.1113}$$

Let's read the graphs of the Figure: ratio $a/b < \sqrt{2}$ first buckles with one half-wave ($m = 1$) and transition to two-half waves for $a/b = \sqrt{2}$. Next transition from two-half waves ($m = 2$) to $m = 3$ half-waves occurs for

$a/b = \sqrt{6}$ and so on. The first buckling mode as function of the ratio a/b is *quantised* as in quantum physics. The corresponding strain energies are also quantised. Note that, after a ratio of, approximately $a/b > 3$, the critical loads are quite close to each other as are also the corresponding modes. Some kind of mode accumulation occurs. This means that, the plate can buckle in any of the modes. Present tiny perturbation can have unexpected effects.

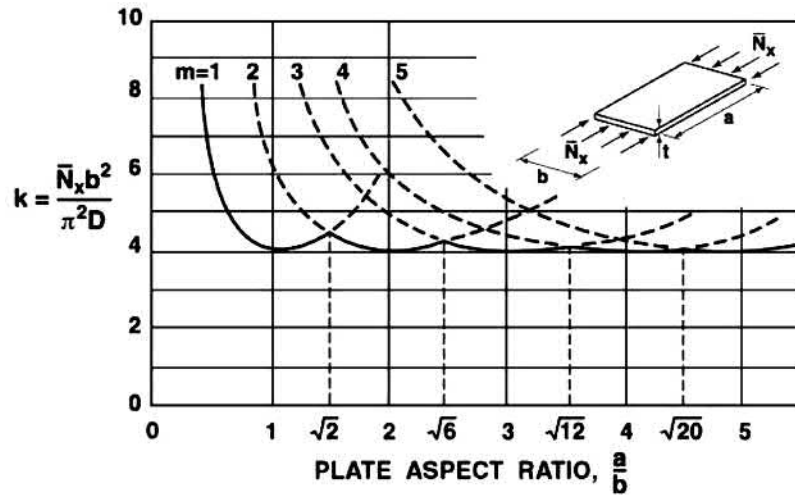


Buckling mode, $m = 2, n = 1$.

Buckling of a simply supported rectangular plate with constrained compression

Consider the plate in Figure (Fig. 1.189) where now the expansion in the orthogonal direction of the loading is fully restrained (Figure 1.191). Because of confinement, the reaction (compressive) in transverse direction will be simply

$$N_{yy}^0 = \nu N_{xx} \tag{1.1114}$$



Normalized buckling load k for simply supported rectangular plates with Various Plate Aspect Ratios

Figure 1.190: Buckling of thin simply supported plate. Buckling coefficient K . (Ref. Robert M. Jones. *Buckling of bars, plates and shells*. Bull Ridge Publishing, 2006.)

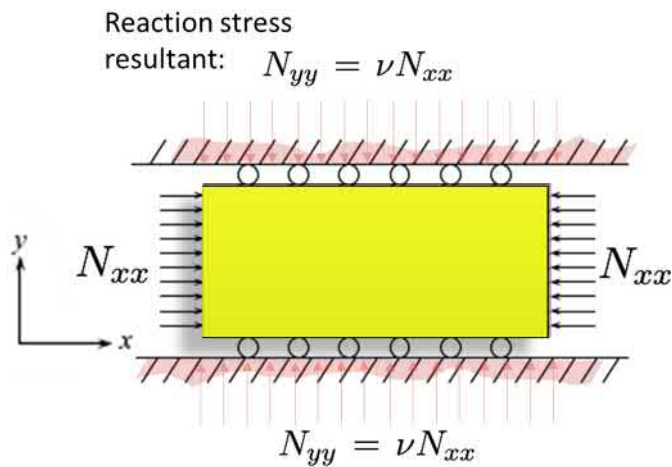


Figure 1.191: Buckling of thin simply supported plate with lateral confinement.

in addition to the original imposed mechanical edge compressive loading N_{xx}^0 . The buckling load will be analogously to Equation (1.1109) with the buckling

coefficient being now

$$K_\sigma = \frac{\left[\left[\frac{mb}{a} \right]^2 + n^2 \right]^2}{\left(\frac{mb}{a} \right)^2 + \nu n^2}. \tag{1.1115}$$

Note that the buckling coefficient is reduced. Now minimising³⁷¹ with respect to m and n one obtains $K_\sigma = 3$ for $a/b = 2$. So, the buckling stress (load) is reduced from $K_\sigma = 4$ for the laterally non-restrained case to 3 for the restrained case.

Buckling of a simply supported rectangular plate - in-plane bending and compression

Let's start by an engineering application having practical importance, especially in metallic constructions: a combined bending and axial compression of beams made from rolled or build-up structural sections. Consider the stress state of a thin web of an I-beam in combined combined compression and bending (Figure 1.192). This stress-state is a consequence of the bending and compression of a beam-column. Just insulate a free-body panel as shown in the figure b) and the stress-state described becomes an evidence. The effect of shear will be treated later. Shear stresses are dominant close to the supports with high shear forces.

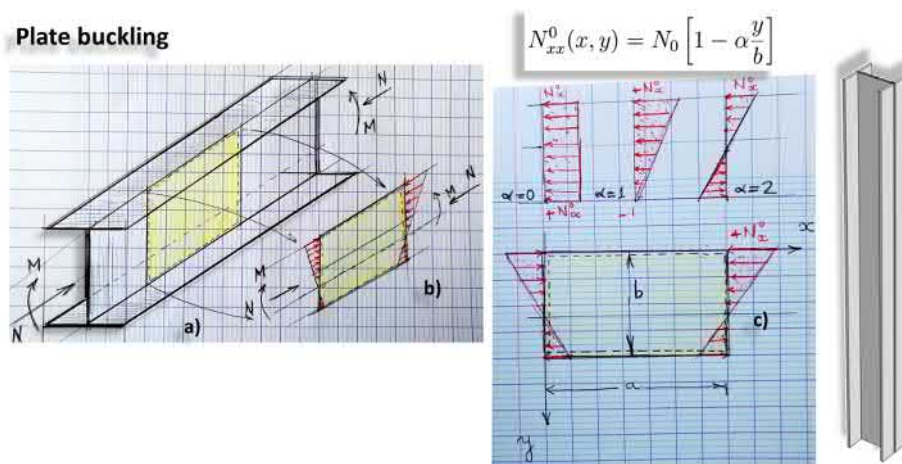


Figure 1.192: Buckling of a web plate section due to bending and compression of the beam-column.

Therefore, the problem consist of buckling problem of the plate depicted in Figure c subjected to combined in-plane axial compression and bending with

³⁷¹Just draw graphs for K_σ in function of m and n and find the smallest value.

initial stress resultant given by

$$N_{xx}^0(x, y) = N_0 \left[1 - \alpha \frac{y}{b} \right], \quad (1.1116)$$

where α is a dimensionless parameter. In this example $0 \leq \alpha \leq 2$ in order to keep superimposed compression³⁷². This problem can be found in Timoshenko's textbook. For $\alpha = 0$ one obtains a uniform compression of the opposite edges. Pure bending is recovered for $\alpha = 2$ (sub-figure *c*). A combined compression and bending occurs for value of α between 0 and 2. The remaining stress components $N_{yy}^0 = N_{xy}^0 = 0$.

For the boundary conditions, let's assume that the insulated panel (the plate of length a and height b) is simply supported at all four edges. *This is of course an approximation leading to a lower-bound for the critical buckling load.* The upper and lower edge-connections of the web-plate to the flanges correspond to those of rotational springs due to their rotational rigidity while the web buckles. This type of boundary condition is not impossible to address even theoretically. However, now we address the problem from a theoretical point of view and assume freely supported from four edges.

A general trial solution is of the type we've seen before: a double sine-series which fulfil the boundary conditions.

$$w(x, y) = \sum_{m=1}^{\infty} \sum_{n=1}^{\infty} a_{mn} \sin \alpha_m x \sin \beta_n y \quad (1.1117)$$

where $\alpha_m = m\pi/a$ and $\beta_n = n\pi/b$, solve already the bending of such thin plate with the above boundary conditions. Let's take the above expansion as a trial solution with indeterminate non-trivial $a_{mn} \neq 0, \forall m, n$ coefficients.

One way to solve for the critical load is to insert the trial solution into (1.1097). However, because of the non-constant in-plane stress-resultant N_{xx}^0 it comes out to be much easier to obtain a solution directly *via* the energetic method by applying the criterion in the form $\Delta\Pi = 0$.

The change in strain energy is simply

$$\Delta U = \frac{D}{2} \frac{ab\pi^4}{4} \sum_{m=1}^{\infty} \sum_{n=1}^{\infty} a_{mn}^2 \left(\frac{m^2}{a^2} + \frac{n^2}{b^2} \right)^2 \quad (1.1118)$$

and the increment of the work of initial stresses

$$\Delta W = \frac{1}{2} \int_0^a \int_0^b N_0 \left(1 - \alpha \frac{y}{b} \right) (w_{,x})^2 dx dy \quad (1.1119)$$

After performing careful integrations and using the criterion $\Delta\Pi = 0$ one obtains

³⁷²For $\alpha > 2$ we start having tension.

the critical load $N_{0,cr}(m, n)$ as³⁷³

$$N_{0,cr} = \frac{D}{2} \sum_{m=1}^{\infty} \sum_{n=1}^{\infty} a_{mn}^2 \left(\frac{m^2}{a^2} + \frac{n^2}{b^2} \right)^2 / \quad (1.1120)$$

$$\left\{ \sum_{m=1}^{\infty} \sum_{n=1}^{\infty} a_{mn}^2 \frac{m^2 \pi^2}{a^2} - \frac{\alpha}{2} \sum_{m=1}^{\infty} \frac{m^2 \pi^2}{a^2} \left[\sum_{n=1}^{\infty} a_{mn}^2 - \frac{32}{\pi^2} \sum_{n=1}^{\infty} \sum_i \frac{a_{mn} a_{mi} n i}{(n^2 - i^2)^2} \right] \right\}. \quad (1.1121)$$

In the above equation, the index i is such that $n \pm i$ is always an odd number. The buckling load will be obtained as the smallest value for $N_{cr}(m, n)$ by taking the derivatives of Equation (1.1121) with respect to each coefficient a_{mn} and equating them to zero. This way, the following set of linear equations is obtained

$$D a_{mn} \pi^4 \left(\frac{m^2}{a^2} + \frac{n^2}{b^2} \right)^2 = N_{0,cr} \left(a_{mn}^2 \frac{m^2 \pi^2}{a^2} - \frac{\alpha}{2} \frac{m^2 \pi^2}{a^2} \left[a_{mn}^2 - \frac{16}{\pi^2} \sum_i \frac{a_{mi} n i}{(n^2 - i^2)^2} \right] \right) \quad (1.1122)$$

This set of equations can be only solved approximately for each value of α and a/b by fixing the number of terms one takes into the series. Once this number being fixed, one obtains a homogeneous system of linear equations for the unknown coefficients a_{mn} . The criticality condition of this system (zero determinant) will provide the smallest critical value for N_{cr} or equivalently $\sigma_{cr} = N_{cr}/h$, where the thickness of the plate being h .

In the following an illustrative example of approximate solution for the above system within less than 1% or relative error in the buckling load by taking only three equations (Timoshenko). For instance, for $\alpha = 2$ (pure bending) and for a square plate ($a = b$), fixing $m = 1$ ³⁷⁴ which means only one half-wave in the corresponding x -direction, one gets

$$\underbrace{\begin{bmatrix} (1 + \frac{a^2}{b^2})^2 & -16\sigma_{cr} \frac{2}{9} \frac{a^2 h}{\pi^4 D} & 0 \\ -16\sigma_{cr} \cdot \frac{2}{9} \frac{a^2 h}{\pi^4 D} & (1 + 4\frac{a^2}{b^2})^2 & -16\sigma_{cr} \cdot \frac{6}{25} \frac{a^2 h}{\pi^4 D} \\ 0 & -16\sigma_{cr} \cdot \frac{6}{25} \frac{a^2 h}{\pi^4 D} & (1 + 9\frac{a^2}{b^2})^2 \end{bmatrix}}_{\det \mathbf{A}(\sigma_{cr})=0} \begin{bmatrix} a_{11} \\ a_{12} \\ a_{13} \end{bmatrix} = \begin{bmatrix} 0 \\ 0 \\ 0 \end{bmatrix}. \quad (1.1123)$$

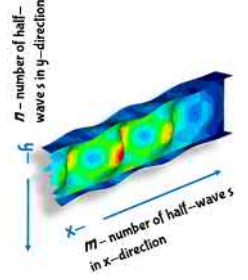
The first zero of the determinant provides

$$\sigma_{cr} = 25.6 \frac{\pi^2 D}{b^2 h}, \quad \text{for } a = b, \alpha = 2 \quad (1.1124)$$

which is which is 6,4 times higher value than for $\alpha = 0$ and $a = b$. Recall that we have obtained previously (for constant compression on one side only) the result $\sigma_{cr} = 4\pi^2 D/(b^2 h)$ (Figure 1.190).

³⁷³Timoshenko, *Theory of Elastic Stability*, 2nd Ed. p.375.

³⁷⁴ $m = 1$ corresponds to a buckling mode of the form $w = \sin \frac{m\pi x}{a} \sum_{n=1}^{\infty} a_{mn} \sin \frac{m\pi y}{b}$.



In general, the critical buckling stresses for various combined loading factor α and ratio a/b is expressed in the canonical form

$$\sigma_{cr} = k \frac{\pi^2 D}{b^2 h} = k \cdot \frac{\pi^2 E}{12(1-\nu^2)} \left[\frac{h}{b} \right]^2, \quad (1.1125)$$

where k being a factor accounting for various values of α and a/b according to Table (1.193) below: Similar tables than the above one (1.193) by Timoshenko

$\alpha \backslash a/b$	0.4	0.5	0.6	0.667	0.75	0.8	0.9	1.0	1.5
2	29.1	25.6	24.1	23.9	24.1	24.4	25.6	25.6	24.1
$\frac{4}{3}$	18.7	12.9	11.5	11.2	11.0	11.5
1	15.1	9.7	8.4	8.1	7.8	8.4
$\frac{2}{3}$	13.3	8.3	7.1	6.9	6.6	7.1
$\frac{1}{3}$	10.8	7.1	6.1	6.0	5.8	6.1

Figure 1.193: Buckling of simply supported thin plate in combined compression and bending. Numerical values for the buckling coefficient k in Equation (1.1125) in the $m = 1$ mode. (ref. Timoshenko & Gere).

are provided our-days for practical design in standards related to structural design of metallic structures. For instance, the standard *EN-1993-1-5, Table 6 (2006)*, provides similar buckling coefficients k tables for combined compression and bending of thin plates for various boundary and loading conditions.

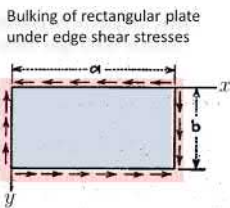
From the analysis and Figure (1.194) it can be seen that a long plate (in a - direction) buckles with half-waves of length approximately $2/3b$. Below the buckling coefficients are given for more cases of loading (Figure 1.195) from the old Finnish standard B7. The table is reproduced because of its clarity, practical analytical expressions for k and historical aspects.

Shear buckling of a rectangular plate

Assume a rectangular thin plate loaded by a shear stresses τ_{xy}^0 and τ_{yx}^0 along the four edges. The stress resultants in the initial state being N_{xy}^0 and N_{yx}^0 , respectively (Figure 1.196). The driving differential becomes

$$D\Delta\Delta w - 2N_{xy}^0 w_{,xy} = 0. \quad (1.1126)$$

The above partial differential equation (1.1126) seems simple to solve analytically. However, it came out that exact solution is available only for an infinitely long strip (Brush & Almroth (1975)). Approximative solutions with double sine-series for the deflection by energy approach gives poor results (Timoshenko &



Shear buckling.

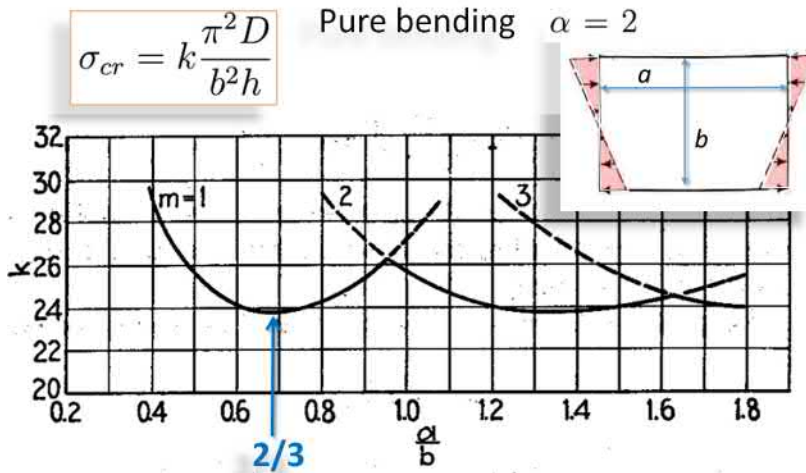


Figure 1.194: Buckling of simply supported thin rectangular plate in pure bending. (Ref. Timoshenko & Gere).

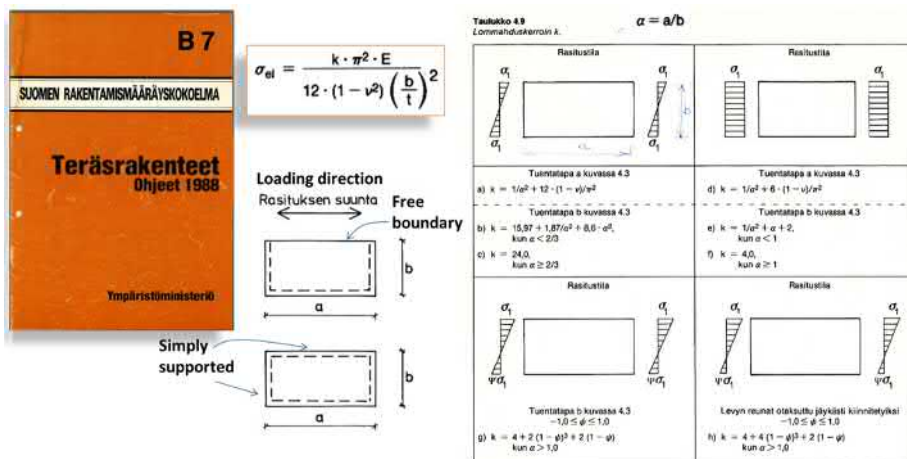


Figure 1.195: Buckling coefficients k of rectangular plate in combined compression and bending. (Ref. B7 - Suomemääräyskokoelma, ohjeet 1988)

Gere (1961)). A solution an infinitely long strip, was obtained by Southwell & Skan (1924), as

$$(N_{xy})_{cr} = k_s \frac{\pi^2 D}{b^2} \implies (\tau_{xy})_{cr} = k_s \cdot \frac{\pi^2 E}{12(1 - \nu^2)} \left[\frac{h}{b} \right]^2, \text{ where} \quad (1.1127)$$

$$\begin{cases} k_s = 5.34, & \text{simply supported} \\ k_s = 8.98, & \text{clamped support.} \end{cases} \quad (1.1128)$$

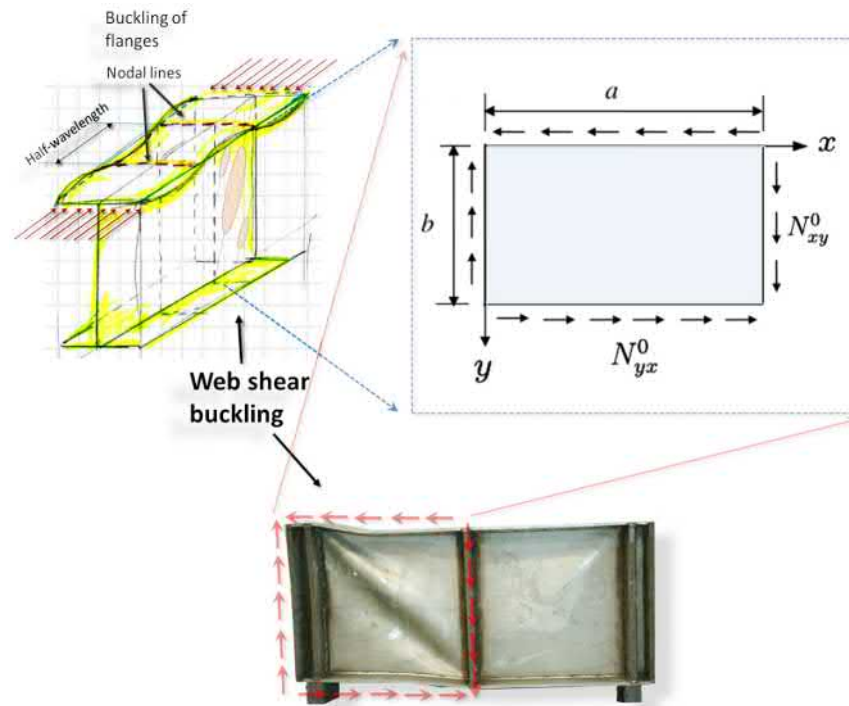


Figure 1.196: Shear buckling of rectangular plates under in-plane shear edge-loading.

For finite dimensions a and b and aspect ratio $\alpha = a/b$, solutions are available *via* computational buckling analysis from which, in Equation (1.1127), following empirical formulas for the shear buckling coefficient k_s are derived (Galambos³⁷⁵ (1998)):

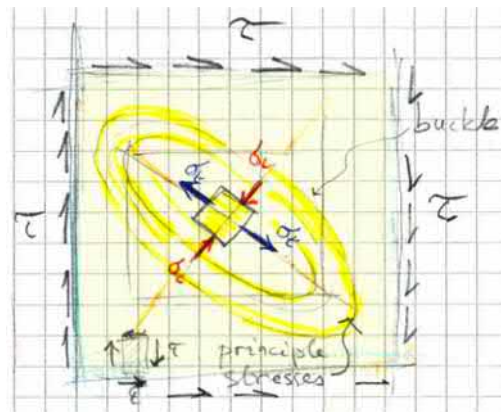
$$\begin{cases} k_s = 4.00 + 5.34/\alpha^2, & \text{for } \alpha \leq 1; \text{ four edges simply supported,} \\ k_s = 5.34 + 4.00/\alpha^2, & \text{for } \alpha \geq 1; \text{ four edges clamped.} \end{cases} \quad (1.1129)$$

For comparison how the above result is implemented in standard for structural design, refer to Figure (1.198) which is reproduced for showing the students the link of theory to practice. For remaining parameters in the formula, please refer to the standard.

1.16.2 Post-buckling response of plates

TO DO Asymptotic analysis ... this may be hard to do by hand. Let's simplify and use reduced model having only few degrees of freedom to be tractable by

³⁷⁵Galambos, T. V. (Ed.). 1998. *Guide to stability design criteria for metal structures*. New York: John & Sons.



Principle stresses under edge shearing:
tension weaken the buckling strength in
the orthogonal compressive direction

Figure 1.197: Principles stresses in Shear buckling of rectangular plates with in-plane shear edge-loading. Tension 'soften' the orthogonal direction against compression.

Standard – EN – 1993 – 1 – 5: 2006

A.3 Shear buckling coefficients

(1) For plates with rigid transverse stiffeners and without long longitudinal stiffeners, the shear buckling coefficient k_{τ} can be obtained

$$k_{\tau} = 5,34 + 4,00 (h_w / a)^2 + k_{\tau s\ell} \quad \text{when } a / h_w \geq 1$$

$$k_{\tau} = 4,00 + 5,34 (h_w / a)^2 + k_{\tau s\ell} \quad \text{when } a / h_w < 1$$

where $k_{\tau s\ell} = 9 \left(\frac{h_w}{a} \right)^2 \sqrt[4]{\left(\frac{I_{s\ell}}{t^3 h_w} \right)^3}$ but not less than $\frac{2,1}{t} \sqrt[3]{\frac{I_{s\ell}}{h_w}}$

Figure 1.198: Shear buckling coefficient k_s for rectangular plates under in-plane shear edge-loading as seen by the standard EN-1993-1-5 (2006).

hand and to capture major post-critical qualitative response, at least³⁷⁶.

So, assume thin plate modelled by a two-degrees of freedom model shown in Figure (XX). The thought-experiment is force controlled: we increase monotonically the edge load axial force P (the resultant of the stress resultant N_{xx}) and solve the displacement to obtain the load-displacement curve and this for pre-

³⁷⁶If I recall correctly the Lorentz (weather) model (Navier-Stokes equations) was simplified to have only three degrees of freedom X , Y and Z (Figure 1.199) to capture successfully the Rayleigh-Bénard convection dynamics (natural convection problem in a plane fluid motion).

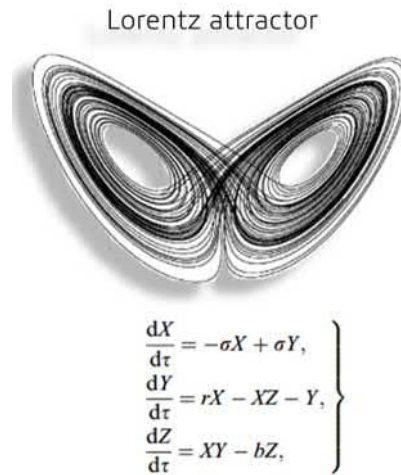


Figure 1.199: Lorenz attractor.

and post-buckling.

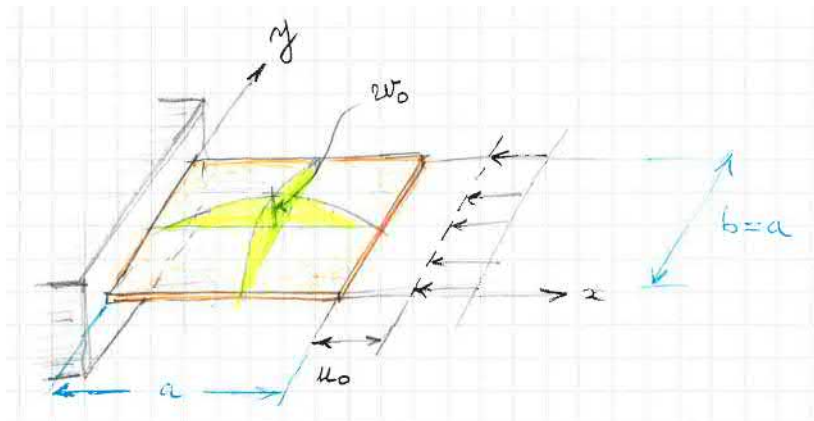


Figure 1.200: Plate axially loaded. The two-parameters model used for Post-buckling analysis.

The pre-buckled state ($w_0 = 0$) is compressive axial load $N_{xx}h = P$. The displacement u_0 is due to compression in the pre-buckled state. The displacement components (bi-axial deformation) in the pre-buckled state are simply

$$u = u_0 \left(1 - \frac{x}{a}\right) \quad (1.1130)$$

$$v = \nu u_0 \frac{y}{a} + f(x) \quad (1.1131)$$

The additional term $f(x)$ is added to fulfil the zero traction boundary condition $N_{yy} = 0$ of the two traction-free edges at $y = 0$ and $y = a$. At bifurcation point

a small perturbation is imposed in the form of out-of-plane deflection simply in the form

$$w(x, y) = w_0 \sin(\pi x/a) \sin(\pi y/b), \text{ we consider square plate } (b = a) \quad (1.1132)$$

The perturbation satisfies the boundary conditions of the simply supported plate at all edges. Next step is to form the change of total potential energy $\Delta\Pi$ and require stationarity for it. However, before doing so, one should resolve the unknown function $f(x)$ from the traction-free boundary conditions $N_{yy}(y = 0) = N_{yy}(y = a)$. Plane stress elasticity provides the membrane stress resultants

$$N_{xx} = C(\epsilon_{xx} + \nu\epsilon_{yy})//N_{yy} = C(\epsilon_{yy} + \nu\epsilon_{xx})//N_{xy} = (1 - \nu)C\epsilon_{xy} \quad (1.1133)$$

where

$$\epsilon_{ij} = \frac{1}{2}(u_{i,j} + u_{j,i}) + \frac{1}{2}w_{,i}w_{,j} \quad (1.1134)$$

where now $\{i, j\} = \{x, y\}$.

Continues ... soit comme MIT ou bien comme je l'ai fais avec l'étude post-critique asymptotique de la colonne

Computational example - linear buckling analysis

Finite Element ...

Note that (Figure 1.201) the plate with ration $a/b = 2$ buckles first with the mode corresponding to *two half-waves* ($m = 2$, Fi).

1.16.3 Computational example

Consider the aluminium plate with specifications shown in Figure (1.204). We will perform both linear buckling analysis and geometrically non-linear post-buckling analysis.

Linear buckling analysis

Linear buckling analysis

The thickness $t = 10$ mm used in the FE-analysis. Note that $\sigma = N/t$. The analytical two-dimensional plate analytical solution for buckling stress $\sigma_{cr,2D} = 4\pi^2 D/b^2 = 103.4$ MPa.

In the following, the FE-simulation is done using the full three-dimensional solid elasticity model (3D-solid elements). So, one will have anyway $\sigma_{cr,2D} > \sigma_{cr,3D}$, accordingly. Here the first four eigenvalues $\sigma_E \equiv \sigma_{cr,1} = 70$ MPa, $\sigma_{cr,2} = 77.3$ MPa, $\sigma_{cr,3} = 104.9$ MPa and $\sigma_{cr,4} = 147.9$ MPa, where the smallest one $\sigma_{cr,1} \equiv \sigma_E = 70$ MPa is the buckling load. Therefore, the ratio of load being $\lambda = N_{cr,i}/N_E = [1, 1.1, 1.5, 2.1]$.

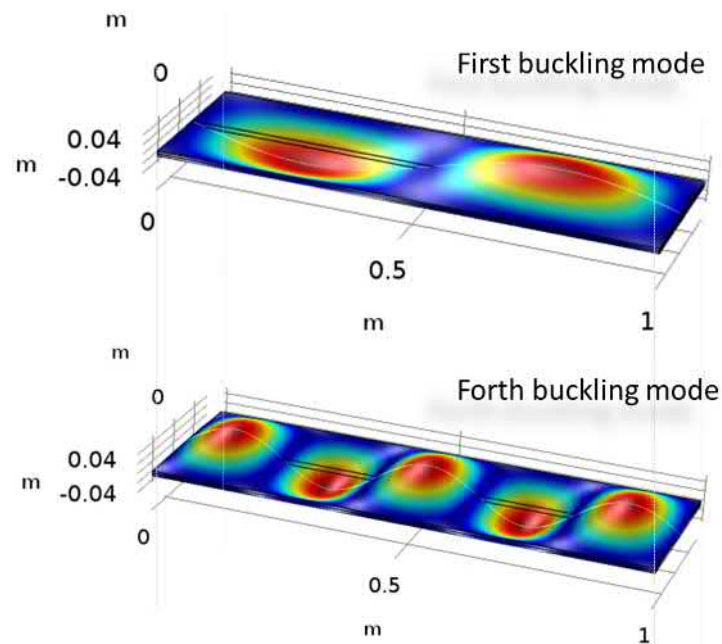


Figure 1.201: Buckling of thin elastic simply supported aluminium plate with in-plane loading N_x [N/m] on the shortest side (numerical simulation). First mode. Aspect ratio $a/b = 1/3$, $E = 70$ GPa, $\nu = 0.33$, thickness $t = 10$ mm, $a = 1$ m, $N_{x,cr}/t = 155$ MPa (1st mode), 211 MPa (4th mode). (Plate-buckling-Analysis-parametric-rectangular-plate-OK-EXAMPLE-2.mph)

Esitä vielä tuossa muodossa $N_{cr} = K \cdot N_{cr,ref}$, jossa referenssiarvo on sen peruslaatakaisten nurjahdusarvo as in (Eq. 1.1062). TO DO.

The corresponding buckling modes are shown in Figure (1.202).

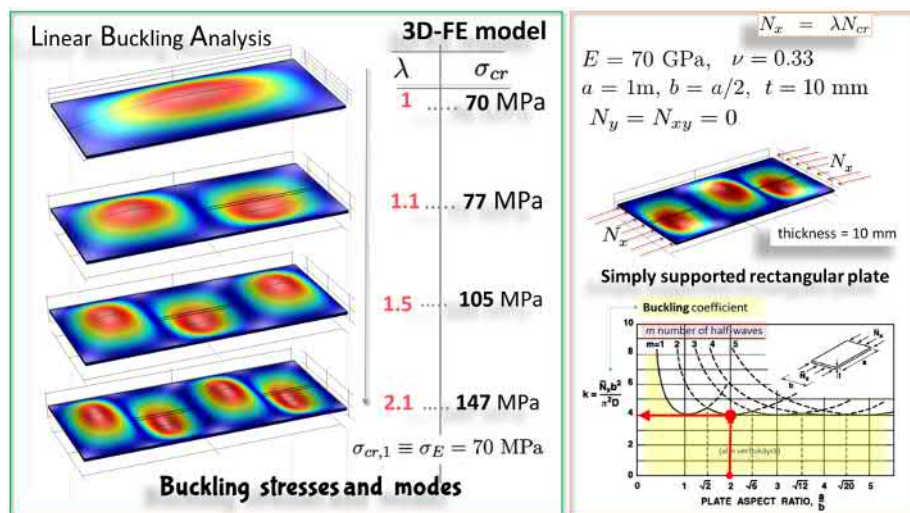


Figure 1.202: Buckling of thin elastic simply supported aluminium plate with in-plane edge loading N_x [N/m] on the shortest side (numerical simulation). Note that $a/b = 2$.

(Plate-buckling-Analysis-parametric-rectangular-plate-OK-2-a-per-b-equal-2.mph)

Post-buckling analysis

Post-buckling³⁷⁷ analysis is also often simply called geometrically non-linear analysis.

I present, in Figure (1.203), a 'poor-man' and for dummies simplified (fast) version

³⁷⁷This note is for the write: Ici, pour par manque de temps, après l'analyse linéaire de bifurcation pour déterminer la charge critique, j'enchaîne sur l'analyse non-linéaire géométrique. Pour cela, 1) j'introduis une imperfection initiale au système sous forme de forces transversales très petites afin d'obtenir une déflexion initiale w_0 correspondante à celle que nous aurions obtenue en 2) introduisons directement une déflexion initial donnée par une combinaison linéaire de N premiers modes propres avec une très petite amplitude $w_0(x, y, z) = \sum_i^N a_i \phi_i(x, y, z)$. Cette première méthode (no 1) s'est avérée plus simple à mettre au point sous Comsol, et je l'adopte. Je laisse la méthode 2) aux étudiants (ils ont plus de temps). Naturellement, les deux méthodes sont équivalentes pour introduire une imperfection initiale. Par exemple, on voudrait ajouter une imperfection de planéité δ/h de la plaque. Pour cela, on peut y arriver au même résultat en rajoutant une force transversale P_{trans} donnant une déflexion maximale équivalente. Cependant, dans le premier cas, nous n'avons pas de tension initial due à la force transversale dans le cas où l'imperfection initiale de géométrie peut ne pas s'accompagner de tensions (une structure moulée, par exemple). Cependant, pour l'analyse non-linéaire de post-bifurcation, cela n'est pas important car l'important est justement une petite perturbation initiale. Quelle soit double : infiniment petites tensions et déplacement transversal. Pour l'étude comportement post-bifurcation (courbe $P-\delta$) la méthode 1) va très bien et est correcte.

how start doing GNA in Comsol and others FEA tools. The difficulty (I mean that one need to read the theory and example manuals or to find by itself how to give initial displacements as tiny imperfections. I have no such time myself.)

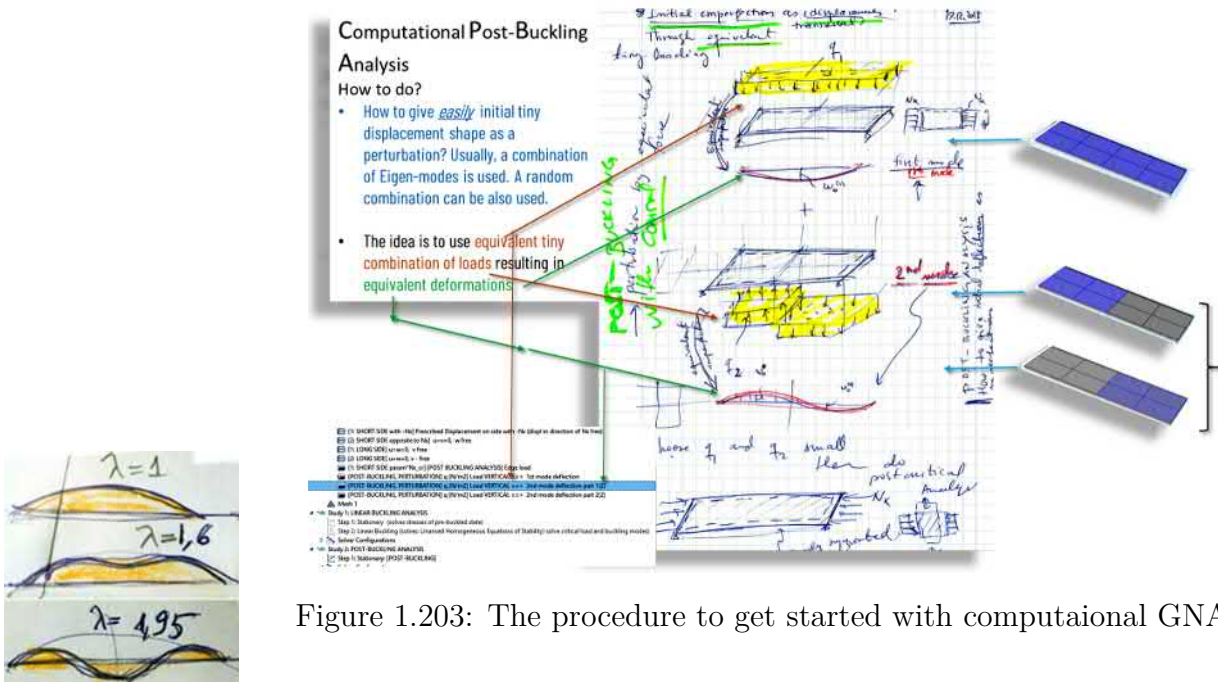


Figure 1.203: The procedure to get started with computational GNA.

GNA-result of simply supported rectangular plate buckling, $N_x = \lambda N_{cr}$, $N_y = N_{xy} = 0$, ($\lambda = 1, 1.6, 1.95$). More in text part.

As an example of geometrically non-linear analysis (GNA), the aluminium plate with specifications shown in Figures (1.204) and (1.205) and is analysed³⁷⁸ to study its post-buckling behaviour in details³⁷⁹

Buckling of orthotropic plates

Assume an *orthotropic material* where the plate coordinate (x, y, z) are oriented in the directions of the principle material axes (x_1, x_2, x_3) . The bending moments are given by the following constitutive relation

$$\begin{bmatrix} M_{xx} \\ M_{yy} \\ M_{xy} \end{bmatrix} = - \begin{bmatrix} D_{11} & D_{12} & 0 \\ D_{12} & D_{22} & 0 \\ 0 & 0 & D_{66} \end{bmatrix} \begin{bmatrix} w_{,xx} \\ w_{,yy} \\ 2w_{,xy} \end{bmatrix} \quad (1.1135)$$

³⁷⁸Plate-buckling-and-POST-Buckling-Analysis-parametric-rectangular-plate-OK-EXAMPLE-2

³⁷⁹In this course, the material behaviour is limited to elastic. However, in practice, material non-linearity has to be included for every-day structural analysis to have a realistic response.

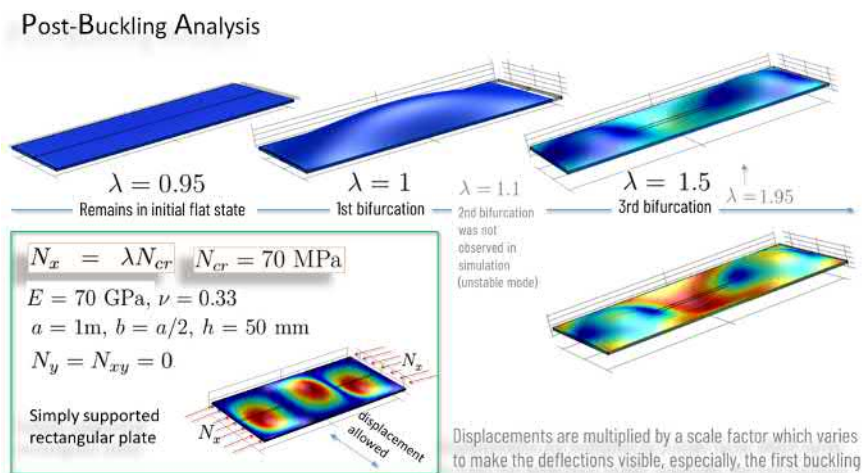


Figure 1.204: Numerical simulation of post-Buckling analysis of rectangular simply supported aluminium plate. No imperfections. The second mode is unstable and not seen in this simulation because a force-control algorithm was used. One should switch to displacement-control algorithm to follow the unstable branch. (Voima ohjattuna / siirtymä-ohjattuna)

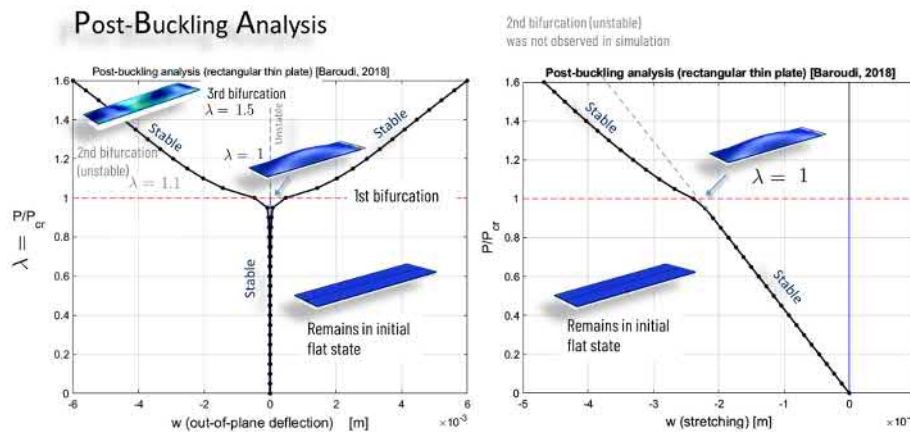


Figure 1.205: Post-Buckling analysis of rectangular simply supported aluminium plate obtained by numerical FE-simulation. Equilibrium paths. Notice that the post-buckling behaviour is stable; 1st & 3rd. The second mode is unstable. The second mode is unstable and not seen in this simulation because a force-control algorithm was used. One should switch to displacement-control algorithm to catch the unstable branch. The plate was ideally perfect.

where

$$D_{11} = \frac{E_1 h^3}{12(1 - \nu_{12}\nu_{21})}, D_{12} = \nu_{21} D_{11}, \tag{1.1136}$$

$$D_{22} = \frac{E_2}{E_1} D_{11}, D_{66} = \frac{G_{12} h^3}{12}. \tag{1.1137}$$

The linearised equations of stability now is

$$D_{11}w_{,xxxx} + 2(D_{12} + 2D_{66})w_{,xxyy} + D_{22}w_{,yyyy} + \quad (1.1138)$$

$$+ \left(N_{xx}^0 w_{,x} + N_{xy}^0 w_{,y} \right)_{,x} + \left(N_{xy}^0 w_{,x} + N_{yy}^0 w_{,y} \right)_{,y} = 0 \quad (1.1139)$$

We will address one or two application examples in order to have an idea what new features orthotropy brings to the stability problems as compared to stability of isotropic plates.

TO DO, DBA 10.1.2019

To be done³⁸⁰ ...

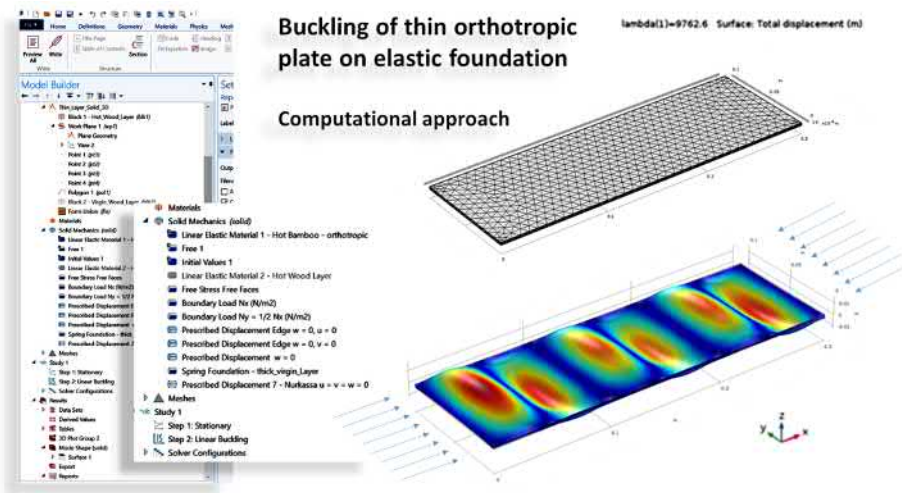


Figure 1.206: Buckling of orthotropic (wood) thin plate on elastic foundation.

1.16.4 Buckling of rectangular plates under uniform bi-axial loading

TO DO

consider here proportional loading; both edge loads increases in the proportion at the same time

³⁸⁰see the ongoing (keskenären) analysis in COMSOL-file Plate-buckling-and-POST-Buckling-Analysis-parametric-rectangular-plate-OK-EXAMPLE-2-OK.

1.16.5 Buckling of rectangular plates under bi-axial loading

TO DO Here the loading sequence can be any 1) consider here proportional loading; both edge loads increases in the proportion at the same time 2) first one then the other ... interaction diagrams

1.16.6 Buckling analysis of square and circular plates on elastic foundations

rectangular plate

Circular plate

... see Figure (1.207) ...

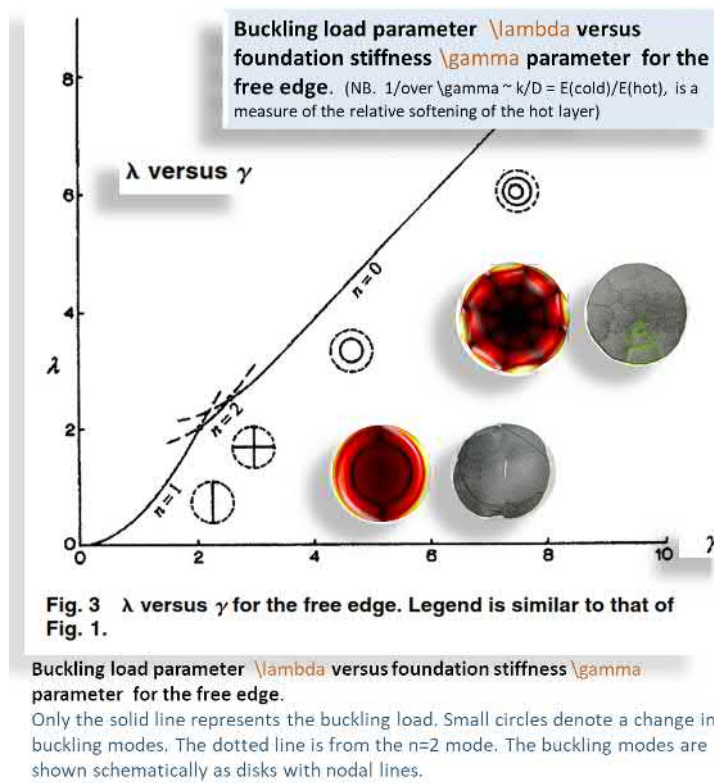


Figure 1.207: Thin circular plate on elastic foundation. Effects of stiffness of the foundation relative to the stiffness of the plate.

Example of a research problem: surface crack patterns on wooden specimens due to surface heating

[Kappale on kseken . . . to be continued . . .]

This short subsection³⁸¹ is to meant to activate student's interest toward importance of theoretical aspects giving by showing an example of application of stability theory to a real engineering problem directly related to *Fire Safety Engineering*. Indeed, the firm understanding of the theory of stability was decisive, for me, to see from an experiment that the cracking behaviour directly results from stability effects. Such hit and clue were hidden for long time to researchers from the field of fire science not having the needed background in structural mechanics. All the previous work, in the field, give shrinkage as the basic mechanism. However, for the particular experiments, it was not true.

What is or are the basic mechanisms for observed various topology of these crack-patterns?

It was believed for long time, till recently, that the driving mechanism was shrinkage of the heated surface. However, such mechanism cannot explain the crack patterns observed on the surface of FIR (Figure 1.208). Shrinkage will result formation of cracks perpendicular to the weakest direction of the wood: parallel to the fibres. However, the observed cracks, in the cone calorimeter experiment performed in a nitrogen atmosphere, are perpendicular to the strongest direction (perpendicular to fibres). Surface instability is 100% in accordance with such observation. This was the first time such novel explanation was given³⁸². It was shown, in the article, that the principle tensional stresses in the buckled state are located along the node-lines of the modes. It is well-known that cracks, when they appear, will be located in tensional regions. So, the node-lines of the buckling modes will correspond to the crack locations. Figure (1.207) shows the effect of foundation stiffness on the buckling modes.

It comes out that, the basic mechanism is Biot surface-instability phenomenon (1.209).

1.16.7 Post-buckling analysis of square and circular plates on elastic foundations

This sections shown an important application problem which solution come up to novel ... explains the topology of surface cracking patterns due to heating of specimens from above of th...

³⁸¹Message to me: pitää lyhentää ja ytemikäistää sekä yhdistää kuvat yhdeksi kuvaksi.

³⁸²D. Baroudi, A. Ferrantelli, K. Y. Li, S. Hostikka. *Combustion and Flame*, 182 (2017) 206–215.

1.18 Stability of cylindrical shells

Computational technology, like Finite Element Method software made complex analysis of shells possible. Combing experimental sciences and computational approach is our-days possible for tackling the complex behaviour of shells³⁸³ the group of green-yellow pixels in the image "a leave", for that you need a conceptual theory which, experiments and simulations alone will not and cannot provide. Only conceptual approach create new intellectual objects (concepts) and give them names (labels). .



Fragment from the past of an old code line of a **computer program** (reikä-nauha & kortti).

The next important observation is good to keep in mind: In general, and this observation is based on experimental evidences for decades, buckling of thin shells is a *localised phenomenon* due to their high imperfection sensitivity. Such imperfections can be localised loading, geometry imperfections of the shell, boundary conditions, local change in rigidity, in curvature, in supporting and load-transfer areas, etc. All this is one of the reasons for which experimental analysis and design of such structures is not avoidable despite availability of computational technology. All these imperfections should be characterized together with heir effects for the specific design of pre-design.

In the following, some classical results and theories will be presented, shortly.

Stability of cylindrical shells

*What makes thin shells special, in structural terms?*³⁸⁴ Recall, may be, for the n^{th} , $n \rightarrow \infty$, time already that *thin shells are imperfection-sensitive structures*. The major reasons is, in short, 1) the *unstable post-buckling behaviour* (Figure 1.214) and 2) mode interaction mechanisms because of mode accumulation (Figure 1.210).

Many buckling modes are close³⁸⁵ to each other, this contribute to make shells very sensitive to imperfections through mode interaction mechanism and

³⁸³So, one may say *where I need theory?*. The answer is to **Elvis Presley**: "*It's now or never.*". "Now" means that, actually, computational approach became already of every use and natural extension of an engineer. For that, we need theoretical understanding of what we are computing and how to cross-check by hand and quickly our results. Not that, the software makes mistakes but more because humans make mistakes, even during the input-phase. Theory provides handles to experiments and simulation. Without, theoretical concepts, the obtained experimental and computational results will be similar to an image of a complex nature landscape shown as a cloud of pixels in a pixel-map. Without conceptual (theoretical) understanding, you have noway to see more than separate pixels which are variously coloured. You cannot discern or "[/name

³⁸⁴Expliques les différences essentielles entre flambage de coques et plaques ou colonnes. Shell: unstable neighbouring bifurcation (snap-through-like branch immediately after bifurcation) and plate stable. First is imperfection-sensitive and the other not. Draw the to diagrams.

³⁸⁵Ref: prof. R. **Kouhia** at <http://www.tut.fi/rakmek/personnel/kouhia/rese/lectio/lectio.html>

this proximity of such many modes is one of the mechanisms for the characteristic *sleepy falling post-buckling path* of such thin-shells (Figure 1.214). This means that at the (Euler) buckling stress, appear practically a *large number of modes* which are all *simultaneously critical* (Cf. Figure 1.210). Yamaki³⁸⁶ illustrates

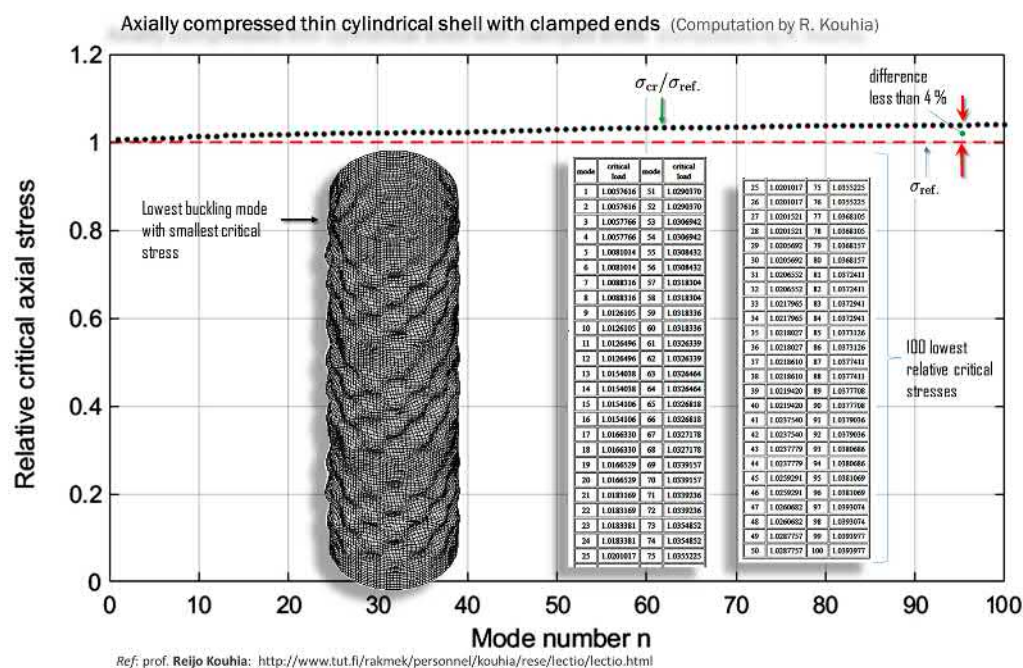


Figure 1.210: Finite Element Linear buckling analysis of an axially compressed thin cylindrical shell with clamped end. The FEA shows that more than 100 buckling modes have corresponding critical loads which differ only by less than 4%! (Reproduced with adaptation with permission of the author).

(Figure 1.211) the post-buckling behaviour of cylindrical shells through experimental results. In such figure, one can see clearly the contribution of such mode accumulation to the unstable post-buckling branch as a function of the **Batdorf** parameter $Z = \sqrt{1 - \nu^2} \cdot L^2 / (Rh)$.

Figure (1.212) shows experimental results of thin-walled cylindrical shell buckling performed at Civil Engineering Laboratory (*Otaniemi*). The tested cylinders are made of aluminium (local beer cans, $h \approx 0.1\text{mm}$) and on steel cylinders. The loading rate was very slow (0.5mm/min). One can see also a saw-shaped load-displacement post-buckling behaviour for the aluminium shells.

The structural design of shells is challenging and demands expertise. For practical design purposes around 100 pp. of the *Eurocode*³⁸⁷ addresses analysis

³⁸⁶N. Yamaki. *Elastic Stability of Circular Cylindrical Shells*. North-Holland (1984).

³⁸⁷**EN 1993-1-6**: Eurocode 3. Design of steel structures. Part 1-6: Strength and stability of shell structures.

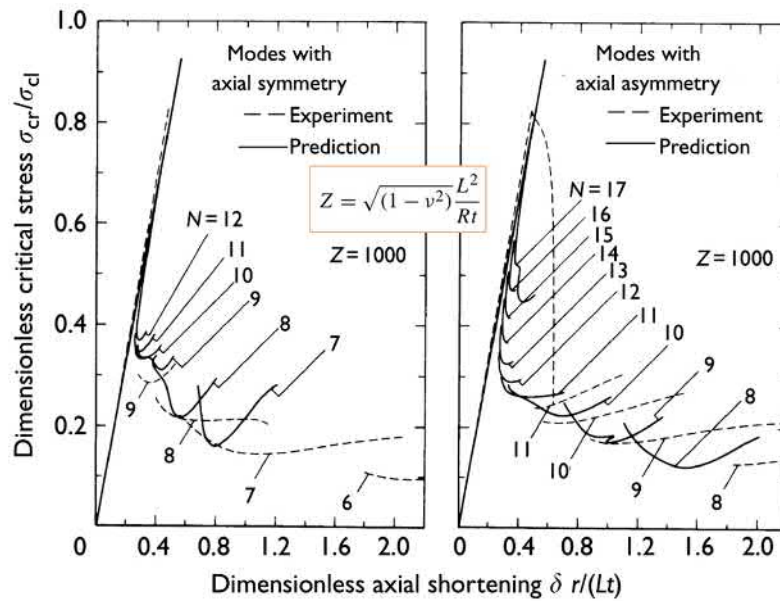


Figure 1.211: Effect of mode accumulation for thin-walled cylindrical shells. In this figure $t \equiv h$, σ_{cr} being the Euler critical stress and σ_{cl} being the collapse stress. figure reproduced from: N. Yamaki. *Elastic Stability of Circular Cylindrical Shells*. North-Holland (1984).

and design aspects of shells.

1.18.1 Shells are imperfection-sensitive structures

The fundamental difference between post-buckling behaviour of thin-shells and other type of basic structures is depicted in Figures (1.214 and 1.213). Flat plates and columns have a post-buckling reserve of strength thanks to their stability after first bifurcation. This makes such structures *imperfection-insensitive*. On the contrary, axially compressed thin-walled cylindrical shell after bifurcation, shows a sharp and sudden unstable post-buckling branch of snap-through like behaviour before, it reaches, at a substantially reduced resistance load value, a stable branch again just after the limit point). This kind of typical behaviour makes the thin-shells *imperfection-sensitive* structure.

Before Koiter's explanation for the imperfection-sensitivity of thin-shells with regard to buckling (collapse) load in compression, **von Kármán**, based on many observations, made a sharp remark³⁸⁸: "*why it much easy to predict the collapse (buckling load) for compressed rods and plates as compared to the experimental value, while predicting the collapse (or buckling) stress of a compressed thin-shell*

³⁸⁸Question which I have freely, translated.

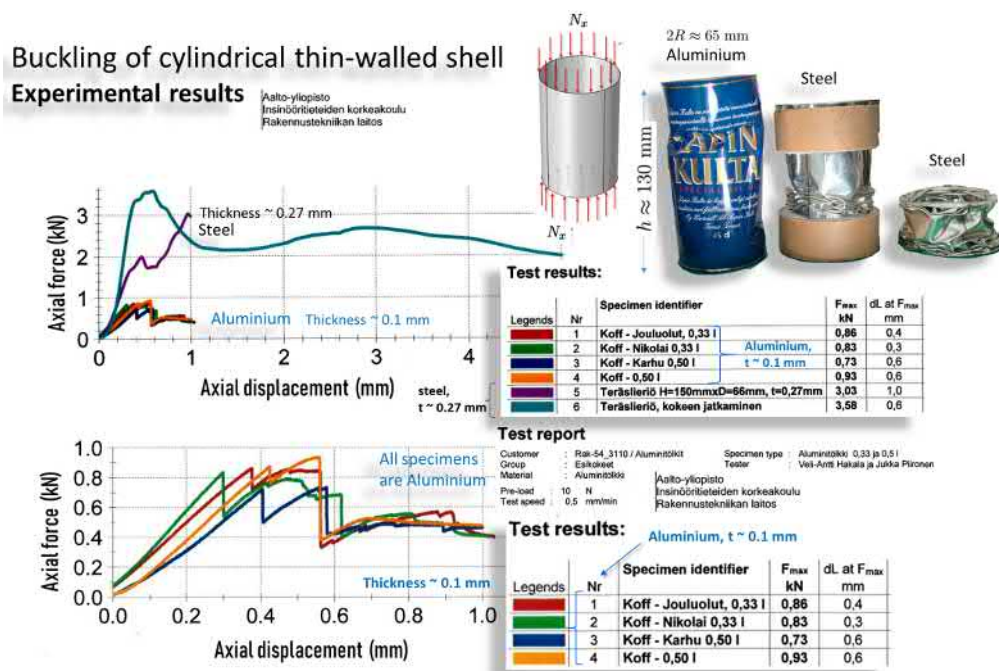


Figure 1.212: Experimental force-displacement curves for cylindrical thin-walled shells. ($t \approx 0.1$ mm, $2R \approx 65$ mm and $h \approx 130$ mm for the beer aluminium can.) (source: Laboratory of Civil Engineering, Aalto-university at Otaniemi; thanks to A. Niemi, V. A. Hakala and J. Pironen, for he data.).

becomes impossible since there is always a substantial difference between prediction and experimental values for thin shells?" von Kármán and Tsien, observed experimentally that collapse load for such shells was systematically much below the predicted theoretical value (Euler stress). This *fundamental difference, in predictability*, puzzled von Kármán and surely, many others working in that experimental field at that time. Interestingly, von Kármán and Tsien (1941) were the first³⁸⁹ to introduce to their analysis initial geometrical imperfections in the shape of buckle patterns they have observed in their experiments after shell collapses.

The non-linear theory of thin shells was initiated by von Kármán and Tsien (1934) and Donnel (1934). A working theory able to tackle the stability of thin shells should account for non-linear terms in displacement³⁹⁰. Such theory of *large-displacement shell equations* was developed separately by von Kármán and Tsien (1934) and Donnel (1934). This theory is actually known as *the von Kármán-Donnel large-displacements shell equations*.

³⁸⁹Elishakoff Isaac E. *Resolution Of The Twentieth Century Conundrum In Elastic Stability*. world Scientific Publishing Co. Pte. Ltd. 2014

³⁹⁰... as introducing initial geometric imperfections.

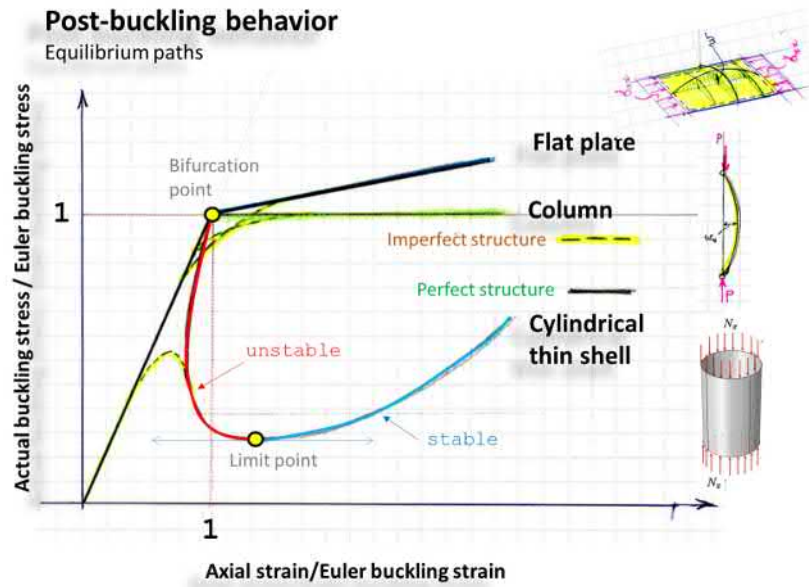
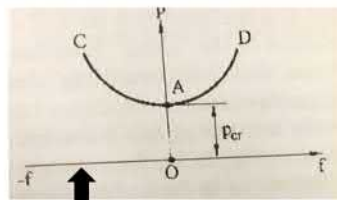


Figure 1.213: Schematic of fundamental characteristics of post-buckling behaviour for plates, columns and thin shells.

Plates and columns
Stable-symmetric bifurcation
Not imperfection sensitive structures



After bifurcation, a stable close neighborhood exists. Consequently, not imperfection sensitive structures

After bifurcation, the close neighborhood is unstable. Very far B-F-D, a stable branch exists. Consequently, imperfection-sensitive structures

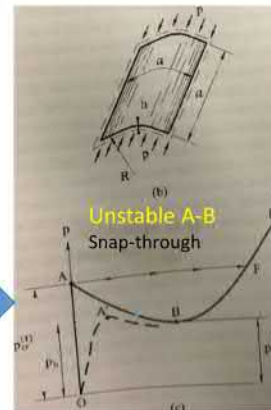


Figure 1.214: what is the main and 'vital' difference, in terms of stability behaviour, between plates, columns and thin shells? Plates are imperfection-insensitive while shells are very sensitive to imperfections because 1) of unstable post-buckling behaviour and 2) some buckling modes are close to each other, mode interaction. (TO DO: a better figure)

Classical results by **Koiter**³⁹¹, others³⁹² have shown that shape imperfection

³⁹¹Initiated the asymptotic theory of initial post-buckling stability.

for thin shells reduced dramatically the critical load as compared to ideally perfect shell. Thin shells are very *imperfection-sensitive*³⁹³ structures.

The relative amplitude of the geometric imperfection is encoded in the ratio

$$\bar{\xi} \equiv \delta/t \quad (1.1140)$$

where t being the thickness of the shell.

The collapse load (limit load) P_s of the imperfect shell is reduced with respect to the critical buckling load P_{cr} of the ideally perfect shell

$$P_s/P_{cr} \dots (\delta/t) \quad \text{find the formula by Koiter} \quad (1.1141)$$

Koiter, in his PhD thesis, analysed the effects of shape imperfections of thin shells on the buckling load of a perfectly shaped sufficiently long shells. He found that the expected theoretical buckling load was reduced dramatically. Through asymptotic analysis (*imperfection-sensitivity analysis*) he arrived to a formula giving such reduction:

$$(1 - \rho_s)^2 - A\rho_s|\bar{\xi}| = 0, \quad (1.1142)$$

where $\rho_s = P_s/P_{cr}$ and $\bar{\xi} = (\delta/t)$ being the non-dimensional amplitude of the imperfection as related to the shell-thickness³⁹⁴ and A a coefficient depending on the case under consideration (type of structure, boundary conditions, ...).

³⁹²Interested readers can consult: 1) von Kármán, T. and Tsien, H. S., "The Buckling of Thin Cylindrical Shells Under Axial Compression," *Journal of the Aeronautical Science*, Vol. 8, No. 8, June 1941, pp. 303-312. 2) Donnell, L. H. and Wan, C. C., "Effect of Imperfections on Buckling of Thin Cylinders and Columns Under Axial Compression." *Journal of Applied Mechanics*, Vol. 17, No. 1, March 1950, pp. 73-83. 3) Koiter, W. T., *On the Stability of Elastic Equilibrium*. (in Dutch), H. J. Paris, Amsterdam, Holland, 1945; translation available as AFFDL-TR-70-25, February, 1970, Wright-Patterson Air Force Base.

³⁹³Koiter WT. 1945. *On the stability of elastic equilibrium*. Dissertation, Delft, The Netherlands. (An English translation is available in 1967. *Tech. Trans. F 10, 833*). and Koiter, W.T., 1963. The effect of axisymmetric imperfections on the buckling of cylindrical shells under axial compression. *Proc. K. Ned. Akad. Wet., Amsterdam*, ser. B, vol. 6; also, Lockheed Missiles and Space Co., Rep. 6-90- 63-86, Palo Alto, California.

³⁹⁴It is found, experimentally and theoretically that stiffened shells have less (or have reduced) imperfection-sensitivity as compared with monocoque cylindrical shells under axial compression. Thanks to the stiffeners: the effective relative thickness $\bar{\xi}_e = \delta/t_e$ of the perturbation of such stiffened shells is reduced. The effective thickness of the stiffened shell t_e increases.

Predictions of sensitivity small initial geometrical imperfections (asymptotic theory)

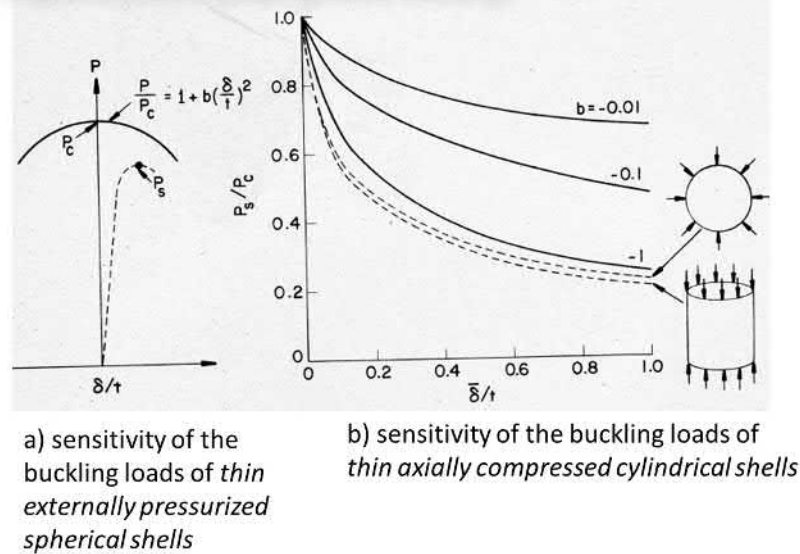


Figure 1.215: Thin shell sensitivity to initial geometrical imperfections. (Ref:https://shellbuckling.com/presentations/buckledShells/pages/page_40.html)

1.18.2 About large-deflection stability equations

Let's stop a short while and have a look downward,³⁹⁵ in time, to the history of *large-deflection equations of thin-walled shells*. This section *shows*³⁹⁶, for general culture of the student, the equation of stability (loss) of thin-walled cylinder buckling under ends torque T , derived for the first³⁹⁷ time by **Donnell** (1933)³⁹⁸. Donnell understood the importance of initial geometrical imperfections for shells and assumed them to be of the same shape (mode) as the perfect shell have at

³⁹⁵Without knowing history we miss our roots. We become as leaves in a tree looking up to the sky without seeing the trunk neither the roots of the tree holding and feeding us. Firmly rooted, it difficult to be *blown by the wind*.

³⁹⁶For derivation, refer to the original. The main idea was to write the equations of equilibrium for an elementary volume of the tube $hdxds$ in the post-buckled configuration. After that, eliminate u and v from the equations of equilibrium of the membrane stress resultants to obtain the eight-order PDE for the increment w of the displacement. Isotropic linear elasticity were assumed.

³⁹⁷Equivalent work by von Kármán and Tsien. Both von Kármán and Donnell contributed largely for understanding and establishing the large-deflection theory for addressing buckling of thin-walled shells (theoretically and experimentally)

³⁹⁸L.H. Donnell. Stability of thin-walled tubes under (uniform) torsion (*NACA Technical Report 479*). (1933)

buckling³⁹⁹.

Donnell large-deflection stability equations of thin-walled torsion

The original Donnell equation will be reproduced just for historical and esthetic curiosity. He derived when studding, both experimentally and theoretically, stability thin-walled tubular shells under a uniform torsion. A constant torque T is applied at both ends of the tube (*Cf.* cited publication; Donnell (1933)). So, considering equilibrium, (geometrical) compatibility between strains and displacement, and linear elastic stress-strain relation, he derived the non-linear equations of stability equations (Donnell large-deflection⁴⁰⁰ equations) keeping just the most meaningful non-linear terms for the perturbed configuration. Neglecting the possible effects of initial deviation from the membrane state close to the boundaries⁴⁰¹, the equations of equilibrium are written for the perturbed adjacent state where the mid-plane displacements u, v, w , deformations and stresses (stress resultants) meaning increments. So, the equations are non-linear by definition. Here a the Donnell large-deflection (stability) equation

$$D\nabla^8 w + \frac{Eh}{R^2} \frac{\partial^4 w}{\partial x^4} + 2Sh\nabla^4 \left(\frac{\partial^2 w}{\partial x \partial s} \right) = 0 \quad (1.1143)$$



Donnell: Report # 479 (1933).

where $D = Eh^2/12(1 - \nu^2)$ being bending rigidity per unit width and $Sh = S^0h = -N_{xs}^0$, the shear stress (constant) from the end-torque T .

The above *beautiful* (PDE) equation is the same as for a flat-plate⁴⁰² except for the second term accounting for shape initial curvature $1/R$ of the cylinder. It allows to determine the critical shear stress $\tau_{xs,cr} \equiv S_{cr}$. The critical torque $T_{cr} = S_{cr}\pi(2R)^2h/2$. To obtain the above equation (1.1143), he eliminated u and v with the help of equilibrium equations of the membrane resultants and of the Hooke's law.

For instance, in a more general loading case with all the initial stress-resultant components N_x^0, N_s^0 and N_{xs}^0 , one can write⁴⁰³, the stability equation for the the

³⁹⁹Robert M. Jones. *Buckling of Bars, Plates, and Shells*. Ed. 2006. Bull Ridge publishing.

⁴⁰⁰It will be more correct to call it *moderate rotation theory* where, for instance, displacements are of order of the shell thickness. Thus, the cosines of the rotations θ_i of the mid-plane normals can be well approximated with $1 - \theta^2/2$ and $\theta \approx w'$, etc. analogously with Euler's *Elastica* for moderate rotations.

⁴⁰¹Such, in practice, impossible to avoid initial bending state close to boundaries, discontinuities or supports can be very local (boundary layer). However, it acts as an initial imperfection which affects highly the stability behaviour of thin-walled shells.

⁴⁰²Which is $D\Delta\Delta w - 2N_{xy}^0 w_{,xy} = 0$. It will be derived later (Equation 1.1126).

⁴⁰³*Cf.* M. Tuomala. *Rakenteiden Stabiilisusteoria*. (stability lecture notes).

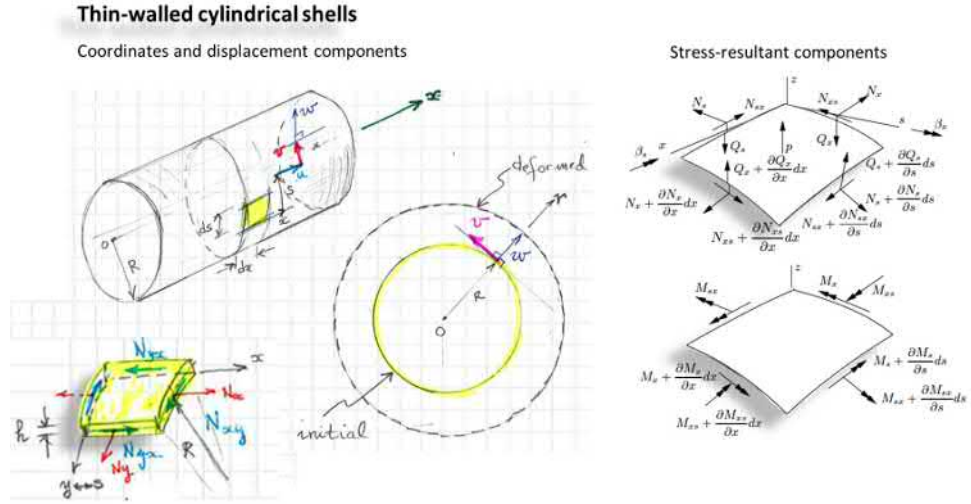


Figure 1.216: Thin-walled cylindrical shell, coordinate system, displacements u, v, w of the mid-plane and stress resultant components. In some writings the coordinate $y \equiv s$). The rotations in the left part of the figure are defined by $\beta_x = -w_{,x}$ and $\beta_s = -w_{,s}$.

increment w of displacement component as

$$D\nabla^8 w + \frac{Eh}{R^2} \frac{\partial^4 w}{\partial x^4} - \nabla^4 \left(N_x^0 \frac{\partial^2 w}{\partial x^2} + 2N_{xs}^0 \frac{\partial^2 w}{\partial x \partial s} + N_s^0 \frac{\partial^2 w}{\partial s^2} \right) = 0 \quad (1.1144)$$

The stress-resultant components N_x^0, N_s^0 and N_{xs}^0 should fulfil equilibrium equation (statically admissible pre-buckling stress state solved before hand).

Donnell-type large-deflection stability equations

Physical problem: thin-walled tubular shell with both axial loading and transversal pressure p . Note that, for instance, given the external pressure p (external loads) we *can solve uniquely* all the displacement components and internal force from the non-linear coupled equilibrium equations (1.1154) for elasticity and given the kinematic relations (& boundary conditions). This set of equations represent large-deflection equilibrium equations which are also valid for the post-buckled configuration, naturally. This set of non-linear coupled equations can expressed with the flexural displacement component w only after eliminating the displacement components u and v from the equilibrium equations and accounting for elasticity and kinematics. Then, through linearisation of these equations, we can obtain the linearised equations of stability (eigenvalue problem) when needed.

Donnell derived this type of *large-deflection theory*⁴⁰⁴ for cylindrical shells in the

⁴⁰⁴There is analogy with the von-Kármán large-deflection plate theory

1930s (see reference).

One can think of writing equilibrium equations in the deformed perturbed configuration where u , v and w being *total displacements*, for instance. Therefore, the obtained non-linear equations are not buckling equations. Or, similarly, consider an initial equilibrium state of the cylinder for which the stress state and displacement field being known (solved). The equations of equilibrium are then written in a slightly perturbed state where the mid-plane displacements u, v, w , deformations and stresses (stress resultants) are now increments. The strain increments (membrane strains of the mid-plane and flexural strains 'curvatures') are

$$\begin{aligned}\epsilon_x &= \frac{\partial u}{\partial x} + \frac{1}{2} \left(\frac{\partial u}{\partial x} \right)^2, & \kappa_x &= -\frac{\partial^2 w}{\partial x^2}, \\ \epsilon_s &= \frac{\partial v}{\partial s} + \frac{w}{R} + \frac{1}{2} \left(\frac{\partial w}{\partial s} \right)^2, & \kappa_s &= -\frac{\partial^2 w}{\partial s^2} \\ \gamma_{xs} &= \frac{\partial u}{\partial s} + \frac{\partial v}{\partial x} + \frac{\partial^2 w}{\partial x \partial s}, & \kappa_{xs} &= -\frac{\partial^2 w}{\partial x \partial s}.\end{aligned}$$

In the above kinematic equations, the membrane deformations ϵ_s , ϵ_x , γ_{xs} refer to the mid-plane ($z = 0$) in-plane deformations and the curvatures κ_x , κ_s and κ_{xs} , are of the mid-plane, too. For instance, a deformation at a location z will be given by $\epsilon_x(z) = \epsilon_x(z = 0) + z\kappa_x$.⁴⁰⁵ The above expressions differ from those of the familiar flat-plate only by the strain term w/R in the circumferential direction s ($y \equiv s$) (Figure 1.216). The relative change in length of the perimeter (for v being constant) is

$$\epsilon_s = \frac{2\pi(R + w) - 2\pi R}{2\pi R} = \frac{w}{R}. \quad (1.1145)$$

For an isotropic elastic material, the constitutive equations for the shell membrane stress-resultants are obtained by integrating over shell thickness h , the stress-components expressed through Hooke law. The membrane stress-resultants are

$$N_x = C(\epsilon_x + \nu\epsilon_s), \quad (1.1146)$$

$$N_s = C(\epsilon_s + \nu\epsilon_x), \quad (1.1147)$$

$$N_{xs} = C(1 - \nu)\epsilon_{xs}, \quad (1.1148)$$

where the membrane rigidity (stiffness) per unit-width

$$C = \frac{Eh}{1 - \nu^2}. \quad (1.1149)$$

⁴⁰⁵Corresponds to kinematics of Love-Kirchhoff for shell or plate.

Correspondingly, the flexural or bending stress-resultants (the moments) are⁴⁰⁶

$$M_x = D(\kappa_x + \nu\kappa_s), \quad (1.1150)$$

$$M_s = D(\kappa_s + \nu\kappa_x), \quad (1.1151)$$

$$M_{xs} = D(1 - \nu)\kappa_{xs}, \quad (1.1152)$$

where the bending rigidity (stiffness) per unit-width being

$$D = \frac{Eh^3}{12(1 - \nu^2)}. \quad (1.1153)$$

Expressing the (three) equations of equilibrium for an element hd_sdx of the shell with the stress-resultants in terms of constitutive laws, on finally, obtains the system of three *coupled* partial differential equations

$$\begin{cases} N_{x,x} + N_{xs,s} = 0 \\ N_{xs,x} + N_{s,s} = 0 \\ D[w_{,xxxx} + 2w_{,xxss} + w_{,ssss}] - [N_x w_{,xx} + 2N_{xs} w_{,xs} + N_s(w_{,ss} - \frac{1}{R})] = p, \end{cases} \quad (1.1154)$$

where the unknowns are the three membrane stress-resultants and radial deflection w . In these *large deflection equations* the membrane stress resultants $N_{\alpha,\beta} = N_{\alpha,\beta}(u, v, w)$, so they depend on actual misplacements.

Equations (1.1154) are the famous *non-linear large-deflection equations* (of Donnell-type) for analysing thin cylindrical shells. (the membrane resultants N_{xx} and N_{ss} are defined positive in tension and p being the external pressure amplitude⁴⁰⁷). These non-linear equations⁴⁰⁸, form a set of coupled three non-linear partial differential equations widely used large-deflection analysis of thin-walled cylindrical shells. When the curvature $1/R \rightarrow 0$, these equations reduce to the von-Kármán large-deflection plate theory.

Compare with flat-plate equations for small displacements, reproduced in (1.1155)

$$D[w_{,xxxx} + 2w_{,xxyy} + w_{,yyyy}] - [N_{xx}w_{,xx} + 2N_{xy}w_{,xy} + N_{yy}w_{,yy}] = p \quad (1.1155)$$

where now $s \equiv y$. The superscript N^0 for initial stress or stress-resultants have also been dropped out since it becomes unnecessary.

N. B. Note that, in Equation (1.1155) the membrane forces $N_{\alpha\beta}$ do not depend on the deflection w . On the contrary, in the *large-deflection equation* (1.1154),

⁴⁰⁶Analogously with those of a flat-plate since they are local as these relations concern an infinitesimal material element hd_sdx as for the plate.

⁴⁰⁷The external pressure p is defined as $\vec{p} = p\vec{e}_R$, where $\vec{e}_R = \vec{R}/R$

⁴⁰⁸Donnell-type large deflection equations (with shallow shell approximation, for in-stance $v/R \ll w_s$), in amplitude.

the membrane stress-resultants depend on the deflection w and the displacement components u and v as well. If one apply the third Donnell equation to a thin slab then one easily obtain the well-known equation for to the geometrically large deflection bending of a beam

$$Dw_{,xxxx} - N_x(x, u, w)w_{,xx} = p(x) \quad (1.1156)$$

where now the normal force N_x depend on deflection w and u for large deflections. If one assume small deflections, then we obtain the not less-known geometrically non-linear beam theory. So, here is the difference. Keep this in mind when we go further in the text.

That's all about the history of such famous equations. Let's go further and return to some classical problems.

* * *

The Linear stability equations: To derive linearised stability loss equations (eigenvalue problem) we consider an infinitely tiny perturbation⁴⁰⁹ of the equilibrium state leading to a transition between the pre-buckled state to buckled equilibrium state. We introduce such a perturbation to the non-linear couples equilibrium equation system (Equation 1.1154) for the purpose of linearise buckling equations in order to determine the lowest critical stress (buckling stress) as from solving the eigenvalue problem. Let for the moment keep in mind that N_x^0 , N_s^0 and N_{xs}^0 are *statically admissible*⁴¹⁰ Then the following perturbation expansion is be used

$$w^* = \underbrace{w^{(0)}}_{=0} + \underbrace{\Delta w}_{\equiv w}, \quad u^* = u^{(0)} + \underbrace{\Delta u}_{\equiv u}, \quad v^* = v^{(0)} + \underbrace{\Delta v}_v \quad (1.1157)$$

$$N_x = N_x^0 + \Delta N_x, \quad N_s^0 + \Delta N_s, \quad N_{xs} = N_{xs}^0 + \Delta N_{xs} \quad (1.1158)$$

Naturally, the perturbed state fulfil the all the three equilibrium equations 1.1154). Inserting this perturbed state to the equilibrium equations and accounting for elasticity and kinematics (plus some simplifications; shallow shell, ...) one obtains the linearised stability equations (For details and the linearised stability equations, refer to our textbook Section 9.4 [Chia Yoo]).

1.18.3 Energy criteria for stability loss of thin-walled cylindrical shell

In the following, Euler approach is adopted and the energy criterion in the Bryan form (Equation 1.143) will be used to derive the equations of stability. So, one

⁴⁰⁹Now, we do not perturb the external load system.

⁴¹⁰The pre-buckling stress resultants are the solution of the plane-stress solution of the equilibrium equations in the pre-buckled state.

should form the increments of strain energy and of the work of initial stresses between the perturbed and the primary state. As compared to flat plates, for shells, the membrane strain energy in the perturbed state should be accounted in addition to the bending strain energy.

Assume the thin-walled cylindrical shell being under a primary equilibrium pre-buckling pure membrane state⁴¹¹ N_x^0 , N_s^0 and N_{xs}^0 . An example of possible such initial bending state is depicted in Figure (1.217), to have a pictured idea.

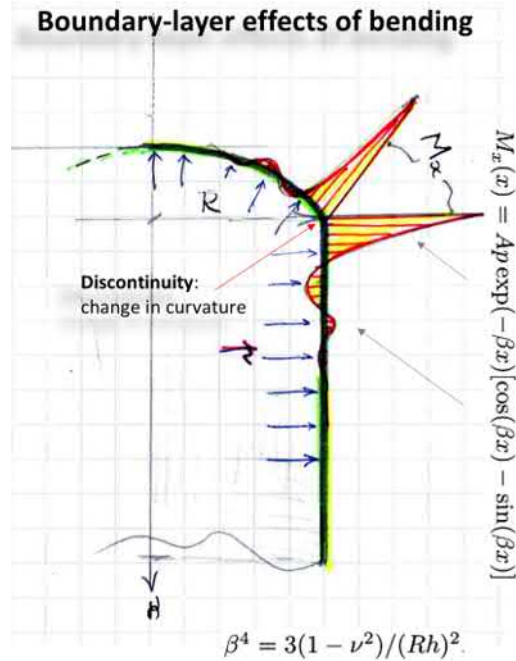


Figure 1.217: Illustration of possible initial bending state (in addition to the membrane state) in thin-walled cylindrical shell at discontinuity boundary.

So, no initial bending in this primary state and N_x^0 , N_s^0 and N_{xs}^0 are statically

⁴¹¹As previously, some footnotes before, we have mentioned that the presence of initial bending state \mathbf{M}^0 are in practice, inherent to thin-shells, and that they act as an initial imperfection. Such initial bending moments are very localised, close to boundaries, edges, discontinuities, supports, etc. They can be generically of the shape $M_i(x) \propto \exp(-\beta x) [\cos(\beta x) + \sin(\beta x)]$, where, the exponent $\exp(-\beta x)$ makes the effect decaying very quickly from the perturbation point and the $\cos(\beta x)$ and $\sin(\beta x)$ shows the periodicity of such effects. The decay coefficient is such that $\beta^4 = 3(1 - \nu^2)/(Rh)^2$, for instance, when a cylinder joins a half-sphere. usually, values of β [1/m] is large, so the decay is very quick. For, example, the bending moment in this case is given by $M_x(x) = Ap \exp(-\beta x) [\cos(\beta x) - \sin(\beta x)]$ This is why, the effect of bending are very localised and called *boundary-layer* effects (reunahäiriö, (sf)). So, in short, the effect of such initial bending state have to be accounted for in real structural design through physical and numerical experimentations.

admissible. The displacement field of the primary state u^0 , v^0 and w^0 are perturbed infinitesimally to a new adjacent equilibrium configuration $u^* = u^0 + u$, $v^* = v^0 + v$ and $w^* = w^0 + w$. The increments of displacements are denoted u , v and w , respectively.

Recall the Bryan form of the increment of the total potential energy in Bryan form (1.143)

$$\Delta\Pi = \underbrace{\frac{1}{2} \int_V \epsilon_1^T \mathbf{E} \epsilon_1 dV}_{\Delta U: \text{membrane + bending}} + \underbrace{\int_V \epsilon_2^T \sigma^0 dV}_{\text{quadratic part in } \Delta W(\sigma^0)} \quad (1.1159)$$

$$= \Delta U_{memb} + \Delta U_{bend} + \Delta W(\sigma^0). \quad (1.1160)$$

The components linear (\mathbf{L}) part of the strain increment ϵ_1 are

$$\begin{aligned} e_x &= \frac{\partial u}{\partial x}, & \kappa_x &= -\frac{\partial^2 w}{\partial x^2}, \\ e_s &= \frac{\partial v}{\partial s} + \frac{w}{R}, & \kappa_s &= -\frac{\partial^2 w}{\partial s^2} \\ \mathbf{L}\gamma_{xs} = 2e_{xs} &= \frac{\partial u}{\partial s} + \frac{\partial v}{\partial x}, & \kappa_{xs} &= -\frac{\partial^2 w}{\partial x \partial s}, \end{aligned}$$

respectively, for membrane deformation and bending of the mid-plane. The curvatures expressions above, except for κ_x , are approximations⁴¹² used in buckling of *shallow cylindrical shells*.

The quadratic part (second-order) of the strain increment ϵ_2 , on which the initial stress works, are

$$\epsilon_x^* \approx \frac{1}{2} \left(\frac{\partial u}{\partial x} \right)^2, \quad (1.1161)$$

$$\epsilon_s^* \approx \frac{1}{2} \left(\frac{\partial w}{\partial s} \right)^2, \quad (1.1162)$$

$$\gamma_{xs}^* \approx \frac{\partial^2 w}{\partial x \partial s}. \quad (1.1163)$$

Finally, as for the flat plate, one obtains

$$\Delta U_{bend} = \frac{1}{2} D \int_A \left[w_{,xx}^2 + w_{,ss}^2 + 2\nu w_{,xx} w_{,ss} + 2(1-\nu) w_{,xs}^2 \right] dA \quad (1.1164)$$

⁴¹²For instance $\kappa_{x\phi} = 1/R[w_{,x\phi} - v_{,x}]$ and $\kappa_s = 1/R^2[w_{,\phi\phi} - v_{,\phi}]$ where $ds = R d\phi$. For shallow shells the . Ref. Alfutov.

and

$$\Delta U_{memb} = \frac{1}{2}C \int_A \left[e_x^2 + e_s^2 + 2\nu e_x e_s + 2(1-\nu)e_{xs}^2 \right] dA \quad (1.1165)$$

$$= \frac{1}{2}C \int_A \left[u_{,x}^2 + v_{,s}^2 + 2\nu u_{,x} v_{,s} + \frac{1-\nu}{2}u_{,s}^2 + \frac{1-\nu}{2}v_{,s}^2 + \right. \quad (1.1166)$$

$$\left. + (1-\nu)u_{,s}v_{,x} + \frac{w^2}{R^2} + 2v_{,s}\frac{w}{R} + 2\nu u_{,x}\frac{w}{R} \right] dA. \quad (1.1167)$$

The increment work of initial pre-stresses, as for the flat plate⁴¹³, is

$$\Delta W(\sigma^0, \epsilon_2) = \int_A \left[N_x^0 \frac{1}{2}w_{,x}^2 + N_s^0 \frac{1}{2}w_{,s}^2 + N_{xs}^0 w_{,x}w_{,s} \right] dA. \quad (1.1168)$$

The linearised stability equations are obtained by requiring⁴¹⁴ that

$$\delta(\Delta\Pi) = 0, \quad \forall \delta u, \delta v, \delta w \quad (1.1169)$$

and provides the three equilibrium equations

$$C \left(u_{,xx} + \frac{1-\nu}{2}u_{,ss} + \frac{1+\nu}{2}v_{,xs} + \frac{\nu}{R}w_{,s} \right) = 0 \quad (1.1170)$$

$$C \left(v_{,ss} + \frac{1-\nu}{2}v_{,xx} + \frac{1+\nu}{2}u_{,xs} + \frac{\nu}{R}w_{,s} \right) = 0 \quad (1.1171)$$

$$D\nabla^4 w + \frac{C}{R} \left(\frac{w}{R} + v_{,s} + \nu u_{,x} \right) - \left(N_x^0 w_{,xx} + 2N_{xs}^0 w_{,x}w_{,s} + N_s^0 w_{,ss} \right) = 0 \quad (1.1172)$$

where the unknown displacement increments u , v and w are coupled. This provides a set of three *coupled* partial differential equations for the increments u , v and w . By eliminating⁴¹⁵ u and v from the obtained third equation of equilibrium

$$\boxed{D\nabla^4 w + \frac{C}{R} \left(\frac{w}{R} + v_{,s} + \nu u_{,x} \right) - \left(N_x^0 w_{,xx} + 2N_{xs}^0 w_{,x}w_{,s} + N_s^0 w_{,ss} \right) = 0} \quad (1.1173)$$

with the help of the two remaining equations of equilibrium one can eliminate u and v through derivations⁴¹⁶, and decouple partially and have

$$\nabla^4 u = \frac{1}{R}v_{,sss} - \frac{\nu}{R}u_{,xxx} \quad (1.1174)$$

$$\nabla^4 v = -\frac{1}{R}v_{,sss} - \frac{2+\nu}{R}u_{,xxs} \quad (1.1175)$$

⁴¹³Recall that we assumed, for the ideal cylindrical thin-walled shell, no initial bending pre-stresses.

⁴¹⁴Requiring that the perturbed state is also an equilibrium state.

⁴¹⁵Not easy to see: one should go through with a paper and a pen to see how the elimination generate the eight-order derivative in w ! Not a trivial task.

⁴¹⁶Higher derivatives needed in the third equation.

to finally, obtain⁴¹⁷ the praised Donnell⁴¹⁸ of stability

$$\boxed{D\nabla^8 w + \frac{Eh}{R^2} w_{,xxxx} - \nabla^4 \left(N_x^0 w_{,xx} + 2N_{xs}^0 w_{,xw,s} + N_s^0 w_{,ss} \right) = 0} \quad (1.1176)$$

Usually, a pressure term p is present (external pressure) and the equation is then written as

$$D\nabla^8 w + \frac{Eh}{R^2} w_{,xxxx} - \nabla^4 \left(N_x^0 w_{,xx} + 2N_{xs}^0 w_{,xw,s} + N_s^0 w_{,ss} \right) = \nabla^4 p \quad (1.1177)$$

The pressure is usually constant and its gradients vanishes. This was the story of genesis of the very well-known stability equation⁴¹⁹. Even though, the real stability behaviour of thin-shells is determined by the huge effect of imperfections, and *accessing this behaviour* becomes realistic only through *experiments* and *computational approaches (FE)*, knowing the concepts makes us, engineers, more 'solid'.

* * *

1.18.4 Cylindrical shells under uniform axial compression

Before even breathing, let's recall that now we deal with a theoretically *perfect* shell. Not less important is to recall work by Koiter⁴²⁰ and many others⁴²¹, showing that by post-buckling analysis and experimentally, the collapse load or buckling load is dramatically reduced from the one obtains for a perfect shell. So, the theoretical approach bellow is useful for at least to reasons: 1) for providing as the control parameters (handlers, dimensionless product, ...) of the system and 2) for cylindrical and spherical shells giving a fact-based estimate for the buckling (or collapse) load of the imperfect shell just by reducing the theoretical value (when the 'formula' is available) of the perfect shell by a factor 3 to 8 as proven by studies. At least, the engineer obtains an estimate which is on the map (order of magnitude).

⁴¹⁷This exercise is left to the student.

⁴¹⁸Donnell derived using approximation of shallow shells a non-linear equation for buckling of thin-walled cylindrical cylinders under end-torsion. He also generalised the model to arbitrary curvature.

⁴¹⁹For details on the full derivation of these *non-linear large deflection equations* of Donnel-type, please refer to literature. The lecture notes by Emeritus M. Tuomala are very detailed on this specific point as is also (Chapter 9) our course textbook by Chai Y.H. and Sung C.L. *Stability of Structures*.

⁴²⁰Koiter, W.T., 1963. The effect of axisymmetric imperfections on the buckling of cylindrical shells under axial compression. *Proc. K. Ned. Akad. Wet., Amsterdam*, ser. B, vol. 6; also, Lockheed Missiles and Space Co., Rep. 6-90- 63-86, Palo Alto, California.

⁴²¹There is an extensive publications addressing this behaviour.



Axial buckling failure in service.

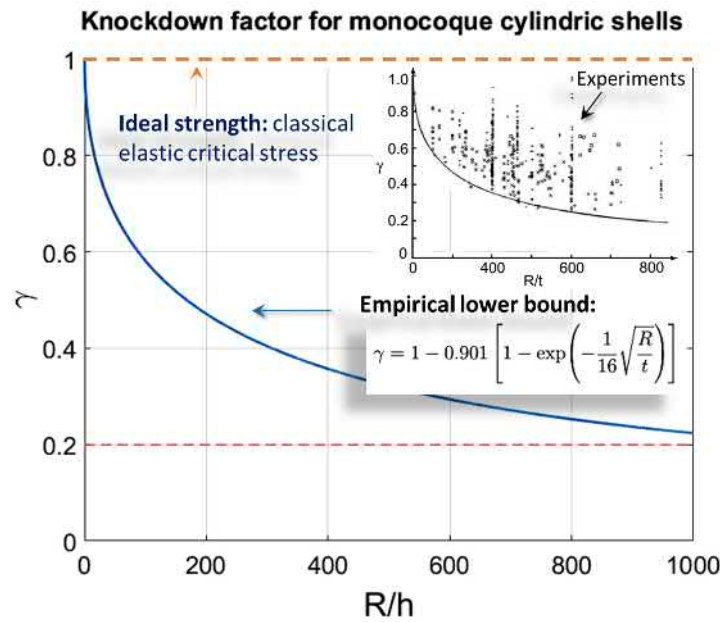


Figure 1.218: Conservative lower bound for the experimentally based *knock-down* factor for reducing the theoretical buckling stress of a perfect cylindrical thin monocoque shell. Ref. for expression of the empirical Buckling Knockdown Factor γ (BKF) : R.M. Jones. *Buckling of Bars, Plates, and Shells*. 2006. See also BKF NASA SP-8007.

So, this methodology of reducing the theoretical buckling by a factor γ is a current practice in design of cylindrical shells again buckling⁴²². Indeed, the actual buckling load P_{cr} of such shells is estimated down⁴²⁴ as

$$P_{cr} = \gamma P_{cr,0} \quad (1.1178)$$

where γ being a *Shell Buckling Knockdown Factor* (SBKF) given by the standards and based which based on experiments. The reference buckling stress (called also as Euler buckling stress) being obtained by a linear bifurcation analyses for simply supported shells, for instance, $\sigma_{cr} = \frac{E}{\sqrt{3(1-\nu^2)}} \frac{h}{R}$. The *knock-down* factor (Figure 1.218) is empirically determined in terms of ratio R/h ⁴²⁵. For instance⁴²⁶, based

⁴²²For your information such 'knock-down'-factor⁴²³ simplified approach approach to shell buckling design is in extensively used in NASA space vehicle design. The reference buckling load can, for instance, be obtained by a linear bifurcation analyses for simply supported shells.

⁴²⁴Lower bound

⁴²⁵NASA SP-8007: NASA Space vehicle design criteria (Structures) *Buckling of thin-walled circular cylinders* (1968)

⁴²⁶R.M. Jones. *Buckling of Bars, Plates, and Shells*. Bull Ridge, Blacksburg. 2006

on an extensive amount of experimentally measured values of the knock-down factor derived provides a lower bound as

$$\gamma = 1 - 0.901 \left[1 - \exp \left(-\frac{1}{16} \sqrt{\frac{R}{t}} \right) \right], \quad \text{for } R/h < 1500 \quad (1.1179)$$

Note that, in both cases of buckling, the kinematic boundary conditions along the radial direction R is such that the lateral expansion, along the edge-meridian of application of load is free (rollers) to move to avoid local bending stresses (so, only membrane initial stress state arise). Otherwise, such (very local) bending should be accounted in the pre-buckling deformation.

Finally, This being said, let's start with the simplest case in complexity. Despite this simplification, the problem is enough challenging to start with and to study key stability behaviour os shells of revolution. Two types of buckling modes will be considered: *ring buckling* and *chessboard buckling*. The first one corresponding axisymmetric and the second, asymmetric modes.

Axisymmetric buckling of circular cylindrical shells under uniform axial compression

A simply supported isotropic thin cylindrical shell of radius R under uniform axial compression $N_x^0 = -N/(2\pi R)$ (with $N > 0$ for compression) will axially shorten and increase in diameter (when no boundary local bending effects) (Figure a) (1.219)). So, the pre-buckling stress state is axisymmetric and we have

$$N_x^0 = -\frac{N}{2\pi R}, \quad N_{xs}^0 = N_s^0 = 0. \quad (1.1180)$$

Inserting the above stress resultants into the Donnell equation (1.1176) we obtain

$$D\nabla^8 w + \frac{Eh}{R^2} w_{,xxxx} - \nabla^4 N_x^0 w_{,xx} = 0 \quad (1.1181)$$

The above Stability loss equation is a linear partial equation with constant coefficients. Taking a trial solution in the form⁴²⁷

$$w(x, s) = A \sin \frac{m\pi x}{\ell} \sin \frac{n\pi s}{\ell} \quad (1.1182)$$

and inserting it into the stability equation (1.1181) leads to an eigenvalue problem which solution gives the buckling stress. We will not proceed this way, in this reading material, but solve the same equation in its simplified form (Equation 1.1183) which can be thought derived by integrating successively four times the stability equation (1.1181). Later, complexity will be added and other buckling modes will come to life.

⁴²⁷So we restrain the buckling mode to this shape. There can be other type of buckling mode. This point will be treated later.

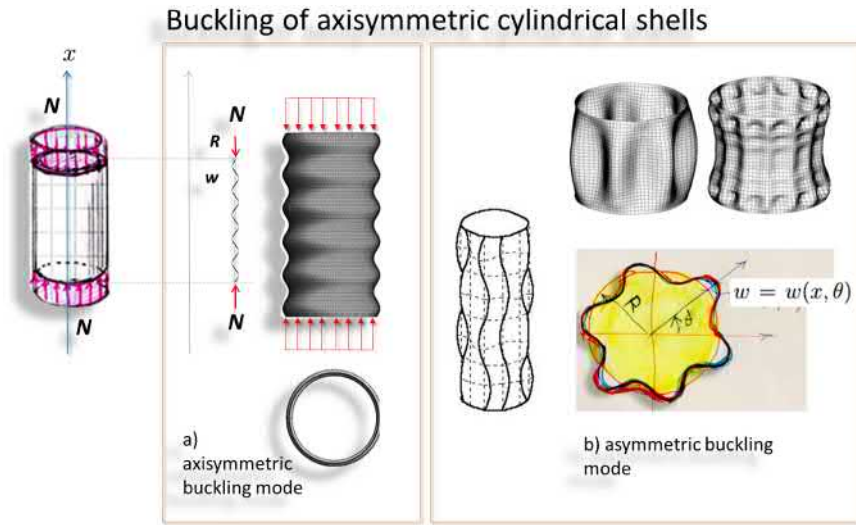
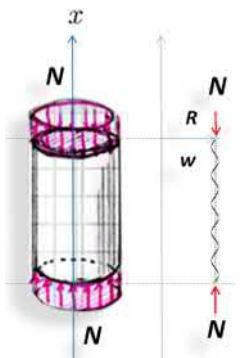


Figure 1.219: Symmetric (*ring patterns*) and asymmetric (*chessboard patterns*) buckling modes of cylindrical shells.



Cylindrical shell under uniform compression. Axisymmetric buckling mode.

So, consider an isotropic thin cylindrical shell of radius R under uniform axial compression buckling in an *axisymmetric mode* (called 'ring mode') (Figure a) (1.219)). Let first give, before hand, the linearised equation of stability, one of its important characteristic related to its mathematical structure and then, a bit later, go back to basics and show how such equation is derived through energy criterion. So, the stability behaviour of such shells is given by the following linearised differential equation (Lorentz, 1908; Timoshenko, 1910)

$$D \frac{d^4 w}{dx^4} + N \frac{d^2 w}{dx^2} + \frac{Eh}{R^2} w = 0, \tag{1.1183}$$

Note that it can be derived from the more general Donnell equation (1.1181). As usual, the bending rigidity per unit width $D = Eh^3/12(1-\nu^2)$, R the radius of the cylinder, $w(x)$ the radial deflection increment and x being the axial coordinate. Recall that axisymmetry means that all the displacements depend only on the x axial coordinate. In case on asymmetric, for instance, $w = w(x, \theta)$, where θ being the angle in cylindrical coordinate system and x the elevation (Figure b) (1.219).

Similarity: Firstly, Equation (1.1183) is analogous with the linearised buckling equation of axially compressed column-beam bounded to an elastic foundation which is (re-call) completely similar with

$$EI \frac{d^4 w}{dx^4} + N \frac{d^2 w}{dx^2} + kw = 0, \tag{1.1184}$$

when we identify

$$D \rightarrow EI, \quad \frac{Eh}{R^2} \rightarrow k. \quad (1.1185)$$

What the similarity⁴²⁸ brings to us? If we know the solutions for the beam on elastic foundation then the solution for the shell under some boundary conditions are the same. The only thing to do is to exchange the physical parameters as given by the relations above. So, in the shell problem, Eh/R^2 plays the role of the stiffness k [N/m] of the elastic foundation for the beam. Therefore $Eh/R^2 w$ is an effective radial reaction for the shell.

The solution: Consider a simply supported cylindrical shell of axial length ℓ being a multiple of the half-sine waves of m mode in the longitudinal direction. Or, assume a relatively very long shell with comparison with its radius R . In these cases, the *simply supported boundary conditions* hold well. This boundary condition requirement means that the initial state is a *membrane* state only. Other type of boundary conditions can lead to a very localised initial bending state that should be accounted for in the initial state. This being said, we continue with a membrane initial state. The fourth-order ordinary differential equation (1.1183) has an exact solution of the form

$$w(x) = w_0 \sin \frac{m\pi x}{\ell} \quad (1.1186)$$

which fulfils automatically the boundary conditions. w_0 is an indeterminate non-zero constant. Following standard solution procedure for the eigenvalue problem and substitution of the solution into the ODE gives the critical load

$$N_{cr} = D \left[\alpha_m^2 + \frac{Eh}{\alpha_m^2 R^2 D} \right], \quad \alpha_m = \frac{m\pi}{\ell}. \quad (1.1187)$$

The buckling load N_{cr} (for an ideally perfect cylinder) corresponds to the smallest positive value in the equation above with respect to m which is

$$\boxed{N_{cr} = \frac{E}{\sqrt{3(1-\nu^2)}} \frac{h^2}{R} \rightarrow \sigma_{cr} = \frac{E}{\sqrt{3(1-\nu^2)}} \frac{h}{R}} \quad (1.1188)$$

obtained for

$$\alpha_{cr} = \frac{m_{cr}\pi}{\ell} = \left[\frac{Eh}{R^2 D} \right]^{1/4}, \quad (1.1189)$$

which corresponds to a buckling mode with a half-wave $m = m_{cr}$.

Keep in mind: Inherently, the geometry of cylindrical shell is not perfect or there is other types of imperfection having the overall effect to reduce the experimentally observed value for the buckling stress. In order to account for

⁴²⁸The similarity starts and stops at the bifurcation point and no extrapolation further even to initial post-buckling behaviour is correct.

this discrepancy, the buckling axial stress is reduced by an empirical factor⁴²⁹ $0 < \gamma < 1$ and is rewritten as

$$\sigma_{cr} = \frac{\gamma E}{\sqrt{3(1-\nu^2)}} \frac{h}{R}. \quad (1.1190)$$

We will come to this reduction after few paragraphs. Now, lets finish the previous talk.

In cases when the length ℓ is not a multiple of half-wave number m the critical load can be found form the lower-bound of the graphs of the critical load $N_{cr}(m)$ (1.1188) as function of m (Figure (TO DO)).

Note that, since we *assumed an axisymmetric buckling mode* and excluded any possible non-axisymmetric mode, the *critical buckling load* given by Equation (1.1188) represents an *upper-bound* for the true collapse load.

The critical stress σ_{cr} depends on the material through E and ν and on the relative thickness h/R . The length of the shell ℓ does not play a role as long as it is not to short.

The more complex case of *non-axisymmetric* buckling mode will be addressed in the following. In such mode all the components of the displacement u (longitudinal), v (tangential) and w (radial) should be included.

Asymmetric buckling of circular cylindrical shells under uniform axial compression

Now, the buckling shape is in for of a chessboard patten (Figure b) & c) 1.220). The displacement increment $w = w(x, \theta)$ has both circumferential and axial contributions in the form⁴³⁰

$$w(x) = w_0 \cdot \sin \frac{m\pi x}{\ell} \cdot \sin n\theta, \quad (1.1191)$$

where $2n$ being the number of half-waves⁴³¹ dividing the circumference. bellow, I reproduce, for memory consolidation, the typical buckling mode types: symmetric and asymmetric (Figure 1.220).

Bellow, I also reproduce for educational purposes, the Matlab-code (1.221) used for plotting the buckling shapes.

The details of establishing the results bellow, will be presented in further coming section. Now, the results are presented directly. Anyway, inserting the

⁴²⁹NASA SP-8007: NASA Space vehicle design criteria (Structures) *Buckling of thin-walled circular cylinders* (1968)

⁴³⁰H.G. Allen and P.S. Bulson. *Background to Buckling*. Mc-Graw-Hill (1980).

⁴³¹So, we have 2π -half waves.

Buckling of axisymmetric cylindrical shells under uniform compression

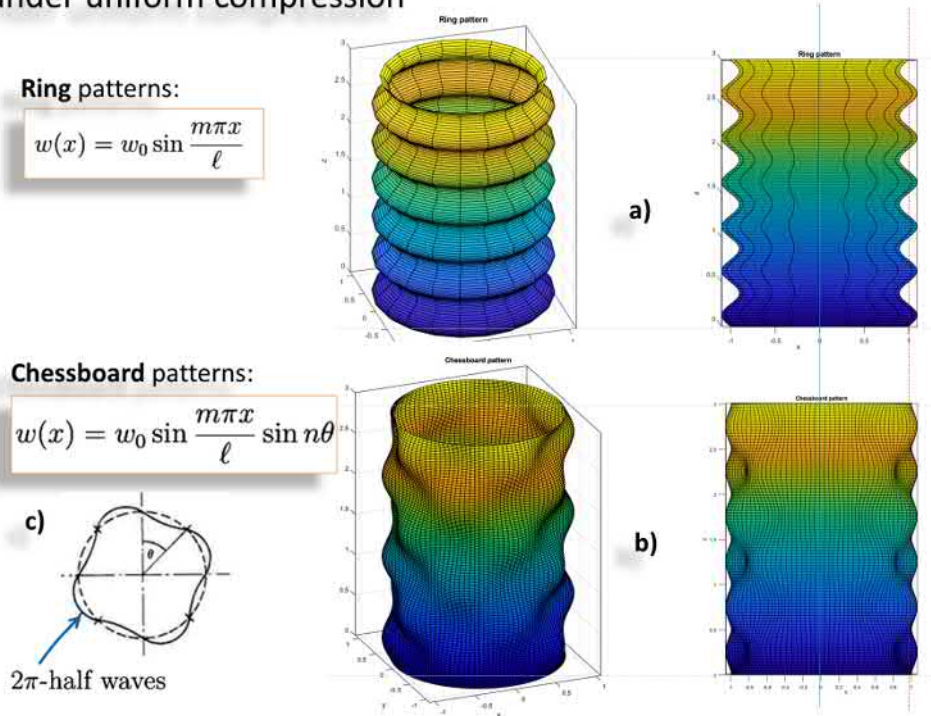


Figure 1.220: Illustration of symmetric and asymmetric buckling modes of cylindrical shells under uniform compression. (The buckling modes are drawn using Matlab (1.221)).

trial buckling mode into the equation of equilibrium⁴³² (in the deformed configuration) on obtains

$$\sigma_{cr} = \frac{Eh^2}{12(1-\nu^2)} \underbrace{\left[\frac{(n^2 + (m\pi R/\ell)^2)^2}{R^2(m\pi R/\ell)^2} + \frac{E(m\pi R/\ell)^2}{(n^2 + (m\pi R/\ell)^2)^2} \right]}_{\min}, \quad (1.1192)$$

Through minimisation, the buckling stress (lower stress) occurs for

$$\frac{n^2 \ell^2 + (m\pi R)^2}{m\pi R \ell} = \frac{n^2 + (m\pi R/\ell)^2}{m\pi R/\ell} = \left[\frac{Eh}{R^2 D} \right]^{1/4}, \quad (1.1193)$$

and gives

$$\sigma_{cr} \equiv \sigma_{\min} = \frac{E}{\sqrt{3(1-\nu^2)}} \frac{h}{R}. \quad (1.1194)$$

⁴³²Note that now we have the asymmetric mode, so partial differential equation is quite complicated. Refer to classical literature⁴³³ for that.

```

1  % asymmetric chessboard bucklin of cylinder-shell
2  % Plotting only.
3  % Author: D. Beroudi, 2019
4  %
5  % Z - cylinder axis Z = [0, L]
6  % THETA - 0:2*pi
7
8  %%
9  RO = 1; % Radius
10 L = 3*RO; % length
11 m = 6; % nbre 1/2-waves in z-direction
12 n = 5; % nbre 1/2-waves in theta direction
13 w0 = RO/10
14 NP = 4 * 30 ;
15
16 theta = linspace(0,2*pi, NP);
17 z = linspace(0,L, NP);
18
19 % Generating the mesh ---
20 z = meshgrid(z);
21 [R, THETA] = meshgrid(z, theta);
22
23 % The radial displacement w(z, theta) at (z, theta) ---
24 w_z_theta = w0 * sin( m * pi * z / L) .* sin(n * THETA);
25
26 % Plotting the cylinder surface ---
27 % 1) Chessboard pattern
28
29 figure
30 surf( (RO + w_z_theta) .* cos(THETA), (RO + w_z_theta) .* sin(THETA), Z);
31 axis square
32 grid on
33 box on
34 title('Chessboard pattern')
35 xlabel('x')
36 ylabel('y')
37 zlabel('z')
38
39 % -----
40 % 2) Ring pattern
41 figure
42 m = 8;
43 [X, Y, Z] = cylinder(RO + w0 * sin( m * pi * z / L));
44 surf(X,Y,Z*L)
45 axis square
46 grid on
47 box on
48 axis equal
49 title('Ring pattern')
50 xlabel('x')
51 ylabel('y')
52 zlabel('z')

```

Figure 1.221: The Matlab-script used to draw the buckling modes in Figure (1.220).

The obtained value (Equation 1.1194) is the same as for ring-type (axisymmetric) buckling when m^2 being large enough. The other surprising thing is that this critical stress does not depend on the length ℓ neither on the number n of buckles in the circumferential direction. However, for short cylinders,⁴³⁴ the number n of lobes affect the critical buckling stress.

Another interesting (not a wished property for a structure) behaviour can be seen: from formula (Equation 1.1193) one sees that we have accumulation of modes and consequently on eigenvalues (critical loads) as the minimisation function being very shallow (Figure 1.222). This unfortunate property render the structure very sensitive to imperfections. One see that, even the *elementary analytical approach* we have performed revealed us a deep hidden *a priori, non-trivial*, at all, property for thin cylindrical shells under compression, at least. So let this be one of the answers to the student *who once was wondering the usefulness of analytical approach*.

Recall, again, that the above obtained theoretical initial buckling formulas (for perfect shells) for critical stresses over-estimates considerably the observed collapse load in tests (Figures 1.218 and 1.224). This dramatic difference is explained when addressing the post-buckling behaviour of such thin shells.

⁴³⁴Timoshenko and Gere.

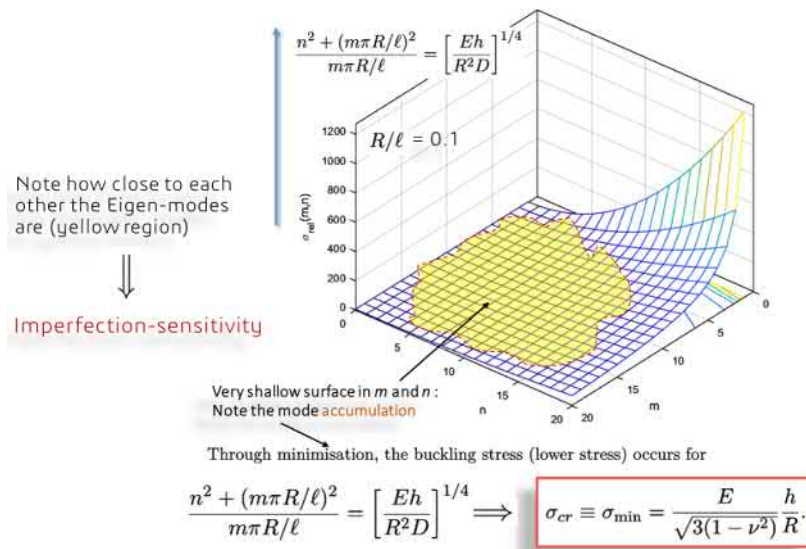


Figure 1.222: Accumulation of modes for m and n . Very shallow surface. Note how close to each other the eigenmodes are (yellow region); this makes the structure imperfection-sensitive.

Solution using Donnell’s linearised buckling equations for axially loaded cylinder

here we solve, for pedagogical purposes, the problem already solved previously using the linearised Donnell’s buckling equations (Eqs. 1.1177) in which now

$$N_x^0 = \sigma_x^0 h \equiv -\bar{\sigma}_x h = -\frac{P}{2\pi R} \quad \text{and} \quad N_{xs}^0 = N_s^0 = 0. \tag{1.1195}$$

The Equation (1.1177) becomes

$$D\nabla^8 w + \frac{Eh}{R^2} w_{,xxxx} - \nabla^4 \left(\underbrace{N_x^0}_{-\frac{P}{2\pi R}} w_{,xx} + \underbrace{2N_{xs}^0 w_{,x} w_{,s} + N_s^0 w_{,ss}}_{=0} \right) = \underbrace{\nabla^4 p}_{=0} \tag{1.1196}$$

$$\implies D\nabla^8 w + \frac{Eh}{R^2} w_{,xxxx} + \underbrace{\frac{P}{2\pi R}}_{\bar{\sigma}_x} \nabla^4 w_{,xx} = 0. \tag{1.1197}$$

The above eigenvalue problem represents an eight-order differential equation with constant coefficients. The trial

$$w(x, s) = A \sin\left(\frac{m\pi x}{\ell}\right) \sin\left(\frac{n\pi s}{\pi R}\right) = A \sin\left(\frac{m\pi x}{\ell}\right) \sin\left(\frac{\beta\pi s}{\ell}\right) \tag{1.1198}$$

is kinematically admissible (simply supported shell). Note the definition $\beta = n\ell/(\pi R)$. Inserting into the equation one obtains

$$D \left(\frac{\pi}{\ell} \right)^8 (m^2 + \beta^2) + \frac{Eh}{R^2} m^4 \left(\frac{\pi}{\ell} \right)^4 - \bar{\sigma}_x h \left(\frac{\pi}{\ell} \right)^6 m^2 (m^2 + \beta^2)^2 = 0. \quad (1.1199)$$

Simplifying a bit the above equation using notation

$$Z = \frac{\ell^2}{Rh} \sqrt{(1 - \nu^2)} \quad \text{and} \quad k_x = \frac{\bar{\sigma}_x h \ell^2}{D\pi^2}, \quad (1.1200)$$

where k_x being the buckling stress parameter and Z known as Batdorf parameter which makes distinction between short and long cylinders. After some *pyörittelyjä* one obtains the critical stress parameter

$$k_x = \frac{(m^2 + \beta^2(n))^2}{m^2} + \frac{12Z^2 m^2}{\pi^4 (m^2 + \beta^2(n))^2}. \quad (1.1201)$$

The buckling stress being the smallest k_x , one need minimisation with respect to m and n (recall that $\beta = \beta(n)$) to obtain *the classical result* we already obtained previously;

$$k_{x,min} = \frac{4\sqrt{3}}{\pi^2} Z \implies \sigma_{cr,min} \equiv \sigma_E = \frac{1}{\sqrt{3(1 - \nu^2)}} \frac{Eh}{R}, \quad (1.1202)$$

where the minimum of k_x is attained when

$$\frac{[m^2 + \beta^2(n)]^2}{m^2} = \sqrt{\frac{12Z^2}{\pi^4}}. \quad (1.1203)$$

For short cylinders ($Z < 2.85$), optimal m and n should be found through trials. ($m = 1$ and $\beta = 0$) seems a limit when $\ell \rightarrow 0$) and gives

$$k_x = 1 + \frac{12Z^2}{\pi^4}. \quad (1.1204)$$

For a very long cylinder, taking the limit for the critical stress as $\ell \rightarrow \infty$ does not, naturally, give the correct Euler buckling load for the flexural buckling of a slender column⁴³⁵

Effect of imperfection on post-buckling behaviour

This section is, for the moment, a collection of well-known results. Later, some analytical asymptotic analysis or Finite Element based post-buckling analysis will be done.

⁴³⁵This is an expectable result; do not wait too much from successive approximations of approximations to find an Euler-Bernoulli beam hidden in the cylindrical shell which wasn't originally there.

Figure (1.223) shows a schematic representation of the typical post-buckling behaviour of axially compressed thin cylindrical shells (Jones, 2006). It is this behaviour is one of the reasons making such shells *imperfection-sensitive* structures as regard to stability. The lowest post-buckling stress, in the Figure, represents a lower bound for the buckling stress for the perfect structure. With imperfections, the lowest value decreases. The sharp pick appears only for ideally perfect shells which, practically, do not exist. For imperfect shell, the pick is smoothed and its value is much lower.

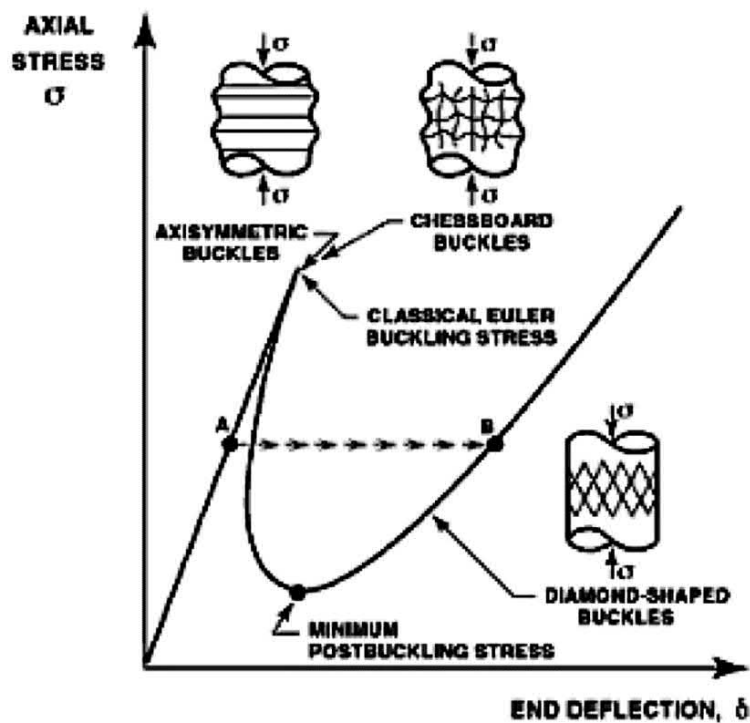


Figure 1.223: Typical post-buckling behaviour of axially compressed ideally perfect thin cylindrical shells (ref. Robert Jones, buckling of bars, plates and shells.). [DRAW by hand]

Figure (1.224) shows the scatter of buckling test results⁴³⁶ of thin cylinders in axial compression. The reduction $\sigma_{\max}/\sigma_{\text{cr}}$ of the measured collapse (buckling) stress σ_{\max} to the theoretical value σ_{cr} of the perfect shell as function of the relative inverse R/h of the thickness h .

Most cylindrical shells are not ideal cylinders. Introducing an initial geometric

⁴³⁶H.G. Allen and P.S. Bulson. *Background to Buckling*. Mc-Graw-Hill (1980).

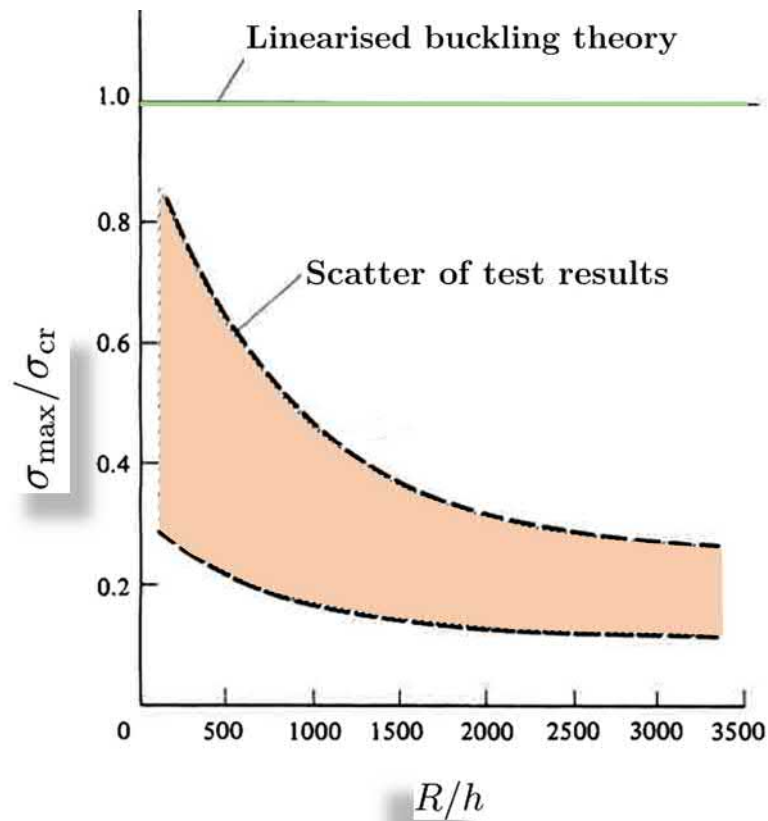


Figure 1.224: Scatter of buckling test results of thin cylindrical shells in axial compression. (Adapted from H.G. Allen and P.S. Bulson. *Background to Buckling*. Mc-Graw-Hill (1980).)

imperfection through a deviation of the deflection as w_0 of the form⁴³⁷

$$w_0 = A_0 \left(\cos \frac{m\pi x}{R} \cos(n\theta) + B_0 \cos \frac{2m\pi x}{R} + C_0 \cos(2n\theta) + D_0 \right) \quad (1.1205)$$

and obtained the sensitivity diagram shown in Figure⁴³⁸ (1.225) in terms of the amplitude of relative imperfection A_0/h .

Koiter⁴³⁹ work on effect of imperfections on post-buckling behaviour is very valuable contribution for structural designers. He investigated the peak stress σ_{\max} in terms of axisymmetric initial displacements and he showed that the reduction of the peak stress (ultimate, collapse stress or experimental value) with

⁴³⁷Donnel and Wan

⁴³⁸T. Von Kármán, H.S. Tsien The buckling of thin cylindrical shells under axial compression. *J. Aeronaut. Sci.*, **8** (303–312) (1941), p. 1941

⁴³⁹His doctoral thesis is available in the internet.

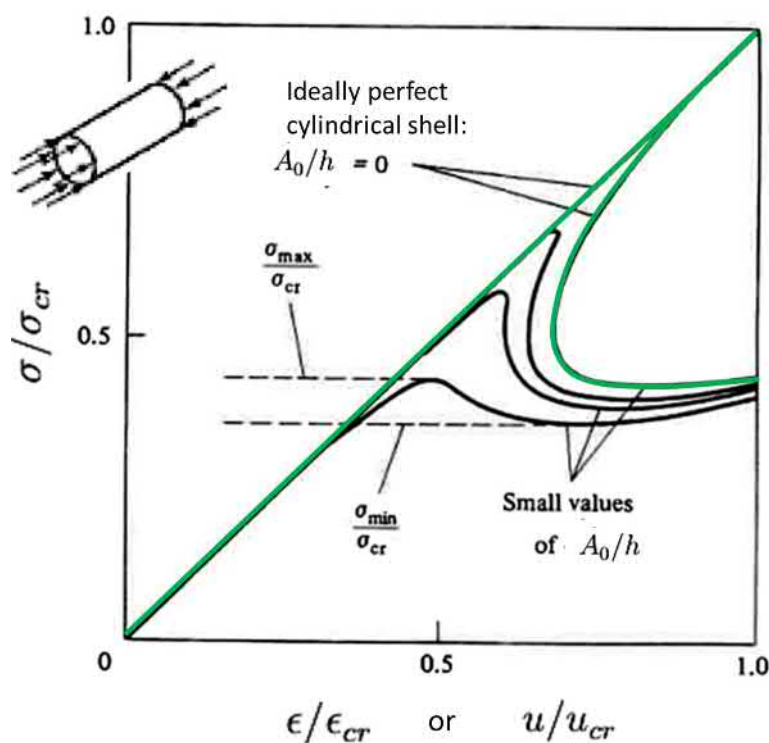


Figure 1.225: Effect of initial geometrical imperfections on post-buckling behaviour of cylindrical shells. (Adapted from Donnel and Wan). Equilibrium paths for geometrically perfect compressed cylindrical shells (green line, from Von Kàlmàn and Tsien (1941)) and for imperfect cylindrical shell (black lines, by Donnel and Wan (1950)). The steeply falling branches are unstable.

respect to the ideal critical stress σ_{cr} for a perfect cylinder in terms of $\sigma_{max.}/\sigma_{cr}$ follows the relation (Cf. to its other form in Equation⁴⁴⁰ (1.1142)

$$\frac{\sigma_{max.}}{\sigma_{cr}} \cdot \frac{w_0}{h} = \left(1 - \frac{\sigma_{max.}}{\sigma_{cr}}\right)^2 \left(\frac{4}{27(1-\nu^2)}\right)^{1/2} \quad (1.1206)$$

where the initial geometrical imperfection amplitude w_0 being relative to shell thickness as w_0/h . The graph of Equation (1.1206) is presented in Figure (1.226)⁴⁴¹. Formula (1.1206) can be re-written in the practical form

$$\left(1 - \frac{\sigma_{max.}}{\sigma_{cr}}\right)^2 - K \left(\frac{\sigma_{max.}}{\sigma_{cr}}\right) \cdot \left(\frac{w_0}{h}\right) = 0 \quad (1.1207)$$

⁴⁴⁰ $(1 - \rho_s)^2 - A\rho_s|\bar{\xi}| = 0.$

⁴⁴¹Koiter, W.T., 1963. The effect of axisymmetric imperfections on the buckling of cylindrical shells under axial compression. *Proc. K. Ned. Akad. Wet.*, Amsterdam, ser. B, vol. **6**; also, *Lockheed Missiles and Space Co.*, Rep. 6-90-63-86, Palo Alto, California.

where K being a constant ($K = 0.4035$ for $\nu = 0.3$). In Koiter's formula⁴⁴², one

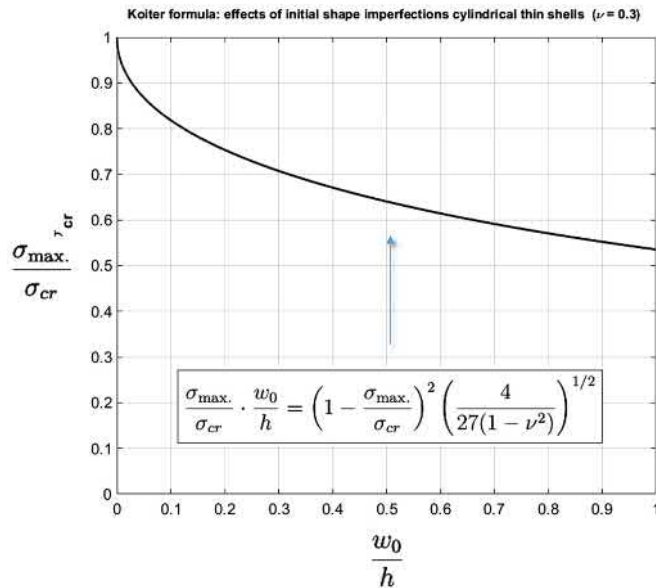


Figure 1.226: Effect of initial geometrical imperfections on post-buckling behaviour of thin-walled cylindrical shells as given by Koiter's formula. ($\nu = 0.3$). [! The formula by Koiter in his dissertation gives different values! (The FORMULA is CORRECT but THIS GRAPH IS not correct,; to be corrected) DB & RK, Selvitä!]

can assume the relative imperfection amplitude w_0/h being proportional to R/h and re-write the formula in terms of R/h .

1.18.5 Finite Element based Linear buckling analysis

Axially compressed simply supported cylindrical thin shell

Let's start with an illustrative example. Figure (1.228) illustrates results of a Finite Element⁴⁴³ linear buckling analysis. The idea was to show that, the buckling loads are really close to each other. This makes the shell structure even highly imperfection and perturbation sensitive. The boundary conditions used

⁴⁴²The formula by Koiter in his dissertation, p. 286, $\lambda^*/\lambda_1 = 1 + 1.24e - \sqrt{(1.24e(2 + 1.24e))}$, where $e = w_0/h$ the initial geometrical imperfection relative amplitude, gives different values when I draw the graphs from the Koiter's formula (Eq. 1.1206)! DB & RK, Selvitä!

⁴⁴³I used here full 3D solid elements because I couldn't figure out what shell theory COMSOL is using. Palataan asiaan myöhemmin paremmalla ajalla. Now, I am in a hurry with time. It is coming out, for me, that I should invest more time and do simulations also in Abaqus.

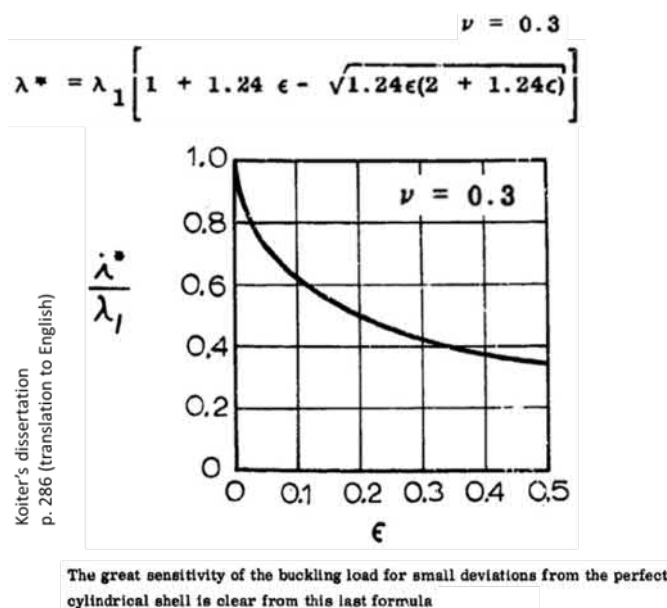


Figure 1.227: Effect of initial geometrical imperfections on post-buckling behaviour of compressed thin-walled cylindrical shells as given by the original Koiter's formula. In this figure, $\epsilon \equiv w_0/h$ and $\lambda^*/\lambda \equiv \sigma_{\max}/\sigma_{cr}$. Published also in: Koiter, W.T., 1963. The effect of axisymmetric imperfections on the buckling of cylindrical shells under axial compression. *Proc. K. Ned. Akad. Wet.*, Amsterdam, ser. B, vol. **6**; also, *Lockheed Missiles and Space Co.*, Rep. 6-90-63-86, Palo Alto, California..

are shown in Figure (1.229).

Buckling of axially compressed thin cylindrical shell

The boundary conditions (kinematic) are those of simply support shell (no initial local bending stresses). Follows the data for geometry and material: $R_{\text{ext}} = 20$ m, shell thickness $h = R_{\text{ext}}/200$, the radius of the shell $R = R_{\text{ext}} - h/2$, $\ell = 3R_{\text{ext}}$, $E = 70$ GPa, $\nu = 0.33$.

FE based linear buckling analysis is performed. The boundary conditions, are in practice, those shown in Figure (1.229). The results, buckling load and corresponding modes, obtained using the FE linear buckling analysis, are depicted in Figure (1.230). The first thing to notice how close are the first six buckling loads.

Axially compressed cylindrical thin shell with free edge

Equivalently, ... $R = 30$ mm, $\ell = 100$ mm, $h = 1$ mm, $E = 210$ MPa, $\nu = 0.3$ (steel). The first buckling modes and loads are shown in Figure (1.231). [TO

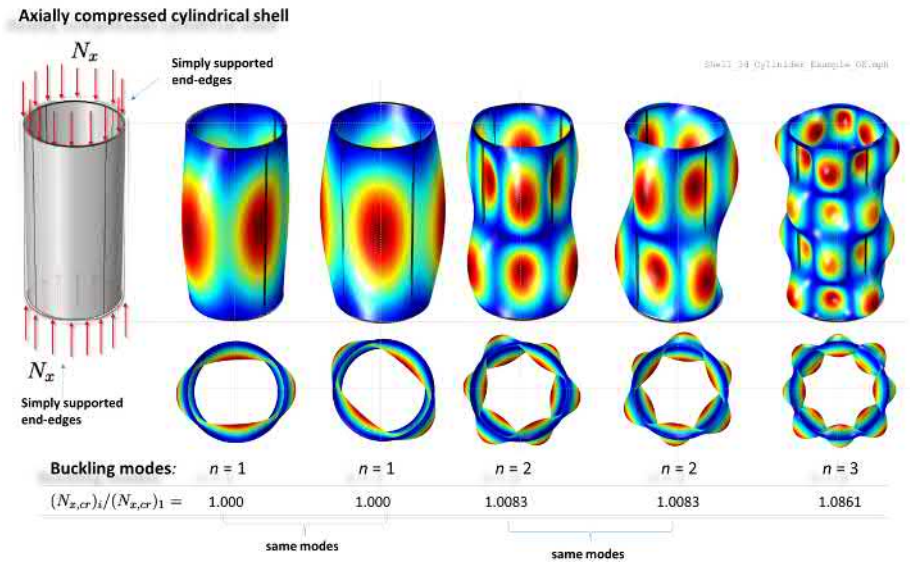


Figure 1.228: Example of buckling modes obtained by FE-buckling analysis for a simply supported cylindrical shell. Notice how close are the buckling loads with respect to the first one.

DO: selostus]

1.18.6 Finite Element based post-buckling analysis

Cylindrical thin-walled shells under compression with various types of imperfections ... (Figure 1.232) ... In order to obtain a robust estimation of the knock-down factors (similar to those in Figure 1.226) experimental validation mixed with finite element simulation is a current practice our days.

[TO DO, 6.2.2019]

1.19 Stability of cylindrical panels

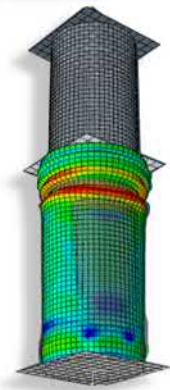
Such panels are usually used as roof structures in buildings and other structures (Figure 1.233). So, they are objects that a student in civil engineering should know how to analyse ...

Coming soon ... [TO DO, 6.2.2019]

1.20 Advanced computational simulations

This section shows some computational simulations which out of the scope of the current course on elastic stability of structures. So, you can escape reading it,

Mild-steel tube crash simulation (Abaqus/Explicit)
[D. Baroudi, 2019]



Simulation: material and geometrical non-linearities and time-dependency. At t_1

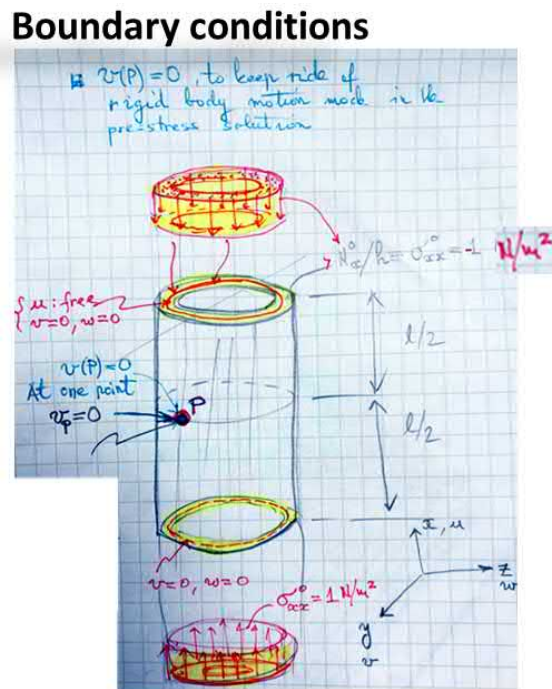


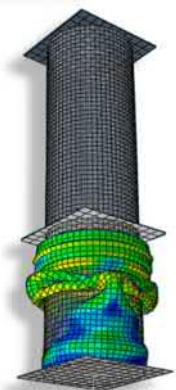
Figure 1.229: Boundary conditions used in the illustration example of Figure (1.228) to simulate simply supported edges for comparing with theoretical results.

totally.

In this particular one, a the continuous crash of a mild-steel tube is simulated (velocity control). The material behaviour is more complex than elastic: rate-dependent (visco-) plasticity with frictional contact. Illustrative results are shown in Figure (1.234) which is reproduced here only for motivating students to come to the course weakly named *material modelling in civil engineering*⁴⁴⁴ A multiplicative Johnson-Cook rate-dependent plasticity model with isotropic hardening was used. Such model is suitable for high strain rate visco-plasticity (see Abaqus manual). The elastic behaviour was modelled with linear elastic isotropic model. The yield stress is given⁴⁴⁵ by

$$\bar{\sigma} = [A + B(\bar{\epsilon}^{pl})^N][1 + C \ln \frac{\dot{\bar{\epsilon}}^{pl}}{\dot{\bar{\epsilon}}_0}][1 - \bar{\theta}^M] \tag{1.1208}$$

Mild-steel tube crash simulation (Abaqus/Explicit) [D. Baroudi, 2019]



Simulation. *idem.* at $t_1 + \Delta t$

⁴⁴⁴Correct name: *Mechanics of constitutive modelling of solids.*

⁴⁴⁵See Abaqus 6.11 User's manual.

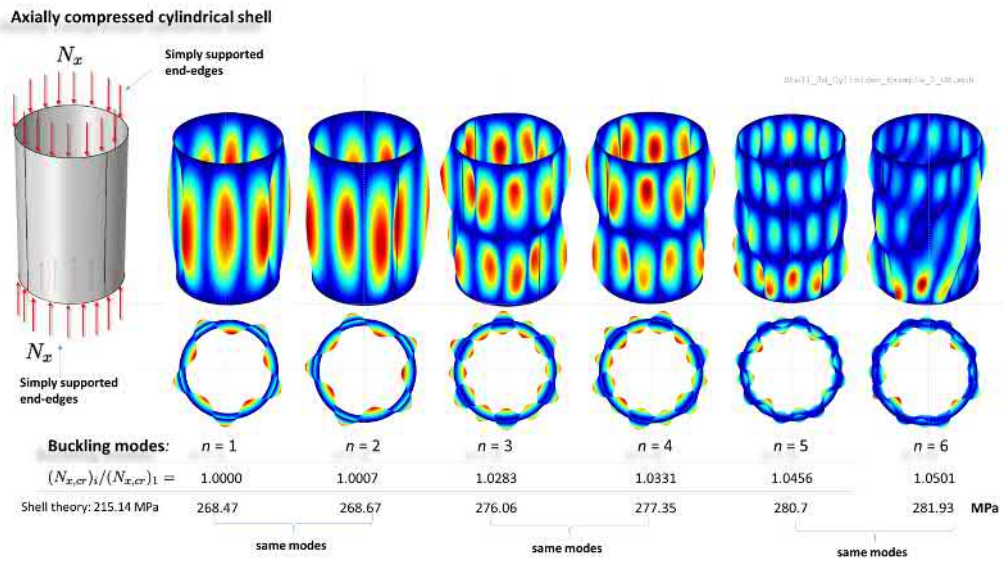


Figure 1.230: Example no 2 of buckling modes obtained by FE-buckling analysis (Comsol) for the simply supported cylindrical shell. Theoretical (Euler) buckling stress as given by equation (1.1194); $\sigma_{cr} = 215.14$ MPa. (Mode 1 and 2 are the same, so are 3 and 4. We have multiple modes.)

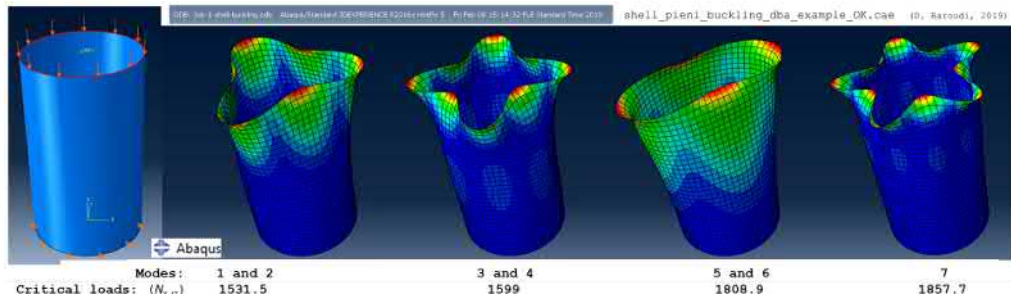


Figure 1.231: First modes, Linear buckling analysis performed by FEA in Abaqus. The shell is simply supported at its bottom but free on the upper loaded edge. Note that we have multiple modes which correspond to simple rotations around the axial symmetry axis of the shell.

where the non-dimensional temperature being defined as

$$\bar{\theta} = \begin{cases} 0, & \theta < \theta_{tr} \\ (\theta - \theta_{tr}) / (\theta_{melt} - \theta_{tr}), & \theta_{tr} \leq \theta < \theta_{melt} \\ 1, & \theta > \theta_{melt} \end{cases} \quad (1.1209)$$

with θ being the current temperature. The material parameters A, B, C, N, M being experimentally determined at or below transition temperature. The con-

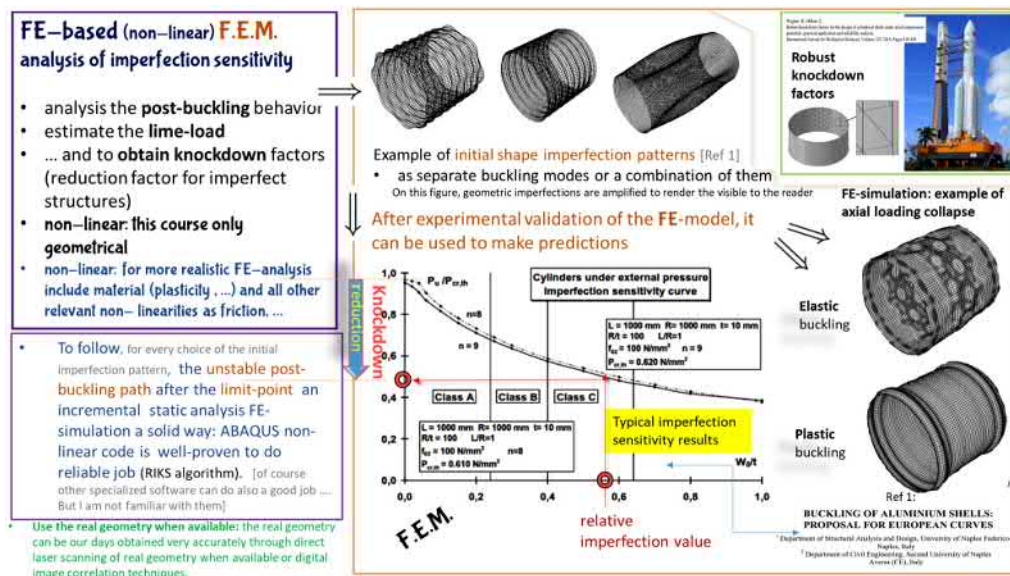


Figure 1.232: Finite Element based knock-down factors numerical estimation and post-buckling analysis.

Cylindrical or barrel shells

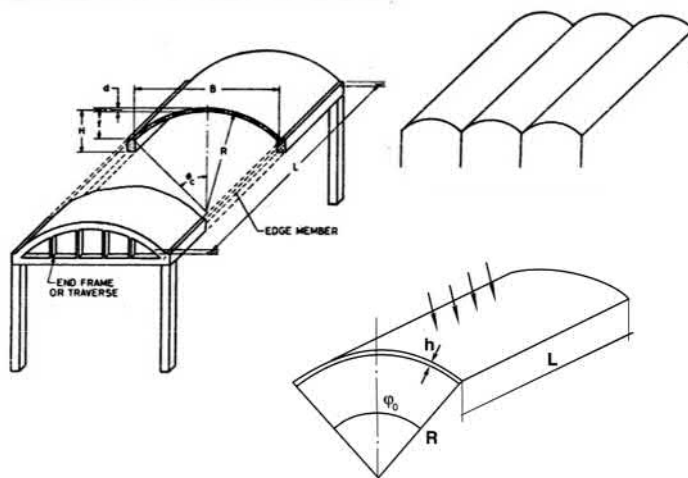


Figure 1.233: Schematic of cylindrical panel or barrel thin-shells.

stitutive model above is a phenomenological *thermo-viscoplastic model* belonging to the family of *decoupled*⁴⁴⁶ *models* (also called *multiplicative models*) having the

⁴⁴⁶As, the reader may guess, there is another family called *coupled models*. However, this constitutive modelling aspects do not belong to this course scope. The reader is encouraged to read or take courses in this exiting subject.

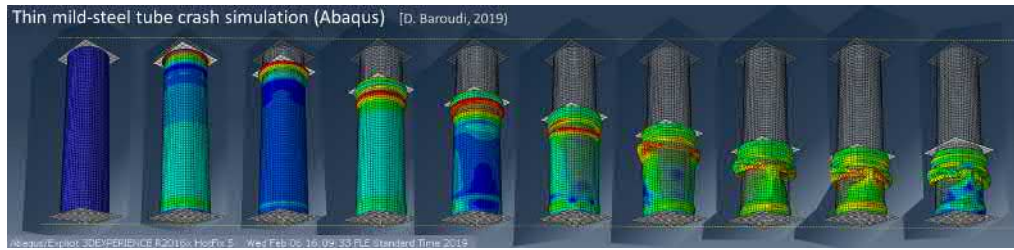


Figure 1.234: Computational simulation of a crash of mild-steel tube (Abaqus/Explicit). The colours code for von-Mises stresses.

general form

$$\sigma = \sigma_\epsilon(\epsilon) \cdot \sigma_{\dot{\epsilon}}(\dot{\epsilon}) \cdot \sigma_T(T) \tag{1.1210}$$

which empirically describes (isotropic) strain hardening, where the effects of strain rate and the influence of temperature are derived empirically from experiments.

(Figure ??)

Between shell walls and the Return of Spring

Enjoy the coming spring I hope this course helped to you to learn what is about in stability and made you curious toward scientific based civil engineering

FIN A MIRACLE OCCURS

$$D\nabla^8 w + \frac{Eh}{R^2} w_{xxxx} - \nabla^4 (N_x^0 w_{,xx} + 2N_{x\theta}^0 w_{,x\theta} + N_\theta^0 w_{,\theta\theta}) = 0$$

Axially compressed cylindrical shell

Simply supported end-edges

Buckling modes:

n = 1	n = 2	n = 3
$(N_{x,xx}) / (N_{x,xx}) = 1.00000$	1.00007	1.02883

Shell theory: 215.14 MPa

Buckling of axisymmetric cylindrical shells under uniform compression

Ring patterns: $w(\theta) = w_0 \sin \frac{n\theta}{2}$

Checkboard patterns: $w(\theta) = w_0 \sin \frac{n\theta}{2} \cos \frac{m\theta}{2}$

2R-half waves

2R = 65 mm Aluminum, Steel, Steel

D, Baroudi, 2019

Stability loss and periodic beauty.

Chapter 2

Geometrically non-linear analysis of Frames

2.1 First words

This chapter covers elastic stability of frame structures and second order effects or in other words, geometric non-linearities. These notes are borrowed in a very short way from the course I am giving on stability of frames. So, dear reader, please consult my detailed lecture notes on this topic in the course *Mechanics of beams and frames*.

As a departure from all other chapters, in this chapter, the buckling equation will not be derived using energy approach. The simple reason for this difference in approach is that, this chapter is borrowed from a previous first year master course covering completely the stability of columns and frames in only two lectures. Yes, we are very efficient at Aalto university. Instead, an equilibrium approach is used to write, directly, new equilibrium equations in the tiny deformed configuration (post-buckled state). This way, one obtains directly the non-linear 'stiffness matrix' $K(\lambda)$ of the system or of its elements, λ being a load parameter.

* * * * *

Primarily, the geometrical non-linear effects considered here rise from shape initial imperfections and load eccentricities or from the effect of sway or tiny lateral loads, for instance. The Effects of initial stress can be accounted too and will be treated later. However, for the perfect structure (frame, column, etc.), the geometrical non-linear effects are the consequence that we write the equations of equilibrium in the deformed geometry (post-buckled state = the adjacent equilibrium configuration). This is why, now axial forces (internal and external) will additionally, work in this tiny departure from initial equilibrium

configuration (pre-buckled state). Recall that, when considering small deformations and rotations, the equilibrium equations are written in the non-deformed configuration.

We apply here, the very well-known among structural engineers, *slope-deflection method*¹ with non-linear stiffness coefficients being magnified by a factor depending on member axial load (the Berry's stability functions). This particular displacement method, which is in fact, a handy analytical (exact) hand-version Finite Element Method, is specially designed as an effective tool for doing structural analysis by hand within an 'A-4' sized paper to catch the 'handels'² of the relevant behaviour before jumping in the boundless complexity of computer models and their endless outputs. One thing, if not more, should be said about this marvellous non-linear *slope-deflection* method (SDM): it produces the full non-linearised eigenvalue problem of buckling while, on the other side of the planet, the finite element method presented in subsection (1.12.12: *Discrete energy method - FEM*) solves only the linearised eigenvalue problem of buckling. So, mathematically speaking, in a generic way, here what is meant:

$$\underbrace{K(\lambda) \cdot u = 0}_{\text{SDM: non-linear eigenvalue problem}}, \quad \underbrace{[K_L - \lambda K_G] \cdot u = 0}_{\text{FEM: linearised eigenvalue problem}}, \quad \lambda\text{-load parameter} \quad (2.1)$$

where K_L and K_G being, respectively, the linearised stiffness matrix and geometric stiffness matrix. This is for the difference. In one word, the slope-deflection method is more accurate than the finite element method for the same discretization level (same number of elements).

2.2 Introduction

Two classes of problems are treated here: 1) the buckling problems in which there are no transversal loads which consist of a Generalised non-linear eigenvalue Problem $K(\lambda)u = 0$, where λ is yet an unknown loading parameter, the buckling load, to be determined and K is the stiffness matrix and u the nodal degrees of freedom. In such case there is neither no eccentricities nor shape imperfections; the geometry of the frame is ideally perfect. 2) the non-linear problem of equilibrium written in terms of nodal displacements with non-zero right hand $K(\lambda)u = f$, where f is nodal force vector.

Two types of planar frames will be treated here: *side-sway* and *non-sway*³. We begin with the nonsway case.

¹Kulmanmuutosmenetelmä, to be short as Finnish is.

²Kahvoja, in Finnish. To understand the importance of handels just think of a big ball (diameter 1 m) made of a heavy material and having a perfectly polished surface. Your task is to rise it about 1 m over the floor by hand. You have a serious problem! There is no handels (ei ole kahvoja) on the ball!

³Sivusiirtyvä ja sivusiirtymätön, in the tongue of Kalevala.

In this chapter the displacement method will be used systematically. For making hand-calculation effective, the elementary stiffness matrix is reduced. The degrees of freedom (dofs) v_1 and v_2 (the nodal deflection) of an beam-element are condensed into one single dof, the relative deflection $\Delta = (v_2 - v_1)$. Instead of Δ , we prefer to use $\Delta/\ell \equiv \psi_{12}$ where $\ell = L_{12}$. The rotation ψ can be seen as the rigid body rotation of the beam. A second simplification is done, namely, it is assumed that the beams are inextensible. This means that the normal force becomes now a reaction and has to be determined from equilibrium equations. Such slightly simplified displacement method carries, in the litterature, the well-known name of *slope-deflection method*.

2.3 Combined axial loading and bending

Here we derive the stiffness matrix of such beam accounting for geometrical nonlinearities. Both cases of compressive and tensile axial loading will be considered.

$$(EIv'')'' \pm Pv'' = q, \quad (2.2)$$

where the '+' and '-' are, respectively, for compression and tension cases. The general solutions are respectively,

$$v(x) = A\sin(kx) + B\cos(kx) + Dx + E + v_0(x) \quad (2.3)$$

and

$$v(x) = A\sinh(kx) + B\cosh(kx) + Dx + E + v_0(x) \quad (2.4)$$

where $v_0(x)$ being the particular solution and $k^2 = N/EI$, $N \equiv |P|$. The reader is encouraged to refer to basic textbooks on elastic stability of frames.

The geometrically non-linear problem (called also in the olde time *the stress-problem*): The equilibrium equation should be written in the deformed configuration. The stiffness matrix is now non-linear. As for bending without axial load, we here solve the BVP with given four boundary conditions at the two nodes (or ends) of the beam where nodal deflections and rotations are given. Solving for the bending moment at end 1, one obtains again the stiffness-equations of the well known and versatile slope-deflection method

Now, in the slope-deflection method the stiffness coefficients are magnified by a factor depending on member compressive/tensional load which are called Stability or Berry's functions.

2.4 Full non-linear analysis of non-sway frame

Essentially, ...The Eigen-Value problem of buckling is now ...
comming soon ...

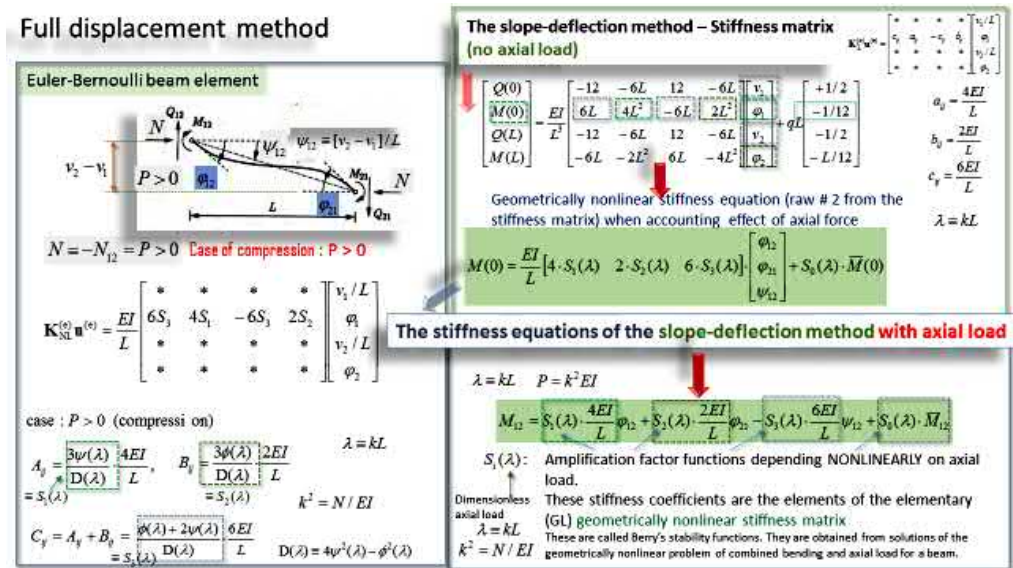


Figure 2.1: The Slope Deflection Method. The derivation of the non-linear stiffness matrix (directly from my lectures slide).

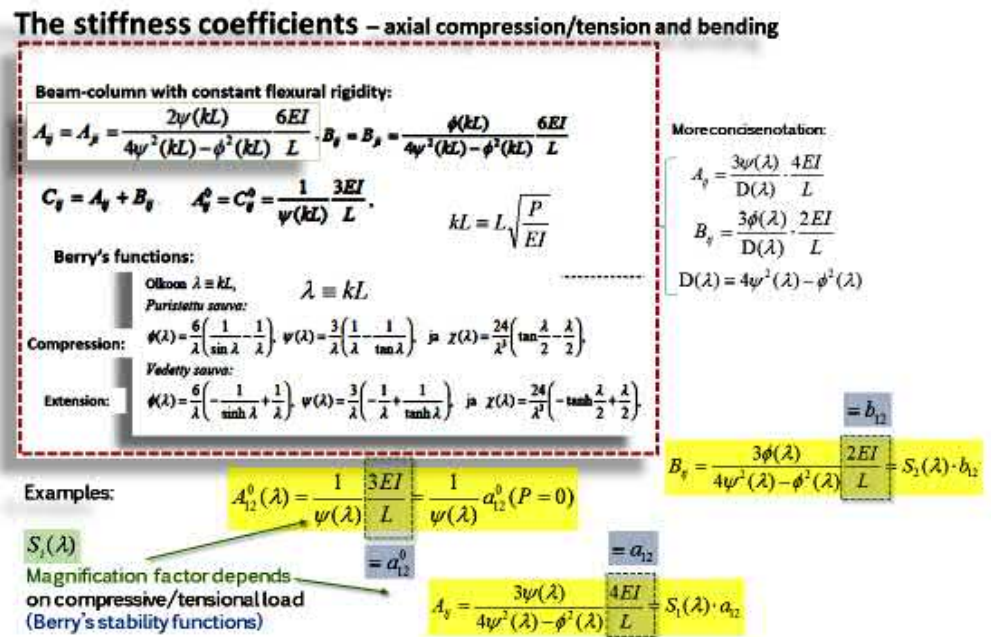


Figure 2.2: Berry's stability functions.

2.4.1 Buckling of continuous beam-column

Solving for the buckling load (the smallest Eigen-Value) one obtains from then equilibrium equation

$$M_{21} + M_{23} = 0, \tag{2.5}$$

giving the criticality condition, in terms of Berry's stability functions, as

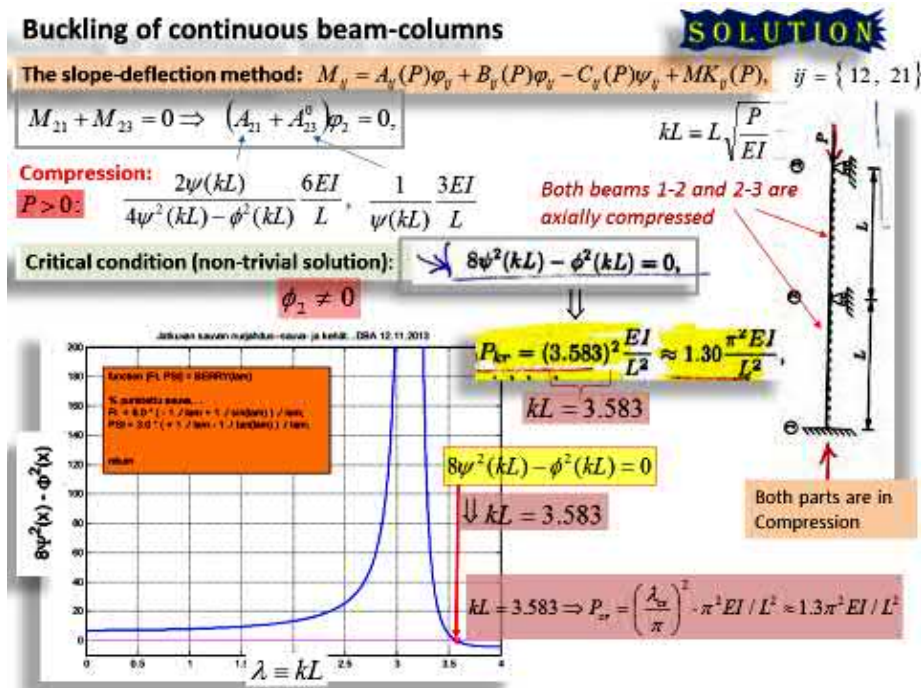


Figure 2.3: Buckling of continuous beam-column.

$$8\psi^2(\lambda) - \phi^2(\lambda) = 0, \tag{2.6}$$

from which the critical load is obtained as the smallest positive zero as shown in the Figure,

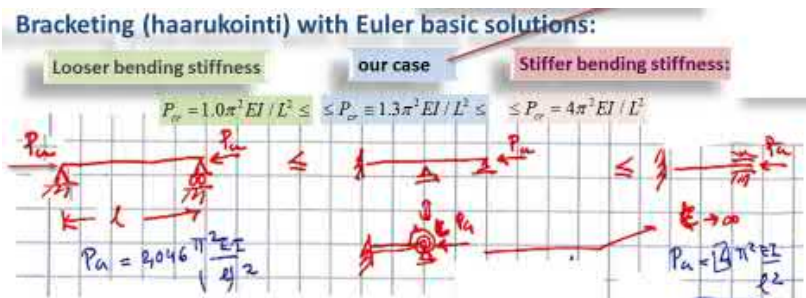


Figure 2.4: Brackets for the buckling load

$$\lambda_{cr} = kL = 3.583 \rightarrow P_{cr} = 1.3\pi^2 EI / L^2. \tag{2.7}$$

One can estimate correctness of this result by giving an estimate bracket using Euler's basic buckling cases (see following Figure).

2.4.2 Buckling of non-sway frame

Solving for the buckling load (the smallest eigenvalue) one obtains from then equilibrium equation

$$M_{21} + M_{23}^0 = 0, \tag{2.8}$$

the criticality condition expressed in terms of Berry's stability functions as

$$12\psi(\lambda) + 16\psi^2(\lambda) - 4\phi^2(\lambda) = 0, \tag{2.9}$$

from which the smallest zero, λ_{cr} , corresponds to the buckling load. The upper equation is non-linear and smart engineer seeks graphically for the smallest zero within a bracket of critical values. See in the following for how such bracket is estimated.

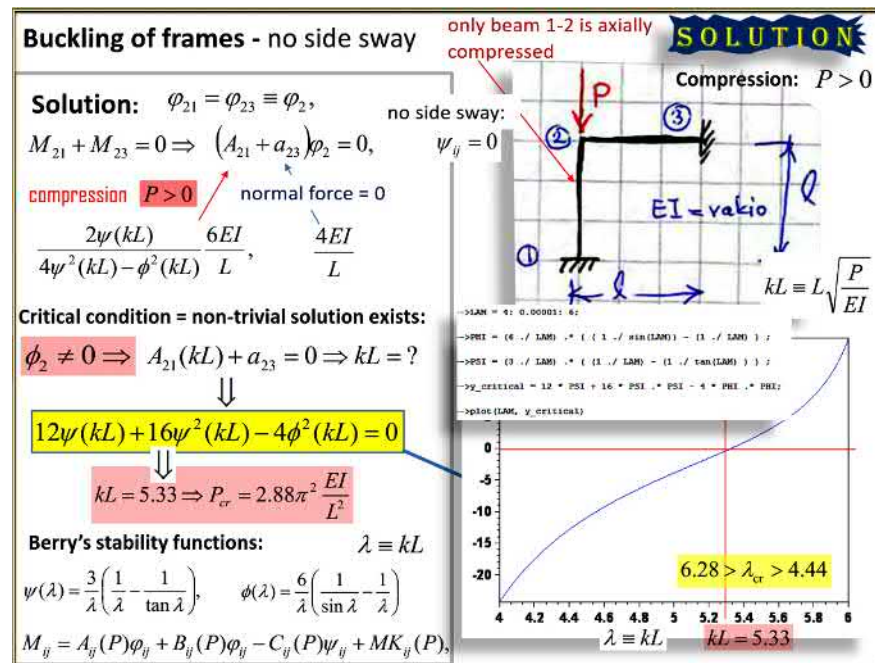


Figure 2.5: Buckling of non-sway frame.

$$\lambda_{cr} = k\ell = 5.33 \rightarrow P_{cr} = \frac{\lambda_{cr}^2}{\pi^2} \cdot \pi^2 EI / \ell^2 \equiv \mu P_E. \tag{2.10}$$

Processing the above result into canonical or more practical form one shows that

$$\mu = \lambda_{cr}^2 / \pi^2 \approx 2.88 \quad \text{and} \quad \ell_{Buckling} = \ell / \sqrt{\mu} \approx 0.59\ell \tag{2.11}$$

Next step is to cross-check our result by bracketing the critical load using well-known basic Euler's buckling cases for a single column with relevant boundary

conditions. One uses here non-side sway basic column cases since our frame have no side-sway. One can easily show that

$$2.046 < \mu = 2.88 < 4, \tag{2.12}$$

refer to the figure.

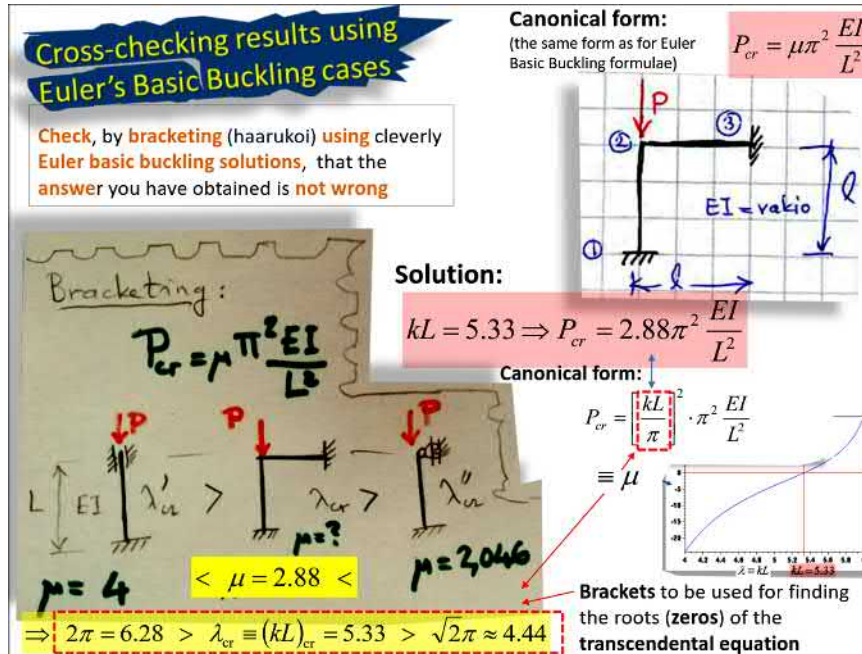


Figure 2.6: Cross-checking for buckling load.

This bracket can be easily expressed in terms of buckling lengths. In left-side column, the rotation *rigidly restrained* and thus the corresponding critical load should be higher than for the frame in which the corner is only *elastically restrained* from rotations. The effect of the ending of the beam is mechanically equivalent to the effect of an elastic rotational spring. Therefore one obtains the upper-bound estimate $P_{E,left} = 4P_E > P_{cr} = 2.88P_E$. On the contrary, the left-side column has *free rotation* at one end and buckles therefore much easily than the elastic-rotational spring case and thus for our frame. Therefore, the corresponding critical load should be higher and one obtains the lower-bound estimate $P_{cr} = 2.88P_E > P_{E,right} = 2.046P_E$.

2.5 Upper- and lower bound estimates for the buckling loads

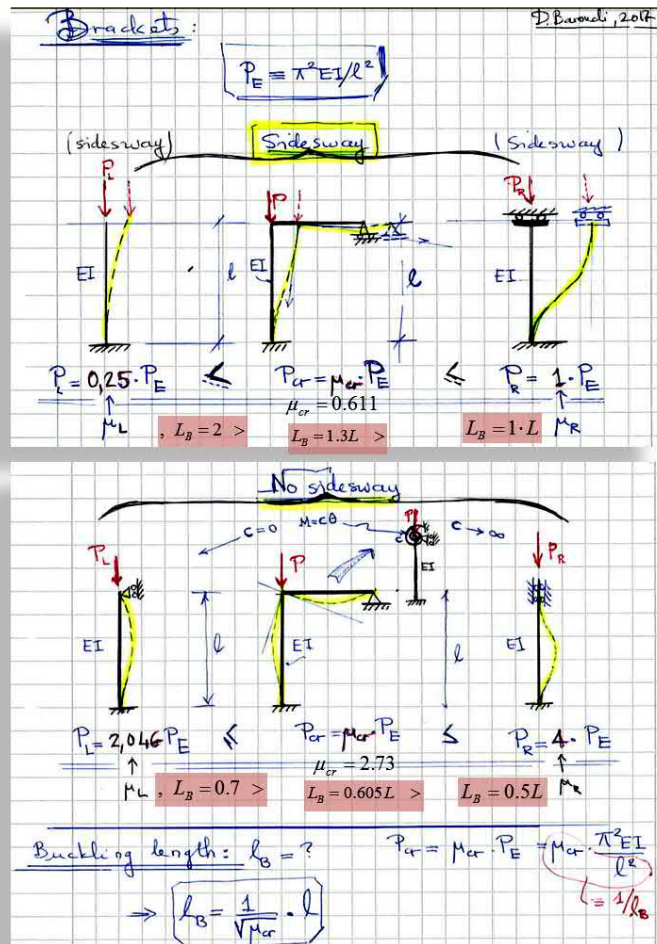


Figure 2.7: Bracketing the buckling load for side-sway and no-sway frames.

Once the buckling load for a frame is estimated, a practical *wisdom* is to *cross-check* and find ways to check for it correctness. One way is to use the Euler's basic buckling cases and some *engineering educated intuition* of how the structures deform in order to resist external loading. As a well educated structural engineer, you should by now, be able to figure out correctly the degree of effective rigidity, stiffness or flexibility of supports or connections at nodes. You must almost feel some *structural behaviour empathy* with the deforming structure, when loaded, in order to estimate correctly the degree of translational or rotational *effective springs* at supports or nodes.

2.6 Full non-linear analysis of side-sway frame

Consider the lateral sway frame shown in figure (Fig. 2.9) having transversal load. Without the transversal load q , the problem is a buckling (stability). We will consider, in the following both cases. The equations of equilibrium are the same for both cases. The only difference is the presence of non-zero right-side for the first case. The compatibility of rotations gives $\phi_{21} = \phi_{23} \equiv \phi_2$. The frame is once side-sway frame since $n = n_{trans.} - n_{constr.} = 3 - 2 = 1$, is the number of independent 'sway-kinematics' or ψ -dofs. Therefore, $\psi_{21} = \psi_{12} \equiv \psi$. The independent kinematical unknowns are then $u = [\phi_2, \psi]^T$. Therefore, one needs two independent equilibrium equations to determine u . These equations are namely, moment equilibrium at node 2

$$M_{21} + M_{23}^0 = 0, \quad (2.13)$$

and shear-equation

$$Q_{21} = 0, \quad (2.14)$$

at section 21 of the column part.

Instead of the shear-equation, one can directly obtain the second independent equilibrium equation through the principle of virtual work. Here one chooses the side sway basic mechanisms as virtual displacements. Consequently, the virtual displacements are those of a rigid body or a kinematic chain or a mechanism. Such displacements can be described by a set of independent rigid body virtual rotation $\delta\psi_i$. One key aspect is to write correctly the increment of virtual work done by external compressive (or extensive) forces.⁴ One should account for the geometric non-linearity in displacements and includes terms up-to second order (quadratic in the independent virtual rotation) in the Taylor expansions of terms including trigonometric functions of the virtual rotations (moderate rotations). Because this approach is very versatile, an example will be provided.

The axial force $N_{12} = -N$ or equivalently the loading parameter $N\ell = \lambda^2$ should be defined by considering equilibrium in the deformed configuration. On the contrary, in the buckling-problem, the normal forces should be determined from the pre-buckled state (membrane state) in which the frame mechanically works as a truss since there is no bending. The normal forces should be defined from the pre-buckled state (membrane state). Here $N_{12} = N_{21} \equiv -N > 0$ and $N_{23} = N_{32} = 0$. The load parameter $\lambda = k\ell$ where $k^2 = N/EI$.

$$(A_{21}(\lambda) + a_{23}^0)\phi_2 - C_{21}(\lambda)\psi = -\bar{M}_{23}^0, \quad (2.15)$$

⁴The vertical virtual displacement at node 2 is $v_2(\ell) = \ell(1 - \cos(\delta\psi))$ and therefore $\delta v_2 = -\ell \sin(\delta\psi) \approx -\ell \delta\psi$ for moderate rotations. Then the external virtual work $\delta W_{ext} = P\delta v_2 = -P\ell\delta\psi$. The internal virtual work increment is $\delta W_{int} = -M_1\delta\psi - M_2\delta\psi$, where M_1 and M_2 being the bending moments at nodes 1 and 2 to be written with the sign convention for end-moments. I let the student establish the final equation of equilibrium.

One need to express Q_{21} in terms of end-moments and therefore in terms of u . For that, one should write the moment equilibrium for the beam 1 – 2 in its deformed geometry and obtain

$$M_{12} + M_{21} + Q_{21} + N\psi\ell = 0, \quad (2.16)$$

Accounting for the shear-equilibrium equation $Q_{21} = 0$ we obtain finally,

$$C_{21}(\lambda)\phi_2 - 2C_{21}(\lambda)\psi + \lambda^2 = 0, \quad (2.17)$$

where $C_{21}(\lambda) = A_{21}(\lambda) + B_{21}(\lambda)$ and $N\ell = \lambda^2$ has been used. The axial force N or $N\ell = \lambda^2$ should be updated in the above equation after each iteration step since they should represent axial forces in the deformed configuration. The initial value for the normal forces can be obtained from the pre-buckled state (membrane state). The normal force is obtained from the equilibrium equation

$$-N = N_{21} = -(P + Q_{23}) \quad (2.18)$$

When multiplied by multiplied by ℓ , one obtains the updating step for the parameter λ in the stiffness matrix (Eq. 2.23) as

$$\lambda^2 \equiv N\ell = -N_{21}\ell = \ell(P + Q_{23}) \quad (2.19)$$

where

$$Q_{23} = q\ell_{23}/2 - M_{23}^0/\ell_{23}, \quad (2.20)$$

$$M_{23}^0 = a_{23}^0\phi_2 + \bar{M}_{23}^0, \quad \text{and} \quad (2.21)$$

$$\bar{M}_{23}^0 = -q\ell_{23}^2/8. \quad (2.22)$$

Re-aranging the non-linear equilibrium equation into matrix form one obtains the problem $K(\lambda)u = f$, namely,

$$\begin{bmatrix} A_{21}(\lambda) + a_{23}^0 & -C_{21}(\lambda) \\ -C_{21}(\lambda) & +2C_{21}(\lambda)\psi - \lambda^2 \end{bmatrix} \begin{bmatrix} \phi_2 \\ \psi \end{bmatrix} = -\bar{M}_{23}^0 \begin{bmatrix} 1 \\ 0 \end{bmatrix} \quad (2.23)$$

This last equation of equilibrium is the geometric non-linear equilibrium equation. Equilibrium equation (2.23) should be solved by iterations by updating the compressive force N according to equation (2.19).

2.6.1 Buckling analysis of side-sway frame

Before solving the non-linear equilibrium equations it is wise to know a bit of the behaviour of the stiffness matrix. Close to critical load (no transverse loading), the matrix goes close to singular before e becoming singular for the buckling load. Therefore, close to buckling load, the solution of the non-linear problem (with non-zero right-hand) begins to diverge and spuriously 'fluctuate'. This

is the reason here why we first solve for this critical load. Close to such load the stiffness matrix becomes singular leading to non-convergent solution since stability loss, at this critical point, means loss of effective stiffness. The tangent at such point is horizontal in equilibrium path curve. Therefore, no solution can be expected since then the increment $K(\lambda)\Delta u$ becomes indeterminate.

The buckling axial load in the column is determined as the smallest eigenvalue of the the non-linear EVP

$$\begin{bmatrix} A_{21}(\lambda) + a_{23}^0 & -C_{21}(\lambda) \\ -C_{21}(\lambda) & +2C_{21}(\lambda)\psi - \lambda^2 \end{bmatrix} \begin{bmatrix} \phi_2 \\ \psi \end{bmatrix} = \begin{bmatrix} 0 \\ 0 \end{bmatrix} \quad (2.24)$$

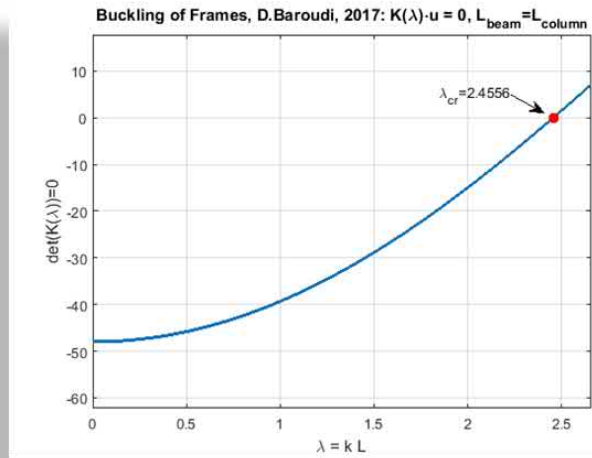
Here follows, a Matlab-script solving the above problem. The criticality conditions is written as $\det(K(\lambda)) = 0$ for the condition to obtain non-trivial solution and thus buckling. Therefore, the critical value corresponds to the smallest zero bellow

$$\lambda_{cr} = \min .\text{sol.}\{\det(K(\lambda)) = 0\}. \quad (2.25)$$

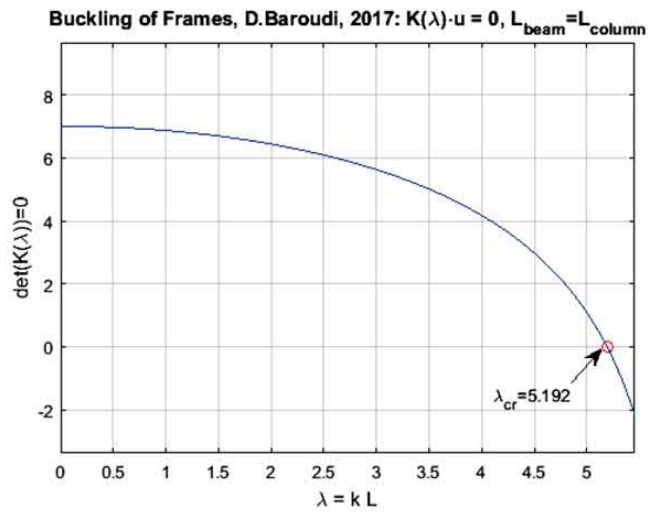
The critical axial force is then $P_{cr} = \lambda_{cr}^2 EI/\ell^2 \approx 0.7\pi^2 EI/\ell^2$ is shown in Figure (2.10).

This is for this hyper-short introduction of the stability analysis of frames, in particular, using the slope-deflection method adapted for geometrically non-linear case.

The general force method and the displacement method, in its version of slope deflection methods, should the best friends of our *Herra Engine-jööri*. The engineer is the computer, not the computer. May be later, we can add a bit more solved examples, especially, related to approximations using energy methods. For the moment *THE END*.



$$\begin{bmatrix} A_{21}(\lambda) + a_{23}^0 & -C_{21}(\lambda) \\ -C_{21}(\lambda) & +2C_{21}(\lambda)\psi - \lambda^2 \end{bmatrix} \begin{bmatrix} \phi_2 \\ \psi \end{bmatrix} = \begin{bmatrix} 0 \\ 0 \end{bmatrix}$$



$$\det(K(\lambda)) = 0 = A_{21}(\lambda) + a_{23}^0 = 0 \Rightarrow \lambda_{cr} = 5.192$$

Figure 2.8: Exact Solutions for the sway- and non-sway buckling load of the frames. The column and the beam have the same length and bending stiffness. This examples are those related to the previous example for estimating the brackets for the critical load of the frame.

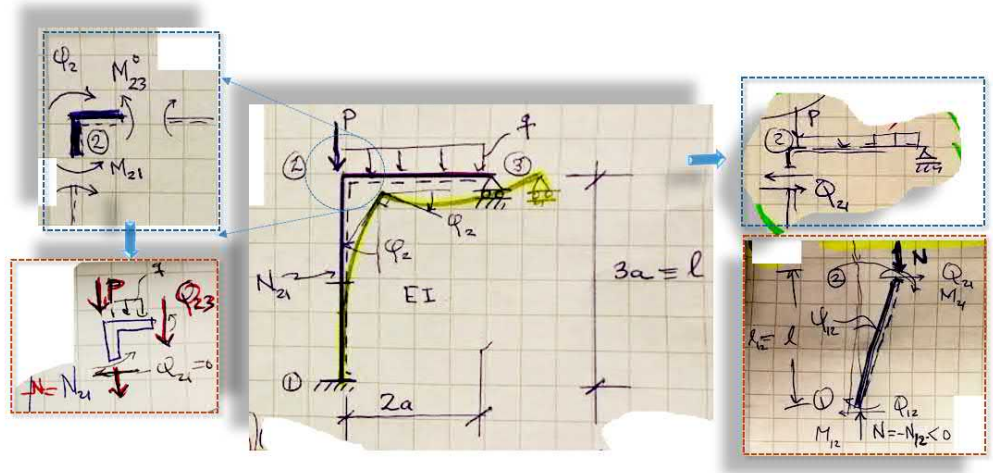


Figure 2.9: Transversally loaded side-sway frame.

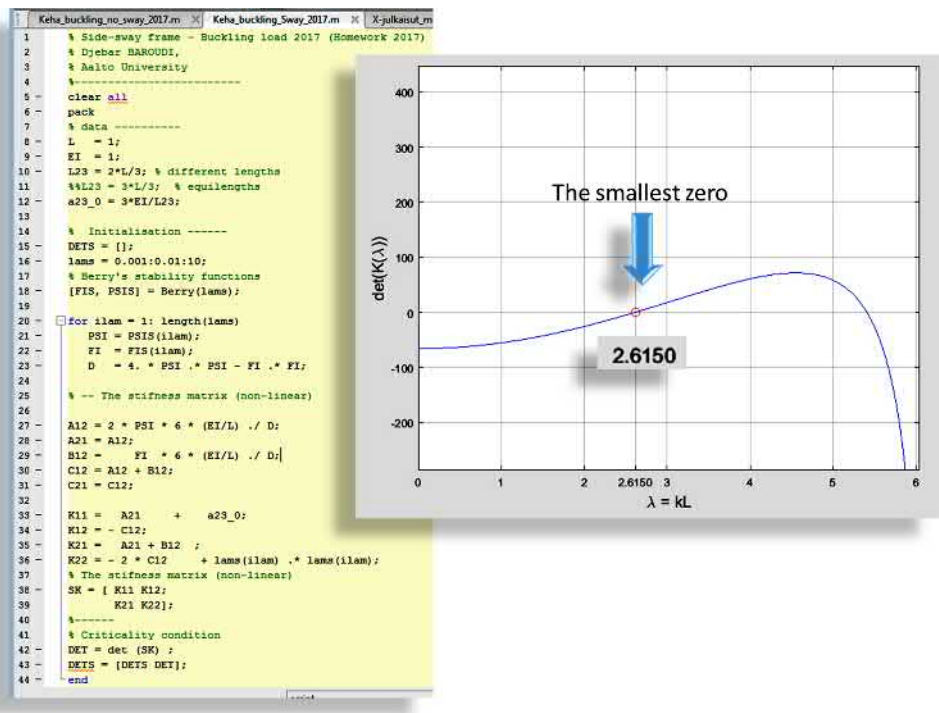


Figure 2.10: Matlab-code for finding graphically the smallest zero of the critical condition. The graph is given by the points $(\lambda, \det(K(\lambda)))$. With $\lambda = 2.615$, the critical load corresponds to $P_{cr} \approx 0.7\pi^2 EI/\ell^2$.

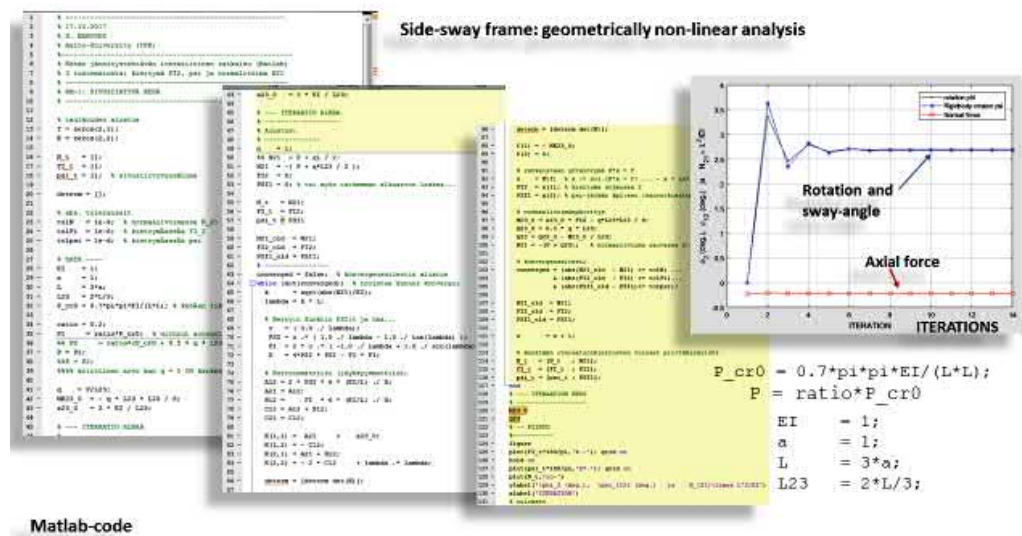


Figure 2.11: Matlab-code iteratively solving the non-linear equation system for $P = 0.2P_{cr}$.

Chapter 3

Torsion of open thin-walled beams

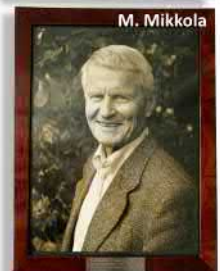
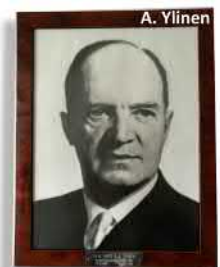
3.1 Introduction

Let's start by the reason for this section¹. I have at hand on my desk, by chance, a Russian textbook belonging to *insinöörieverstiluutnantti* Professor **Arvo Ylinen** (1902–1975)⁵ of *Strength of Material* by **Beliaev**. The textbook landed on my desk through Emeritus professor of *Structural Mechanics* **Martti Mikkola** (1936–) a former student of A. Ylinen and also my teacher of Structural Mechanics at **TKK - HUT**⁶, known originally as *Suomen Teknillinen Korkeakoulu* in the 80's. There is still one last student of Emir Professor Martti Mikkola, actually professor **Reijo Kouhia**, teaching Mechanics: Structural Mechanics, Mechanics of Materials, Mechanics of Solids, . . . at Tampere University. This is for the short history. $M_x = M_t + M_\omega \rightarrow \tau = \tau_t + \tau_\omega$

So now I come back to the Beliaev book. So, I was reading a chapter about deformation of *open thin-walled beams* in *bending* and *torsion* and I liked enormously the paragraph in which the kinematics of warping was modelled and explained, primarily, in *geometrical terms*. This is what I want to share with students. I liked the clear and concise *physical-based well graphically illustrated* explanation and visualisation of the key kinematic relating axial displacement; *the deplanation* differential $du(x, s)$ to the differential of torsion angle $d\theta(x)$ along the beam axis *assuming no-shearing* of the shell-beam mid-plane, assumption which is known, our-days, as the *Vlassov assumption* [**Vlassov**, Chap. 1]–*Torsion of thin-walled beam-shells of open section*:

$$\gamma_{xs} = 0. \tag{3.1}$$

¹Tämä luku on raakeli. Sitä huolimatta, se osa joka käsittelee Vlassovin teoriaa on ihan OK, anakin minulle.



⁵ **A. Ylinen:** *Timoshenko* of Finland. Father of famous strength of materials twin-textbooks *Kimmo- ja lujuusoppi I-II* (1948–1950).



⁶ **TKK – MIT** of Finland.

3.2 The geometry of motion: the value of observation

Let's be clear: Teaching the mechanics of thin-walled beams and of restrained warping is not simple. Classically, teacher starts from equations, continue explaining with the help of equations and at the end they obtains equations to compute the stress in function of the sectorial coordinate. Every one is happy; the teacher who teach and the future engineer who has a *formula* to use to compute warping stresses. Stop a moment! Did anyone understood the underlying physics of deformation in such warping? How this stress-formula relates to the physics of restraining the axial deformation? In reality, neither the teacher nor the student understood the physics of warping!

What is missing? The physics is missing. One should start from observations. The physics of deformation, the physics of the stresses resisting such deformation. Yes, to enhance understanding the teacher should starts from the physics and the equation just follow naturally. Not the contrary.

Yes, I can use equations, in my teaching, without any drawing relating deplanation motion and this kinematic assumptions. However, both understanding and motivation of the students will decrease asymptotically toward zero, almost surely.

In the following, I propose to use, in teaching, the primary Vlassov's assumption and to show its geometrical meaning, as regarded to motion: its represents a rigid body motion of a differential element of the mid-surface of the shell-beam. Prior to the previous step, I will demonstrate them using a physical reduced model of such thin-walled beam with an open section, that indeed, torsion results in axial displacements and that, in addition, a square plotted on the (very) thin wall will remain square and will have only rigid body rotation. Therefore, I should present first the experimental observations prior formulating the Vlassov kinematic assumption. The student is not obliged to believe all what I tell even if I have formula to convince him. He should see with his own eyes to be convinced. This is call *experimental observations* validating or invalidating the hypothesis (here, the used kinematic hypothesis). This is a must step. It is classically, the way in teaching, with the **Euler-Bernoulli's**, *i.e.*, we shoe students reduced models of beams with use it explicitly and draw the geometry of motion to derive, in pure bending, the axial displacement of any point P on a fibre at height y from the neutral axis, as $u(x, y) = -y \cdot \sin \theta(x) \approx -y \cdot \theta(x)$, where $\theta(x)$ being the rotation of the section around the neutral axis. The derivation of such formula is completely using the geometry and the geometry only of the kinematic assumptions. Why for warping, we just state that the Vlassov's kinematic assumptions is this '*bla bla, bla bla bl*' and then by 'pure mathematics', derive the relation between the deplanation and a *mysterious coordinate* $\omega(s)$, which is a function indeed, and which is postulated in the beginning without even knowing

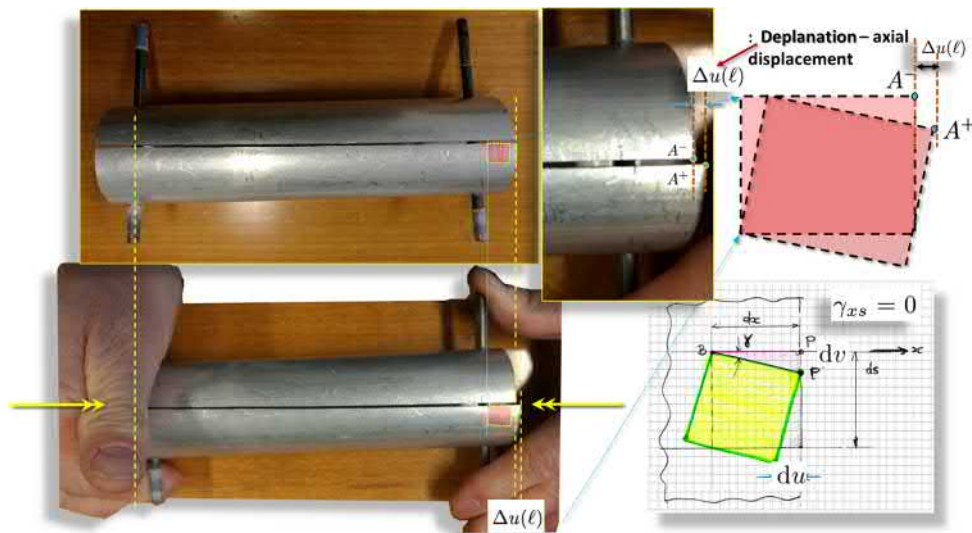


Figure 3.1: Experiment illustrating the deformation.

Bernoulli's hypothesis

Kinematics

0. vertical lines perpendicular to NA are incompressible (or inextensible) $\Rightarrow AB = \text{const.}$
 $\rightarrow \epsilon_{yy} = 0$

1. plane cross-sections before deformation ...

... remain plane after deformation

2. ... and perpendicular to the Neutral Axis (NA)

Perpendiculars

Remain perpendicular

Simple Bending

Bernoulli kinemaattiset hypoteesit

Initial state: Unloaded beam

Final state: deformed state after loading

Plane cross-section

Neutral axis

F

$\theta(x)$

fishbone model

$$\vec{u}(s, y) = (u_0(s) - y \sin \theta(s)) \vec{e}_s$$

$$y \sin \theta(s) \approx y \theta(s) = y \frac{dv}{ds} = yv'(s)$$

Figure 3.2: Experimental illustrating of the Euler-Bernoulli hypothesis during class. *N.B.* the rigid body rotation of the material element $dx dy$ on the beam in bending; it Cf. to the Vlassov same assumption for no-shearing of the mid-plane element $dx ds$.

why!², straightforward from the geometry of the motion of an infinitesimal surface-element $dxds$ of the mid-plan and results primarily from the simple physical observation of that this mid-plan of the thin-walled beam in torsion happens in plan sx with *no shape distortion* which is the *Vlassov's kinematic hypothesis* I mean for the student. There is a complete equivalence, in teaching, between the two cases. As a teacher, I will follow what I am proposing while teaching the warping. No derivations which follow directly from mathematics only, will be accepted. I want that the student understand the underlying physics first.

My reason is to make for students the notion of *warping* and its synonym **deplanation** easier to understand (*käsittää* = catch, FI) through the geometry of motion. Then to show that such mechanical phenomenon and a main related concept known as, for instance, the *sectorial coordinate* $\omega(s)$ follows, primarily from the hypothesis (an experimental observation) known as *Vlassov assumption for zero shearing of the mid-surface*. The way it is actually taught without figures explaining the geometry of motion of the mid-plan and relying solely on the mathematics of the **Vlassov assumption** for no shearing of the mid-plan makes it hard for students to understand since teaching starts now from the end of the logical chain of events *stating that there is no distortion of the mid-plane* that is $\gamma_{xs} = 0$. This is the so called Vlassov assumption. While this is true, this alone will not help students *figure out* the kinematics because teachers present no schematics, no drawings for the kinematics of thin-walled sections giving rise to the axial displacement leading to **deplanation** and thus **warping**.

This chapter is adapted from the Russian textbook of **N. M. Beliaev**, 1959 of *Strength of Material*. *Why such choice?* For many reasons. However, if I have to produce only one then here it is: the book is on my desk and it has a simple and clear *physically based explanation and consequently straight-forward modelling of the deplanation*, in this order. ⁷



⁷ I will present the **Vlassov** derivations in his theory of torsion of open thin-walled beams as soon as I can. Chap. 1 of the Vlassov's book *Torsion of thin-walled beam-shells of open section*.

²Of course, this all staff follows *mathematically* and naturally from the Vlassov's constraint $\gamma_{sx} = 0$ for *pure warping torsion* by integrating $\frac{\partial u}{\partial s}$ etc. However, this is not the point because the kinematics is hidden inside the formula. I am stressing here that the starting point is the *physics of the motion* and not its mathematics and this is exactly what I wanted to *unhide* for the students. Of course without mathematics, we cannot go enough far, for engineers at least. We know that mathematics can sometimes lead to discovery of physical objects even before any physical observation as for instance the **Higgs** bosons or much before that, **Einstein**, using pure mathematics with no observations at all, showed that the light should be *bended* by gravity, long, long before such observation validating his theory - in other words, the mathematical formula (Einstein's general theory of relativity) - were validated by the very famous direct observation during the solar total eclipse. It was proved that indeed, gravity bends the light! This was done first by mathematics and proved later by experimentation. So mathematics is much more than what we understand. Many teacher forget to mention to their students about physics-based arguments and possibly to sketch the related motion.

3.2.1 My teaching goal in starting teaching warping

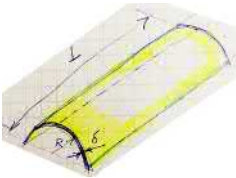
So, why I hope to share this description of the almost *mythical* warping? It is because when I was a student, my teachers started the lesson introducing warping by first defining a completely new and strange object named **sectorial coordinate** $\omega(s)$. . . after what I lost the handles of understanding the true physics and then just tried to remember the equations and formulas needed to handle such problems in order to survive the soon coming exam. Why this was impossible to understand? Because some teachers just explained the thing backward: they started from the *end* and never reached the *beginning!* This is called making simple things difficult. So, this is the reason why I hope to start from the beginning and to share with the young students the joy of discovering that they can indeed follow and understand well this most difficult subject; one have to just attentively follow the *motion*. However, after introducing the warping as in the following sections and ensured that the students are now comfortable with the subject, one need to explore - through mathematics - a more detailed kinematics of the cross section, especially what deformation occurs across the the thin-wall by enriching the displacement field by local 'bubble' like additional displacement fields. The only systematic and error-free method to derive consistent equilibrium equations and the corresponding boundary conditions is without any doubt is to use the *virtual work principle*. At this point, I join firmly the teaching of my teachers. Now that you stated the physical problem correctly go and use this versatile *variational principle*.

But I have to be more correct for my teachers. They were often, indeed, consolidating a new branch of Structural Mechanics which I call *Theoretical Structural Mechanics*. It was not anymore starting from considering the equilibrium of a free-body as in Newtonian (vectorial) Mechanics but by hypothesising a cinematically displacement field and *via* variational principles or directly virtual work principle, they obtain the **Euler** or equilibrium equations. This last methodology can be classed as *theoretical mechanics* ³

³Known also as *analytical mechanics*. In such approach, let say the Lagrangian is first established then its stationarity leads to the field equations (motion equations). This is usually done by, first, hypothesising an admissible displacement field from which the velocity field is obtained. Then we write the kinetic and the potential energy of the system in order to write the complete Lagrangian. Analogously, in the *theoretical Structural Mechanics*, we state a cinematically admissible displacement field then from this determine the variations of the strains (virtual strains) and input them often directly to the *virtual work principle* (virtual work of internal and external forces) which can be seen as a stationarity conditions for the total potential energy of the system. In elastic stability problems, we instead prefer to work directly with the total potential energy change between to two neighbouring equilibrium configurations for the system. Here why I call this branch os structural mechanics *Theoretical Structural Mechanics* because together with the *Lagrangian* or the *Hamiltonian* approaches of theoretical mechanics they rely all on *variational principles* (scalar) in contrast to Newtonian (or vectorial) mechanics formulation.

3.3 Deplanation – demystifying the warping

Now that you have well studied *uniform torsion* comes the time to move further a bit and discover a new aspect called **deplanation** or **warping**. The mechanics, and more specifically, the specialised kinematics of a special type of hemicylindrical or prismatic shells, called by **Vlassov** as *thin-walled beams*, is considered here. Such thin-walled beam structures may be seen as having $t/R \leq 1/10$ and $R/L \leq 1/10$, where t being the wall thickness, R some characteristic width of the section and L the length of the beam. It is assumed that the material is isotropic and elastic. This is not a limitation but should be viewed as the definition for the wise operating limits of such thin-walled beam.



As a student, *I remember it like this was yesterday*⁸ when I've heard for the first time this term *deplanation* in Russian, I then understood, that we were moving to *higher engineering off-plan concepts* as it was the case when we have been moved from high-school-level mathematics to the university-level mathematics. The step was small but dramatic and we met for the first time the double- and triple-integral $\iint_A dx dy$, $\iiint_V dx dy dz$ or even more, the integral over a closed-path $\oint f(s) ds$! I was fascinated and simply I was transported into the fourth dimension of mind by these mathematics. As these was surely doing higher mathematics. So, does **deplanation** or equivalently **warping**, represents higher engineering structural mechanics? Anyway, it makes you off-plane.

⁸ **M. Feraoun:** "« Je me souviens, comme si cela datait d'hier de mon entrée à l'école.

I'll stop now remembering and come down to the plane. Let a long elastic rod be under some torsional loading. Assume that the cross-sections of the rod is open thin-walled. Let further assume, that the engineer, a former student from HUT, who's is designing the beam, remembers well his lessons in structural mechanics and understood to use uniformly distributed along the beam, stiffeners (or diaphragms) to ensure that the cross-sections, or more precisely the shape of its projection onto a spatial plan taken orthogonal to the length of the beam at x , are not distorted during deformation of the rod. The torsion of the rod produces axial displacement of material points on the same cross-section. This phenomenon is called *deplanation*⁹ or warping. When this deplanation or warping is uniform or non-constrained, we speak of *uniform torsion*. When such axial displacement is constrained and vary along the beam axis, this case is termed as *non-uniform torsion* with contrast to the *free-torsion = uniform torsion* or S^T Venant's torsion.

⁹ *Deplanation* means *out-of-plane motion*. Therefore, material points which were on the same cross-section plane before torsion do not any more remain on a same plane after a rotation of this cross-section as a rigid body by a small amount $d\theta(x)$.

Let's now come back to the problem setting in the classical Vlassov theory. A schematic for the torsion problem setting is shown in the above Figure. Assume a twist moment M_x is acting at the ends of the shell-beam. By virtue of superposition principle, one can decompose the total twist moment into two parts $M_x = M_t + M_\omega$. The uniform torsion part M_t is the one resulting in shearing of a mid-plane element $dx ds$ ($\gamma_{xs} \neq 0$) and, oppositely, the warping torsional moment M_ω is the one resulting in zero shearing ($\gamma_{xs} = 0$). *Nota bene* that in the

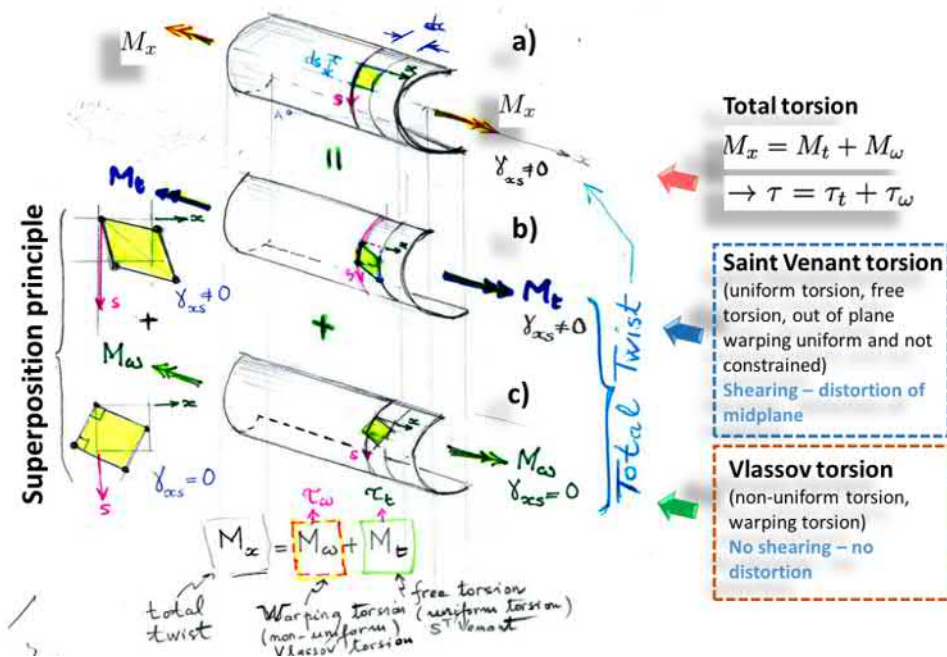


Figure 3.3: A schematic for the total torsion problem. Assume a twist moment M_x is acting at the ends of the shell-beam. By superposition we decompose the total twist moment as $M_x = M_t + M_w$. *Nota bene* that in this presentation of *Vlassov theory*, we consider only the contribution of torsion moment M_w leading to zero distortion of the mid-plane xs .

Vlassov theory, one considers only the part of torsion moment, M_w , leading to zero distortion of the mid-plane xs . The contribution from the uniform torsion should be added, later, by superposition. So, I want to stress that, the *Vlassov theory is not wrong* because it says that there is no shearing (distortion) of the mid-plane. It is the usual reading of the Vlassov’s assumption which is usually wrong or too quick. Vlassov just separates the two contributions of the twist moments M_t and M_w – the shearing and no-shearing one. Vlassov considers, first, the contribution of the warping torsional moment which is by construction not mechanical action leading to zero distortion of the mid-plane. ⁴

⁴Compare to the Bernoulli-Euler theory of bending: the kinematic assumptions lead the shear strain to vanish and therefore also the should, consistently, vanish the corresponding shear stress. However, *via* equilibrium equations (not pure bending) one finds that the shear force does not vanish and consequently, the non-zero shear stress leads logically to non-zero shear strains. The shear strains and stresses should be added through equilibrium equation and constitutive equation $\tau = G\gamma$. Equivalently, since you know already that, in an open thin-walled section, the maximum value of the Saint Venant’s shear stress varies linearly across the thickness $t(s)$ between values $\tau_t = \pm\tau_t = M_t/I_t t(s)$, you superpose it to $\tau_{xz}\omega$ to obtain the total shear stress.

3.4 Geometry of the motion of points on the cross-section



Let start by the description of the geometry of the motion⁵ of the points laying on an arbitrary the cross-section at x along the axis of th beam. To fix the motion, let us first chose two systems of coordinates; one global (xyz) they other local, (xs) on the cross-section. Let fix a section at x and a material point $P(x, s)$ on

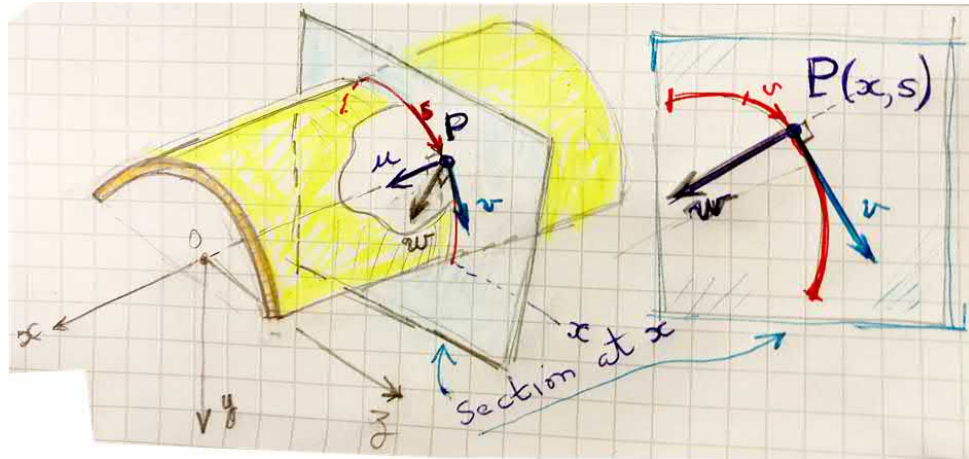


Figure 3.4: The two coordinate systems: global and local.

the cross-section. Along the mid-plane of the cross-section runs the curvilinear coordinate s . Consider the displacements in the plan of the section plan. The displacement component u is tangent to s

So a material point P on the mid-surface at (x, s) will have a displacement differential projection between x and $x + dx$ of $dw(P) = \rho \times d\theta$. Projecting again onto the tangent unit vector e_s of the mid-surface one obtains finally the needed increment component $du(P) = dw(P) \cdot \vec{e}_s$. This last displacement component will be needed when deriving the mythical relation between deplanation motion $u(x, s)$ and the sectorial coordinate $\omega(s)$. It will be shown that, indeed $u(x, s) \propto \omega(s)$. But, *what is this proportionality factor?*

⁵This kinematic assumption has exactly the role as **Euler-Bernoulli** kinematics hypothesis saying that, in bending, *planes before deformation remain planes and right angles are not distorted during deformation*. It is as a direct consequence of this assumption that the displacement hypothesis, $u_x(x, y, z) = z\theta_y - y\theta_z(x)$, is derived. Therefore, for the kinematics of thin-walled beams, one should follow the same logical steps: show graphically what in terms of motion what the Vlassov's assumption means and relate it to axial displacement (deplanation), and then, derive the resulting axial displacement field. Firstly, the students need experimental motivation of the assumption, figures and schematics, and only then, equations and mathematical manipulations, in this order. (add a side figure here for this kinematic).

3.5 The sect – $\omega(s)$

Here the idea to demystify and uncloth the notion of warping takes as much as a half-a-line to derive it from a stamp-sized schematic of the surface kinematics of thin-walled beam in torsion: Consider the experiment of twisting a rod made of open thin-walled section (Fig. 3.1). Note that, the two ends A^+ and A^- move an amount of $\Delta u(\ell)$ one to another because of torque. *Imagine* now, a small material square drawn on the mid-surface deforming in twist as a rigid body. This is approximately, what an observer sees if he draw a small square with ink on the surface. Therefore, this basic kinematic assumption, the **Vlassov's** zero-shear of the mid-plane, is based on observation. The rigid-body rotation induces an axial differential displacement which is integrated to obtain the deplanation. Solving for the axial displacement in function of the shear angle γ and the twist rate θ' gives us a result saying the $u(x, s) = -\theta'(x) \int_s r(s) ds$ where the defined integral will be called ω the *sectorial coordinate*. This is what I call the logical chronology of developing the model. Let now re-start from the beginning with *formulas and equations*, the bread of the engineers.

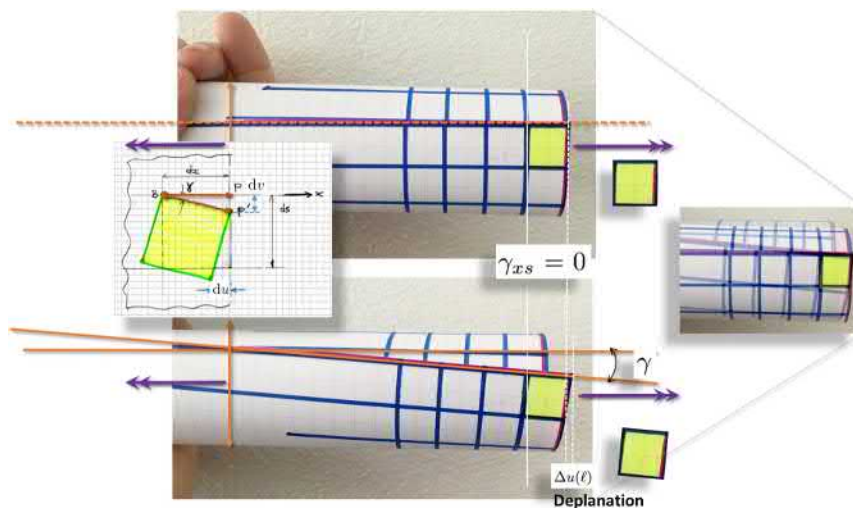


Figure 3.5: Zero shearing of the mid-plane (**Vlassov's** kinematic hypothesis) - experimental evidence.

Without loss of generality, Vlassov's theory is presented here for a straight beam aligned along its x -axis. Assume only torque force applied. The effect of bending and stretching is achieved, later, *via* superposition principle. Consider of a material point $P(x, s)$ moving to a new position P' after the applying a torque or a rotation differential of $d\theta(x)$

$$d\vec{\theta}(x) = [d\theta_x, \quad 0, \quad 0]^T \equiv d\theta(x)\vec{i}, \quad (3.2)$$

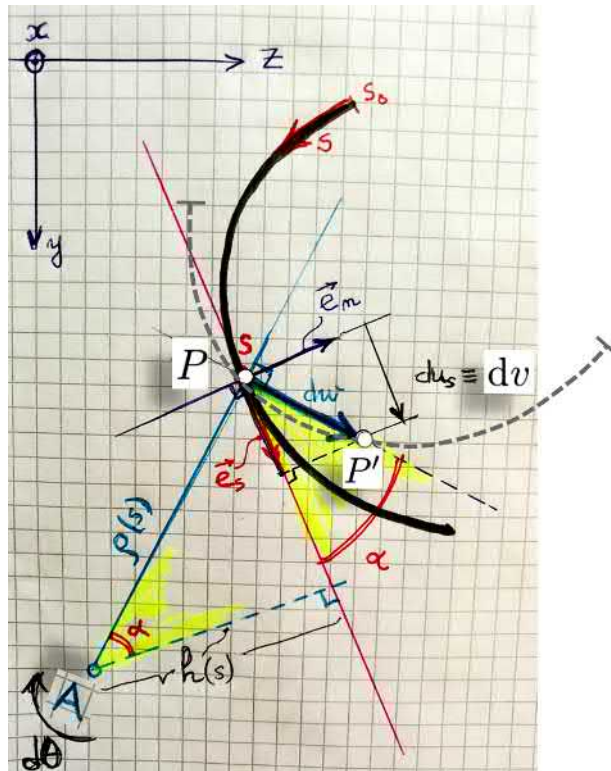


Figure 3.6: Infinitesimal rigid-body motion of a point in the plane (y, z) of Cross-section.

between two adjacent sections separated by a distance dx around the *shear centre*¹⁰ A of coordinates (y_A, z_A) . Consider now, the incremental displacement $du_s \equiv dv$ in this plane $y - z$ of such point $P(x, s) \rightarrow P'$, (Fig. 3.6). As a consequence of such infinitesimal rotation of the section, this point $P(x, s)$ will have an incremental displacement of such point will be

$$d\vec{w} = P\vec{P}' = [d\theta(x)\vec{i}] \times \vec{\rho}(s), \quad (3.3)$$

where

$$\vec{\rho}(s) = (y - y_A)\vec{j} + (z - z_A)\vec{k}. \quad (3.4)$$

The main idea: Express the deplanation differential such that it can be integrated to obtain the axial displacement $u(x, s)$ at any point $P(x, s)$ of the section at on the mid-plane. In order to achieve this task, one has to find an expression for the deplanation differential $du(x, s)$, one should express du in terms of dv which is at its turn expressed in terms of $\gamma(x) = dv/dx$, (Fig. 3.1). This is what we will do in the following.

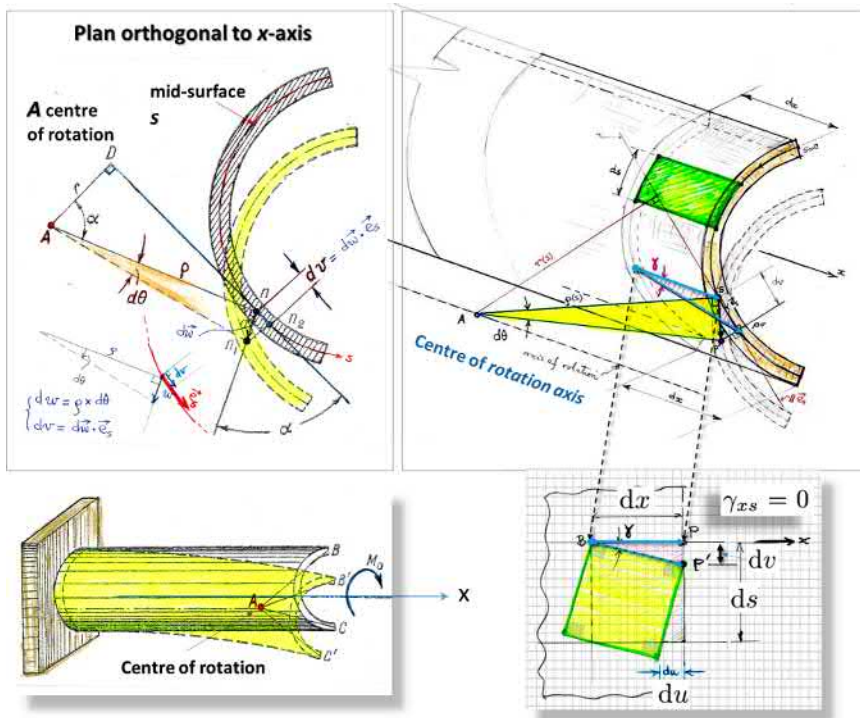


Figure 3.7: Kinematics of the displacement. Due to an external torque, the projection of the section has a rigid body motion: a rotation around an axis of rotation passing through point A and parallel to x -axis. (This figure is freely adapted from N. M. Beliaev, 1959).

The complete story of the warping: Deriving the deplanation from only geometric meaning of Vlassov's kinematic hypothesis

From geometry, (Fig. 3.6), one have

$$\boxed{r(s) \equiv h(s) = \rho(s) \cos \alpha}. \quad (3.5)$$

Projecting $d\vec{w}$ on the undeformed geometry (small displacement theory)

$$dv = d\vec{w} \cdot \vec{e}_s \quad (3.6)$$

$$= \rho(s) \cos \alpha \cdot d\theta(x), \quad (3.7)$$

$$= r(s) d\theta(x). \quad (3.8)$$

From the kinematics, (Fig. 3.7), we write that increment of the axial off-plane displacement (deplanation) du of any point on the mid-plane (component in the direction of x -axis of the total displacement under twist only) as

$$\boxed{du = -ds \cdot \sin \gamma \approx -\gamma ds}, \quad (3.9)$$

where the rigid-body motion for the point P on the mid-plane follows directly from **Vlassov's kinematic assumption** (differential element $dx ds$ have a rigid body rotation in pure twist of the section) $\gamma_{xs} = 0 \implies$, displacement vertical and horizontal components in section plane are

$$dv = dx \cdot \sin \gamma \approx \gamma dx, \quad (3.10)$$

$$du = -ds \cdot \sin \gamma \approx -\gamma ds, \quad (3.11)$$

where γ is a small rotation angle between two adjacent cross-sections. Combining the above equation, finally, one obtains the needed relation for the axial increment of displacement

$$\Rightarrow du = \gamma ds = \left(\frac{dv}{dx}\right) ds \quad (3.12)$$

$$\gamma = \frac{dv}{dx} = \underbrace{\rho(s) \cos \alpha}_{\equiv r(s)} \cdot \frac{d\theta(x)}{dx} = r(s) \theta'(x). \quad (3.13)$$

Inserting this 'shear angle' expression into the boxed equation one obtains

$$du(x, s) = -r(s) \cdot \theta'(x) \cdot ds. \quad (3.14)$$

Finally integrating along the curvilinear coordinate from a freely chosen *polus* or starting- point $s_0 = 0$ to s one obtains the axial displacement due to torsion as

$$\boxed{u(x, s) = - \int_s r(s) \theta'(x) ds = -\theta'(x) \int_s r(s) ds \equiv -\theta'(x) \cdot \omega(s)}. \quad (3.15)$$

Finally we have obtained both *i*) the definition of the *sectorial coordinate* $\omega(s)$:

$$\boxed{\omega_A(s) \equiv \int_s r(s) ds}. \quad (3.16)$$

and *ii*) an equation above for computing the axial displacement due to torsion - $u(x, s)$ - which is called *deplanation* or *warping*.

3.5.1 Normal Stress resultant from Vlassov twist

Now we consider the normal strains and stresses due only to the twist. The axial strain will be

$$\epsilon_{xx}(x, s) = \frac{d}{dx}u(x, s) = -\theta''(x) \cdot \omega(s) \quad (3.17)$$

and accounting for elasticity one obtains the resulting axial stress, called *warping normal stress* or Vlassov's normal stress, is

$$\sigma_\omega(x, s) = E\epsilon_{xx}(x, s) = -E\omega(s)\theta''(x) \quad (3.18)$$

Writing the cross section is in equilibrium one obtains

$$\int_A \sigma_\omega(x, s)dA = - \int_A E\omega(s)\theta''(x)dA = -E\theta''(x) \int_A \omega(s)dA = 0. \quad (3.19)$$

The geometric entity

$$\int_A \omega(s)dA \equiv S_\omega \quad (3.20)$$

is called the *sectorial static moment* of the cross-section. This relation will serve to correctly scale an initial $\omega(s)$ determined with respect to an arbitrary *polus* or pole s_0 . See later the details. We should also, for the section to be in equilibrium, ask for the linear moments of $\sigma_{\omega x}\omega$ around the axes y and z to vanish;

$$\int_A \sigma_\omega y dA = -E\theta''(x) \int_A \omega(s)y(s)dA = 0, \quad (3.21)$$

$$\int_A \sigma_\omega z dA = -E\theta''(x) \int_A \omega(s)z(s)dA = 0. \quad (3.22)$$

This gives us the definitions of next sectorial linear moments

$$S_{\omega y} = \int_A \omega(s)y(s)dA, \quad (3.23)$$

$$S_{\omega z} = \int_A \omega(s)z(s)dA. \quad (3.24)$$

It comes out that the sectorial moment of the Vlassov normal stresses, called $B(x)$, does not vanish. This last one is called the *Bi-moment* and defined as

$$B(x) = \int_A \sigma_{xx}\omega dA = -E\theta''(x) \int_A \omega^2(s)dA. \quad (3.25)$$

Again, a geometric entity emerges, i.e., the *sectorial moment of inertia*

$$I_\omega = \int_A \omega^2(s)dA. \quad (3.26)$$

Again, again, a beautiful formula for the warping normal stress emerges, equivalently as for the bending stresses as

$$\boxed{\sigma_\omega(x, s) = B(x) \cdot \frac{\omega(s)}{I_\omega}.} \quad (3.27)$$

This formula is analogous for the one for bending stresses, for instance, $\sigma_{xx} = M_y \cdot \frac{z(s)}{I_y}$.

3.5.2 Shear stresses

We have seen that Vlassov torsion (or non-uniform torsion) results in additional the warping shear normal warping stresses σ_ω . Considering the equilibrium of an elementary volume element, $t(s)dxds$, we see that corresponding additional shear stress component τ_ω should be added to equilibrate the additional warping normal stresses. This shear stress τ_ω is called *warping shear stress* or *Vlassov shear stress*. Therefore, by virtue of the superposition principle we say that the shear stresses due to only free torsion or *Saint Venant shear stresses* τ_t accumulate with the warping shear stresses τ_ω .

$$\tau = \tau_t + \tau_\omega, \quad (3.28)$$

where Saint Venant shear stresses are linearly distributed across the wall-thickness $t(s)$ and re-calling, from your basic courses, their maximum amplitude

$$\tau_t = \frac{M_t}{I_t} \cdot t(s) \quad (3.29)$$

3.5.3 Torsion, Bending and Stretching

When the beam is subject, in addition to torsion (T), to bending (B) and stretching axial forces (N), the *total axial displacement* field at any point $P(x, y, z)$ of the cross-section will be of the form

$$\vec{u}(x, y, z) \equiv \vec{u}(P) = \vec{u}_N(P) + \vec{u}_B(P) + \vec{u}_T(P). \quad (3.30)$$

The displacement field, at the mid-plane of the section, due to torsion only will be

$$u_T(x, s) = -\theta'_x(x) \cdot \omega(s)\vec{i} + u_0(x)\vec{i} + (z - z_A)\theta_x(x)\vec{j} + (z - z_A)\theta(x)\vec{k}. \quad (3.31)$$

The bending and stretching part will be

$$\vec{u}_{N,T}(x, y, z) = u_0(x)\vec{i} + z\theta_y(x)\vec{i} - y\theta_z(x)\vec{i}. \quad (3.32)$$

In addition the deflection of the centre-line (elastic-line) $\vec{w}(x, y = 0, z = 0)$ should be added to \vec{u} .

$$\vec{w}(x, y = 0, z = 0) = w_y(x)\vec{j} + w_z(x)\vec{k}. \quad (3.33)$$

Therefore, the total displacement field will be finally,

$$\vec{U}(x, y, z) = \vec{w}(x) + \vec{u}(x, y, z). \quad (3.34)$$

Note that, for all the equations, we are in the principle inertia axes. Now that the displacement field is obtained, the strains are easily determined from their definitions (small or engineering strains). After this, one determines the corresponding

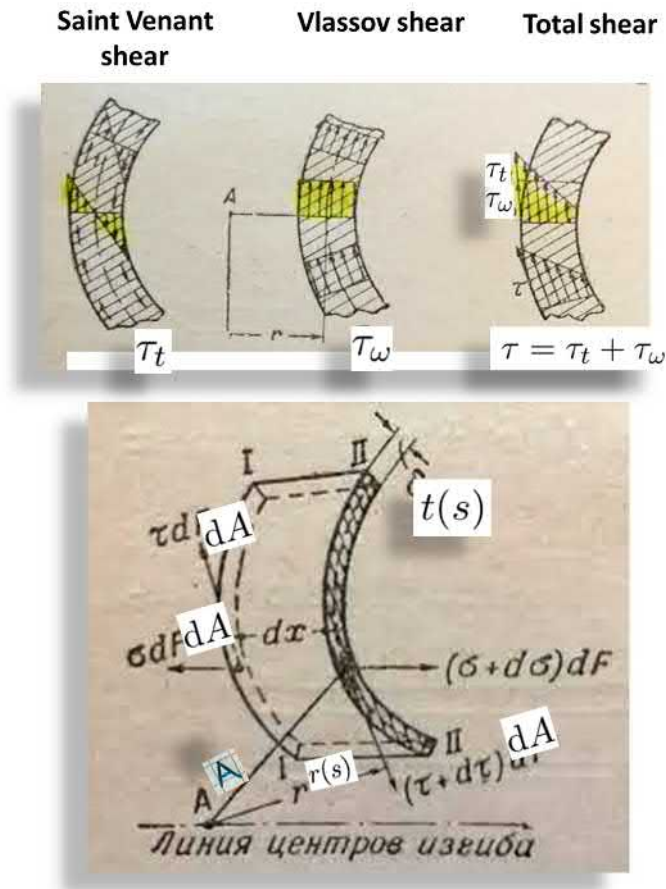


Figure 3.8: Shear stresses from free-torsion (Saint Venant) and non-uniform torsion (Vlassov). (these figures were adapted from **Belaiev** (1959).)

virtual strains that he injects in the virtual work principle to obtain finally, the equilibrium equations. Note that the stresses are obtained through the strains using elasticity relations. Therefore, the whole problem is solved. CQFD.

So the answer to the primary question of what is this proportionality factor? is the sectorial coordinate $\omega(s)$.

That short is the story of the *sectorial*- ω and of the deplanation $u(x, s) = -\theta'(x) \cdot \omega(s)$. From here forward, once the true centre of rotation T is being determined, it will be just a question of scaling ω_A with respect to the true centre of torsion such $S_{\omega_T} = 0$ or in other words that $\omega_T = \omega_A - S_{\omega_A}/A$. (The student should train to determine the centre of rotation and to draw the distribution of the final scaled sectorial coordinate). Now emerges many new meta-concepts in

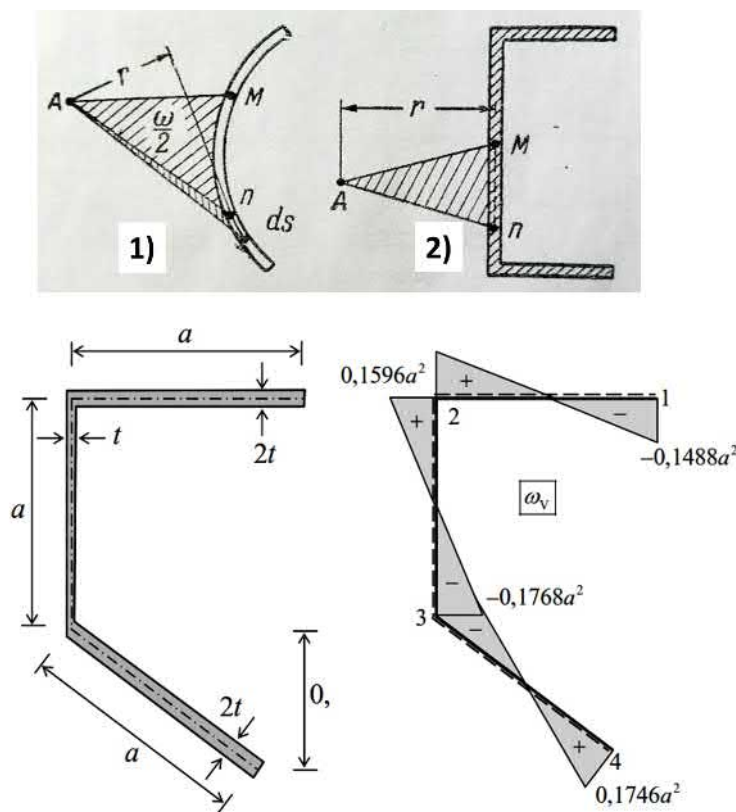


Figure 3.9: Example of geometrical meaning of the sectorial coordinates (from **Beliaev**). Another example of a computed distribution of the sectorial coordinate for the given profile (This last figure from Emeritus professor **Jukka Aalto** lecture-notes).

the form of *design handles* – as the result of dimension reduction from a cylindrical shell to a *thin-walled shell-beam of open section* – as

$$S_\omega = \int_A \omega(s) dA = \int_s \omega(s) t(s) ds, \tag{3.35}$$

$$I_\omega = \int_A \omega^2(s) dA = \int_s \omega^2(s) t(s) ds, \tag{3.36}$$

the warping normal and shear stresses

$$\sigma_\omega(x, s) = -E\omega(s)\theta''(x) = \frac{B(x)\omega(s)}{I_\omega}, \tag{3.37}$$

$$\tau_\omega(x, s) = \frac{B'(x)S_\omega(s)}{t(s)I_\omega} = \frac{M_\omega(x)S_\omega(s)}{t(s)I_\omega}, \tag{3.38}$$

and the bi-moment and the warping moment (torsional)

$$B(x) = -EI_\omega \theta''(x), \quad M_\omega = B' = -EI_\omega \theta''', \quad (3.39)$$

Consequentially, additional *warping shear stresses* τ_ω also emerges to equilibrate the additional warping normal stress $\sigma_\omega(x, s)$. So this is a rich family of 100%-useful engineering handles for structural designers to separate and *give names*¹¹ means to various contributions to the overall stress state.

¹¹ Things and concepts exist only after giving them names.

I think that now the problem is set well. *The kinematics is demystified.* Remains to write equilibrium equations and to set the problem as a boundary value-problem. This job, I let it for you as a homework. Just use free-body diagrams or preferentially, the *virtual work principle* and you should end up with

$$-EI_\omega \theta^{(IV)}(x) + GI_t \theta'' = m, \quad (3.40)$$

and the constitutive relations

$$M_t = GI_t \theta', \quad B = -EI_\omega \theta'', \quad M_\omega = B' = -EI_\omega \theta'''. \quad (3.41)$$

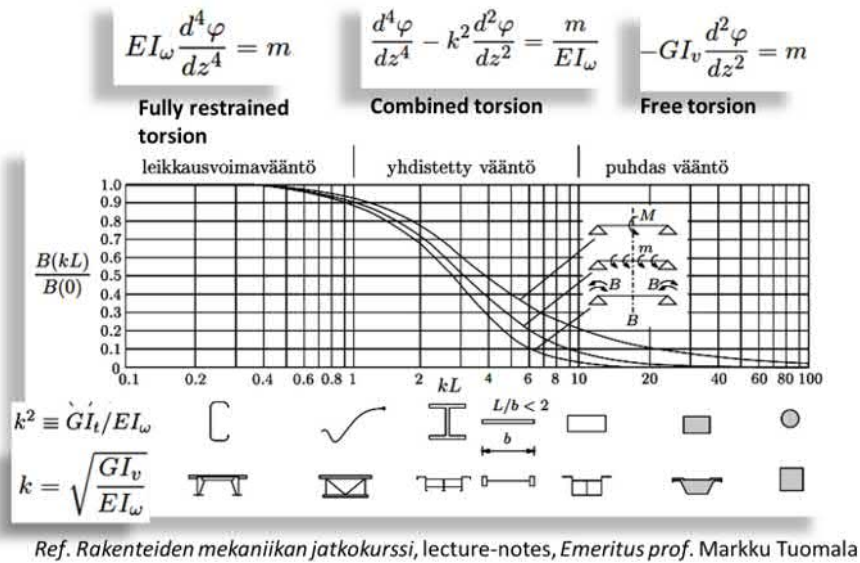


Figure 3.10: Torsion - regimes.

For modern presentation of the Vlassov's theory, please refer to modern courses.

This figure will be moved to the *plasticity* chapter.

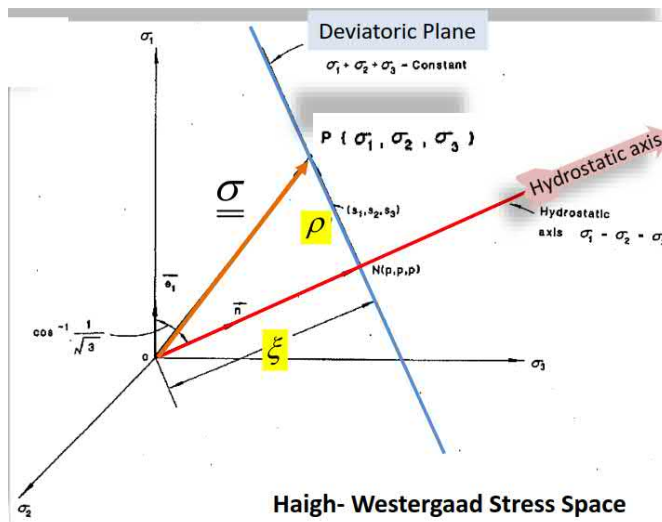


Figure 3.11: Haigh-Westergaard Stress Space

Chapter 4

On Euler's Elastica

The study of *Elastica*¹² is meant as a classical and natural introduction to the geometrically non-linear problems we will address, in next chapters, while analysing frames with large displacements and large rotations and the so-called *second-order* or more commonly *geometrically non-linear effects*.

Consider a planar straight homogeneous flexible slender rod having constant cross-section with a constant static load acting at its end with no torsion. Because of the slenderness, the displacement and rotations are not any more small. They are Finite. The deformation are assumed to remain in the elastic domain even for large displacements. Thus the strains remain small. This is a typical case of *large displacement with small strains*. This is the case for very slender rods, as instance hairs, a slender pole, or a slender fishing rod.

In order to account for large displacements and rotations one should write equilibrium equations in the deformed configuration. The material coordinates denoted by $X(s)$ and $Y(s)$ and the spatial coordinates, respectively, by $x(s)$ and $y(s)$ where

$$x(s) = X(s) + u(s), \quad y(s) = Y(s) + v(s) \quad (4.1)$$

and the curvilinear coordinate along the deformed rod being s . The displacement vector being (u, v) . The rod is assumed inextensible.

Equilibrium Equations

Moment Equilibrium around section A gives

$$M(s) - M(s + \Delta s) - F_x \Delta y + F_y \Delta x = 0, \quad (4.2)$$

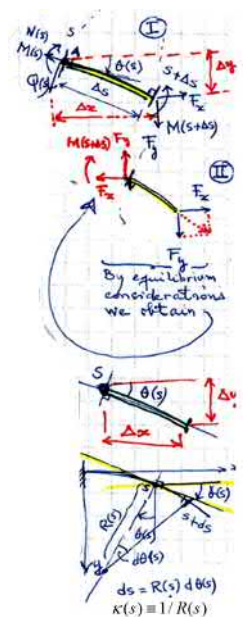
where

$$\Delta x(s) = \Delta s \cos(\theta(s)), \quad \Delta y(s) = \Delta s \sin(\theta(s)). \quad (4.3)$$

After insertion of the above geometrical relations, the moment equation becomes

$$M(s) - M(s + \Delta s) - F_x \sin(\theta(s))\Delta s + F_y \cos(\theta(s))\Delta s = 0, \quad (4.4)$$

¹² This problem was proposed by Jacob Bernoulli (1691). Daniel Bernoulli derived the Elastica energy functional and the minimal principle. Using that, Euler (1744) solved the *Elastica* problem by setting it as an *isoperimetrical* problem and developed for that a new field in mathematics *variational calculus* and also the elliptic integral theory.



and taking the limit as $\Delta s \rightarrow 0$, one finally have

$$-M'(s) - F_x \sin(\theta(s)) + F_y \cos(\theta(s)) = 0. \quad (4.5)$$

Accounting for elasticity and bending moment-curvature relation $M = EI\kappa = -EI\theta'$ where the prime is derivative with respect to s , one obtains the classical Elastica differential equation of the cantilever

$$\boxed{(EI\theta'(s))' - F_x \sin(\theta(s)) + F_y \cos(\theta(s)) = 0} \quad (4.6)$$

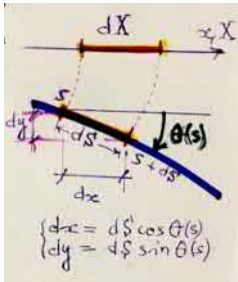
with boundary conditions

$$\theta(0) = 0, \quad M(\ell) = (EI\theta')(\ell) = 0. \quad (4.7)$$

The rotation $\theta(s)$ is obtained as a solution of the boundary-value problem (BVP) (4.6) using appropriate boundary conditions (4.7).

The analytical solution involves elliptic integrals which are not obtainable in a close form. One can also numerically solve the BVP as a constrained minimisation problem of the total potential energy $\Pi(\theta(s))$

$$\Pi(\theta(s)) = \frac{1}{2} \int_0^\ell (EI\theta'(s))^2 ds - F_x u(\ell) - F_y v(\ell), \quad (4.8)$$



where $x(\ell) = \int_0^\ell \cos(\theta(s)) ds$ and $y(\ell) = \int_0^\ell \sin(\theta(s)) ds$. For instance, by approximating piece-wisely the curvature $\theta'(s)$ or directly the rotation $\theta(s)$. The minimum order of required continuity for the curvature is piece-wise constant within each-element. The constraint being $\theta(0) = 0$. Now, if one assumes the Euler-Bernoulli kinematics, then $\sin \theta = v' \implies \theta = \arcsin(v')$ and

$$(EIv'')' - F_x \sin(\theta) + F_y \cos(\theta) = 0, \quad (4.9)$$

which, after derivation further, the equilibrium equation takes a more familiar look as

$$(EIv''') - F_x \cos(\theta) - F_y \sin(\theta) = 0, \quad (4.10)$$

The displacement vector components (u, v) at some section $s_i \in [0, \ell]$ will be determined from the rotation θ via integrating spatial coordinates from relations (4.1) as

$$u(s_i) = x(s_i) - X(s_i), \quad v(s_i) = y(s_i) - Y(s_i). \quad (4.11)$$

Noticing from geometry that we have the relations $\sin(\theta(s)) = dy(s)/ds$ and $\cos(\theta(s)) = dx(s)/ds$ one obtains

$$u(s_i) = x(0) + \int_0^{s_i} \cos(\theta(s)) ds - X(s_i), \quad (4.12)$$

$$v(s_i) = y(0) + \int_0^{s_i} \sin(\theta(s)) ds - Y(s_i). \quad (4.13)$$



Boubka.

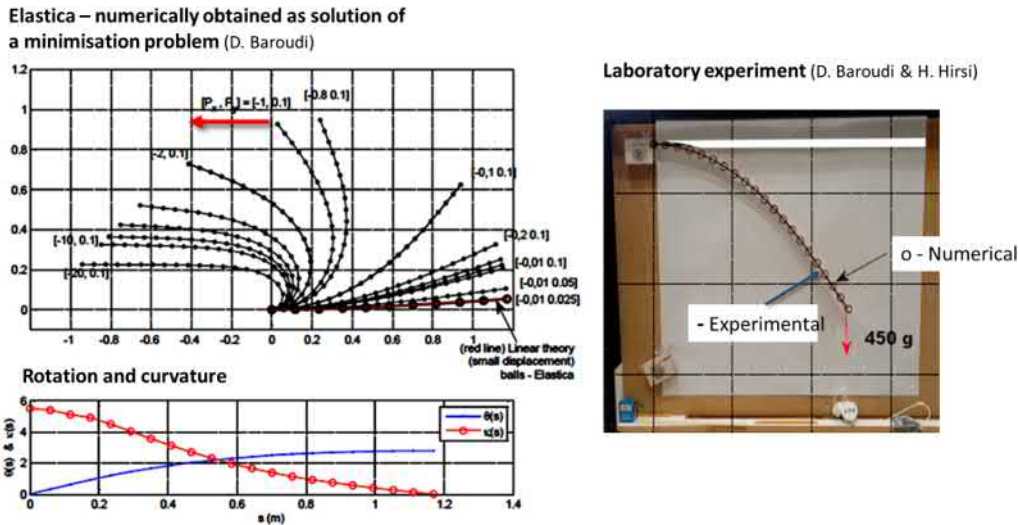


Figure 4.1: Numerically obtained Elastica under various loading as compared to experiment.

Remember that in the Elastica problem, we assumed that the rod was inextensible. Therefore, the axial strain from *material* deformation is zero (no *stretching*). The only contribution to axial deformation results from *bending*, in other words, from the *geometrical non-linearity* induced by the finite Lagrangian¹

$$\kappa \equiv \frac{d\theta}{ds} = -\frac{d^2v}{dx^2} \frac{1}{\left[1 - \left(\frac{dv}{dx}\right)^2\right]^{1/2}}. \tag{4.14}$$

The total axial displacement component $u(\ell) \approx u_b(\ell)$ is due to bending contribution from v . One can show further that, *par exemple*, the relative shortening of the centreline due to bending is

$$\epsilon_s = \frac{du}{ds} = \frac{d}{ds} \int_0^s \cos(\theta(s)) ds = \cos(\theta(s)) \tag{4.15}$$

$$\approx \left(1 - \frac{1}{2}\theta^2\right) = 1 - \frac{1}{2}v'^2(s). \tag{4.16}$$

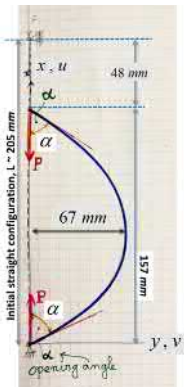
Example: Analytical solution of Elastica

What is the shape of a stringed initially straight bow? Or what is the shape of Sergey Boubka's¹³ pole? The answer is given by the solution of the BVP (4.6).

Analytical expressions (4.12) and (4.13) involves elliptic integrals and are not obtainable in a close form. We should anyway use numerical quadrature to estimate these integrals when solving the BVP (4.6).

¹The Eulerian curvature is given by $\kappa = -\frac{d^2v}{dx^2} / \left[1 + \left(\frac{dv}{dx}\right)^2\right]^{3/2}$.

¹³ **Sergey Boubka** is a legendary Ukrainian pole vaulter having the world record 35 times! His latest record is 6m15 in 1993. Finally, **Renald Lavellenie** got 6m16 in 2014.



True deformed shape of a stringed elastic ruler.

The analytical form of *Elastica* using elliptic integrals is here reminded shortly for the interested students. Here how it goes:

Consider a slender bow or pole with zero bending moments at ends. The boundary conditions correspond to those of hinged ends. Let the rotation angles $\theta(0) = \alpha$ and $\theta(\ell) = -\alpha$, where $\alpha > 0$ is the opening angle at the ends. Note that the rotation angle θ is a *monotonically* increasing (decreasing) from one end to the opposite one. The boundary conditions fix the constant of integration. Then, for constant EI and constant $(F_x, F_y) = (-P, 0)$, $P > 0$, multiplying by $d\theta/ds$ the BVP

$$EI\theta'' - P \cos(\theta) = 0 \tag{4.17}$$

and then integrating with respect to s yield to

$$\frac{1}{2}EI\theta'^2 = +P \cos(\theta) + C. \tag{4.18}$$

Inserting all 'this and that' into (4.18) and denoting $P/EI \equiv k > 0$ we obtain

$$\left(\frac{d\theta}{ds}\right)^2 = 2k^2(\cos \theta - \cos \alpha) \rightarrow ds = d\theta/[k\sqrt{2(\cos \theta - \cos \alpha)}] \tag{4.19}$$

which yield to the elliptic integral for solving the shape s of the pole or bow parametrized by θ ¹⁴

$$s(\theta) = \frac{1}{k} \int_{\theta}^{\alpha} d\theta/[\sqrt{2(\cos \theta - \cos \alpha)}]. \tag{4.20}$$

This integral should be evaluated numerically, for each $\theta_i \in [\theta = -\alpha : \Delta\theta : \alpha]$ where $\Delta\theta$ is some chosen discretisation step. The end-values of the opening angle α is kept fixed. When $\theta = -\alpha$, the integral is equal to ℓ , the total length of the pole. This constraint provides a relation between α and $P/P_E \equiv \ell^2 k/\pi$, where the classical Euler's buckling load being P_E .

The Cartesian coordinates¹⁵ x and y are then easily derived as

$$x = \frac{1}{k} \int_{\theta}^{\alpha} \cos(\theta)/[\sqrt{2(\cos \theta - \cos \alpha)}]d\theta \tag{4.21}$$

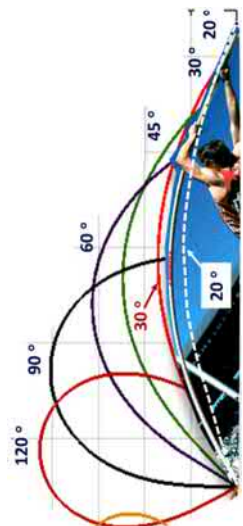
and

$$y = \frac{1}{k}[\sqrt{2(\cos \theta - \cos \alpha)}]. \tag{4.22}$$

The algorithm for integrating numerically (4.21) reads:

- **fix** a value for $\alpha > 0$ and k .
- **set** $\theta(0) = -\alpha, \theta(\ell) = \alpha$

$$\begin{aligned} \frac{dx}{ds} &= \cos(\theta(s)) \\ \frac{dy}{ds} &= \sin(\theta(s)). \end{aligned}$$



Boubka's pole follows the shape of the *Elastica*.

- **determine** the length ℓ of the rod *via* numerical quadrature of the arch-length $\ell = s(\theta = -\alpha) = \frac{1}{k} \int_{\theta=-\alpha}^{\alpha} d\theta / [\sqrt{2(\cos \theta - \cos \alpha)}]$.
- **chose** a discretisation step $\Delta\theta = \alpha/N$, where N the number of intervals or arch-segments being fixed, let's say $N = 10 \dots 1000$.
- **discretize** the interval $[\theta(0), \theta(\ell)]$, with a step $\Delta\theta$
 $(\theta(s_1) \equiv \theta_1 = -\alpha, \quad \theta(s_N) \equiv \theta_N = +\alpha)$
- **for** $i = 1 : N$ **do**
- **increment** $\theta_{i+1} = \theta_i + \Delta\theta$
- **for each** $\theta_i \in$ **integrate numerically**. Here, I use Gauss¹⁶ quadrature the following integral for the Cartesian coordinates of the Elastica: $x(\theta_i)$ and the expression of $y(\theta_i)$

¹⁶ $I = \int_a^b f(z)dz \approx \sum_{k=1}^{NG} f(z_k)w(z_k)$; $NG, z_k, w(z_k)$ are number, coordinates and weight of the integration points, respectively.

$$x(\theta_i) = \frac{1}{k} \int_{\theta_i}^{\alpha} \cos(\theta) / [\sqrt{2(\cos \theta - \cos \alpha)}] d\theta, \tag{4.23}$$

$$y(\theta_i) = \frac{1}{k} [\sqrt{2(\cos \theta_i - \cos \alpha)}]. \tag{4.24}$$

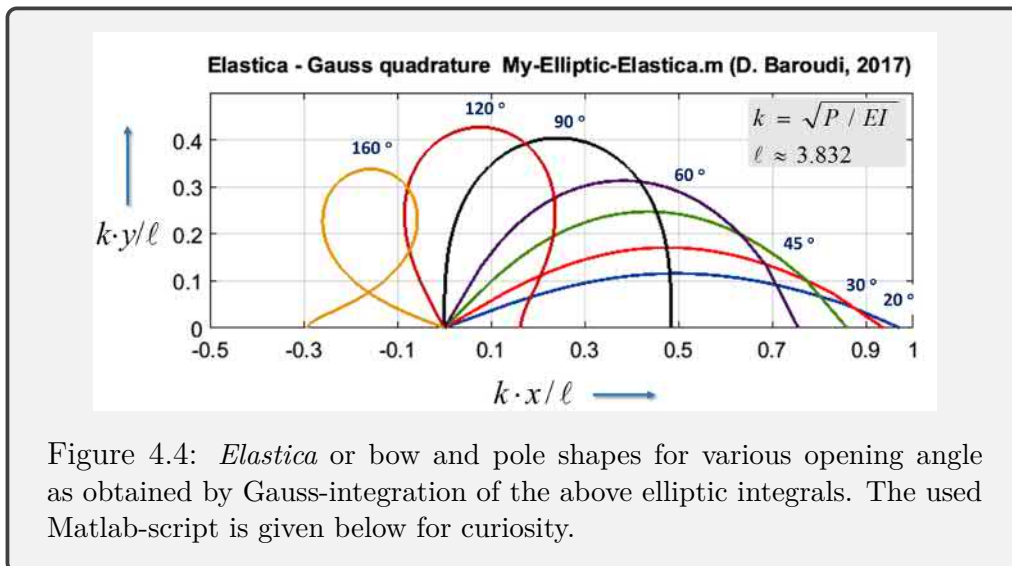


Figure 4.4: *Elastica* or bow and pole shapes for various opening angle as obtained by Gauss-integration of the above elliptic integrals. The used Matlab-script is given below for curiosity.

So, this was this Chapter to introduce Euler's Elastica.